Adaptive Methods for Time Domain Boundary Integral Equations

A Thesis Submitted for the Degree of Doctor of Philosophy

by Matthias Gläfke

School of Information Systems, Computing and Mathematics

Brunel University

December 2012

Abstract

This thesis is concerned with the study of transient scattering of acoustic waves by an obstacle in an infinite domain, where the scattered wave is represented in terms of time domain boundary layer potentials. The problem of finding the unknown solution of the scattering problem is thus reduced to the problem of finding the unknown density of the time domain boundary layer operators on the obstacle's boundary, subject to the boundary data of the known incident wave.

Using a Galerkin approach, the unknown density is replaced by a piecewise polynomial approximation, the coefficients of which can be found by solving a linear system. The entries of the system matrix of this linear system involve, for the case of a two dimensional scattering problem, integrals over four dimensional space-time manifolds. An accurate computation of these integrals is crucial for the stability of this method. Using piecewise polynomials of low order, the two temporal integrals can be evaluated analytically, leading to kernel functions for the spatial integrals with complicated domains of piecewise support. These spatial kernel functions are generalised into a class of admissible kernel functions. A quadrature scheme for the approximation of the two dimensional spatial integrals with admissible kernel functions is presented and proven to converge exponentially by using the theory of countably normed spaces. A priori error estimates for the Galerkin approximation scheme are recalled, enhanced and discussed. In particular, the scattered wave's energy is studied as an alternative error measure.

The numerical schemes are presented in such a way that allows the use of non-uniform meshes in space and time, in order to be used with adaptive methods that are based on a posteriori error indicators and which modify the computational domain according to the values of these error indicators. The theoretical analysis of these schemes demands the study of generalised mapping properties of time domain boundary layer potentials and integral operators, analogously to the well known results for elliptic problems. These mapping properties are shown for both two and three space dimensions. Using the generalised mapping properties, three types of a posteriori error estimators are adopted from the literature on elliptic problems and studied within the context of the two dimensional transient problem. Some comments on the three dimensional case are also given. Advantages and disadvantages of each of these a posteriori error estimates are discussed and compared to the a priori error estimates.

The thesis concludes with the presentation of two adaptive schemes for the two dimensional scattering problem and some corresponding numerical experiments.

Acknowledgements

Life is mainly grief and labour.
Two things get you through.
Chortling when it hits your neighbour,
Whingeing when it's you.

Sir Kingsley Amis (1922-1995)

The last three years were indeed quite laborious. Thankfully I had the good fortune to have some people around me who made sure that there never was too much grief.

The most important one of them is my supervisor, Matthias Maischak, who was always ready to discuss the progress of my work and who helped me a lot with his guidance and experience. His research code *maiprogs* has provided a much more than just solid foundation for the code I developed for the numerical experiments conducted in this work.

The Department of Mathematical Sciences at Brunel University funded my research with a generous grant and allowed me to work in a friendly atmosphere. All of the technical and administrative staff were always kind and helpful. I also enjoyed the company of my fellow students a lot.

I would further like to thank Layal Hakim and Lothar Banz, who both read draft versions of this thesis and pointed out several errors. I am, however, solely responsible for the remaining ones. Layal and Lothar were also always interested in discussing my mathematical problems, for which I am additionally grateful.

Contents

List of Figures

List of Tables

List of Algorithms

Nomenclature

$\mathbb{1}_A$	indicator function for some set A
$\delta_{i,j}$	Kronecker delta
$\mathfrak{R}, \mathfrak{I}$	real and imaginary part of a complex number
H	Heaviside function
δ	Dirac impulse
$\star$	convolution operator
$\frac{\partial}{\partial s}$	differentiation with respect to the arc length
$\mathcal{B}$	boundary data of a function
$\Box$	d'Alembert operator, see equation (1.1a)
G	fundamental solution of the wave equation, see Lemma 1.2
S, D	wave equation Single and Double Layer potential, see Definition 1.3
V, K', K, W	wave equation Single Layer, adjoint Double Layer, Double Layer and hypersingular operator, see Definition 1.4
$\gamma_0^{\text{in}}, \gamma_0^{\text{ex}}, \gamma_1^{\text{in}}, \gamma_1^{\text{ex}}$	interior and exterior trace, and normal derivative operator, see Definition 1.5
$[\![\gamma_0]\!]_\Gamma, [\![\gamma_1]\!]_\Gamma$	jump, and jump of the normal derivative across Γ, see Definition 1.5
$\mathcal{T}_S, \mathcal{T}_T, \mathcal{T}_{S,T}$	spatial and temporal mesh, and combined space-time mesh, see Section 2.1 (p. 19)
Γ_i, T_j	boundary element and temporal element (time slab), see Section 2.1 (p. 19)
$h_i, h, \Delta t_j, \Delta t$	local and global spatial and temporal mesh widths, see Section 2.1 (p. 19)
$h(\mathcal{T}_S), \Delta t(\mathcal{T}_T)$	mesh widths functions, see Section 2.1 (p. 19)
$K(\mathcal{T}_S)$	maximum quotient of sizes of neighbouring elements in spatial mesh, see equation (2.3)
$q(\mathcal{T}_S)$	maximum quotient of element sizes in spatial mesh, see equation (2.4)
$V_h^p, V_{\Delta t}^q, V_N$	spatial and temporal discretisation space, and their tensor product, see Section 2.2 (p. 20)
γ^m, β^m	piecewise constant and piecewise linear temporal basis function, see equations (2.8) and (2.9)

P	abstract wave equation boundary integral operator, see equation (2.11)
$\langle\cdot,\cdot\rangle$	duality product/$L^2(\Gamma)$ inner product, see equation (2.14)
$\Upsilon^{q;\,m,n}, \Upsilon^{m,n}, \Upsilon^m_\alpha$	temporal part of the discrete general kernel, see equations (2.11), (2.20) and (2.34)
r	distance of points $\vec{x}, \vec{y} \in \Gamma$, see p. 22, below equation (2.18)
E_l, D_l	discrete light ring and disc, see equations (2.22) and (2.23)
$\mathcal{U}^{m,n}$	system matrix block, see equation (2.27)
$\vec{m}_i, \vec{d}_i, \vec{x}_i, \vec{x}_{i+1}$	data of arbitrary boundary edge Γ_i, see equation (2.37) and Figure 2.2a
$\vec{a} \times \vec{b}$	two dimensional cross product, see equation (2.38)
$D^i_{l-1}, D^j_{l-1}(\vec{x})$	discrete light disc of a boundary edge and a point $\vec{x}$, see equations (2.53) and (2.54)
$E^i_{l-1}, E^j_{l-1}(\vec{x})$	discrete light ring of a boundary edge and a point $\vec{x}$, see equations (2.56) and (2.57)
$E(r_1, r_2; \vec{x}), E(r_1, r_2; \Gamma_j)$	domain of influence of a point $\vec{x}$ and a boundary edge Γ_j, see equations (2.60) and (2.63), and Figure 2.5
$\mathcal{E}_{\Gamma_j}$	boundary edge ray of a boundary edge Γ_j, see equation (2.61)
$\operatorname{dist}(\vec{x}, \Gamma_j)$	minimum distance of a point $\vec{x}$ and a boundary edge Γ_j, see equation (2.62)
$P_{R,e}[\varphi]$	time domain boundary layer potential with discrete support, see equation (2.71)
$n!!$	double factorial, see equation (2.93)
C^k_{pw}	set of piecewise C^k-curves, see p. 47, below Remark 2.9
$\mathcal{B}^l_\beta(\Omega_{\mathrm{ref}})$	countably normed space for the reference element, see Definition 2.13
$\mathcal{F}_t, \mathcal{F}_x, \mathcal{L}_t$	Fourier transform with respect to the time and space variable, and Fourier-Laplace transform with respect to the time variable, see equations (3.1), (3.2) and (3.3)
$\mathcal{S}(\mathbb{R}^N), \mathcal{S}(E)$	space of tempered $\mathbb{R}^N$- and E-valued functions, see Definitions 3.2 and 3.4
$LT, LT(E)$	space of Laplace transformable distributions and Laplace transformable distributions with values in E, see Definitions 3.2 and 3.4
Λ^s	temporal derivative/anti-derivative operator, see equation (3.4)
G_ω	fundamental solution of the Helmholtz equation, see Lemma 3.7
S_ω, D_ω	Helmholtz equation Single and Double Layer potential, see Definition 3.8
$V_\omega, K'_\omega, K_\omega, W_\omega$	Helmholtz equation Single Layer, adjoint Double Layer, Double Layer and hypersingular operator, see Section 3.2 (p. 78)
E_Ω	energy in the domain Ω, see equation (3.11)
$H^s(\mathcal{O}),\ \|\cdot\|_{H^s(\mathcal{O})},\ \|\cdot\|_{s,\omega,\mathcal{O}}$	Sobolev space with corresponding usual and weighted norm, with $\mathcal{O} \in \{\mathbb{R}^N, \Omega, \Gamma\}$, see equations (3.13) and (3.14)
a^V_ω, a^W_ω	bilinear forms for the Helmholtz Dirichlet and Neumann problem, see equations (3.44) and (3.45)

N_ω, N	Helmholtz and wave equation Newton potential, see equations (3.50) and (3.51)
$\mathcal{P}_\omega, \mathcal{P}_\omega^*$	Helmholtz and adjoint Helmholtz operator, see equations (3.59a) and (3.88a)
$\mathcal{H}_\sigma^k(\mathbb{R}, E),\ \|\cdot\|_{\sigma,k,E}$	classical space-time Sobolev space with corresponding norm, see Definition 3.37
$H_{\sigma,\mathcal{O}}^{k;\,s,s},\ \|\cdot\|_{\sigma,\mathcal{O};\,k;\,s,s}$	energy space-time Sobolev space with corresponding norm, with $\mathcal{O} \in \{\Omega, \Gamma\}$, see Definition 3.39
$H_{\mathcal{O}}^{r,s},\ \|\cdot\|_{\mathcal{O};\,r,s}$	anisotropic space-time Sobolev space with corresponding norm, with $\mathcal{O} \in \{\mathbb{R}^N, \Omega, \Gamma\}$, see Remark 3.40 c)
$H_{\mathcal{O}}^{k;\,s,s},\ \|\cdot\|_{\mathcal{O};\,k;\,s,s}$	generalised anisotropic space-time Sobolev space with corresponding norm, with $\mathcal{O} \in \{\mathbb{R}^N, \Omega, \Gamma\}$, see Definition 3.41 c)
$\langle\!\langle \cdot, \cdot \rangle\!\rangle_\sigma$	$\mathcal{H}_\sigma^k(\mathbb{R}, E)$- and $H_{\sigma,\mathcal{O}}^{k;\,s,s}$-duality product, see equation (3.119)
a_σ^V, a_σ^W	bilinear forms for the scattering Dirichlet and Neumann problem, see equations (3.154)/(4.1) and (3.155)
$\Pi_{h,\Delta t;\,s,k}^{m_1,m_2}$	projection operator, see (3.158)
$\|\!\|\!\|\cdot\|\!\|\!\|$	energy norm, see (4.14)
$\bar{k}, K, \tilde{K}, K_\alpha$	auxilary integrals, see equations (A.1) - (A.4)
S, L	auxilary functions, see equation (A.22)

Chapter 1

Introduction

Let $\Omega^- \subseteq \mathbb{R}^n$ be a bounded open domain, with $n = 1, 2, 3$ denoting the number of spatial dimensions. Its complement is given by $\Omega := \mathbb{R}^n \setminus \Omega^-$, with boundary $\Gamma := \partial\Omega$. In the present work, we consider the boundary-initial value problem [127]

$$
\text{(P)} \quad \left\{ \begin{array}{l} \text{Find } u : \Omega \times \mathbb{R}_{\geq 0} \to \mathbb{R} \text{ such that} \\ \\ \qquad\qquad \Box u := \dfrac{\partial^2 u}{\partial t^2} - \Delta u = 0 \text{ in } \Omega \times \mathbb{R}_{\geq 0} \qquad (1.1a) \\ \qquad\qquad u(x,0) = 0 \text{ in } \Omega \qquad (1.1b) \\ \qquad\qquad \dfrac{\partial u}{\partial t}(x,0) = 0 \text{ in } \Omega \qquad (1.1c) \\ \qquad\qquad \mathcal{B}[u](x,t) = g(x,t) \text{ on } \Gamma \times \mathbb{R}_{\geq 0} \qquad (1.1d) \\ \\ \text{where } g : \Gamma \times \mathbb{R}_{\geq 0} \to \mathbb{R} \text{ is a given function.} \end{array} \right.
$$

The hyperbolic partial differential equation (1.1a) is known as the (homogeneous) *wave equation* or *d'Alembert's equation* [154]. By Δ in (1.1a) we denote the *Laplace operator* $\Delta = \sum_{i=1}^{n} \frac{\partial^2}{\partial x_i^2}$. The operator $\Box$ in (1.1a) is known as the *d'Alembert operator* or the *wave operator*. The initial conditions (1.1b), (1.1c) are called *homogeneous* and correspond to the assumption of a quiescent past. In the literature, (1.1a) subject to the initial conditions (1.1b) and (1.1c) is referred to as the *homogeneous wave equation*.

The boundary condition (1.1d) is called *Dirichlet boundary condition* if $\mathcal{B}[u] = u$, whereas it is called *Neumann boundary condition* if $\mathcal{B}[u] = \frac{\partial u}{\partial n}$. In the first case, the scatterer is said to be *sound-soft* or *acoustically soft*. In the latter case, it is called *sound-hard* or *acoustically rigid* [126, pp. 345ff.].

If $\mathcal{B}[u] = \frac{\partial u}{\partial n} - \alpha \frac{\partial u}{\partial t}$, the boundary condition (1.1d) is called *Robin boundary condition* or *impedance boundary condition* [51, p. 2], and the scatterer is then called *absorbing* [81, 82], with impedance function $\alpha : \Gamma \to \mathbb{R}_{\geq 0}$. The assumption of $\alpha(x) \geq 0$ for all $x \in \Gamma$ ensures that (P) is well-posed in this case [82]. However, we only consider the first two types of boundary conditions in this work.

Physically, the unknown solution $u = u^{\text{sc}}$ of problem (P) corresponds to the scattered wave reflected by the obstacle Ω^- when it is hit by an incident wave u^{inc}, if the boundary condition is chosen as $\mathcal{B}[u] = -\mathcal{B}[u^{\text{inc}}]$. This physical problem is illustrated in Figure 1.1.

The scattering problem (P) is a model problem for various (acoustic, electromagnetic and elastic) wave propagation problems with numerous engineering applications, such as aero-acoustics, bio-acoustics, hydro-acoustics, optoelectronic communication, radar detection, tomography and

ultrasound imaging [23, 54, 81, 134, 150].

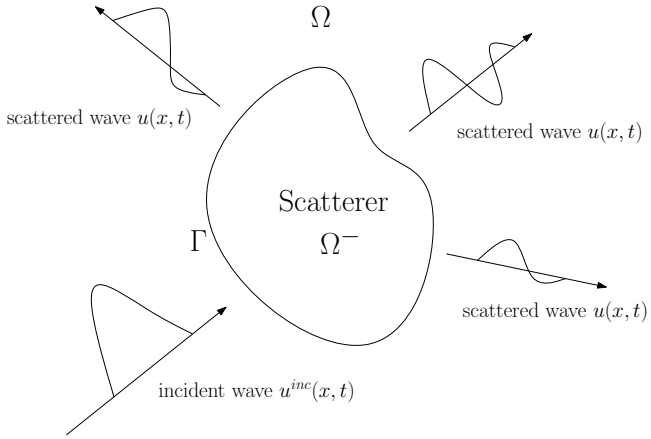

Figure 1.1: The physical problem that corresponds to problem (P): The scatterer Ω^- is hit by an incident wave u^{inc} and reflects the scattered wave $u = u^{\text{sc}}$.

Remark 1.1 (Sound Velocity / Huygens' Principle)
a) In general, the homogeneous wave equation (1.1a) *is*

$$\frac{1}{c^2}\frac{\partial^2 u}{\partial t^2} - \Delta u = 0$$

where c is the velocity of sound in the medium Ω under consideration. Choosing appropriate units allows us, as in (1.1a)*, to assume $c = 1$ without loss of generality [82, p. 1847].*

b) There is a well known fundamental difference in the nature of the scattered wave in different space dimensions n. In the three dimensional case, and in fact for every odd $n > 1$, the scattered wave travels in the form of a sphere, with a sharp front and a sharp cutoff, which means that the excited state in the neighbourhood $\mathbb{B}_\varepsilon(x)$ of a point $x \in \Omega$, $\epsilon \ll 1$, persists only for $t = dist(x, \Omega^-)$. Once the wave has passed a point, it returns to its previous quiescent state. On the other hand, in two space dimensions, and equally for every even $n \geq 2$, the excited state persists indefinitely at every point the wave has passed, i.e. for every time $t \geq dist(x, \Omega^-)$. The scattered wave therefore has, in this case, a sharp front, but it is not a sharp signal as a whole, with diffusions in its infinite tail. These physical phenomena, which are illustrated in Figure 1.2, are known as Huygens' principle*.*

Popular examples that illustrate Huygens' principle are the propagation of a sound, that does not persist once it has passed a receiver, for the three dimensional case, and the drop of a rock into a pond of water, which stimulates a propagating circular front, with wavelets remaining in its interior, for the two dimensional case [34, Remarque 3.1].

These physical differences are also reflected in the structure of the fundamental solutions, which are given in Lemma 1.2 below: The support of the two dimensional fundamental solution is the entire forward light cone

$$\Sigma_+ = \{\ (x,t) \in \mathbb{R}^n \times \mathbb{R}_{\geq 0}\ \mid\ |x| \leq t\ \}$$

whereas the support of the three dimensional fundamental solution is only the boundary of Σ_+ [151, Chapter 8]. This is the mathematical statement of Huygens' principle.

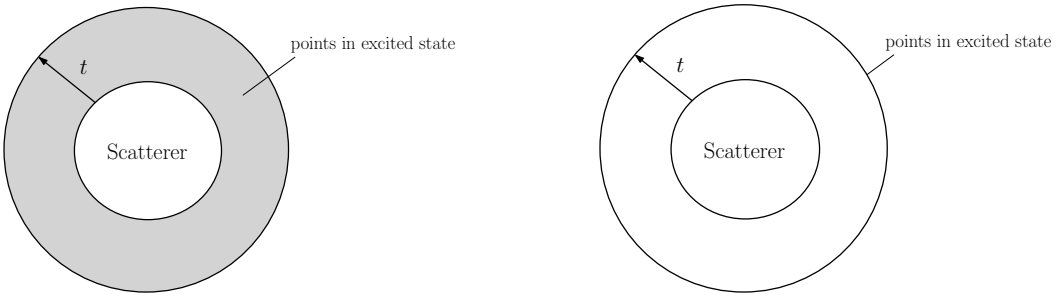

(a) Two dimensional case (b) Three dimensional case

Figure 1.2: Illustration of Huygens' principle in two and three space dimensions for a circular and a spherical scatterer (shown in a plane), respectively.

1.1 Literature Review on the Time Domain Boundary Element Method and Space-Time Adaptive Methods

This work is concerned with a posteriori error estimates and adaptive methods for the time domain Boundary Element Method for the hyperbolic initial-boundary value problem (P). To the best of the author's knowledge, these topics have not been addressed in this setup so far.

In order to establish this work within the existing scientific framework, we give brief reviews on these two fields; the time domain Boundary Element Method, and a posteriori error estimates and adaptive methods for hyperbolic problems and time dependent problems in general.

1.1.1 The Time Domain Boundary Element Method

The *time domain Boundary Element Method (TD-BEM)* has been the subject of research within the numerical analysis community for at least 50 years [46, 84], beginning with articles by Friedman and Shaw [73] and Mitzner [120]. A detailed review of these early developments can be found in [142]. For thorough self-contained introductions to the subject, we refer to the review papers by Costabel [54] and Ha-Duong [81], and to a set of lecture notes by Sayas [136] that covers more recent developments. For some short reports on state-of-the-art research and recent trends in this field, we further refer to [89, 90].

When compared to volumetric methods such as Finite Elements Methods or Finite Difference Methods that deal directly with the partial differential equations, time domain Boundary Element Methods, which are concerned with the corresponding space-time boundary integral equations (also known as *retarded potential boundary integral equations*), have some striking advantages. Similarly to Boundary Element Methods for elliptic problems, they allow the reduction of a problem in an unbounded exterior domain to a problem on the domain's boundary, and thus a reduction in dimensionality by one. In particular, when dealing with unbounded domains, time domain Boundary Element Methods do not require the introduction of an artificial boundary on which an additional non-reflecting boundary condition has to be imposed, which is necessary for volumetric methods. Further, they implicitly impose radiation conditions at infinity. All these features make time domain Boundary Element Methods particularly well suited for free-field scattering problems with known fundamental solution. An illustration of the different computational domains for volumetric methods and Boundary Element Methods is given in Figure 1.3.

On the discrete level, the reduction to the boundary implies that the unknown solution does not need to be approximated throughout any homogeneous volumes, while the reduction in dimensionality corresponds to much smaller linear systems [5, 19, 30, 87, 100]. Additionally

time domain Boundary Element Methods provide simple pre- and post-processing for input and output data, and (potentially) permit to achieve high computational accuracy [5].

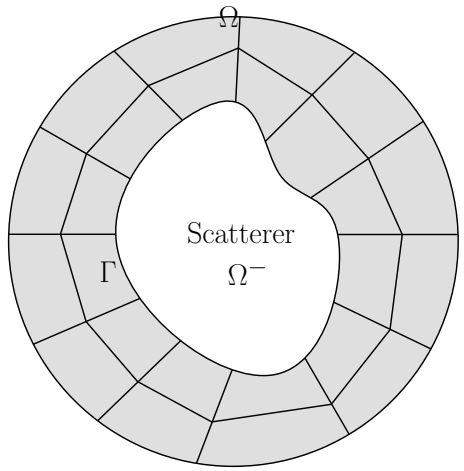

(a) Scatterer with artificial boundary and Finite Element mesh. The computational domain is printed in grey.

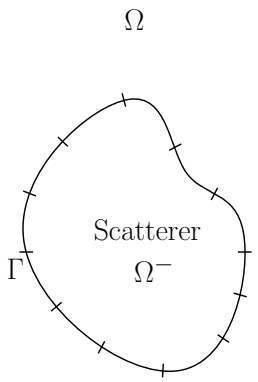

(b) Scatterer with Boundary Element mesh.

Figure 1.3: Two possible discretisations of unbounded domains. After [48, Figure 1] and [126, Figures 2,3].

There are two major branches that can be distinguished within the field of time domain Boundary Element Methods.

The first one comprises *collocation methods*, which are relatively easy to implement, but which are hard to analyse mathematically and therefore lack theoretical underpinning [54, Section 2.5].

The second branch are the *variational methods*. The vast majority of all publications on the subject of time domain Boundary Element Methods within the numerical analysis community deals with these methods. Again, there are two major approaches to distinguish here. Both of them lead to a certain type of semi-implicit scheme of linear systems if a uniform temporal grid is used, known as a *marching-on-in-time (MOT)* scheme.

The first approach are the *Galerkin methods* that emerged from the French school around Bamberger and Ha-Doung. Their groundbreaking work [20, 21] has been the foundation for all subsequent research in this area. A drawback of Bamberger's and Ha-Duong's work is the presence of a weight factor $e^{-\sigma t}$ with $\sigma > 0$ in their variational formulations. In all common practical computations, however, this weight factor is neglected, which corresponds to setting $\sigma = 0$. This inconsistency motivated the recent research by Aimi et al. [4, 5, 6], who introduced a method that they call the *Energetic Galerkin Boundary Element Method*. It deals with the same bilinear forms that are used for computations, i.e. the ones with $\sigma = 0$, in both theory and practice.

The second variational approach is called the *Convolution Quadrature method*, also known as the *Operational Quadrature method*. It was introduced by Lubich [108] and makes use of the time convolution structure of the time domain boundary layer potentials and the corresponding time domain boundary integral operators involved in the governing boundary integral equations to realise the time discretisation. The spatial discretisation is usually done by a Galerkin Boundary Element Method. Reviews on this method have been given by Banjai and Schanz [30] and Lubich [109].

Discussions on advantages and disadvantages of the two variational approaches can be found

in, amongst others, [29, 46, 84]. The basic idea of the Galerkin approach is more straightforward than the Convolution Quadrature method, and its computational complexity and storage requirements are more modest [84, Tables 1 and 2]. On the other hand, the computation of the matrix entries in a space-time Galerkin method requires special quadrature schemes for the integration domains involved, that emerge from the intersections of boundary elements and discrete light cones if standard piecewise polynomial basis functions in time are used. This issue makes the implementation of an accurate and stable space-time Galerkin method a very challenging task, particularly in three space dimensions [127]. In the Convolution Quadrature method, the spatial integration domains are simply the boundary elements themselves [46, 84], and no additional effort needs to be made for this part of the implementation. Another type of compactly supported, infinitely smooth temporal basis functions, which form a so-called PUM space, has recently been introduced by Sauter and Veit [134, 152] . This choice of basis functions circumvents the problem of computing intersections of discrete light cones with the spatial mesh. On the other hand, it is not entirely clear whether a full space-time implementation of this method exists yet, and how the computation times compete. We remark, however, that the method seems to be particularly well suited to be used with higher temporal polynomial degrees, since the involved analytical computation of temporal integrals is avoided. The method is further inherently suitable for temporal adaptivity. Fast quadrature techniques for this approach are considered in [98].

Research into the reduction of computation costs for both methods has received considerable attention in recent years. For the Galerkin approach, most of these works can be found in the engineering literature. A separate paragraph on research activities in this community is given below. For developments regarding the fast computation of Convolution Quadrature matrices, we refer to [27, 46, 84] and the references cited therein. Note that the Convolution Quadrature method has very recently been extended to variable time step sizes [106, 107].

Solid theoretical frameworks are available for both methods. After about three and two decades, respectively, of research activity on space-time Galerkin methods and the Convolution Quadrature method there seems to be a general consensus that both have reached a state of relative maturity today [90]. However, compared to Boundary Element Methods for elliptic problems, time domain Boundary Element Methods are still by far less well studied.

For completeness, we also give a brief review of research activities regarding time domain Boundary Element Methods in the engineering community. One major focus has been the fast computation of the matrices appearing in the classical MOT schemes that arise from space-time Galerkin methods. The *plane wave time domain algorithm (PWTD)* [62, 118] is an adaption of the fast multipole method that has been used for time harmonic scattering problems. The *time domain adaptive integral method (TD-AIM)* [19, 155] extends the frequency domain adaptive integral method to the time domain. We remark that the term 'adaptive' does not refer to adaptive mesh refinements based on error estimators here. Instead, the method's name is due to the adaptive integration in space featured in the algorithm. For each quadrature point, the inner integration domain is split into a near and a far field, where the near field contains those points that are close to the given point. In the mathematical literature, El Gharib [59, Chapter III] follows a similar approach. The *Burton-Miller formulation* is another approach that has been adopted from time independent problems to the time domain in order to reduce instabilities [63]. This approach has also been analysed in a mathematical context [47].

Another relatively recent development in the engineering community is the use of globally supported basis functions in time, such as Laguerre polynomials [50, 95, 97] or Hermite polynomials [143]. The corresponding schemes are known as *marching-on-in-degree (MOD)* or *marching-on-in-order (MOO)* schemes. They were introduced to compensate for long-term instabilities which have been reported to occur often when using MOT schemes based on space-time Galerkin meth-

ods. Similarly to MOT schemes, accelerators for MOO schemes have been investigated [156]. Apparently, MOO schemes have solely been used in the engineering community so far and have not been the subject of any mathematical research yet. State-of-the-art reviews on different choices of basis functions in time from an engineering perspective are given by Geranmayeh et al. [75, 76]. In particular, [75] provides an extensive list of references on this topic.

1.1.2 A Posteriori Error Estimation and Self-Adaptive Methods for Time Dependent Problems

Adaptive Finite Element Methods steered by error indicators for elliptic and parabolic problems have been studied extensively for at last 30 years [85, 126, 133, 157], starting with the pioneering works by Babuška and Rheinboldt [15, 16]. They also appear to have been the first authors to define an 'optimal' mesh as one in which the error is approximately equally distributed over the mesh elements [16, p. 748]. If the computational domain is simply uniformly remeshed to reduce the approximation error, this sort of optimality can normally not be achieved.

Adaptive methods are usually based on local a posteriori error estimates. A disadvantage of a priori error estimates is that they usually feature the solution of the problem, or at least regularity assumptions on it, which are, in most cases, unknown. A posteriori error estimates, on the other hand, include only known quantities, such as the given input data and the computed approximate solution. In order to use them with adaptive methods, one needs a posteriori error bounds that can be localised and which can thus serve as error indicators [25, p. 57f.]. To summarise, localisable a posteriori error estimates serve two purposes:

(i) they can be used to estimate the approximation error and therewith to quantify the approximation's quality, in particular if the exact solution is unknown

(ii) they can be used as local error indicators to flag elements with very small or very large error contributions for modification.

For introductions to adaptive Finite Element Methods for elliptic problems, we refer to the monographs [7, 17, 26, 64, 153]. For parabolic problems, we refer to the research article by Schmich and Vexler [137] and the references cited therein, in particular [37, 65]. We further mention the reviews on a posteriori error estimation by Oden et al. [126] and on adaptive methods by Thompson [149, Section VIII], which both focus on time harmonic acoustics.

The literature on adaptive Finite Element Methods for second-order hyperbolic problems is not as vast, yet rich [74, p. 1], [85, p. 2], [130, p. 1]. Bangerth et al. [22] provide a recent review on this topic. In the words of Georgoulis et al. [74, p. 16], '[t]he design and implementation of adaptive algorithms for the wave equation based on rigorous a posteriori error estimators is a largely unexplored subject, despite the importance of these problems in the modelling of a number of physical phenomena. The numerical implementation of the proposed bounds in the context of adaptive algorithm design for second order hyperbolic problems remains a challenge that deserves special attention [...]'. Bangerth and Rannacher [24] report that '[d]espite the common perception that adaptivity is crucial to the efficient solution of the wave equation, there does not exist much literature on a posteriori error estimates and practical implementations', even though '[...] solutions to the wave equation often have very localized features, such as wave fronts [so] that efficient algorithms need to employ some kind of adaptivity in the choice of computational grids'. Thompson and He [150] remark that '[a]daptive meshes provide for controllable accuracy with the least amount of elements, thus providing computational speedup and reduced memory requirements' and allow 'unstructured mesh distributions [in which] elements are refined near

wave fronts, and unrefined where the solution is smooth or quiescent [...] as local wave pulses propagate throughout the mesh'.

The adaptive schemes proposed in the literature are relatively diverse. There are, generally speaking, two possible strategies for time dependent problems. Conceptual schemes of both are sketched in Figure 1.4. The first option is to carry out the computations throughout the full time interval as usual. Once the computations have ended, the error can be estimated and the mesh can be refined, according to local error indicators. This process can be iterated until a given error tolerance is reached (Figure 1.4a). Alternatively, the error can be estimated after each time step, and re-meshing is then carried out immediately. The computations are therefore normally not completely restarted, and no time step is revisited once the corresponding adaptions have been done (Figure 1.4b). There are numerous variants of these two strategies, particularly of the latter. Schmidt and Siebert [138, p. 49], for example, citing Bänsch [31, Section 4], specify four different possible variants. These four variants all concern spatial mesh adaptions, to which some authors restrict themselves while using a fixed temporal mesh, for example Bangerth and Rannacher [24]. Some authors allow refinements only, but no coarsening, for example Rademacher [130]. In so-called r-methods or moving mesh methods, which are described in the monograph by Huang and Russell [93], the number of mesh elements remains fixed and thus restricts the choice of possible refinements and coarsenings. Besides all these variants, there are many other kinds of error indicators which have been used in practice; some of them heuristically motivated and some derived within theoretical frameworks.

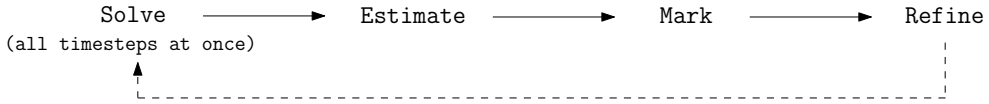

(a) Strategy 1: Solve the problem for all time steps and refine the mesh after the computations have ended.

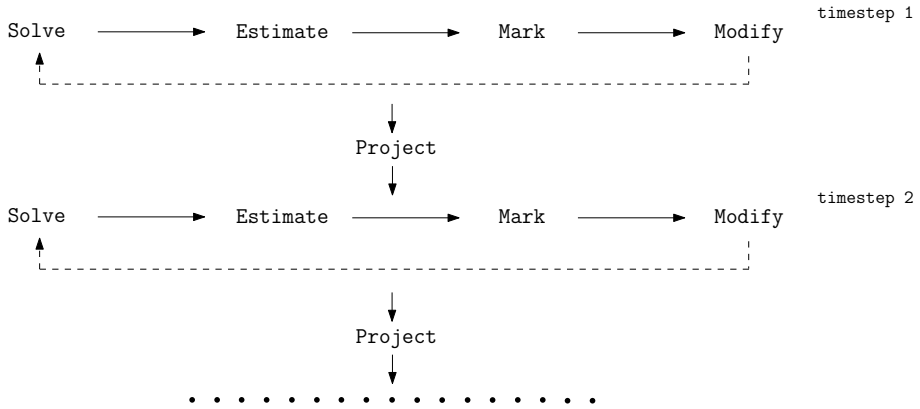

(b) Strategy 2: Modify the mesh after the computations for one time step have ended.

Figure 1.4: Two possible adaptive strategies for time dependent problems.

It appears to be impossible to say which of these two methods is generally preferable. Clearly, adaptive schemes that are based on the second kind of mesh adaption processes described in the previous paragraph, i.e. the ones that adapt the mesh immediately after each time step, seem to be particularly suitable for time-marching schemes. They are able to 'track' the areas of the computational domain where the highest errors occur throughout the entire computation period.

On the other hand, they can leave the mesh heavily refined in the region where it was refined at the start, due to initial errors being propagated throughout the entire computation period. Mesh-coarsening is, in general, also harder to implement, since it requires a tree-like data structure for the organisation of the mesh elements to allow the reconstruction of previous meshes. Further, solutions from previous time steps may need to be projected to different grids, possibly causing additional errors. The first kind of mesh adaption process mentioned, on the other hand, i.e. the one that modifies the mesh after the computations have ended, is more suitable for use with methods that solve the entire problem 'at once'. Here, every step within the mesh-adaption loop is effectively equal to a restart of the computation from the initial time step, and this method is therefore more costly. If it is used with a time-marching scheme, it may also suffer from the accumulation of errors throughout the computation period, leading to more strongly refined meshes towards its end. We discuss both methods for our particular setup in Chapter 6.

Note that most papers address adaptive methods for interior wave problems instead of scattering problems, including the references [24, 25, 36, 74, 94, 96, 132]. We believe that the works by Thompson and He [88, 150] and by Bangerth et al. [23] are the closest to the studies presented in this work. Thompson and He [88, 150] consider an exterior scattering problem in two space dimensions similar to (P). Unlike us, they introduce an artificial circular boundary around the scatterer and discretise the finite domain in between the scatterer and the artificial boundary by a finite element mesh. The discretisation in time is done by a Discontinuous Galerkin method. A clear advantage of their approach is its unconditional stability, owing to the use of the Discontinuous Galerkin method, making it particularly suitable for adaptive methods, since it is not subject to a CFL condition that would impose a bound on the ratio of spatial and temporal mesh sizes [150, p. 1948]. Bangerth et al. [23] consider a scattering problem of the same kind, but in three space dimensions. They also introduce an artificial boundary and use Finite Elements for the spatial discretisation. They further use the Crank-Nicolson scheme for the time discretisation, which is also unconditionally stable. Nevertheless, their algorithm performs an automatic time mesh modification if the spatial mesh is modified [23, p. 2470], thus prohibiting independent refinements and coarsenings of both meshes.

Other temporal discretisations that have been applied in this context include the Backward-Euler method [36] and Petrov-Galerkin methods [130]. In addition, Bernardi and Süli [36] provide a thorough analysis of a posteriori error estimates for an interior wave problem, but do not conduct any numerical experiments and do not address adaptivity. Discontinuous Galerkin methods have also been used in the frequently cited works by Hughes and Hulbert [94] and Johnson [96]. For completeness, we remark that adaptive methods for the wave equation have also received attention in the optimisation community, for example in [102, 137].

No work on a posteriori error estimates and adaptive methods for time domain Boundary Element Methods appears to have been done previously, neither for hyperbolic problems such as ours, nor for parabolic problems. For elliptic problems, a vast literature on this topic exists. However, Sauter and Schwab [133, p. 517] observe that 'for boundary element methods, the nonlocal character of the integral operator and the nonlocal fractional Sobolev norms cause difficulties in the mathematical derivation of local error indicators and much fewer authors have investigated local a posteriori error estimates for integral equations [than for finite element methods]'. An introduction to this topic that mostly focusses on one particular type of error indicators, the Faermann indicators, is given in Chapter 9 of the monograph by Sauter and Schwab [133]. Carstensen and Faermann [39] provide a more general review on adaptive methods for Boundary Element Methods for elliptic problems. Another review on various error indicators that includes numerous numerical examples is given by Erath et al. [60].

1.2 Time Domain Boundary Layer Potentials and Integral Operators for the Wave Equation

In this section, we derive the usual time domain boundary integral equations for the scattering problem (P). For the definition of the time domain boundary layer potentials and integral operators involved, we state the fundamental solutions of the wave equation in Lemma 1.2.

Lemma 1.2 (Fundamental Solutions of the Wave Equation)
The fundamental solution of the wave equation (1.1a) *is given by [77, (1.2), (1.3), (1.4)], [151, (7.7), (8.12), (8.16)]*

$$\textit{(1D)}: \qquad G(t,s,x,y) = G(t-s,|x-y|) = \frac{1}{2}H(t-s-|x-y|) \tag{1.2}$$

$$\textit{(2D)}: \qquad G(t,s,x,y) = G(t-s,|x-y|) = \frac{1}{2\pi}\frac{H(t-s-|x-y|)}{\sqrt{(t-s)^2-|x-y|^2}} \tag{1.3}$$

$$\textit{(3D)}: \qquad G(t,s,x,y) = G(t-s,|x-y|) = \frac{1}{4\pi}\frac{\delta(t-s-|x-y|)}{|x-y|} \tag{1.4}$$

where H is the Heaviside function

$$H(x) = \mathbb{1}_{\mathbb{R}_{>0}}(x) = \begin{cases} 0 & , \quad x \le 0 \\ 1 & , \quad x > 0 \end{cases} \tag{1.5}$$

and δ is the Dirac impulse.

We now define the usual time domain boundary layer potentials, also known as retarded potentials, for the wave equation, and the corresponding boundary integral operators. For the time being, we only define these as operators and do not give any comments on mapping properties. This is done thoroughly in Section 3.3.

Definition 1.3 (Time Domain Boundary Layer Potentials [34, (18), (19)])
Let $(x,t) \in (\mathbb{R}^n \setminus \Gamma) \times \mathbb{R}_{\ge 0}$. For appropriate densities $p, \varphi : \Gamma \times \mathbb{R}_{\ge 0} \to \mathbb{R}$, the time domain *or* retarded Single Layer potential *is given by*

$$S[p](x,t) := \int_\Gamma \int_{\mathbb{R}_{\ge 0}} G(t-s,|x-y|)p(y,s)\,ds\;ds_y \tag{1.6}$$

and the time domain *or* retarded Double Layer potential *by*

$$D[\varphi](x,t) := \int_\Gamma \int_{\mathbb{R}_{\ge 0}} \frac{\partial G}{\partial n_y}(t-s,|x-y|)\varphi(y,s)\,ds\;ds_y = \int_\Gamma \int_{\mathbb{R}_{\ge 0}} n_y \cdot \nabla_x G(t-s,|x-y|)\varphi(y,s)\,ds\;ds_y\,. \tag{1.7}$$

The origin of the term 'retarded potential' is the delayed or *retarded* time argument in their integrands [57, p. 1167]. In order to take the limits of the potentials S and D to the boundary, the following boundary integral operators are defined.

Definition 1.4 (Time Domain Boundary Integral Operators [34, (26), (31), (32)])
Let $(x,t) \in \Gamma \times \mathbb{R}_{\ge 0}$. For appropriate densities $p, \varphi : \Gamma \times \mathbb{R}_{\ge 0} \to \mathbb{R}$, the following time domain boundary integral operators are called time domain *or* retarded potential boundary integral operators.

a) time domain Single Layer operator

$$V[p](x,t) := \int_\Gamma \int_{\mathbb{R}_{\ge 0}} G(t-s,|x-y|)p(y,s)\,ds\;ds_y \tag{1.8}$$

b) time domain adjoint Double Layer operator

$$K'[p](x,t) \coloneqq \int_\Gamma \int_{\mathbb{R}_{\geq 0}} n_x \cdot \nabla_x G(t-s,|x-y|) p(y,s)\, ds\ ds_y \tag{1.9}$$

c) time domain Double Layer operator

$$K[\varphi](x,t) \coloneqq \int_\Gamma \int_{\mathbb{R}_{\geq 0}} n_y \cdot \nabla_x G(t-s,|x-y|) \varphi(y,s)\, ds\ ds_y \tag{1.10}$$

d) time domain hypersingular boundary integral operator

$$W[\varphi](x,t) \coloneqq -\lim_{x' \in \Omega \to x} n_x \cdot \nabla_{x'} D[\varphi](x',t) \tag{1.11}$$

We further denote the identity integral operator *by I, i.e. $I[p](x,t) \coloneqq p(x,t)$.*

We emphasise that the space and time variables in the kernels of the time domain boundary layer potentials and integral operators that correspond to the fundamental solutions (1.2), (1.3), (1.4) are interwoven [80, p. 493]. One can therefore, in general, not 'get rid' of the temporal integral in order to consider time domain boundary integral operators as time dependent boundary integral operators only on Γ [81, p. 8].

Definition 1.5 (Traces and Jumps)
For any function w, its jump *and the* jump of its normal derivative $\frac{\partial w}{\partial n}$ *across Γ are defined by*

$$[\![\ \gamma_0[w]\ ]\!]_\Gamma \coloneqq \gamma_0^+[w] - \gamma_0^-[w] \quad , \quad [\![\ \gamma_1[w]\ ]\!]_\Gamma = \left[\!\!\left[\frac{\partial w}{\partial n} \right]\!\!\right]_\Gamma \coloneqq \gamma_1^+[w] - \gamma_1^-[w]$$

where $\gamma_0^+[w]$, $\gamma_0^-[w]$ denote the boundary limits *of w on Γ from Ω and Ω^-, respectively, i.e.*

$$\gamma_0^+[w](x) \coloneqq \gamma_0^{ex}[w](x) \coloneqq \lim_{y \in \Omega \to x} w(y) \quad , \quad \gamma_0^-[w](x) \coloneqq \gamma_0^{in}[w](x) \coloneqq \lim_{y \in \Omega^- \to x} w(y)$$

for $x \in \Gamma$. γ_0^+ and γ_0^- are known as the interior *and* exterior trace operator*. Similarly, the* interior *and* exterior normal derivative operators *are*

$$\begin{aligned} \gamma_1^+[w](x) &\coloneqq \gamma_1^{ex}[w](x) \coloneqq n_x \gamma_0^+[\nabla w] = \lim_{y \in \Omega \to x} n_x \cdot \nabla w(y) \\ \gamma_1^-[w](x) &\coloneqq \gamma_1^{in}[w](x) \coloneqq n_x \gamma_0^-[\nabla w] = \lim_{y \in \Omega^- \to x} n_x \cdot \nabla w(y) \end{aligned}$$

for $x \in \Gamma$.

As in [114, p. 142] we write $\gamma_0[w] \coloneqq \gamma_0^+[w] = \gamma_0^-[w]$ if $[\![\ \gamma_0[w]\ ]\!]_\Gamma = 0$ and $\gamma_1[w] \coloneqq \gamma_1^+[w] = \gamma_1^-[w]$ if $[\![\ \gamma_1[w]\ ]\!]_\Gamma = 0$. $\gamma_0[w]$ and $\gamma_1[w] = \gamma_0\left[\frac{\partial w}{\partial n}\right]$ are called the trace *of w and $\frac{\partial w}{\partial n}$, respectively. If the setup is clear we simply write w and $\frac{\partial w}{\partial n}$ instead of $\gamma_0[w]$ and $\gamma_1[w]$.*

By [79, Lemma 3, Lemma 4a], [54, p. 7], the boundary limits of the time domain boundary layer potentials given in Definition 1.3 are similar to the well known boundary limits of the boundary layer potentials for elliptic problems [145, Section 6.6].

Lemma 1.6 (Boundary Limits of the Time Domain Boundary Layer Potentials)
Taking the limits of the time domain boundary layer potentials given in Definition 1.3 to the boundary, there holds

a) $\gamma_0^{ex}[S[p]](x,t) = \gamma_0^{in}[S[p]](x,t) = V[p](x,t)$

b) $\gamma_1^{in}[S[p]](x,t) = (K' + \frac{1}{2}I)[p](x,t)$

c) $\gamma_1^{ex}[S[p]](x,t) = (K' - \frac{1}{2}I)[p](x,t)$

d) $\gamma_0^{in}[D[\varphi]](x,t) = (K - \frac{1}{2}I)[\varphi](x,t)$

e) $\gamma_0^{ex}[D[\varphi]](x,t) = (K + \frac{1}{2}I)[\varphi](x,t)$

f) $\gamma_1^{in}[D[\varphi]](x,t) = \gamma_1^{ex}[D[\varphi]](x,t) = W[\varphi](x,t)$

for $(x,t) \in \Gamma \times \mathbb{R}_{\geq 0}$.

An immediate consequence of Lemma 1.6 are the jumps of the time domain boundary layer potentials and their normal derivatives, which are again similar to the jumps of the boundary layer potentials for elliptic problems [114, Theorem 6.11].

Corollary 1.7 (Jumps of the Time Domain Boundary Layer Potentials)
For the time domain boundary layer potentials given in Definition 1.3, there hold the jump relations

a) $[\![\ \gamma_0[S[p]]\ ]\!]_\Gamma = 0$

b) $[\![\ \gamma_1[S[p]]\ ]\!]_\Gamma = -p$

c) $[\![\ \gamma_0[D[\varphi]]\ ]\!]_\Gamma = \varphi$

d) $[\![\ \gamma_1[D[\varphi]]\ ]\!]_\Gamma = 0$

There are several ways to represent the unknown solution u in the exterior domain in terms of time domain boundary layer potentials. We consider the following three representations of u:

(I) *Representation Formula*: Any solution u of the homogeneous wave equation (1.1a) can be written as [34, p. 18 (iii)], [77, (1.9) and Theorem 5, (1.12)], [82, (11)]

$$u = S\left[\ \left[\!\left[\frac{\partial u}{\partial n}\right]\!\right]_\Gamma\ \right] - D[\ [\![u]\!]_\Gamma\ ] \qquad \text{in } (\Omega \cup \Omega^-) \times \mathbb{R}_{\geq 0}.$$

This representation formula is also known as *Kirchhoff's formula*. If one assumes that the solution of the scattering problem (P) is extended by zero inside the scatterer, one obtains [34, p. 17 (i)], [77, (1.8)]

$$u = D[\ u|_\Gamma\ ] - S\left[\ \left.\frac{\partial u}{\partial n}\right|_\Gamma\ \right] \qquad \text{in } \Omega \times \mathbb{R}_{\geq 0}.$$

This changes to [77, (1.7)]

$$-u = D[\ u|_\Gamma\ ] - S\left[\ \left.\frac{\partial u}{\partial n}\right|_\Gamma\ \right] \qquad \text{in } \Omega^- \times \mathbb{R}_{\geq 0}$$

for interior wave problems.

(II) *Single Layer ansatz*: Using some unknown density p, the solution of (P) is represented as

$$u = S[p] \qquad \text{in } \Omega \times \mathbb{R}_{\geq 0}.$$

(III) *Double Layer ansatz*: Using some unknown density φ, the solution of (P) is represented as

$$u = D[\varphi] \qquad \text{in } \Omega \times \mathbb{R}_{\geq 0}.$$

(II), (III) are called *indirect methods* whereas (I) is a *direct method*.

Passing (I), (II), (III) from the exterior domain Ω to the boundary Γ (with γ_0^{ex} and γ_1^{ex}, respectively) and using Lemma 1.6, we obtain the time domain boundary integral equations

$$\left(K - \frac{1}{2}I\right)[\, u|_\Gamma \,] = V\left[\, \left.\frac{\partial u}{\partial n}\right|_\Gamma \,\right] \qquad \left(K' + \frac{1}{2}I\right)\left[\, \left.\frac{\partial u}{\partial n}\right|_\Gamma \,\right] = W[\, u|_\Gamma \,] \tag{1.12}$$

$$u|_\Gamma = V[p] \qquad \left.\frac{\partial u}{\partial n}\right|_\Gamma = \left(K' - \frac{1}{2}I\right)[p] \tag{1.13}$$

$$u|_\Gamma = \left(K + \frac{1}{2}I\right)[\varphi] \qquad \left.\frac{\partial u}{\partial n}\right|_\Gamma = W[\varphi] \tag{1.14}$$

on $\Gamma \times \mathbb{R}_{\geq 0}$. By inserting the known boundary data (1.1d), one obtains a boundary integral equation with unknown trace (for (1.12)) or density (for (1.13) and (1.14)).

In accordance with the terms for representations (I)-(III) above, equations (1.12) are called *Direct Integral Equations*, whereas equations (1.13), (1.14) are called *Indirect Integral Equations*. (1.12), (1.13).1 and (1.14).2 are *integral equations of the first kind*, whereas (1.13).2 and (1.14).1 are *integral equations of the second kind* [54, p. 6f.], [78, p. 6].

We note that the direct integral equations (1.12) involve only physical quantities, while the indirect integral equations (1.13) and (1.14) involve the unknown densities p and φ that have no physical interpretation. Direct integral equations are, therefore, advantageous for experimental validations of programme codes if an exact solution is known. However, their computation is more expensive, since the corresponding matrices of two boundary integral operators need to be computed. Steinbach [145, Remark 7.2] remarks that, generally, 'depending on the application and on the discretisation scheme to be used, each [type of integral equation] may have their advantages or disadvantages'.

1.3 Some Examples of Waves

Upon reaching the end of this chapter, we now consider some examples of waves that will serve as test cases for our numerical experiments later on.

1.3.1 Circular Waves

Let $\Omega_C := \left\{ x \in \mathbb{R}^2 \;\middle|\; |x| = R \right\}$ be a circle of radius R with boundary $\Gamma_C = \partial\Omega_C$. The Laplace operator in polar coordinates (r, θ) is given by $\Delta_{(r,\theta)} = \frac{\partial^2}{\partial r^2} + \frac{1}{r}\frac{\partial}{\partial r} + \frac{1}{r^2}\frac{\partial^2}{\partial \theta^2}$, and so the wave equation (1.1a) for waves with polar symmetric motion, i.e. those that do not depend on θ, reads

$$\Box_{(r,\theta)} u = \frac{\partial^2 u}{\partial r^2} + \frac{1}{r}\frac{\partial u}{\partial r} - \frac{\partial^2 u}{\partial t^2} = 0. \tag{1.15}$$

A *circular wave* is of the form [99, (6.65)]

$$u(r,t) = \frac{1}{\sqrt{r}} f\,(t - r + c) \tag{1.16}$$

for an arbitrary function f, any $c \in \mathbb{R}$ and $r \geq R$. For such circular waves, there holds

$$\Box_{(r,\theta)} u = \frac{1}{4} r^{-\frac{5}{2}} f\,(t - r + c) \quad \sim \quad \mathcal{O}(\sqrt{\frac{1}{r^5}})$$

which means that u solves the homogeneous wave equation (1.1a) for $r \gg 1$. Circular waves may be seen as a two dimensional version of the spherical waves that are considered for the numerical experiments in [45, 127].

Since $u(r,t) = (x_1^2 + x_2^2)^{-\frac{1}{4}} f(t - (x_1^2 + x_2^2)^{\frac{1}{2}} + c)$,

$$\begin{aligned} \frac{\partial u}{\partial x_1} &= -\frac{1}{4}(x_1^2 + x_2^2)^{-\frac{5}{4}}\, 2x_1 f(t - r + c) + \frac{1}{\sqrt{r}} f'(t - r + c)(-1)\frac{1}{2}(x_1^2 + x_2^2)^{-\frac{1}{2}} 2x_1 \\ &= -r^{-\frac{3}{2}} x_1 \left(\frac{1}{2r} f(t - r + c) + f'(t - r + c)\right) \end{aligned}$$

the gradient of u is

$$\nabla_x u(x,t) = -\frac{1}{\sqrt{r^3}} \left(\frac{1}{2r} f(t - R + c) + f'(t - r + c)\right) x. \tag{1.17}$$

Choosing a normal vector of unit length $n_x = (\cos\theta, \sin\theta)$ for $x = R(\cos\theta, \sin\theta)$, there holds $x \cdot n_x = R$, and thus, on Γ_C,

$$\frac{\partial u}{\partial n_x}(t) = -\frac{1}{\sqrt{R}} \left(\frac{1}{2R} f(t - R + c) + f'(t - R + c)\right). \tag{1.18}$$

As

$$\begin{aligned} \|u(\cdot,t)\|^2_{L^2(\Gamma_C)} &= \int_{\Gamma_C} u(x,t)^2 ds_x = \int_{\Gamma_C} \left(\frac{1}{\sqrt{r}} f\,(t - r + c)\Big|_{r=R}\right)^2 dr = |\Gamma_C| \,\frac{f(t - R + c)^2}{R} \\ &= 2\pi f(t - R + c)^2 \end{aligned}$$

and

$$\begin{aligned} \left\| \frac{\partial u}{\partial n_x}(\cdot,t) \right\|^2_{L^2(\Gamma_C)} &= \int_{\Gamma_C} \frac{\partial u}{\partial n}(x,t)^2 ds_x = \int_{\Gamma_C} \left(-\frac{1}{\sqrt{R}} \left(\frac{1}{2R} f(t - R + c) + f'(t - R + c)\right)\right)^2 dr \\ &= |\Gamma_C| \frac{1}{R} \left(\frac{1}{2R} f(t - R + c) + f'(t - R + c)\right)^2 \\ &= 2\pi \left(\frac{1}{2R} f(t - R + c) + f'(t - R + c)\right)^2 \end{aligned}$$

the $L^2(\Gamma_C)$ norms of u and $\frac{\partial u}{\partial n_x}$ are given by

$$\|u(\cdot,t)\|_{L^2(\Gamma_C)} = \sqrt{2\pi}\,|f(t - R + c)| \tag{1.19}$$

$$\left\| \frac{\partial u}{\partial n_x}(\cdot,t) \right\|_{L^2(\Gamma_C)} = \sqrt{2\pi} \left|\frac{1}{2R} f(t - R + c) + f'(t - R + c)\right|. \tag{1.20}$$

In order to satisfy the initial conditions, we need to choose a function f such that

$$u(r, t = 0) = \frac{1}{\sqrt{r}} f\,(-r + c) = 0 \quad \text{and} \quad \dot{u}(r, t = 0) = \frac{1}{\sqrt{r}} f'\,(-r + c) = 0 \tag{1.21}$$

for $r \geq R$.

If we choose $c = R$ we may seek a function f that satisfies $f(x) = f'(x) = 0$ for $x < 0$. We choose

$$f(x) = \left(\frac{3}{4} - \cos\left(\frac{\pi}{2}x\right) + \frac{1}{4}\cos(\pi x)\right)(H(x) - H(x-4k)) \tag{1.22}$$

with

$$f'(x) = \left(\frac{\pi}{2}\sin\left(\frac{\pi}{2}x\right) - \frac{\pi}{4}\sin(\pi x)\right)(H(x) - H(x-4k))$$

which satisfies $f(4k) = f'(4k) = 0$ for $k \in \mathbb{Z}$. The scatterer radiates a signal at r for $t \in (r-R, 4k+r-R)$, in particular for $t \in (0, 4k)$ on Γ_C. Plots of a circular wave of this type at different times are shown in Figure 1.5.

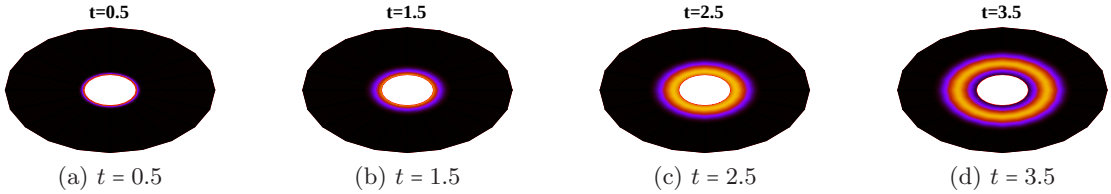

(a) $t = 0.5$ (b) $t = 1.5$ (c) $t = 2.5$ (d) $t = 3.5$

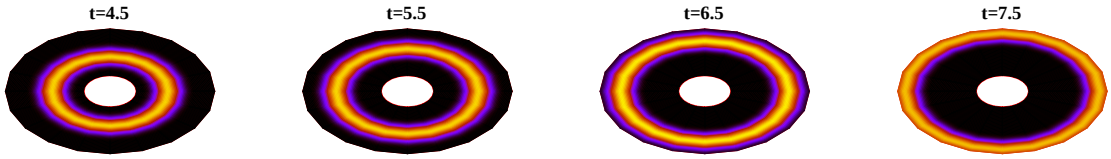

(e) $t = 4.5$ (f) $t = 5.5$ (g) $t = 6.5$ (h) $t = 7.5$

Figure 1.5: Circular wave of type (1.22) progressing away from the scatterer (the white circle in the centre) at times $t = 0.5$, $t = 1.5$, ..., $t = 7.5$ in the truncated exterior domain.

The derivatives in general, for $m \geq 1$, are

$$f^{(m)}(x) = \begin{cases} (H(x) - H(x-4k))\left(\left(\frac{\pi}{2}\right)^m \cos\left(\frac{\pi}{2}x\right) - \frac{\pi^m}{4}\cos(\pi x)\right)(-1)^{l-1} & m = 2l \\ (H(x) - H(x-4k))\left(\left(\frac{\pi}{2}\right)^m \sin\left(\frac{\pi}{2}x\right) - \frac{\pi^m}{4}\sin(\pi x)\right)(-1)^{l} & m = 2l+1 \end{cases}.$$

The function thus possesses jumps at $x = 0$ and $x = 4k$ in its even-numbered derivatives $f^{(2l)}$ for $l \geq 2$. These jumps are of order $\mathcal{O}\left(-\frac{\pi^{2l}}{4}\left(1 - \frac{1}{4^{l-1}}\right)\right) \sim \mathcal{O}\left(-\frac{\pi^{2l}}{4}\right)$.

1.3.2 Box Pulses

We call a function of the type

$$\begin{aligned} f_\lambda(x = (x_1, x_2), t) &= H(x_1 + x_2 + 2 - t + \lambda) - H(x_1 + x_2 + 2 - t) \\ &= \begin{cases} 1 & , \quad t - 2 \geq x_1 + x_2 \geq t - 2 - \lambda \\ 0 & , \quad \text{else} \end{cases}. \end{aligned} \tag{1.23}$$

a *box pulse* with length $\lambda > 0$. A pulse of this type is shown in Figure 1.6a.

Introducing another variable $\alpha > 0$, we generalise (1.23) to

$$\begin{aligned} f_{\lambda,\alpha}(x, t) &= H(x_1 + x_2 + 2 - \alpha t + \lambda) - H(x_1 + x_2 + 2 - \alpha t) \\ &= \begin{cases} 1 & , \quad \alpha t - 2 \geq x_1 + x_2 \geq \alpha t - 2 - \lambda \\ 0 & , \quad \text{else} \end{cases}. \end{aligned} \tag{1.24}$$

The additional parameter α allows to control the pulse's speed: The front of $f_{\lambda,\alpha}$, given by $x_1 + x_2 = \alpha t - 2$, arrives at the line $x_1 + x_2 = 0$ at $t = \frac{2}{\alpha}$. It arrives at the line $x_1 + x_2 = 2$ at $t = \frac{4}{\alpha}$. This is illustrated in Figure 1.6b. Hence the front of $f_{\lambda,\alpha}$ travels from $(0,0)$ to $(1,1)$, a distance of $\sqrt{2}$, in $\Delta t = \frac{4}{\alpha} - \frac{2}{\alpha} = \frac{2}{\alpha}$, and hence the pulse's speed is $\frac{\sqrt{2}}{\frac{2}{\alpha}} = \frac{\alpha}{\sqrt{2}}$. The pulse thus moves rapidly for $\alpha \gg 1$ and very slowly for $\alpha \ll 1$.

With regard to applications, we are particularly interested in choosing pulses of type (1.24) as incident waves in (P), i.e. $g = -\mathcal{B}[f_{\lambda,\alpha}]$ in (1.1d). As an example, let us consider the case of a square scatter $\Omega^- = [-1,1]^2$, as illustrated in Figure 1.6c. Since the scatterer's edge length is 2, the pulse has passed it completely at $t = 2 + \lambda$ for $\alpha = 1$.

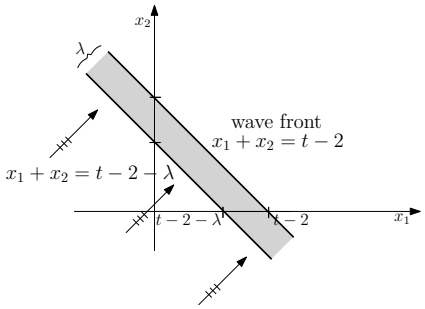

(a) box pulse $f_\lambda(x,t)$

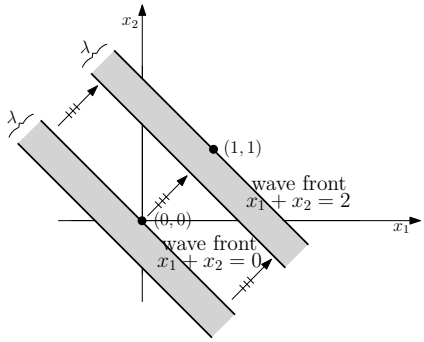

(b) illustration of the pulse's speed

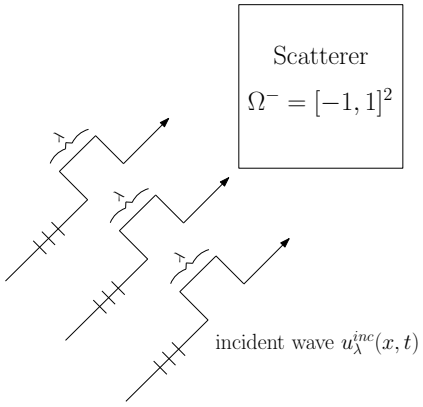

(c) square scatterer hit by a box pulse

Figure 1.6: A box pulse of type (1.23).

1.3.3 Plane Waves

Let us consider *plane waves* of the type

$$p(x,t) = \Re\left(Ae^{i(k\cdot x+\varphi_0)}e^{-i\omega t}\right) = A\cos\left(k\cdot x + \varphi_0 - \omega t\right) \tag{1.25}$$

where $k \in \mathbb{R}^2$ and $\omega \in \mathbb{R}$ with $|k|^2 = \omega^2$, and $A, \varphi_0 \in \mathbb{R}$.

Since $\frac{\partial^2 p}{\partial t^2} = -\omega^2 p$ and $\Delta p = -|k|^2 p$, any plane wave of type (1.25) is a solution of the homogeneous wave equation (1.1a). ω is known as the *wave speed* of p, and k as the wave's *direction vector*. Further, the *wave length* of p is $\lambda = \frac{2\pi}{\omega}$, and its frequency is $f = \frac{\omega}{2\pi}$. The wave's velocity

therefore is $\nu = \lambda f = 1$. Note that the box pulse (1.23) is a special case of a plane wave with $|k| = \omega = \varphi_0 = 0$ and $A = 1$. Obviously, the wave p is equal to zero along the lines

$$k \cdot x - \omega t + \varphi_0 = \frac{\pi}{2} + l\pi \tag{1.26}$$

for every $l \in \mathbb{Z}$. Our aim is to introduce a *front* and a *tail* to the plane wave p. We multiply p by a box pulse similar to (1.23) and obtain

$$\begin{aligned} p_{m_F,m_T}(x,t) &= \left(H(k \cdot x - \omega t + m_T) - H(k \cdot x - \omega t + m_F)\right) p(x,t) \\ &= \begin{cases} A\cos\left(k \cdot x + \varphi_0 - \omega t\right) & , \quad \omega t - m_F \geq k \cdot x \geq \omega t - m_T \\ 0 & , \quad \text{else} \end{cases} \end{aligned} \tag{1.27}$$

with front and tail at $k \cdot x = \omega t - m_F$ and $k \cdot x = \omega t - m_T$, respectively, where $m_F, m_T \in \mathbb{R}$ with $m_T > m_F$. To make the function continuous, we require $p_{m_F,m_T}(x,t) = 0$ along the front and tail. Hence, using (1.26), we demand

$$\varphi_0 - m_F = \frac{\pi}{2} + l_F\pi \qquad \varphi_0 - m_T = \frac{\pi}{2} + l_T\pi$$

for $l_F, l_T \in \mathbb{Z}$. For arbitrary l_F we need to take $l_T = l_F + \frac{m_F - m_T}{\pi}$. Note that the choices of l_F and l_T correspond to $\frac{l_T - l_F}{2}$ full phases of the cosine function. We further note that the derivatives of p_{m_F,m_T} are not continuous along the front and tail, since, for $i = 1, 2$,

$$|\dot{p}_{m_F,m_T}(x,t)| = |A\omega| \quad \text{and} \quad \left|\frac{\partial p_{m_F,m_T}}{\partial x_i}(x,t)\right| = |Ak_i| \tag{1.28}$$

for x, t such that $k \cdot x = \omega t - m_F$ and $k \cdot x = \omega t - m_T$.

We call a function of the type (1.27) that meets the requirements stated above a *plane wave packet* with support

$$\operatorname{supp} p_{m_F,m_T} = \left\{ x \in \mathbb{R}^2 \;\middle|\; \omega t - m_F \geq k \cdot x \geq \omega t - m_T \right\}.$$

The size of the support is the distance of front and tail and is found to be $|\operatorname{supp} p_{m_F,m_T}| = \frac{|m_T - m_F|}{\|k\|}$. We can construct combinations of wave packages with different frequencies.

Example 1.8

a) $k = \pi(1,1)$, $\omega = \sqrt{2}\pi$, $m_F = 2\pi$, $m_T = 4\pi$, $\varphi_0 = \frac{7}{2}\pi$. *In this case,* $|\operatorname{supp} p_{m_F,m_T}| = \sqrt{2}$.

b) Take $k_1 = \pi(1,1)$, $\omega_1 = \sqrt{2}\pi$, $m_F^1 = 2\pi$, $m_T^1 = 4\pi$, $\varphi_0 = \frac{7}{2}\pi$ *as in a). For the second wave we take* $k_2 = mk_1$ *and* $\omega_2 = m\omega_1$. *To make the second wave follow the first one immediately we have to demand*

$$\omega_1 t - \frac{m_F^2}{m} = \omega_1 t - m_T^1$$

which yields $4\pi = m_T^1 = \frac{m_F^2}{m}$. *If we choose* $m = 4$ *we thus get* $m_F^2 = 16\pi$.

(i) Choosing $m_T^2 = 20\pi$, *we have* $\left|\operatorname{supp} p_{m_F^2,m_T^2}\right| = \frac{1}{\sqrt{2}}$.

(ii) Choosing $m_T^2 = 24\pi$, *we have* $\left|\operatorname{supp} p_{m_F^2,m_T^2}\right| = \sqrt{2}$.

1.3.4 Gaussian Plane Waves

If we multiply the plane wave (1.25) by

$$\exp\left(-\sigma^2\left(t-\frac{1}{\omega}k\cdot x-B\right)^2\right)=\exp\left(-\left(\frac{\sigma}{\omega}\right)^2(k\cdot x+\omega B-\omega t)^2\right)$$

with $\sigma, B\in\mathbb{R}$, we obtain a *Gaussian plane wave* or *Gaussian pulse* [27, (6.1)], [75, (6.2)]

$$g(x,t)=A\cos(k\cdot x+\varphi_0-\omega t)\exp\left(-\sigma^2\left(t-\frac{1}{\omega}k\cdot x-B\right)^2\right). \tag{1.29}$$

One can verify that Gaussian pulses are solutions of the homogeneous wave equation (1.1a) when $|k|^2=\omega^2$.

The Gaussian plane waves, similarly to the plane waves introduced in Section 1.3.3, are equal to zero along the lines (1.26) and, analogously to (1.27), we can define *Gaussian plane wave packets* g_{m_F,m_T}. These wave packets are continuous along the front and tail, but their derivatives are not, with, for $i=1,2$,

$$\begin{aligned}|\dot{g}_{m_F,m_T}(x,t)| &= |A\omega|\exp\left(-\left(\frac{\sigma}{\omega}\right)^2\left(\frac{\pi}{2}+l\pi-\varphi_0+\omega B\right)^2\right)\\ \left|\frac{\partial p_{m_F,m_T}}{\partial x_i}(x,t)\right| &= |Ak_i|\exp\left(-\left(\frac{\sigma}{\omega}\right)^2\left(\frac{\pi}{2}+l\pi-\varphi_0+\omega B\right)^2\right)\end{aligned} \tag{1.30}$$

for x,t such that $k\cdot x=\omega t-m_F$ and $k\cdot x=\omega t-m_T$.

Chapter 2

Approximation of Two Dimensional Time Domain Boundary Potential Operators

In this chapter, we introduce the variational formulation and an approximation scheme for the time domain boundary integral equations corresponding to the scattering problem presented in Chapter 1.

In Sections 2.1 and 2.2, the discretisations of the space and time domains are described, and piecewise polynomial functions which are used to approximate the solutions of the time domain boundary integral equations are introduced.

The variational formulation of a model time domain boundary integral equation, of which all integral equations given in Chapter 1 are realisations, is derived in Section 2.3. After discretising the variational formulation, the computation of the entries of the system matrix of the linear system that has to be solved to obtain the approximation's coefficient vector is addressed. The entries of the system matrix feature four integrals, of which two are spatial and two are temporal. Similarly to Ostermann [127], who considers the three dimensional case, we seek to perform the two temporal integrations analytically and the two spatial integrations using a quadrature method.

The analytical computation of the temporal integrals is treated, in general, in Section 2.3. These computations are rather technical for the explicit examples that we are concerned with, and are therefore treated separately in Appendix A. The general considerations reveal that the analytically computed solutions of the temporal integrals, which appear as the kernel function of the spatial double integral, have piecewise finite support. The special nature of these kernel functions therefore require an appropriate quadrature scheme, which is studied in Section 2.4. This involves concepts from computational geometry that are not commonly needed for Boundary Element Methods for time independent problems, and which are therefore amply treated. All these considerations result in a full quadrature scheme for the computation of the Galerkin matrices, given in Algorithm 2.6. We establish the exponential convergence of this quadrature scheme by the theory of countably normed spaces in Section 2.5.

The chapter ends with some first numerical experiments to validate our computational scheme in Section 2.6.

2.1 Discretisation of the Space and Time Domains

Let us assume that $\Gamma \subseteq \mathbb{R}^2$ is the boundary of a polygonal domain. If Γ is not polygonal (a circle, for instance) we approximate it by a polygon, and write Γ again for the approximation, for the sake of simplicity in the notation. We discretise Γ by a mesh of non-overlapping straight edges $\mathcal{T}_S = \{\Gamma_1, \dots, \Gamma_N\}$, with $\Gamma = \bigcup_{i=1}^N \Gamma_i$. We write $h_i := |\Gamma_i|$ for the length of an edge Γ_i. For a uniform spatial mesh, i.e. if $h_i = h_j$ for all $i, j = 1, \dots, N$, we drop the index, and simply write h.

We further consider a finite subinterval $[0, T)$ of the infinite time domain $\mathbb{R}_{\geq 0}$. We decompose $[0, T)$ by a time mesh $\mathcal{T}_T = \{[0, t_1), [t_1, t_2), \dots, [t_{M-1}, T)\}$ of M elements. For convenience, we set $t_0 := 0$ and $t_M := T$. Further, $\Delta t_j := t_j - t_{j-1}$, $j = 1, \dots, M$, denotes the *length of the j-th time interval* $T_j := [t_{j-1}, t_j)$. As for the spatial discretisation, if $\Delta t_i = \Delta t_j$ for all $i, j = 1, \dots, M$, we drop the index and write Δt.

We call the most general type of space-time meshes we consider *pseudo-3D meshes*. These are allowed to feature arbitrary non-overlapping triangulations (by squares) of the space-time cylinder $\Gamma \times [0, T] \subseteq \mathbb{R}^3$, i.e.

$$\mathcal{T}_{S,T} = \{\ S_k \quad | \quad k \geq 0\ \} \tag{2.1}$$

where, for each $k \geq 0$, $S_k = \Gamma_k \times [t_k^1, t_k^2) \subseteq \mathbb{R}^2$, with $\Gamma_k \subseteq \Gamma$ and $0 \leq t_k^1 < t_k^2 \leq T$, is a square on the surface of the space-time cylinder $\Gamma \times [0, T]$, and $\bigcup_{k \geq 0} S_k = \Gamma \times [0, T]$. A mesh of this type is sketched in Figure 6.1b.

If the temporal mesh is uniform, i.e. if $t_k^2 - t_k^1 = \Delta t$ for every $k \geq 0$, $\mathcal{T}_{S,T}$ can be rewritten as

$$\mathcal{T}_{S,T} = \bigcup_{j=1}^{M} \mathcal{T}_S^j \times [t_{j-1}, t_j) \tag{2.2}$$

after renumbering the mesh elements, with $\mathcal{T}_S^j \neq \mathcal{T}_S^k$ for $j \neq k$ in general. A mesh of this type is sketched in Figure 6.1a.

The simplest form of space-time meshes we consider are of the type $\mathcal{T}_{S,T} = \mathcal{T}_S \times \mathcal{T}_T$. In particular, if $\mathcal{T}_S$ and $\mathcal{T}_T$ are both uniform meshes, $\mathcal{T}_{S,T}$ is a uniform space-time mesh.

We further define piecewise constant functions

$$h(\mathcal{T}_S) : \Gamma \to \mathbb{R}_{>0} \quad , \quad h(\mathcal{T}_S)|_{\Gamma_i} := |\Gamma_i| = h_i.$$

and

$$\Delta t(\mathcal{T}_T) : [0, T] \to \mathbb{R}_{>0} \quad , \quad \Delta t(\mathcal{T}_T)|_{[t_{j-1}, t_j)} := |t_j - t_{j-1}| = \Delta t_j.$$

Piecewise constant functions $h(\mathcal{T}_{S,T})$ and $\Delta t(\mathcal{T}_{S,T})$ are defined similarly.

The *local mesh ratio* $K(\mathcal{T}_S)$ of a mesh $\mathcal{T}_S$ is defined as the smallest number K that satisfies [39, (2.9)]

$$\frac{1}{K} \leq \frac{|\Gamma_i|}{|\Gamma_j|} \leq K \tag{2.3}$$

for all $\Gamma_i, \Gamma_j \in \mathcal{T}_S$ with $\Gamma_i \cap \Gamma_j \neq \varnothing$. The definition of $K_T(\mathcal{T}_{S,T}) := K(\mathcal{T}_T)$ is analogous.

Similarly to [133, Definition 4.3], we define a constant that describes the *quasi-uniformity* of $\mathcal{T}_S$ by

$$q(\mathcal{T}_S) := \max\left\{ \frac{|\Gamma_i|}{|\Gamma_j|} \quad | \quad \Gamma_i, \Gamma_j \in \mathcal{T}_S \right\} \geq 1. \tag{2.4}$$

Obviously $q(\mathcal{T}_S) = 1$ for uniform meshes, whereas a large number $q(\mathcal{T}_S)$ indicates a strongly non-uniform mesh. A constant $q(\mathcal{T}_T)$ is defined analogously. We further set

$$q(\mathcal{T}_{S,T}) := \max\left\{ \max\left\{ \frac{|\Gamma_i|}{|T_j|}, \frac{|T_j|}{|\Gamma_i|} \right\} \quad | \quad \Gamma_i, T_j \in \mathcal{T}_{S,T} \right\}. \tag{2.5}$$

2.2 Approximation Spaces

We choose a basis $\{\varphi_1^p, \ldots, \varphi_{N_S}^p\}$ of the space V_h^p of piecewise polynomial functions of degree p in space, and a basis $\{\beta^{1,q}, \ldots, \beta^{M_T,q}\}$ of the space $V_{\Delta t}^q$ of piecewise polynomial functions of degree q in time. Note that $M = M_T + 1$ is the number of time mesh points we consider for the approximation (including the initial time $t_0 = 0$).

If the simplest type of meshes introduced in Section 2.1, $\mathcal{T}_{S,T} = \mathcal{T}_S \times \mathcal{T}_T$, is considered, the space of piecewise polynomials in space and time is simply the tensor product of the approximation spaces in space and time, V_h^p and $V_{\Delta t}^q$, and we write [53, p. 535]

$$V_N := V_{h,\Delta t}^{p,q} := V_h^p \otimes V_{\Delta t}^q.$$

Approximation properties of these spaces are considered in Section 3.4. For meshes of type (2.2), the approximation space is

$$V_N = \bigcup_{j=1}^{M_T} V_h^p(j) \otimes \left\{\beta^{j,q}\right\} \tag{2.6}$$

and for the pseudo-3D meshes (2.1),

$$\begin{aligned} V_N \;=\; \text{span}\{\; \psi \;\mid\; & \psi \text{ has piecewise support on } \mathcal{T}_{S,T} \text{ and } \psi|_{S_k} \text{ is a poly-} \\ & \text{nomial of degree} \le p \text{ in } x \text{ and} \le q \text{ in } t \text{ for any } k \ge 0 \;\} \end{aligned} \tag{2.7}$$

where the basis functions ψ are associated with the mesh elements or the nodes of $\mathcal{T}_{S,T}$.
Note that we write $\gamma^m = \beta^{m,0}$, $m = 1, \ldots, M_T$, for piecewise constant functions in time, and $\beta^m = \beta^{m,1}$, $m = 1, \ldots, M_T$, for piecewise linear functions in time. As usual, for $q = 0, 1$, we use basis functions with piecewise support and $\beta^{m,q}(t_n) = \delta_{m,n}$ for each time mesh point t_n. For $q \ge 2$, one would use the space of piecewise linear basis functions ($q = 1$), enriched by so-called *bubble function* α_q^m that have support on only one time slab, namely $\operatorname{supp} \alpha_q^m = [t_{m-1}, t_m)$, and with $\alpha_q^m(t_n) = 0$ for all m, n. Thus, for $q \ge 2$, $V_{\Delta t}^q = V_{\Delta t}^1 \oplus \text{span}\left\{\alpha_q^1, \ldots, \alpha_q^{M_t - |V_{\Delta t}^q|}\right\}$.

The *hat functions* $\beta^m = \beta^{m,1}$, $m = 1, \ldots, M_T - 1$, have support on two time slabs, namely $\operatorname{supp} \beta^m = [t_{m-1}, t_m) \cup [t_m, t_{m+1})$, and are given explicitly by

$$\beta^m(t) = \begin{cases} \frac{1}{\Delta t_m}(t - t_{m-1}) & , \quad t \in [t_{m-1}, t_m) \\ \frac{1}{\Delta t_{m+1}}(t_{m+1} - t) & , \quad t \in [t_m, t_{m+1}) \\ 0 & , \quad t \notin [t_{m-1}, t_m) \cup [t_m, t_{m+1}) \end{cases}. \tag{2.8}$$

The *brick functions* $\gamma^m = \beta^{m,0}$, $m = 1, \ldots, M_T$, have support on only one time slab, namely $\operatorname{supp} \gamma^m = [t_{m-1}, t_m)$, and are given explicitly by

$$\gamma^m(t) = \mathbb{1}_{[t_{m-1}, t_m)}(t) = \begin{cases} 1 & , \quad t \in [t_{m-1}, t_m) \\ 0 & , \quad t \notin [t_{m-1}, t_m) \end{cases}. \tag{2.9}$$

We note that one can rewrite all the basis functions in terms of Heaviside (and hence of indicator) functions,

$$\begin{aligned} \gamma^m(t) &= H(t - t_{m-1}) - H(t - t_m) \\ \beta^m(t) &= (H(t - t_{m-1}) - H(t - t_m))\frac{t - t_{m-1}}{\Delta t_m} + (H(t - t_m) - H(t - t_{m+1}))\frac{t_{m+1} - t}{\Delta t_{m+1}} \\ &= \frac{1}{\Delta t_m}(t - t_{m-1})\gamma^m(t) + \frac{1}{\Delta t_{m+1}}(t_{m+1} - t)\gamma^{m+1}(t) \\ \alpha_q^m(t) &= (H(t - t_{m-1}) - H(t - t_m))p_q^m(t) = \gamma^m(t)p_q^m(t) \qquad (q \ge 2) \end{aligned} \tag{2.10}$$

where p_m^q is a polynomial of degree q with $p_m^q(t_{m-1}) = p_m^q(t_m) = 0$. We further note that we understand the derivatives of γ^m in the distributional sense as the the difference of two Dirac impulses, i.e.

$$\dot{\gamma}^m(t) = \delta_{t_{m-1}}(t) - \delta_{t_m}(t).$$

2.3 Model Problem and Analytical Temporal Integration for Time Domain Boundary Element Matrices in Two Space Dimensions

Let us consider a model problem of which the six standard time domain boundary integral equations (1.12)-(1.14) are realisations.

For $(x,t) \in \Gamma \times \mathbb{R}_{\geq 0}$, let

$$P[p](x,t) := \int_\Gamma \int_{\mathbb{R}_{\geq 0}} H(t-s-|x-y|)\kappa(s,t;|x-y|)p(y,s)\ ds\ ds_y \tag{2.11}$$

be an arbitrary time domain boundary integral operator. Note that all the time domain boundary integral operators defined in Definition 1.4 are of this type, at least after integrating by parts or in their weak form; see also (A.60) and (A.88).

Let $f(x,t) : \Gamma \times \mathbb{R}_{\geq 0} \to \mathbb{R}$ be some given function, and V some function space. We aim to solve the *model problem*

$$\text{(RPIE)} \quad \begin{cases} \text{Find } p \text{ with } P[p] \in V \text{ such that} \\ \\ \qquad P[p](x,t) = f(x,t) \\ \\ \text{for all } (x,t) \in \Gamma \times \mathbb{R}_{\geq 0}. \end{cases} \tag{2.12}$$

In order to find a weak formulation, we multiply (2.12) by a test function $q \in V'$ and integrate over Γ and $\mathbb{R}_{\geq 0}$. The weak formulation of (RPIE) then reads

$$\text{(RPIE)}_{\text{V}} \quad \begin{cases} \text{Find } p \text{ with } P[p] \in V \text{ such that} \\ \\ \qquad \int_{\mathbb{R}_{\geq 0}} \langle P[p](\cdot,t), q(\cdot,t)\rangle\ dt = \int_{\mathbb{R}_{\geq 0}} \langle f(\cdot,t), q(\cdot,t)\rangle\ dt \\ \\ \text{for all } q \in V'. \end{cases} \tag{2.13}$$

Here, $\langle \cdot, \cdot \rangle$ stands for the duality product

$$\langle g, h\rangle := \int_\Gamma g(x)h(x)\ ds_x \tag{2.14}$$

that coincides with the $L^2(\Gamma)$ inner product for $g, h \in L^2(\Gamma)$.

On the left hand side of (2.13), we have to deal with integrals of the type (see Section A.2 for some explicit examples)

$$\int_{\mathbb{R}_{\geq 0}} \langle P[p](\cdot,t), q(\cdot,t)\rangle\ dt = \iint_{\Gamma\times\Gamma} \iint_{\mathbb{R}_{\geq 0}\times\mathbb{R}_{\geq 0}} H(t-s-|x-y|)\kappa(s,t;|x-y|)\ p(y,s)q(x,t)\ ds\ dt\ ds_x\ ds_y. \tag{2.15}$$

Next we replace p by an approximation p_N, given by

$$p_N(y,s) = \sum_{m=1}^{M_T} \sum_{i=1}^{N_S} p_i^m \beta^{m,q_1}(s)\varphi_i^{p_1}(y) \ \in\ V_{h,\Delta t}^{p_1,q_1}. \tag{2.16}$$

We further write $p_N^m(y) = p_N(y, t_m) := \sum_{i=1}^{N_S} p_i^m \varphi_i^{p_1}(y)$, $1 \le m \le M_T$. This is the approximation to the solution at time step t_m, i.e. $p(\cdot, t_m) \approx p_N^m$.

Analogously, we replace q in (2.13) by a discrete test function

$$q_N(x,t) = \beta^{n,q_2}(t)\varphi_j^{p_2}(x) \ \in \ V_{h,\Delta t}^{p_2,q_2}. \tag{2.17}$$

The functions $\beta^{m,q_1} \in V_{\Delta t}^{q_1}$, $\beta^{n,q_2} \in V_{\Delta t}^{q_2}$, $\varphi_i^{p_1} \in V_h^{p_1}$, $\varphi_j^{p_2} \in V_h^{p_2}$ in (2.16) and (2.17) are basis functions with piecewise support, as indicated in Section 2.2. Note that the subscript N in p_N and q_N is meant to indicate discrete functions. It does not refer to the dimension of the underlying discrete spaces, which can be different for p_N and q_N.

Writing $q = (q_1, q_2)$, let us define the integral

$$\Upsilon^{q;\,m,n}(r) := \int_0^\infty \int_0^\infty H(t-s-r)\kappa(s,t;r)\ \beta^{m,q_1}(s)\beta^{n,q_2}(t)\ ds\ dt \tag{2.18}$$

where $r = r(x,y) := |x-y|$ for $x, y \in \Gamma$. We discussed in Section 2.2 that, for $q_1, q_2 \ge 0$ (for the special case $q_2 = -1$, see Section 2.3.1 below) all temporal basis functions can be rewritten in terms of indicator functions, We hence consider, without loss of generality, integrals of the type

$$\iint_{\Gamma\times\Gamma} \int_{t_{n-1}}^{t_n} \int_{t_{m-1}}^{t_m} H(t-s-r)k(s,t;r)\ ds\ dt\ \varphi(y)\psi(x)\ ds_x\ ds_y \tag{2.19}$$

with $k(s,t;r) := \kappa(s,t;r)\ \beta^{m,q_1}(s)|_{[t_{m-1},t_m)}\beta^{n,q_2}(t)|_{[t_{n-1},t_n)}$, where we aim to compute the integral

$$\Upsilon^{m,n}(r) := \int_{t_{n-1}}^{t_n} \int_{t_{m-1}}^{t_m} H(t-s-r)k(s,t;r)\ ds\ dt. \tag{2.20}$$

analytically. The integral (2.18) can be rewritten as the sum of at most four integrals of the type (2.20). In computing the temporal integrals (2.20) analytically, we follow Ostermann [127], who considers the three dimensional case. For simpler reference, we thus use the same notation as [127] where it is possible. The challenges that we face here are, however, of quite a different nature compared to the three dimensional case. In our case, the two temporal integrals in (2.20) are, for $q_1, q_2 \ge 0$, 'genuine', as opposed to the three dimensional case where one temporal integral appears only formally, due to the presence of the delta function in the fundamental solution; see Lemma 1.2.

In what follows, we derive a general scheme to compute the terms (2.20) analytically. Explicit calculations for particular types of basis functions (Section A.1) and kernel functions (Section A.2) are given in Appendix A. For the evaluation of (2.20), we distinguish four different cases, depending on r. A similar construction is used in [110, Section 4.4] for a particular choice of basis functions and kernel. We write $l := n - m$ in what follows.

(i) $r > t_{l+1} = t_n - t_{m-1}$

Here $t - s - r < t_n - t_{m-1} - (t_n - t_{m-1}) = 0$, and thus $H(t-s-r) = \Upsilon^{m,n}(r) = 0$.

(ii) $r \le t_{l-1} = t_{n-1} - t_m$

Here $t - r \ge t_{n-1} - t_{l-1} = t_m$, and so $t - s - r = (t-r) - s \ge t_m - t_m = 0$. Thus $H(t-s-r) = 1$.

(iii) $t_{n-1} - t_m = t_{l-1} < r \le t_l = t_{n-1} - t_{m-1} = t_n - t_m$

Here $t_{l-1} = t_{n-1} - t_m \le r$ and $t_l = t_n - t_m \ge r$, and so $t_{n-1} \le r + t_m \le t_n$. This allows us to split $[t_{n-1}, t_n] = [t_{n-1}, r + t_m] \cup [r + t_m, t_n]$. The integration domain then becomes

$$[t_{m-1}, t_m] \times [t_{n-1}, t_n] = ([t_{m-1}, t_m] \times [t_{n-1}, r + t_m]) \cup ([t_{m-1}, t_m] \times [r + t_m, t_n]).$$

(a) $(s,t) \in [t_{m-1}, t_m] \times [t_{n-1}, r+t_m]$. Then $t-r \le r+t_m-r = t_m$ and $t-r \ge t_{n-1}-r \ge t_{n-1}-t_l = t_{m-1}$, which allows us to split $[t_{m-1}, t_m] = [t_{m-1}, t-r] \cup [t-r, t_m]$.

(aa) $(s,t) \in [t_{m-1}, t-r] \times [t_{n-1}, r+t_m]$. Then $t-s-r \ge t-(t-r)-r = 0$.

(ab) $(s,t) \in [t-r, t_m] \times [t_{n-1}, r+t_m]$. Then $t-s-r \le t-(t-r)-r = 0$.

(b) $(s,t) \in [t_{m-1}, t_m] \times [r+t_m, t_n]$. Then $t-s-r \ge r+t_m-r-s = t_m-s \ge t_m-t_m = 0$.

Thus $H(t-s-r) = 1$ for $(s,t) \in ([t_{m-1}, t-r] \times [t_{n-1}, r+t_m]) \cup ([t_{m-1}, t_m] \times [r+t_m, t_n])$ and $H(t-s-r) = 0$ for $(s,t) \in [t-r, t_m] \times [t_{n-1}, r+t_m]$.

(iv) $t_n - t_m = t_l < r \le t_{l+1} = t_n - t_{m-1}$

Here $t_l = t_{n-1} - t_{m-1} \le r$ and $t_{l+1} = t_n - t_{m-1} \ge r$, and so $t_{n-1} \le r + t_{m-1} \le t_n$. This allows us to split $[t_{n-1}, t_n] = [t_{n-1}, r+t_{m-1}] \cup [r+t_{m-1}, t_n]$. The integration domain then becomes

$$[t_{m-1}, t_m] \times [t_{n-1}, t_n] = ([t_{m-1}, t_m] \times [t_{n-1}, r+t_{m-1}]) \cup ([t_{m-1}, t_m] \times [r+t_{m-1}, t_n]).$$

(a) $(s,t) \in [t_{m-1}, t_m] \times [t_{n-1}, r+t_{m-1}]$. Then $t-s-r \le (r+t_{m-1}) - t_{m-1} - r = 0$.

(b) $(s,t) \in [t_{m-1}, t_m] \times [r+t_{m-1}, t_n]$. Then $t-r \le t_n - r < t_n - t_l = t_m$ and $t-r \ge r+t_{m-1}-r = t_{m-1}$, which allows us to split $[t_{m-1}, t_m] = [t_{m-1}, t-r] \cup [t-r, t_m]$.

(ba) $(s,t) \in [t_{m-1}, t-r] \times [r+t_{m-1}, t_n]$. Then $t-s-r \ge t-(t-r)-r = 0$.

(bb) $(s,t) \in [t-r, t_m] \times [r+t_{m-1}, t_n]$. Then $t-s-r \le t-(t-r)-r = 0$.

Thus $H(t-s-r) = 1$ for $(s,t) \in [t_{m-1}, t-r] \times [r+t_{m-1}, t_n]$ and $H(t-s-r) = 0$ for $(s,t) \in ([t_{m-1}, t_m] \times [t_{n-1}, r+t_{m-1}]) \cup ([t-r, t_m] \times [r+t_{m-1}, t_n])$.

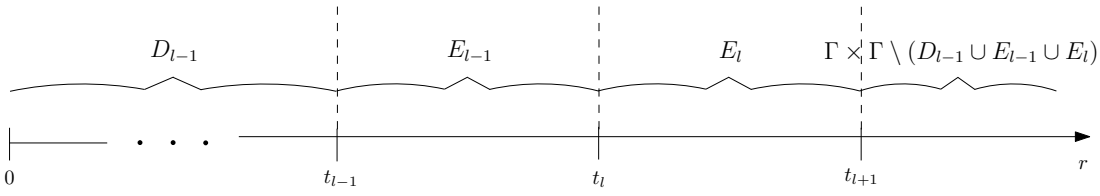

Figure 2.1: Decomposition of $\Gamma \times \Gamma$ with respect to r into non-overlapping domains as in (2.21).

Writing $l := n - m$, $\Upsilon^{m,n}(r)$ can now be rewritten as the sum of four integrals over the non-overlapping domains discussed above, namely

$$\Gamma \times \Gamma = D_{l-1} \cup E_{l-1} \cup E_l \cup (\Gamma \times \Gamma \setminus (D_{l-1} \cup E_{l-1} \cup E_l)) \tag{2.21}$$

where

$$E_l := \{\ (x,y) \in \Gamma \times \Gamma \ \mid\ t_l \le |x-y| \le t_{l+1}\ \} \tag{2.22}$$

is called a *discrete light ring* and

$$D_l := \{\ (x,y) \in \Gamma \times \Gamma \ \mid\ |x-y| \le t_l\ \} \tag{2.23}$$

is called a *discrete light disc*. The decomposition is illustrated in Figure 2.1. By the discussion above, we can rewrite the integral (2.20) as

$$\begin{aligned}\Upsilon^{m,n}(r) &= \mathbb{1}_{D_{l-1}}(r)\int_{t_{n-1}}^{t_n}\int_{t_{m-1}}^{t_m} k(s,t;r)\ ds\ dt \\ &\quad +\mathbb{1}_{E_{l-1}}(r)\left(\int_{t_{n-1}}^{r+t_m}\int_{t_{m-1}}^{t-r} k(s,t;r)\ ds\ dt + \int_{r+t_m}^{t_n}\int_{t_{m-1}}^{t_m} k(s,t;r)\ ds\ dt\right) \\ &\quad +\mathbb{1}_{E_l}(r)\int_{r+t_{m-1}}^{t_n}\int_{t_{m-1}}^{t-r} k(s,t;r)\ ds\ dt \\ &=: \mathbb{1}_{D_{l-1}}(r)F^{m,n}_{D_{l-1}}(r) + \mathbb{1}_{E_{l-1}}(r)F^{m,n}_{E_{l-1}}(r) + \mathbb{1}_{E_l}(r)F^{m,n}_{E_l}(r). \end{aligned} \tag{2.24}$$

Obviously, $\operatorname{supp}\Upsilon^{m,n} = D_{l-1}\cup E_{l-1}\cup E_l$. As Section A.1 shows, all kernel functions of interest yield integrals that depend only on the difference $l = n-m$, so that $F^{m,n}_{D_{l-1}} = F^{l}_{D_{l-1}}$, $F^{m,n}_{E_{l-1}} = F^{l}_{E_{l-1}}$ and $F^{m,n}_{E_l} = F^{l}_{E_l}$. Crucially, we are therefore allowed to write $\Upsilon^l = \Upsilon^{n-m}$ instead of $\Upsilon^{m,n}$ in (2.20) and (2.24), and $\Upsilon^{q;l}$ instead of $\Upsilon^{q;m,n}$ in (2.18), which implies a considerable simplification in the structure of the corresponding linear system, outlined below (2.30).

The discussion above showed that we may restrict ourselves to the case $n \geq m$; for if $m > n$, we have $l \leq -1$, and thus $t_{l+1} < 0$. But then $r > t_{l+1}$ for any pair (x,y), and hence $D_{l-1} = E_{l-1} = E_l = \varnothing$, yielding $\Upsilon^l(r) = 0$.

In the case of a non-uniform temporal mesh, there is one more case to consider. If $t_n - t_m \geq t_{n-1} - t_{m-1}$,

$$\begin{aligned}[0,\infty) &= [0, t_{n-1}-t_m] \cup (t_{n-1}-t_m, t_{n-1}-t_{m-1}] \cup (t_{n-1}-t_{m-1}, t_n - t_m] \\ &\quad \cup (t_n - t_m, t_n - t_{m-1}] \cup (t_n - t_{m-1}, \infty). \end{aligned} \tag{2.25}$$

The case $t_n - t_m \leq t_{n-1} - t_{m-1}$ is covered by renaming the variables. In (2.25), the first, second, fourth and fifth subintervals are covered by cases (ii), (iii), (iv) and (i) above, respectively. If a uniform temporal mesh is used, the third subinterval $(t_{n-1}-t_{m-1}, t_n - t_m]$ is empty. Otherwise, one can use a splitting similar to cases (iii) and (iv):

(v) $t_{n-1} - t_{m-1} \leq r \leq t_n - t_m$

Here $t_{n-1} \leq r + t_{m-1} \leq r + t_m \leq t_n$. This allows us to split $[t_{n-1}, t_n] = [t_{n-1}, r+t_{m-1}] \cup [r + t_{m-1}, r+t_m] \cup [r+t_m, t_n]$. The integration domain then becomes

$$\begin{aligned}[t_{m-1},t_m]\times[t_{n-1},t_n] &= ([t_{m-1},t_m]\times[t_{n-1},r+t_{m-1}]) \cup ([t_{m-1},t_m]\times[t_{n-1},r+t_m]) \\ &\quad \cup ([t_{m-1},t_m]\times[r+t_m,t_n]). \end{aligned}$$

(a) $(s,t) \in [t_{m-1},t_m]\times[t_{n-1},r+t_{m-1}]$. Then $t - s - r \leq (r+t_{m-1}) - t_{m-1} - r = 0$.

(b) $(s,t) \in [t_{m-1},t_m]\times[r+t_{m-1},r+t_m]$. Then $t - r \in [t_{m-1},t_m]$, which allows us to split $[t_{m-1},t_m] = [t_{m-1}, t-r] \cup [t-r, t_m]$.

(ba) $(s,t) \in [t_{m-1}, t-r]\times[r+t_{m-1}, r+t_m]$. Then $t - s - r \geq t - (t-r) - r = 0$.

(bb) $(s,t) \in [t-r, t_m]\times[r+t_{m-1}, r+t_m]$. Then $t - s - r \leq t - (t-r) - r = 0$.

(c) $(s,t) \in [t_{m-1},t_m]\times[r+t_m,t_n]$. Then $t - s - r \geq (r+t_m) - t_m - r = 0$.

Thus $H(t-s-r) = 1$ for $(s,t) \in ([t_{m-1}, t-r]\times[r+t_{m-1}, r+t_m]) \cup ([t_{m-1},t_m]\times[r+t_m,t_n])$ and $H(t-s-r) = 0$ for $(s,t) \in ([t_{m-1},t_m]\times[t_{n-1},r+t_{m-1}]) \cup ([t-r,t_m]\times[r+t_{m-1},r+t_m])$.

We now return to the approximation of (2.15). Replacing p and q in (2.15) by their approximations p_N and q_N, given in (2.16) and (2.17), we obtain

$$\int_0^\infty \langle P[p_N](\cdot,t), q_N(\cdot,t)\rangle \; dt = \sum_{m=1}^{M_T}\sum_{i=1}^{N_S} p_i^m \iint_{\Gamma\times\Gamma} \Upsilon^{q;n-m}(r)\varphi_i^{p_1}(y)\varphi_j^{p_2}(x)\; ds_x\; ds_y \tag{2.26}$$

for all $j = 1,\dots,N_S$, $n = 1,\dots,M_T$. We define matrices $\mathcal{U}^{m,n} \in \mathbb{R}^{N_S\times N_S}$ by

$$\mathcal{U}^{m,n} = \mathcal{U}^{n-m} = \mathcal{U}^l := \left(\iint_{\Gamma\times\Gamma} \Upsilon^{q;\,m,n}(r)\varphi_i^{p_1}(y)\varphi_j^{p_2}(x)\; ds_x\; ds_y\right)_{i,j=1}^{N_S}. \tag{2.27}$$

The subdomains D_{l-1}, E_{l-1}, E_l in (2.24) correspond to three submatrices $\mathcal{U}^l_{D_{l-1}}, \mathcal{U}^l_{E_{l-1}}, \mathcal{U}^l_{E_l}$. Since the discrete light discs D_l grow with l, the corresponding matrices $\mathcal{U}^l_{D_{l-1}}$ become increasingly populated with increasing time step l. The matrices $\mathcal{U}^l_{E_{l-1}}, \mathcal{U}^l_{E_l}$, on the other hand, are equal to zero for $t_l \geq \operatorname{diam}\Omega^-$.

Obviously, $\mathcal{U}^l = 0$ for $l < 0$. Therefore, for all $j = 1,\dots,N_S$, $n = 1,\dots,M_T$,

$$\int_0^\infty \langle P[p_N](\cdot,t), q_N(\cdot,t)\rangle \; dt = \sum_{m=1}^{M_T}\sum_{i=1}^{N_S} p_i^m \mathcal{U}_{i,j}^{m,n}. \tag{2.28}$$

Similarly, we use discrete basis functions to approximate the right hand side of (2.13), and obtain

$$\int_0^\infty \langle f(\cdot,t), q_N(\cdot,t)\rangle \; dt = \int_0^\infty \int_\Gamma f(x,t)\varphi_j^{p_2}(x)\; ds_x \beta^{n,q_2}(t)\; dt =: b_j^n \tag{2.29}$$

for all $j = 1,\dots,N_S$, $n = 1,\dots,M_T$. The approximation of (2.29) is addressed in Section A.5. Writing $\vec{b}^n := \left(b_j^n\right)_{j=1}^{M_T}$, the unknown coefficient vectors $\vec{p}^1,\dots,\vec{p}^{M_T}$ are then the solution of the linear system

$$\begin{pmatrix} \mathcal{U}^{1,1} & 0 & 0 & \cdots & 0 \\ \mathcal{U}^{1,2} & \mathcal{U}^{2,2} & 0 & \cdots & 0 \\ \mathcal{U}^{1,3} & \mathcal{U}^{2,3} & \mathcal{U}^{3,3} & \cdots & 0 \\ \vdots & \vdots & \vdots & \ddots & \vdots \\ \mathcal{U}^{1,M_T} & \mathcal{U}^{2,M_T} & \mathcal{U}^{3,M_T} & \dots & \mathcal{U}^{M_T,M_T} \end{pmatrix} \begin{pmatrix} \vec{p}^1 \\ \vec{p}^2 \\ \vec{p}^3 \\ \vdots \\ \vec{p}^{M_T} \end{pmatrix} = \begin{pmatrix} \vec{b}^1 \\ \vec{b}^2 \\ \vec{b}^3 \\ \vdots \\ \vec{b}^{M_T} \end{pmatrix} \tag{2.30}$$

which is of size $M_T N_S \times M_T N_S$. If a uniform temporal mesh is chosen, i.e. if $\Delta t_i = \Delta t_j$ for each $i,j = 1,\dots,M_T$, we have $\mathcal{U}^{1,1} = \mathcal{U}^{2,2} = \dots = \mathcal{U}^{M_T,M_T} = \mathcal{U}^0$, $\mathcal{U}^{1,2} = \mathcal{U}^{2,3} = \dots = \mathcal{U}^{M_T-1,M_T} = \mathcal{U}^1$, and so on. In this case, the solution of the linear system (2.30) becomes considerably easier, since it can be rewritten as a sequence of M_T linear systems of size N_S, namely

$$\sum_{m=1}^{M_T} \mathcal{U}^{n-m}\vec{p}^m = \sum_{m=1}^{n} \mathcal{U}^{n-m}\vec{p}^m = \mathcal{U}^0\vec{p}^n + \sum_{m=1}^{n-1} \mathcal{U}^{n-m}\vec{p}^m = \vec{b}^n \tag{2.31}$$

for every $n = 1,\dots,M_T$. Additionally, instead of storing $\frac{M_T(M_T+1)}{2}$ matrix blocks, we only need to store the M_T matrix blocks in the last line of the system matrix of (2.30), which reduces the storage requirements considerably.

To find the unknown coefficient vectors $\vec{p}^n$ for any time step $1 \leq n \leq M_T$, one then uses the semi-implicit scheme

$$\mathcal{U}^0\vec{p}^n = \vec{b}^n - \sum_{m=1}^{n-1} \mathcal{U}^{n-m}\vec{p}^m. \tag{2.32}$$

This scheme is widely known as a *marching-on-in-time scheme* (*MOT scheme*). Its storage requirements and computation times are considerably smaller, compared to the full linear system (2.30), and uniform temporal meshes are therefore used throughout most of the literature on time domain Boundary Element Methods. The MOT scheme is summarised comprehensively in Algorithm 2.1 below.

Note that it is still possible to use some kind of MOT scheme with meshes of the type (2.2), even though this is more costly than the classical one. This topic is addressed in more detail in Section 6.1.1. For non-uniform temporal meshes, however, the full linear system (2.30) has to be solved, and its large system matrix has to be stored.

Algorithm 2.1 Classical MOT scheme

Input: number of time steps M_T, time step size Δt, number of space basis functions N_S
Output: sequence of approximations p_h^n for each time step t_n, $n = 1, \dots, M_T$, represented by $\vec{p}^n$

```
compute system matrix U^0 and the first right hand side vector b^1
compute the approximation at t_1, p_h^1, by solving the linear system U^0 p^1 = b^1
store U^0, p^1
for n = 2, ..., M_T do
    compute new matrix U^{n-1}
    compute new right hand side vector b^n
    compute the approximation at t_n, p_h^n, by solving the linear system (2.32)
    store U^{n-1}, p^n
end for
```

Remark 2.1

a) The matrix $\mathcal{U}^0$ is the system matrix *of the MOT scheme, i.e. the matrix on the left hand side of the linear system* (2.32)*, for each time step.*

In order to reduce the cost of solving the linear systems, one could therefore store the inverse matrix to $\mathcal{U}^0$, or use a decomposition method. The, by far, most expensive part of the computations within a MOT scheme is, however, the computation of the matrices $\mathcal{U}^l$, and a reduction in the time to solve the linear systems has little effect on the computation time of the entire MOT scheme.

b) Obviously, $D_l = D_{l-1} \cup E_{l-1}$. However, due to the l-dependence of the functions $F^l_{D_{l-1}}$, $F^l_{E_{l-1}}$ and $F^l_{E_l}$, it is in general impossible to obtain $\Upsilon^{q;\,l}$ from the previously computed $\Upsilon^{q;\,l-1}$ and an additional term. In practice, every corresponding matrix therefore has to be fully computed.

c) Clearly, $|x - y| \leq$ diam Ω^- for all $(x, y) \in \Gamma \times \Gamma$. Hence, if $t_l \geq$ diam Ω^-, $E_{l-1} = E_l = \varnothing$ and $D_{l-1} = \Gamma \times \Gamma$. In this case, we say that the discrete light rings have passed the scatterer *and that the boundary has become* entirely illuminated*. Due to the l-dependence of the kernel function, the corresponding matrices still change, although the integration domain remains unchanged.*

This is a fundamental difference to the three dimensional case, where no discrete light discs exist. In this case, the boundary becomes entirely darkened *for $t_l \geq$ diam Ω^-, and no more matrices need to be computed from that time step onwards. In fact, these algebraic differences are the manifestations of the physical differences outlined in Huygens' principle; see Remark 1.1.*

d) Guardasoni et al. [3, 5, 77] use a different decomposition of the integrals (2.24)*, which results in sums of integrals over several light discs; see, for instance, [77, (4.11)-(4.16)]. For reasons*

that become apparent in Section 2.4, their decomposition simplifies the computation of the spatial integrals (2.27)*, but it is disadvantageous in other respects. It requires, independently of* l*, the computation of four integrals, which increases the overall quadrature error and the computation time. In particular, and as outlined in c), for* $t_l \geq \operatorname{diam} \Omega^-$*, all but one of the terms in* (2.24) *vanish. Therefore, only one integral needs to be computed in this case, whereas four integrals need to be computed when the decomposition [77, (4.11)] is applied. The decomposition* (2.24) *further often allows to cancel some terms in the kernel functions. We note, however, that [77, (4.11)] can be rearranged to obtain a decomposition into a single light disc and two light rings, which then coincides with* (A.47)*.*

2.3.1 The Special Case of Derivatives of Piecewise Constant Test Functions

The case of $q_2 = -1$ in (2.18) corresponds to derivatives of piecewise constant basis functions as test functions. In this case, $\beta^{n,-1} = \dot{\gamma}^n(t) = \delta_{t_{n-1}}(t) - \delta_{t_n}(t)$, and thus

$$\begin{aligned}
&\Upsilon^{(q_1,-1);\,m,n}(r)\\
&= \int_0^\infty \int_0^\infty H(t-s-r)\kappa(s,t;r)\ \beta^{m,q_1}(s)\beta^{n,-1}(t)\ ds\ dt\\
&= \int_0^\infty \left(H(t_{n-1}-s-r)\kappa(s,t_{n-1};r) - H(t_n-s-r)\kappa(s,t_n;r)\right)\ \beta^{m,q_1}(s)\ ds\\
&= \sum_{j=0,1} (-1)^{j+1} \int_0^\infty H(t_{n-j}-s-r)\kappa(s,t_{n-j};r)\ \beta^{m,q_1}(s)\ ds. \qquad (2.33)
\end{aligned}$$

Here we aim to compute integrals of the type

$$\Upsilon_\alpha^m(r) = \int_{t_{m-1}}^{t_m} H(\alpha-s-r)k(s,\alpha;r)\ ds \qquad (2.34)$$

analytically, with $k(s,\alpha;r) := \kappa(s,\alpha;r)\beta^{m,q_1}(s)|_{[t_{m-1},t_m)}$ and $\alpha = t_{n-j}$ in (2.33), instead of the integrals of type (2.20). Obviously $\Upsilon^{(q_1,-1);\,m,n}$ can be written as the sum of at most 4 integrals of type (2.34).

Regarding Υ_α^m, we distinguish three cases in $\alpha - r$:

(i) $\alpha - r \geq t_m$, hence $\alpha - s - r \geq t_m - s \geq 0$ and thus $H(\alpha - s - r) = 1$ always in this case.

(ii) $t_m \geq \alpha - r \geq t_{m-1}$, and thus $H(\alpha - s - r) = 1$ only for $s \leq \alpha - r$ in this case.

(iii) $\alpha - r \leq t_{m-1}$, hence $\alpha - s - r \leq t_{m-1} - s \leq 0$ and thus $H(\alpha - s - r) = 0$ always in this case.

Consequently,

$$\Upsilon_\alpha^m(r) = \begin{cases} \int_{t_{m-1}}^{t_m} k(s,\alpha;r)\,ds & \text{if } r \leq \alpha - t_m \\ \int_{t_{m-1}}^{\alpha-r} k(s,\alpha;r)\,ds & \text{if } \alpha - t_m \leq r \leq \alpha - t_{m-1} \\ 0 & \text{if } r \geq \alpha - t_{m-1} \end{cases}. \qquad (2.35)$$

For $\alpha = t_{n-j}$, we thus distinguish $r < t_{l-j}$ and $t_{l-j} < r < t_{l-j+1}$. Then

$$\begin{aligned}
\Upsilon_{t_{n-j}}^m(r) &= \mathbb{1}_{D_{l-j}}(r) \int_{t_{m-1}}^{t_m} k(s,t_{n-j};r)\ ds + \mathbb{1}_{E_{l-j}}(r) \int_{t_{m-1}}^{t_{n-j}-r} k(s,t_{n-j};r)\ ds\\
&=: \mathbb{1}_{D_{l-j}}(r) F_{D_{l-j}}^{m,n}(r) + \mathbb{1}_{E_{l-j}}(r) F_{E_{l-j}}^{m,n}(r). \qquad (2.36)
\end{aligned}$$

As for (2.24), it is shown in Section A.1 that $F_{D_{l-j}}^{m,n} = F_{D_{l-j}}^{l}$ and $F_{E_{l-j}}^{m,n} = F_{E_{l-j}}^{l}$ in all the cases that we consider, and we therefore write Υ_j^l instead of $\Upsilon_{t_{n-j}}^m$.

2.4 Efficient Implementation of the Integration in Space

Our next task is to consider the computation of the entries of the Galerkin matrices $\mathcal{U}^{m,n}$ that are given by (2.27). Since the temporal integrals are assumed to have been computed analytically, only the spatial integration remains to be done. For this purpose we present a quadrature scheme that enables us to compute the entries of the Galerkin matrices $\mathcal{U}^{m,n}$ efficiently and precisely, by detecting zero entries a-priori and by a precise determination of the integration domain in space before the actual quadrature routine is carried out. The latter task is of particular importance, since Galerkin methods for time domain boundary integral equations are very sensitive to instabilities that arise from imprecise computations of the matrix entries. In contrast to the three dimensional setting of [127] (see Sections 3.2.3 and 3.2.4 therein in particular), we are able to establish a full quadrature scheme, due to the considerably easier geometrical setting.

In what follows, we introduce all the operations necessary for this full quadrature scheme, which is given in Algorithm 2.6 in Section 2.4.3. The rate of convergence of Algorithm 2.6 is the subject of Section 2.5.

2.4.1 Some Geometrical Preliminaries

We begin this section with some geometrical studies within our discrete setup of two dimensional Boundary Element Methods.

Suppose that the boundary edges $\Gamma_i, \Gamma_j \in \mathcal{T}_S$ are given by their midpoints $\vec{m}_i, \vec{m}_j$ and their direction vectors $\vec{d}_i, \vec{d}_j$, respectively, as

$$\begin{aligned} \Gamma_i &= \left\{ \vec{x} = \vec{m}_i + \mu \vec{d}_i \;\middle|\; \mu \in [-1,1] \right\} \\ \Gamma_j &= \left\{ \vec{x} = \vec{m}_j + \nu \vec{d}_j \;\middle|\; \nu \in [-1,1] \right\}. \end{aligned} \tag{2.37}$$

Their end points are denoted by $\vec{x}_i$, $\vec{x}_{i+1}$ and $\vec{x}_j$, $\vec{x}_{j+1}$, respectively. We further write $\vec{\Delta}_i = 2\vec{d}_i$ and $\vec{\Delta}_j = 2\vec{d}_j$. The notation for a boundary edge Γ_i is illustrated in Figure 2.2(a). We use the notation

$$\vec{a} \times \vec{b} := a_1 b_2 - a_2 b_1 \tag{2.38}$$

for the cross product of $\vec{a}, \vec{b} \in \mathbb{R}^2$.

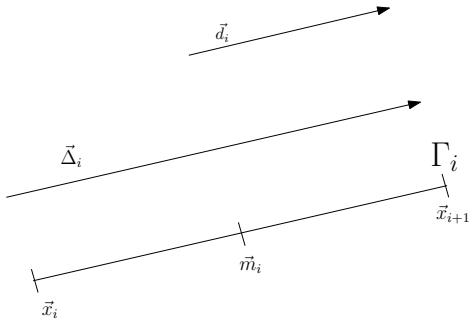

(a) boundary edge Γ_i

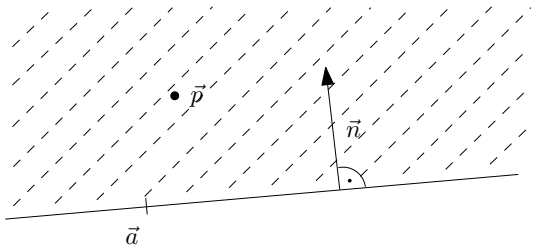

(b) left half space of a line through $\vec{a}$ with normal vector $\vec{n}$

Figure 2.2: Boundary edge Γ_i and corresponding left half space.

Next we recall some trivial yet important methods from the field of computational geometry which are needed for the implementation of the quadrature scheme.

The Halfspace Given by a Line

Let a line l through a point $\vec{a}$ with normal vector $\vec{n}$ be given. It is well known that a point $\vec{p} \in \mathbb{R}^2$ is on l if and only if $(\vec{p} - \vec{a}) \cdot \vec{n} = 0$, which is the so-called *Hesse normal form* of a line. For each point $\vec{p} \in \mathbb{R}^2$, we can find a point $\vec{b}$ on l which is perpendicular to $\vec{p}$, such that $\vec{p} = \vec{b} + \nu\vec{n}$ for $\nu \in \mathbb{R}$. Obviously $\left(\vec{p} - \vec{b}\right) \cdot \vec{n} = \nu|\vec{n}|^2$, and so $\vec{p}$ is on the same side of l as the normal vector, i.e. $\nu > 0$, if and only if $\left(\vec{p} - \vec{b}\right) \cdot \vec{n} > 0$. We call the set of all these points the *left half space of a line*,

$$\left\{ \vec{p} \in \mathbb{R}^2 \;\middle|\; (\vec{p} - \vec{a}) \cdot \vec{n} > 0 \right\} \tag{2.39}$$

for some arbitrary $\vec{a}$ on l. This set is sketched in Figure 2.2(b).

The Intersection Point of a Boundary Element Γ_i and an Arbitrary Line

Let Γ_i be given as in (2.37), and let another line l be given by

$$l = \left\{ \vec{y} = \vec{p} + \nu\vec{d} \;\middle|\; \nu \in [-1, 1] \right\}. \tag{2.40}$$

To find the intersection point of Γ_i and l, if there is one, we need to solve the linear system

$$\mu\vec{d}_i - \nu\vec{d} = \vec{p} - \vec{m}_i. \tag{2.41}$$

The linear system (2.41) is uniquely solvable, i.e. there is an intersection point, if and only if $\vec{d}_i \times \vec{d} \neq 0$ and $\mu, \nu \in [-1, 1]$. In this case, the solution is given by

$$\mu = \frac{1}{\vec{d}_i \times \vec{d}} \left((\vec{p} - \vec{m}_i) \times \vec{d} \right) \quad \text{and} \quad \nu = \frac{1}{\vec{d} \times \vec{d}_i} \left((\vec{p} - \vec{m}_i) \times \vec{d}_i \right) \tag{2.42}$$

in the local coordinates of Γ_i and l, respectively.

The Intersection Point(s) of a Line and a Semicircle

Let Γ_i be given as in (2.37), and let a semicircle C, in clockwise orientation, with radius r, start point $\vec{c} + \frac{r}{|\vec{a}|}\vec{a}$ and end point $\vec{c} - \frac{r}{|\vec{a}|}\vec{a}$, be given by

$$C = \left\{ \vec{y} = \vec{c} + r \left(\frac{\cos\nu}{|\vec{a}|}\vec{a} + \frac{\sin\nu}{|\vec{b}|}\vec{b} \right) \;\middle|\; \nu \in [0, \pi] \right\} \tag{2.43}$$

with $\vec{a} \cdot \vec{b} = 0$. The geometrical setup for C is illustrated in Figure 2.3(a).
Note that C is equally represented by

$$C = \left\{ \vec{y} \in \mathbb{R}^2 \;\middle|\; |\vec{c} - \vec{y}| = r \text{ and } (\vec{y} - \vec{c}) \cdot \vec{b} \geq 0 \right\}.$$

This representation is more suitable to check whether a point is contained in C. To find the intersection points of Γ_i and C, we square the equation $\vec{m}_i + \mu\vec{d}_i = \vec{c} + r\left(\frac{\cos\nu}{|\vec{a}|}\vec{a} + \frac{\sin\nu}{|\vec{b}|}\vec{b}\right)$ and arrive at [139, Section 7.3.2]

$$\mu_{1,2} = \frac{1}{\vec{d}_i^2} \left(-(\vec{m}_i - \vec{c})\,\vec{d}_i \pm \sqrt{\left((\vec{m}_i - \vec{c})\,\vec{d}_i\right)^2 - \left((\vec{m}_i - \vec{c})^2 - r^2\right)\vec{d}_i^2} \right). \tag{2.44}$$

The pseudocode to determine the intersection points of Γ_i and C, if there are any, is given in Algorithm 2.2.

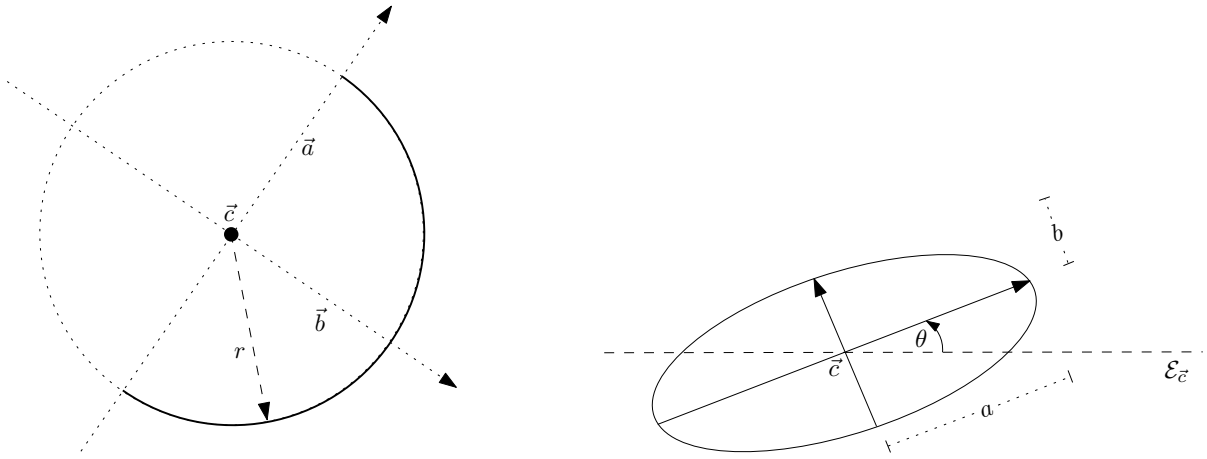

(a) semicircle

(b) ellipse (after [139], Fig. 5.16), with $\mathcal{E}_{\vec{c}} := \mathbb{R} \times \{c_2\}$

Figure 2.3: A semicircle and an ellipse as in (2.43) and (2.46), respectively.

Algorithm 2.2 Intersection points of a boundary edge Γ_i and a semicircle C

Input: boundary edge Γ_i, as in (2.37); semicircle C, as in (2.43)
Output: existence of intersection points of Γ_i and C; intersection points, if any

```
if ((m_i − c) d_i)^2 − ((m_i − c)^2 − r^2) d_i^2 < 0 then
    return false
else
    compute μ_1, μ_2 by (2.44)
    intersection ← false
    for l = 1, 2 do
        if (x(μ_l) − c) · b ≥ 0 and μ_l ∈ [−1, 1] then
            intersection ← true
            return x(μ_l) = m_i + μ_l d_i
        end if
    end for
    return intersection
end if
```

The Intersection Point(s) of a Line and an Ellipse

Let Γ_i be given as in (2.37), with end points $\vec{x}_i$ and $\vec{x}_{i+1}$. We denote the end point of Γ_i with larger x_2-value, i.e. the one which is 'above' $\vec{m}_i$, as illustrated in Figure 2.4, by $\vec{x}_{i,E}$. It is given by

$$\vec{x}_{i,E} = \begin{cases} \vec{x}_{i+1} & , \quad d_i^2 \geq 0 \\ \vec{x}_i & , \quad d_i^2 < 0 \end{cases}.$$

The *angle* θ of Γ_i and the x_1-axis, shown in Figure 2.4, is then given by

$$\sin\theta = \frac{2|m_i^2 - x_{i,E}^2|}{|\Gamma_i|} = \frac{|m_i^2 - x_{i,E}^2|}{|\vec{d}_i|} \tag{2.45}$$

where $\vec{m}_i = \left(m_i^1, m_i^2\right)$ and $\vec{x}_{i,E} = \left(x_{i,E}^1, x_{i,E}^2\right)$.

(a) $\vec{x}_{i,E}$ is the right end point of Γ_i

(b) $\vec{x}_{i,E}$ is the left end point of Γ_i

Figure 2.4: Angle of a boundary edge Γ_i and the x_1-axis, with $\mathcal{E}_{\vec{m}_i} := \mathbb{R} \times \{m_i^2\}$.

The general form of an ellipse E with centre $\vec{c}$ and axes $\vec{a}$, $\vec{b}$ with lengths a, b such that $|\vec{c} - \vec{a}| = a$, $|\vec{c} - \vec{b}| = b$, and an angle θ with the x_1-axis, is given by [139, Section 5.5.2]

$$E = \left\{ \vec{x} \in \mathbb{R}^2 \;\middle|\; (\vec{x} - \vec{c})^T R^T D R (\vec{x} - \vec{c}) = 1 \right\}. \tag{2.46}$$

The geometrical setup for E is illustrated in Figure 2.3(b). Here $D = \begin{pmatrix} \frac{1}{a^2} & 0 \\ 0 & \frac{1}{b^2} \end{pmatrix}$, and R denotes the *rotation matrix* that describes a counter-clockwise rotation of the coordinate system by θ, namely $R = \begin{pmatrix} \cos\theta & \sin\theta \\ -\sin\theta & \cos\theta \end{pmatrix}$. Then

$$\begin{aligned} R^T D R &= \begin{pmatrix} \cos\theta & -\sin\theta \\ \sin\theta & \cos\theta \end{pmatrix} \begin{pmatrix} \frac{1}{a^2} & 0 \\ 0 & \frac{1}{b^2} \end{pmatrix} \begin{pmatrix} \cos\theta & \sin\theta \\ -\sin\theta & \cos\theta \end{pmatrix} \\ &= \begin{pmatrix} \frac{1}{a^2}\cos^2\theta + \frac{1}{b^2}\sin^2\theta & \left(\frac{1}{a^2} - \frac{1}{b^2}\right)\sin\theta\cos\theta \\ \left(\frac{1}{a^2} - \frac{1}{b^2}\right)\sin\theta\cos\theta & \frac{1}{a^2}\sin^2\theta + \frac{1}{b^2}\cos^2 \end{pmatrix} =: \begin{pmatrix} a(\theta) & c(\theta) \\ c(\theta) & b(\theta) \end{pmatrix}. \end{aligned}$$

Let $\vec{x} \in \Gamma_i$, so that $\vec{x} = \vec{m}_i + \mu \vec{d}_i$ with $\mu \in [-1, 1]$. To find the intersection points of Γ_i and the ellipse E, if there are any, we insert $\vec{x}$ into the equation defining E,

$$\begin{aligned} 1 &= (\vec{x} - \vec{c})^T R^T D R (\vec{x} - \vec{c}) \\ &= (\vec{m}_i - \vec{c} + \mu\vec{d}_i)^T \begin{pmatrix} a(\theta) & c(\theta) \\ c(\theta) & b(\theta) \end{pmatrix} (\vec{m}_i - \vec{c} + \mu\vec{d}_i) \\ &= a(\theta)\left((m_i^1 - c^1)^2 + 2(m_i^1 - c^1)d_i^1\mu + \mu^2(d_i^1)^2\right) \\ &\quad + 2c(\theta)\left((m_i^1 - c^1)(m_i^2 - c^2) + d_i^1 d_i^2 \mu^2 + \left((m_i^1 - c^1)d_i^2 + (m_i^2 - c^2)d_i^1\right)\mu\right) \\ &\quad + b(\theta)\left((m_i^2 - c^2)^2 + 2(m_i^2 - c^2)d_i^2\mu + \mu^2(d_i^2)^2\right). \end{aligned} \tag{2.47}$$

To find the intersection points in local coordinates $\mu_{1,2}$ of Γ_i, we solve the quadratic equation

$$\begin{aligned} &\underbrace{\left\{a(\theta)(d_i^1)^2 + b(\theta)(d_i^2)^2 + 2c(\theta)d_i^1 d_i^2\right\}}_{:=A(\theta)}\mu^2 \\ &+ \underbrace{2\left\{a(\theta)(m_i^1 - c^1)d_i^1 + b(\theta)(m_i^2 - c^2)d_i^2 + c(\theta)\left((m_i^1 - c^1)d_i^2 + (m_i^2 - c^2)d_i^1\right)\right\}}_{:=B(\theta)}\mu \\ &+ \underbrace{\left\{a(\theta)(m_i^1 - c^1)^2 + b(\theta)(m_i^2 - c^2)^2 + 2c(\theta)(m_i^1 - c^1)(m_i^2 - c^2) - 1\right\}}_{:=C(\theta)} = 0 \end{aligned} \tag{2.48}$$

by the well known formula

$$\mu_{1,2} = \frac{1}{2A(\theta)}\left(-B(\theta) \pm \sqrt{B(\theta)^2 - 4A(\theta)C(\theta)}\right). \tag{2.49}$$

The pseudocode to determine the intersection points of Γ_i and E, if there are any, is similar to Algorithm 2.2. It is given in Algorithm 2.3.

Algorithm 2.3 Intersection points of a boundary edge Γ_i and an ellipse E

Input: boundary edge Γ_i, as in (2.37); ellipse E, as in (2.46)
Output: existence of intersection points of Γ_i and E; intersection points, if any

```
1  if B(θ)^2 − 4A(θ)C(θ) < 0 then { A(θ), B(θ), C(θ) as in (2.48) }
2    return false
3  else
4    compute μ_1, μ_2 by (2.49)
5    intersection ← false
6    for l = 1, 2 do
7      if μ_l ∈ [−1, 1] then
8        intersection ← true
9        return x(μ_l) = m_i + μ_l d_i
10     end if
11   end for
12   return intersection
13 end if
```

2.4.2 Decomposition of Boundary Elements in Terms of the Discrete Light Disc and Rings

Having the elementary geometrical operations presented in Section 2.4.1 at hand, we can now proceed to the actual computation of the matrix entries. Let Γ_i, Γ_j be some boundary edges. We consider the integral

$$\int_{\Gamma_i} \int_{\Gamma_j} \Upsilon(\vec{x}, \vec{y}) \varphi(\vec{y}) ds_{\vec{y}} \; \psi(\vec{x}) \; ds_{\vec{x}} \tag{2.50}$$

that corresponds to (2.19), with kernel $\Upsilon(\vec{x}, \vec{y})$ as given by (2.20) respectively (2.24). Γ_i is called the *outer integration domain* or *test element*, and Γ_j is called the *inner integration domain* or *ansatz element*. The functions φ and ψ in (2.50) are assumed to have support on the whole of Γ_j and Γ_i, respectively, as it is the case for piecewise polynomial boundary element functions.

Obviously, we are only interested in the subset of $\Gamma_i \times \Gamma_j$ that actually contributes to the integral, namely $(\operatorname{supp} \Upsilon(\vec{x}, \vec{y})) \cap \Gamma_i \times \Gamma_j$ or, without loss of generality,

$$\{ \, (\vec{x}, \vec{y}) \in \Gamma_i \times \Gamma_j \;\; | \;\; \Upsilon(\vec{x}, \vec{y}) \neq 0 \, \} = (\Gamma_i \times \Gamma_j \cap D_{l-1}) \cup (\Gamma_i \times \Gamma_j \cap E_{l-1}). \tag{2.51}$$

We decompose, similarly to [127, Section 4],

$$\begin{aligned} \Gamma_i \times \Gamma_j \cap D_{l-1} &= \{ \, (\vec{x}, \vec{y}) \in \Gamma_i \times \Gamma_j \;\; | \;\; |\vec{x} - \vec{y}| \leq t_{l-1} \, \} \\ &= \{ \, \vec{x} \in \Gamma_i \;\; | \;\; \exists \vec{y} \in \Gamma_j : |\vec{x} - \vec{y}| \leq t_{l-1} \, \} \times \{ \, \vec{y} \in \Gamma_j \;\; | \;\; |\vec{x} - \vec{y}| \leq t_{l-1} \, \} \\ &= \bigcup_{\vec{x} \in D^i_{l-1}(\Gamma_j)} \{\vec{x}\} \times D^j_{l-1}(\vec{x}) \end{aligned} \tag{2.52}$$

where we have written

$$D^i_{l-1}(\Gamma_j) := \{ \, \vec{x} \in \Gamma_i \;\; | \;\; \exists \vec{y} \in \Gamma_j : |\vec{x} - \vec{y}| \leq t_{l-1} \, \} \subseteq \Gamma_i \tag{2.53}$$

and

$$D^j_{l-1}(\vec{x}) := \{ \, \vec{y} \in \Gamma_j \;\; | \;\; |\vec{x} - \vec{y}| \leq t_{l-1} \, \} \subseteq \Gamma_j \tag{2.54}$$

for given $\vec{x} \in D^i_{l-1}(\Gamma_j)$. We emphasise that the second set depends on the given point $\vec{x} \in \Gamma_i$, whereas the first set depends on the given edge Γ_j. Analogously,

$$\Gamma_i \times \Gamma_j \cap E_{l-1} = \bigcup_{\vec{x} \in E^i_{l-1}(\Gamma_j)} \{\vec{x}\} \times E^j_{l-1}(\vec{x}) \tag{2.55}$$

with

$$E^i_{l-1}(\Gamma_j) := \{\ \vec{x} \in \Gamma_i \ \mid\ \exists \vec{y} \in \Gamma_j : t_{l-1} \le |\vec{x} - \vec{y}| \le t_l\ \} \subseteq \Gamma_i \tag{2.56}$$

and

$$E^j_{l-1}(\vec{x}) := \{\ \vec{y} \in \Gamma_j \ \mid\ t_{l-1} \le |\vec{x} - \vec{y}| \le t_l\ \} \subseteq \Gamma_j \tag{2.57}$$

for given $\vec{x} \in E^i_{l-1}(\Gamma_j)$. We present algorithms for the computation of the domains $D^j_{l-1}(\vec{x}), E^j_{l-1}(\vec{x})$ and $D^i_{l-1}(\Gamma_j), E^i_{l-1}(\Gamma_j)$ in the next two subsections.

2.4.2.1 The Domains $D^j_{l-1}(\vec{x})$ and $E^j_{l-1}(\vec{x})$

Let the boundary edges Γ_i, Γ_j be given as in (2.37), and let $\vec{x} = \vec{x}(\mu) \in \Gamma_i$ be some given point, represented by $\mu \in [-1,1]$. To find the subset $D^j_{l-1}(\vec{x}) \subseteq \Gamma_j$, we observe that we can find the (at most two) points $\vec{y}_{\vec{x},1}$, $\vec{y}_{\vec{x},2} \in \Gamma_j$, represented by $\nu_1, \nu_2 \in [-1,1]$, respectively, such that $|\vec{x} - \vec{y}_{\vec{x},1}| = |\vec{x} - \vec{y}_{\vec{x},2}| = t_{l-1}$, as the roots of the quadratic equation

$$|\vec{x} - \vec{y}|^2 = |\vec{x} - \vec{m}_j - \nu \vec{d}_j|^2 = t^2_{l-1}$$

which yields

$$\nu^2 \underbrace{\vec{d}_j^{\,2}}_{:=a} + \underbrace{(-2\vec{d}_j(\vec{x} - \vec{m}_j))}_{:=b=b(\mu)} \nu + \underbrace{(\vec{x} - \vec{m}_j)^2 - t^2_{l-1}}_{:=c=c(\mu)} = 0 \tag{2.58}$$

with solutions $\nu_{1,2} = -\frac{b}{2a} \mp \sqrt{\frac{b^2-4ac}{4a^2}}$, so that $\nu_1 < \nu_2$. This allows us to rewrite the set $D^j_{l-1}(\vec{x})$ explicitly in terms of the local coordinates μ, ν as $D^j_{l-1}(\mu) \subseteq \{\nu \in [-1,1]\}$. There are five cases to distinguish:

(i) $\nu_1, \nu_2 \in [-1,1]$. In this case, $D^j_{l-1}(\mu) = [\nu_1, \nu_2]$.

(ii) $\nu_1 > 1$ or $\nu_2 < -1$. In this case, $D^j_{l-1}(\mu) = \varnothing$.

(iii) $\nu_1 < -1$, $\nu_2 > 1$. In this case, $D^j_{l-1}(\mu) = [-1,1]$.

(iv) $\nu_1 < -1$, $\nu_2 \in [-1,1]$. In this case, $D^j_{l-1}(\mu) = [-1,\nu_2]$.

(v) $\nu_1 \in [-1,1]$, $\nu_2 > 1$. In this case, $D^j_{l-1}(\mu) = [\nu_1, 1]$.

We can therefore rewrite $D^j_{l-1}(\vec{x})$ explicitly as

$$D^j_{l-1}(\vec{x}) = \left\{\ \vec{y}(\nu) = \vec{m}_j + \nu \vec{d}_j \ \mid\ \nu \in [\max\{\nu_1, -1\}, \min\{\nu_2, 1\}] \cap [-1,1]\ \right\}. \tag{2.59}$$

It is straightforward to consider the general situation from here onwards. We define the (annular) *domain of influence* of a point $\vec{x} \in \Gamma_i$ by

$$E(r_1, r_2; \vec{x}) := \left\{\ \vec{z} \in \mathbb{R}^2 \ \mid\ r_1 \le |\vec{x} - \vec{z}| \le r_2\ \right\} \tag{2.60}$$

which is sketched in Figure 2.5(b). Obviously $D^j_{l-1}(\vec{x}) = \Gamma_j \cap E(0, t_{l-1}; \vec{x})$ and $E^j_{l-1}(\vec{x}) = \Gamma_j \cap E(t_{l-1}, t_l; \vec{x})$. We have dealt with the case $r_1 = 0$ above. In the case when $r_1 \neq 0$, $\vec{x}$ might

illuminate two subintervals of Γ_j. Let the local coordinates of the, at most, four solutions of the quadratic equations (2.58) with t_{l-1} and t_l on the ray $\mathcal{E}_{\Gamma_j}$ be denoted by $\nu_1^l < \nu_1^{l-1} < \nu_2^{l-1} < \nu_2^l$. Here, the *boundary edge ray* $\mathcal{E}_{\Gamma_j}$ that contains Γ_j is defined as

$$\mathcal{E}_{\Gamma_j} = \left\{ \vec{m}_j + \mu \vec{d}_j \;\middle|\; \mu \in \mathbb{R} \right\} = \left\{ \vec{z} \in \mathbb{R}^2 \;\middle|\; \vec{n} \cdot (\vec{z} - \vec{p}) = 0 \right\} \tag{2.61}$$

for any arbitrary point $\vec{p} \in \Gamma_j$. The illuminated subintervals of $\mathcal{E}_{\Gamma_j}$ are, in local coordinates, $[\nu_1^l, \nu_1^{l-1}]$, $[\nu_2^{l-1}, \nu_2^l]$, and $E_{l-1}^j(\vec{x})$ can consequently be found similarly to (2.59).

Remark 2.2

a) For any $\vec{x} \in \mathbb{R}^2$, let $\vec{x}' = \vec{x} - \frac{(\vec{x}-\vec{m}_j)\cdot\vec{n}_j}{|\vec{n}_j|^2}\vec{n}_j$ be the projection of $\vec{x}$ onto $\mathcal{E}_{\Gamma_j}$. Then

$$\operatorname{dist}(\vec{x}, \Gamma_j) := |\vec{x} - \vec{x}'| = \frac{|(\vec{x} - \vec{m}_j) \cdot \vec{n}_j|}{|\vec{n}_j|} \tag{2.62}$$

is the minimum distance of $\vec{x}$ and Γ_j. Obviously $E_{l-1}^j(\vec{x}) = \varnothing$ if $\operatorname{dist}(\vec{x}, \Gamma_j) > t_l$.

b) If $t_l \geq \operatorname{dist}(\vec{x}, \Gamma_j) > t_{l-1}$, there exist no points ν_1^{l-1}, ν_2^{l-1}, and thus $\vec{x}$ illuminates only the subinterval $[\nu_1^l, \nu_2^l]$.

c) By a) and b), there can only be more than two intersection points if $\operatorname{dist}(\vec{x}, \Gamma_j) \leq t_{l-1}$, which can be verified intuitively from Figure 2.5(b).

Illustrations of exemplary situations for all three cases are shown in Figure 2.6.

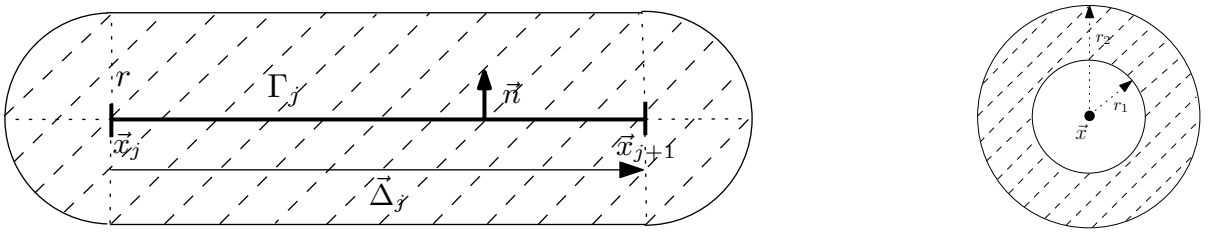

(a) domain of influence $E(0, r; \Gamma_j)$ of a boundary edge Γ_j

(b) domain of influence $E(r_1, r_2; \vec{x})$ of a point $\vec{x}$

Figure 2.5: Domains of influence of a boundary edge and of a point.

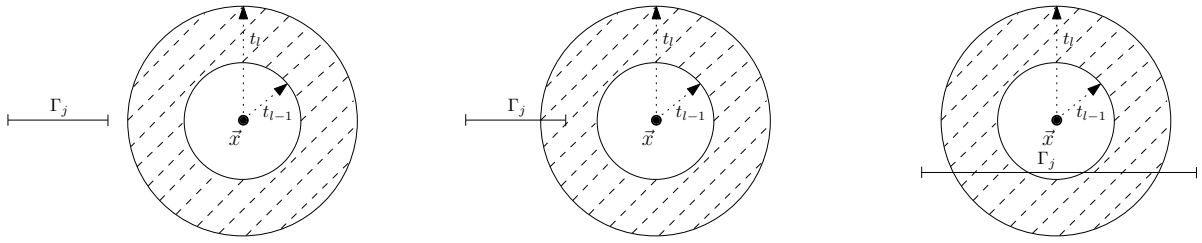

(a) $\operatorname{dist}(\vec{x}, \Gamma_j) > t_l$

(b) $t_l \geq \operatorname{dist}(\vec{x}, \Gamma_j) > t_{l-1}$

(c) $t_l \geq \operatorname{dist}(\vec{x}, \Gamma_j) > t_{l-1}$

Figure 2.6: Different scenarios for the domain of influence $E(t_{l-1}, t_l; \vec{x})$ and boundary edge Γ_i, discussed in Remark 2.2.

All these considerations result in the pseudocode given in Algorithm 2.4, which computes the domain $E_{l-1}^j(\vec{x}) \subseteq \Gamma_j$. It can also be used to compute the domain $D_{l-1}^j(\vec{x}) \subseteq \Gamma_j$ by setting $t_{l-1} := 0$ and $t_l := t_{l-1}$, as outlined above, and lines 16 to 23 can then be omitted.

Algorithm 2.4 Computation of the domain $E_{l-1}^{j}(\vec{x}) \subseteq \Gamma_j$ for arbitrary $\vec{x} \in \mathbb{R}^2$

Input: boundary edge Γ_j, as in (2.37); point $\vec{x} \in \mathbb{R}^2$

Output: the set $E_{l-1}^{j}(\vec{x})$, i.e. the subinterval(s) of Γ_j that is (are) illuminated by $\vec{x}$, if any

if $\operatorname{dist}(\vec{x}, \Gamma_j) > t_l$ **then** { a priori check has failed; there is no illuminated subinterval, see Remark 2.2 a) }
  return $E_{l-1}^{j}(\vec{x}) = \varnothing$
else
  intersection $\leftarrow$ **false**
  if $t_{l-1} \le \operatorname{dist}(\vec{x}, \Gamma_j) \le t_l$ **then** { two intersections with outer boundary at most, no intersection with inner boundary, see Remark 2.2 b) }
    compute ν_1^l, ν_2^l by (2.58), with t_{l-1} replaced by t_l therein
    for $i = 1, 2$ **do**
      if $\nu_i^l \in [-1, 1]$ **then**
        store ν_i^l
        intersection $\leftarrow$ **true**
      end if
    end for
    if (**not** intersection) **then** { no intersection points found }
      check if Γ_j is fully contained in $E(t_{l-1}, t_l; \vec{x})$ and **return** $E_{l-1}^{j}(\vec{x}) = \varnothing$
      or **return** $E_{l-1}^{j}(\vec{x}) = \Gamma_j$, accordingly
    end if
  else { $\operatorname{dist}(\vec{x}, \Gamma_j) < t_{l-1}$, see Remark 2.2 c) }
    compute ν_1^l, ν_1^{l-1}, ν_2^{l-1}, ν_2^l by (2.58)
    for $i = 1, 2$ **do**
      for $j = 0, 1$ **do**
        if $\nu_i^{l-j} \in [-1, 1]$ **then**
          store ν_i^{l-j}
        end if
      end for
    end for
    if (**not** intersection) **then** { no intersection points found, $\Gamma_j \notin E(t_{l-1}, t_l; \vec{x})$ }
      return $E_{l-1}^{j}(\vec{x}) = \varnothing$
    end if
  end if
  the one or two illuminated subintervals of which $E_{l-1}^{j}(\vec{x})$ is composed are now computed by (2.59), using the stored values of ν_i^{l-j}, $i = 1, 2$, $j = 0, 1$
  return $E_{l-1}^{j}(\vec{x})$
end if

2.4.2.2 The Domains $D^i_{l-1}(\Gamma_j)$ and $E^i_{l-1}(\Gamma_j)$

We are still lacking a representation of the sets $D^i_{l-1}(\Gamma_j) \subseteq \Gamma_i$ and $E^i_{l-1}(\Gamma_j) \subseteq \Gamma_i$. We define the *domain of influence* of an edge Γ_j by

$$E(r_1, r_2; \Gamma_j) := \left\{ \vec{z} \in \mathbb{R}^2 \;\middle|\; \exists \vec{y} \in \Gamma_j : r_1 \le |\vec{z} - \vec{y}| \le r_2 \right\} = \bigcup_{\vec{y} \in \Gamma_j} E(r_1, r_2; \vec{y}). \tag{2.63}$$

Obviously $D^i_{l-1}(\Gamma_j) = \Gamma_i \cap E(0, t_{l-1}; \Gamma_j)$ and $E^i_{l-1}(\Gamma_j) = \Gamma_i \cap E(t_{l-1}, t_l; \Gamma_j)$.

Let us consider the case $r_1 = 0$, which corresponds to a discrete light disc, first. In this case, we simply write r instead of r_2. The domain $E(0, r; \Gamma_j)$ is sketched in Figure 2.5(a). The algebraic condition for any $\vec{z} \in \mathbb{R}^2$ to be contained in the set $E(0, r; \Gamma_j)$ is

$$\begin{aligned} \vec{z} \in E(0, r; \Gamma_j) \quad \text{iff.} \quad & \Bigg(-\left(\vec{z} - \left(\vec{m}_j + \frac{r}{|\vec{n}_j|}\vec{n}_j\right)\right) \cdot \vec{n}_j \ge 0 \wedge -(\vec{z} - \vec{x}_{j+1}) \cdot \vec{d}_j \ge 0 \\ & \quad \wedge \quad \left(\vec{z} - \left(\vec{m}_j - \frac{r}{|\vec{n}_j|}\vec{n}_j\right)\right) \cdot \vec{n}_j \ge 0 \wedge (\vec{z} - \vec{x}_j) \cdot \vec{d}_j \ge 0 \Bigg) \\ & \vee \quad \left(|\vec{x}_{j+1} - \vec{z}| \le r \wedge (\vec{z} - \vec{x}_{j+1}) \cdot \vec{d}_j \ge 0\right) \\ & \vee \quad \left(|\vec{x}_j - \vec{z}| \le r \wedge -(\vec{z} - \vec{x}_j) \cdot \vec{d}_j \ge 0\right). \end{aligned} \tag{2.64}$$

The boundary of $E(0, r; \Gamma_j)$ is composed of two semicircles and two lines. Its explicit form is, clockwise,

$$\begin{aligned} & \partial E(0, r; \Gamma_j) \\ = \; & \left\{ \vec{m}_j + \frac{r}{|\vec{n}|}\vec{n} + \mu\vec{d}_j \;\middle|\; \mu \in [-1, 1] \right\} \cup \left\{ \vec{x}_{j+1} + \frac{r}{|\vec{d}_j|} \sin\mu \; \vec{d}_j + \frac{r}{|\vec{n}|} \cos\mu \; \vec{n} \;\middle|\; \mu \in [0, \pi] \right\} \\ & \left\{ \vec{m}_j - \frac{r}{|\vec{n}|}\vec{n} - \mu\vec{d}_j \;\middle|\; \mu \in [-1, 1] \right\} \cup \left\{ \vec{x}_{j+1} - \frac{r}{|\vec{d}_j|} \sin\mu \; \vec{d}_j - \frac{r}{|\vec{n}|} \cos\mu \; \vec{n} \;\middle|\; \mu \in [0, \pi] \right\}. \end{aligned} \tag{2.65}$$

Let us now consider the algebraic representation of the discrete light ring $E(r_1, r_2; \Gamma_j)$ with $r_1 > 0$. Due to geometric considerations, which are justified mathematically below, we distinguish two cases: If $r_1 \le \frac{1}{2}|\Gamma_j|$, we simply have $E(r_1, r_2; \Gamma_j) = E(0, r_2; \Gamma_j)$, and the domain is fully described by equations (2.64) and (2.65) above.

For the second case, we assume $r_1 > \frac{1}{2}|\Gamma_j|$. The outer boundary of the domain of influence is then the same as before, but in this case, there is an ellipse-shaped hole $\mathbb{H}$ inside it, as shown in Figure 2.7. The domain of influence $E(r_1, r_2; \Gamma_j)$ can then be written as

$$E(r_1, r_2; \Gamma_j) = E(0, r_2; \Gamma_j) \setminus \mathbb{H}_j(r_1). \tag{2.66}$$

We use the notation $\mathbb{H}_j(r_1)$ here, since the size and shape of the hole only depends on the edge Γ_j and on r_1, but not on r_2. The four axis points of the ellipse that bound $\mathbb{H}_j(r_1)$ are given by the respective intersection points of the circles $\mathbb{B}_{r_1}(\vec{x}_j)$ and $\mathbb{B}_{r_1}(\vec{x}_{j+1})$ with the boundary edge ray $\mathcal{E}_{\Gamma_j}$, and by the intersection points of the circles themselves.

Using [139, Section 7.3.2], the local parameters of the intersection points of $\mathcal{E}_{\Gamma_j}$ and $\mathbb{B}_{r_1}(\vec{x}_j)$ are, in local coordinates of $\mathcal{E}_{\Gamma_j}$,

$$\mu_{1,2} = -1 \pm \frac{r_1}{|\vec{d}_j|} = -1 \pm 2\frac{r_1}{|\Gamma_j|}$$

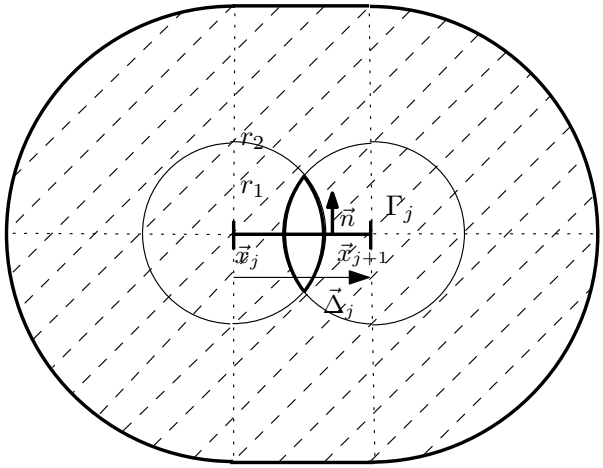

Figure 2.7: Domain of influence of a boundary edge Γ_j, for $r_1 > \frac{1}{2}|\Gamma_j|$.

and, consequently, the intersection points in global coordinates are

$$\vec{x}_{1,2}^{E,j} = \vec{x}_j \pm \frac{r_1}{|\vec{d}_j|}\vec{d}_j = \vec{x}_j \pm 2\frac{r_1}{|\Gamma_j|}\vec{d}_j.$$

Analogously, the local parameters of the intersection points of $\mathcal{E}_{\Gamma_j}$ and $\mathbb{B}_{r_1}(\vec{x}_{j+1})$ are

$$\mu_{1,2} = 1 \pm \frac{r_1}{|\vec{d}_j|} = 1 \pm 2\frac{r_1}{|\Gamma_j|}.$$

Out of these four points, the two intersection points that are possibly on Γ_j are

$$\vec{x}_j + \frac{r_1}{|\vec{d}_j|}\vec{d}_j \qquad \text{and} \qquad \vec{x}_{j+1} - \frac{r_1}{|\vec{d}_j|}\vec{d}_j. \tag{2.67}$$

If $r_1 > |\Gamma_j|$, the edge Γ_j does not illuminate itself at all, since $\frac{r_1}{|\vec{d}_j|} > 2$ in this case. Alternatively, this can also be concluded by geometric considerations. For $\frac{1}{2}|\Gamma_j| < r_1 \leq |\Gamma_j|$, we have $1 \leq \frac{r_1}{|\vec{d}_j|} < 2$, and the intersection points given in (2.67) are then both on Γ_j.

We now need to compute the intersection points of the two circles $\mathbb{B}_{r_1}(\vec{x}_j)$ and $\mathbb{B}_{r_1}(\vec{x}_{j+1})$. In the notation of [139, Section 7.5.2], let $\vec{u} := \vec{x}_{j+1} - \vec{x}_j = 2\vec{d}_j$ and $\vec{v} := \frac{2|\vec{d}_j|}{|\vec{n}|}\vec{n}$. The intersection points then are

$$\vec{x}_{1,2} = \vec{x}_j + \mu\vec{u} + \nu_{1,2}\vec{v}$$

where by [139, (7.5), (7.6)],

$$\mu = \frac{1}{2} \qquad \text{and} \qquad \nu_{1,2}^2 = -\frac{\left(4|\vec{d}_j|^2 - 4r_1^2\right)4|\vec{d}_j|^2}{4(2|\vec{d}_j|)^4} = \frac{r_1^2 - |\vec{d}_j|^2}{4|\vec{d}_j|^2}.$$

Hence $\nu_{1,2} = \pm\frac{1}{2|\vec{d}_j|}\sqrt{r_1^2 - |\vec{d}_j|^2}$, and so the two intersection points of the circles $\mathbb{B}_{r_1}(\vec{x}_j)$ and $\mathbb{B}_{r_1}(\vec{x}_{j+1})$ are

$$\vec{x}_{1,2}^{C} = \vec{m}_j \pm \frac{\sqrt{r_1^2 - |\vec{d}_j|^2}}{|\vec{n}_j|}\vec{n}_j.$$

Note that the two circles intersect if and only if $r_1^2 - |\vec{d}_j|^2 \geq 0$, i.e. if and only if $r_1 \geq \frac{1}{2}|\Gamma_j|$, which justifies the distinction of cases we have chosen above. The axis end points of the ellipse-shaped domain $\mathbb{H}_j(r_1)$ with midpoint m_j thus are, in clockwise orientation,

$$\vec{m}_j + \frac{\sqrt{r_1^2 - |\vec{d}_j|^2}}{|\vec{n}_j|}\vec{n}_j \quad , \quad \vec{x}_j + \frac{r_1}{|\vec{d}_j|}\vec{d}_j \quad , \quad \vec{m}_j - \frac{\sqrt{r_1^2 - |\vec{d}_j|^2}}{|\vec{n}_j|}\vec{n}_j \quad , \quad \vec{x}_{j+1} - \frac{r_1}{|\vec{d}_j|}\vec{d}_j \tag{2.68}$$

with midpoint $\vec{m}_j$. The lengths of the axes, in the notation of Figure 2.3(b), are

$$a = \left|\vec{m}_j - \left(\vec{x}_j + \frac{r_1}{|\vec{d}_j|}\vec{d}_j\right)\right| = \left|\left(1 - \frac{r_1}{|\vec{d}_j|}\right)\vec{d}_j\right| = |r_1 - |\vec{d}_j|| = \frac{1}{2}|2r_1 - |\Gamma_j|| \tag{2.69}$$

$$b = \left|\vec{m}_j - \left(\vec{m}_j + \frac{\sqrt{r_1^2 - |\vec{d}_j|^2}}{|\vec{n}_j|}\vec{n}_j\right)\right| = \left|\frac{\sqrt{r_1^2 - |\vec{d}_j|^2}}{|\vec{n}_j|}\vec{n}_j\right| = \sqrt{r_1^2 - |\vec{d}_j|^2} = \frac{1}{2}\sqrt{4r_1^2 - |\Gamma_j|^2}. \tag{2.70}$$

This completes the description of the ellipse-shaped hole $\mathbb{H}_j(r_1)$ in the domain of influence $E(r_1, r_2; \Gamma_j)$ for the case $r_1 > \frac{|\Gamma_j|}{2}$. In summary, $\mathbb{H}_j(r_1)$ is an ellipse of type (2.46) with centre $\vec{m}_j$ and axis lengths $a = a(r_1)$ and $b = b(r_1)$, given by (2.69) and (2.70). The pseudocode for the computation of $E_{l-1}^i(\Gamma_j)$ is given in Algorithm 2.5.

Algorithm 2.5 Computation of the domain $E_{l-1}^i(\Gamma_j) \subseteq \Gamma_i$ for arbitrary boundary edge Γ_j

Input: boundary edges Γ_j, Γ_i, as in (2.37)
Output: the set $E_{l-1}^i(\Gamma_j)$, i.e. the subinterval(s) of Γ_i that is (are) illuminated by Γ_j, if any

intersection ← **false**
if Γ_i intersects the outer boundary (2.65) of $E(t_{l-1}, t_l; \Gamma_j)$ **then** { compute intersections with outer boundary by (2.42) and Algorithm 2.2 }
  store the intersection points
  intersection ← **true**
end if
if $r_1 > \frac{1}{2}|\Gamma_j|$ **then**
  if Γ_i intersects the boundary of $\mathbb{H}_j(t_{l-1})$ **then** { compute intersections with boundary of ellipse-shaped hole by Algorithm 2.3 }
    store the intersection points
    intersection ← **true**
  end if
end if
if (**not** intersection) **then** { no intersections with inner or outer boundary found }
  perform check by taking arbitrary point on Γ_i and use (2.64)
  if Γ_i is fully contained in $E(t_{l-1}, t_l; \Gamma_j)$ **then**
    return $E_{l-1}^i(\Gamma_j) = \Gamma_i$ { fully contained }
  else
    return $E_{l-1}^i(\Gamma_j) = \varnothing$ { not contained }
  end if
else { at least one intersection with one of the boundaries was found }
  construct the one or two subintervals of Γ_i that are illuminated by Γ_j, using the stored intersection points
  return E_{l-1}^i
end if

2.4.3 The Full Quadrature Scheme

We are now in a position to state the full spatial quadrature scheme for the computation of the entries of the Galerkin matrices $\mathcal{U}^{m,n}$. We recall that, by (2.27),

$$\begin{aligned}\mathcal{U}_{i,j}^{m,n} &= \iint_{\Gamma\times\Gamma} \Upsilon^{q;\,m,n}(r)\varphi_i^{p_1}(y)\varphi_j^{p_2}(x)\; ds_x\; ds_y \\ &= \sum_{\substack{\Gamma_k\subseteq\operatorname{supp}\varphi_i^{p_1}\\ \Gamma_l\subseteq\operatorname{supp}\varphi_j^{p_2}}} \iint_{\Gamma_k\times\Gamma_l} \Upsilon^{q;\,m,n}(r)\varphi_i^{p_1}(y)\varphi_j^{p_2}(x)\; ds_x\; ds_y\end{aligned}$$

for $i,j = 1,\dots,N_S$. The integrals inside the sum are all of type (2.50). The pseudocode for the computation of the Galerkin matrices is given in Algorithm 2.6.

In the next section, we show that Algorithm 2.6 convergences exponentially for a class of kernel functions that includes the kernel functions that are relevant to us. They are given and characterised in Appendices A.2 and A.3, respectively. The statements about the inner and outer quadrature schemes in lines 7 and 10 refer to grading schemes that are designed to handle singularities that occur on the ansatz and test element for these kernel functions.

Algorithm 2.6 Computation of the Galerkin matrices $\mathcal{U}^{m,n}$ (after [10, Algorithm 2])

Input: time indices m,n
Output: corresponding Galerkin matrix $\mathcal{U}^{m,n}$, as given by (2.27)

1 $\mathcal{U}^{m,n} \leftarrow 0$
2 **if** $n-m \geq 0$ **then**
3 **for** $i,j = 1,\dots,N_S$ **do**
4 **for** k,l with $\Gamma_k \subseteq \operatorname{supp}\varphi_i^{p_1}, \Gamma_l \subseteq \operatorname{supp}\varphi_j^{p_2}$ **do**
5 compute $D_{n-m-1}^k(\Gamma_l)$ by Algorithm 2.5
6 **if** $D_{n-m-1}^k(\Gamma_l) \subseteq \Gamma_k \neq \varnothing$ **then**
7 use the grading scheme outlined in Section 2.5.3.1 to construct a quadrature mesh on $D_{n-m-1}^k(\Gamma_l)$ {outer quadrature}
8 **for** each quadrature point $\vec{x}^k \in D_{n-m-1}^k(\Gamma_l)$ **do**
9 compute $D_{n-m-1}^l(\vec{x}^k)$ by Algorithm 2.4
10 use the grading scheme outlined in Section 2.5.3.2 to construct a quadrature mesh on $D_{n-m-1}^l(\vec{x}^k) \subseteq \Gamma_l$ {inner quadrature}
11 perform the inner quadrature and update $\mathcal{U}_{i,j}^{m,n}$
12 **end for**
13 **end if**
14 **end for**
15 repeat the procedure outlined in lines 4-14 for all possible discrete light rings E_{n-m-1}^k
16 **end for**
17 **end if**
18 **return** $\mathcal{U}^{m,n}$

2.5 Regularity of Time Domain Boundary Layer Potentials with Discrete Support in Two Space Dimensions

In order to give convergence estimates for the quadrature method presented in Algorithm 2.6, we analyse a typical *time domain boundary layer potential with discrete support*. To this end,

we define an arbitrary integral potential with discrete integration domain, kernel function k and density $\varphi \in L^\infty(e)$,

$$P_{R,e}[\varphi](\vec{x}) \coloneqq \int_{e \cap \mathbb{B}_R(\vec{x})} k(\vec{x} - \vec{y})\ \varphi(\vec{y})\ ds_{\vec{y}} \tag{2.71}$$

for $\vec{x} \in \mathbb{R}^2$, where e is an arbitrary boundary edge. We observed in Section 2.4.2 that $\operatorname{supp} P_{R,e}[\varphi] = E(0, R; e)$. For the moment, we do not specify the kernel function any further, and present some results that hold for arbitrary kernel functions of type $k(\vec{x} - \vec{y})$.

Due to the presence of the Heaviside function in the fundamental solution of the two dimensional wave equation, we observed (see equations (2.54) and (2.57) in particular) that the inner integration domain of the matrix entries (2.50) is the intersection of the ansatz element and a domain of the type

$$D_{l-1}(\vec{x}) = \mathbb{B}_{t_l}(\vec{x}) \qquad \text{or} \qquad E_{l-1}(\vec{x}) = \mathbb{B}_{t_l}(\vec{x}) \setminus \mathbb{B}_{t_{l-1}}(\vec{x}) \tag{2.72}$$

for $\vec{x} \in \Gamma$. For the second case, we note that one can, since

$$e \cap E_{l-1}(\vec{x}) = (e \cap \mathbb{B}_{t_l}(\vec{x})) \setminus (e \cap \mathbb{B}_{t_{l-1}}(\vec{x})) \tag{2.73}$$

rewrite any inner integral of the matrix entries (2.50) with integration domain $e \cap E_{l-1}(\vec{x})$ as the difference of two integral operators of type (2.71).

In the matrix entries (2.50), $P_{R,e}[\varphi]$ is multiplied by a test function $\psi \in L^\infty(\Gamma_i)$ and integrated over a test element Γ_i, which means that terms of the type

$$\int_{\Gamma_i} P_{R,e}[\varphi](\vec{x}) \psi(\vec{x})\ ds_{\vec{x}}$$

need to be computed. The convergence of quadrature methods for the approximation of these integrals depends on the regularity of $P_{R,e}[\varphi]$ [141]. In what follows, we compute the derivatives of $P_{R,e}[\varphi]$ and specify the locations of singularities in the derivatives for a class of kernel functions in order to establish its regularity in countably normed spaces, and thus obtain a theoretical convergence estimate for Algorithm 2.6.

The three dimensional counterpart of $P_{R,e}[\varphi]$,

$$P_{R,T}[\varphi](\vec{x}) \coloneqq \int_{T \cap \mathbb{B}_R(\vec{x})} k(\vec{x} - \vec{y})\ \varphi(\vec{y})\ ds_{\vec{y}}$$

for $\vec{x} \in \mathbb{R}^3$, where $T \subseteq \mathbb{R}^3$ is a triangle, has been thoroughly analysed in [127]. The integrals $P_{R,e}[\varphi]$ studied here are similar to the edge integrals $I_{e_i}[\varphi]$, where e_i is one of the edges of T, that appear in the gradient of $P_{R,T}[\varphi]$. They are analysed in [127, Section 3.2.1].

Our analysis follows [127] but is considerably simpler, because it is restricted to the two dimensional plane. In another aspect, however, it is more general. We study a wider class of kernel functions, that includes the spatial kernel functions of the time domain Single Layer, Double Layer and hypersingular operators for temporal basis functions of low polynomial order, as given in Appendix A. The analysis in [127], on the other hand, is restricted to the kernel function of the time domain Single Layer operator.

2.5.1 Derivatives of Time Domain Boundary Layer Potentials with Discrete Support

Let us consider a boundary edge parametrised by μ as in (2.37), namely

$$e = \left\{ \vec{m} + \mu \vec{d} \ \mid \ \mu \in [-1, 1] \right\}. \tag{2.74}$$

We denote the two end points of e, corresponding to local coordinates $\mu = -1$ and $\mu = 1$, respectively, by $\vec{a}$ and $\vec{b}$. The normal vector to e is denoted by $\vec{n}$, with $|\vec{n}| = 1$. The *ray* that contains e was given by (2.61),

$$\mathcal{E}_e = \left\{ \vec{m} + \mu\vec{d} \;\middle|\; \mu \in \mathbb{R} \right\} = \left\{ \vec{z} \in \mathbb{R}^2 \;\middle|\; \vec{n} \cdot (\vec{z} - \vec{p}) = 0 \right\} \tag{2.75}$$

for any arbitrary point $\vec{p} \in \mathcal{E}_e$. We recall that we stated in Remark 2.2 that, for any $\vec{x} \in \mathbb{R}^2$, we can find the point $\vec{x}' \in \mathcal{E}_e$ which is perpendicular to $\vec{x}$ by

$$\vec{x}' = \vec{x} - \big((\vec{x} - \vec{p}) \cdot \vec{n}\big)\, \vec{n}. \tag{2.76}$$

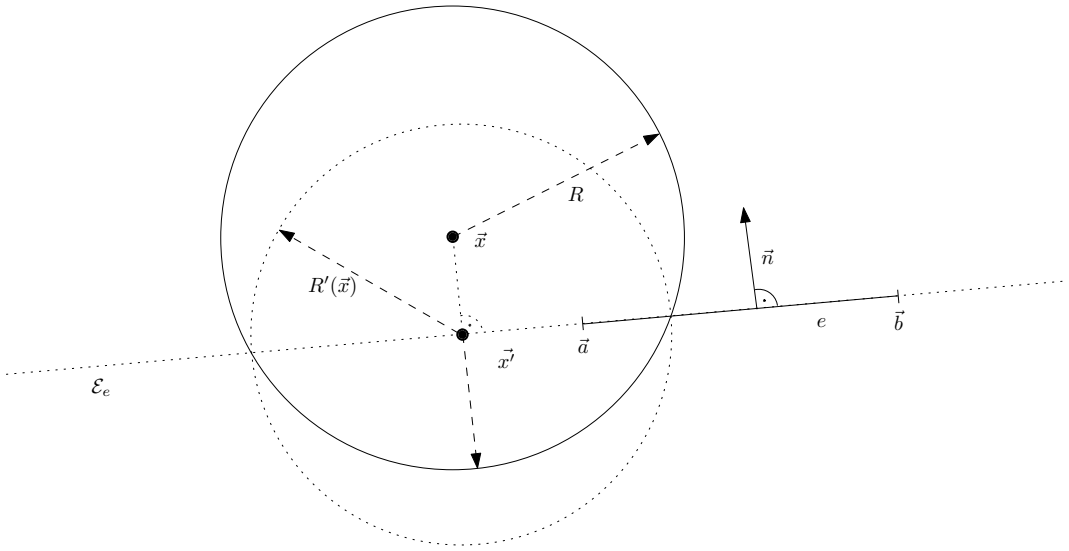

Figure 2.8: Boundary edge e with circular domains $\mathbb{B}_R(\vec{x})$ and $\mathbb{B}_{R'(\vec{x})}(\vec{x}')$.

Due to (2.76), $|\vec{x} - \vec{x}'| = |\,(\vec{x} - \vec{p}) \cdot \vec{n}|$, and

$$|\vec{x} - \vec{y}|^2 = \left|\vec{x}' - \vec{y} - \big((\vec{p} - \vec{x}) \cdot \vec{n}\big)\, \vec{n}\right|^2 = |\vec{x}' - \vec{y}|^2 + \big((\vec{p} - \vec{x}) \cdot \vec{n}\big)^2$$

for each $\vec{y} \in \mathcal{E}_e$, as $(\vec{x}' - \vec{y}) \cdot \vec{n} = 0$. Setting $R'(\vec{x}) := \sqrt{R^2 - \big((\vec{p} - \vec{x}) \cdot \vec{n}\big)^2}$, there holds $|\vec{x} - \vec{y}| \le R$ if and only if $|\vec{x}' - \vec{y}| \le R'(\vec{x})$ or, in terms of indicator functions,

$$\mathbb{1}_{\mathbb{B}_R(\vec{x})}(\vec{y}) = \mathbb{1}_{\mathbb{B}_{R'(\vec{x})}(\vec{x}')}(\vec{y}) \tag{2.77}$$

for $\vec{y} \in \mathcal{E}_e$. An illustration of the described setup is given in Figure 2.8. Writing $\vec{\Delta} := 2\vec{d}$, the indicator function of the set which is on the same side of the line perpendicular to e through $\vec{a}$ as $\vec{\Delta}$ is pointing to is $H\left((\vec{y} - \vec{a}) \cdot \vec{\Delta}\right)$; see (2.39). Therefore

$$\mathbb{1}_e(\vec{y}) = \mathbb{1}_{\mathcal{E}_e}(\vec{y})\, H\left((\vec{y} - \vec{a}) \cdot \vec{\Delta}\right) H\left(-\left(\vec{y} - \vec{b}\right) \cdot \vec{\Delta}\right). \tag{2.78}$$

Using (2.77) and (2.78), we rewrite (2.71) as

$$P_{R,e}[\varphi](\vec{x}) = \int_{\mathcal{E}_e} H\left(R'(\vec{x}) - |\vec{x}' - \vec{y}|\right) H\left((\vec{y} - \vec{a}) \cdot \vec{\Delta}\right) H\left(-\left(\vec{y} - \vec{b}\right) \cdot \vec{\Delta}\right) k(\vec{x} - \vec{y})\; \varphi(\vec{y})\; ds_{\vec{y}}. \tag{2.79}$$

Writing $|\vec{x}' - \vec{y}| = \sqrt{(\vec{x}' - \vec{y}) \cdot (\vec{x}' - \vec{y})}$ and using

$$\nabla_{\vec{x}} \left(\vec{y} \cdot \vec{x}' \right) = \vec{y} - (\vec{y} \cdot \vec{n})\, \vec{n} \qquad \text{and} \qquad \nabla_{\vec{x}} \left(\vec{x}' \cdot \vec{x}' \right) = 2 \left(\vec{x} - (\vec{x} \cdot \vec{n})\, \vec{n} \right).$$

for any $\vec{y} \in \mathbb{R}^2$, we obtain

$$\nabla_{\vec{x}} |\vec{x}' - \vec{y}| = \frac{1}{|\vec{x}' - \vec{y}|} \left(\vec{x} - \vec{y} - ((\vec{x} - \vec{y}) \cdot \vec{n})\, \vec{n} \right) = \frac{1}{|\vec{x}' - \vec{y}|} \left(\vec{x}' - \vec{y} \right)$$

for any $\vec{y} \in \mathcal{E}_e$. One can further compute

$$\nabla_{\vec{y}} |\vec{x}' - \vec{y}| = -\frac{1}{|\vec{x}' - \vec{y}|} \left(\vec{x}' - \vec{y} \right) = -\nabla_{\vec{x}} |\vec{x}' - \vec{y}|$$

for $\vec{y} \in \mathcal{E}_e$, and

$$\nabla_{\vec{x}} R'(\vec{x}) = \frac{1}{R'(\vec{x})} \left((\vec{p} - \vec{x}) \cdot \vec{n} \right) \vec{n}. \tag{2.80}$$

Using

$$\nabla_{\vec{x}} H \left(R'(\vec{x}) - |\vec{x}' - \vec{y}| \right) = \delta \left(R'(\vec{x}) - |\vec{x}' - \vec{y}| \right) \nabla_{\vec{x}} \left(R'(\vec{x}) - |\vec{x}' - \vec{y}| \right)$$

and

$$\nabla_{\vec{y}} H \left(R'(\vec{x}) - |\vec{x}' - \vec{y}| \right) = \delta \left(R'(\vec{x}) - |\vec{x}' - \vec{y}| \right) \nabla_{\vec{y}} \left(-|\vec{x}' - \vec{y}| \right) = \delta \left(R'(\vec{x}) - |\vec{x}' - \vec{y}| \right) \nabla_{\vec{x}} \left(|\vec{x}' - \vec{y}| \right)$$

with (2.80), we obtain

$$\nabla_{\vec{x}} H \left(R'(\vec{x}) - |\vec{x}' - \vec{y}| \right) = \delta \left(R'(\vec{x}) - |\vec{x}' - \vec{y}| \right) \frac{1}{R'(\vec{x})} \left(\left((\vec{p} - \vec{x}) \cdot \vec{n} \right) \right) \vec{n} - \nabla_{\vec{y}} H \left(R'(\vec{x}) - |\vec{x}' - \vec{y}| \right) \tag{2.81}$$

for $\vec{y} \in \mathcal{E}_e$. Since $\nabla_{\vec{x}} k(\vec{x} - \vec{y}) = -\nabla_{\vec{y}} k(\vec{x} - \vec{y})$, we consequently have

$$\begin{aligned}
& \nabla_{\vec{x}} \left\{ H \left(R'(\vec{x}) - |\vec{x}' - \vec{y}| \right) k(\vec{x} - \vec{y}) \right\} \\
= \;& \nabla_{\vec{x}} \left\{ H \left(R'(\vec{x}) - |\vec{x}' - \vec{y}| \right) \right\} k(\vec{x} - \vec{y}) - H \left(R'(\vec{x}) - |\vec{x}' - \vec{y}| \right) \nabla_{\vec{y}} \left\{ k(\vec{x} - \vec{y}) \right\} \\
= \;& \delta \left(R'(\vec{x}) - |\vec{x}' - \vec{y}| \right) \frac{1}{R'(\vec{x})} \left(\left((\vec{p} - \vec{x}) \cdot \vec{n} \right) \right) \vec{n} - \nabla_{\vec{y}} \left\{ H \left(R'(\vec{x}) - |\vec{x}' - \vec{y}| \right) k(\vec{x} - \vec{y}) \right\}.
\end{aligned} \tag{2.82}$$

Using the representation (2.79) of $P_{R,e}[\varphi]$ and (2.82), we obtain

$$\begin{aligned}
& \nabla_{\vec{x}} \left(P_{R,e}[\varphi] \right) (\vec{x}) \\
= \;& \frac{(\vec{p} - \vec{x}) \cdot \vec{n}}{R'(\vec{x})} \int_{\mathcal{E}_e} \delta(R'(\vec{x}) - |\vec{x}' - \vec{y}|) H \left((\vec{y} - \vec{a}) \cdot \vec{\Delta} \right) H \left(- \left(\vec{y} - \vec{b} \right) \cdot \vec{\Delta} \right) \; k(\vec{x} - \vec{y}) \varphi(\vec{y}) \; ds_{\vec{y}} \; \vec{n} \\
& - \int_{\mathcal{E}_e} \nabla_{\vec{y}} \left\{ H(R'(\vec{x}) - |\vec{x}' - \vec{y}|) \; k(\vec{x} - \vec{y}) \right\} H \left((\vec{y} - \vec{a}) \cdot \vec{\Delta} \right) H \left(- \left(\vec{y} - \vec{b} \right) \cdot \vec{\Delta} \right) \varphi(\vec{y}) \; ds_{\vec{y}}
\end{aligned} \tag{2.83}$$

which is a two dimensional analogue of [127, (3.7)]. Since $R'(\vec{x}) - |\vec{x}' - \vec{y}| = 0$ if and only if $|\vec{x} - \vec{y}| = R$ for $\vec{y} \in \mathcal{E}_e$, the first integral in (2.83) is

$$\int_{\mathcal{E}_e} \delta(R'(\vec{x}) - |\vec{x}' - \vec{y}|) H \left((\vec{y} - \vec{a}) \cdot \vec{\Delta} \right) H \left(- \left(\vec{y} - \vec{b} \right) \cdot \vec{\Delta} \right) \; k(\vec{x} - \vec{y}) \varphi(\vec{y}) \; ds_{\vec{y}} = \sum_{\vec{y} \in e \cap \partial \mathbb{B}_R(\vec{x})} k(\vec{x} - \vec{y}) \varphi(\vec{y}).$$

Regarding the second term, we can use the product rule for differentiation and the fact that, for any F with bounded support, $\int_{\mathcal{E}_e} \nabla_{\vec{y}} F \; ds_{\vec{y}} = 0$, and obtain

$$\begin{aligned}
& \int_{\mathcal{E}_e} \nabla_{\vec{y}} \left\{ H(R'(\vec{x}) - |\vec{x}' - \vec{y}|) \; k(\vec{x} - \vec{y}) \right\} \; H \left((\vec{y} - \vec{a}) \cdot \vec{\Delta} \right) H \left(- \left(\vec{y} - \vec{b} \right) \cdot \vec{\Delta} \right) \varphi(\vec{y}) \; ds_{\vec{y}} \\
= \;& - \int_{\mathcal{E}_e} \nabla_{\vec{y}} \left\{ H \left((\vec{y} - \vec{a}) \cdot \vec{\Delta} \right) H \left(- \left(\vec{y} - \vec{b} \right) \cdot \vec{\Delta} \right) \varphi(\vec{y}) \right\} \; H(R'(\vec{x}) - |\vec{x}' - \vec{y}|) \; k(\vec{x} - \vec{y}) \; ds_{\vec{y}}
\end{aligned}$$

where

$$\begin{aligned}
&\nabla_{\vec{y}} \left\{ H\left((\vec{y}-\vec{a})\cdot\vec{\Delta}\right) H\left(-\left(\vec{y}-\vec{b}\right)\cdot\vec{\Delta}\right)\varphi(\vec{y})\right\} \\
= \quad & \left(\delta\left((\vec{y}-\vec{a})\cdot\vec{\Delta}\right) H\left(-\left(\vec{y}-\vec{b}\right)\cdot\vec{\Delta}\right) - H\left((\vec{y}-\vec{a})\cdot\vec{\Delta}\right)\delta\left(-\left(\vec{y}-\vec{b}\right)\cdot\vec{\Delta}\right)\right)\ \varphi(\vec{y})\vec{\Delta} \\
& + H\left((\vec{y}-\vec{a})\cdot\vec{\Delta}\right) H\left(-\left(\vec{y}-\vec{b}\right)\cdot\vec{\Delta}\right)\ \nabla_{\vec{y}}\varphi(\vec{y}).
\end{aligned}$$

Since $(\vec{y}-\vec{a})\cdot\vec{\Delta} = 0$ if and only if $\vec{y} = \vec{a}$ (similarly for $\vec{b}$), we have thus shown a two dimensional version of [127, Lemma 3.2].

Lemma 2.3 (Gradient of $P_{R,e}[\varphi]$)
For a boundary integral operator $P_{R,e}[\varphi]$ of type (2.71) with $R > 0$ and boundary edge e of type (2.74) there holds, with arbitrary $\vec{p} \in \mathcal{E}_e$,

$$\begin{aligned}
\nabla_{\vec{x}} \left(P_{R,e}[\varphi]\right)(\vec{x}) \quad = \quad & \int_{e\cap\mathbb{B}_R(\vec{x})} k(\vec{x}-\vec{y})\ \nabla_{\vec{y}}\varphi(\vec{y})\ ds_{\vec{y}} \\
& -\left(\mathbb{1}_{\mathbb{B}_R(\vec{b})}(\vec{x})\ k(\vec{x}-\vec{b})\varphi(\vec{b}) - \mathbb{1}_{\mathbb{B}_R(\vec{a})}(\vec{x})\ k(\vec{x}-\vec{a})\varphi(\vec{a})\right)\ \left(\vec{b}-\vec{a}\right) \\
& + \frac{(\vec{p}-\vec{x})\cdot\vec{n}}{R'(\vec{x})} \sum_{\vec{y}\in e\cap\partial\mathbb{B}_R(\vec{x})} k(\vec{x}-\vec{y})\varphi(\vec{y})\ \vec{n}
\end{aligned} \tag{2.84}$$

for any $\vec{x} \in \mathbb{R}^2$ and density $\varphi \in L^\infty(e)$.

We note that the first term in (2.84) is

$$h_1(\vec{x}) := \int_{e\cap\mathbb{B}_R(\vec{x})} k(\vec{x}-\vec{y})\ \nabla_{\vec{y}}\varphi(\vec{y})\ ds_{\vec{y}} = P_{R,e}\left[\nabla_{\vec{y}}\varphi\right](\vec{x}). \tag{2.85}$$

The singularities of h_1 are located at the same points as the singularities of $P_{R,e}[\varphi]$, and no further considerations are needed for this term. The terms in the second line,

$$h_2(\vec{x}) := \mathbb{1}_{\mathbb{B}_R(\vec{b})}(\vec{x})\ k(\vec{x}-\vec{b})\varphi(\vec{b}) - \mathbb{1}_{\mathbb{B}_R(\vec{a})}(\vec{x})\ k(\vec{x}-\vec{a})\varphi(\vec{a}) \tag{2.86}$$

are non-zero if the evaluation point $\vec{x}$ is contained within the circle of radius of R around the respective end point of e. The last term

$$h_3(\vec{x}) := \frac{(\vec{p}-\vec{x})\cdot\vec{n}}{R'(\vec{x})} \sum_{\vec{y}\in e\cap\partial\mathbb{B}_R(\vec{x})} k(\vec{x}-\vec{y})\varphi(\vec{y}) \tag{2.87}$$

is non-zero if $\mathbb{B}_R(\vec{x})$ intersects e. The sum contains two terms at most, since the edge e can intersect $\mathbb{B}_R(\vec{x})$ in at most two points.

In order to compute the second derivatives of $P_{R,e}[\varphi]$, we consider the derivatives of h_2 and h_3. Using

$$\nabla_{\vec{x}}\mathbb{1}_{\mathbb{B}_R(\vec{b})}(\vec{x}) = -\delta(R-|\vec{x}-\vec{b}|)\ \nabla_{\vec{x}}|\vec{x}-\vec{b}| = -\mathbb{1}_{\partial\mathbb{B}_R(\vec{b})}(\vec{x})\frac{1}{|\vec{x}-\vec{b}|}\left(\vec{x}-\vec{b}\right)$$

we obtain

$$\begin{aligned}
\nabla_{\vec{x}} h_2(\vec{x}) \quad = \quad & \mathbb{1}_{\mathbb{B}_R(\vec{b})}(\vec{x})\varphi(\vec{b})\ \nabla_{\vec{x}}k(\vec{x}-\vec{b}) - \ \mathbb{1}_{\partial\mathbb{B}_R(\vec{b})}(\vec{x})\frac{k(\vec{x}-\vec{b})}{|\vec{x}-\vec{b}|}\varphi(\vec{b})\ \left(\vec{x}-\vec{b}\right) \\
& -\mathbb{1}_{\mathbb{B}_R(\vec{a})}(\vec{x})\varphi(\vec{a})\ \nabla_{\vec{x}}k(\vec{x}-\vec{a}) + \mathbb{1}_{\partial\mathbb{B}_R(\vec{a})}(\vec{x})\frac{k(\vec{x}-\vec{a})}{|\vec{x}-\vec{a}|}\varphi(\vec{a})\ \left(\vec{x}-\vec{a}\right).
\end{aligned} \tag{2.88}$$

Further, using (2.80), there holds

$$\nabla_{\vec{x}} \left(\frac{(\vec{p}-\vec{x})\cdot\vec{n}}{R'(\vec{x})} \right) = -\left(\frac{1}{R'(\vec{x})} + \frac{((\vec{p}-\vec{x})\cdot\vec{n})^2}{R'(\vec{x})^3} \right) \vec{n} = -\frac{R^2}{R'(\vec{x})^3}\vec{n} \tag{2.89}$$

and therefore

$$\nabla_{\vec{x}} h_3(\vec{x}) = \frac{(\vec{p}-\vec{x})\cdot\vec{n}}{R'(\vec{x})} \sum_{\vec{y}\in e\cap\partial\mathbb{B}_R(\vec{x})} \varphi(\vec{y}) \;\; \nabla_{\vec{x}} k(\vec{x}-\vec{y}) \;\; - \;\; \frac{R^2}{R'(\vec{x})^3} \sum_{\vec{y}\in e\cap\partial\mathbb{B}_R(\vec{x})} k(\vec{x}-\vec{y})\varphi(\vec{y}) \;\; \vec{n} \tag{2.90}$$

where we used $\nabla_{\vec{x}} \mathbb{1}_{\partial\mathbb{B}_R(\vec{y})}(\vec{x}) = 0$. By Lemma 2.3, there holds

$$\frac{\partial^2}{\partial x_i \partial x_j} \left(P_{R,e}[\varphi] \right)(\vec{x}) = \frac{\partial}{\partial x_i} P_{R,e}\left[\frac{\partial \varphi}{\partial y_j} \right](\vec{x}) - \left(\frac{\partial}{\partial x_i} h_2(\vec{x}) \right)(b_j - a_j) + \left(\frac{\partial}{\partial x_i} h_3(\vec{x}) \right) n_j$$

for $i, j = 1, 2$. Using Lemma 2.3, (2.88) and (2.90), we obtain Lemma 2.4.

Lemma 2.4 (Second Derivatives of $P_{R,e}[\varphi]$)
Under the assumptions of Lemma 2.3, there holds

$$\begin{aligned}
&\frac{\partial^2}{\partial x_i \partial x_j} \left(P_{R,e}[\varphi] \right)(\vec{x}) \\
= \;& \int_{e\cap\mathbb{B}_R(\vec{x})} k(\vec{x}-\vec{y}) \;\; \frac{\partial^2 \varphi}{\partial y_i \partial y_j}(\vec{y}) \; ds_{\vec{y}} \\
& - \mathbb{1}_{\mathbb{B}_R(\vec{b})}(\vec{x}) \left((b_i - a_i) \; k(\vec{x}-\vec{b}) \; \frac{\partial \varphi}{\partial x_j}(\vec{b}) \; + (b_j - a_j) \; \frac{\partial k}{\partial x_i}(\vec{x}-\vec{b}) \; \varphi(\vec{b}) \right) \\
& + \mathbb{1}_{\mathbb{B}_R(\vec{a})}(\vec{x}) \left((b_i - a_i) \; k(\vec{x}-\vec{a}) \; \frac{\partial \varphi}{\partial x_j}(\vec{a}) + (b_j - a_j) \; \frac{\partial k}{\partial x_i}(\vec{x}-\vec{a}) \; \varphi(\vec{a}) \right) \\
& + \left\{ \mathbb{1}_{\partial\mathbb{B}_R(\vec{b})}(\vec{x}) \; \frac{x_i - b_i}{|\vec{x}-\vec{b}|} \; k(\vec{x}-\vec{b}) \; \varphi(\vec{b}) - \mathbb{1}_{\partial\mathbb{B}_R(\vec{a})}(\vec{x}) \; \frac{x_i - a_i}{|\vec{x}-\vec{a}|} \; k(\vec{x}-\vec{a}) \; \varphi(\vec{a}) \right\} \; (b_j - a_j) \\
& + \frac{(\vec{p}-\vec{x})\cdot\vec{n}}{R'(\vec{x})} \left\{ \sum_{\vec{y}\in e\cap\partial\mathbb{B}_R(\vec{x})} n_i \; k(\vec{x}-\vec{y}) \; \frac{\partial \varphi}{\partial y_j}(\vec{y}) \; + \; n_j \; \frac{\partial k}{\partial x_i}(\vec{x}-\vec{y}) \; \varphi(\vec{y}) \right\} \\
& - \frac{R^2}{R'(\vec{x})^3} \sum_{\vec{y}\in e\cap\partial\mathbb{B}_R(\vec{x})} n_i n_j \; k(\vec{x}-\vec{y}) \; \varphi(\vec{y})
\end{aligned} \tag{2.91}$$

for $i, j = 1, 2$.

Derivatives of $P_{R,e}[\varphi]$ of higher order can be be found iteratively, as demonstrated in [127, Theorem 3.4]. In particular, the subdomains involved are the same as the ones in (2.91).

2.5.2 Singularities of Time Domain Boundary Layer Potentials with Discrete Support

Our next aim is to study the singularities of the derivatives of $P_{R,e}[\varphi]$. We restrict ourselves to a certain class of kernel functions that includes the spatial kernel functions that result from the analytical temporal integration for temporal basis functions of low polynomial order, characterised in Section A.3. Beforehand, however, we notice that the gradient of $P_{R,e}[\varphi]$ contains a term that is singular independently of the kernel function:

Let $\vec{x} = \vec{m} + \mu\vec{d} \pm R\vec{n}$. We can choose $\vec{p} = \vec{m}$ in (2.84), which gives $(\vec{p} - \vec{x}) \cdot \vec{n} = \mp R$. On the other hand, $R'(\vec{x}) = 0$ for these points. This means that, independently of the kernel function, the term $\frac{(\vec{p}-\vec{x})\cdot\vec{n}}{R'(\vec{x})}$ in the gradient of $P_{R,e}[\varphi]$ is singular on the two edges parallel to e at distance R. We characterise these singularities in a more general and more formal way in Lemma 2.18.

2.5.2.1 A Class of Admissible Kernel Functions

In order to give a more detailed analysis of the singularities of $P_{R,e}[\varphi]$, we now restrict ourselves to a certain class of kernel functions.

Assumption 2.5 (On the Kernel Function)
The kernel k of $P_{R,e}[\varphi]$ is either of the form

$$k(\vec{x} - \vec{y}) = \kappa(R; |\vec{x} - \vec{y}|) = \kappa(R; r)$$

or of the form

$$k(\vec{x} - \vec{y}, \vec{n}_{\vec{y}}) = (\vec{x} - \vec{y}) \cdot \vec{n}_{\vec{y}}\ \kappa(R; |\vec{x} - \vec{y}|) = (\vec{x} - \vec{y}) \cdot \vec{n}_{\vec{y}}\ \kappa(R; r)$$

or of the form

$$k(\vec{x} - \vec{y}, \vec{n}_{\vec{x}}, \vec{n}_{\vec{y}}) = \vec{n}_{\vec{x}} \cdot \vec{n}_{\vec{y}}\ \kappa(R; |\vec{x} - \vec{y}|) = \vec{n}_{\vec{x}} \cdot \vec{n}_{\vec{y}}\ \kappa(R; r)$$

where we assume $\nabla_{\vec{x}}\vec{n}_{\vec{x}} = 0$, which is guaranteed to hold if $\vec{x}$ is a point on a straight boundary edge. In short,

$$k(\vec{x} - \vec{y}, \vec{n}_{\vec{x}}, \vec{n}_{\vec{y}}) = \kappa(R; |\vec{x} - \vec{y}|) f_k(\vec{x} - \vec{y}, \vec{n}_{\vec{x}}, \vec{n}_{\vec{y}}) \tag{2.92}$$

where either $f_k(\vec{x} - \vec{y}, \vec{n}_{\vec{x}}, \vec{n}_{\vec{y}}) \equiv 1$ or $f_k(\vec{x} - \vec{y}, \vec{n}_{\vec{x}}, \vec{n}_{\vec{y}}) = (\vec{x} - \vec{y}) \cdot \vec{n}_{\vec{y}}$ or $f_k(\vec{x} - \vec{y}, \vec{n}_{\vec{x}}, \vec{n}_{\vec{y}}) = \vec{n}_{\vec{x}} \cdot \vec{n}_{\vec{y}}$.

There holds $\kappa(R; R) \in \mathbb{R}$, but the derivative of κ can be weakly singular for $|\vec{x} - \vec{y}| = R$. Additionally, κ can be weakly singular for $|\vec{x} - \vec{y}| = 0$. Formally, there hold the Calderón-Zygmund inequalities

$$\left| f_k(\vec{x} - \vec{y}, \vec{n}_{\vec{x}}, \vec{n}_{\vec{y}}) \frac{d^n}{dr^n} \kappa(R; r) \right| \leq C_{1,1} C_{1,2}^n\ n!\ r^{\min\{\kappa_1 - n, 0\}}$$

with $\kappa_1 \geq -1$ for any $n \geq 0$ and any $\vec{x}, \vec{y} \in \Gamma$ with $|\vec{x} - \vec{y}| = r < \varepsilon$, and

$$\left| f_k(\vec{x} - \vec{y}, \vec{n}_{\vec{x}}, \vec{n}_{\vec{y}}) \frac{d^n}{dr^n} \kappa(R; r) \right| \leq C_{2,1} C_{2,2}^n\ n!\ |r - R|^{\min\{\kappa_2 - n, 0\}}$$

with $\kappa_2 \geq 0$ for any $n \geq 0$ and any $\vec{x}, \vec{y} \in \Gamma$ with $R - \varepsilon < |\vec{x} - \vec{y}| = r < R + \varepsilon$. The constants $C_{i,j} > 0$, $i, j = 1, 2$, are independent of n.

Remark 2.6 (On Assumption 2.5)

a) *Even though the second type of kernel function specified in Assumption 2.5 is non-symmetric, there still holds $\nabla_{\vec{x}} k(\vec{x} - \vec{y}, \vec{n}_{\vec{y}}) = -\nabla_{\vec{y}} k(\vec{x} - \vec{y}, \vec{n}_{\vec{y}})$, and therefore the formulas for the derivatives given in Section 2.5.1 remain valid.*

b) *The third class of kernel functions, with $f_k(\vec{x} - \vec{y}, \vec{n}_{\vec{x}}, \vec{n}_{\vec{y}}) = \vec{n}_{\vec{x}} \cdot \vec{n}_{\vec{y}}$, is included in Assumption 2.5 to cover the case of the hypersingular integral operator after integrating by parts; see* (A.87). *This class is meaningless if $\vec{x}$ is contained in a genuine two dimensional manifold, as when dealing with the Newton potential; see also Remark 2.19.*

Definition 2.7 (Admissible Kernel Function)
A kernel function k for which Assumption 2.5 holds is called an admissible kernel function.

We now consider some examples of admissible kernel functions. These are typical kernel functions that arise after an analytical temporal integration of the matrix entries; see Section A.3. In what follows, we use the notation

$$n!! = \begin{cases} n \cdot (n-2) \cdot (n-4) \cdot \cdots \cdot 2 \cdot 1 & n \text{ even} \\ n \cdot (n-2) \cdot (n-4) \cdot \cdots \cdot 3 \cdot 1 & n \text{ odd} \end{cases} \tag{2.93}$$

for any $n \geq 1$. There obviously holds $(2n)!! = 2^n n!$.

Example 2.8 (Admissible Kernel Functions)

a) Let

$$k(\vec{x}-\vec{y},\vec{n}_{\vec{x}},\vec{n}_{\vec{y}}) = S(R;|\vec{x}-\vec{y}|) = \sqrt{R^2-|\vec{x}-\vec{y}|^2} = \kappa(R;|\vec{x}-\vec{y}|).$$

There holds $\kappa(R;R) = 0$ *and* $\frac{d}{dr}\kappa(R;r) = -r(R^2-r^2)^{-1/2}$. *Since*

$$\frac{d\left(R^2-r^2\right)^{-\frac{2n+1}{2}}}{dr} = (2n+1)\, r\left(R^2-r^2\right)^{-\frac{2n+3}{2}}$$

the leading (regarding the order of the singularity at $r = R$*) terms in* $\frac{d^n}{dr^n}\kappa(R;r)$ *are of the form*

$$(2n-3)!!\; r^n (R^2-r^2)^{-\frac{2n-1}{2}}$$

for $n \geq 2$, *and the kernel function is therefore admissible with* $\kappa_2 = \frac{1}{2}$.

b) Let

$$k(\vec{x}-\vec{y},\vec{n}_{\vec{x}},\vec{n}_{\vec{y}}) = L(R;|\vec{x}-\vec{y}|) = \ln\left(R+\sqrt{R^2-|\vec{x}-\vec{y}|^2}\right) = \kappa(R;|\vec{x}-\vec{y}|).$$

There holds $\kappa(R;R) = \ln R$ *and*

$$\frac{d}{dr}\kappa(R;r) = -\left(R+\sqrt{R^2-r^2}\right)^{-1}(R^2-r^2)^{-1/2}\, r.$$

Arguing as in a), the leading terms in $\frac{d^n}{dr^n}\kappa(R;r)$ *are of the form*

$$(2n-3)!!\; r^n \left(R+\sqrt{R^2-r^2}\right)^{-1}(R^2-r^2)^{-\frac{2n-1}{2}}$$

for $n \geq 2$, *and the kernel function is therefore admissible with* $\kappa_2 = \frac{1}{2}$.

c) Let

$$k(\vec{x}-\vec{y},\vec{n}_{\vec{x}},\vec{n}_{\vec{y}}) = \ln|\vec{x}-\vec{y}| = \kappa(R;|\vec{x}-\vec{y}|).$$

In this case there simply holds

$$\frac{d^n}{dr^n}\kappa(R;r) = (-1)^{n-1}(n-1)!\, r^{-n}$$

for $n \geq 1$, *and the kernel function is therefore admissible with* $\kappa_1 = 0$.

d) Let

$$k(\vec{x}-\vec{y},\vec{n}_{\vec{x}},\vec{n}_{\vec{y}}) = \frac{(\vec{x}-\vec{y})\cdot\vec{n}_{\vec{y}}}{|\vec{x}-\vec{y}|}\frac{1}{|\vec{x}-\vec{y}|} = (\vec{x}-\vec{y})\cdot\vec{n}_{\vec{y}}\;\frac{1}{|\vec{x}-\vec{y}|^2} = f_k(\vec{x}-\vec{y},\vec{n}_{\vec{x}},\vec{n}_{\vec{y}})\kappa(R;|\vec{x}-\vec{y}|).$$

Similarly to c) there simply holds

$$\frac{d^n}{dr^n}\kappa(R;r) = (-1)^n(n+1)!\, r^{-n-2}$$

for $n \geq 1$, *and, using* $(n+1)! \leq 2^n n!$, *the kernel function is therefore admissible with* $\kappa_1 = -1$.

Remark 2.9 (Relevant Admissible Kernel Functions)
The spatial kernel functions that result from the analytical temporal integration for temporal basis functions of low polynomial order were characterised in Section A.3. The kernel functions of the Single Layer and hypersingular operator are sums of the functions considered in Example 2.8 a)-c), and therefore admissible. The kernel functions of the Double Layer operator, given by (A.68), (A.79) *and* (A.85)*, additionally involve products of functions considered in part a)-b) (first factor) and part d) (second factor) of Example 2.8. These are also admissible.*

It is well known that the Single Layer potential for the Laplace equation is continuous in $\mathbb{R}^2$ and that the Laplace Double Layer operator is continuous on Γ for $\Gamma \in C^2_{\mathrm{pw}}$; see, for instance, [83, Theorems 8.1.7 and 8.2.5] or [133, Theorem 3.3.5]. Here, for $k \in \mathbb{N} \cup \{\infty\}$, C^k_{pw} denotes the *set of piecewise C^k-curves*, with $\Gamma \in C^k_{\mathrm{pw}}$ if and only if [83, Definition 7.1.10], [133, Definition 2.2.10]

(i) Γ is a Lipschitz boundary, and

(ii) there exists a partition $\mathcal{G}$ of Γ such that

  (a) every $\tau \in \mathcal{G}$ is a C^k curve

  (b) the elements of $\mathcal{G}$ are open and disjoint

  (c) $\cup_{\tau \in \mathcal{G}} \bar{\tau} = \Gamma$.

If, for instance, Γ is a polygon, there holds $\Gamma \in C^\infty_{\mathrm{pw}}$. In the proof of [127, Proposition 3.21], it is observed that the proofs of these statements rely on a decomposition of the 'domain of integration [of the integral operator] into a neighbourhood of $\vec{x}$ and its complement', which can still be applied for the integration domain $T \cap \mathbb{B}_R(\vec{x})$ of $P_{T,e}[\varphi]$. We therefore conclude that $P_{R,e}[\varphi]$ is continuous.

Lemma 2.10 (Continuity of $P_{R,e}[\varphi]$)
Let k be an admissible kernel function, $\varphi \in L^\infty(e)$, and let $\Gamma \in C^2_{pw}$. Then $P_{R,e}[\varphi]$ defines a continuous function on Γ.

2.5.2.2 Classification of Typical Singularities

Due to Lemma 2.10, singularities appear only in the derivatives of $P_{R,e}[\varphi]$. We now characterise these singularities for admissible kernel functions.

Let k be an admissible kernel function. Due to Assumption 2.5, for $f_k \equiv 1$,

$$h_3(\vec{x}) = \frac{(\vec{p}-\vec{x})\cdot\vec{n}}{R'(\vec{x})} \sum_{\vec{y}\in e\cap\partial\mathbb{B}_R(\vec{x})} \kappa(R;R)\varphi(\vec{y}) = |e\cap\partial\mathbb{B}_R(\vec{x})|\,\frac{(\vec{p}-\vec{x})\cdot\vec{n}}{R'(\vec{x})}\kappa(R;R) \tag{2.94}$$

since $\vec{y} \in e \cap \partial\mathbb{B}_R(\vec{x})$ if and only if $|\vec{x}-\vec{y}| = R$. As we pointed out previously, the factor $\frac{(\vec{p}-\vec{x})\cdot\vec{n}}{R'(\vec{x})}$ is singular at the two edges parallel to e at distance R, independently of the kernel function.

Further, the function h_2 can be rewritten as

$$h_2(\vec{x}) = \mathbb{1}_{\mathbb{B}_R(\vec{b})}(\vec{x})\ \kappa(R;|\vec{x}-\vec{b}|) f_k(\vec{x}-\vec{b},\vec{n}_{\vec{x}},\vec{n})\varphi(\vec{b}) - \mathbb{1}_{\mathbb{B}_R(\vec{a})}(\vec{x})\ \kappa(R;|\vec{x}-\vec{a}|) f_k(\vec{x}-\vec{a},\vec{n}_{\vec{x}},\vec{n})\varphi(\vec{a}). \tag{2.95}$$

The gradient of h_2, given by (2.88), is singular for $\vec{x} \in \partial\mathbb{B}_R(\vec{a})$ and $\vec{x} \in \partial\mathbb{B}_R(\vec{b})$. If, additionally, k is singular at the origin $r = 0$, h_2 is singular for $\vec{x} = \vec{a}$ and $\vec{x} = \vec{b}$, i.e. at the end points $\vec{a}$, $\vec{b}$ of e.

We can therefore identify three locations at which the derivatives of $P_{R,e}[\varphi]$ can possibly be singular:

(i) on the two edges parallel to e at distance R

(ii) on the boundaries of the circles $\mathbb{B}_R(\vec{a})$ and $\mathbb{B}_R(\vec{b})$ around the end points of e

(iii) at the end points of e.

Similarly to [127, Definition 3.18], we classify these singularities in Definition 2.11.

Definition 2.11 (Types of Singularities of $P_{R,e}[\varphi]$)
We call the singularities that appear at location (i) planar light disc singularities*, the singularities that appear at location (ii)* circular light disc singularities *and the singularities that appear at location (iii)* end point *or* classical singularities*.*

We study the singularities given in Definition 2.11 for two typical kernel functions in Example 2.12.

Example 2.12 (Kernel Functions of the Single Layer Operator)
We consider the admissible kernel functions

$$S(R;|\vec{x}-\vec{y}|) = \sqrt{R^2-|\vec{x}-\vec{y}|^2} \qquad \text{and} \qquad L(R;|\vec{x}-\vec{y}|) = \ln\left(R+\sqrt{R^2-|\vec{x}-\vec{y}|^2}\right)$$

that were defined in (A.22)*; see Example 2.8 a)-b) as well. We observed in Section A.3 that the spatial kernel functions for the Single Layer operator are sums of functions of this type.*

Contour plots of $P_{R,e}[\varphi]$ with these kernel functions and constant density $\varphi \equiv 1$ are shown in Figure 2.9. The function values of $P_{R,e}[\varphi]$ are computed by the adaptive quadrature routines provided in QUADPACK *[129] which are exact up to double precision for an appropriately chosen error tolerance.*

We note that $S(R;|\vec{x}-\vec{y}|) = R'(\vec{x})$ for $\vec{y} \in e \cap \partial\mathbb{B}_R(\vec{x})$, and consequently, by (2.94)*, $h_3(\vec{x})$ is non-singular in this case, with $|h_3(\vec{x})| = R$. The gradient of $P_{R,e}[\varphi]$ is therefore also non-singular for this kernel function. The second derivatives of $P_{R,e}[\varphi]$ are, however, singular; the strongest ones being the planar light disc singularities.*

For the second kernel function, we have $L(R;R) = \ln R$ for $\vec{y} \in e \cap \partial\mathbb{B}_R(\vec{x})$, and consequently planar light disc singularities appear in the gradient of $P_{R,e}[\varphi]$. The contour lines in Figure 2.9b are, therefore, very dense at these points, but one can also observe the circular light disc singularities which appear in the second derivatives of $P_{R,e}[\varphi]$.

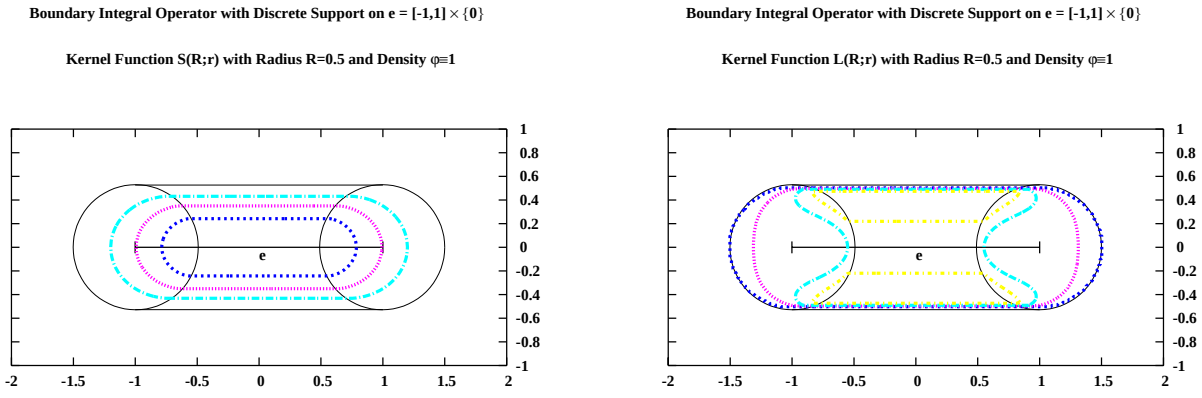

(a) kernel function $S(R;|\vec{x}-\vec{y}|)$ (b) kernel function $L(R;|\vec{x}-\vec{y}|)$

Figure 2.9: Contour plots of $P_{R,e}[\varphi \equiv 1]$ with $e = [-1,1] \times \{0\}$ and $R = 0.5$.

2.5.2.3 Analysis of Time Domain Boundary Layer Potentials with Discrete Support in Countably Normed Spaces

Exponential convergence of a class of composite quadrature methods of variable order was proven in [141] for functions that belong to countably normed spaces. Ostermann showed in [127, Section 3.2.1] that edge integrals of type $P_{R,e}[\varphi]$ are elements of these spaces when the support of $P_{R,e}[\varphi]$ is restricted to a plane. This setup coincides with the two dimensional case considered in this work if the plane is parallel to the edge with distance zero. While some of the results of [127] can be adopted immediately with minimal modifications, we also need to carefully incorporate the wider class of kernel functions specified in Definition 2.7 into our analysis.

Definition 2.13 (Countably Normed Spaces $\mathcal{B}^l_\beta(\Omega_{\text{ref}})$ [141])
Let $\Omega_{ref} := (0,1)^2 \subseteq \mathbb{R}^2$ be the two dimensional reference element. For $l \in \mathbb{N}_0$ and $\beta \in (0,1)$ we define countably normed spaces *by*

$$\mathcal{B}^l_\beta(\Omega_{ref}) := \left\{ u \in H^{l-1}(\Omega_{ref}) \;\middle|\; \left\| \frac{\partial^{\alpha_1+\alpha_2} u}{\partial x_1^{\alpha_1} \partial x_2^{\alpha_2}} \, \Phi_{\beta,\vec{\alpha},l} \right\|_{L^2(\Omega_{ref})} \leq C d^{|\vec{\alpha}|-l} (|\vec{\alpha}|-l)! \right.$$
$$\left. \text{for any } \vec{\alpha} = (\alpha_1,\alpha_2) \text{ with } |\vec{\alpha}| \geq l \right\} \tag{2.96}$$

for $l \geq 1$ and

$$\mathcal{B}^0_\beta(\Omega_{ref}) := \left\{ u \;\middle|\; \left\| \frac{\partial^{\alpha_1+\alpha_2} u}{\partial x_1^{\alpha_1} \partial x_2^{\alpha_2}} \, \Phi_{\beta,\vec{\alpha},0} \right\|_{L^2(\Omega_{ref})} \leq C d^{|\vec{\alpha}|} |\vec{\alpha}|! \text{ for any } \vec{\alpha} = (\alpha_1,\alpha_2) \in \mathbb{N}_0^2 \right\}$$

for $l = 0$, where $C = C(u) \geq 0$ and $d = d(u) \geq 1$ are independent of $|\vec{\alpha}|$, and $\Phi_{\beta,\vec{\alpha},l}$ is the weight function

$$\Phi_{\beta,\vec{\alpha},l}(\vec{x}) := |\vec{x}|^{\beta+\alpha_1+\alpha_2-l}.$$

Remark 2.14 (On Countably Normed Spaces)
a) The definition of $\mathcal{B}^l_\beta(\Omega_{ref})$, $l \in \mathbb{N}_0$, for the one dimensional reference element $\Omega_{ref} := (0,1) \subseteq \mathbb{R}$ is similar [14]. The countably normed spaces on Ω_{ref} are then given by

$$\mathcal{B}^l_\beta(\Omega_{ref}) := \left\{ u \in H^{l-1}(\Omega_{ref}) \;\middle|\; \left\| \frac{d^n u}{dx^n} \, \Phi_{\beta,n,l} \right\|_{L^2(\Omega_{ref})} \leq C d^{n-l} (n-l)! \text{ for any } n \geq l \right\} \tag{2.97}$$

for $l \geq 1$ and

$$\mathcal{B}^0_\beta(\Omega_{ref}) := \left\{ u \;\middle|\; \left\| \frac{d^n u}{dx^n} \, \Phi_{\beta,\vec{\alpha},0} \right\|_{L^2(\Omega_{ref})} \leq C d^n n! \text{ for any } n \geq 0 \right\}$$

for $l = 0$, with weight function $\Phi_{\beta,n,l}(x) := |x|^{\beta+n-l}$.

b) In polar coordinates around the point singularity (the origin), the space $\mathcal{B}^l_\beta(\Omega_{ref})$ is characterised equivalently by the growth condition [13, Theorem 1.1], [141, Proposition A.1]

$$\left\| r^{\frac{1}{2}} \frac{\partial^{\alpha_1+\alpha_2} u}{\partial r^{\alpha_1} \partial \theta^{\alpha_2}} \, \Phi_{\beta,\alpha_1,l} \right\|_{L^2(\Omega_{ref})} \leq C d^{|\vec{\alpha}|-l} (|\vec{\alpha}|-l)! \tag{2.98}$$

with weight function

$$\Phi_{\beta,\alpha_1,l}(r) := r^{\beta+\alpha_1-l}.$$

c) *[141, Remark 5.4] points out that singularities along lines demand the use of anisotropic weight functions. If the integrand is singular along the edge $x_1 = 0$, the corresponding anisotropic weight function is $\Phi_{\beta,\alpha_1,l}(\vec{x}) = x_1^{\beta+\alpha_1-l}$.*

d) *The spaces $\mathcal{B}^l_\beta(\Omega_{ref})$ and the weight functions $\Phi_{\beta,\vec{\alpha},l}$ are designed to examine functions characterised by the order of growth of their derivatives that are singular at one single point, which in this case is the origin. A generalisation to arbitrary domains Ω and point singularities in arbitrary locations is straightforward. If a function is singular at two points in an integration domain Ω, the integration domain is split into two subdomains Ω_1 and Ω_2 such that each Ω_i contains only one singular point. The function then belongs to the two spaces $\mathcal{B}^l_\beta(\Omega_i)$. These splits also need to be realised in the implementation of the composite quadrature method investigated in [141]; see Section 2.5.3 as well.*

e) *It follows immediately from Assumption 2.5 and the chain rule that admissible kernel functions belong to certain classes $\mathcal{B}^l_\beta$ as one dimensional integrands on boundary edges e and for given evaluation point $\vec{x} \in \mathbb{R}^2$. After possibly subdiving $e = \bigcup_{m\geq 1} e_m$ in a way that guarantees that each edge $e_m \subseteq e$ contains only one singularity, there holds, in the local variable μ of e, $k(\vec{x} - \cdot) = k(\vec{x} - \cdot)(\mu) \in \mathcal{B}^l_\beta(e_m)$ for some $l \geq 0$ that depends on κ_1 and κ_2. See the proof of Theorem 2.22 for technical details.*

Different types of singularities of $P_{R,e}[\varphi]$ were classified in Definition 2.11. These singularities only occur in certain subregions of $E(0, R; e)$, and we therefore introduce a decomposition of $E(0, R; e)$ in terms of $\mathbb{B}_R(\vec{a})$ and $\mathbb{B}_R(\vec{b})$ that is similar to [127, Lemma 3.6]:

$$S_1 := \mathbb{B}_R(\vec{a}) \setminus \overline{\mathbb{B}}_R(\vec{b}) \qquad S_2 := \mathbb{B}_R(\vec{b}) \setminus \overline{\mathbb{B}}_R(\vec{a}) \qquad S_3 := \mathbb{B}_R(\vec{a}) \cap \mathbb{B}_R(\vec{b})$$
$$S_4 := E(0, R; e) \setminus \left(\bar{S}_1 \cup \bar{S}_2 \cup \bar{S}_3\right). \tag{2.99}$$

The decomposition is illustrated in Figure 2.10. The domain S_3 corresponds to the ellipse-shaped hole (2.66) and vanishes for $R \leq \frac{|e|}{2}$.

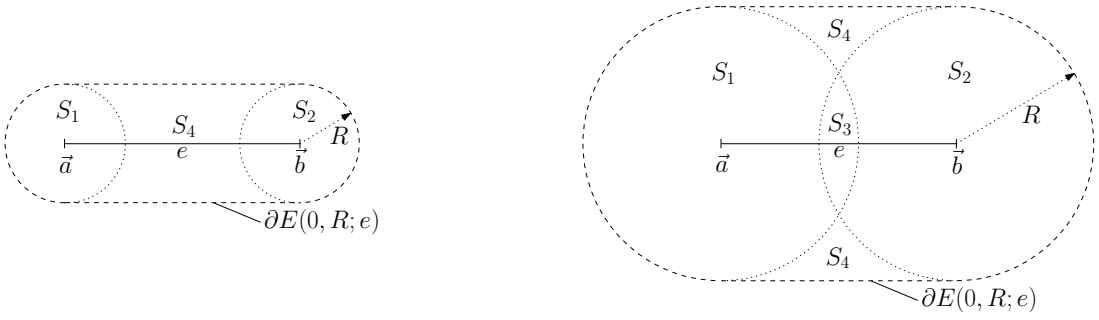

(a) decomposition of $E(0, R; e)$ for $R \leq \frac{|e|}{2}$ (b) decomposition of $E(0, R; e)$ for $R > \frac{|e|}{2}$

Figure 2.10: Decomposition (2.99) of $E(0, R; e)$ for different values of R. After [127, Figure 3.8].

The gradient of $P_{R,e}[\varphi]$, which was given in Lemma 2.3, can be written as

$$\nabla_{\vec{x}} \left(P_{R,e}[\varphi]\right)(\vec{x}) = \tag{2.100}$$
$$\begin{cases} P_{R,e}[\nabla_{\vec{x}}\varphi](\vec{x}) + k(\vec{x} - \vec{a}, \vec{n}_{\vec{x}}, \vec{n})\varphi(\vec{a})(\vec{b} - \vec{a}) + \sum_{\vec{y}\in e\cap\partial\mathbb{B}_R(\vec{x})} k(\vec{x} - \vec{y}, \vec{n}_{\vec{x}}, \vec{n})\varphi(\vec{y}) \left(\nabla_{\vec{x}} R'(\vec{x})\right) & \vec{x} \in S_1 \\ P_{R,e}[\nabla_{\vec{x}}\varphi](\vec{x}) - k(\vec{x} - \vec{b}, \vec{n}_{\vec{x}}, \vec{n})\varphi(\vec{b})(\vec{b} - \vec{a}) + \sum_{\vec{y}\in e\cap\partial\mathbb{B}_R(\vec{x})} k(\vec{x} - \vec{y}, \vec{n}_{\vec{x}}, \vec{n})\varphi(\vec{y}) \left(\nabla_{\vec{x}} R'(\vec{x})\right) & \vec{x} \in S_2 \\ P_{R,e}[\nabla_{\vec{x}}\varphi](\vec{x}) & \vec{x} \in S_3 \\ P_{R,e}[\nabla_{\vec{x}}\varphi](\vec{x}) + \left(\nabla_{\vec{x}} R'(\vec{x})\right) \sum_{\vec{y}\in e\cap\partial\mathbb{B}_R(\vec{x})} k(\vec{x} - \vec{y}, \vec{n}_{\vec{x}}, \vec{n})\varphi(\vec{y}) & \vec{x} \in S_4. \end{cases}$$

Regarding derivatives of higher order, we note that $P_{R,e}[\nabla_{\vec{x}}\varphi](\vec{x})$ simply reiterates the same terms with the density φ replaced by its corresponding derivative, and needs no further consideration. Further,

$$\sum_{\vec{y}\in e\cap\partial\mathbb{B}_R(\vec{x})} k(\vec{x}-\vec{y},\vec{n}_{\vec{x}},\vec{n}_{\vec{y}})\varphi(\vec{y}) = \kappa(R;R) \sum_{\vec{y}\in e\cap\partial\mathbb{B}_R(\vec{x})} f_k(\vec{x}-\vec{y},\vec{n}_{\vec{x}},\vec{n}_{\vec{y}})$$

due to (2.92). The term $\kappa(R;R)$ exists by assumption, while $f_k(\vec{x}-\vec{y},\vec{n}_{\vec{x}},\vec{n}_{\vec{y}})$ is regular with vanishing second derivative. We conclude that the regularity of $\nabla_{\vec{x}}\,(P_{R,e}[\varphi])$, and therewith of $P_{R,e}[\varphi]$, depends crucially on the regularity of R' in S_1, S_2 and S_4, and on the regularity of the kernel function k, which is weakly singular for $|\vec{x}-\vec{y}| = R$ and can be weakly singular for $|\vec{x}-\vec{y}| = 0$, in S_1 and S_2. If k is indeed weakly singular for $|\vec{x}-\vec{y}| = 0$, we subdivide S_1 and S_2 as

$$S_1 = \big(\overline{\mathbb{B}}_{r_1}(\vec{a})\cap S_1\big)\cup\big(S_1\setminus\overline{\mathbb{B}}_{r_1}(\vec{a})\big) =: S_{1,1}\cup S_{1,2} \quad \text{and} \quad S_2 = \big(\overline{\mathbb{B}}_{r_1}(\vec{b})\cap S_2\big)\cup S_2\setminus\overline{\mathbb{B}}_{r_1}(\vec{b}) =: S_{2,1}\cup S_{2,2} \tag{2.101}$$

where $r_1 < R$. In what follows, we specify countably normed spaces with suitable weight functions in local coordinates for each of the domains S_i in order to establish the regularity of $P_{R,e}[\varphi]$ on them.

Regularity on S_1 and S_2

Let us consider the domain S_1 and the end point singularities first. We introduce a local polar coordinate system with centre $\vec{a}$ so that

$$\vec{x} = \vec{a} + r\cos\theta\ \vec{n} + r\sin\theta\frac{1}{|\vec{d}|}\,\vec{d} \qquad\qquad 0\le\theta<2\pi,\ 0\le r\le R \tag{2.102}$$

for every $\vec{x}\in S_1$, with $0\le r\le r_1$ for $\vec{x}\in S_{1,1}$ and $r_1 < r\le R$ for $\vec{x}\in S_{1,2}$. Obviously, $|\vec{x}-\vec{a}| = r$, and thus $\kappa(R;|\vec{x}-\vec{a}|) = \kappa(R;r)$ for any $\vec{x}\in S_1$. Due to Assumption 2.5, $k(\vec{x}-\vec{a},\vec{n}_{\vec{x}},\vec{n}) = \kappa(R;|\vec{x}-\vec{a}|)f_k(\vec{x}-\vec{a},\vec{n}_{\vec{x}},\vec{n})$ with $f_k(\vec{x}-\vec{a},\vec{n}_{\vec{x}},\vec{n})\equiv 1$ or $f_k(\vec{x}-\vec{a},\vec{n}_{\vec{x}},\vec{n}) = (\vec{x}-\vec{a})\cdot\vec{n}_{\vec{y}}$ or $f_k(\vec{x}-\vec{a},\vec{n}_{\vec{x}},\vec{n}) = \vec{n}_{\vec{x}}\cdot\vec{n}$. For $f_k\equiv 1$, the kernel function k is simply equal to the θ-independent function κ. Secondly, $f_k(\vec{x}-\vec{a},\vec{n}_{\vec{x}},\vec{n}) = (\vec{x}-\vec{a})\cdot\vec{n} = r\cos\theta$ in polar coordinates. Finally, for $f_k(\vec{x}-\vec{a},\vec{n}_{\vec{x}},\vec{n}) = \vec{n}_{\vec{x}}\cdot\vec{n}$, we assume that $\vec{n}_{\vec{x}}$ is the normal vector of a given boundary edge and therefore independent of r and θ. We conclude that, in all three cases,

$$\left|\frac{\partial^{\alpha_1+\alpha_2}}{\partial r^{\alpha_1}\partial\theta^{\alpha_2}}k(\vec{x}-\vec{a},\vec{n}_{\vec{x}},\vec{n})\right| \le 2\left|f_k(\vec{x}-\vec{a},\vec{n}_{\vec{x}},\vec{n})\frac{d^{\alpha_1}}{dr^{\alpha_1}}\kappa(R;r)\right| \le 2C_{1,1}C_{1,2}^{\alpha_1}\ \alpha_1!\ r^{\min\{\kappa_1-\alpha_1,0\}} \tag{2.103}$$

for $(r,\theta)\in S_{1,1}$ and therefore

$$\left\|\frac{\partial^{\alpha_1+\alpha_2}}{\partial r^{\alpha_1}\partial\theta^{\alpha_2}}k(\vec{x}-\vec{a},\vec{n}_{\vec{x}},\vec{n})\,\Phi_{\beta,\vec{\alpha},l}\right\|^2_{L^2(S_{1,1})} \le 4\pi C_{1,1}^2C_{1,2}^{\alpha_1}\ \alpha_1!^2\int_0^{r_1} r^{\min\{2(\kappa_1-\alpha_1),0\}}\left(\Phi_{\beta,\vec{\alpha},l}(r)\right)^2\,dr \tag{2.104}$$

for any $\vec{\alpha}\in\mathbb{N}_0^2$. With $\Phi_{\beta,\vec{\alpha},l}(r) = r^{\beta+\alpha_1-l}$, the integral in (2.104) is finite if and only if $\beta > l-\kappa_1-\frac{1}{2}$. In Example 2.8 c) and d), we considered two kernel functions with $\kappa_1 = 0$ and $\kappa_1 = -1$, respectively. For these two kernel functions, we have $k\in\mathcal{B}^0_\beta(S_{1,1})$ for $\kappa_1 = -1$ and $\beta > \frac{1}{2}$, and $k\in\mathcal{B}^1_\beta(S_{1,1})$ for $\kappa_1 = 0$ and $\beta > \frac{1}{2}$, where

$$\mathcal{B}^l_\beta(S_{1,1}) = \left\{ u\in H^{l-1}(S_{1,1}) \ \middle|\ \left\|\frac{\partial^{\alpha_1+\alpha_2}u}{\partial r^{\alpha_1}\partial\theta^{\alpha_2}}\ \Phi_{\beta,\vec{\alpha},l}\right\|_{L^2(S_{1,1})} \le Cd^{|\vec{\alpha}|-l}(|\vec{\alpha}|-l)!\ \forall|\vec{\alpha}| = |(\alpha_1,\alpha_2)|\ge l \right\} \tag{2.105}$$

for $l \geq 1$ and

$$\mathcal{B}^0_\beta(S_{1,1}) = \left\{ u \;\middle|\; \left\| \frac{\partial^{\alpha_1+\alpha_2} u}{\partial r^{\alpha_1} \partial \theta^{\alpha_2}} \, \Phi_{\beta,\vec{\alpha},0} \right\|_{L^2(S_{1,1})} \leq C d^{|\vec{\alpha}|} |\vec{\alpha}|! \text{ for any } \vec{\alpha} = (\alpha_1, \alpha_2) \in \mathbb{N}_0^2 \right\}$$

for $l = 0$, where $C = C(u) \geq 0$ and $d = d(u) \geq 1$ are independent of $|\vec{\alpha}|$.

Regarding the circular light disc singularities on $S_{1,2}$ we have, similarly to (2.103),

$$\left| \frac{\partial^{\alpha_1+\alpha_2}}{\partial r^{\alpha_1} \partial \theta^{\alpha_2}} k(\vec{x} - \vec{a}, \vec{n}_{\vec{x}}, \vec{n}) \right| \leq C_{2,1} \left(\max\{1, R - r\} + C_{2,2}^{-1} \max\{R, 1\} \right) C_{2,2}^{\alpha_1} \, \alpha_1! \, (R - r)^{\min\{\kappa_2 - \alpha_1, 0\}}$$

for $(r, \theta) \in S_{1,2}$, and therefore

$$\left\| \frac{\partial^{\alpha_1+\alpha_2}}{\partial r^{\alpha_1} \partial \theta^{\alpha_2}} k(\vec{x} - \vec{a}, \vec{n}_{\vec{x}}, \vec{n}) \, \Phi_{\beta,\vec{\alpha},l} \right\|^2_{L^2(S_{1,2})} \leq 4\pi \tilde{C}_{2,1}^2 C_{2,2}^{2\alpha_1} \, \alpha_1!^2 \int_{r_1}^{R} (R-r)^{\min\{2(\kappa_2 - \alpha_1), 0\}} \left(\Phi_{\beta,\vec{\alpha},l}(r) \right)^2 \, dr \tag{2.106}$$

for any $\vec{\alpha} \in \mathbb{N}_0^2$, with $\tilde{C}_{2,1} := C_{2,1} \left(\max\{1, R - r_1\} + C_{2,2}^{-1} \max\{R, 1\} \right)$. With $\Phi_{\beta,\vec{\alpha},l}(r) = (R - r)^{\beta+\alpha_1-l}$, the integral in (2.106) is finite if and only if $\beta > l - \kappa_2 - \frac{1}{2}$. In Example 2.8 a) and b), we considered two kernel functions with $\kappa_2 = \frac{1}{2}$. For these kernel functions, there holds $k \in \mathcal{B}^1_\beta(S_{1,2})$ for $\beta > 0$, where $\mathcal{B}^l_\beta(S_{1,2})$ is defined similarly to (2.105).

This finishes the analysis of the end point and circular light disc singularities on S_1 and S_2. We summarise our results in Lemma 2.15.

Lemma 2.15 (Regularity of $k(\vec{x} - \vec{a}, \vec{n}_{\vec{x}}, \vec{n})$ on S_1 and of $k(\vec{x} - \vec{b}, \vec{n}_{\vec{x}}, \vec{n})$ on S_2)
Let k be an admissible kernel function. For the term $k(\vec{x} - \vec{a}, \vec{n}_{\vec{x}}, \vec{n})$ that appears in the gradient of $P_{R,e}[\varphi]$ on S_1, see (2.100), there holds

a) $k(\vec{x} - \vec{a}, \vec{n}_{\vec{x}}, \vec{n}) \in \mathcal{B}^1_\beta(S_{1,2})$ for $\beta > \frac{1}{2} - \kappa_2$ if $0 \leq \kappa_2 \leq \frac{1}{2}$, and $k(\vec{x} - \vec{a}, \vec{n}_{\vec{x}}, \vec{n}) \in \mathcal{B}^2_\beta(S_{1,2})$ for $\beta > \frac{3}{2} - \kappa_2$ if $\frac{1}{2} < \kappa_2 \leq \frac{3}{2}$, with weight function $\Phi_{\beta,\vec{\alpha},l}(r) = (R - r)^{\beta+\alpha_1-l}$ for $l = 1$ and $l = 2$, respectively

b) $k(\vec{x} - \vec{a}, \vec{n}_{\vec{x}}, \vec{n}) \in \mathcal{B}^0_\beta(S_{1,1})$ for $\beta > -\kappa_1 - \frac{1}{2}$ if $-1 \leq \kappa_1 \leq -\frac{1}{2}$, and $k(\vec{x} - \vec{a}, \vec{n}_{\vec{x}}, \vec{n}) \in \mathcal{B}^1_\beta(S_{1,1})$ for $\beta > -\kappa_1 + \frac{1}{2}$ if $-\frac{1}{2} < \kappa_1 \leq \frac{1}{2}$, with weight function $\Phi_{\beta,\vec{\alpha},l}(r) = r^{\beta+\alpha_1-l}$ for $l = -1$ and $l = 0$, respectively

where the spaces $\mathcal{B}^l_\beta(S_{i,j})$ are given by (2.105). Analogous results hold for the term $k(\vec{x} - \vec{b}, \vec{n}_{\vec{x}}, \vec{n})$ that appears in the gradient of $P_{R,e}[\varphi]$ on S_2.

We note that the planar light disc singularities in S_1 and S_2, i.e. the singularities of $R'(\vec{x}) = \sqrt{R^2 - |\vec{x} - \vec{x}'|}$, are point singularities in $\vec{x} = \vec{a} \pm R\vec{n} \in \partial S_1$ and $\vec{x} = \vec{b} \pm R\vec{n} \in \partial S_2$, respectively. In the polar coordinates of S_1, these are the points $(r, \theta) = (R, 0)$ and $(r, \theta) = (R, \pi)$. Since these point singularities of R' appear on lines parallel to $\vec{d}$, the tangential derivatives, which correspond to singularities with respect to θ in polar coordinates, in these points are also singular, as we find below. This affects the regularity of the function R', and therewith the regularity of $P_{R,e}[\varphi]$. We introduce two additional lunar subdomains $S^1_{1,2}$ and $S^2_{1,2}$ to separate these singularities from the rest of the domain, where only circular light disc singularities appear,

$$S^1_{1,2} := S_{1,2} \cap \mathbb{B}_\varepsilon(\vec{a} + R\vec{n}) \subseteq S_{1,2} \quad \text{and} \quad S^2_{1,2} := S_{1,2} \cap \mathbb{B}_\varepsilon(\vec{a} - R\vec{n}) \subseteq S_{1,2} \tag{2.107}$$

with $\varepsilon > 0$. The subdomains $S^1_{2,2}$ and $S^2_{2,2}$ of $S_{2,2}$ are defined in the same way.

There obviously holds $\vec{x}' = \vec{a} + r\sin\theta\frac{1}{|\vec{d}|}\vec{d}$ for every $\vec{x} \in S_1$, and therefore

$$|\vec{x} - \vec{x}'|^2 = |r\cos\theta\ \vec{n} + (r-R)\sin\theta\frac{1}{|\vec{d}|}\vec{d}|^2 = r^2\cos^2\theta + (R-r)^2\sin^2\theta.$$

Consequently,

$$R'(\vec{x}) = \sqrt{R^2 - |\vec{x} - \vec{x}'|^2} = \sqrt{R^2 - (R-r)^2 - (r^2 - (R-r)^2)\cos^2\theta} = R'(r,\theta) \tag{2.108}$$

for $\vec{x} \in S_1$. Obviously $R' \in L^2(S_1)$. The derivatives with respect to r and θ are given by

$$\frac{\partial R'}{\partial r} = \left(R^2 - (R-r)^2 - (r^2 - (R-r)^2)\cos^2\theta\right)^{-1/2} \underbrace{(R - r - R\cos^2\theta)}_{=-r+R\sin^2\theta}$$

and

$$\frac{\partial R'}{\partial \theta} = \left(R^2 - (R-r)^2 - (r^2 - (R-r)^2)\cos^2\theta\right)^{-1/2} \underbrace{(r^2 - (R-r)^2)}_{R(2r-R)}\sin\theta\,\cos\theta$$

respectively. To simplify the notation, we set

$$f(r,\theta) := R^2 - (R-r)^2 - (r^2 - (R-r)^2)\cos^2\theta = r(2R-r) - R(2r-R)\cos^2\theta$$

The second derivatives of R' are

$$\begin{aligned}
\frac{\partial^2 R'}{\partial r^2} &= -f(r,\theta)^{-3/2}(-r + R\sin^2\theta)^2 - f(r,\theta)^{-1/2} = -f(r,\theta)^{-3/2}\left((-r+R\sin^2\theta)^2 + f(r,\theta)\right) \\
&= -R^2\left(\sin^4\theta + \cos^2\theta\right)f(r,\theta)^{-3/2} \\
\frac{\partial^2 R'}{\partial r\partial\theta} &= -f(r,\theta)^{-3/2}(-r + R\sin^2\theta)R(2r-R)\,\sin\theta\,\cos\theta + 2R\,\sin\theta\,\cos\theta f(r,\theta)^{-1/2} \\
&= -f(r,\theta)^{-3/2}R\sin\theta\,\cos\theta\left((-r+R\sin^2\theta)(2r-R) - 2f(r,\theta)\right) \\
&= -R^2\sin\theta\,\cos\theta\left((2r-R)(\sin^2\theta + 2\cos^2\theta) - 3r\right)f(r,\theta)^{-3/2} \\
\frac{\partial^2 R'}{\partial\theta^2} &= -f(r,\theta)^{-3/2}\left(R(2r-R)\,\sin\theta\,\cos\theta\right)^2 + \left(\cos^2\theta - \sin^2\theta\right)R(2r-R)f(r,\theta)^{-1/2} \\
&= -f(r,\theta)^{-3/2}\left\{(R(2r-R)\,\sin\theta\,\cos\theta)^2 - \left(\cos^2\theta - \sin^2\theta\right)R(2r-R)f(r,\theta)\right\} \\
&= -R(2r-R)\left(r(2R-r)(\sin^2\theta - \cos^2\theta) + (2r-R)\cos^4\theta\right)f(r,\theta)^{-3/2}.
\end{aligned}$$

Introducing the analytical function $\zeta(\theta) := \frac{\sin\theta}{\theta}$, we have $\sin\theta = \zeta(\theta)\theta$ and $\cos^2\theta = 1 - \sin^2\theta = 1 - \theta^2\zeta(\theta)^2$. Hence

$$f(r,\theta) = R^2 - (R-r)^2 - (r^2 - (R-r)^2)\left(1 - \theta^2\zeta(\theta)^2\right) = R^2 - r^2 + \theta^2\zeta(\theta)^2R(2r-R) \geq \theta^2\zeta(\theta)^2R(2r-R) \tag{2.109}$$

on $S^1_{1,2}$. Consequently

$$\left|\frac{\partial R'}{\partial\theta}\right| \leq \left|\theta^2\zeta(\theta)^2R(2r-R)\right|^{-1/2}R|2r-R|\,|\sin\theta\cos\theta| = \sqrt{R}\sqrt{|2r-R|}|\cos\theta| \leq R \tag{2.110}$$

on $S^1_{1,2}$. However, the derivative $\frac{\partial^2 R'}{\partial\theta^2}$ is not bounded in the same way, due to the presence of the $\cos^2\theta$-term in the second term in the first line. Every even-numbered derivative with respect to θ is of a similar form, and we need to choose the weight functions with this in mind.

To simplify the presentation, we introduce the new variable $\delta(r) := R - r \in [0, \varepsilon)$. Using (2.109), there holds

$$f(r,\theta) = \delta(2R-\delta) + \theta^2\zeta(\theta)^2 R(R-2\delta) = R(R-2\delta)\left(\frac{2R-\delta}{R(R-2\delta)}\delta + \theta^2\zeta(\theta)^2\right) \tag{2.111}$$

with $R - 2\varepsilon < R - 2\delta \leq R$ and $\frac{2R-\varepsilon}{R^2} < \frac{2R-\delta}{R(R-2\delta)} < \frac{2}{R-2\varepsilon}$. Choosing $\varepsilon < \frac{R}{N}$ with $N > 2$ there holds $\frac{N-2}{N}R < R - 2\delta \leq R$ and $\frac{2N-1}{N}\frac{1}{R} < \frac{2}{R-2\varepsilon} < \frac{2N}{N-2}\frac{1}{R}$. Introducing

$$h(\delta,\theta) := \left(\delta + \theta^2\right)^{1/2} \tag{2.112}$$

we have, from (2.111),

$$R'(r,\theta) = (f(r,\theta))^{1/2} = (R(R-2\delta))^{1/2}\; h\left(\frac{2R-\delta}{R(R-2\delta)}\delta, \theta\zeta(\theta)\right) \tag{2.113}$$

on $S^1_{1,2}$. The singularity of R' in $(r,\theta) = (R,0)$ correspond to a singularity at $(\delta,\theta) = (0,0)$. Since the additional factors in (2.113) are bounded and since ζ is analytic, it follows from the chain and product rules that the function h and its derivatives describe the leading order singularities in the derivatives of R' in the normal and tangential directions sufficiently. We therefore study the function h from here onwards.

Trivially,

$$\frac{\partial^{\alpha_1} h}{\partial \delta^{\alpha_1}} = (-1)^{\alpha_1+1}\frac{1}{2^{\alpha_1}}(2\alpha_1 - 3)!!\left(\delta+\theta^2\right)^{-\frac{2\alpha_1-1}{2}} \tag{2.114}$$

for $\alpha_1 \geq 1$, with $(-1)!! := 1$. The derivatives with respect to θ are of a more involved form. We set

$$g_m(r,\theta) := \left(\delta+\theta^2\right)^{-\frac{2m-1}{2}} \tag{2.115}$$

for $m \geq 0$, so that $h = g_0$ and $\frac{\partial^{\alpha_1} h}{\partial \delta^{\alpha_1}} = (-1)^{\alpha_1+1}\frac{1}{2^{\alpha_1}}(2\alpha_1-3)!!\, g_{\alpha_1}$. We first compute a recursion formula for the derivatives of g_1.

Lemma 2.16 (Derivatives of g_1)
The derivatives of g_1 are given by

$$\frac{\partial^{2n}}{\partial\theta^{2n}} g_1(r,\theta) = \sum_{k=0}^{n} (4n-2k-1)!!\; a(n,k)\; \left(\delta+\theta^2\right)^{-\frac{4n-2k+1}{2}}\; \theta^{2(n-k)} \tag{2.116}$$

and

$$\frac{\partial^{2n+1}}{\partial\theta^{2n+1}} g_1(r,\theta) = \sum_{k=0}^{n} (4n-2k+1)!!\; b(n,k)\; \left(\delta+\theta^2\right)^{-\frac{4n-2k+3}{2}}\; \theta^{2(n-k)+1} \tag{2.117}$$

for $n \geq 0$. The coefficients $a(n,k)$ are given recursively by

$$a(n,k) = a(n-1,k) - (4(n-k)+1)\, a(n-1,k-1) + 2((n-k)+1)(2(n-k)+1)\, a(n-1,k-2) \tag{2.118}$$

with $a(0,0) := 1$ and $a(n,k) := 0$ for $k < 0$ and $k > n$. The coefficients $b(n,k)$ are given by

$$b(n,k) = -a(n,k) + 2(n-k+1)\, a(n,k-1) \tag{2.119}$$

For convinience in the notation, we further set $(-1)!! := 1$. Clearly, (2.118) and (2.119) immediately imply $a(n,0) = 1$ and $b(n,0) = -1$ for any $n \geq 0$.

There hold the estimates

$$\sum_{k=0}^{n} (4n-2k-1)!!\,|a(n,k)| \le 3^n (4n-1)!! \tag{2.120}$$

and

$$\sum_{k=0}^{n} (4n-2k+1)!!\,|b(n,k)| \le 3^{n+1} (4n+1)!!. \tag{2.121}$$

Proof
The formula (2.116) clearly holds for $n = 0$. The induction step is

$$\begin{aligned}
&\frac{\partial^2}{\partial\theta^2}\left(\frac{\partial^{2n}}{\partial\theta^{2n}} g_1(r,\theta)\right) \\
= \;& \frac{\partial}{\partial\theta}\Bigg\{ \sum_{k=0}^{n} (4n-2k+1)!!\;(-1)\,a(n,k)\,\left(\delta+\theta^2\right)^{-\frac{4n-2k+3}{2}}\;\theta^{2(n-k)+1} \\
&\qquad + \sum_{k=0}^{n-1} (4n-2k-1)!!\;2(n-k)\,a(n,k)\,\left(\delta+\theta^2\right)^{-\frac{4n-2k+1}{2}}\;\theta^{2(n-k)-1}\Bigg\} \\
= \;& \sum_{k=0}^{n} (4n-2k+3)!!\,a(n,k)\,\left(\delta+\theta^2\right)^{-\frac{4n-2k+5}{2}}\;\theta^{2(n-k)+2} \\
&+ \sum_{k=0}^{n-1} (4n-2k+1)!!\;(2(n-k)+1)\;(-1)\,a(n,k)\,\left(\delta+\theta^2\right)^{-\frac{4n-2k+3}{2}}\;\theta^{2(n-k)} \\
&+ \sum_{k=0}^{n-1} (4n-2k+1)!!\;2(n-k)\;(-1)\,a(n,k)\,\left(\delta+\theta^2\right)^{-\frac{4n-2k+3}{2}}\;\theta^{2(n-k)} \\
&+ \sum_{k=0}^{n-2} (4n-2k-1)!!\;2(n-k)(2(n-k)-1)\,a(n,k)\,\left(\delta+\theta^2\right)^{-\frac{4n-2k+1}{2}}\;\theta^{2(n-k-1)}
\end{aligned}$$

which is (2.116), after shifting the index in the second and third sum by one, und by two in the fourth sum, and rearranging the terms, with coefficients

$$a(n+1,k) = \begin{cases} a(n,0) & k=0 \\ a(n,1) - (4n+1)a(n,0) & k=1 \\ a(n,k) - (4(n-k)+5)a(n,k-1) + 2(n-k+2)(2(n-k)+3)a(n,k-2) & 2 \le k \le n \\ -a(n,n) + 2a(n,n-1) & k = n+1 \end{cases}$$

These can be rewritten as (2.118), and (2.117) follows immediately from the proof of (2.116).

It remains to show (2.120). We set $S(n) := \sum_{k=0}^{n} (4n-2k-1)!!\,|a(n,k)|$. Obviously $S(0) = 1$. Using (2.118), we obtain

$$\begin{aligned}
S(n) \;\le\; & \sum_{k=0}^{n-1} (4n-2k-1)!!\,|a(n-1,k)| \;+\; \sum_{k=1}^{n} (4n-2k-1)!!\,(4(n-k)+1)\,|a(n-1,k-1)| \\
&+ \sum_{k=2}^{n} (4n-2k-1)!!\,2((n-k)+1)(2(n-k)+1)\,|a(n-1,k-2)| \;=:\; S_1 + S_2 + S_3
\end{aligned}$$

with

$$S_1 = \sum_{k=0}^{n-1} (4(n-1)-2k-1)!!\,(4(n-1)-2k-1)(4(n-1)-2k-3)\,|a(n-1,k)| \le (4n-3)(4n-1)\,S(n-1)$$

and

$$\begin{aligned} S_2 &= \sum_{k=0}^{n-1} (4n-2(k+1)-1)!!\,(4(n-(k+1))+1)\,|a(n-1,k)| \\ &= \sum_{k=0}^{n-1} (4(n-1)-2k-1)!!\,(4(n-1)-2k+1)(4(n-k)-3)\,|a(n-1,k)| \\ &\le (4n-3)(4n-1)\,S(n-1) \end{aligned}$$

and

$$\begin{aligned} S_3 &= \sum_{k=0}^{n-2} (4n-2(k+2)-1)!!\,2((n-(k+2))+1)(2(n-(k+2))+1)\,|a(n-1,k)| \\ &= \sum_{k=0}^{n-2} (4(n-1)-2k-1)!!\,2(n-k-1)(2(n-k)-3)\,|a(n-1,k)| \\ &\le 2(n-1)(2n-3)S(n-1) \le (4n-1)(4n-3)S(n-1) \end{aligned}$$

for any $n \ge 1$. Hence

$$S(n) \le 3(4n-1)(4n-3)\,S(n-1)$$

for any $n \ge 1$. This estimate can be iterated to obtain (2.120).

To show (2.121), we observe that

$$\begin{aligned} &\sum_{k=0}^{n} (4n-2k+1)!!\,|b(n,k)| \\ \le\ & \sum_{k=0}^{n} (4n-2k+1)!!\,|a(n,k)| + \sum_{k=1}^{n} (4n-2k+1)!!\,2(n-k+1)\,|a(n,k-1)| \\ =\ & \sum_{k=0}^{n} (4n-2k-1)!!\,(4n-2k+1)\,|a(n,k)| + \sum_{k=0}^{n-1} (4n-2k-1)!!\,2(n-k)\,|a(n,k)| \\ \le\ & (4n+1)\,S(n) + 2n\,S(n) \le 3(4n+1)\,S(n). \end{aligned}$$

(2.121) now follows immediately from (2.120). ∎

In the same way, we obtain a general formula for the derivatives of g_m.

Corollary 2.17 (Derivatives of g_m)
The derivatives of g_m with $m \ge 0$ are given by

$$\frac{\partial^{2n}}{\partial\theta^{2n}} g_m(r,\theta) = \frac{1}{(2m-1)!!} \sum_{k=0}^{n} (2m+4n-2k-3)!!\ a(n,k)\ \left(\delta+\theta^2\right)^{-\frac{2m-1+4n-2k}{2}}\ \theta^{2(n-k)} \tag{2.122}$$

and

$$\frac{\partial^{2n+1}}{\partial\theta^{2n+1}} g_m(r,\theta) = \frac{1}{(2m+1)!!} \sum_{k=0}^{n} (2m+4n-2k-1)!!\ b(n,k)\ \left(\delta+\theta^2\right)^{-\frac{2m+1+4n-2k}{2}}\ \theta^{2(n-k)+1} \tag{2.123}$$

for $n \ge 0$. The coefficients $a(n,k)$ and $b(n,k)$ are the same as the ones in Lemma 2.16 and are given by (2.118) *and* (2.119)*, respectively.*

There hold the estimates

$$\sum_{k=0}^{n} (2m+4n-2k-3)!!\,|a(n,k)| \le 3^n (2m+4n-3)!! \tag{2.124}$$

and

$$\sum_{k=0}^{n} (2m+4n-2k-1)!!\,|b(n,k)| \le 3^{n+1}(2m+4n-1)!!. \tag{2.125}$$

Using (2.114), we obtain

$$\frac{\partial^{\alpha_1+\alpha_2} h}{\partial\delta^{\alpha_1}\partial\theta^{\alpha_2}} = (-1)^{\alpha_1+1}\frac{1}{2^{\alpha_1}}(2\alpha_1-3)!!\,\frac{\partial^{\alpha_2}}{\partial\theta^{\alpha_2}} g_{\alpha_1} \tag{2.126}$$

where the term $\frac{\partial^{\alpha_2}}{\partial\theta^{\alpha_2}} g_{\alpha_1}$ is now known from Corollary 2.17. We observe that $\frac{\partial^{\alpha_1+\alpha_2} h}{\partial\delta^{\alpha_1}\partial\theta^{\alpha_2}}$ involves terms of the type

$$\left(\delta+\theta^2\right)^{-\frac{2\alpha_1-1+2\alpha_2-2k}{2}} \theta^{\alpha_2-2k} = \left(\delta+\theta^2\right)^{-\frac{2\alpha_1-1}{2}} \left(\delta+\theta^2\right)^{-(\alpha_2-k)} \theta^{\alpha_2-2k}$$

for $0 \le k \le \left\lfloor \frac{\alpha_2}{2} \right\rfloor$. Let us assume that $\alpha_1, \alpha_2 \ge 1$, so that the exponents of the $\left(\delta+\theta^2\right)$-terms are both negative. This is no loss of generality since, if $\alpha_1 = 0$ or $\alpha_2 = 0$, the corresponding terms are bounded. Using $\delta+\theta^2 \ge \delta$ and $\delta+\theta^2 \ge \theta^2$, there holds

$$\left(\delta+\theta^2\right)^{-\frac{2\alpha_1-1+2\alpha_2-2k}{2}} \theta^{\alpha_2-2k} \le \delta^{-\alpha_1+\frac{1}{2}}\,\theta^{-\alpha_2} \tag{2.127}$$

This suggest to choose weight functions of type $\delta^{\alpha_1+\beta-l}\theta^{\alpha_2+\beta-l}$ for any $\vec{\alpha} \in \mathbb{N}_0^2$. In the original coordinates, these correspond to weight functions $(R-r)^{\alpha_1+\beta-l}\,\theta^{\alpha_2+\beta-l}$.

Formally, combining (2.126) and (2.127) with Corollary 2.17 with $2n = \alpha_2$ or $2n+1 = \alpha_2$ and $m = \alpha_1$,

$$\left|\frac{\partial^{\alpha_1+\alpha_2} h}{\partial\delta^{\alpha_1}\partial\theta^{\alpha_2}}\,\delta^{\alpha_1+\beta-l}\theta^{\alpha_2+\beta-l}\right| \le \left(\frac{1}{2}\right)^{\alpha_1} 3^{\alpha_2}\,(2\alpha_1+2\alpha_2-1)!!\,\delta^{\frac{1}{2}+\beta-l}\theta^{\beta-l}$$

where $(2\alpha_1+2\alpha_2-1)!! \le 2^{|\vec{\alpha}|}\,|\vec{\alpha}|! \le 4^{|\vec{\alpha}|}\,(|\vec{\alpha}|-1)!$, and hence

$$\left|\frac{\partial^{\alpha_1+\alpha_2} h}{\partial\delta^{\alpha_1}\partial\theta^{\alpha_2}}\,\delta^{\alpha_1+\beta-l}\theta^{\alpha_2+\beta-l}\right| \le 12^{|\vec{\alpha}|+1}\,(|\vec{\alpha}|-1)!\,\delta^{\frac{1}{2}+\beta-l}\theta^{\beta-l}.$$

Choosing $l = 1$ and $\beta > 0$, there holds $\left\| \frac{\partial^{\alpha_1+\alpha_2} h}{\partial\delta^{\alpha_1}\partial\theta^{\alpha_2}}\,\delta^{\alpha_1+\beta-1}\theta^{\alpha_2+\beta-1} \right\|_{L^2(S^1_{1,2})} < 12^{|\vec{\alpha}|+1}\,(|\vec{\alpha}|-1)!$ for any $\vec{\alpha} \in \mathbb{N}_0^2$, and therefore $h \in \mathcal{B}^1_\beta(S^1_{1,2})$ for any $\beta > 0$. We discussed above that the singularities of leading order in the derivatives of R' are sufficiently described by the singularities in the corresponding singularities of h. We therefore conclude the regularity of R' in Lemma 2.18.

Lemma 2.18 (Regularity of R' on $S^k_{1,2}$ and $S^k_{2,2}$ for $k = 1, 2$)
For the function R' that appears in the gradient of $P_{R,e}[\varphi]$ on S_i, see (2.100), there holds $R' \in \mathcal{B}^1_\beta(S^k_{i,2})$ for $\beta > 0$ with weight function $\Phi_{\beta,\vec{\alpha},1}(r,\theta) = (R-r)^{\beta+\alpha_1-1}\,\theta^{\beta+\alpha_2-1}$ for $i = 1, 2$ and $k = 1, 2$, where the spaces $\mathcal{B}^1_\beta(S^k_{i,2})$ are given by (2.105).

Remark 2.19 (On the Weight Functions on $S_{1,2}$ and $S_{2,2}$)
The weight function $(R-r)^{\beta+\alpha_1-1}\,\theta^{\beta+\alpha_2-1}$ used in Lemma 2.18 reproduces the weight function $(R-r)^{\beta+\alpha_1-l}$ that was introduced for the circular light disc singularities in Lemma 2.15 a) as one of its factors. Regarding the implementation of quadrature schemes on $S_{i,2}$, $i = 1, 2$, this means that the corresponding quadrature meshes overlap. In the context of this work, this is of no particular interest, since we only need to implement one dimensional quadrature methods on edges that are intersected with $E(0, R; e)$, as in Theorem 2.22. For problems that involve the Newton potential, however, we need to consider intersections of $E(0, R; e)$ and triangles or squares, and two dimensional quadrature meshes then become crucial.

Regularity on S_4

On S_4, we only need to analyse the planar light disc singularities that are induced by R'. We note that S_4 can be written as

$$S_4 = \left\{ \vec{m}_i + \mu\vec{d} + \nu\vec{n} \;\;\middle|\;\; -R \le \nu \le R\,,\ -1 \le \mu \le 1\,,\ (\mu+1)^2 + \nu^2 > R^2\,,\ (\mu-1)^2 + \nu^2 > R^2 \right\} \tag{2.128}$$

where the last two conditions express $|\vec{x} - \vec{a}|^2 > R^2$ and $|\vec{x} - \vec{b}|^2 > R^2$ for any $\vec{x} \in S_4$. We define countably normed spaces $\mathcal{B}^l_\beta(S_4)$ with weight function $\Phi_{\beta,\vec{\alpha},l}$ by

$$\mathcal{B}^l_\beta(S_4) = \left\{ u \in H^{l-1}(S_4) \;\;\middle|\;\; \left\| \frac{\partial^{\alpha_1+\alpha_2} u}{\partial\mu^{\alpha_1}\partial\nu^{\alpha_2}}\ \Phi_{\beta,\vec{\alpha},l} \right\|_{L^2(S_4)} \le C d^{|\vec{\alpha}|-l} (|\vec{\alpha}| - l)!\ \forall |\vec{\alpha}| = |(\alpha_1,\alpha_2)| \ge l \right\} \tag{2.129}$$

for $l \ge 1$ and

$$\mathcal{B}^0_\beta(S_4) = \left\{ u \;\;\middle|\;\; \left\| \frac{\partial^{\alpha_1+\alpha_2} u}{\partial\mu^{\alpha_1}\partial\nu^{\alpha_2}}\ \Phi_{\beta,\vec{\alpha},0} \right\|_{L^2(S_4)} \le C d^{|\vec{\alpha}|} |\vec{\alpha}|! \text{ for any } \vec{\alpha} = (\alpha_1,\alpha_2) \in \mathbb{N}_0^2 \right\}$$

for $l = 0$, where $C = C(u) \ge 0$ and $d = d(u) \ge 1$ are independent of $|\vec{\alpha}|$.

Since $\vec{x}' = \vec{m}_i + \mu\vec{d}$, there holds $|\vec{x} - \vec{x}'|^2 = \nu^2$ for any $\vec{x} \in S_4$, and therefore

$$R'(\vec{x}) = \sqrt{R^2 - ((\vec{p} - \vec{x}) \cdot \vec{n})^2} = \sqrt{R^2 - |\vec{x} - \vec{x}'|^2} = \sqrt{R^2 - \nu^2} = R'(\nu) \tag{2.130}$$

for any $\vec{x} \in S_4$. In order to separate the two locations of the singularities, we subdivide S_4 as

$$S_4 = \{\, \vec{x} \in S_4 \;\mid\; \nu \ge 0 \,\} \cup \{\, \vec{x} \in S_4 \;\mid\; \nu < 0 \,\} =: S_{4,1} \cup S_{4,2} = S_{4,1} \cup (S_4 \setminus S_{4,2})\,. \tag{2.131}$$

There clearly holds $R' \in L^2(S_{4,i})$ for $i = 1, 2$. It was shown in [127, p. 34] that

$$\frac{d^n R'}{d\nu^n} = \left(R^2 - \nu^2\right)^{-\frac{2n-1}{2}} p_n(\nu) \tag{2.132}$$

for $n \ge 0$, where p_n is a polynomial of degree n with $|p_n(\nu)| \le C \max\left\{1, R^2\right\}^{n-1} (n-1)!\ \max|\nu|^n$. Alternatively, one can conclude a similar bound from Corollary 2.17. Clearly, $\frac{\partial^{|\vec{\alpha}|} R'}{\partial^{\alpha_1}\nu\partial^{\alpha_2}\mu} = 0$ for $\alpha_2 \ne 0$, and therefore, for any $\vec{\alpha} \in \mathbb{N}_0^2$,

$$\begin{aligned} \left\| \frac{\partial^{|\vec{\alpha}|} R'}{\partial^{\alpha_1}\nu\partial^{\alpha_2}\mu} \Phi_{\beta,\vec{\alpha},l} \right\|_{L^2(S_{4,1})} &\le \left\| \frac{d^{\alpha_1} R'}{d^{\alpha_1}\nu} \Phi_{\beta,\vec{\alpha},l} \right\|_{L^2(S_{4,1})} \\ &\le C \max\left\{1, R^2\right\}^{\alpha_1 - 1} (\alpha_1 - 1)!\, R^{\alpha_1} \left(\int_{-1}^{1} \int_0^R \left(R^2 - \nu^2\right)^{-(2\alpha_1 - 1)} \Phi^2_{\beta,\vec{\alpha},l}(\nu)\, d\nu\, d\mu \right)^{1/2} \end{aligned} \tag{2.133}$$

where the integral on the right hand side is finite if the weight function $\Phi_{\beta,\vec{\alpha},l}(\nu) = (R - \nu)^{\beta + \alpha_1 - l}$ with $l = 1$ and $\beta > 0$ is chosen. Hence $R' \in \mathcal{B}^1_\beta(S_{4,i})$ for $i = 1, 2$. We summarise our results in Lemma 2.20.

Lemma 2.20 (Regularity of R' on S_4)
For the function R' that appears in the gradient of $P_{R,e}[\varphi]$ on S_4, see (2.100)*, there holds $R' \in \mathcal{B}^1_\beta(S_{4,i})$ for $\beta > 0$ with weight function $\Phi_{\beta,\vec{\alpha},1}(\nu) = \left(R^2 - \nu^2\right)^{\beta+\alpha_1-1}$ for $i = 1, 2$, where the spaces $\mathcal{B}^1_\beta(S_{4,i})$ are given by* (2.129)*.*

We finally obtain a full characterisation of $P_{R,e}[\varphi]$ on the subdomains considered above. We recall that, beginning from (2.99), we divided $E(0,R;e)$ via (2.101), (2.107) and (2.131) into pairwise disjoint subsets

$$E(0,R;e) = \bigcup_{S\in\mathcal{S}} S \qquad \text{with} \qquad \mathcal{S} := \bigcup_{i=1,2} \left\{ S_{i,1}, S_{i,2}^1, S_{i,2}^2, S_{i,3}, S_{4,i} \right\} \cup \{S_3\} \tag{2.134}$$

with, for $r_1 = \frac{R}{2}$,

$$\begin{aligned}
S_{1,1} &:= \bar{\mathbb{B}}_{\frac{R}{2}}(\vec{a}) \setminus \bar{\mathbb{B}}_R(\vec{b}) \qquad S_{1,2}^1 := \bar{\mathbb{B}}_R(\vec{a}) \cap \mathbb{B}_\varepsilon(\vec{a}+R\vec{n}) \qquad S_{1,2}^2 := \bar{\mathbb{B}}_R(\vec{a}) \cap \mathbb{B}_\varepsilon(\vec{a}-R\vec{n}) \\
S_{1,3} &:= \left(\bar{\mathbb{B}}_R(\vec{a}) \setminus \bar{\mathbb{B}}_R(\vec{b})\right) \setminus \left(\bar{\mathbb{B}}_{\frac{R}{2}}(\vec{a}) \cup S_{i,2}^1 \cup S_{i,2}^2\right) \\
S_3 &:= \mathbb{B}_R(\vec{a}) \cap \mathbb{B}_R(\vec{b}) \\
S_{4,1} &:= \left(E(0,R;e) \setminus \left(\bar{S}_1 \cup \bar{S}_2 \cup \bar{S}_3\right)\right) \cap \{\, \vec{x} \in E(0,R;e) \;\mid\; (\vec{x}-\vec{m})\cdot\vec{n} \geq 0 \,\} \\
S_{4,2} &:= \left(E(0,R;e) \setminus \left(\bar{S}_1 \cup \bar{S}_2 \cup \bar{S}_3\right)\right) \cap \{\, \vec{x} \in E(0,R;e) \;\mid\; (\vec{x}-\vec{m})\cdot\vec{n} < 0 \,\}
\end{aligned}$$

where we have written $S_i = S_{i,1} \cup S_{i,2}^1 \cup S_{i,2}^2 \cup S_{i,3}$ for $i = 1,2$ again to define the last two sets. The sets $S_{2,1}$, $S_{2,2}^1$, $S_{2,2}^2$ and $S_{2,3}$ are obtained by interchanging $\vec{a}$ and $\vec{b}$ in $S_{1,1}$, $S_{1,2}^1$, $S_{1,2}^2$ and $S_{1,3}$. The sets $S_{i,2}$, defined in (2.101), are given by $S_{i,2} = S_{i,2}^1 \cup S_{i,2}^2 \cup S_{i,3}$ for $i = 1,2$. The final decomposition (2.134) is illustrated in Figure 2.11.

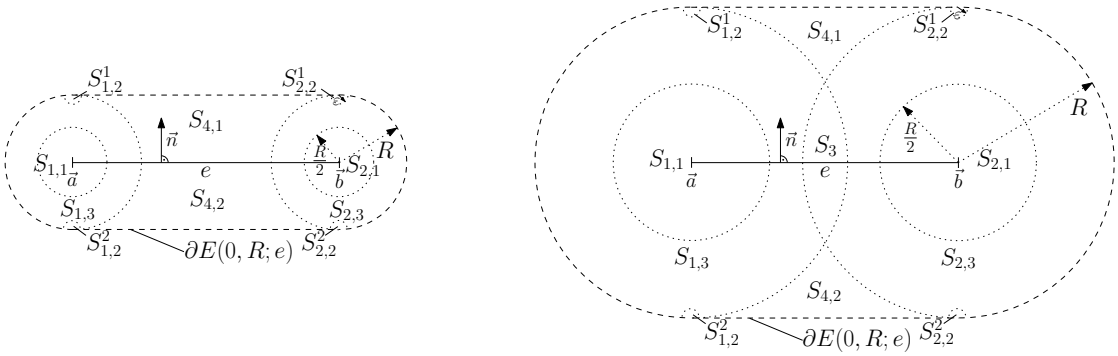

(a) decomposition of $E(0,R;e)$ for $R \leq \frac{|e|}{2}$

(b) decomposition of $E(0,R;e)$ for $R > \frac{|e|}{2}$

Figure 2.11: Final decomposition (2.134) of $E(0,R;e)$ for different values of R. The initial decomposition is shown in Figure 2.10.

The regularity of $P_{R,e}[\varphi]$ on the subdomains $S \in \mathcal{S}$ specified in (2.134) is summarised in Theorem 2.21.

Theorem 2.21 (Regularity of $P_{R,e}[\varphi]$ on $E(0,R;e)$)
Let $P_{R,e}[\varphi]$ be an integral operator of type (2.71) with $\varphi \in L^\infty(e)$ and admissible kernel function. Then

a) $P_{R,e}[\varphi] \in \mathcal{B}_\beta^1(S_{i,2}^k)$ for $i,k = 1,2$, where

$$\mathcal{B}_\beta^l(S_{i,2}^k) = \left\{ u \in H^{l-1}(S_{i,2}^k) \;\mid\; \left\| \frac{\partial^{\alpha_1+\alpha_2} u}{\partial r^{\alpha_1} \partial\theta^{\alpha_2}} \; \Phi_{\beta,\vec{\alpha},l} \right\|_{L^2(S_{i,2}^k)} \leq C d^{|\vec{\alpha}|-l} (|\vec{\alpha}|-l)! \; \forall \vec{\alpha} \in \mathbb{N}_0^2 \text{ with } |\vec{\alpha}| \geq l \right\} \tag{2.135}$$

for $l \geq 1$ and $C = C(u) \geq 0$, $d = d(u) > 1$ are independent of $|\vec{\alpha}|$, in the local polar coordinate system (r,θ) defined by (2.102). The weight function is given by $\Phi_{\beta,\vec{\alpha},1}(r,\theta) = (R-r)^{\beta+\alpha_1-1}\,\theta^{\beta+\alpha_2-1}$ for any $\beta > 0$.

b) $P_{R,e}[\varphi] \in \mathcal{B}^2_\beta(S_{i,3})$ *for* $\beta > \frac{1}{2} - \kappa_2$ *if* $0 \le \kappa_2 \le \frac{1}{2}$ *and* $P_{R,e}[\varphi] \in \mathcal{B}^3_\beta(S_{i,3})$ *for* $\beta > \frac{3}{2} - \kappa_2$ *if* $\frac{1}{2} < \kappa_2 \le \frac{3}{2}$ *for* $i = 1, 2$*, where the spaces* $\mathcal{B}^l_\beta(S_{i,3})$*,* $l = 2, 3$*, are defined similarly to* (2.135)*. The weight function is given by* $\Phi_{\beta,\vec{\alpha},l}(r) = \Phi_{\beta,\alpha_1,l}(r) = (R - r)^{\beta+\alpha_1-l}$*,* $l = 2, 3$*.*

c) $P_{R,e}[\varphi] \in \mathcal{B}^1_\beta(S_{i,1})$ *for* $\beta > -\frac{1}{2} - \kappa_1$ *if* $-1 \le \kappa_1 \le -\frac{1}{2}$ *and* $P_{R,e}[\varphi] \in \mathcal{B}^2_\beta(S_{i,1})$ *for* $\beta > \frac{1}{2} - \kappa_1$ *if* $-\frac{1}{2} < \kappa_1 \le \frac{1}{2}$ *for* $i = 1, 2$*, where the spaces* $\mathcal{B}^l_\beta(S_{i,1})$*,* $l = 1, 2$*, are defined similarly to* (2.135)*. The weight function is given by* $\Phi_{\beta,\vec{\alpha},l}(r) = \Phi_{\beta,\alpha_1,l}(r) = r^{\beta+\alpha_1-l}$*,* $l = 1, 2$*.*

d) $P_{R,e}[\varphi] \in \mathcal{B}^1_\beta(S_{4,i})$ *for* $i = 1, 2$*, where*

$$\mathcal{B}^l_\beta(S_{4,i}) = \left\{ u \in H^{l-1}(S_{4,i}) \;\middle|\; \left\| \frac{\partial^{\alpha_1+\alpha_2} u}{\partial \mu^{\alpha_1} \partial \nu^{\alpha_2}} \; \Phi_{\beta,\vec{\alpha},l} \right\|_{L^2(S_{4,i})} \le C d^{|\vec{\alpha}|-l} (|\vec{\alpha}| - l)! \; \forall \vec{\alpha} \in \mathbb{N}_0^2 \text{ with } |\vec{\alpha}| \ge l \right\}$$

for $l \ge 1$ *and* $C = C(u) \ge 0$*,* $d = d(u) > 1$ *are independent of* $|\vec{\alpha}|$*, in the local coordinate system* (μ, ν) *defined by* (2.128)*. The weight function is given by* $\Phi_{\beta,\vec{\alpha},1}(\nu) = \Phi_{\beta,\alpha_1,1}(\nu) = (R - \nu)^{\beta+\alpha_1-1}$ *for any* $\beta > 0$*.*

Proof
a) follows from Lemmas 2.15 and 2.18. b) and c) follow from Lemma 2.15. d) follows from Lemma 2.20. ∎

Regularity on the Test Element

We have, up to now, studied the regularity of $P_{R,e}[\varphi]$ on two dimensional domains. For the computation of the matrix entries, however, we intersect $E(0, R; e)$ and therewith, by (2.134), the domains $S \in \mathcal{S}$ with boundary edges and compute integrals over the resulting subedges $S \cap \Gamma_j$, i.e. over one dimensional manifolds. We study the regularity of $P_{R,e}[\varphi]$ on each of the subedges $S \cap \Gamma_j$ with $S \in \mathcal{S}$, similarly to Theorem 2.21. Examples of these decompositions of $E(0, R; e) \cap \Gamma_j$ into subedges are illustrated in Figure 2.13. Due to the domain decomposition (2.134), every subedge $S \cap \Gamma_j$ contains at most one singular point for $S \notin \{S_{i,1}, S_{i,3} \mid i = 1, 2\}$. If $S = S_{i,1}$ or $S = S_{i,3}$, the subedge $S \cap \Gamma_j$ can be split in half to produce two edges that contain one singularity each.

The local coordinate system with parameter ν on $S \cap \Gamma_j$ can be chosen such that the one singular point on $S \cap \Gamma_j$ coincides with $\nu = 0$. We define countably normed spaces $\mathcal{B}^l_\beta(S \cap \Gamma_j)$ with weight function $\Phi_{\beta,n,l}(\nu) = \nu^{\beta+n-1}$ by

$$\mathcal{B}^l_\beta(S \cap \Gamma_j) = \left\{ u \in H^{l-1}(S \cap \Gamma_j) \;\middle|\; \left\| \frac{d^n u}{d\nu^n} \; \Phi_{\beta,n,l} \right\|_{L^2(S \cap \Gamma_j)} \le C d^{n-l} (n - l)! \text{ for } n \ge l \right\} \tag{2.136}$$

for $S \in \mathcal{S}$, $l \ge 1$, $\beta > 0$ and $C = C(u) \ge 0$, $d = d(u) > 1$ independent of n, and prove the following result that complements Theorem 2.21.

Theorem 2.22 (Regularity of $P_{R,e}[\varphi]$ on $E(0, R; e) \cap \Gamma_j$)
Let $P_{R,e}[\varphi]$ *be an integral operator of type* (2.71) *with* $\varphi \in L^\infty(e)$ *and admissible kernel function, and let* Γ_j *be a boundary edge with local parameter* ν*. Then*

a) $P_{R,e}[\varphi] \in \mathcal{B}^1_\beta(S^k_{i,2} \cap \Gamma_j)$ *for any* $\beta > 0$ *for* $i, k = 1, 2$*.*

b) $P_{R,e}[\varphi] \in \mathcal{B}^2_\beta(S_{i,3} \cap \Gamma_j)$ *for* $\beta > \frac{1}{2} - \kappa_2$ *if* $0 \le \kappa_2 \le \frac{1}{2}$ *and* $P_{R,e}[\varphi] \in \mathcal{B}^3_\beta(S_{i,3} \cap \Gamma_j)$ *for* $\beta > \frac{3}{2} - \kappa_2$ *if* $\frac{1}{2} < \kappa_2 \le \frac{3}{2}$ *for* $i = 1, 2$*.*

c) $P_{R,e}[\varphi] \in \mathcal{B}^1_\beta(S_{i,1} \cap \Gamma_j)$ *for* $\beta > -\frac{1}{2} - \kappa_1$ *if* $-1 \le \kappa_1 \le -\frac{1}{2}$ *and* $P_{R,e}[\varphi] \in \mathcal{B}^2_\beta(S_{i,1})$ *for* $\beta > \frac{1}{2} - \kappa_1$ *if* $-\frac{1}{2} < \kappa_1 \le \frac{1}{2}$ *for* $i = 1, 2$.

d) $P_{R,e}[\varphi] \in \mathcal{B}^1_\beta(S_{4,i} \cap \Gamma_j)$ *for any* $\beta > 0$ *for* $i = 1, 2$.

Proof
We begin with $S = S_{1,1}$. We assume, without loss of generality, that $\vec{a} \in \Gamma_j$, since $P_{R,e}[\varphi]$ would be non-singular on $S_{1,1} \cap \Gamma_j$ otherwise. By choosing a direction vector $\vec{d}_j$ of appropriate length,

$$S_{1,1} \cap \Gamma_j = \left\{ \vec{a} + \nu \vec{d}_j \;\; | \;\; 0 \le \nu \le 1 \right\}$$

and therefore $|\vec{x} - \vec{a}| = \nu |\vec{d}_j| =: r(\nu)$ for any $\vec{x} \in S_{1,1} \cap \Gamma_j$. The geometrical setup is illustrated in Figure 2.12a. By the chain rule, $\frac{d}{d\nu}\kappa(R; r(\nu)) = |\vec{d}_j| \frac{d}{dr}\kappa(R; r)$ and, in general,

$$\frac{d^n}{d\nu^n}\kappa(R; r(\nu)) = |\vec{d}_j|^n \frac{d^n}{dr^n}\kappa(R; r) \tag{2.137}$$

for any $n \ge 0$. Using Assumption 2.5, we obtain, similarly to (2.103),

$$\begin{aligned} \left| \frac{d^n}{d\nu^n} k(\vec{x} - \vec{a}, \vec{n}_{\vec{x}}, \vec{n}) \right| &\le 2C_{1,1} \left(C_{1,2} |\vec{d}_j| \right)^n n!\, r(\nu)^{\min\{\kappa_1 - n, 0\}} \\ &= 2C_{1,1} |\vec{d}_j|^{n + \min\{\kappa_1 - n, 0\}} C_{1,2}^n\, n!\, \nu^{\min\{\kappa_1 - n, 0\}} \end{aligned} \tag{2.138}$$

for any $\vec{x} \in S_{1,1} \cap \Gamma_j$, and therefore

$$\begin{aligned} &\left\| \frac{d^n}{d\nu^n} k(\vec{x} - \vec{a}, \vec{n}_{\vec{x}}, \vec{n}) \Phi_{\beta,n,l} \right\|_{L^2(S_{1,1} \cap \Gamma_j)} \\ \le\;& 2C_{1,1} |\vec{d}_j|^{n + \min\{\kappa_1 - n, 0\}} C_{1,2}^n\, n! \left(\int_0^1 \nu^{\min\{2(\kappa_1 - n), 0\}} \Phi^2_{\beta,n,l}(\nu)\, d\nu \right)^{\frac{1}{2}} \end{aligned} \tag{2.139}$$

for any $n \ge 0$, which is similar to (2.104). With $\Phi_{\beta,n,l}(\nu) = \nu^{\beta + n - l}$, the integral in (2.139) is finite if and only if $\beta > l - \kappa_1 - \frac{1}{2}$. This proves c).

Now let $S = S_{1,2}$. We assume, without loss of generality, that there exists a point $\vec{x}_j \in \Gamma_j$ such that $|\vec{x}_j - \vec{a}| = R$, i.e. $\vec{x}_j \in \partial \mathbb{B}_R(\vec{a})$, since $P_{R,e}[\varphi]$ would be non-singular on $S_{1,2} \cap \Gamma_j$ otherwise. By choosing a direction vector $\vec{d}_j$ of appropriate length,

$$S_{1,2} \cap \Gamma_j = \left\{ \vec{x}_j + \nu \vec{d}_j \;\; | \;\; 0 \le \nu \le 1 \right\}.$$

If $(\vec{x}_j - \vec{a}) \cdot \vec{d}_j = 0$, then $S_{1,2} \cap \Gamma_j = \{\vec{x}_j\}$, and this case can therefore be neglected. Otherwise, there exist a second point $\vec{\tilde{x}}_j \in \mathcal{E}_{\Gamma_j}$ such that $|\vec{\tilde{x}}_j - \vec{a}| = R$. By geometrical considerations, the midpoint of the line from $\vec{x}_j$ to $\vec{\tilde{x}}_j$ is the point on $\mathcal{E}_{\Gamma_j}$ with the smallest distance to $\vec{a}$, i.e. the projection of $\vec{a}$ onto $\mathcal{E}_{\Gamma_j}$. By Remark 2.2, it is given by

$$\vec{a}' = \vec{a} - ((\vec{a} - \vec{x}_j) \cdot \vec{n}_j) \vec{n}_j.$$

On the other hand, $\vec{a}' = \vec{x}_j + \nu_{\vec{a}} \vec{d}_j$ for some $\nu_{\vec{a}} > 0$. Hence $\vec{x} - \vec{a} = (\vec{x} - \vec{a}') + (\vec{a}' - \vec{a}) = (\nu - \nu_{\vec{a}}) \vec{d}_j + ((\vec{a} - \vec{x}_j) \cdot \vec{n}_j) \vec{n}_j$ for any $\vec{x} \in S_{1,2} \cap \Gamma_j$, and therefore

$$r(\nu) := |\vec{x} - \vec{a}| = \sqrt{(\vec{x} - \vec{a}) \cdot (\vec{x} - \vec{a})} = \sqrt{(\nu - \nu_{\vec{a}})^2 |\vec{d}_j|^2 + ((\vec{a} - \vec{x}_j) \cdot \vec{n}_j)^2} = \sqrt{R^2 + \nu(\nu - 2\nu_{\vec{a}}) |\vec{d}_j|^2}$$

for any $\vec{x} \in S_{1,2} \cap \Gamma_j$. The geometrical setup is illustrated in Figure 2.12b.

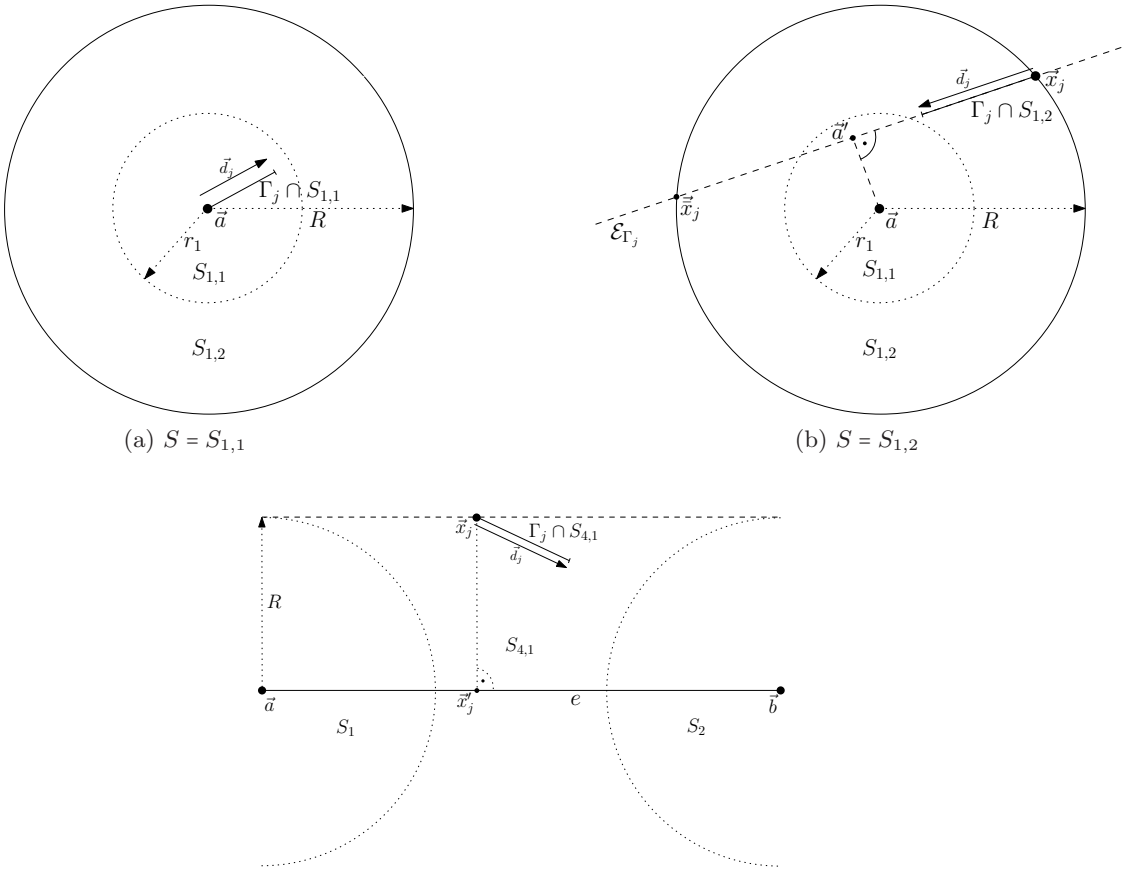

(a) $S = S_{1,1}$ (b) $S = S_{1,2}$

(c) $S = S_{4,1}$

Figure 2.12: Parameterisation of boundary edge $\Gamma_j \subseteq S$ for $S \in \{S_{1,1}, S_{1,2}, S_{4,1}\}$.

Since $0 < r_1 \leq r(\nu) \leq R$ for any $\nu \in [0,1]$, the derivatives of $r(\nu)$ are bounded with

$$\left|\frac{d^n r}{d\nu^n}\right| \leq C(r_1, R)^n \tag{2.140}$$

where $C(r_1, R)$ depends on r_1 and R but not on n. It follows from the chain and product rule that the singularities of leading order in $\frac{d^n \kappa(R;r(\nu))}{d\nu^n}$ are given by $\frac{d^n \kappa(R;r)}{dr^n}$. Using Assumption 2.5, we conclude that

$$\left|\frac{d^n}{d\nu^n} k(\vec{x} - \vec{a}, \vec{n}_{\vec{x}}, \vec{n})\right| \leq 2n\, C(r_1, R)^n \left|\frac{d^n \kappa(R;r)}{dr^n}\right| \leq 2n\, C(r_1, R)^n\, C_{2,1} C_{2,2}^n\, n!\, |r(\nu) - R|^{\min\{\kappa_2 - n, 0\}} \tag{2.141}$$

with $|r(\nu) - R|^{\min\{\kappa_2 - n, 0\}} = (R - r(\nu))^{\min\{\kappa_2 - n, 0\}}$. Therefore

$$\begin{aligned} &\left\| \frac{d^n}{d\nu^n} k(\vec{x} - \vec{a}, \vec{n}_{\vec{x}}, \vec{n}) \Phi_{\beta,n,l} \right\|_{L^2(S_{1,2} \cap \Gamma_j)} \\ \leq\ & 2nC_{2,1} |\vec{d}_j| C(r_1, R)^n C_{2,2}^n\, n! \left(\int_0^1 (R - r(\nu))^{\min\{2(\kappa_2 - n), 0\}} \Phi_{\beta,n,l}^2(\nu)\, d\nu \right)^{\frac{1}{2}} \end{aligned} \tag{2.142}$$

for any $n \geq 0$, which is similar to (2.106). By l'Hôpital's rule and using $r'(\nu) = \frac{(\nu - \nu_{\vec{a}})|\vec{d}_j|}{r(\nu)}$,

$$\lim_{\nu \to 0} \frac{\nu}{R - r(\nu)} = -\lim_{\nu \to 0} \frac{1}{r'(\nu)} = -\lim_{\nu \to 0} \frac{r(\nu)}{(\nu - \nu_{\vec{a}})|\vec{d}_j|} = \frac{R}{|\vec{a}' - \vec{x}_j|} =: \bar{C}(\Gamma_j, R) < \infty \tag{2.143}$$

Let $\Phi_{\beta,n,l}(\nu) = \nu^{\beta+n-l}$ with $\beta > l - \kappa_2 - \frac{1}{2}$, so that $2(\beta - l) = -2\kappa_2 - 1 + \varepsilon$ with $\varepsilon > 0$. The integrand in (2.142) for $\kappa_2 < n$ then is

$$(R - r(\nu))^{2(\kappa_2 - n)} \Phi^2_{\beta,n,l}(\nu) = \left(\frac{\nu}{R - r(\nu)} \right)^{2(n-\kappa_2)} \nu^{-1+\varepsilon}$$

By (2.143), the integral in (2.142) is finite for this choice of weight function. This proves b).

Now let $S = S_{4,1}$. We assume, without loss of generality, that there exists a point $\vec{x}_j \in \Gamma_j$ such that $|\vec{x}_j - \vec{a}| = R$, located on the edge parallel to e at distance R, since $P_{R,e}[\varphi]$ would be non-singular on $S_{4,1} \cap \Gamma_j$ otherwise. By choosing a direction vector $\vec{d}_j$ of appropriate length,

$$S_{4,1} \cap \Gamma_j = \left\{ \vec{x}_j + \nu \vec{d}_j \;\; | \;\; 0 \le \nu \le 1 \right\}.$$

Let $\vec{x}'_j = \vec{x}_j - R\vec{n}$ be the projection of $\vec{x}_j$ onto e. The geometrical setup is illustrated in Figure 2.12c. For any other $\vec{x} \in S_{4,1} \cap \Gamma_j$, the projection $\vec{x}'$ of $\vec{x}$ onto e is, by Remark 2.2,

$$\vec{x}' = \vec{x} - ((\vec{x} - \vec{x}'_j) \cdot \vec{n})\vec{n}$$

Therefore, using the notation $\vec{x}^2 = \vec{x} \cdot \vec{x}$,

$$(\vec{x} - \vec{x}')^2 = (((\vec{x} - \vec{x}'_j) \cdot \vec{n})\vec{n})^2 = (((R\vec{n} + \nu\vec{d}_j) \cdot \vec{n})\vec{n})^2 = (R\vec{n} + \nu(\vec{d}_j \cdot \vec{n})\vec{n})^2 = R^2 + 2\nu(\vec{d}_j \cdot \vec{n})R + \nu^2(\vec{d}_j \cdot \vec{n})^2$$

for any $\vec{x} \in S_{4,1} \cap \Gamma_j$. Hence, similarly to (2.130),

$$R'(\vec{x}) = \sqrt{R^2 - |\vec{x} - \vec{x}'|^2} = \sqrt{-\nu(\vec{d}_j \cdot \vec{n})} \sqrt{2R + \nu(\vec{d}_j \cdot \vec{n})} = R'(\nu)$$

for any $\vec{x} \in S_{4,1} \cap \Gamma_j$, with $0 = R'(0) \le R'(\nu) \le R$. We note that $\vec{d}_j \cdot \vec{n} = 0$ corresponds to the case when Γ_j is parallel to e, with distance R. We further note that $\vec{d}_j \cdot \vec{n} = |\vec{d}_j| \cos\theta$, where θ is the angle between $\vec{d}_j$ and $\vec{n}$. By geometric considerations, $\frac{\pi}{2} \le \theta \le \pi$ and therefore $-1 \le \cos\theta \le 0$. We conclude that $0 < \sqrt{2R + \nu(\vec{d}_j \cdot \vec{n})} \le \sqrt{2R}$, where the first inequality holds since $R'(\nu) = 0$ if and only if $\nu = 0$. By the product rule and using $\frac{d^n \sqrt{\delta}}{d\delta^n} = \frac{(-1)^{n+1}}{2^n} (2n-3)!! \, \delta^{-\frac{2n-1}{2}}$ for $n \ge 1$, with $(-1)!! := 1$,

$$\frac{d^n R'}{d\nu^n} = \sum_{m=0}^{n} \binom{n}{m} \frac{(-1)^n}{2^n} (2m-3)!! \, (2(n-m)-3)!! \left(-\nu(\vec{d}_j \cdot \vec{n}) \right)^{-\frac{2m-1}{2}} \left(2R + \nu(\vec{d}_j \cdot \vec{n}) \right)^{-\frac{2(n-m)-1}{2}}$$

and therefore

$$\left| \frac{d^n R'}{d\nu^n} \right| \le n! \sum_{m=0}^{n} \nu^{-\frac{2m-1}{2}} \left(\vec{d}_j \cdot \vec{n} \right)^{-\frac{2m-1}{2}} \left(2R + \nu(\vec{d}_j \cdot \vec{n}) \right)^{-\frac{2(n-m)-1}{2}} \le C(\Gamma_j, R)^n \, n! \sum_{m=0}^{n} \nu^{-\frac{2m-1}{2}}$$

where $C(\Gamma_j, R)$ depends on Γ_j and R but not on n. The singularity of leading order in $\left| \frac{d^n R'}{d\nu^n} \right|$ is $\nu^{-\frac{2n-1}{2}}$. Hence

$$\left\| \frac{d^n R'}{d\nu^n} \Phi_{\beta,n,l} \right\|_{L^2(S_{4,1} \cap \Gamma_j)} \le C(\Gamma_j, R)^n \, n! \sum_{m=0}^{n} \left(\int_0^1 \nu^{-(2m-1)} \Phi^2_{\beta,n,l}(\nu) \, d\nu \right)^{\frac{1}{2}}$$

for any $n \ge 0$, which is similar to (2.133). With $\Phi_{\beta,n,l}(\nu) = \nu^{\beta+n-l}$, the integrals in (2.144) are finite for $l = 1$ and $\beta > 0$. This proves d).

Finally, a) follows from b) and d). For $S = S^1_{1,2}$, the singularity is located at $\vec{x}_j = \vec{a} + R\vec{n}$; the point at which the circular and planar light disc singularities coincide. ∎

2.5.3 Grading Strategies for the Computation of Time Domain Boundary Layer Potentials with Discrete Support

We now consider the approximation of the matrix entries (2.50) with ansatz element $\Gamma_j = e$ and test element Γ_i, i.e.

$$\int_{\Gamma_i} P_{R,e}[\varphi](\vec{x})\psi(\vec{x})\, ds_{\vec{x}} \tag{2.144}$$

where the kernel function of $P_{R,e}[\varphi]$ is admissible. Similarly to (2.53), we denote the part of Γ_i that is illuminated by e by $\tilde{\Gamma}_i = \Gamma_i \cap E(0, R; e)$, so that

$$\int_{\Gamma_i} P_{R,e}[\varphi](\vec{x})\psi(\vec{x})\, ds_{\vec{x}} = \int_{\tilde{\Gamma}_i} P_{R,e}[\varphi](\vec{x})\psi(\vec{x})\, ds_{\vec{x}}.$$

Due to the singularities in the kernel functions and in the derivatives of $P_{R,e}[\varphi]$, a grading strategy for the quadrature meshes on e and $\tilde{\Gamma}_i$ is crucial. Some typical locations of singularities on the test and ansatz element are illustrated in Figures 2.13 and 2.14, respectively.

We note that Guardasoni et al. [3, 77] observe singularities 'along the oblique boundary of the double integration domain' [77, p. 91] experimentally for a certain kernel function, which corresponds to the singularities in the derivatives of $P_{R,e}[\varphi]$ observed here. Their observations and quadrature schemes are fully described in local coordinates of the test and ansatz element, which somewhat blurs the geometrical and physical background, and they do not provide any general theoretical arguments for the occurrence of these singularities. Consequently, no estimate on the order of convergence for their quadrature scheme is given. Their quadrature schemes [77, Section 4.4] take full account of possible end point singularities of the kernel function and of the boundary integral operators involved. However, regarding the additional singularities at $r = R$, they only apply an appropriate quadrature scheme (a regularisation procedure) on the ansatz element. Since the accuracy of standard Gaussian quadrature is affected by the singularities of $P_{R,e}[\varphi]$ on the test element method, we proceed more carefully.

In the grading strategies described in what follows, we often state that the quadrature mesh on an edge 'needs to be graded towards' certain points on it. Assume that there are $\tilde{n}$ such points on an edge Γ_l. After eliminating points that have possibly been multiply flagged, one is left with n points on Γ_l towards which the quadrature mesh on Γ_l is supposed to be graded. The local coordinates μ_i, $i = 0, \dots, n-1$, of these points are assumed to be in ascending order. If $\mu_0 = -1$ or $\mu_{n-1} = 1$, one or two of the end points of Γ_l have been flagged. Γ_l is divided into N subintervals, where $N = 2n$ if $\mu_0 \neq -1$ and $\mu_{n-1} \neq 1$, $N = 2n-1$ if $\mu_0 = -1$ and $\mu_{n-1} \neq 1$ or $\mu_0 \neq -1$ and $\mu_{n-1} = 1$, and $N = 2n-2$ if $\mu_0 = -1$ and $\mu_{n-1} = 1$. These are chosen such that each of the N subintervals of Γ_l contains only one point, its left or its right end point, towards which the quadrature mesh on it has to be graded. Let N_Q be the number of quadrature points, and $\sigma \in (0,1)$ the grading parameter. Then the local coordinates $\nu \in [0,1]$ of the quadrature points on each subinterval are given by [141, (3.1)]

$$\nu_0 := 0 \quad , \quad \nu_k = \sigma^{N_Q-1-k} \text{ for } k = 1, \dots, N_Q - 1 \tag{2.145}$$

if the quadrature mesh needs to be graded towards its left end point, and by $\tilde{\nu}_k = 1 - \nu_{N_Q-1-k}$ for $k = 0, \dots, N_Q - 1$ if the quadrature mesh needs to be graded towards its right end point. It is well known [141, Section 6] that the optimal grading parameter is $\sigma = (\sqrt{2}-1)^2$. A standard Gaussian quadrature mesh is used if $n = 0$.

2.5.3.1 Grading Strategies for the Test Element (Outer Quadrature)

The kernel function of $P_{R,e}[\varphi]$ is assumed to be admissible, and we can therefore restrict ourselves to the singularities specified in Definition 2.11. In what follows, we say that a test element $\tilde{\Gamma}_i$ is

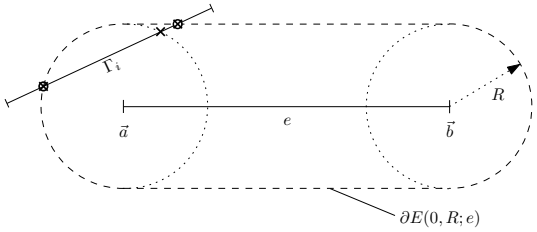

(a) Two circular and one planar light disc singularities

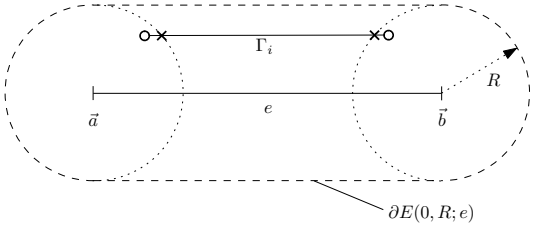

(b) Two circular light disc singularities

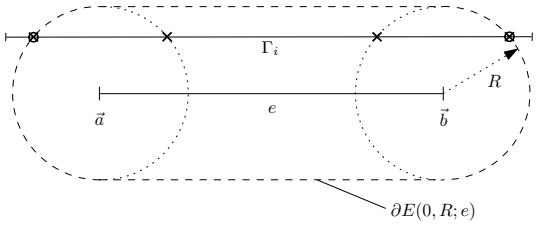

(c) Four circular light disc singularities

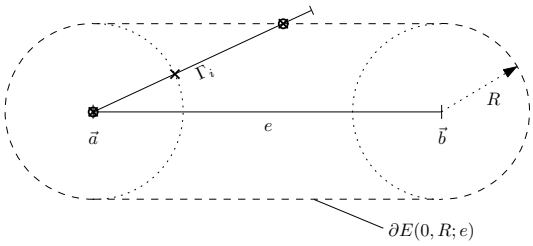

(d) One end point singularity, and one circular and one planar light disc singularity

Figure 2.13: Examples of singularities on the outer integration domain $\tilde{\Gamma}_i$. The end points of $\tilde{\Gamma}_i$ are denoted by $\circ$, and singularities on $\tilde{\Gamma}_i$ are denoted by $\times$. If end points coincide with singularities, this is denoted by $\otimes$.

contained in the *near field* of the ansatz element e if it is sufficiently close to it. Otherwise, it is said to be contained in the *far field* of e.

Similarly, a test element $\tilde{\Gamma}_i$ is said to be contained in the *R-planar near field* of e if its distance to any of the two parallel edges to e at distance R is sufficiently small. It is said to be contained in the *R-circular near field* of e if its distance to any of the two circles of radius R around the end points of e is sufficiently small.

- The *end point singularities* of $P_{R,e}[\varphi]$ at $r = 0$ can be treated by a classical grading strategy towards the end points of $\tilde{\Gamma}_i$.
  - If $\tilde{\Gamma}_i$ is contained in the far field of e, no such grading is needed.
  - If $\tilde{\Gamma}_i$ is contained in the near field of e, $\tilde{\Gamma}_i$ is graded towards the point on it that is closest to e. In particular, if Γ_i and e are neighbouring elements, i.e. if $\tilde{\Gamma}_i \cap e \in \{\vec{a}, \vec{b}\}$, $\tilde{\Gamma}_i$ is graded towards the respective intersection point.
  - For $e = \Gamma_i$, there holds $\tilde{\Gamma}_i = \Gamma_i$, since e fully illuminates itself for any $R > 0$. The quadrature mesh on $\tilde{\Gamma}_i = \Gamma_i$ is therefore graded towards both end points.
- The *planar* and *circular light disc singularities* of $P_{R,e}[\varphi]$ at at $r = R$ demand another grading strategy.
  - For $e = \Gamma_i$, there holds $\tilde{\Gamma}_i = \Gamma_i$, since e fully illuminates itself for any $R > 0$. Planar light disc singularities do not occur in this case. Regarding the circular light disc singularities, several cases can be distinguished. For $R > |\Gamma_i|$, $\partial\mathbb{B}_R(\vec{a}) \cap \Gamma_i = \partial\mathbb{B}_R(\vec{b}) \cap \Gamma_i = \emptyset$, and consequently there are no circular light disc singularities on Γ_i. For $R = \frac{|\Gamma_i|}{2}$, one circular light disc singularity appears at the midpoint of Γ_i, and the quadrature mesh on Γ_i is graded towards it. For all other $0 < R \leq |\Gamma_i|$, the quadrature mesh on Γ_i

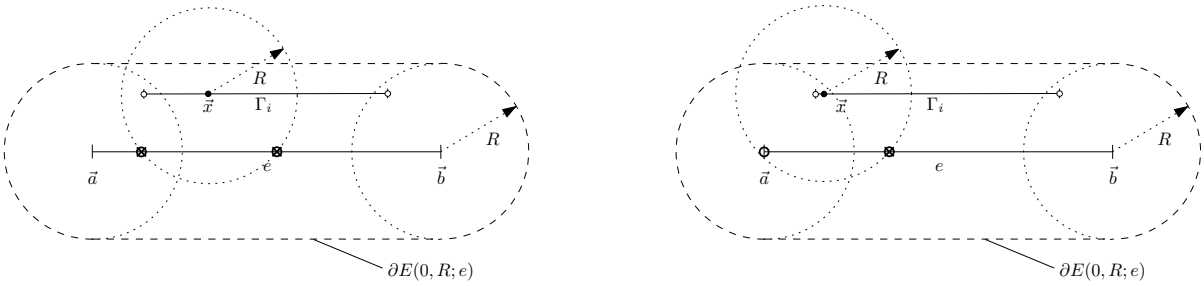

(a) Two kernel singularities at $r = R$

(b) One kernel singularities at $r = R$

Figure 2.14: Examples of singularities on the inner integration domain $e \cap \mathbb{B}_R(\vec{x})$, for given $\vec{x} \in \tilde{\Gamma}_i$. The end points of $\tilde{\Gamma}_i$ and of $e \cap \mathbb{B}_R(\vec{x})$ are denoted by $\circ$, and singularities on $e \cap \mathbb{B}_R(\vec{x})$ are denoted by $\times$. If end points coincide with singularities, this is denoted by $\otimes$.

is graded towards the two intersection points of $\Gamma_i \cap \partial\mathbb{B}_R(\vec{a})$ and $\Gamma_i \cap \partial\mathbb{B}_R(\vec{b})$. In the limiting case $R = |\Gamma_i|$, the two intersection points coincide with the two end points of e.

– For $e \neq \Gamma_i$, there can be up to four points on $\tilde{\Gamma}_i$ that intersect the locations of the planar and circular light disc singularities. The quadrature mesh on $\tilde{\Gamma}_i$ has to be graded towards each of these points. They can, but not not necessarily do, coincide with the end points of $\tilde{\Gamma}_i$. If $\tilde{\Gamma}_i$ does not intersect the locations of these singularities, it can still be contained in the R-planar or R-circular near field of e, and the quadrature mesh on $\tilde{\Gamma}_i$ is then graded towards the point on it whose distance to the location of the respective singularity is closest to R.

The grading strategy obviously corresponds to the decomposition (2.134) of $E(0, R; e)$ that was used in Theorem 2.21.

2.5.3.2 Grading Strategies for the Ansatz Element (Inner Quadrature)

Regarding the quadrature mesh on e to compute the inner integral $P_{R,e}[\varphi](\vec{x})$ for given $\vec{x} \in \tilde{\Gamma}_i$, the grading strategy is less involved. Similarly to Section 2.5.3.1, we say that e is contained in the *near field* of $\vec{x}$ if e is sufficiently close to $\vec{x}$, and we say that e is contained in the *R-near field* of $\vec{x}$ if e is sufficiently close to $\partial\mathbb{B}_R(\vec{x})$.

- If the kernel function k is singular at the origin $r = 0$, the quadrature mesh on e is graded towards the evaluation point $\vec{x}$ if $\vec{x} \in e$, i.e. if $\Gamma_i = e$, or towards the point on e that $\vec{x}$ is closest to if e is contained in the near field of $\vec{x}$.

- Regarding the singularities of k at $r = R$, the quadrature mesh on $e \cap \mathbb{B}_R(\vec{x})$ has to be graded towards the at most two points $\vec{y} \in e \cap \partial\mathbb{B}_R(\vec{x})$, if they exist, or to the point on e that $\mathbb{B}_R(\vec{x})$ is closest to if e is contained in the R-near field of $\vec{x}$. If any intersection point $\vec{y} \in e \cap \partial\mathbb{B}_R(\vec{x})$ exists, it coincides with one of the end points of the integration domain $e \cap \mathbb{B}_R(\vec{x})$. For the special case $e = \Gamma_i$, we can distinguish two sub cases. If $R > |e|$, there holds $e \cap \mathbb{B}_R(\vec{x}) = e$ and $e \cap \partial\mathbb{B}_R(\vec{x}) = \varnothing$, and consequently no grading is needed. For the case $e = \Gamma_i$ and $\frac{|e|}{2} < R \leq |e|$, there is only one intersection point.

2.5.4 Error Analysis for the Computation of Time Domain Boundary Layer Potentials with Discrete Support

Similarly to [127, Theorem 4.11] and due to [141, (5.4)], the quadrature scheme described in Algorithm 2.6 to approximate the entries of the Galerkin matrices converges exponentially.

Theorem 2.23 (Exponential Convergence of Algorithm 2.6)
Let $\tilde{\mathcal{U}}_{i,j}^{m,n}$ be the approximation to $\mathcal{U}_{i,j}^{m,n}$, computed by Algorithm 2.6, using N_Q quadrature points and the composite grading schemes outlined in Section 2.5.3. Then there holds the error estimate

$$\left|\tilde{\mathcal{U}}_{i,j}^{m,n} - \mathcal{U}_{i,j}^{m,n}\right| \leq Ce^{-b\sqrt{N_Q}} \tag{2.146}$$

where $b \in \mathbb{R}_{>0}$ is independent of N_Q, and C depends only on the admissible kernel function k and on the grading parameter σ.

Proof
For simplicity, we consider the approximation of (2.144), from which (2.146) follows. We denote the term (2.144) by I, and its approximation by $\tilde{I}$. As in the proof of [127, Theorem 4.11], one can use the triangle inequality to split the quadrature error $|I-\tilde{I}|$ into the sum of the quadrature error on the ansatz element for the approximation of $P_{R,e}[\varphi](\vec{x})$ for given $\vec{x} \in \tilde{\Gamma}_i$, and the quadrature error on the test element for the approximation of $\int_{\Gamma_i} P_{R,e}[\varphi](\vec{x})\psi(\vec{x})\, ds_{\vec{x}}$.

By assumption, k is an admissible kernel function. Let $\vec{x} \in \tilde{\Gamma}_i$ be given. After possibly subdividing the inner integration element $e \cap \mathbb{B}_R(\vec{x})$ into subelements $e \cap \mathbb{B}_R(\vec{x}) = \bigcup_{m\geq 1} e_m$, as outlined in Section 2.5.3.2 and Remark 2.14 b), there holds, in the local variable μ of e, $k(\vec{x}-\cdot) = k(\vec{x}-\cdot)(\mu) \in \mathcal{B}_\beta^l(e_m)$ for each $m \geq 1$ and $l \geq 0$, with the latter depending on κ_1 and κ_2. [141, (5.4)] therefore implies exponential convergence of the first quadrature error term.

The second quadrature error also convergences exponentially due to [141, (5.4)], since, by Theorem 2.22, $P_{R,e}[\varphi] \in \mathcal{B}_\beta^l(S \cap \tilde{\Gamma}_i)$ with $l \geq 1$ for each of the subdomains $S \subseteq E(0,R;e)$ specified in (2.134). This decomposition corresponds to the possible locations of singularities towards which the quadrature mesh needs to be graded, as discussed in Section 2.5.3.1. ∎

We close this section with an example that shows the effects of the grading strategy in the values of the matrix entries for two typical kernel functions.

Example 2.24 (Exponential Convergence of the Quadrature Scheme)
We consider the same kernel functions as in Example 2.12,

$$S(R;|\vec{x}-\vec{y}|) = \sqrt{R^2-|\vec{x}-\vec{y}|^2} \qquad \text{and} \qquad L(R;|\vec{x}-\vec{y}|) = \ln\left(R+\sqrt{R^2-|\vec{x}-\vec{y}|^2}\right).$$

We approximate matrix entries of the type (2.144) *with piecewise constant ansatz and test function, i.e.*

$$a_{i,e,R} := \int_{\Gamma_i} P_{R,e}[\varphi](\vec{x})\psi(\vec{x})\, ds_{\vec{x}} \tag{2.147}$$

with $\varphi \equiv \psi \equiv 1$ and $e = [-1,1]\times\{0\}$, for given radius R and test element Γ_i, using the grading strategy presented in Section 2.5.3. We denote the end points of Γ_i by $\vec{x}_{i,0}$ and $\vec{x}_{i,1}$, where $\vec{x}_{i,0}$ is always chosen as the end point that is closer to the boundary of $E(0,R;e)$.

We choose $R = 0.5$ and the test elements Γ_0 with end points $\vec{x}_{0,0} = (0,0.5)$ and $\vec{x}_{0,1} = (0,R-0.2) = (0,0.3)$, and Γ_1 with end points $\vec{x}_{1,0} = (-1,0)+\frac{R}{\sqrt{2}}(-1,1)$ and $\vec{x}_{1,1} = (-1,0)+\frac{R-0.2}{\sqrt{2}}(-1,1) = (-1,0)+\frac{0.3}{\sqrt{2}}(-1,1)$. We note that the end point $\vec{x}_{0,0}$ of Γ_0 is located at the planar light disc singularity on the line $e = [-1,1]\times\{R\} \subseteq E(0,R;e)$, and the end point $\vec{x}_{1,0}$ of Γ_1 is located at the circular light disc singularity on the semicircle $\partial\mathbb{B}_R((-1,0)) \cap \{\,\vec{x} \mid x_1 \leq -1\,\} \subseteq E(0,R;e)$.

The quadrature errors for increasing numbers of quadrature points are shown in Figure 2.15. We observe that the convergence is indeed of exponential order for both test elements Γ_0 (Figure 2.15a) and Γ_1 (Figure 2.15b). The exact value of the integral is correct up to single precision and is obtained from the same routine as the other approximations $a_{i,e,R}$, using a sufficient number of quadrature points to ensure convergence of the approximated value up to singular precision.

2.6 First Numerical Experiment

In order to validate our implementation, we consider the example of a circular wave that was presented in Section 1.3.1, with $k = 1$ in (1.22). This is the only interesting example with a known exact solution we are aware of. Technical data on the code and on the equipment the experiments were performed on are given in Section 6.2. We use the direct formulations (1.12) and lowest-order approximations in space and time, and measure the approximation error in the space-time L^2-norm, which can be computed in a straightforward manner, for both the Dirichlet and Neumann problems. We use a uniform $h\Delta t$-version, halving the spatial and temporal mesh width in each step. The experimental convergence rate is then computed as follows:

Given two approximations p_{N_1}, p_{N_2}, corresponding to uniform spatial and temporal mesh widths $h_1, \Delta t_1$ and $h_2, \Delta t_2$, we write

$$e_k := \|p - p_{N_k}\|_{L^2([0,T],L^2(\Gamma))}.$$

for the corresponding error terms. We further assume that the experimental convergence rate $\alpha_{h,\Delta t}$ can be estimated by using the asymptotic expansion

$$e = C\,(h + \Delta t)^{\alpha_{h,\Delta t}} + \text{high order terms}.$$

Neglecting the high order terms, we have $e = C\,(h + \Delta t)^{\alpha_{h,\Delta t}}$, and hence

$$\alpha_{h,\Delta t} = -\frac{\log \frac{e_2}{e_1}}{\log \frac{h_1+\Delta t_1}{h_2+\Delta t_2}}. \tag{2.148}$$

For the uniform $h\Delta t$-version, this term becomes

$$\alpha_{h,\Delta t} = -\frac{\log \frac{e_2}{e_1}}{\log 2}. \tag{2.149}$$

We observe an experimental convergence rate of order $\mathcal{O}(h + \Delta t)$ for both the Dirichlet and the Neumann problem, see Tables 2.1 and 2.2 and Figures 2.18 and 2.19. The error is computed on the time interval $[0, 4]$, for which the solution is non-zero on the boundary. In Figures 2.16 and 2.17, we show the $L^2(\Gamma)$-norm of the exact solution, computed by (1.19) and (1.20), and the $L^2(\Gamma)$-norms of the approximations on the time interval $[0, 4.5]$ for both types of boundary data.

As another means of validation, we have also implemented a simple realisation of the *Convolution Quadrature Boundary Element Method (CQ-BEM)*. Details on the implementation of this method are given in Appendix B. We obtain the same order of convergence as for the Galerkin Boundary Element Method for both the Dirichlet and the Neumann problem.

Since uniform time step sizes are used, the computations can be done via the MOT scheme outlined in Algorithm 2.1. The number *total DOF* in Tables 2.1 and 2.2 corresponds to the size of the full linear system (2.30).

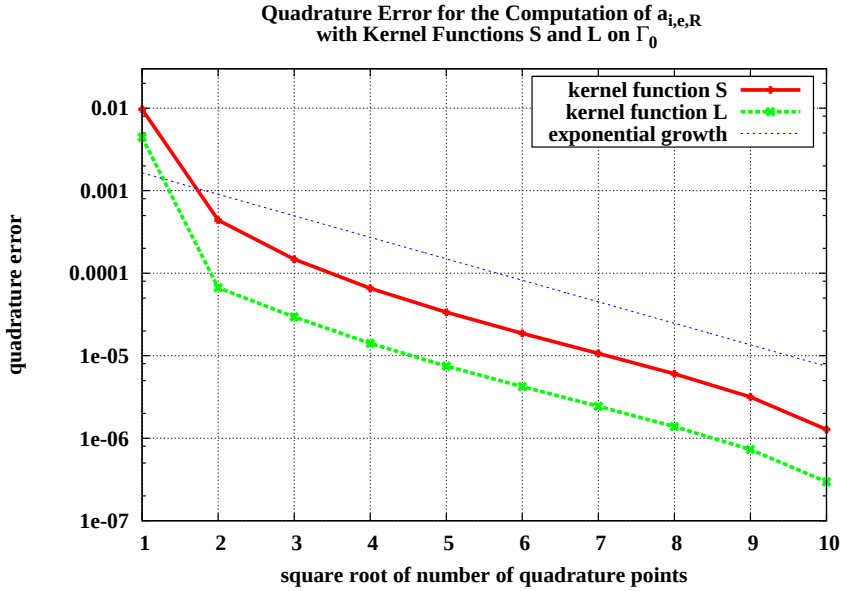

(a) test element Γ_0

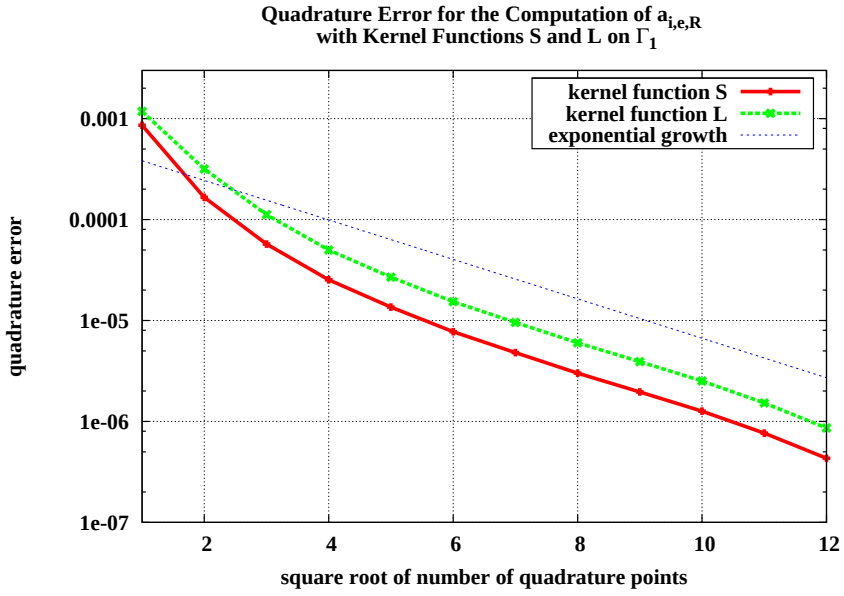

(b) test element Γ_1

Figure 2.15: Quadrature errors for the computation of $a_{i,e,R}$ with kernel functions S and L, with $e = [-1,1] \times \{0\}$ and $R = 0.5$. The end points of test edge Γ_0 are $\vec{x}_{0,0} = (0, 0.5)$ and $\vec{x}_{0,1} = (0, 0.3)$, and the end points of test edge Γ_1 are $\vec{x}_{1,0} = (-1, 0) + \frac{R}{\sqrt{2}}(-1, 1)$ and $\vec{x}_{1,1} = (-1, 0) + \frac{R-0.2}{\sqrt{2}}(-1, 1)$.

degrees of freedom (DOF)			$L^2([0,4],L^2(\Gamma))$-error			
total DOF	spatial DOF	no. of time steps	Galerkin BEM	$\alpha_{h,\Delta t}$	CQ-BEM	$\alpha_{h,\Delta t}$
320	64	5	2.6774159	-	4.5873064	-
1280	128	10	1.4052234	0.93	2.7124512	0.76
5120	256	20	0.7115031	0.98	1.4142800	0.94
20480	512	40	0.3571216	1.00	0.7140314	0.99
81920	1024	80	0.1800194	0.99	0.3579140	1.00
327680	2048	160	0.0904268	0.99	0.1793608	1.00

Table 2.1: $L^2([0,4],L^2(\Gamma))$-error and experimental convergence rates $\alpha_{h,\Delta t}$ for the Dirichlet problem, using the Galerkin Boundary Element Method (Galerkin BEM) and the Convolution Quadrature Boundary Method (CQ-BEM).

degrees of freedom (DOF)			$L^2([0,4],L^2(\Gamma))$-error			
total DOF	spatial DOF	no. of time steps	Galerkin BEM	$\alpha_{h,\Delta t}$	CQ-BEM	$\alpha_{h,\Delta t}$
320	64	5	4.7301870	-	3.1620926	-
1280	128	10	2.5235496	0.91	1.5709787	1.01
5120	256	20	1.2815138	0.98	0.7430721	1.08
20480	512	40	0.6399670	1.00	0.3592204	1.05
81920	1024	80	0.3259086	0.97	0.1762172	1.03
327680	2048	160	0.1688831	0.95	0.0864535	1.03

Table 2.2: $L^2([0,4],L^2(\Gamma))$-error and experimental convergence rates $\alpha_{h,\Delta t}$ for the Neumann problem, using the Galerkin Boundary Element Method (Galerkin BEM) and the Convolution Quadrature Boundary Method (CQ-BEM).

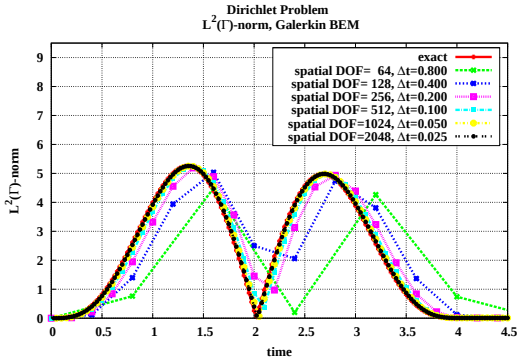

(a) Galerkin Boundary Element Method

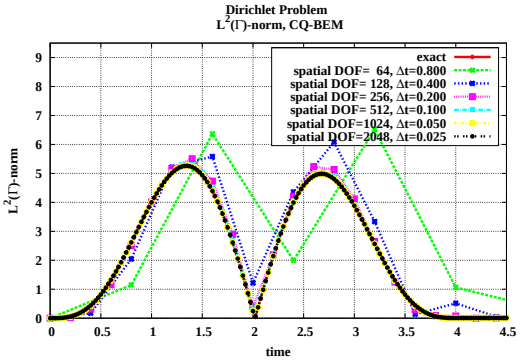

(b) Convolution Quadrature Boundary Element Method

Figure 2.16: Exact $L^2(\Gamma)$-norm and $L^2(\Gamma)$-norms of the approximations plotted versus time, using the Galerkin Boundary Element Method (Galerkin BEM) and the Convolution Quadrature Boundary Method (CQ-BEM), Dirichlet Problem.

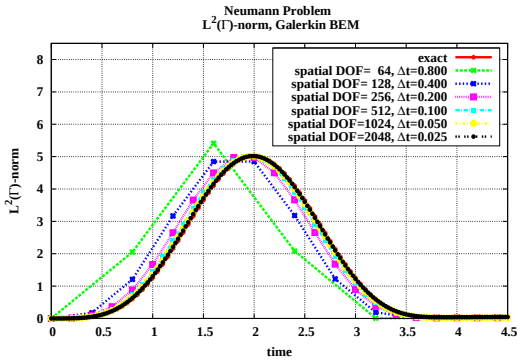

(a) Galerkin Boundary Element Method

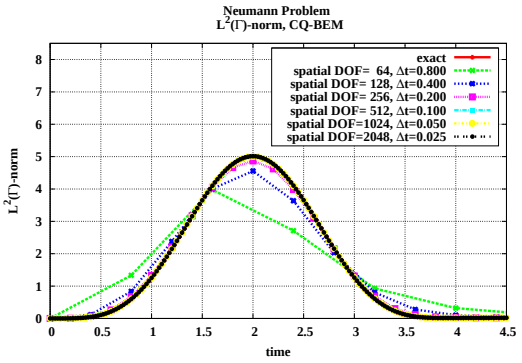

(b) Convolution Quadrature Boundary Element Method

Figure 2.17: Exact $L^2(\Gamma)$-norm and $L^2(\Gamma)$-norms of the approximations plotted versus time, using the Galerkin Boundary Element Method (Galerkin BEM) and the Convolution Quadrature Boundary Method (CQ-BEM), Neumann Problem.

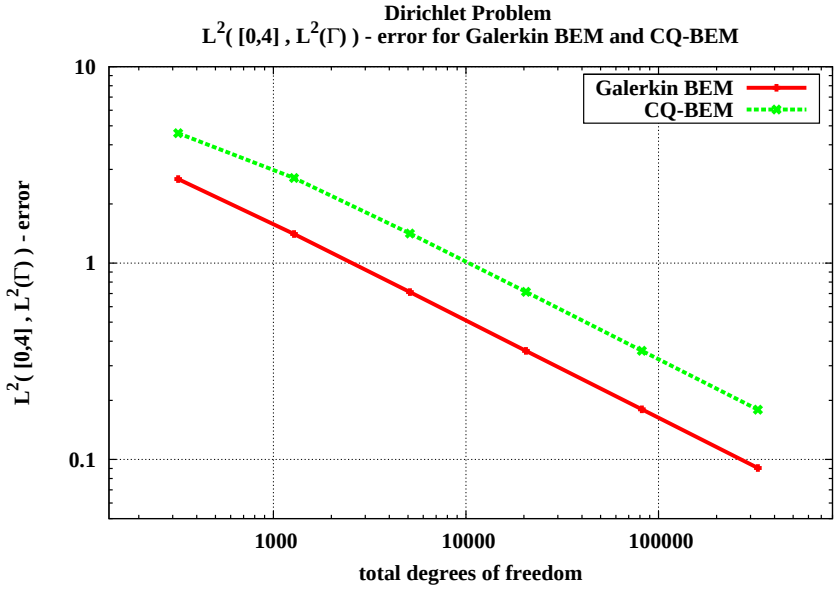

Figure 2.18: $L^2([0,4], L^2(\Gamma))$-error for the Dirichlet problem, using the Galerkin Boundary Element Method (Galerkin BEM) and the Convolution Quadrature Boundary Method (CQ-BEM).

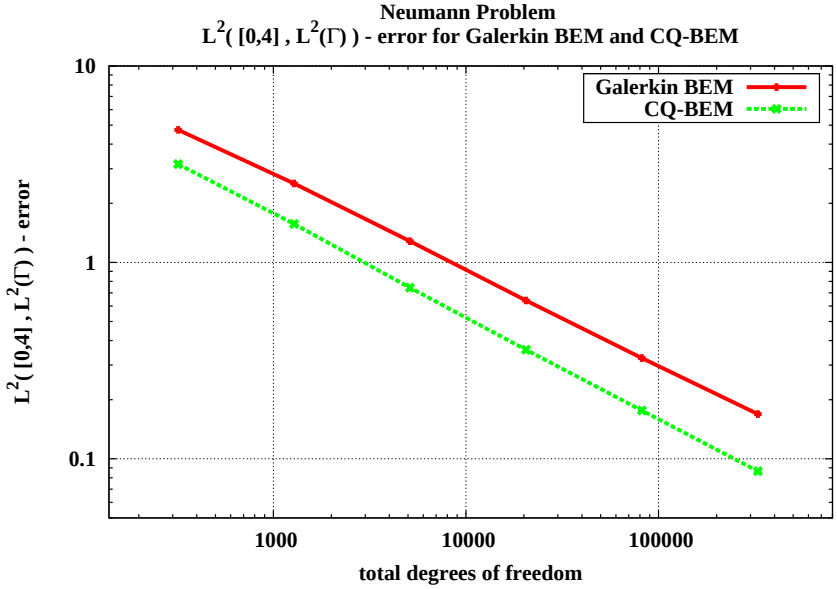

Figure 2.19: $L^2([0,4], L^2(\Gamma))$-error for the Neumann problem, using the Galerkin Boundary Element Method (Galerkin BEM) and the Convolution Quadrature Boundary Method (CQ-BEM).

Chapter 3

Functional Analysis for Time Domain Boundary Element Methods

In this chapter, we introduce function spaces for the analysis of time domain Boundary Element Methods. The first results in this branch of applied analysis were published by Bamberger and Ha-Duong [20, 21] in 1986. Their method, which can, in short, be summarised as applying the Laplace transform to the transient problem, analysing the resulting time harmonic problem explicitly in terms of the wavenumber and then transferring the results back to the time dependent problem, has since then been adapted by other authors, and is well established in this field.

In Section 3.1, a brief review of the Fourier transform and the Laplace transform is given. Both are important tools for analysing time domain boundary layer potentials and the corresponding time domain boundary integral operators.

In Section 3.2, the Laplace transform is used to map the original transient problem (P) to a time independent boundary value problem of the Helmholtz type in the Laplace domain. In Section 3.2.1, a wavenumber-dependent norm that is equivalent to the usual $H^s(\Gamma)$-norms is introduced. This equivalent norm is closely related to the energy of the function under consideration. In Section 3.2.1.1, some classic results are translated to the context of the wavenumber-dependent energy norms. In particular, the dependence of these estimates on the wavenumber is investigated. Section 3.2.2 deals with the boundary potentials and the corresponding boundary integral operators for the Helmholtz problem. In Section 3.2.2.1, mapping properties in the natural norms for the Helmholtz boundary integral operators are collected from the literature. These mapping properties are generalised to a novel result that covers a wider range of spaces in Section 3.2.2.2 and that, again, explicitly states the dependence on the wavenumber.

In Section 3.3, we return to the space-time domain. Space-time function spaces are introduced and reviewed in Section 3.3.1. The classical space-time Sobolev spaces, based on the classical norms in $H^s(\Omega)$ and $H^s(\Gamma)$, are considered in Section 3.3.1.1. The energy space-time Sobolev spaces considered in Section 3.3.1.2 are the space-time counterpart of the energy-related equivalent norm that was presented for the time harmonic case in Section 3.2.1. In Section 3.3.2, the new results on mapping properties for the time harmonic case, obtained in Section 3.2.2.2, are transferred to the space-time domain which, in turn, results in novel, generalised mapping properties for the time domain boundary integral operators.

Approximation properties for different types of space-time function spaces are considered in Section 3.4.

3.1 The Fourier and Laplace Transforms

In this section, we recall the definitions of the Fourier transform and of the Laplace transform (in the distributional sense). The spaces $\mathcal{S}(\mathbb{R}^N)$ and LT are already used in the definitions of the respective transforms, although they are only introduced in Definition 3.2 below.

For $u(t,\cdot) \in \mathcal{S}(\mathbb{R})$ and $\eta \in \mathbb{R}$, the (one dimensional) *Fourier transform with respect to the time variables* is given by

$$\mathcal{F}_t[u(t,\cdot)](\eta,\cdot) := \int_{\mathbb{R}} e^{i\eta t} u(t,\cdot)\, dt. \tag{3.1}$$

Analogously, for $u(\cdot,x) \in \mathcal{S}(\mathbb{R}^N)$ and $\xi \in \mathbb{R}^N$, the (multi dimensional) *Fourier transform with respect to the space variables* is given by

$$\mathcal{F}_x[u(\cdot,x)](\cdot,\xi) := \int_{\mathbb{R}^N} e^{i\ \xi\cdot x} u(\cdot,x)\, dx. \tag{3.2}$$

We sometimes write $\tilde{u}$ instead of $\mathcal{F}_x[u]$. Partial Fourier transforms with respect to k spatial variables $x' := x'_k := (x_{i_1},\dots,x_{i_k})$ with $1 \le i_j < i_{j+1} \le N$ for $1 \le j \le k-1$ are defined analogously in an obvious way. In the distributional sense, $\mathcal{F} : \mathcal{S}(\mathbb{R}^N) \to \mathcal{S}(\mathbb{R}^N)$ [145, p. 30], [151, p. 34].

Finally, for $\omega = \eta + i\sigma \in \mathbb{C}$ and for $u(t,\cdot) \in LT$, the *Fourier-Laplace transform with respect to the time variables* is given by

$$\mathcal{L}_t[u(t,\cdot)](\omega,\cdot) := \int_{\mathbb{R}} e^{i\omega t} u(t,\cdot)\, dt. \tag{3.3}$$

We sometimes write $\hat{u}$ instead of $\mathcal{L}_t[u]$.

Remark 3.1 (On the Laplace and Fourier Transforms)
a) [54, p. 16] The Laplace transform is often defined as, for $s \in \mathbb{C}$,

$$\mathcal{L}_t[u(t,\cdot)](s,\cdot) := \int_{\mathbb{R}} e^{-st} u(t,\cdot)\, dt.$$

This definition coincides with (3.3) *for $-s = i\omega$ or, respectively, for $\omega = is$.*

b) We note that, for $\omega = \eta + i\sigma \in \mathbb{C}$,

$$\mathcal{L}_t[u(t,\cdot)](\omega,\cdot) = \mathcal{F}_t[e^{-\sigma t} u(t,\cdot)](\eta,\cdot).$$

c) For $k \in \mathbb{N}$, there holds

$$\mathcal{L}_t\left[\frac{\partial^k}{\partial t^k} u(t,\cdot)\right](\omega,\cdot) = (-i\omega)^k \mathcal{L}_t[u(t,\cdot)](\omega,\cdot).$$

We use the following obvious notation for combined space-time transforms, for example for $(\tau,\xi) \in \mathbb{R}\times\mathbb{R}^N$,

$$\mathcal{F}_{x,t}[u(t,x)](\tau,\xi) := \mathcal{F}_{t,x}[u(t,x)](\tau,\xi) := \mathcal{F}_t[\ \mathcal{F}_x[u(t,x)](t,\xi)\ ](\tau,\xi)$$

or for $(\omega,\xi) \in \mathbb{C}\times\mathbb{R}^N$ with $\omega = \eta + i\sigma$,

$$\mathcal{F}\mathcal{L}_{x,t}[u(t,x)](\omega,\xi) := \mathcal{F}_x[\ \mathcal{L}_t[u(t,x)](\omega,x)\ ](\omega,\xi) = \mathcal{F}_{x,t}[e^{-\sigma t} u(t,x)](\eta,\xi)$$

We now return to some formal definitions. Above we have used the spaces $\mathcal{S}(\mathbb{R}^N)$ and LT without defining them. This is done in Definition 3.2.

Definition 3.2 (Tempered and Laplace Transformable Functions and Distributions)
a) [145, Definition 2.11] Let $\|\varphi\|_{k,l} \coloneqq \sup_{x\in\mathbb{R}^N}(|x|^k+1)\sum_{|\alpha|\le l}|D^\alpha\varphi(x)|$ *for* $k,l\ge 0$ *and any multi-index* α*. Then*

$$\mathcal{S}(\mathbb{R}^N) \coloneqq \left\{\ \varphi\in C^\infty(\mathbb{R}^N)\ \ \middle|\ \ \|\varphi\|_{k,l}<\infty \text{ for all } k,l\in\mathbb{N}_0\ \right\}$$

is called the space of tempered functions*. It is also known as the* space of rapidly decreasing/decaying (towards infinity) functions*. Note that the definition*

$$\mathcal{S}(\mathbb{R}^N) = \left\{\ \varphi\in C^\infty(\mathbb{R}^N)\ \ \middle|\ \ \sup_{x\in\mathbb{R}^N}\left|x^\alpha\partial^\beta\varphi(x)\right|<\infty \text{ for all multi-indices } \alpha,\beta\ \right\}$$

is equivalent [114, p. 72], [131, p. 184].

b) The dual space of $\mathcal{S}(\mathbb{R}^N)$ *(the space of all distributions on* $\mathcal{S}(\mathbb{R}^N)$*), denoted by* $\mathcal{S}^*(\mathbb{R}^N)$*, is called the* space of tempered distributions *or the* space of slowly growing distributions*.*

c) [114, p. 65] We set $\mathcal{D}(\mathbb{R}^N)\coloneqq C^\infty_{\text{comp}}(\mathbb{R}^N)$*, with* $C^\infty_{\text{comp}}(\mathbb{R}^N)$ *as in [114, p. 61].*

d) Let $N=1$*. By* $\mathcal{D}^*_+(\mathbb{R})$*, we denote the* space of causal distributions*, i.e. the space of distributions with support in* $[0,\infty)$*, and by* $\mathcal{S}^*_+(\mathbb{R})$ *the* space of causal tempered distributions*. Using Remark 3.1 b), the use of the Laplace transform makes sense for* $f\in\mathcal{D}^*_+(\mathbb{R})$ *with* $e^{-\sigma_0 t}f\in\mathcal{S}^*_+(\mathbb{R})$ *for some* $\sigma_0\in\mathbb{R}$*.*

In this case, i.e. if $f\in\mathcal{D}^*_+(\mathbb{R})$*,* $\mathcal{L}[f](\omega)$ *is holomorphic for* $\omega=\mu+i\sigma$ *with* $\Im(\omega)=\sigma>\sigma_0$*. We thus have the set LT of* Laplace transformable distributions *given by [151, p. 417]*

$$LT \coloneqq \bigcup_{\sigma_0\in\mathbb{R}} LT(\sigma_0)$$

where, for any $\sigma_0\in\mathbb{R}$*,*

$$LT(\sigma_0)\coloneqq\left\{\ f\in\mathcal{D}^*_+(\mathbb{R})\ \ \middle|\ \ e^{-\sigma_0 t}f\in\mathcal{S}^*_+(\mathbb{R})\ \right\}.$$

For any $f\in LT$*, we set* $\sigma(f)\coloneqq\inf\{\ \sigma_0\mid f\in LT(\sigma_0)\ \}$*.*

Remark 3.3 (On Definition 3.2)
[114, p. 72] There holds $\mathcal{D}(\mathbb{R}^N)\subseteq\mathcal{S}(\mathbb{R}^N)$ *and* $\mathcal{S}^*(\mathbb{R}^N)\subseteq\mathcal{D}^*(\mathbb{R}^N)$*.*

Similar definitions for domains $\Omega\subseteq\mathbb{R}^N$ can be found in any textbook on functional analysis. Here we need to extend the definitions above to functions and distributions valued in Banach spaces, as in [151, Section 39] and used in [20, 81].

Definition 3.4 (Generalisation of Definition 3.2 to Banach Spaces)
Let E *be a Banach space.*

a) [151, (39.15)] Let $\|f\|_{k,l}\coloneqq\sup_{t\in\mathbb{R}}(t^2+1)^k\sum_{|\alpha|\le l}\|D^\alpha f(\cdot,t)\|_E$ *for* $k,l\ge 0$ *and any multi-index* α*. Then*

$$\mathcal{S}(E)\coloneqq\left\{\ f(\cdot,t)\in C^\infty(\mathbb{R}),\ \text{valued in } E\ \ \middle|\ \ \|f(\cdot,t)\|_{k,l}<\infty \text{ for all } k,l\in\mathbb{N}_0\ \right\}$$

is called the space of tempered E-valued functions*. Again,* $\mathcal{F}:\mathcal{S}(E)\to\mathcal{S}(E)$ *is an isomorphism.*

b) *The dual space of $\mathcal{S}(E)$ (the space of all distributions on $\mathcal{S}(E)$), denoted by $\mathcal{S}^*(E)$, is called the* space of tempered E-valued distributions *or the* space of E-valued distributions of slow growth. *An equivalent definition can be found in [151, p. 417]. Again, $\mathcal{S}^*(E)$ can be identified with a subspace of $\mathcal{D}^*(E)$. For causal distributions, i.e. those with support on $[0,\infty)$, the respective spaces are again denoted by $\mathcal{S}_+^*(E)$ and $\mathcal{D}_+^*(E)$.*

c) *[34, p. 25], [81, p. 16] The set $LT(E)$ of* Laplace transformable distributions with values in E *is given by*

$$LT(E) := \bigcup_{\sigma_0 \in \mathbb{R}} LT(\sigma_0, E)$$

where, for any $\sigma_0 \in \mathbb{R}$,

$$LT(\sigma_0, E) := \left\{ f(\cdot,t) \in \mathcal{D}_+^*(E) \;\middle|\; e^{-\sigma_0 t} f(\cdot,t) \in \mathcal{S}_+^*(E) \right\}.$$

Again, for any $f \in LT(E)$, we set $\sigma(f) := \inf\{ \sigma_0 \mid f \in LT(\sigma_0, E) \}$.

For reference, we state the well known Paley-Wiener Theorem and the Parseval-Plancherel identity. Lemma 3.5 allows to map results on existence and uniqueness obtained in the frequency domain to the space-time domain [20, p. 415], and Lemma 3.6 can be used to deduce mapping properties of time dependent operators from the mapping properties of time independent operators.

Lemma 3.5 (Paley-Wiener Theorem [81, Theorem 1.1], [151, Theorem 43.1])
Let the E-valued function $\hat{f}(\cdot,\omega) = \hat{f}(\cdot,\mu+i\sigma)$ be holomorphic in the half-plane

$$\mathbb{C}_{\sigma_0} := \{ \omega \in \mathbb{C} \mid \Im(\omega) = \sigma > \sigma_0 \}$$

for $\sigma_0 \in \mathbb{R}$. Then the following conditions are equivalent:

a) *There exists a distribution $f \in LT(E)$ such that $\mathcal{L}_t[f(t,\cdot)](\omega,\cdot) = \hat{f}(\omega,\cdot)$.*

b) *There exists some $\sigma_1 > \sigma_0$, some $C > 0$ and $k \geq 0$ such that*

$$\|\hat{f}(\cdot,\omega)\|_E \leq C(1+|\omega|)^k$$

for all ω with $\Im(\omega) \geq \sigma_1$.

Lemma 3.6 (Parseval-Plancherel Identity [81, Theorem 1(3)], [114, Theorem 3.12])
Let E be a Hilbert space, $\omega = \mu + i\sigma$ and $f, g \in LT(E) \cap L^1_{loc}(\mathbb{R}, E)$. Then

$$\frac{1}{2\pi}\int_{\mathbb{R}+i\sigma} \left(\hat{f}(\omega), \hat{g}(\omega)\right)_E \, d\omega = \frac{1}{2\pi}\int_{\mathbb{R}} \left(\hat{f}(\mu+i\sigma), \hat{g}(\mu+i\sigma)\right)_E \, d\mu = \int_{\mathbb{R}} e^{-2\sigma t} \left(f(t), g(t)\right)_E \, dt.$$

With $\sigma = 0$, we obtain

$$\frac{1}{2\pi}\int_{\mathbb{R}} \left(\tilde{f}(\mu), \tilde{g}(\mu)\right)_E \, d\mu = \int_{\mathbb{R}} \left(f(t), g(t)\right)_E \, dt$$

for the Fourier transform.

As in [20, p. 415], we further define an operator Λ^s implicitly by

$$\Lambda^s[f] := \mathcal{L}^{-1}\left[(-i\omega)^s \hat{f}(\omega)\right] \tag{3.4}$$

for any $s \in \mathbb{R}$. For $s = k$ with $k \in \mathbb{N}$, this is the k-th temporal derivative of f, whereas for $s = -k$ with $k \in \mathbb{N}$, this is the k-th temporal anti-derivative of f.

3.2 Analysis in the Laplace Domain

As we mentioned in the introduction to this chapter, we use the classical approach for the analysis of the time domain boundary layer potentials and the corresponding time domain boundary integral operators that was introduced by Bamberger and Ha-Duong [20, 21]. This means that we analyse the potentials and operators in the Laplace domain first, after mapping the original problem (P) to the Laplace domain by means of the Laplace transform. The results we obtain there are transferred back to the space-time domain in Section 3.3.

Reviews on this method have been published in the form of research papers, such as the ones by Ha-Duong (2003) [81] or Laliena and Sayas (2009) [103], or in the form of lecture notes, such as the ones by Bécache (1994) [34] or, most recently, Sayas (2011) [136].

Let us recall how the transient problem (P) is related to the time harmonic Helmholtz problem first. Assume that u solves (P), and let $\hat{u} := \mathcal{L}_t[u]$. Then $\hat{u}$ solves the exterior *Helmholtz boundary value problem*

$$
\text{(HH)} \quad \left\{ \begin{array}{l} \text{Find } u : \Omega \to \mathbb{R} \text{ such that} \\ \\ \qquad\qquad \Delta u + \omega^2 u = 0 \text{ in } \Omega \qquad (3.5a) \\ \qquad\qquad \mathcal{B}[u] = \hat{g} \text{ on } \Gamma \qquad (3.5b) \\ \qquad\qquad \lim\limits_{R\to\infty} \int_{\partial\mathbb{B}_R(0)} |\nabla u \cdot n_x - i\omega u|^2 \, ds_x = 0 \qquad (3.5c) \\ \\ \text{where } \hat{g} := \mathcal{L}_t[g] : \Gamma \to \mathbb{R}, \text{ with } g \text{ as in (P).} \end{array} \right.
$$

Equation (3.5a) is known as the homogeneous *Helmholtz equation*, while condition (3.5c) is called the *Sommerfeld radiation condition*. It corresponds [148, p. 26] to the causality conditions (1.1b) and (1.1c) of the transient problem (P).

We note that there are at least two different versions of the Sommerfeld radiation condition by which (3.5c) could be replaced; see [92, (2.1.2) and (2.1.3)] or [122, 2.6.142]. For the definition of the boundary layer potentials and integral operators, we state the fundamental solutions of the Helmholtz equation in Lemma 3.7.

Lemma 3.7 (Fundamental Solutions of the Helmholtz Equation)
The fundamental solution of the Helmholtz equation (3.5a) *is given by [51, (2.6), (3.60)], [122, (2.3.4), (2.3.8)]*

$$
\textit{(1D)}: \qquad G_\omega(x,y) = G_\omega(|x-y|) = -\frac{1}{2i\omega} e^{i\omega|x-y|} \qquad (3.6)
$$

$$
\textit{(2D)}: \qquad G_\omega(x,y) = G_\omega(|x-y|) = \frac{i}{4} H_0^{(1)}(\omega|x-y|) \qquad (3.7)
$$

$$
\textit{(3D)}: \qquad G_\omega(x,y) = G_\omega(|x-y|) = \frac{1}{4\pi} \frac{e^{i\omega|x-y|}}{|x-y|} \qquad (3.8)
$$

with $\omega \in \mathbb{C}$, where $H_0^{(1)}$ denotes the Hankel function *of order zero of the first kind.*

The boundary potentials for the Helmholtz Problem (HH) are defined similarly to the time domain boundary layer potentials given in Definition 1.3.

Definition 3.8 (Boundary Layer Potentials for the Helmholtz Problem)
Let $x \in (\mathbb{R}^n \setminus \Gamma)$. For appropriate densities $p, \varphi : \Gamma \to \mathbb{R}$, the Helmholtz Single Layer potential *is given by*

$$
S_\omega[p](x) = \int_\Gamma G_\omega(|x-y|)\; p(y)\, ds_y \qquad (3.9)
$$

and the Helmholtz Double Layer potential *by*

$$D_\omega[\varphi](x) = \int_\Gamma n_y \cdot \nabla_x G_\omega(|x-y|)\ \varphi(y)\, ds_y\,. \tag{3.10}$$

As in Definition 1.3, we do not specify the regularity of p and φ here. We conduct an explicit analysis that takes the dependency on the wave number ω into account in Section 3.2.2.2. We further refer to [52] for mapping properties of arbitrary elliptic boundary integral operators.

The corresponding boundary integral operators V_ω, K_ω, K'_ω and W_ω are defined analogously to Definition 1.4. Note that the Helmholtz boundary potentials and operators are the Laplace transforms of their transient counterparts, e.g. $S_\omega[\hat{p}] = \mathcal{L}_t\,[S[p]]$.

In the rest of this chapter, we restrict ourselves to the three dimensional case, even though we conduct our studies on a posteriori error estimates in Section 5 and our numerical experiments in two space dimensions. This distinction can be justified by the fact that the fundamental solution of the two dimensional Helmholtz equation is much more complicated than its three dimensional counterpart, and therefore dealing with it would lead to many additional technical difficulties. Other authors have followed these two different routes in theory and practice for the same reason [49, Section 4]. The new generalised mapping properties studied in Section 3.2.2.2, however, also hold in two space dimensions; see Remark 3.26 in particular.

Note that we omit the hat while working in the Laplace domain and write u instead of $\hat{u}$ if its correct meaning is clear and there is no danger of confusion.

3.2.1 An Equivalent Norm in Sobolev Spaces

For some domain Ω, the energy of u in Ω is given by [20, (3.2)], [81, p. 10]

$$E_\Omega[u](t) \coloneqq \frac{1}{2}\int_\Omega |\nabla u(x,t)|^2 + \dot{u}(x,t)^2\ dx. \tag{3.11}$$

By the Parseval-Plancherel identity (Lemma 3.6),

$$\int_{\mathbb{R}} e^{-2\sigma t} E_\Omega[u](t)\ dt = \frac{1}{4\pi}\int_{\mathbb{R}+i\sigma}\int_\Omega |\nabla \hat{u}(x)|^2 + \left(\omega \hat{u}(x)\right)^2\ dx\, d\omega. \tag{3.12}$$

This relation motivates [18, p. 264] the definition of the following energy-related norms.

Recall the definition of the usual $H^s(\mathbb{R}^N)$-norm [114, p. 76], [122, (2.5.55)]

$$\|u\|^2_{H^s(\mathbb{R}^N)} = \int_{\mathbb{R}^N} (1+|\xi|^2)^s |\tilde{u}(\xi)|^2\ d\xi. \tag{3.13}$$

Now, to guarantee $\omega \neq 0$, let $\Im(\omega) > \sigma_0$ for some $\sigma_0 \in \mathbb{R}_{>0}$. Then the norm [34, p. 28], [81, p. 10], [116, p. 1874]

$$\|u\|^2_{s,\omega,\mathbb{R}^N} = \int_{\mathbb{R}^N} (|\omega|^2 + |\xi|^2)^s |\tilde{u}(\xi)|^2\ d\xi \tag{3.14}$$

is equivalent to the $\|\cdot\|_{H^s(\mathbb{R}^N)}$-norm. We often refer to these norms as the *wavenumber-dependent norms* or $|\omega|$*-dependent norms*.

The norms $\|\cdot\|^2_{s,\omega,\Omega}$ and $\|\cdot\|^2_{s,\omega,\Gamma}$ are defined analogously by using an atlas; see, for instance, [81, p. 10] or [125, p. 16]. We write $\|\cdot\|_{s,\omega,\mathcal{O}}$ and $H^s(\mathcal{O})$ when we deal with statements and results that hold for all $\mathcal{O} \in \left\{\mathbb{R}^N, \Omega, \Gamma\right\}$.

Remark 3.9 (Equivalence Estimates for the Classical and $|\omega|$-Dependent Norms) *Note that the* equivalence of the norms is $|\omega|$-dependent *[34, (67)-(69)]. We have, for* $s \geq 0$,

$$\left(|\omega|^2 + |\xi|^2\right)^s \geq \left(\sigma_0^2 + |\xi|^2\right)^s \geq \min\left\{1, \sigma_0^{2s}\right\}\left(1+|\xi|^2\right)^s$$

but only

$$\left(|\omega|^2+|\xi|^2\right)^s \le \left(|\omega|^2+\frac{1}{\sigma_0^2}|\omega|^2|\xi|^2\right)^s \le \max\left\{1,\frac{1}{\sigma_0^{2s}}\right\}|\omega|^{2s}\left(1+|\xi|^2\right)^s$$

and hence, in summary,

$$\min\left\{1,\sigma_0^{2s}\right\}\left(1+|\xi|^2\right)^s \;\le\; \left(|\omega|^2+|\xi|^2\right)^s \;\le\; \max\left\{1,\frac{1}{\sigma_0^{2s}}\right\}|\omega|^{2s}\left(1+|\xi|^2\right)^s. \tag{3.15}$$

Correspondingly, for $s \le 0$,

$$\min\left\{1,\sigma_0^{2s}\right\}|\omega|^{2s}\left(1+|\xi|^2\right)^s \;\le\; \left(|\omega|^2+|\xi|^2\right)^s \;\le\; \max\left\{1,\frac{1}{\sigma_0^{2s}}\right\}\left(1+|\xi|^2\right)^s. \tag{3.16}$$

(3.15) *and* (3.16) *can be summarised as*

$$C_1(\sigma_0)\left(|\omega|^{2s}\right)^{H(-s)}\left(1+|\xi|^2\right)^s \;\le\; \left(|\omega|^2+|\xi|^2\right)^s \;\le\; C_2(\sigma_0)\left(|\omega|^{2s}\right)^{H(s)}\left(1+|\xi|^2\right)^s \tag{3.17}$$

for any $s \in \mathbb{R}$. *Norm equivalences of the type [136, (2.13)]*

$$C(\sigma_0)\|u\|_{H^1(\mathcal{O})} \le \|u\|_{1,\omega,\mathcal{O}} \le \tilde{C}(\sigma_0)|\omega|\|u\|_{H^1(\mathcal{O})} \tag{3.18}$$

for $\mathcal{O} \in \left\{\mathbb{R}^N,\Omega,\Gamma\right\}$ *can be concluded from* (3.17).

Example 3.10 (Norm Equivalences)
a) For $s = 1$ *[117, (1.2a)]*

$$\|u\|^2_{1,\omega,\mathbb{R}^N} = |\omega|^2\int_{\mathbb{R}^N}|\tilde{u}(\xi)|^2\,d\xi + \int_{\mathbb{R}^N}|\nabla\tilde{u}(\xi)|^2\,d\xi = |\omega|^2\|u\|^2_{L^2(\mathbb{R}^N)} + |u|^2_{H^1(\mathbb{R}^N)}.$$

Similarly, for $s = 2$,

$$\|u\|^2_{2,\omega,\mathbb{R}^N} = |\omega|^4\|u\|^2_{L^2(\mathbb{R}^N)} + 2|\omega|^2|u|^2_{H^1(\mathbb{R}^N)} + |u|^2_{H^2(\mathbb{R}^N)}.$$

b) Since, for $a,b \ge 0$, $\sqrt{\frac{1}{2}}(a+b) \le \sqrt{a^2+b^2} \le a+b$, *there holds*

$$\sqrt{\frac{1}{2}}\left(|\omega|\|u\|^2_{L^2(\mathbb{R}^N)} + |u|^2_{H^{1/2}(\mathbb{R}^N)}\right) \le \|u\|^2_{1/2,\omega,\mathbb{R}^N} \le |\omega|\|u\|^2_{L^2(\mathbb{R}^N)} + |u|^2_{H^{1/2}(\mathbb{R}^N)}$$

and therefore equivalence of these two norms; see also [117, (1.2b)].

Due to the $|\omega|$-dependence of the equivalence estimates illustrated in Remark 3.9, we cannot deduce, for instance, the trace theorem for the $|\omega|$-dependent norms directly from the results for the standard norms without any 'losses' regarding powers of $|\omega|$. We prove these results separately in Section 3.2.1.1.

3.2.1.1 The Trace Theorem for the $|\omega|$-Dependent Norms

The proofs of the following results are all similar to the ones of the original results given in [114]. For the particular case $s = 1$, a result similar to Lemma 3.11 below is given in [35, Lemma 3.1], based on the proof of [56, Theorem 2] for the standard norms. These are also collected in Lemma 3.17 below. We give outlines of the proofs here for completeness and to demonstrate the (minor) differences to the original proofs. The term 'generalisation' is appropriate in the sense that we obtain the classical theorems (see, for instance, [133, Theorems 2.6.8, 2.6.9] or [145, Theorem 2.21]) again for $|\omega| = 1$.

Lemma 3.11 (Generalisation of [114, Lemma 3.35] and [114, Theorem 3.37])
a) For $s > \frac{1}{2}$, the trace operator $\gamma : \mathcal{D}(\mathbb{R}^n) \to \mathcal{D}(\mathbb{R}^{n-1})$, given by

$$\gamma[u](x) = \gamma[u](x', x_n) := u(x', 0)$$

has a unique extension to a bounded linear operator

$$\gamma : H^s(\mathbb{R}^n) \to H^{s-1/2}(\mathbb{R}^{n-1})$$

where the continuity constant with respect to the $|\omega|$-dependent norm $\|\cdot\|_{s,\omega,\mathcal{O}}$ depends on s but not on $|\omega|$, i.e. there exists a $|\omega|$-independent constant $C = C(s) > 0$ such that

$$\|\gamma[u]\|_{s-1/2,\omega,\mathbb{R}^{n-1}} \leq C\|u\|_{s,\omega,\mathbb{R}^n} \tag{3.19}$$

for $u \in H^s(\mathbb{R}^n)$.

b) Let Ω be a $C^{k,1}$ domain and $\frac{1}{2} < s \leq k + 1$. Then the trace operator $\gamma : \mathcal{D}(\bar{\Omega}) \to \mathcal{D}(\Gamma)$, defined by $\gamma[u] := u|_\Gamma$, has an extension to a linear bounded operator

$$\gamma : H^s(\Omega) \to H^{s-1/2}(\Gamma)$$

where the continuity constant with respect to the $|\omega|$-dependent norms $\|\cdot\|_{s,\omega,\mathcal{O}}$, $\mathcal{O} \in \{\Omega, \Gamma\}$, depends on s, σ_0 and Γ but not on $|\omega|$ in the sense of part a).

Proof
Part b) is a consequence of part a), using a technique called 'flattening of the boundary' described in the proof of [114, Theorem 3.37]. It is thus enough to show part a).

We write $x = (x', x_n)$ and $\xi = (\xi', \xi_n)$ for $x, \xi \in \mathbb{R}^n$. Since

$$\tilde{u}(\xi) := \mathcal{F}_x[u](\xi) = \mathcal{F}_{x_n}\left[\mathcal{F}_{x'}[u](\xi', x_n)\right](\xi', \xi_n)$$

there holds, by the definition of the inverse Fourier transform,

$$\mathcal{F}_{x_n}^{-1}\left[\tilde{u}\right](\xi', x_n) = \int_{\mathbb{R}} e^{i\,2\pi\,\xi_n x_n} \tilde{u}(\xi', \xi_n)\, d\xi_n = \mathcal{F}_{x'}[u](\xi', x_n).$$

By the definition, $\gamma[u](x) = \gamma[u](x') = u(x', 0)$ and thus

$$\mathcal{F}_{x'}\left[\gamma[u]\right](\xi') = \int_{\mathbb{R}} \tilde{u}(\xi', \xi_n)\, d\xi_n = \int_{\mathbb{R}} \left(|\omega|^2 + |\xi|^2\right)^{-s/2} \left(|\omega|^2 + |\xi|^2\right)^{s/2} \tilde{u}(\xi', \xi_n)\, d\xi_n. \tag{3.20}$$

By the Cauchy-Schwarz inequality for integrals, we obtain

$$\left|\mathcal{F}_{x'}\left[\gamma[u]\right](\xi')\right|^2 \leq M_s^\omega(\xi') \int_{\mathbb{R}} \left(|\omega|^2 + |\xi|^2\right)^s \left|\tilde{u}(\xi', \xi_n)\right|^2\, d\xi_n. \tag{3.21}$$

where

$$M_s^\omega(\xi') := \int_{\mathbb{R}} \left(|\omega|^2 + |\xi|^2\right)^{-s} \, d\xi_n = \left(|\omega|^2 + |\xi'|^2\right)^{1/2-s} \int_{\mathbb{R}} (t^2+1)^{-s} \, dt \tag{3.22}$$

via the substitution $t(\xi_n) := \xi_n \left(|\omega|^2 + |\xi'|^2\right)^{-1/2}$ that gives $d\xi_n = \left(|\omega|^2 + |\xi'|^2\right)^{1/2} \, dt$ and $|\omega|^2 + |\xi|^2 = (1+t^2)\left(|\omega|^2 + |\xi'|^2\right)$. By [114, p. 100], there holds, for $s > 1/2$,

$$C_s := \int_{\mathbb{R}} (t^2+1)^{-s} \, dt < \infty$$

where the constant C_s is obviously $|\omega|$-independent. Combining (3.21) and (3.22), we obtain

$$\left(|\omega|^2 + |\xi'|^2\right)^{s-1/2} \left|\mathcal{F}_{x'}\left[\gamma[u]\right](\xi')\right|^2 \le C_s \int_{\mathbb{R}} \left(|\omega|^2 + |\xi|^2\right)^s \left|\tilde{u}(\xi', \xi_n)\right|^2 \, d\xi_n. \tag{3.23}$$

Taking the integral $\int_{\mathbb{R}^{n-1}} \, d\xi'$ in (3.23) proves the claimed result via the definitions of the respective norms. ∎

Since a Lipschitz boundary is $C^{0,1}$, the result above can only be applied for $\frac{1}{2} < s \le 1$ in this case. In fact it can be extended to the range $1 < s < \frac{3}{2}$, as the following result shows. The proof is again similar to the original ones of [52, Lemma 3.6] and [114, Theorem 3.38].

Lemma 3.12 (Generalisation of [114, Theorem 3.38])
Let Ω be a Lipschitz domain and $\frac{1}{2} < s < \frac{3}{2}$. Then the trace operator defined in Lemma 3.11 b) is bounded independently of $|\omega|$ as an operator mapping $H^s(\Omega)$ to $H^{s-1/2}(\Gamma)$ in the same way as in Lemma 3.11 b), i.e. with a continuity constant that depends only on s, σ_0 and Γ.

The following result is an immediate consequence of Lemma 3.12 and the fact that the norms of a linear operator and of its dual operator are equal; see, for instance, [114, Lemma 2.9] or [133, Proposition 2.1.4].

Corollary 3.13
Let Ω be a Lipschitz domain and $\frac{1}{2} < s < \frac{3}{2}$. Then the adjoint operator γ^* to the trace operator γ defined in Lemma 3.11 b) is bounded independently of ω as an operator mapping $\left(H^{s-1/2}(\Gamma)\right)^* = H^{1/2-s}(\Gamma)$ to $\left(H^s(\Omega)\right)^* = H^{-s}(\Omega)$ in the same way as in Lemma 3.12.

Proof (of Lemma 3.12)
First we define an anisotropic Sobolev space E_ω^s via the norm

$$\|u\|_{E_\omega^s}^2 := \int_{\mathbb{R}} |\xi_n|^{2s} \|\mathcal{F}_{x_n}[u(\cdot, x_n)](\cdot, \xi_n)\|_{L^2(\mathbb{R}^{n-1})}^2 + |\xi_n|^{2(s-1)} \|\mathcal{F}_{x_n}[u(\cdot, x_n)](\cdot, \xi_n)\|_{1,\omega,\mathbb{R}^{n-1}}^2 \, d\xi_n.$$

By the definitions of the norms, there holds

$$\|u\|_{E_\omega^s}^2 = \int_{\mathbb{R}^n} |\xi_n|^{2(s-1)} \left(|\omega|^2 + |\xi|^2\right) |\tilde{u}(\xi)|^2 \, d\xi_n$$

where, as in the proof of Lemma 3.11, $\tilde{u} := \mathcal{F}_x[u]$. Writing $x = (x', x_n)$ and $\xi = (\xi', \xi_n)$ for $x, \xi \in \mathbb{R}^n$ again, we define

$$u_\zeta(x) := u(x', \zeta(x') + x_n)$$

where ζ is the Lipschitz-continuous function whose graph is Γ, see [114, p. 89f.]. Then, by the definition,

$$\|\gamma[u]\|_{s-1/2,\omega,\Gamma} = \|u_\zeta(\cdot, 0)\|_{s-1/2,\omega,\mathbb{R}^{n-1}}. \tag{3.24}$$

Analogously to the proof of [114, Theorem 3.38], there hold the inequalities

$$\|u_\zeta\|_{E^s_\omega} \le C\|u\|_{E^s_\omega} \tag{3.25}$$

and

$$\|u\|_{E^s_\omega} \le \|u\|_{s,\omega,\mathbb{R}^n} \tag{3.26}$$

where $C = C(\Omega)$ is $|\omega|$-independent. Further, by the definition and (3.20), and by the Cauchy-Schwarz inequality for integrals,

$$\begin{aligned}
\|u(\cdot,0)\|^2_{s-1/2,\omega,\mathbb{R}^{n-1}} &= \int_{\mathbb{R}^{n-1}} \left(|\omega|^2+|\xi'|^2\right)^{s-1/2} \left|\int_{\mathbb{R}} \tilde{u}(\xi)\, d\xi_n\right|^2 d\xi' \\
&\le \int_{\mathbb{R}^{n-1}} \left(|\omega|^2+|\xi'|^2\right)^{s-1/2} \left(\int_{\mathbb{R}} |\xi_n|^{2(1-s)} \left(|\omega|^2+|\xi|^2\right)^{-1} d\xi_n\right) \\
&\qquad \int_{\mathbb{R}} |\xi_n|^{2(s-1)} \left(|\omega|^2+|\xi|^2\right) |\tilde{u}(\xi)|^2\, d\xi_n\ d\xi'.
\end{aligned}$$

Using the same substitution as in the proof of Lemma 3.11, we obtain

$$\begin{aligned}
&\int_{\mathbb{R}} |\xi_n|^{2(1-s)} \left(|\omega|^2+|\xi|^2\right)^{-1} d\xi_n \\
&= \int_{\mathbb{R}} t^{2(1-s)} \left(|\omega|^2+|\xi'|^2\right)^{1-s} (t^2+1)^{-1} \left(|\omega|^2+|\xi'|^2\right)^{-1} \left(|\omega|^2+|\xi'|^2\right)^{1/2} dt \\
&= \left(|\omega|^2+|\xi'|^2\right)^{1/2-s} \int_{\mathbb{R}} (t^2+1)^{-1}\ t^{2(1-s)}\, dt =: \left(|\omega|^2+|\xi'|^2\right)^{1/2-s} C_s
\end{aligned}$$

where the constant $C_s < \infty$ is obviously $|\omega|$-independent. Thus

$$\begin{aligned}
&\|u(\cdot,0)\|^2_{s-1/2,\omega,\mathbb{R}^{n-1}} \\
&\le \int_{\mathbb{R}^{n-1}} \left(|\omega|^2+|\xi'|^2\right)^{s-1/2} C_s \left(|\omega|^2+|\xi'|^2\right)^{1/2-s} \int_{\mathbb{R}} |\xi_n|^{2(s-1)} \left(|\omega|^2+|\xi|^2\right) |\tilde{u}(\xi)|^2\, d\xi_n\ d\xi' \\
&= C_s \int_{\mathbb{R}^n} |\xi_n|^{2(s-1)} \left(|\omega|^2+|\xi|^2\right) |\tilde{u}(\xi)|^2\, d\xi \ = \ C_s \|u\|^2_{E^s_\omega}.
\end{aligned} \tag{3.27}$$

Combining estimates (3.24), (3.27), (3.25) and (3.26), we obtain

$$\|\gamma[u]\|_{s-1/2,\omega,\Gamma} = \|u_\zeta(\cdot,0)\|_{s-1/2,\omega,\mathbb{R}^{n-1}} \le \sqrt{C_s}\|u_\zeta\|_{E^s_\omega} \le \sqrt{C_s} C \|u\|_{E^s_\omega} \le \sqrt{C_s} C \|u\|_{s,\omega,\mathbb{R}^n}$$

which proves the claim. ∎

The next result is about the inverse to γ, the so-called extension operator. As before, the proofs follow the respective ones given in [114] closely.

Lemma 3.14 (Generalisation of [114, Lemma 3.36] and [114, Theorem 3.37])
a) For each $j \in \mathbb{Z}_{\ge 0}$, there exists an $|\omega|$-dependent bounded linear operator

$$\eta^\omega_j : H^{s-j-1/2}(\mathbb{R}^{n-1}) \to H^s(\mathbb{R}^n)$$

where the continuity constant with respect to the $|\omega|$-dependent norm $\|\cdot\|_{s,\omega,\mathbb{R}^N}$ depends on s, but not on $|\omega|$ in the sense of Lemma 3.11 a), i.e. there exists a $|\omega|$-independent constant $C = C(s) > 0$ such that

$$\|\eta^\omega_j[u]\|_{s,\omega,\mathbb{R}^n} \le C\|u\|_{s-j-1/2,\omega,\mathbb{R}^{n-1}} \tag{3.28}$$

for $u \in H^{s-j-1/2}(\mathbb{R}^{n-1})$.

b) Let Ω be a $C^{k,1}$ domain and $\frac{1}{2} < s \le k+1$. Then there exists a $|\omega|$-dependent bounded linear operator

$$Z_\Omega^\omega : H^{s-1/2}(\Gamma) \to H^s(\Omega)$$

which is a right inverse to γ, i.e. $(\gamma \circ Z_\Omega^\omega)[\varphi] \equiv \varphi$ for $\varphi \in H^{s-1/2}(\Gamma)$. The continuity constant with respect to the $|\omega|$-dependent norms $\|\cdot\|_{s,\omega,\mathcal{O}}$, $\mathcal{O} \in \{\Omega, \Gamma\}$, depends on s, σ_0 and Γ, but not on $|\omega|$ in the sense of part a). Z_Ω^ω is sometimes called the extension operator *to φ.*

Proof
Part b) is a consequence of part a); taking $Z_\Omega^\omega = \eta_0^\omega$ and using the same technique as in the proof of Lemma 3.11 b). It is thus enough to show part a).

Take $\theta_j \in \mathcal{D}(\mathbb{R})$ such that $\theta_j(y) = \frac{y^j}{j!}$ for $|y| \le 1$. The operator η_j^ω is defined by, for $x \in \mathbb{R}^n$,

$$\eta_j^\omega[u](x) := \int_{\mathbb{R}^{n-1}} \frac{\tilde{u}(\xi')\,\theta_j\left((|\omega|^2 + |\xi'|^2)^{1/2} x_n\right)}{(|\omega|^2 + |\xi'|^2)^{j/2}} e^{i\,2\pi\,\xi'\cdot x'}\, d\xi' \tag{3.29}$$

where, in this case, $\tilde{u} = \mathcal{F}_{x'}[u]$.
Then

$$\begin{aligned}
&\mathcal{F}_{x_n}\left[\eta_j^\omega[u]\right](x', \xi_n) = \int_{\mathbb{R}} \eta_j^\omega[u](x', x_n)\; e^{-i\,2\pi\,x_n\xi_n}\, dx_n \\
= &\int_{\mathbb{R}^{n-1}} \int_{\mathbb{R}} \theta_j\left((|\omega|^2 + |\xi'|^2)^{1/2} x_n\right)\; e^{-i\,2\pi\,x_n\xi_n}\, dx_n\; \frac{\tilde{u}(\xi')}{(|\omega|^2 + |\xi'|^2)^{j/2}}\; e^{i\,2\pi\,\xi'\cdot x'}\, d\xi' \\
= &\mathcal{F}_{x'}^{-1}\left[\frac{\tilde{u}(\xi')}{(|\omega|^2 + |\xi'|^2)^{j/2}} \int_{\mathbb{R}} \theta_j\left((|\omega|^2 + |\xi'|^2)^{1/2} x_n\right)\; e^{-i\,2\pi\,x_n\xi_n}\, dx_n\right](x', \xi_n)
\end{aligned}$$

and thus

$$\begin{aligned}
\mathcal{F}_x\left[\eta_j^\omega[u]\right](\xi) &= \mathcal{F}_{x'}\left[\mathcal{F}_{x_n}\left[\eta_j^\omega[u]\right](x', \xi_n)\right](\xi', \xi_n) \\
&= \frac{\tilde{u}(\xi')}{(|\omega|^2 + |\xi'|^2)^{j/2}} \int_{\mathbb{R}} \theta_j\left((|\omega|^2 + |\xi'|^2)^{1/2} x_n\right)\; e^{-i\,2\pi\,x_n\xi_n}\, dx_n.
\end{aligned}$$

Substituting $y(x_n) := \left(|\omega|^2 + |\xi'|^2\right)^{1/2} x_n$, we obtain, with $dx_n = \left(|\omega|^2 + |\xi'|^2\right)^{-1/2} dy$,

$$\begin{aligned}
&\int_{\mathbb{R}} \theta_j\left((|\omega|^2 + |\xi'|^2)^{1/2} x_n\right)\; e^{-i\,2\pi\,x_n\xi_n}\, dx_n \\
= &\left((|\omega|^2 + |\xi'|^2)^{-1/2} \int_{\mathbb{R}} \theta_j(y)\; e^{-i\,2\pi\,y\left(\xi_n\left(|\omega|^2+|\xi'|^2\right)^{-1/2}\right)}\, dy \right. \\
= &\left(|\omega|^2 + |\xi'|^2\right)^{-1/2} \mathcal{F}_{x_n}[\theta_j]\left(\xi_n\left(|\omega|^2 + |\xi'|^2\right)^{-1/2}\right)
\end{aligned}$$

and hence

$$\mathcal{F}_x\left[\eta_j^\omega[u]\right](\xi) = \tilde{u}(\xi')\; \left(|\omega|^2 + |\xi'|^2\right)^{-(j+1)/2}\; \mathcal{F}_{x_n}[\theta_j]\left(\xi_n\left(|\omega|^2 + |\xi'|^2\right)^{-1/2}\right).$$

Now

$$\begin{aligned}
&\|\eta_j^\omega[u]\|_{s,\omega,\mathbb{R}^n}^2 = \int_{\mathbb{R}^n} \left(|\omega|^2 + |\xi|^2\right)^s \left|\mathcal{F}_x\left[\eta_j^\omega[u]\right](\xi)\right|^2\, d\xi \\
= &\int_{\mathbb{R}^{n-1}} \frac{|\tilde{u}(\xi')|^2}{(|\omega|^2 + |\xi'|^2)^{j+1}} \int_{\mathbb{R}} \left(|\omega|^2 + |\xi|^2\right)^s \left|\mathcal{F}_{x_n}[\theta_j]\left(\xi_n\left(|\omega|^2 + |\xi'|^2\right)^{-1/2}\right)\right|^2\, d\xi_n\, d\xi'.
\end{aligned}$$

Using the same substitution as in the proof of Lemma 3.11, we obtain

$$\begin{aligned}
&\|\eta_j^\omega[u]\|^2_{s,\omega,\mathbb{R}^n} \\
= &\int_{\mathbb{R}^{n-1}} \frac{|\tilde{u}(\xi')|^2}{\left(|\omega|^2+|\xi'|^2\right)^{j+1}} \int_{\mathbb{R}} \left(|\omega|^2+|\xi'|^2\right)^s (1+t^2)^s \left(|\omega|^2+|\xi'|^2\right)^{1/2} |\mathcal{F}_{x_n}[\theta_j](t)|^2 \; dt\, d\xi' \\
= &\int_{\mathbb{R}^{n-1}} |\tilde{u}(\xi')|^2 \left(|\omega|^2+|\xi'|^2\right)^{s-j-1/2} \int_{\mathbb{R}} (1+t^2)^s |\mathcal{F}_{x_n}[\theta_j](t)|^2 \; dt\, d\xi'
\end{aligned}$$

where the integral $\int_{\mathbb{R}}(1+t^2)^s |\mathcal{F}_{x_n}[\theta_j](t)|^2 \; dt =: C_s < \infty$ is bounded independently of $|\omega|$ for all $s \in \mathbb{R}$ [114, p. 102] and thus finally

$$\|\eta_j^\omega[u]\|^2_{s,\omega,\mathbb{R}^n} = C_s \|\eta_j^\omega[u]\|^2_{s-j-1/2,\omega,\mathbb{R}^{n-1}}.$$

This completes the proof. ∎

3.2.1.2 A Brief Remark on Interpolation

We close our observations on the $|\omega|$-dependent norms with some brief remarks on interpolation. We use the notation $[X,Y]_\theta$ with $\theta \in (0,1)$ for interpolation spaces here, where X, Y are Banach spaces with $X \subseteq Y$. Without providing any technical details, we first cite a result for future reference.

Lemma 3.15 (Interpolation Estimate [114, Lemma B.1])
For any $u \in X \subseteq Y$, there holds

$$\|u\|_{[X,Y]_\theta} \leq \|u\|_X^{1/2-\theta} \|u\|_Y^{1/2+\theta}.$$

We now return to our specific setup. It is well established that $[H^{s_0}(\mathcal{O}), H^{s_1}(\mathcal{O})]_\theta = H^s(\mathcal{O})$ for $s = (1-\theta)s_0 + \theta s_1$, $\theta \in (0,1)$ and $\mathcal{O} \in \{\mathbb{R}^N, \Omega, \Gamma\}$; see, for instance, [114, Theorem B.7]. In what follows, we need:

Theorem 3.16 (Interpolation for Sobolev Spaces $H^s(\mathcal{O})$ [114, Theorem B.2])
Let the linear operator A be bounded as $A : H^{s_0}(\mathcal{O}) \to H^{t_0}(\mathcal{O})$ and as $A : H^{s_1}(\mathcal{O}) \to H^{t_1}(\mathcal{O})$ with

$$\|A[u]\|_{H^{t_j}(\mathcal{O})} \leq M_j \|u\|_{H^{s_j}(\mathcal{O})}$$

for $j = 0, 1$. Then

$$\|A[u]\|_{H^t(\mathcal{O})} \leq M_0^{1-\theta} M_1^\theta \|u\|_{H^s(\mathcal{O})} \tag{3.30}$$

for $s = (1-\theta)s_0 + \theta s_1$, $t = (1-\theta)t_0 + \theta t_1$ and $\theta \in (0,1)$, i.e. $A : H^s(\mathcal{O}) \to H^t(\mathcal{O})$ is also a bounded map for these numbers s, t.

Theorem 3.16 is stated in [114, Theorem B.2] and [133, Theorem 2.1.62] in general, but it is cited here for the special case of Sobolev spaces. In what follows, it is shown that Theorem 3.16 still holds without any additional $|\omega|$-dependent factors in (3.30) if the wave number dependent norms are used. To do this, we follow the proofs in [114]. Let

$$K\left(t, u; (H^{s_0}(\mathbb{R}^n), H^{s_1}(\mathbb{R}^n))\right) := \inf_{\substack{u=u_0+u_1 \\ u_0 \in H^{s_0}(\mathbb{R}^n), u_1 \in H^{s_1}(\mathbb{R}^n)}} \left(\|u_0\|^2_{H^{s_0}(\mathbb{R}^n)} + t^2 \|u_1\|^2_{H^{s_1}(\mathbb{R}^n)}\right)$$

for $t > 0$ and $u \in H^{s_0}(\mathbb{R}^n) + H^{s_1}(\mathbb{R}^n)$. It is shown in [114, Theorem B.7] that

$$K\left(t, u; (H^{s_0}(\mathbb{R}^n), H^{s_1}(\mathbb{R}^n))\right) = \int_{\mathbb{R}^n} (1+|\xi|^2)^{s_0} \left(f\left(a(\xi)t\right)\right)^2 |\tilde{u}(\xi)|^2 \, d\xi$$

with $a(\xi) = (1+|\xi|^2)^{(s_1-s_0)/2}$ and $f(t) = \frac{t}{\sqrt{1+t^2}}$, and

$$\|K(\cdot,u;(H^{s_0}(\mathbb{R}^n),H^{s_1}(\mathbb{R}^n)))\|_{\theta,2} = \left(\frac{\pi}{2\sin(\pi\theta)}\right)^{1/2} \|u\|_{H^s(\mathbb{R}^n)} =: N_{\theta,2}\|u\|_{H^s(\mathbb{R}^n)}$$

where $\|\cdot\|_{\theta,2}$ is a weighted L_2 norm,

$$\|f\|_{\theta,2}^2 := \int_{\mathbb{R}_{\geq 0}} \frac{|t^{-\theta}f(t)|^2}{t}\,dt.$$

Note that $\|u\|_{K_{\theta,2}(H^{s_0}(\mathbb{R}^n),H^{s_1}(\mathbb{R}^n))} = N_{\theta,2}\|K(\cdot,u;(H^{s_0}(\mathbb{R}^n),H^{s_1}(\mathbb{R}^n)))\|_{\theta,2}$ is the norm of the interpolation space $[H^{s_0}(\mathbb{R}^n),H^{s_1}(\mathbb{R}^n)]_\theta = K_{\theta,2}((H^{s_0}(\mathbb{R}^n),H^{s_1}(\mathbb{R}^n)))$ that corresponds to θ [114, p. 319].

Repeating the proof of [114, Theorem B.7] line by line, we find that, for

$$K_\omega(t,u;(H^{s_0}(\mathbb{R}^n),H^{s_1}(\mathbb{R}^n))) := \inf_{\substack{u=u_0+u_1 \\ u_0\in H^{s_0}(\mathbb{R}^n),u_1\in H^{s_1}(\mathbb{R}^n)}} \left(\|u_0\|_{s_0,\omega,\mathbb{R}^n}^2 + t^2\|u_1\|_{s_1,\omega,\mathbb{R}^n}^2\right)$$

there holds

$$K_\omega(t,u;(H^{s_0}(\mathbb{R}^n),H^{s_1}(\mathbb{R}^n))) = \int_{\mathbb{R}^n} (|\omega|^2+|\xi|^2)^{s_0} \left(f(a_\omega(\xi)t)\right)^2 |\tilde{u}(\xi)|^2\,d\xi$$

with $a(\xi) = (|\omega|^2+|\xi|^2)^{(s_1-s_0)/2}$ and

$$\|K_\omega(\cdot,u;(H^{s_0}(\mathbb{R}^n),H^{s_1}(\mathbb{R}^n)))\|_{\theta,2} = N_{\theta,2}\|u\|_{s,\omega,\mathbb{R}^n}.$$

We can thus use the interpolation result Theorem 3.16 in the usual way for the $|\omega|$-dependent norms, without any additional factors of $|\omega|$ appearing in the interpolation estimates.

3.2.2 Mapping Properties of the Boundary Potentials and Boundary Integral Operators for the Helmholtz Problem

In this section, we deal with the mapping properties of the boundary layer potentials given in Definition 3.8, and of the corresponding boundary integral operators for the Helmholtz problem. The bounds are explicit with respect to the wave number ω, which is going to prove to be important in the next section, where we consider the mapping properties of the time domain boundary layer potentials and the corresponding time domain boundary integral operators.

We first collect estimates with respect to the natural (or energy) norms that have been proven in the literature. By natural norms, we mean the spaces $H^1(\Omega)$, $H^{1/2}(\Gamma)$ and $H^{-1/2}(\Gamma)$ equipped with either the classical norms or with the $|\omega|$-dependent norms introduced in Section 3.2.1. We then use Costabel's technique [52] to generalise these results to a wider range of Sobolev spaces. The mapping properties themselves are well known; the new contribution is the explicitness in $|\omega|$.

3.2.2.1 A Review on Estimates with respect to the Natural Norms

We state the mapping properties in the classical Sobolev norms and in the equivalent $|\omega|$-dependent norms. The differences we observe are merely a result of the differences in part b) and c) of the following lemma. In the estimates, ω is the argument of the Laplace transform. The differences in the estimates with respect to this variable are crucial, as their powers correspond to the orders of the time derivatives in the space-time estimates via the Parseval-Plancherel identity (Lemma 3.6).

Lemma 3.17 (Trace Theorem; Trace Extension Lemma)
Let Ω be a Lipschitz domain. Then the following results hold.

a) Trace Theorem

(i) [34, Lemme 5.1] For $u \in H^1(\Omega)$, with $C = C(\Gamma)$,

$$\|\gamma[u]\|_{H^{1/2}(\Gamma)} \leq C\|u\|_{H^1(\Omega)}.$$

(ii) [32, p. 50], [81, Lemma 1(1)] For $u \in H^1(\Omega)$, with $C = C(\Gamma, \sigma_0)$,

$$\|\gamma[u]\|_{1/2,\omega,\Gamma} \leq C\|u\|_{1,\omega,\Omega}.$$

b) Trace Extension Lemma

(i) [34, Lemme 5.2], [20, Lemme 1] For $\varphi \in H^{1/2}(\Gamma)$, there exists an extension $u = \mathcal{R}[\varphi]$ into Ω, for which

$$\|u\|_{1,\omega,\Omega} \leq C|\omega|^{1/2}\|\varphi\|_{H^{1/2}(\Gamma)}$$

with $C = C(\Gamma)$.

(ii) [81, Lemma 1(2)] For $\varphi \in H^{1/2}(\Gamma)$, there exists an extension $u = \mathcal{R}[\varphi]$ into Ω, for which

$$\|u\|_{1,\omega,\Omega} \leq C\|\varphi\|_{1/2,\omega,\Gamma}$$

with $C = C(\Gamma, \sigma_0)$.

c) Bound for the normal derivative

(i) [20, (2.9)], [136, Proposition 2.5.2] Let u solve the homogeneous Helmholtz equation (3.5a)*. Then, with $C = C(\Gamma, \sigma_0)$,*

$$\left\|\frac{\partial u}{\partial n}\right\|_{H^{-1/2}(\Gamma)} \leq C|\omega|^{1/2}\|u\|_{1,\omega,\Omega}.$$

A similar result is given in [115, Lemma 4.6], but there the factor on the right hand side is $|\omega|$ instead of $|\omega|^{1/2}$.

(ii) [81, Lemma 2] Let u solve the homogeneous Helmholtz equation (3.5a)*. Then, with $C = C(\Gamma, \sigma_0)$,*

$$\left\|\frac{\partial u}{\partial n}\right\|_{-1/2,\omega,\Gamma} \leq C\|u\|_{1,\omega,\Omega}.$$

Remark 3.18 (On Lemma 3.17)
a) [81, Remark 1(2)] These estimates are optimal with respect to $|\omega|$.

b) Note that estimates b) (ii) and c) (ii) yield estimates b) (i) and c) (i) in Lemma 3.17, respectively, via Remark 3.9.

The following two lemmas are consequences of Lemma 3.17.

Lemma 3.19 (Mapping Properties, Classical Norms, Helmholtz Problem)
Let Ω be a Lipschitz domain. Let $p \in H^{-1/2}(\Gamma)$ and $\varphi \in H^{1/2}(\Gamma)$. Then [34, p. 37f.], [103, Table 1]

$$\begin{aligned}
\|S_\omega[p]\|_{H^1(\Omega)} &\leq C|\omega|\|p\|_{H^{-1/2}(\Gamma)} && (3.31)\\
\|V_\omega[p]\|_{H^{1/2}(\Gamma)} &\leq C|\omega|\|p\|_{H^{-1/2}(\Gamma)} && (3.32)\\
\|K'_\omega[p]\|_{H^{-1/2}(\Gamma)} &\leq C|\omega|^{3/2}\|p\|_{H^{-1/2}(\Gamma)} && (3.33)\\
\|D_\omega[\varphi]\|_{H^1(\Omega)} &\leq C|\omega|^{3/2}\|\varphi\|_{H^{1/2}(\Gamma)} && (3.34)\\
\|K_\omega[\varphi]\|_{H^{1/2}(\Gamma)} &\leq C|\omega|^{3/2}\|\varphi\|_{H^{1/2}(\Gamma)} && (3.35)\\
\|W_\omega[\varphi]\|_{H^{-1/2}(\Gamma)} &\leq C|\omega|^{2}\|\varphi\|_{H^{1/2}(\Gamma)} && (3.36)
\end{aligned}$$

with $C = C(\Gamma, \sigma_0)$.

The Single Layer operator V_ω is further bounded independently of $|\omega|$ when it is considered as an operator mapping from $L^2(\Gamma)$ to $L^2(\Gamma)$ in three space dimensions: For $p \in L^2(\Gamma)$ there holds [20, (2.13)], [43, Theorem 3.3]

$$\|V_\omega[p]\|_{L^2(\Gamma)} \leq C\|p\|_{L^2(\Gamma)} \tag{3.37}$$

with $C = C(\Gamma)$.

In two space dimensions, one can replace the bound $C\|p\|_{L^2(\Gamma)}$ in (3.37) by $\tilde{C}|\omega|^{-1/3}\|p\|_{L^2(\Gamma)}$, with $\tilde{C} = \tilde{C}(\Gamma)$ again. Note that $|\omega|^{-1/3} \leq \sigma_0^{-1/3}$, and therefore (3.37) also holds in two space dimensions, with $C = C(\Gamma, \sigma_0)$.

Lemma 3.20 (Mapping Properties, $|\omega|$-Dependent Norms, Helmholtz Problem)
Let Ω be a Lipschitz domain. Let $p \in H^{-1/2}(\Gamma)$ and $\varphi \in H^{1/2}(\Gamma)$. Then [34, p. 37f.], [81, (26)-(28) and (31)-(33)]

$$\begin{aligned}
\|S_\omega[p]\|_{1,\omega,\Omega} &\leq C|\omega|\|p\|_{-1/2,\omega,\Gamma} && (3.38)\\
\|V_\omega[p]\|_{1/2,\omega,\Gamma} &\leq C|\omega|\|p\|_{-1/2,\omega,\Gamma} && (3.39)\\
\|K'_\omega[p]\|_{-1/2,\omega,\Gamma} &\leq C|\omega|\|p\|_{-1/2,\omega,\Gamma} && (3.40)\\
\|D_\omega[\varphi]\|_{1,\omega,\Omega} &\leq C|\omega|\|\varphi\|_{1/2,\omega,\Gamma} && (3.41)\\
\|K_\omega[\varphi]\|_{1/2,\omega,\Gamma} &\leq C|\omega|\|\varphi\|_{1/2,\omega,\Gamma} && (3.42)\\
\|W_\omega[\varphi]\|_{-1/2,\omega,\Gamma} &\leq C|\omega|\|\varphi\|_{1/2,\omega,\Gamma} && (3.43)
\end{aligned}$$

with $C = C(\Gamma, \sigma_0)$.

We define bilinear forms $a_\omega^V(\cdot,\cdot)$ and $a_\omega^W(\cdot,\cdot)$ by

$$a_\omega^V(p,q) := \langle -i\omega V_\omega[p], q\rangle \tag{3.44}$$

for $p, q \in H^{-1/2}(\Gamma)$, and

$$a_\omega^W(\varphi,\psi) := \langle W_\omega[\varphi], -i\omega\psi\rangle \tag{3.45}$$

for $\varphi, \psi \in H^{1/2}(\Gamma)$. Then there hold the coercivity estimates stated in Lemma 3.21.

Lemma 3.21 (Coercivity Estimates, Helmholtz Problem Bilinear Forms)
a) Let $p \in H^{-1/2}(\Gamma)$. Then, with $C = C(\Gamma, \sigma_0)$,

(i) [20, (2.10)], [136, Proposition 2.6.1]

$$\Re\left(a_\omega^V(p,p)\right) \geq C|\omega|^{-1}\|p\|^2_{H^{-1/2}(\Gamma)}.$$

(ii) [81, (40)]

$$\Re\big(a_\omega^V(p,p)\big) \geq C\|p\|^2_{-1/2,\omega,\Gamma}.$$

b) Let $\varphi \in H^{1/2}(\Gamma)$. Then, with $C = C(\Gamma,\sigma_0)$,

(i) [21, (2.12)]

$$\Re\big(a_\omega^W(\varphi,\varphi)\big) \geq C\|\varphi\|^2_{H^{1/2}(\Gamma)}.$$

(ii) [34, p. 37]

$$\Re\big(a_\omega^W(\varphi,\varphi)\big) \geq C\|\varphi\|^2_{1/2,\omega,\Gamma}.$$

The continuity estimates stated in Corollary 3.22 are an immediate consequence of Lemmas 3.19 and 3.20.

Corollary 3.22 (Continuity Estimates, Helmholtz Problem Bilinear Forms)
a) Let $p,q \in H^{-1/2}(\Gamma)$. Then, with $C = C(\Gamma,\sigma_0)$,

(i)

$$|a_\omega^V(p,q)| \leq C|\omega|^2\|p\|_{H^{-1/2}(\Gamma)}\|q\|_{H^{-1/2}(\Gamma)}.$$

(ii)

$$|a_\omega^V(p,q)| \leq C|\omega|^2\|p\|_{-1/2,\omega,\Gamma}\|q\|_{-1/2,\omega,\Gamma}.$$

b) Let $\varphi,\psi \in H^{1/2}(\Gamma)$. Then, with $C = C(\Gamma,\sigma_0)$,

(i)

$$|a_\omega^W(\varphi,\psi)| \leq C|\omega|^3\|\varphi\|_{H^{1/2}(\Gamma)}\|\psi\|_{H^{1/2}(\Gamma)}.$$

(ii)

$$|a_\omega^W(\varphi,\psi)| \leq C|\omega|^2\|\varphi\|_{1/2,\omega,\Gamma}\|\psi\|_{1/2,\omega,\Gamma}.$$

We note that we gain one power of $|\omega|$ in the coercivity estimates for $a_\omega^V(\cdot,\cdot)$, but none for the continuity estimate when $|\omega|$-dependent Sobolev spaces are used instead of classical Sobolev spaces. Regarding $a_\omega^W(\cdot,\cdot)$, it is the other way round.

In both cases, the presence of powers of $|\omega|$ in the continuity estimates and their absence in the coercivity estimates means that we have coercivity and continuity on two different spaces in the space-time framework. In the frequency domain though, $|\omega|$ is just another constant, and one can apply the Lax-Milgram Theorem as usual in this context.

The inverse operator to V_ω is denoted by N^ω in [20]. As mentioned in the proof of [20, Preposition 3], there hold

$$V_\omega N^\omega = \mathrm{Id}|_{H^{1/2}(\Gamma)} \qquad \text{and} \qquad N^\omega V_\omega = \mathrm{Id}|_{H^{-1/2}(\Gamma)}$$

and hence we simply write V_ω^{-1} instead of N^ω here, in particular to avoid confusion with the Newton potential, which is defined in (3.50) below. Some properties of V_ω^{-1} are collected in Lemma 3.23.

Lemma 3.23 (Boundedness and Coercivity of V_ω^{-1})
Let $g \in H^{1/2}(\Gamma)$. Then [20, (2.7), (2.8)], [136, Proposition 2.6.1]

$$\|V_\omega^{-1}[g]\|_{H^{-1/2}(\Gamma)} \leq C|\omega|^2\|g\|_{H^{1/2}(\Gamma)} \tag{3.46}$$

$$\|V_\omega^{-1}[g]\|_{-1/2,\omega,\Gamma} \leq C|\omega|\|g\|_{1/2,\omega,\Gamma} \tag{3.47}$$

$$\Re\big\langle V_\omega^{-1}[g], -i\omega g\big\rangle \geq C\|g\|^2_{H^{1/2}(\Gamma)} \tag{3.48}$$

$$\Re\big\langle V_\omega^{-1}[g], -i\omega g\big\rangle \geq C\|g\|^2_{1/2,\omega,\Gamma} \tag{3.49}$$

with $C = C(\Gamma, \sigma_0)$.

Equations (3.47) and (3.49) are proven below. A bound similar to (3.46) on W_ω^{-1} can be found in [136, Proposition 3.4.1].

Proof (of equations (3.47) **and** (3.49) **in Lemma 3.23)**
(3.49) follows just as in the proof of [20, Proposition 2], by using Lemma 3.17 a) (ii) instead of (i).

To prove (3.47), we modify the proof of [20, Proposition 2]: Instead of [20, (2.9)], which is Lemma 3.17 c) (i), we take (ii). The term $\|u\|_{1,\omega,\Omega}$ can be estimated by [81, below (36)]. Hence we obtain

$$\left\| \frac{\partial u}{\partial n} \right\|_{-1/2,\omega,\Gamma} \leq C\|u\|_{1,\omega,\Omega} \leq C|\omega|\|g\|_{1/2,\omega,\Gamma}$$

and thus (3.47). ∎

With regard to the inhomogeneous Helmholtz equation the *Newton potential* (or *volume potential*) is given by [92, (9.1.6)], [116, (2.7)]

$$N_\omega[f](x) = \int_\Omega G_\omega(|x-y|)\ f(y)\ dy \tag{3.50}$$

for $x \in \mathbb{R}^N$. Correspondingly, the Newton potential for the wave equation is [34, (11)]

$$N[f](x,t) = \int_{\mathbb{R}_{\geq 0}} \int_\Omega G(t-s, |x-y|)\ f(y,s)\ dy\ dt \tag{3.51}$$

for $(x,t) \in \mathbb{R}^N \times \mathbb{R}_{\geq 0}$. To simplify the notation, and in contrast to (P) and (HH), Ω denotes a bounded domain here. In the context of (P) and (HH), Ω would be the scatterer, which is denoted by Ω^- there.

Melenk and Sauter [116, Lemma 3.5] show that

$$\omega^4\|N_\omega[f]\|^2_{L^2(\Omega)} + \omega^2|N_\omega[f]|^2_{H^1(\Omega)} + |N_\omega[f]|^2_{H^2(\Omega)} \leq C|\omega|^2\|f\|^2_{L^2(\Omega)}$$

for $f \in L^2(\Omega)$, with $C = C(R, \sigma_0)$ respectively $C = C(\Gamma, \sigma_0)$. As an immediate consequence we obtain a bound on N_ω.

Lemma 3.24 (Boundedness of N_ω)
Let $f \in L^2(\Omega)$. *Then*

$$\|N_\omega[f]\|_{2,\omega,\Omega} \leq C|\omega|\|f\|_{L^2(\Omega)} \tag{3.52}$$

with $C = C(\Gamma, \sigma_0)$.

3.2.2.2 Generalised Mapping Properties

Up to now we have only presented results on the boundedness of the Helmholtz boundary layer potentials and boundary integral operators with respect to their respective natural energy spaces $H^1(\Omega)$, $H^{1/2}(\Gamma)$ and $H^{-1/2}(\Gamma)$. However, generalised mapping properties are of interest as well, in particular in the context of a posteriori error estimation. The groundbreaking work on the boundary integral operators for a class of elliptic problems that includes the Laplace, Helmholtz and Lamé problem was done by Costabel in [52]. In [53], he subsequently extended his analysis to the boundary integral operators for the heat equation. We further refer to [114] for a presentation of the results of [52] in the context of a text book.

It is well known that the Helmholtz boundary integral operators have the same mapping properties as their Laplace counterparts. What is unknown though is how the respective estimates depend on the wave number ω when the spaces are not the respective natural energy spaces. Here we mimic Costabel's arguments in order to obtain bounds which are explicit in $|\omega|$.

We begin with a generalisation of Lemma 3.24.

Lemma 3.25 (Generalised Boundedness of N_ω)
Let $s \in \mathbb{R}$ and $f \in H^s(\Omega)$. Then

$$\|N_\omega[f]\|_{s+2,\omega,\Omega} \leq C|\omega|\|f\|_{s,\omega,\Omega} \tag{3.53}$$

where the constant $C = C(\Gamma, \sigma_0)$ is $|\omega|$-independent.

The boundedness of the Helmholtz Newton potential N_ω as stated in Lemma 3.25 is well known; see, for instance, [133, Theorem 3.1.2 and Remark 3.1.3], [145, Section 6.9]. In contrast to the aforementioned references, the bound in Lemma 3.25 is explicit in terms of $|\omega|$.

In the proof of Lemma 3.25, we need estimates of terms of the form $|s^k \iota_\omega(s)|$ for $k = 0, 1, 2$, where for three space dimensions [116, (3.34) and p. 1873]

$$\iota_\omega(s) := \int_{\mathbb{R}_{\geq 0}} \frac{\sin(rs)}{s} e^{i\omega r} \mu(r)\, dr \tag{3.54}$$

with μ being a cutoff function defined in the proof below, and $s \geq 0$. The estimates we need are given in [116, Lemma 3.7 (i)-(iii)],

$$(i)\quad |\iota_\omega(s)| \leq C_0|\omega|^{-1} \qquad (ii)\quad |s\iota_\omega(s)| \leq C_1 \qquad (iii)\quad |s^2\iota_\omega(s)| \leq C_2|\omega| \tag{3.55}$$

with $C_i = C_i(R)$ for $i = 0, 1$ and $C_2 = C_2(R, \sigma_0)$, with R such that $\Omega \subseteq B_R(0)$, and therefore equivalently $C_i = C_i(\Gamma)$ for $i = 0, 1$ and $C_2 = C_2(\Gamma, \sigma_0)$. In particular, C_0, C_1, C_2 are all $|\omega|$-independent.

Note that the estimates (3.55) are proven for $\omega \in \mathbb{R}$ in [116]. However, the estimates can be adapted to $\omega \in \mathbb{C}$ immediately.

Remark 3.26 (Bounds in Two Space Dimensions)
Of the estimates (3.55)*, (i) always holds in two space dimensions as well. To guarantee (ii) and (iii), on the other hand, one needs $|\omega| > \frac{1}{4R}$. However, since $|\omega| \geq \sigma_0 > 0$ with arbitrary but fixed σ_0, one can always choose R large enough so that this condition holds, and the estimates proven in what follows therefore also hold in two space dimensions.*

The proof of Lemma 3.25 is now similar to the one of [116, Lemma 3.5], which itself is similar to the respective proof for the Laplace Newton potential; see, for instance, [145, Theorem 6.1].

Proof (of Lemma 3.25)
We assume $\Omega \subseteq B_R(0)$ and use the short-hand notation $v(x) := N_\omega[f](x) = (G_\omega \star f)(x)$. Let $\mu \in C^\infty(\mathbb{R}_{\geq 0})$ be a cutoff function as in [116, (3.27)] and define

$$v_\mu(x) := \int_\Omega \mu(|x-y|) G_\omega(|x-y|) f(y)\, dy = ((G_\omega \mu) \star f)(x) \tag{3.56}$$

for $x \in \Omega$. Due to the properties of μ, there holds $v_\mu \equiv v|_\Omega$ and thus

$$\|v\|_{s,\omega,\Omega} = \|v_\mu\|_{s,\omega,\Omega} \tag{3.57}$$

for all $s \in \mathbb{R}$. By (3.56),

$$\tilde{v}_\mu(\xi) := \mathcal{F}_x[v_\mu](\xi) = \mathcal{F}_x\left[G_\omega \mu\right](\xi)\ \tilde{f}(\xi)$$

where

$$\mathcal{F}_x\left[G_\omega \mu\right](\xi) = (2\pi)^{-3/2} \int_{\mathbb{R}^3} e^{i\,\xi\cdot z} G_\omega(|z|)\mu(|z|)\ dz =: (2\pi)^{-3/2} I_\omega(\xi)$$

for $\xi \in \mathbb{R}^3$. Arguing as in [145, p. 113], we restrict ourselves to the case $\xi = (0, 0, |\xi|)$, i.e. $I_\omega(\xi) = I_\omega(|\xi|)$. Introducing spherical coordinates, we obtain $I_\omega(|\xi|) = \iota_\omega(|\xi|)$, with ι_ω as defined in (3.54). Hence

$$\tilde{v}_\mu(\xi) = (2\pi)^{-3/2} \iota_\omega(|\xi|)\tilde{f}(\xi). \tag{3.58}$$

By (3.57), the definition of $\|\cdot\|_{s,\omega,\Omega}$ and (3.58), we obtain

$$\begin{aligned}
\|v\|^2_{s,\omega,\Omega} = \|v_\mu\|^2_{s,\omega,\Omega} &= \int_\Omega \left(|\omega|^2 + |\xi|^2\right)^s |\tilde{v}_\mu(\xi)|^2\ d\xi \\
&= (2\pi)^{-3/2} \int_\Omega \left(|\omega|^2 + |\xi|^2\right)^s |\iota_\omega(|\xi|)|^2 \left|\tilde{f}(\xi)\right|^2\ d\xi \\
&= (2\pi)^{-3/2} \int_\Omega \left(|\omega|^2 + |\xi|^2\right)^{s-2} \left|\left(|\omega|^2 + |\xi|^2\right) \iota_\omega(|\xi|)\right|^2 \left|\tilde{f}(\xi)\right|^2\ d\xi.
\end{aligned}$$

Now, by (3.55),

$$\begin{aligned}
\left|\left(|\omega|^2 + |\xi|^2\right) \iota_\omega(|\xi|)\right|^2 &= \left||\omega|^4 \iota_\omega(|\xi|)^2 + 2|\omega|^2 \left(|\xi|\iota_\omega(|\xi|)\right)^2 + \left(|\xi|^2 \iota_\omega(|\xi|)\right)^2\right| \\
&\leq \max\left\{C_0, C_1, C_2\right\} \left(|\omega|^4 |\omega|^{-2} + 2|\omega|^2 + |\omega|^2\right) =: C|\omega|^2
\end{aligned}$$

with $C_i = C_i(\Gamma)$ for $i = 0, 1$ and $C_2 = C_2(\Gamma, \sigma_0)$, so that $C = C(\Gamma, \sigma_0)$ does not depend on $|\omega|$. Hence

$$\|v\|^2_{s,\omega,\Omega} \leq (2\pi)^{-3/2} C\ |\omega|^2 \int_\Omega \left(|\omega|^2 + |\xi|^2\right)^{s-2} \left|\tilde{f}(\xi)\right|^2\ d\xi = (2\pi)^{-3/2} C\ |\omega|^2 \|f\|^2_{s-2,\omega,\Omega}$$

which ends the proof. ∎

Let Ω be a bounded domain. The next lemma is about the solution operator to the interior Helmholtz Dirichlet problem

$$\text{(DP)} \quad \begin{cases} \text{Find } u : \Omega \to \mathbb{R} \text{ such that} \\ \qquad\qquad \mathcal{P}_\omega[u] := \Delta u + \omega^2 u = 0 \text{ in } \Omega & \text{(3.59a)} \\ \qquad\qquad u = g \text{ on } \Gamma & \text{(3.59b)} \\ \text{for given } g : \Gamma \to \mathbb{R}. \end{cases}$$

It is stated explicitly here to relate our problem to the context of [52, 114, 133].

Lemma 3.27 (The Solution Operator to Problem (DP) [81, p. 14])
Let Ω be a Lipschitz domain. Then there exists a continuous solution operator $\mathcal{U} : H^{1/2}(\Gamma) \to H^1(\Omega)$ *that maps the Dirichlet data $g \in H^{1/2}(\Gamma)$ to the solution u of (DP) with*

$$\|\mathcal{U}[g]\|_{1,\omega,\Omega} \leq C_1 |\omega| \|g\|_{1/2,\omega,\Gamma} \tag{3.60}$$

with $C_1 = C_1(\Gamma, \sigma_0)$. The Steklov-Poincaré operator $\gamma_1 \circ \mathcal{U} : H^{1/2}(\Gamma) \to H^{-1/2}(\Gamma)$ *is bounded with*

$$\|\left(\gamma_1 \circ \mathcal{U}\right)[g]\|_{-1/2,\omega,\Omega} \leq C_2 |\omega| \|g\|_{1/2,\omega,\Gamma} \tag{3.61}$$

with $C_2 = C_2(\Gamma, \sigma_0)$. In particular, both constants C_1 and C_2 are $|\omega|$-independent.

Remark 3.28 (On Lemma 3.27)

a) As an immediate consequence of the proof of Lemma 3.27, we obtain the bound [81, Lemma 2]

$$\|\gamma_1[u]\|_{-1/2,\omega,\Omega} \leq C\|u\|_{1,\omega,\Omega}$$

on the solution u of (DP), where the constant $C = C(\Gamma, \sigma_0)$ is $|\omega|$-independent.

b) Similar bounds on the solution operator for the Neumann problem can be found in [34, Théorème 5.1].

c) In terms of powers of $|\omega|$, the estimate in Lemma 3.27 looks worse than that in Lemma 3.17 b). However, Lemma 3.17 b) is about the 'lifting' of an arbitrary function, whereas Lemma 3.27 gives an estimate for the solution of the Helmholtz problem (DP).

d) Via Remark 3.9, we also get the estimates

$$\|\mathcal{U}[g]\|_{1,\omega,\Omega} \leq \tilde{C}_1|\omega|^{3/2}\|g\|_{H^{1/2}(\Gamma)}$$

and

$$\|\left(\gamma_1 \circ \mathcal{U}\right)[g]\|_{H^{-1/2}(\Gamma)} \leq \tilde{C}_2|\omega|^2\|g\|_{H^{1/2}(\Gamma)}$$

with $\tilde{C}_i = \tilde{C}_i(\Gamma, \sigma_0)$ for $i = 1, 2$. These are the original results given in [20, Propositions 1 and 2].

The proof of Lemma 3.27 follows the ones of [20, Proposition 1] and [133, p. 73].

Proof (of Lemma 3.27)

Define a bilinear form $a_\omega(u, v) := \int_\Omega -\nabla u \cdot \nabla \bar{v} + \omega^2 u\bar{v}\, dx$. Since $\omega = \mu + i\omega$, there holds $i\bar{\omega} = \sigma + i\mu$ and $i\omega = -\sigma + i\mu$. Hence

$$i\bar{\omega}a_\omega(u,u) = \int_\Omega -(\sigma + i\mu)\,|\nabla u|^2 + (-\sigma + i\mu)|\omega|^2|u|^2\, dx = -\sigma\|u\|^2_{1,\omega,\Omega} + i\mu \int_\Omega -|\nabla u|^2 + |\omega|^2|u|^2\, dx$$

and thus

$$\Re\left(-i\bar{\omega}a_\omega(u,u)\right) = \sigma\|u\|^2_{1,\omega,\Omega}. \tag{3.62}$$

As $\Im(\omega) = \sigma \geq \sigma_0$, there holds

$$\sigma_0\|u\|^2_{1,\omega,\Omega} \leq \sigma\|u\|^2_{1,\omega,\Omega} = |\Re\left(-i\bar{\omega}a_\omega(u,u)\right)| \leq |\omega||a_\omega(u,u)|. \tag{3.63}$$

Now set $u_1 := Z^\omega_\Omega[g]$, with Z^ω_Ω as in Lemma 3.14 b), and $u_0 := u - u_1 \in H^1(\Omega)$. We obtain

$$\Delta u_0 + \omega^2 u_0 = -\left(\Delta u_1 + \omega^2 u_1\right) \text{ in } \Omega \tag{3.64a}$$

$$u_0 = 0 \text{ on } \Gamma \tag{3.64b}$$

Then, for every $v \in H^1_0(\Omega)$, $a_\omega(u_0, v) = -a_\omega(u_1, v)$. In particular, for $v = u_0 \in H^1_0(\Omega)$, $a_\omega(u_0, u_0) = -a_\omega(u_1, u_0)$. Using (3.63), we obtain

$$\sigma_0\|u_0\|^2_{1,\omega,\Omega} \leq |\omega||a_\omega(u_0,u_1)| \leq |\omega|\; C_1\|u_0\|_{1,\omega,\Omega}\|u_1\|_{1,\omega,\Omega} \tag{3.65}$$

with $C_1 = C_1(\sigma_0)$, and hence

$$\|u_0\|_{1,\omega,\Omega} \leq \tilde{C}_1|\omega|\|u_1\|_{1,\omega,\Omega}$$

with $\tilde{C}_1 = \tilde{C}_1(\sigma_0)$. Hence

$$\|u\|_{1,\omega,\Omega} \leq \|u_0\|_{1,\omega,\Omega} + \|u_1\|_{1,\omega,\Omega} \leq \left(\tilde{C}_1|\omega| + 1\right)\|u_1\|_{1,\omega,\Omega} \leq \tilde{\tilde{C}}_1|\omega|\|u_1\|_{1,\omega,\Omega}$$

with $\tilde{\tilde{C}}_1 = \tilde{\tilde{C}}_1(\sigma_0)$. Using the continuity of $u_1 = Z_\Omega^\omega[g]$ (Lemma 3.14 b) with $s = 1$), we thus obtain

$$\|\mathcal{U}[g]\|_{1,\omega,\Omega} = \|u\|_{1,\omega,\Omega} \le \tilde{\tilde{C}}_1 C_2 |\omega| \|g\|_{1/2,\omega,\Omega} \tag{3.66}$$

with $C_2 = C_2(\Gamma, \sigma_0)$. This proves (3.60).

We obtain a bound on the normal derivative as in [81, Lemma 2]: As, for every $v \in H^1(\Omega)$, $a_\omega(u,v) = -\int_\Gamma \gamma_1[u] v \, ds_\Gamma = -\langle \gamma_1[u], v \rangle$, we obtain, by (3.65),

$$|\langle \gamma_1[u], \gamma_0[v] \rangle| = |a_\omega(u,v)| \le C_3 \|u\|_{1,\omega,\Omega} \|v\|_{1,\omega,\Omega} \tag{3.67}$$

with $C_3 = C_3(\sigma_0)$. For arbitrary $\psi \in H^{1/2}(\Gamma)$, let $w := Z_\Omega^\omega[\psi] \in H^1(\Omega)$, so that $\gamma_0[w] = \psi$. The desired bounds on $\|\gamma_1[u]\|_{-1/2,\omega,\Omega} = \|(\gamma_1 \circ \mathcal{U})[g]\|_{-1/2,\omega,\Omega}$ stated in (3.61) and in Remark 3.28 a) then follow by the definition of the dual norm and (3.67) with $v = w$, combined with (3.66) and the continuity of $w = Z_\Omega^\omega[\psi]$, respectively. ∎

Note that, in the language of [52, (2.2)], [114, p. 113], the variables of the Helmholtz differential operator $\mathcal{P}_\omega$ defined in (3.59a) are

$$m = 1, \quad (A_\omega)_{jk} = (A)_{jk} = -\delta_{jk}, \quad (A_\omega)_j = (A)_j = 0, \quad A_\omega = \omega^2, \quad j,k = 1,2,3. \tag{3.68}$$

As in [52, p. 617], let

$$\mathcal{P}_\omega^0[u] = \mathcal{P}^0[u] := -\Delta u + \lambda \tag{3.69}$$

with $\lambda > 0$ such that $\mathcal{P}^0$ is positive on $H^1(\Omega)$, be an operator with the same principal part as $\mathcal{P}_\omega$. Note that one could simply use $\lambda = 0$ as well, since the semi-norm $|\cdot|_{H^1(\Omega)}$ and the norm $\|\cdot\|_{H^1(\Omega)}$ are equivalent on $H_0^1(\Omega)$ [114, p. 118ff.]. Consequently, $\mathcal{P}^0[u] = -\Delta u$ in [114]. The constant λ in (3.69) then corresponds to the coercivity constant C on [114, p. 118].

Costabel [52] studies the solution operator $\mathcal{U}^0$ for the interior Dirichlet problem

$$(\mathrm{DP})^0 \quad \begin{cases} \text{Find } u : \Omega \to \mathbb{R} \text{ such that} & \\ \qquad \mathcal{P}^0[u] = 0 \text{ in } \Omega & \text{(3.70a)} \\ \qquad u = v \text{ on } \Gamma & \text{(3.70b)} \\ \text{for given } v : \Gamma \to \mathbb{R}. & \end{cases}$$

Since the differential operator $\mathcal{P}^0$ does not depend on ω, all the estimates on it are ω-independent. Note further that γ_1 can be expressed in terms of $\left(\gamma_1 \circ \mathcal{U}^0\right)^*$, γ_0, $\left(\mathcal{U}^0\right)^*$ and $\mathcal{P}^0$, namely [52, (4.16)], [133, (2.127)]

$$\gamma_1 = \left(\gamma_1 \circ \mathcal{U}^0\right)^* \circ \gamma_0 - \left(\mathcal{U}^0\right)^* \circ \mathcal{P}^0$$

where e.g. $\left(\mathcal{U}^0\right)^*$ is the adjoint operator to $\left(\mathcal{U}^0\right)^*$, i.e. $\left\langle \mathcal{U}^0[v], w \right\rangle = \left\langle v, \left(\mathcal{U}^0\right)^*[w] \right\rangle$. This is a consequence of the fact that the normal derivative depends only on the principal part of an differential operator [133, Remark 2.7.9]. As all the operators in this representation are independent of $|\omega|$, we conclude Lemma 3.29.

Lemma 3.29 (Bounds on γ_1)
Let $u \in H^s(\Omega)$ for $\frac{1}{2} < s < \frac{3}{2}$. Then

$$\|\gamma_1[u]\|_{H^{s-3/2}(\Gamma)} \le C_1 \|u\|_{H^s(\Omega)} \tag{3.71}$$

with $C_1 = C_1(\Gamma, s)$ and

$$\|\gamma_1[u]\|_{s-3/2,\omega,\Gamma} \le C_2 \|u\|_{s,\omega,\Omega} \tag{3.72}$$

with $C_2 = C_2(\Gamma, \sigma_0, s)$. In particular, the constants C_1 and C_2 are $|\omega|$-independent.

Proof
The first statement (3.71) is [52, Lemma 4.3]. The second estimate (3.72) is a consequence of (3.71) and Remark 3.9: Since $s - 3/2 < 0$ and $s > 0$, there holds

$$C\|\gamma_1[u]\|_{s-3/2,\omega,\Gamma} \le \|\gamma_1[u]\|_{H^{s-3/2}(\Gamma)} \le C_1\|u\|_{H^s(\Omega)} \le C_1\tilde{C}\|u\|_{s,\omega,\Omega}$$

with $C = C(\sigma_0)$ and $\tilde{C} = \tilde{C}(\sigma_0)$, which gives (3.72). ∎

We are now able to prove the enhanced mapping properties of the Helmholtz boundary layer potentials and operators.

Theorem 3.30 (Enhanced Mapping Properties, $|\omega|$-Dependent Norms, Helmholtz P.) *Let Ω be a Lipschitz domain and $-\frac{1}{2} < s < \frac{1}{2}$. Let $p \in H^{-1/2+s}(\Gamma)$ and $\varphi \in H^{1/2+s}(\Gamma)$. Then*

$$\|S_\omega[p]\|_{s+1,\omega,\Omega} \le C|\omega|\|p\|_{s-1/2,\omega,\Gamma} \tag{3.73}$$
$$\|V_\omega[p]\|_{s+1/2,\omega,\Gamma} \le C|\omega|\|p\|_{s-1/2,\omega,\Gamma} \tag{3.74}$$
$$\|K'_\omega[p]\|_{s-1/2,\omega,\Gamma} \le C|\omega|\|p\|_{s-1/2,\omega,\Gamma} \tag{3.75}$$
$$\|D_\omega[\varphi]\|_{s+1,\omega,\Omega} \le C|\omega|\|\varphi\|_{s+1/2,\omega,\Gamma} \tag{3.76}$$
$$\|K_\omega[\varphi]\|_{s+1/2,\omega,\Gamma} \le C|\omega|\|\varphi\|_{s+1/2,\omega,\Gamma} \tag{3.77}$$
$$\|W_\omega[\varphi]\|_{s-1/2,\omega,\Gamma} \le C|\omega|\|\varphi\|_{s+1/2,\omega,\Gamma} \tag{3.78}$$

with $C = C(\Gamma, \sigma_0, s)$. In particular, the constants C are $|\omega|$-independent.

Theorem 3.30 is a generalisation of Lemma 3.20. We observe that the powers of $|\omega|$ in the estimates do not change. In the space-time context, this means that the time regularity does not change for different assumptions on the space regularity.

For a comment on the limiting cases $s = -\frac{1}{2}$ and $s = \frac{1}{2}$, we refer to [114, p. 209].

Proof (of Theorem 3.30)
By the definition, $S_\omega[p](x) = (N_\omega \circ \gamma_0')[p](x)$ for $x \in \mathbb{R}^N \setminus \Gamma$ [52, (2.5)], [133, Definition 3.1.5]. Hence, by Lemma 3.25 and Corollary 3.13, and for $\frac{1}{2} < \tilde{s} < \frac{3}{2}$,

$$\|S_\omega[p]\|_{2-\tilde{s},\omega,\Omega} = \|N_\omega\left[\gamma_0'[p]\right]\|_{2-\tilde{s},\omega,\Omega} \le C_{N_\omega}\ |\omega|\|\gamma_0'[p]\|_{-\tilde{s},\omega,\Gamma} \le C_{N_\omega}\ C_{\gamma_0'}\ |\omega|\|p\|_{1/2-\tilde{s},\omega,\Gamma}.$$

Setting $s := 1 - \tilde{s}$ and $C := C_{N_\omega}C_{\gamma'}$, so that $C = C(\Gamma, \sigma_0, s)$, we thus obtain, for $-\frac{1}{2} < s < \frac{1}{2}$,

$$\|S_\omega[p]\|_{1+s,\omega,\Omega} \le C\ |\omega|\|p\|_{-1/2+s,\omega,\Gamma}.$$

where C is $|\omega|$-independent. This is (3.73).

As an immediate consequence, and since $V_\omega[p](x) = (\gamma_0 \circ S_\omega)[p](x)$ for $x \in \Gamma$ [52, (2.8)], [133, (3.6)], we obtain (3.74) from Lemma 3.12. In the same way, since $K'_\omega[p](x) = (\gamma_1 \circ S_\omega)[p](x)$ for $x \in \Gamma$, we obtain (3.75) from Lemma 3.29.

There holds $D_\omega[\varphi](x) = (N_\omega \circ \gamma_1')[\varphi](x)$ for $x \in \mathbb{R}^N \setminus \Gamma$ by the definition [52, (2.6)], [133, Definition 3.1.5]. (3.76) hence follows from Lemma 3.25 and Lemma 3.29.

Finally, (3.77) and (3.78) follow from (3.76), since $K_\omega[\varphi](x) = (\gamma_0 \circ D_\omega)[\varphi](x)$ and $W_\omega[\varphi](x) = -(\gamma_1 \circ D_\omega)[\varphi](x)$ for $x \in \Gamma$. ∎

The next result follows immediately from Theorem 3.30 and Remark 3.9. It generalises Lemma 3.19.

Theorem 3.31 (Enhanced Mapping Properties, Classical Norms, Helmholtz P.)
Let Ω be a Lipschitz domain and $-\frac{1}{2} < s < \frac{1}{2}$. Let $p \in H^{-1/2+s}(\Gamma)$, $\varphi \in H^{1/2+s}(\Gamma)$. Then

$$\begin{aligned}
\|S_\omega[p]\|_{H^{s+1}(\Omega)} &\leq C|\omega|\|p\|_{H^{s-1/2}(\Gamma)} && (3.79)\\
\|V_\omega[p]\|_{H^{s+1/2}(\Gamma)} &\leq C|\omega|\|p\|_{H^{s-1/2}(\Gamma)} && (3.80)\\
\|K'_\omega[p]\|_{H^{s-1/2}(\Gamma)} &\leq C|\omega|^{3/2-s}\|p\|_{H^{s-1/2}(\Gamma)} && (3.81)\\
\|D_\omega[\varphi]\|_{H^{s+1}(\Omega)} &\leq C|\omega|^{3/2+s}\|\varphi\|_{H^{s+1/2}(\Gamma)} && (3.82)\\
\|K_\omega[\varphi]\|_{H^{s+1/2}(\Gamma)} &\leq C|\omega|^{3/2+s}\|\varphi\|_{H^{s+1/2}(\Gamma)} && (3.83)\\
\|W_\omega[\varphi]\|_{H^{s-1/2}(\Gamma)} &\leq C|\omega|^{2}\|\varphi\|_{H^{s+1/2}(\Gamma)} && (3.84)
\end{aligned}$$

with $C = C(\Gamma, \sigma_0, s)$. In particular, the constants C are $|\omega|$-independent.

In Lemma 3.23, we cited two bounds on V_ω^{-1}, one in the energy norm and one in the classical norm, that are both explicit in $|\omega|$. Similarly to Theorems 3.30 and 3.31, we now aim to generalise this bound. By the Inverse Mapping Theorem [8, Satz 5.8], $V_\omega^{-1} : H^{1/2+s}(\Gamma) \to H^{-1/2+s}(\Gamma)$ is a bounded linear operator for $-\frac{1}{2} < s < \frac{1}{2}$. Unfortunately, the Inverse Mapping Theorem does not provide any information on the continuity constant since its proof is not constructive, and hence we cannot conclude the $|\omega|$-dependence directly.

As in Lemma 3.27, let $\mathcal{U}$ be the solution operator to problem (DP). Using a Single Layer representation for the solution $\mathcal{U}[g] = u = S_\omega[\psi]$ with $-\psi = [\gamma_1[u]]_\Gamma$, there holds, by the jump relations (Corollary 1.7),

$$[\gamma_1[u]]_\Gamma = [\gamma_1 \circ \mathcal{U}[g]]_\Gamma = -\psi = -V_\omega^{-1}[g]$$

and hence

$$-V_\omega^{-1} = [\gamma_1 \circ \mathcal{U}]_\Gamma . \tag{3.85}$$

It thus suffices to generalise the mapping properties of the Steklov-Poincaré operator $\gamma_1 \circ \mathcal{U}$ introduced in Lemma 3.27.

First we cite a result that can be found in [114].

Theorem 3.32 ([114, Theorem 4.24])
Assume that Ω is a Lipschitz domain. Let $\mathcal{P}$ be a strongly elliptic linear second-order partial differential operator as in [114, (4.1)] with self-adjoint principal part. Let $u \in H^1(\Omega)$, $\gamma_0[u] \in H^1(\Gamma)$ and $\mathcal{P}[u] = 0$ in Ω.

Then

$$\|\gamma_1[u]\|_{L^2(\Gamma)} \leq C_1\|\gamma_0[u]\|_{H^1(\Gamma)} + C_2\|u\|_{H^1(\Omega)}.$$

In particular, $\mathcal{P}_\omega$ is strongly elliptic and its principal part $\mathcal{P}_\omega^0 = \Delta u$ is self-adjoint [114, pp. 246 and 277]. But the result does not state in which way the constants C_1 and C_2 in the estimate depend on the coefficients of the differential operator $\mathcal{P}$. A closer inspection of the proof of [114, Theorem 4.24] leads to Lemma 3.33.

Lemma 3.33 (Theorem 3.32 for the Helmholtz Problem)
Assume that Ω is a Lipschitz domain. Let $u \in H^1(\Omega)$ with $\gamma_0[u] \in H^1(\Gamma)$ and $\mathcal{P}_\omega[u] = 0$ in Ω.

Then

$$\|\gamma_1[u]\|_{L^2(\Gamma)} \leq C_1\|\gamma_0[u]\|_{1,\omega,\Gamma} + C_2|\omega|\|u\|_{1,\omega,\Omega} \tag{3.86}$$

with $|\omega|$-independent constants $C_i = C_i(\Omega, \sigma_0)$ for $i = 1, 2$.

Proof
As already stated in (3.68), we have, in the language of [114, p. 113],

$$m = 1, \quad (A_\omega)_{jk} = (A)_{jk} = \delta_{jk}, \quad (A_\omega)_j = (A)_j = 0, \quad A_\omega = \omega^2, \quad j,k = 1,2,3$$

for the operator $\mathcal{P}_\omega$ defined in (DP). The associated sesquilinear form Φ is [114, (4.2)]

$$\Phi_\omega(u,v) = \int_\Omega \nabla u \cdot \nabla \bar{v} - \omega^2 u\bar{v}\, dx$$

similar to the form $a(u,v)$ in the proof of Lemma 3.27, and $\Phi^0_\omega(u,v) = \int_\Omega \nabla u \cdot \nabla \bar{v}\, dx$ [114, p. 118]. We need to choose $\lambda = \omega^2$ in the estimate

$$\Phi_\omega(u,u) + \lambda \|u\|^2_{L^2(\Omega)^m} \geq c\|u\|^2_{H^1_0(\Omega)^m}$$

for $u \in H^1_0(\Omega)^m$ on [114, p. 150], with $c = 1$. The dependence of the estimates on λ is therefore of particular interest to us. The first part of the proof (before 'Now we drop the requirement ...') depends only on the ($|\omega|$-independent) principal part, and is thus independent of $|\omega|$. The constants C_1 and C_2 in the bound [114, p. 151(5)]

$$\|u\|_{H^1(\Omega_r)} \leq C_1 \|f + \lambda u\|_{\tilde{H}^{-1}(\Omega_r)} + C_2 \|\gamma_r[g]\|_{H^1(\Gamma_r)}$$

are found to be independent of λ respectively $|\omega|$, and so are all the constants that appear before. Note that f denotes the right hand side of the differential operator in the original proof, i.e. $f \equiv 0$ here. As a consequence, we obtain

$$\|\gamma_1[u]\|_{L^2(\Gamma_r)} \leq c_1 \|\gamma_0[u]\|_{H^1(\Gamma)} + c_2 \|f\|_{L^2(\Omega)} + c_3 |\lambda| \|u\|_{L^2(\Omega)}$$

where, again, the constants c_1, c_2, c_3 are all independent of λ respectively $|\omega|$. Since $|\lambda| = |\omega^2| = |\omega|^2$ and $\|u\|^2_{1,\omega,\mathcal{O}} = |\omega|^2 \|u\|^2_{L^2(\mathcal{O})} + |u|^2_{H^1(\mathcal{O})}$, the claim (3.86) follows after some convergence considerations that cause no further problems. ∎

We can now apply estimate (3.86) to the Steklov–Poincaré operator $\gamma_1 \circ \mathcal{U}$ associated with (DP) and obtain the bound

$$\| (\gamma_1 \circ \mathcal{U})[g] \|_{0,\omega,\Gamma} \leq C \left(\|g\|_{1,\omega,\Gamma} + |\omega| \|\mathcal{U}[g]\|_{1,\omega,\Omega} \right)$$

where $C = \max\{C_1, C_2\}$ is $|\omega|$-independent. By Lemma 3.27, we thus obtain

$$\| (\gamma_1 \circ \mathcal{U})[g] \|_{0,\omega,\Gamma} \leq C \left(\|g\|_{1,\omega,\Gamma} + |\omega|^2 \|g\|_{1/2,\omega,\Omega} \right) \leq \tilde{C} |\omega|^2 \|g\|_{1,\omega,\Gamma} \tag{3.87}$$

with $\tilde{C} = \tilde{C}(\Gamma, \sigma_0)$, which means that the Steklov-Poincaré operator $\gamma_1 \circ \mathcal{U} : H^1(\Gamma) \to L^2(\Gamma)$ is bounded with a higher order of $|\omega|$, namely $|\omega|^2$ instead of $|\omega|$, than the Steklov-Poincaré operator $\gamma_1 \circ \mathcal{U} : H^{1/2}(\Gamma) \to H^{-1/2}(\Gamma)$.

The *adjoint operator* to $\mathcal{P}_\omega$ is $\mathcal{P}^*_\omega[v] := \Delta v + \bar{\omega}^2 v$, and the corresponding adjoint problem to (DP) is

$$(\mathrm{DP})^* \quad \begin{cases} \text{Find } v : \Omega \to \mathbb{R} \text{ such that} \\ \qquad \mathcal{P}^*_\omega[v] = \Delta v + \bar{\omega}^2 v = 0 \text{ in } \Omega & (3.88a) \\ \qquad v = h \text{ on } \Gamma & (3.88b) \\ \text{for given } h : \Gamma \to \mathbb{R}. \end{cases}$$

The solution operator for $(\mathrm{DP})^*$ is denoted by $\mathcal{V}$. $\mathcal{V}$ and $\gamma_1 \circ \mathcal{V}$ are bounded just as $\mathcal{U}$ and $\gamma_1 \circ \mathcal{U}$, i.e.

$$\|\mathcal{V}[h]\|_{1,\omega,\Omega} \leq C_1|\omega|\|h\|_{1/2,\omega,\Gamma}.$$

and

$$\|\left(\gamma_1 \circ \mathcal{V}\right)[h]\|_{-1/2,\omega,\Omega} \leq C_2|\omega|\|h\|_{1/2,\omega,\Gamma} \tag{3.89}$$

where both constants $C_i = C_i(\Omega, \sigma_0)$ for $i = 1, 2$ are $|\omega|$-independent. The proof is identical to the one of Lemma 3.27. We further get an analogue to (3.87), namely

$$\|\left(\gamma_1 \circ \mathcal{V}\right)[h]\|_{0,\omega,\Gamma} \leq C|\omega|^2\|h\|_{1,\omega,\Gamma} \tag{3.90}$$

where $C = C(\Omega, \sigma_0)$ is $|\omega|$-independent. By [114, (4.39)], $\gamma_1 \circ \mathcal{V}$ is the adjoint operator to $\gamma_1 \circ \mathcal{U}$, i.e. $\langle\left(\gamma_1 \circ \mathcal{U}\right)[g], h\rangle = \langle g, \left(\gamma_1 \circ \mathcal{V}\right)[h]\rangle$. Hence, by the Cauchy-Schwarz inequality,

$$\|\left(\gamma_1 \circ \mathcal{U}\right)[g]\|_{-1,\omega,\Gamma} = \sup_{h \in H^1(\Gamma)} \frac{\langle\left(\gamma_1 \circ \mathcal{U}\right)[g], h\rangle}{\|h\|_{1,\omega,\Gamma}} = \sup_{h \in H^1(\Gamma)} \frac{\langle g, \left(\gamma_1 \circ \mathcal{V}\right)[h]\rangle}{\|h\|_{1,\omega,\Gamma}} \leq C|\omega|^2\|g\|_{0,\omega,\Gamma} \tag{3.91}$$

where $C = C(\Gamma, \sigma_0)$ is $|\omega|$-independent. The results of Lemma 3.27, (3.87) and (3.91) are collected in Corollary 3.34.

Corollary 3.34
Let $s \in \left\{-1, -\frac{1}{2}, 0\right\}$ and $g \in H^{s+1}(\Gamma)$. Then

$$\|\left(\gamma_1 \circ \mathcal{U}\right)[g]\|_{s,\omega,\Gamma} \leq C|\omega||\omega|^{2|s+1/2|}\|g\|_{s+1,\omega,\Gamma}$$

where $C = C(\Gamma, \sigma_0)$ is $|\omega|$-independent.

By interpolation (Theorem 3.16), we can generalise Corollary 3.34 to the following result.

Lemma 3.35 ([52, Lemmas 3.7 and 4.2] for the Helmholtz Problem)
a) Let $-\frac{1}{2} \leq s \leq \frac{1}{2}$ and $g \in H^{s+1/2}(\Gamma)$. Then

$$\|\left(\gamma_1 \circ \mathcal{U}\right)[g]\|_{s-1/2,\omega,\Gamma} \leq C_1|\omega||\omega|^{2|s|}\|g\|_{s+1/2,\omega,\Gamma}$$

where $C_1 = C_1(\Gamma, \sigma_0)$ is $|\omega|$-independent.

b) Further, for $-\frac{1}{2} < s < \frac{1}{2}$,

$$\|\mathcal{U}[g]\|_{s+1,\omega,\Omega} \leq C_2|\omega|^2|\omega|^{2|s|}\|g\|_{s+1/2,\omega,\Gamma}$$

where $C_2 = C_2(\Gamma, \sigma_0)$ is $|\omega|$-independent.

We note that Lemma 3.35 a) generalises the first estimate in Lemma 3.27, which states the same result for the special case $s = 0$. Lemma 3.35 b) is a consequence of Theorem 3.30 and Lemma 3.36, since $\mathcal{U} = S_\omega \circ V_\omega^{-1}$ In what follows, we do not need this bound on $\mathcal{U}$, but we state it for information nevertheless.

We note further that the estimate in Lemma 3.35 b) is 'worse' than its counterpart in Lemma 3.27, which is about the special case $s = 0$, in the sense that there is an additional factor of $|\omega|$ on the right hand side. This suggests that there might a better bound than b), of the same same order as the one in Lemma 3.27. However, we have not been able to prove such a bound.

Using (3.85), Lemma 3.35 a) immediately implies the generalised bound on V_ω^{-1} we were after. This can be seen as an addendum to Theorems 3.30 and 3.31.

Lemma 3.36 (Enhanced Mapping Properties of V_ω^{-1}, Helmholtz Problem)
Let Ω be a Lipschitz domain and $-\frac{1}{2} \le s \le \frac{1}{2}$. Let $\varphi \in H^{1/2+s}(\Gamma)$. Then

$$\|V_\omega^{-1}[\varphi]\|_{s-1/2,\omega,\Gamma} \le C|\omega||\omega|^{2|s|}\|\varphi\|_{s+1/2,\omega,\Gamma} \tag{3.92}$$

$$\|V_\omega^{-1}[\varphi]\|_{H^{s-1/2}(\Gamma)} \le C|\omega|^2|\omega|^{2|s|}\|\varphi\|_{H^{s+1/2}(\Gamma)} \tag{3.93}$$

where the constants $C = C(\Gamma, \sigma_0, s)$ are $|\omega|$-independent.

These bounds are again counter-intuitive: Why is the power of $|\omega|$ always larger (except for $s = 0$) than the one in the bound on V_ω? Why does the bound in $|\omega|$ depend on s now, while it did not before? Once again, we stress that there might be better and more intuitive bounds, but the techniques we used here only allowed us to prove the ones stated here.

3.3 Analysis in the Space-Time Domain

In this section, we introduce the function spaces that we use for the analysis in the space-time domain. We then transfer the results obtained in the Laplace domain in the previous section to the space-time domain.

3.3.1 Space-Time Sobolev Spaces

In this section, we introduce the two types of function spaces that have been used in the literature for the analysis of time domain Boundary Element Methods; the classical space-time Sobolev spaces (Section 3.3.1.1) and the space-time Sobolev spaces with an interweaved space-time norm, or energy space-time Sobolev spaces (Section 3.3.1.2). The former ones are merely the classical norms with an additional time weight factor, whereas the latter ones are based on the wavenumber-dependent norms introduced in Section 3.2 for the time harmonic problem. We define the respective spaces and relate them to the context of the anisotropic Sobolev spaces that are used for the analysis of time domain Boundary Element Methods for parabolic problems in [53, 125]. In Section 3.3.1.3, we briefly investigate the dual spaces for these function spaces.

3.3.1.1 Classical Space-Time Sobolev Spaces

We begin with the definition of the classical space-time Sobolev spaces. These are the spaces that are used to derive a priori error estimates for the time domain Boundary Element Method in [20, 21].

Definition 3.37 (Classical Space-Time Sobolev Spaces [20, p. 416], [34, p. 38])
Let $\sigma > 0$, $k \in \mathbb{R}$ and E be a Banach space. The classical space-time Sobolev spaces *are given by*

$$\mathcal{H}^k_\sigma(\mathbb{R}, E) := \left\{ u \in LT(E) \;\middle|\; \|u\|_{\sigma,k,E} < \infty \right\} \tag{3.94}$$

with norm [34, p. 40], [81, p. 17]

$$\|u\|^2_{\sigma,k,E} := \int_{\mathbb{R}+i\sigma} |\omega|^{2k}\|\hat{u}(\omega,\cdot)\|^2_E \, d\omega. \tag{3.95}$$

Remark 3.38 (On Definition 3.37)
a) [20, p. 416] For $k \in \mathbb{N}$,

$$\|u\|^2_{\sigma,k,E} = 2\pi \int_{\mathbb{R}} e^{-2\sigma t} \left\| \frac{\partial^k}{\partial t^k} u(t,\cdot) \right\|^2_E dt$$

by the Parseval-Plancherel identity (Lemma 3.6).

b) For $k \in \mathbb{N}$,

$$\|u\|_{\sigma,k,E} = \left\| \frac{\partial^k}{\partial t^k} u(t,\cdot) \right\|_{\sigma,0,E}$$

which implies [69, p. 3] that $u \in \mathcal{H}^k_\sigma(\mathbb{R},E)$ if and only if $e^{-\sigma t}\frac{\partial^k u}{\partial t^k} \in L^2(\mathbb{R},E)$. For $k \in \mathbb{R}\setminus\mathbb{N}$, this involves fractional order derivatives [20, p. 415], [81, p. 17] that can be expressed in terms of the operator Λ^k defined in (3.4), and there holds

$$\|f\|_{\sigma,k,E} = \|\Lambda^k[f]\|_{\sigma,0,E}$$

for any $k \in \mathbb{R}$.

c) For $k = 0$, we also write $\mathcal{H}^0_\sigma(\mathbb{R},E) = \mathcal{L}^2_\sigma(\mathbb{R},E)$.

d) $\|\cdot\|_{\sigma,k,E}$ is a norm and a semi-norm on $\mathcal{H}^k_\sigma(\mathbb{R},E)$: For any $u \in \mathcal{H}^k_\sigma(\mathbb{R},E)$, there holds

$$\|u\|^2_{\sigma,k,E} \geq \sigma^2 \int_{\mathbb{R}+i\sigma} |\omega|^{2(k-1)} \|\hat{u}(\omega,\cdot)\|^2_E \, d\omega = \sigma^2 \|u\|^2_{\sigma,k-1,E}, \tag{3.96}$$

and therefore $\|u\|_{\sigma,k,E} \geq \sigma\|u\|_{\sigma,k-1,E}$. On the other hand, let $|||u|||^2_{\sigma,k,E} := \sum_{l=0}^{\lfloor k\rfloor} \|u\|^2_{\sigma,l,E} + \|u\|^2_{\sigma,k,E}$ where $\lfloor k\rfloor := \max\{\, m \in \mathbb{Z} \;\mid\; m < k \,\}$. For $k \in \mathbb{Z}$, this simply gives $|||u|||^2_{\sigma,k,E} = \sum_{l=0}^{k} \|u\|^2_{\sigma,l,E}$. Obviously $|||u|||_{\sigma,k,E} \geq \|u\|_{\sigma,k,E}$ but also, by (3.96) and for $k \in \mathbb{Z}$,

$$|||u|||^2_{\sigma,k,E} \leq \sum_{l=0}^{k} \sigma^{-2l} \|u\|^2_{\sigma,k,E}.$$

With $C(k,\sigma) = \sqrt{k\frac{1-(\sigma^{-2})^{k+1}}{1-\sigma^{-2}}}$, we obtain

$$\|u\|_{\sigma,k,E} \leq |||u|||_{\sigma,k,E} \leq C(k,\sigma)\|u\|_{\sigma,k,E}. \tag{3.97}$$

This means that the semi-norm and the norm are equivalent. The relation (3.97) holds analogously for $k \notin \mathbb{Z}$. This can be seen as an analogue to the Poincaré-Friedrichs inequality in $H^1_0(\Omega)$; see, for instance, [2, Theorem 6.30 and Corollary 6.31] or [133, Theorem 2.5.7].

e) By [104, (9.24)], there holds

$$[H^{s_1}(\Omega;X), H^{s_2}(\Omega;Y)]_\theta = H^{(1-\theta)s_1+\theta s_2}(\Omega;[X,Y]_\theta)$$

for $s_1 > 0$, $s_2 < s_1$ and $\theta \in (0,1)$. Consequently, we conclude that

$$\left[\mathcal{H}^{k_1}_\sigma(\mathbb{R},E_1), \mathcal{H}^{k_2}_\sigma(\mathbb{R},E_2)\right]_\theta = \mathcal{H}^{(1-\theta)k_1+\theta k_2}_\sigma(\mathbb{R},[E_1,E_2]_\theta) \tag{3.98}$$

as well.

3.3.1.2 Energy Space-Time Sobolev Spaces

We now define an alternative space-time Sobolev norm and corresponding spaces which are directly related to the wave's energy (3.11). These norms were first introduced by Terrasse [147].

Definition 3.39 (Energy Space-Time Sobolev Spaces [34, p. 41], [81, p. 18f.])
Let $\sigma > 0$, $s \in \mathbb{R}_{\geq 0}$ and $k \in \mathbb{R}$. The energy space-time Sobolev spaces *are given by*

$$H^{k;\,s,s}_{\sigma,\Gamma} := \left\{ u \in LT(H^s(\Gamma)) \;\middle|\; \|u\|_{\sigma,\Gamma;\,k;\,s,s} < \infty \right\} \tag{3.99}$$

with norm [147, p. 35]

$$\|u\|^2_{\sigma,\Gamma;\,k;\,s,s} := \int_{\mathbb{R}+i\sigma} |\omega|^{2k} \|\hat{u}(\omega,\cdot)\|^2_{s,\omega,\Gamma}\, d\omega. \tag{3.100}$$

The definitions of $\|\cdot\|_{\sigma,\Omega;\,k;\,s,s}$ and $H^{k;\,s,s}_{\sigma,\Omega}$ are analogous.

In this context, we now obtain, by (3.12),

$$\int_{\mathbb{R}} e^{-2\sigma t} E_\Omega[u](t)\, dt = \frac{1}{4\pi} \int_{\mathbb{R}+i\sigma} \|\hat{u}(\omega,\cdot)\|^2_{1,\omega,\Omega}\, d\omega = \frac{1}{4\pi} \|u\|^2_{\sigma,\Omega;\,0;\,1,1} \tag{3.101}$$

which demonstrates the relation of these spaces to the wave's energy $E_\Omega[u]$. It is also obvious that there holds

$$\int_{\mathbb{R}} e^{-2\sigma t} E_\Omega[\dot{u}](t)\, dt = \frac{1}{4\pi} \|\dot{u}\|^2_{\sigma,\Omega;\,0;\,1,1} = \frac{1}{4\pi} \|u\|^2_{\sigma,\Omega;\,1;\,1,1} \geq \frac{\sigma^2}{4\pi} \|u\|^2_{\sigma,\Omega;\,0;\,1,1}$$

or simply

$$\|u\|_{\sigma,\Omega;\,1;\,1,1} \geq \sigma \|u\|_{\sigma,\Omega;\,0;\,1,1}$$

and generally, for $s \in \mathbb{R}_{\geq 0}$, $k \in \mathbb{Z}_{\geq 0}$,

$$\|u\|_{\sigma,\mathcal{O};\,k+1;\,s,s} \geq \sigma \|u\|_{\sigma,\mathcal{O};\,k;\,s,s}\,. \tag{3.102}$$

Similarly to Remark 3.38 d), this shows that $\|\cdot\|_{\sigma,\mathcal{O};\,k;\,s,s}$ is a norm and a semi-norm on $H^{k;\,s,s}_{\sigma,\mathcal{O}}$.

Remark 3.40 (On Definition 3.39)
a) $H^{0;\,0,0}_{\sigma,\mathcal{O}} = \mathcal{H}^0_\sigma(\mathbb{R}, L^2(\mathcal{O})) = \mathcal{L}^2_\sigma(\mathbb{R}, L^2(\mathcal{O}))$. In this case, we also write $L^2_{\sigma,\mathcal{O}} := H^{0;\,0,0}_{\sigma,\mathcal{O}}$.

b) For $k \in \mathbb{N}$, $\|u\|_{\sigma,\mathcal{O};\,k;\,s,s} = \left\| \frac{\partial^k}{\partial t^k} u(t,\cdot) \right\|_{\sigma,\mathcal{O};\,0;\,s,s}$ by the Parseval-Plancherel identity (Lemma 3.6).

c) The spaces $H^{k;\,s,s}_{\sigma,\mathcal{O}}$ are in fact intermediate spaces between the classical spaces $\mathcal{H}^k_\sigma(\mathbb{R}, H^s(\mathcal{O}))$. More precisely, by (3.18)*, there holds*

$$\mathcal{H}^1_\sigma(\mathbb{R}, H^1(\Omega)) \subseteq H^{0;\,1,1}_{\sigma,\Omega} \subseteq \mathcal{H}^0_\sigma(\mathbb{R}, H^1(\Omega)).$$

More generally, by Remark 3.9,

$$\mathcal{H}^{k+s}_\sigma(\mathbb{R}, H^s(\mathcal{O})) \subseteq H^{k;\,s,s}_{\sigma,\mathcal{O}} \subseteq \mathcal{H}^k_\sigma(\mathbb{R}, H^s(\mathcal{O})). \tag{3.103}$$

A further characterisation is given in (3.113) *below.*

The reason for using the space index s twice in the notation of the norm (3.100) is to show the relation to the *anisotropic Sobolev spaces* that are used in the analysis of parabolic Boundary Element Methods [53, 105, 125]. These spaces are, for $r, s \geq 0$, given by [53, p. 502], [105, Chapter 4, (2.1)], [125, p. 8]

$$H^{r,s}_{\mathbb{R}^N} := L^2(\mathbb{R}, H^r(\mathbb{R}^N)) \cap H^s(\mathbb{R}, L^2(\mathbb{R}^N)) \tag{3.104}$$

with equivalent norm

$$\|u\|^2_{\mathbb{R}^N;\,r,s} := \int_{\mathbb{R}} \int_{\mathbb{R}^N} \left((1+|\xi|^2)^r + (1+|\tau|^2)^s \right) |\mathcal{F}_{x,t}[u](\xi,\tau)|^2\, d\xi\, d\tau. \tag{3.105}$$

Again, similar norms for spaces $H^{r,s}(\Omega\times\mathbb{R})$ and $H^{r,s}(\Gamma\times\mathbb{R})$ can be defined via restrictions [105, Chapter 4, (2.11)], [125, p. 12]. We further note that there holds the interpolation result [105, Chapter 4, Proposition 2.1]

$$\left[H_\Omega^{r,s}, H_\Omega^{\rho,\sigma}\right]_\theta = H_\Omega^{(1-\theta)r+\theta\rho,(1-\theta)s+\theta\sigma} \tag{3.106}$$

for $r,s,\rho,\sigma\geq 0$ and $\theta\in(0,1)$.

The respective dual spaces are denoted by $\left(H_{\mathcal{O}}^{r,s}\right)^\star = H_{\mathcal{O}}^{-r,-s}$ for $r,s\geq 0$ [125, p. 11], and one can show that $H_{\mathcal{O}}^{-r,-s} = L^2(\mathbb{R},H^{-r}(\mathbb{R}^N))\cap H^{-s}(\mathbb{R},L^2(\mathbb{R}^N))$.

In the next definition, we generalise these anisotropic Sobolev spaces to spaces that allow more rigorous assumptions on the temporal regularity.

Definition 3.41 (Generalised Anisotropic Sobolev Spaces)
Let $s,k\in\mathbb{R}$. Analogously to (3.104) *and* (3.105)*,*

$$H_{\mathbb{R}^N}^{k;\,s,s} := H^k(\mathbb{R},H^s(\mathbb{R}^N))\cap H^{s+k}(\mathbb{R},L^2(\mathbb{R}^N)) \tag{3.107}$$

with equivalent norm

$$\|u\|_{\mathbb{R}^N;\,k;\,s,s}^2 := \int_{\mathbb{R}}\int_{\mathbb{R}^N}\left((1+|\xi|^2)^s(1+|\tau|^2)^k + (1+|\tau|^2)^{s+k}\right)|\mathcal{F}_{x,t}[u](\xi,\tau)|^2\,d\xi\,d\tau. \tag{3.108}$$

The respective spaces for Ω and Γ are denoted by $H_\Omega^{k;\,s,s}$ and $H_\Gamma^{k;\,s,s}$.

Remark 3.42 (On Definition 3.41)
a) Obviously $H_{\mathcal{O}}^{0;\,s,s} = H_{\mathcal{O}}^{s,s}$ for all s and $\mathcal{O}\in\{\mathbb{R}^N,\Omega,\Gamma\}$.

b) By the definition, $\left\|\frac{\partial^k}{\partial t^k}u(\cdot,t)\right\|_{\mathcal{O};\,0;\,s,s} = \|u\|_{\mathcal{O};\,k;\,s,s}$, and thus $u\in H_{\mathcal{O}}^{k;\,s,s}$ if and only if $\frac{\partial^k u}{\partial t^k}\in H_{\mathcal{O}}^{s,s}$.

c) We conclude from (3.106) *that*

$$\left[H_{\mathcal{O}}^{k;\,s,s}, H_{\mathcal{O}}^{\kappa;\,\sigma,\sigma}\right]_\theta = H_{\mathcal{O}}^{(1-\theta)k+\theta\kappa;\,(1-\theta)s+\theta\sigma,(1-\theta)s+\theta\sigma} \tag{3.109}$$

for $k,s,\kappa,\sigma\geq 0$, $\theta\in(0,1)$ and $\mathcal{O}\in\{\mathbb{R}^N,\Omega,\Gamma\}$.

For a further characterisation of the spaces $H_{\sigma,\mathcal{O}}^{k;\,s,s}$, the following result, established in [81, (51)] for $s=1/2$, is needed.

Lemma 3.43
Let $a\in\mathbb{R}_{\geq 0}$ and $s\in\mathbb{R}_{\geq 0}$. Further, let $\Im(\omega)>\sigma_0$ for some $\sigma_0\in\mathbb{R}_{>0}$, as established in Section 3.2.1. Then there exist $|\omega|$-independent constants $C_1 = C_1(s)$ and $C_2 = C_2(s,\sigma_0)$ such that

$$C_1\left(a+|\omega|^2\right)^s \leq (1+a)^s + \left(1+|\omega|^2\right)^s \leq C_2\left(a+|\omega|^2\right)^s. \tag{3.110}$$

Proof
The first inequality in (3.110) holds for $s=0$ with $C_1=1$. For $s\in(0,1)$,

$$\left(a+|\omega|^2\right)^s \leq a^s + \left(|\omega|^2\right)^s \leq (1+a)^s + \left(1+|\omega|^2\right)^s$$

and thus the first inequality in (3.110) with $C_1=1$, where the first inequality is [86, Theorem 28] and the second is obvious. Finally, for $s\geq 1$,

$$2^{1-s}\left(a+|\omega|^2\right)^s \leq a^s + \left(|\omega|^2\right)^s \leq (1+a)^s + \left(1+|\omega|^2\right)^s$$

and thus the first inequality in (3.110) with $C_1 = 2^{1-s}$, where the first inequality is Jensen's inequality.

Similarly, for $s \geq 1$,

$$(1+a)^s + \left(1+|\omega|^2\right)^s < \left(1+a+1+|\omega|^2\right)^s < \left(a+\left(\frac{2}{\sigma_0^2}+1\right)|\omega|^2\right)^s < \left(\frac{2}{\sigma_0^2}+1\right)^s \left(a+|\omega|^2\right)^s$$

and thus the second inequality in (3.110) with $C_2 = \left(\frac{2}{\sigma_0^2}+1\right)^s$, where the the first inequality is [86, Theorem 27]. For $s = 0$, the second inequality in (3.110) trivially holds with $C_2 = 2$. Finally, let $s \in (0,1)$. Then

$$(1+a)^s < \left(\frac{1}{\sigma_0^2}|\omega|^2 + a\right)^s \leq \max\left\{\frac{1}{\sigma_0^{2s}}, 1\right\}\left(a+|\omega|^2\right)^s$$

and

$$\left(1+|\omega|^2\right)^s \leq \left(a+1+|\omega|^2\right)^s < \left(a+\left(\frac{1}{\sigma_0^2}+1\right)|\omega|^2\right)^s \leq \left(1+\frac{1}{\sigma_0^2}\right)^s \left(a+|\omega|^2\right)^s.$$

Hence

$$(1+a)^s + \left(1+|\omega|^2\right)^s \leq \left(\max\left\{\frac{1}{\sigma_0^{2s}}, 1\right\} + \left(1+\frac{1}{\sigma_0^2}\right)^s\right)\left(a+|\omega|^2\right)^s$$

and thus the second inequality in (3.110) with $C_2 = \max\left\{\frac{1}{\sigma_0^{2s}}, 1\right\} + \left(1+\frac{1}{\sigma_0^2}\right)^s$. ∎

Using the inequality in Lemma 3.43 with $a = |\xi|^2$, one can show that, for $s \in \mathbb{R}_{\geq 0}$,

$$u \in H^{k;s,s}_{\sigma,\mathcal{O}} \qquad \text{if and only if} \qquad e^{-\sigma t}u \in H^{k;s,s}_{\mathcal{O}}. \tag{3.111}$$

For negative s, we obtain the same result by duality. We can therefore give a further characterisation of the relation (3.103) of the classical Sobolev spaces $\mathcal{H}^k_\sigma(\mathbb{R}, H^s(\mathcal{O}))$ and the energy spaces $H^{k;s,s}_{\sigma,\mathcal{O}}$ stated in Remark 3.40 c): By (3.107) and (3.111),

$$u \in H^{k;s,s}_{\sigma,\mathcal{O}} \qquad \text{if and only if} \qquad e^{-\sigma t}u \in H^k(\mathbb{R}, H^s(\mathcal{O})) \cap H^{s+k}(\mathbb{R}, L^2(\mathcal{O})) \tag{3.112}$$

which is the case if and only if $e^{-\sigma t}\frac{\partial^k u}{\partial t^k} \in L^2(\mathbb{R}, H^s(\mathcal{O}))$ and $e^{-\sigma t}\frac{\partial^{s+k} u}{\partial t^{s+k}} \in L^2(\mathbb{R}, L^2(\mathcal{O}))$, and therefore, using Remark 3.38 b),

$$H^{k;s,s}_{\sigma,\mathcal{O}} = \mathcal{H}^k_\sigma(\mathbb{R}, H^s(\mathcal{O})) \cap \mathcal{H}^{s+k}_\sigma(\mathbb{R}, L^2(\mathcal{O})). \tag{3.113}$$

For $s = 1, k = 0$, (3.113) corresponds to [81, p. 17], and for $s = 0$ and arbitrary k, we obtain $H^{k;0,0}_{\sigma,\mathcal{O}} = \mathcal{H}^k_\sigma(\mathbb{R}, L^2(\mathcal{O}))$ [18, p. 264].

Note that (3.113) implies that one can use

$$\|u\|^2_{\sigma,\mathcal{O};k;s,s} = \|u\|^2_{\sigma,k,H^s(\mathcal{O})} + \|u\|^2_{\sigma,s+k,L^2(\mathcal{O})} \tag{3.114}$$

as an equivalent norm on $H^{k;s,s}_{\sigma,\mathcal{O}}$.

Further, by (3.109) and (3.111), we conclude that

$$\left[H^{k;s,s}_{\sigma,\mathcal{O}}, H^{\kappa;\sigma,\sigma}_{\sigma,\mathcal{O}}\right]_\theta = H^{(1-\theta)k+\theta\kappa;\,(1-\theta)s+\theta\sigma,(1-\theta)s+\theta\sigma}_{\sigma,\mathcal{O}} \tag{3.115}$$

for $k, s, \kappa, \sigma \geq 0$, $\theta \in (0,1)$ and $\mathcal{O} \in \left\{\mathbb{R}^N, \Omega, \Gamma\right\}$.

3.3.1.3 The Space-Time Dual Spaces

Having introduced the space-time Sobolev spaces used in the analysis of the time domain Boundary Element Method and their relations to each other, we finally consider their dual spaces for completeness.

As usual, we write $\left(\mathcal{H}^k_\sigma(\mathbb{R},E)\right)^* = \mathfrak{L}\left(\mathcal{H}^k_\sigma(\mathbb{R},E),\mathbb{R}\right)$ for $E \in \left\{H^s(\mathbb{R}^N), H^s(\Omega), H^s(\Gamma)\right\}$ and $\left(H^{k;\,s,s}_{\sigma,\mathcal{O}}\right)^* = \mathfrak{L}\left(H^{k;\,s,s}_{\sigma,\mathcal{O}},\mathbb{R}\right)$ for $\mathcal{O} \in \left\{\mathbb{R}^N,\Omega,\Gamma\right\}$. The norms on $\left(\mathcal{H}^k_\sigma(\mathbb{R},E)\right)^*$ and $\left(H^{k;\,s,s}_{\sigma,\mathcal{O}}\right)^*$ are given by

$$\|g\|_{\mathfrak{L}(\mathcal{H}^k_\sigma(\mathbb{R},E),\mathbb{R})} = \sup_{\mathcal{H}^k_\sigma(\mathbb{R},E)} \frac{|\,(f,g)_{\mathcal{H}^k_\sigma(\mathbb{R},H^s(\mathbb{R}^N))}\,|}{\|f\|_{\sigma,k,E}}$$

and

$$\|g\|_{\mathfrak{L}(H^{k;\,s,s}_{\sigma,\mathcal{O}},\mathbb{R})} = \sup_{f\in H^{k;\,s,s}_{\sigma,\mathcal{O}}} \frac{|\,(f,g)_{\mathcal{H}^k_\sigma(\mathbb{R},H^s(\mathbb{R}^N))}\,|}{\|f\|_{\sigma,\mathcal{O};\,k;\,s,s}}$$

where $(\cdot,\cdot)_{\mathcal{H}^k_\sigma(\mathbb{R},H^s(\mathbb{R}^N))}$ stands for the respective inner product, see (3.121) below. We give a further characterisation of these spaces in Lemma 3.44.

Lemma 3.44 (Space-Time Dual Spaces)
The dual spaces of $\mathcal{H}^k_\sigma(\mathbb{R},E)$ with $E \in \left\{H^s(\mathbb{R}^N), H^s(\Omega), H^s(\Gamma)\right\}$ and $H^{k;\,s,s}_{\sigma,\mathcal{O}}$ with $\mathcal{O} \in \left\{\mathbb{R}^N,\Omega,\Gamma\right\}$ are given by

$$\left(\mathcal{H}^k_\sigma(\mathbb{R},E)\right)^* \cong \mathcal{H}^{-k}_\sigma(\mathbb{R},E^*) \qquad \text{and} \qquad \left(H^{k;\,s,s}_{\sigma,\mathcal{O}}\right)^* \cong H^{-k;-s,-s}_{\sigma,\mathcal{O}} \tag{3.116}$$

for $s \in \mathbb{R}_{\geq 0}, k \in \mathbb{Z}_{\geq 0}$, where $\cong$ means 'equal up to an isometric isomorphism'. We hence identify $\left(\mathcal{H}^k_\sigma(\mathbb{R},E)\right)^*$ with $\mathcal{H}^{-k}_\sigma(\mathbb{R},E^*)$ and $\left(H^{k;\,s,s}_{\sigma,\mathcal{O}}\right)^*$ with $H^{-k;-s,-s}_{\sigma,\mathcal{O}}$.

Consequently, there holds a generalised Cauchy-Schwarz inequality in both cases: Let $f \in \mathcal{H}^k_\sigma(\mathbb{R},E)$ and $g \in \mathcal{H}^{-k}_\sigma(\mathbb{R},E^*)$ or $f \in H^{k;\,s,s}_{\sigma,\mathcal{O}}$ and $g \in H^{-k;-s,-s}_{\sigma,\mathcal{O}}$, respectively. Then

$$|\langle\!\langle f,g\rangle\!\rangle_\sigma| \leq \|f\|_{\sigma,k,E}\|g\|_{\sigma,-k,E^*} \tag{3.117}$$

and

$$|\langle\!\langle f,g\rangle\!\rangle_\sigma| \leq \|f\|_{\sigma,\mathcal{O};\,k;\,s,s}\|g\|_{\sigma,\mathcal{O};\,-k;\,-s,-s}. \tag{3.118}$$

where $\langle\!\langle\cdot,\cdot\rangle\!\rangle_\sigma$ stands for the duality product

$$\langle\!\langle f,g\rangle\!\rangle_\sigma := \int_{\mathbb{R}_{\geq 0}} e^{-2\sigma t}\,\langle f(\cdot,t), g(\cdot,t)\rangle\; dt. \tag{3.119}$$

Proof
We consider the case $\mathcal{H}^k_\sigma(\mathbb{R},H^s(\mathbb{R}^N))$ here; the proofs for the other cases are all similar.

As mentioned in Section 3.1 we write $\tilde{u}(\xi,\cdot) = \mathcal{F}_x[u](\xi,\cdot)$ for the Fourier transform of u with respect to x and $\hat{u}(\cdot,\omega) = \mathcal{L}_t[u](\cdot,\omega)$ for the Fourier-Laplace transform with respect to t. We write $\hat{\tilde{u}}(\xi,\omega) = \mathcal{L}\mathcal{F}_{t,x}[u](\xi,\omega) = \mathcal{L}_t[\;\mathcal{F}_x[u](\xi,t)\;](\xi,\omega)$ for the respective combined space-time transform. Recall that, for $s \geq 0$ and by (3.13),

$$\|u\|^2_{H^s(\mathbb{R}^N)} = \int_{\mathbb{R}^N} \left(1+|\xi|^2\right)^s |\tilde{u}(\xi)|^2\; d\xi.$$

Hence, due to the Parseval-Plancherel identity (Lemma 3.6),

$$\|u\|^2_{\mathcal{H}^k_\sigma(\mathbb{R},H^s(\mathbb{R}^N))} = \|u\|^2_{\sigma,k,H^s(\mathbb{R}^N)} = \left(\frac{1}{2\pi}\right)^2 \int_{\mathbb{R}+i\sigma}\int_{\mathbb{R}^N} |\omega|^{2k}\left(1+|\xi|^2\right)^s \left|\hat{\tilde{u}}^2(\xi,\omega)\right|^2\; d\xi\; d\omega. \tag{3.120}$$

This space is equipped with the inner product

$$(u,v)_{\mathcal{H}^k_\sigma(\mathbb{R},H^s(\mathbb{R}^N))} = \left(\frac{1}{2\pi}\right)^2 \int_{\mathbb{R}+i\sigma}\int_{\mathbb{R}^N} |\omega|^{2k}\left(1+|\xi|^2\right)^s \hat{\tilde{u}}(\xi,\omega)\hat{\tilde{v}}(\xi,\omega)\,d\xi\,d\omega. \tag{3.121}$$

so that $(u,u)_{\mathcal{H}^k_\sigma(\mathbb{R},H^s(\mathbb{R}^N))} = \|u\|^2_{\sigma,k,H^s(\mathbb{R}^N)}$. We further define, for $s,k\geq 0$,

$$\|u\|^2_{\sigma,-k,H^{-s}(\mathbb{R}^N)} := \left(\frac{1}{2\pi}\right)^2 \int_{\mathbb{R}+i\sigma}\int_{\mathbb{R}^N} |\omega|^{-2k}\left(1+|\xi|^2\right)^{-s} \hat{\tilde{u}}^2(\xi,\omega)\,d\xi\,d\omega \tag{3.122}$$

as the norm on $\mathcal{H}^{-k}_\sigma(\mathbb{R},H^{-s}(\mathbb{R}^N))$. Let us define a mapping

$$j:\left\{\begin{array}{lll} \mathcal{H}^{-k}_\sigma(\mathbb{R},H^{-s}(\mathbb{R}^N)) & \to & \left(\mathcal{H}^k_\sigma(\mathbb{R},H^s(\mathbb{R}^N))\right)^* \\ f & \mapsto & j[f](v) := \int_{\mathbb{R}} e^{-2\sigma t}\int_{\mathbb{R}^N} f(x,t)v(x,t)\,dx\,dt =: (f,v) \\ & & \qquad \text{for } v\in\mathcal{H}^k_\sigma(\mathbb{R},H^s(\mathbb{R}^N)) \end{array}\right.$$

Then, for any $v\in\mathcal{H}^k_\sigma(\mathbb{R},H^s(\mathbb{R}^N))$,

$$\begin{aligned} |j[f](v)| &= |(f,v)| = \frac{1}{2\pi}\left|\left(\tilde{f},\tilde{v}\right)\right| = \left(\frac{1}{2\pi}\right)^2\left|\int_{\mathbb{R}+i\sigma}\int_{\mathbb{R}^N}\hat{\tilde{f}}(\xi,\omega)\hat{\tilde{v}}(\xi,\omega)\,d\xi\,d\omega\right| \\ &= \left(\frac{1}{2\pi}\right)^2\left|\int_{\mathbb{R}+i\sigma}\int_{\mathbb{R}^N}\left(1+|\xi|^2\right)^{-s/2}\hat{\tilde{f}}(\xi,\omega)\left(1+|\xi|^2\right)^{s/2}\hat{\tilde{v}}(\xi,\omega)\,d\xi\,d\omega\right| \\ &\leq \frac{1}{2\pi}\int_{\mathbb{R}+i\sigma}\sqrt{\frac{1}{2\pi}\int_{\mathbb{R}^N}(1+|\xi|^2)^{-s}\,\hat{\tilde{f}}^2(\xi,\omega)\,d\xi}\sqrt{\frac{1}{2\pi}\int_{\mathbb{R}^N}(1+|\xi|^2)^{s}\,\hat{\tilde{v}}^2(\xi,\omega)\,d\xi}\,d\omega \\ &= \frac{1}{2\pi}\int_{\mathbb{R}+i\sigma}|\omega|^{-k}\|\tilde{f}\|_{H^{-s}(\mathbb{R}^N)}\,|\omega|^k\|\tilde{v}\|_{H^s(\mathbb{R}^N)}\,d\omega \\ &\leq \sqrt{\frac{1}{2\pi}\int_{\mathbb{R}+i\sigma}|\omega|^{-2k}\|\tilde{f}\|^2_{H^{-s}(\mathbb{R}^N)}\,d\omega}\sqrt{\frac{1}{2\pi}\int_{\mathbb{R}+i\sigma}|\omega|^{2k}\|\tilde{v}\|^2_{H^s(\mathbb{R}^N)}\,d\omega} \\ &= \|f\|_{\sigma,-k,H^{-s}(\mathbb{R}^N)}\,\|v\|_{\sigma,k,H^s(\mathbb{R}^N)} \end{aligned} \tag{3.123}$$

where the second and third identity are due to the Parseval-Plancherel identity (Lemma 3.6) and the inequalities are due to the Cauchy-Schwarz inequality for integrals. As a consequence, we obtain

$$\|j[f]\|_{(\mathcal{H}^k_\sigma(\mathbb{R},H^s(\mathbb{R}^N)))^*} = \sup_{v\in\mathcal{H}^k_\sigma(\mathbb{R},H^s(\mathbb{R}^N))}\frac{|j[f](v)|}{\|v\|_{\sigma,k,H^s(\mathbb{R}^N)}} \leq \|f\|_{\sigma,-k,H^{-s}(\mathbb{R}^N)} < \infty \tag{3.124}$$

for any $f\in\mathcal{H}^{-k}_\sigma(\mathbb{R},H^{-s}(\mathbb{R}^N))$, and hence j is well-defined.

Next we show that j is a surjective mapping. Let $G\in\left(\mathcal{H}^k_\sigma(\mathbb{R},H^s(\mathbb{R}^N))\right)^*$. We need to find $g\in\mathcal{H}^{-k}_\sigma(\mathbb{R},H^{-s}(\mathbb{R}^N))$ such that $j[g]\equiv G$. By the Riesz representation theorem [114, Theorem 2.30], there exists a $u_G\in\mathcal{H}^k_\sigma(\mathbb{R},H^s(\mathbb{R}^N))$ to G such that

$$\|G\|_{(\mathcal{H}^k_\sigma(\mathbb{R},H^s(\mathbb{R}^N)))^*} = \|u_G\|_{\sigma,k,H^s(\mathbb{R}^N)} \tag{3.125}$$

and

$$\langle G,v\rangle_{(\mathcal{H}^k_\sigma(\mathbb{R},H^s(\mathbb{R}^N)))^*\times\mathcal{H}^k_\sigma(\mathbb{R},H^s(\mathbb{R}^N))} = (u_G,v)_{\mathcal{H}^k_\sigma(\mathbb{R},H^s(\mathbb{R}^N))} \tag{3.126}$$

for all $v\in\mathcal{H}^k_\sigma(\mathbb{R},H^s(\mathbb{R}^N))$.

This yields, with (3.121),

$$\begin{aligned}\langle G, v\rangle_{(\mathcal{H}^k_\sigma(\mathbb{R},H^s(\mathbb{R}^N)))^*\times\mathcal{H}^k_\sigma(\mathbb{R},H^s(\mathbb{R}^N))} &= (u_G, v)_{\mathcal{H}^k_\sigma(\mathbb{R},H^s(\mathbb{R}^N))}\\ = \left(\frac{1}{2\pi}\right)^2 \int_{\mathbb{R}+i\sigma}\int_{\mathbb{R}^N} |\omega|^{2k}\left(1+|\xi|^2\right)^s \hat{u}_G(\xi,\omega)\hat{v}(\xi,\omega)\,d\xi\,d\omega &= \left(\frac{1}{2\pi}\right)^2 \left(\hat{\hat{g}},\hat{\hat{v}}\right) \end{aligned} \tag{3.127}$$

for any $v \in \mathcal{H}^k_\sigma(\mathbb{R}, H^s(\mathbb{R}^N))$, where $\hat{\hat{g}} := |\omega|^{2k}\left(1+|\xi|^2\right)^s \hat{u}_G$. We set $g(x,t) := \mathcal{LF}^{-1}_{t,x}[\hat{\hat{g}}](x,t)$. Then

$$\left(\frac{1}{2\pi}\right)^2 \left(\hat{\hat{g}},\hat{\hat{v}}\right) = (g,v) = j[g](v) = \langle j[g], v\rangle_{(\mathcal{H}^k_\sigma(\mathbb{R},H^s(\mathbb{R}^N)))^*\times\mathcal{H}^k_\sigma(\mathbb{R},H^s(\mathbb{R}^N))} \tag{3.128}$$

where the first identity is due to the Parseval-Plancherel identity (Lemma 3.6) and the second and third are the definition of j. Combining equations (3.127) and (3.128), we obtain

$$\langle G, v\rangle_{(\mathcal{H}^k_\sigma(\mathbb{R},H^s(\mathbb{R}^N)))^*\times\mathcal{H}^k_\sigma(\mathbb{R},H^s(\mathbb{R}^N))} = \langle j[g], v\rangle_{(\mathcal{H}^k_\sigma(\mathbb{R},H^s(\mathbb{R}^N)))^*\times\mathcal{H}^k_\sigma(\mathbb{R},H^s(\mathbb{R}^N))} \tag{3.129}$$

or $G(v) = j[g](v)$ for any $v \in \mathcal{H}^k_\sigma(\mathbb{R}, H^s(\mathbb{R}^N))$, hence $G \equiv j[g]$. Finally, by the definition of g and since $u_G \in \mathcal{H}^k_\sigma(\mathbb{R}, H^s(\mathbb{R}^N))$,

$$\begin{aligned}\|g\|^2_{\sigma,-k,H^{-s}(\mathbb{R}^N)} &= \left(\frac{1}{2\pi}\right)^2 \int_{\mathbb{R}+i\sigma}\int_{\mathbb{R}^N} |\omega|^{-2k}\left(1+|\xi|^2\right)^{-s} \hat{\hat{g}}^2(\xi,\omega)\,d\xi\,d\omega\\ &= \left(\frac{1}{2\pi}\right)^2 \int_{\mathbb{R}+i\sigma}\int_{\mathbb{R}^N} |\omega|^{2k}\left(1+|\xi|^2\right)^{s} \hat{u}^2_G(\xi,\omega)\,d\xi\,d\omega\\ &= \|u_G\|^2_{\sigma,k,H^s(\mathbb{R}^N)} < \infty \end{aligned} \tag{3.130}$$

and so $g \in \mathcal{H}^{-k}_\sigma(\mathbb{R}, H^{-s}(\mathbb{R}^N))$, which is what we needed to show.

The discussion above further shows that j is an isometry: By (3.125) and (3.130),

$$\|g\|_{\sigma,-k,H^{-s}(\mathbb{R}^N)} = \|u_G\|_{\sigma,k,H^s(\mathbb{R}^N)} = \|G\|_{(\mathcal{H}^k_\sigma(\mathbb{R},H^s(\mathbb{R}^N)))^*} = \|j[g]\|_{(\mathcal{H}^k_\sigma(\mathbb{R},H^s(\mathbb{R}^N)))^*} \tag{3.131}$$

and hence, for every $g \in \mathcal{H}^{-k}_\sigma(\mathbb{R}, H^{-s}(\mathbb{R}^N))$,

$$\|j[g]\|_{(\mathcal{H}^k_\sigma(\mathbb{R},H^s(\mathbb{R}^N)))^*} = \|g\|_{\sigma,-k,H^{-s}(\mathbb{R}^N)} \tag{3.132}$$

which is the definition of an isometry. Since every isometry is injective (this is indeed obvious from the definition of j as well), we have shown that j is an isometric isomorphism and hence we can identify $\left(\mathcal{H}^k_\sigma(\mathbb{R}, H^s(\mathbb{R}^N))\right)^*$ with $\mathcal{H}^{-k}_\sigma(\mathbb{R}, H^{-s}(\mathbb{R}^N))$.

The Cauchy-Schwarz inequality (3.117) is indeed (3.123). ∎

3.3.2 Mapping Properties of the Time Domain Boundary Layer Potentials and Integral Operators

We now transfer the results of Section 3.2.2 to the space-time domain, using the Parseval-Plancherel identity (Lemma 3.6). All the constants $C > 0$ that appear in the results depend on σ_0.

The first result is an immediate consequence of Lemma 3.19 (for $s = 0$) and its generalisation, Theorem 3.31.

Theorem 3.45 (Enhanced Space-Time Mapping Properties, Classical Spaces)
Let Ω be a Lipschitz domain and $-\frac{1}{2} < s < \frac{1}{2}$. Let $p \in \mathcal{H}^1_\sigma(\mathbb{R}, H^{s-1/2}(\Gamma))$ for (3.133), (3.134) or $p \in \mathcal{H}^{3/2-s}_\sigma(\mathbb{R}, H^{s-1/2}(\Gamma))$ for (3.135), and let $\varphi \in \mathcal{H}^{3/2+s}_\sigma(\mathbb{R}, H^{s+1/2}(\Gamma))$ for (3.136), (3.137) or $\varphi \in \mathcal{H}^2_\sigma(\mathbb{R}, H^{s+1/2}(\Gamma))$ for (3.138). Then

$$\begin{aligned}
\|S[p]\|_{\sigma,0,H^{s+1}(\Omega)} &\leq C\|p\|_{\sigma,1,H^{s-1/2}(\Gamma)} && (3.133)\\
\|V[p]\|_{\sigma,0,H^{s+1/2}(\Gamma)} &\leq C\|p\|_{\sigma,1,H^{s-1/2}(\Gamma)} && (3.134)\\
\|K'[p]\|_{\sigma,0,H^{s-1/2}(\Gamma)} &\leq C\|p\|_{\sigma,3/2-s,H^{s-1/2}(\Gamma)} && (3.135)\\
\|D[\varphi]\|_{\sigma,0,H^{s+1}(\Omega)} &\leq C\|\varphi\|_{\sigma,3/2+s,H^{s+1/2}(\Gamma)} && (3.136)\\
\|K[\varphi]\|_{\sigma,0,H^{s+1/2}(\Gamma)} &\leq C\|\varphi\|_{\sigma,3/2+s,H^{s+1/2}(\Gamma)} && (3.137)\\
\|W[\varphi]\|_{\sigma,0,H^{s-1/2}(\Gamma)} &\leq C\|\varphi\|_{\sigma,2,H^{s+1/2}(\Gamma)} && (3.138)
\end{aligned}$$

with $C = C(\Gamma, \sigma_0, s)$. For $s = 0$, see [20, (3.4)] for (3.134), and [21, (2.13)], [34, (96)] for (3.138).

The next result follows immediately from Lemma 3.20 (for $s = 0$) and its generalisation, Theorem 3.30.

Theorem 3.46 (Enhanced Space-Time Mapping Properties, Energy Spaces)
Let Ω be a Lipschitz domain and $-\frac{1}{2} < s < \frac{1}{2}$. Let $p \in H^{1;\,-1/2+s,-1/2+s}_{\sigma,\Gamma}$ and $\varphi \in H^{1;\,1/2+s,\,1/2+s}_{\sigma,\Gamma}$. Then

$$\begin{aligned}
\|S[p]\|_{\sigma,\Omega;\,0;\,s+1,s+1} &\leq C\|p\|_{\sigma,\Gamma;\,1;\,s-1/2,s-1/2} && (3.139)\\
\|V[p]\|_{\sigma,\Gamma;\,0;\,s+1/2,s+1/2} &\leq C\|p\|_{\sigma,\Gamma;\,1;\,s-1/2,s-1/2} && (3.140)\\
\|K'[p]\|_{\sigma,\Gamma;\,0;\,s-1/2,s-1/2} &\leq C\|p\|_{\sigma,\Gamma;\,1;\,s-1/2,s-1/2} && (3.141)\\
\|D[\varphi]\|_{\sigma,\Omega;\,0;\,s+1,s+1} &\leq C\|\varphi\|_{\sigma,\Gamma;\,1;\,s+1/2,\,s+1/2} && (3.142)\\
\|K[\varphi]\|_{\sigma,\Gamma;\,0;\,s+1/2,s+1/2} &\leq C\|\varphi\|_{\sigma,\Gamma;\,1;\,s+1/2,\,s+1/2} && (3.143)\\
\|W[\varphi]\|_{\sigma,\Gamma;\,0;\,s-1/2,s-1/2} &\leq C\|\varphi\|_{\sigma,\Gamma;\,1;\,s+1/2,\,s+1/2} && (3.144)
\end{aligned}$$

with $C = C(\Gamma, \sigma_0, s)$. For $s = 0$, see [81, Theorem 3(1)] for (3.140) and [81, Theorem 2(1)] for (3.143).

The next result transfers the results of Lemma 3.23 (for $s = 0$) and its generalisation, Lemma 3.36, from the frequency domain to the space-time domain.

Lemma 3.47 (Boundedness and Positiveness of V^{-1})
Let Ω be a Lipschitz domain and $-\frac{1}{2} \leq s \leq \frac{1}{2}$. Let $g \in \mathcal{H}^{2+2|s|}_\sigma(\mathbb{R}, H^{1/2+s}(\Gamma))$ for (3.145) or $g \in H^{1;\,1/2+s,\,1/2+s}_{\sigma,\Gamma}$ for (3.146), and let $g \in \mathcal{H}^0_\sigma(\mathbb{R}, H^{1/2}(\Gamma))$ for (3.147) or $g \in H^{0;\,1/2,\,1/2}_{\sigma,\Gamma}$ for (3.148). Then

$$\begin{aligned}
\|V^{-1}[g]\|_{\sigma,0,H^{s-1/2}(\Gamma)} &\leq C\|g\|_{\sigma,2+2|s|,H^{s+1/2}(\Gamma)} && (3.145)\\
\|V^{-1}[g]\|_{\sigma,\Gamma;\,0;\,s-1/2,s-1/2} &\leq C\|g\|_{\sigma,\Gamma;\,1+2|s|;\,s+1/2,s+1/2} && (3.146)\\
\int_{\mathbb{R}} e^{-2\sigma t}\left\langle V^{-1}[g](\cdot,t), \dot{g}(\cdot,t)\right\rangle\, dt &\geq C\|g\|^2_{\sigma,0,H^{1/2}(\Gamma)} && (3.147)\\
\int_{\mathbb{R}} e^{-2\sigma t}\left\langle V^{-1}[g](\cdot,t), \dot{g}(\cdot,t)\right\rangle\, dt &\geq C\|g\|^2_{\sigma,\Gamma;\,0;\,1/2,1/2} && (3.148)
\end{aligned}$$

with $C = C(\Gamma, \sigma_0, s)$ for (3.145) and (3.146), and $C = C(\Gamma, \sigma_0)$ for (3.147) and (3.148). For $s = 0$, see [20, (3.3)], [54, Theorem 2.4 (i)] for (3.145), and [20, Proposition 4] for (3.147).

The space-time equivalent of Lemma 3.25 is Lemma 3.48.

Lemma 3.48 (Boundedness of N)
Let $f \in H^{1;s,s}_{\sigma,\Omega}$. Then

$$\|N[f]\|_{\omega,\Omega;\,0;\,s+2,s+2} \leq C\|f\|_{\omega,\Omega;\,1;\,s,s} \tag{3.149}$$

with $C = C(\Gamma, \sigma_0)$.

Remark 3.49 (On Theorems 3.45 and 3.46 and Lemmas 3.47 and 3.48)

a) *Note that we could also allow variable time regularity in all the results obtained in this section so far (Theorems 3.45 and 3.46 and Lemmas 3.47 and 3.48). Instead of* (3.139)*, for example, we could take*

$$\|S[p]\|_{\sigma,\Omega;\,k;\,s+1,s+1} \leq C\|p\|_{\sigma,\Gamma;\,k+1;\,s-1/2,s-1/2}$$

for $p \in H^{k+1;\,-1/2+s,-1/2+s}_{\sigma,\Gamma}$, or

$$\|V^{-1}[p]\|_{\sigma,\Gamma;\,k;\,s-1/2,s-1/2} \leq C\|p\|_{\sigma,\Gamma;\,k+1+2|s|;\,s+1/2,s+1/2}$$

for $p \in H^{k+1+2|s|;\,1/2+s,1/2+s}_{\sigma,\Gamma}$, instead of (3.146)*.*

b) *Note that one looses regularity in time for* both *the Single Layer operator V and its inverse V^{-1}; see also [49, Remark 5]. In particular, we* do not *have bounded mappings $V : X \to Y$ and $V^{-1} : Y \to X$. In fact, for $s = 0$, only the mappings*

$$\begin{aligned} V^{-1} \circ V &: \mathcal{H}^3_\sigma(\mathbb{R}, H^{-1/2}(\Gamma)) \to \mathcal{H}^0_\sigma(\mathbb{R}, H^{-1/2}(\Gamma)) \\ V \circ V^{-1} &: \mathcal{H}^3_\sigma(\mathbb{R}, H^{1/2}(\Gamma)) \to \mathcal{H}^0_\sigma(\mathbb{R}, H^{1/2}(\Gamma)) \end{aligned} \tag{3.150}$$

and

$$V^{-1} \circ V : H^{2;\,-1/2,-1/2}_{\sigma,\Gamma} \to H^{0;\,-1/2,-1/2}_{\sigma,\Gamma} \qquad V \circ V^{-1} : H^{2;\,1/2,1/2}_{\sigma,\Gamma} \to H^{0;\,1/2,1/2}_{\sigma,\Gamma} \tag{3.151}$$

are bounded. For variable s and k,

$$\begin{aligned} V^{-1} \circ V &: \mathcal{H}^{k+3+2|s|}_\sigma(\mathbb{R}, H^{-1/2+s}(\Gamma)) \to \mathcal{H}^k_\sigma(\mathbb{R}, H^{1/2+s}(\Gamma)) \\ V \circ V^{-1} &: \mathcal{H}^{k+3+2|s|}_\sigma(\mathbb{R}, H^{1/2+s}(\Gamma)) \to \mathcal{H}^0_\sigma(\mathbb{R}, H^{1/2+s}(\Gamma)) \end{aligned} \tag{3.152}$$

and

$$\begin{aligned} V^{-1} \circ V &: H^{k+2+2|s|;\,-1/2+s,-1/2+s}_{\sigma,\Gamma} \to H^{k;\,-1/2+s,-1/2+s}_{\sigma,\Gamma} \\ V \circ V^{-1} &: H^{k+2+2|s|;\,1/2+s,1/2+s}_{\sigma,\Gamma} \to H^{k;\,1/2+s,1/2+s}_{\sigma,\Gamma} \end{aligned} \tag{3.153}$$

are bounded.

On this issue, Costabel [54, p. 10] remarks that the 'loss of regularity in time is the price that needs to be paid for the application of elliptic methods to the hyperbolic problem'. Similarly, Monk et al. [49, Remark 5] state that '[t]he loss of time regularity both for [V] and its inverse is seemingly contradictory. The reason is that the mapping properties of both operators are established through bounds in the frequency domain'. Ha-Duong [81, Remark 3] adds that these problems (i.e. the loss of regularity) 'may be due to the chosen functional framework where time and space variables are treated separately'. But 'the search for a better framework to analyse the equations and their discretisations [is] difficult'. He adds that the use of the energy spaces might be a step in the right direction, since time and space are 'interweaved' in the space norm for these already.

c) Likewise, the mapping properties of the Newton potential N are not the ones one would expect. The d'Alembert operator reduces the orders in both space and time by two. The operator N recovers the two orders of regularity in space, but even loses another one in time.

We now define space-time bilinear forms $a_\sigma^V(\cdot,\cdot)$ and $a_\sigma^W(\cdot,\cdot)$ that correspond to the time independent bilinear forms (3.44) and (3.45) defined in the previous section,

$$a_\sigma^V(p,q) := \int_{\mathbb{R}_{\geq 0}} e^{-2\sigma t} \left\langle V[\dot{p}](\cdot,t), q(\cdot,t)\right\rangle \, dt = \frac{1}{2\pi} \int_{\mathbb{R}+i\sigma} a_\omega^V(\hat{p},\hat{q}) \, d\omega \tag{3.154}$$

for p, q in appropriate spaces (see below), and

$$a_\sigma^W(\varphi,\psi) := \int_{\mathbb{R}_{\geq 0}} e^{-2\sigma t} \left\langle W[\varphi](\cdot,t), \dot{\psi}(\cdot,t)\right\rangle \, dt = \frac{1}{2\pi} \int_{\mathbb{R}+i\sigma} a_\omega^W(\hat{\phi},\hat{\psi}) \, d\omega \tag{3.155}$$

for φ, ψ in appropriate spaces (see below). The coercivity and continuity estimates follow obviously from their time independent counterparts (Lemma 3.21).

Corollary 3.50 (Coercivity Estimates, Space-Time Bilinear Forms)
a) Let $p \in \mathcal{H}_\sigma^{-1/2}(\mathbb{R}, H^{-1/2}(\Gamma))$ or $p \in H_{\sigma,\Gamma}^{0;\,-1/2,-1/2}$, respectively. Then, with $C = C(\Gamma,\sigma_0)$,

(i) [20, (3.5)]

$$a_\sigma^V(p,p) \geq C\|p\|^2_{\sigma,-1/2,H^{-1/2}(\Gamma)}.$$

(ii) [81, (54)]

$$a_\sigma^V(p,p) \geq C\|p\|^2_{\sigma,\Gamma;\,0;-1/2,-1/2}.$$

b) Let $\varphi \in \mathcal{H}_\sigma^0(\mathbb{R}, H^{1/2}(\Gamma))$ or $\varphi \in H_{\sigma,\Gamma}^{0;\,1/2,1/2}$, respectively. Then, with $C = C(\Gamma,\sigma_0)$,

(i) [21, (2.13)], [34, (97)]

$$a_\sigma^W(\varphi,\varphi) \geq C\|\varphi\|^2_{\sigma,0,H^{1/2}(\Gamma)}.$$

(ii)

$$a_\sigma^W(\varphi,\varphi) \geq C\|\varphi\|^2_{\sigma,\Gamma;\,0;\,1/2,1/2}.$$

Corollary 3.51 (Continuity Estimates, Space-Time Bilinear Forms)
a) Let $p, q \in \mathcal{H}_\sigma^1(\mathbb{R}, H^{-1/2}(\Gamma))$ or $p, q \in H_{\sigma,\Gamma}^{1;\,-1/2,-1/2}$, respectively. Then, with $C = C(\Gamma,\sigma_0)$,

(i)

$$|a_\sigma^V(p,q)| \leq C\|p\|_{\sigma,1,H^{-1/2}(\Gamma)}\|q\|_{\sigma,1,H^{-1/2}(\Gamma)}.$$

(ii)

$$|a_\sigma^V(p,q)| \leq C\|p\|_{\sigma,\Gamma;\,1;\,-1/2,-1/2}\ \|q\|_{\sigma,\Gamma;\,1;-1/2,-1/2}.$$

b) Let $\varphi \in \mathcal{H}_\sigma^2(\mathbb{R}, H^{1/2}(\Gamma))$, $\psi \in \mathcal{H}_\sigma^1(\mathbb{R}, H^{1/2}(\Gamma))$ or $\varphi, \psi \in H_{\sigma,\Gamma}^{1;\,1/2,1/2}$, respectively. Then, with $C = C(\Gamma,\sigma_0)$,

(i)

$$|a_\sigma^W(\varphi,\psi)| \leq C\|\varphi\|_{\sigma,2,H^{1/2}(\Gamma)}\|\psi\|_{\sigma,1,H^{1/2}(\Gamma)}.$$

(ii)

$$|a_\sigma^W(\varphi,\psi)| \leq C\|\varphi\|_{\sigma,\Gamma;\,1;\,1/2,1/2}\|\psi\|_{\sigma,\Gamma;\,1;\,1/2,1/2}.$$

3.4 Approximation Properties

In this last section of the present chapter, we investigate approximation properties for the space-time function spaces introduced in Section 3.3.1. Our analysis follows the works of Costabel and Noon [53, 125] for the parabolic case.

The approximation spaces of piecewise polynomials in space and time, V_h^p and $V_{\Delta t}^q$, were defined in Section 2.2. The space-time approximation space in which we seek an approximation to the solution of (P) was denoted by V_N. Let $u \in H^s(\Gamma)$ and q_{h,m_1}^s be the ($H^s(\Gamma)$-) projection operator onto the space of piecewise polynomial functions with mesh width h and polynomial degree m_1, i.e. $q_{h,m_1}^s : H^s(\Gamma) \to V_h^{m_1}$. Note that, since $V_h^{m_1} \subseteq H^\sigma(\Gamma)$ for $\sigma \in [m_1 - 1, m_1]$, the projection operator is stable with respect to the $H^s(\Gamma)$-norm [145, Chapter 10]. The approximation property (3.156) holds for the $L^2(\Gamma)$ projection operator $q_{h,m_1}^0 : L^2(\Gamma) \to V_h^{m_1}$ and other lower order projection orders as well, but stability can only be proven for the $H^s(\Gamma)$-projection operator.

Given these assumptions, there holds the approximation property [133, Theorems 4.3.19 and 4.3.22], [145, Theorem 10.2, Corollary 10.3 and Lemma 10.8]

$$\|u - q_{h,m_1}^s[u]\|_{H^r(\Gamma)} \leq C h^{s-r} |u|_{H^s(\Gamma)} \tag{3.156}$$

with $m_1 - 1 \leq r \leq m_1$ and $r \leq s \leq m_1 + 1$, where the constant $C = C(m_1)$ depends only on the polynomial degree m_1 in the two dimensional case under the assumption of a polygonal boundary Γ.

For some interval $I \subseteq \mathbb{R}_{\geq 0}$, let $u \in H^k(I)$ and $r_{\Delta t,m_2}^k : H^k(I) \to V_{\Delta t}^{m_2}$ be the projection operator (the Taylor polynomial) onto the space of piecewise polynomial functions with mesh width Δt and polynomial degree m_2. Then there holds the approximation property [53, (5.16)], [125, (7.1)]

$$\|u - r_{\Delta t,m_2}^k[u]\|_{H^l(I)} \leq C \Delta t^{k-l} |u|_{H^k(I)} \tag{3.157}$$

with $m_2 - 1 \leq l \leq m_2$ and $l \leq k \leq m_2 + 1$, where the constant $C = C(m_2)$ depends only on the polynomial degree m_2.

We call

$$\Pi_{h,\Delta t;\, s,k}^{m_1,m_2} := r_{\Delta t,m_2}^k \circ q_{h,m_1}^s = q_{h,m_1}^s \circ r_{\Delta t,m_2}^k \tag{3.158}$$

the *projection operator* of polynomial degree m_1 in space and m_2 in time. For $s = k = 0$, we simply write $\Pi_{h,\Delta t}^{m_1,m_2}$ instead of $\Pi_{h,\Delta t;\,0,0}^{m_1,m_2}$.

The spaces $H_\Gamma^{r,s}$ with norm $\|\cdot\|_{\Gamma;\,r,s}$ are given by (3.104) and (3.105). Mind that, contrary to our usual notation, r stands for the space regularity here, while s stands for time regularity. This notation is used for easier reference to the literature. The approximation property for the spaces $H_\Gamma^{r,s}$ is given by [53, Proposition 5.3], [125, Lemmas 7.1-7.3].

Proposition 3.52 (Approximation Property for $H_\Gamma^{r,s}$ [53, Proposition 5.3])
Let $u \in H_\Gamma^{r,s}$ with $0 < r \leq m_1 + 1$ and $0 < s \leq m_2 + 1$. Let $p \leq r$ and $q \leq s$ such that $pq \geq 0$. Then

$$\|u - \Pi_{h,\Delta t}^{m_1,m_2}[u]\|_{\Gamma;\,p,q} \leq C \left(h^\alpha + \Delta t^\beta\right) \|u\|_{\Gamma;\,r,s} \tag{3.159}$$

with $C = C(p,q,r,s,m_1,m_2) > 0$ and $\alpha = \min\left\{r - p, r - \frac{r}{s}q\right\}$, $\beta = \min\left\{s - q, s - \frac{s}{r}p\right\}$.

Note that $\alpha = r - p$ if and only if $sp \leq rq$, and $\beta = s - q$ if and only if $sp \geq rq$.

Remark 3.53 (On Proposition 3.52)
Note that the interpolation result

$$\left[L^2(\mathbb{R}, H^r(\Gamma)), H^s(\mathbb{R}, L^2(\Gamma))\right]_\theta = H^{\theta s}(\mathbb{R}, H^{(1-\theta)r}(\Gamma)) \tag{3.160}$$

for $\theta \in [0,1]$ [105, Chapter 4, Proposition 2.1] is needed for the proof of Proposition 3.52. Inspecting the proof, we find that (3.160) *can be extended to*

$$\left[H^k(\mathbb{R}, H^s(\Gamma)), H^{s+k}(\mathbb{R}, L^2(\Gamma))\right]_\theta = H^{k+\theta s}(\mathbb{R}, H^{(1-\theta)s}(\Gamma)) \tag{3.161}$$

if we replace $\mathcal{H} = L^2(\mathbb{R}, L^2(\Gamma))$ by $\mathcal{H} = H^k(\mathbb{R}, L^2(\Gamma))$ (notation of the original proof in [105]). The rest of the proof remains unchanged.

By (3.156) and (3.157), respectively, we obtain semi-discrete approximation properties in the space-time norms. We use the same notation as in [53, (5.20), (5.21)] here for easier reference. For $u \in H^\mu(I, H^\rho(\Gamma))$, taking $r = \kappa$, $s = \rho$ in (3.156),

$$\|u - q^\kappa_{h,m_1}[u]\|_{H^\mu(I,H^\kappa(\Gamma))} \le C(m_1) h^{\rho-\kappa} \|u\|_{H^\mu(I,H^\rho(\Gamma))} \tag{3.162}$$

and for $u \in H^\sigma(I, H^\mu(\Gamma))$, taking $l = \lambda$, $k = \sigma$ in (3.157),

$$\|u - r^\lambda_{\Delta t,m_2}[u]\|_{H^\lambda(I,H^\mu(\Gamma))} \le C(m_2) h^{\sigma-\lambda} \|u\|_{H^\sigma(I,H^\mu(\Gamma))} \tag{3.163}$$

where $H^\mu(I, H^\kappa(\Gamma))$ is the obvious modification of the space $H^\mu(\mathbb{R}, H^\kappa(\Gamma))$.

The next result is similar to Proposition 3.52, but deals with the spaces $H_\Gamma^{k;s,s}$ given by (3.107) and (3.108). It may look 'too favourable' in terms of convergence orders when compared to Proposition 3.52 at first glance, but one needs to keep in mind that the elements of $H_\Gamma^{k;s,s}$ are of higher temporal regularity, which follows immediately from the definition (3.107). For $k = l = 0$, (3.164) corresponds to $p = q$ and $r = s$ in (3.159).

Proposition 3.54 (Approximation Property for $H_\Gamma^{k;s,s}$)
Let $u \in H_\Gamma^{k;s,s}$ with $0 < s \le m_1 + 1$ and $0 < k \le m_2 + 1$. Let $r \le s$ and $l \le k$ such that $lr \ge 0$. Then, if $l, r \le 0$,

$$\|u - \Pi^{m_1,m_2}_{h,\Delta t}[u]\|_{\Gamma;l;r,r} \le C\left(h^\alpha + \Delta t^\beta\right) \|u\|_{\Gamma;k;s,s} \tag{3.164}$$

with $C = C(l, r, k, s, m_1, m_2) > 0$ and $\alpha = \min\left\{s - r, s - \frac{s(l+r)}{s+k}\right\}$, $\beta = \min\left\{s + k - (l + r), s + k - \frac{s+k}{s} r\right\}$.

For $l, r > 0$, we need to replace $\Pi^{m_1,m_2}_{h,\Delta t}$ in (3.164) by $\Pi^{m_1,m_2}_{h,\Delta t;0,l}$ to guarantee the continuity estimate (3.168) *in the proof. Further, $\beta = s + k - (l + r)$ in this case.*

The symmetric case is, as in Proposition 3.52, $rk = sl$.

Proof
Recall the definition (3.107) of $H_\Gamma^{k;s,s}$,

$$H_\Gamma^{k;s,s} = H^k(\mathbb{R}, H^s(\Gamma)) \cap H^{s+k}(\mathbb{R}, L^2(\Gamma)).$$

Using (3.162) with $\mu = k$, $\kappa = 0$, $\rho = s$, we find that

$$\|u - q_{h,m_1}[u]\|_{L^2(I,L^2(\Gamma))} \le C(m_1) h^s \|u\|_{H^k(\mathbb{R},H^s(\Gamma))}$$

and by (3.163) with $\mu = \lambda = 0$, $\sigma = s + k$,

$$\|u - r_{\Delta t,m_2}[u]\|_{L^2(I,L^2(\Gamma))} \le C(m_2) \Delta t^{s+k} \|u\|_{H^{s+k}(I,L^2(\Gamma))}.$$

Hence

$$\|u - \Pi^{m_1,m_2}_{h,\Delta t}[u]\|_{\Gamma;0;0,0} \le C(m_1, m_2)\left(h^s + \Delta t^{s+k}\right) \|u\|_{\Gamma;k;s,s}$$

which proves the result for the case $l = r = 0$.

For $l, r < 0$, we obtain, in place of [53, (5.24)],

$$\|u - \Pi_{h,\Delta t}^{m_1,m_2}[u]\|_{\Gamma;\, l;\, r,r} \le C(m_1,m_2)\left(h^{-r} + \Delta t^{-(l+r)}\right)\left(h^s + \Delta t^{s+k}\right)\|u\|_{\Gamma;\, k;\, s,s}.$$

Using Young's inequality with $p = \frac{r-s}{r}$ and $p' = \frac{s-r}{s}$, we obtain

$$h^{-r}\Delta t^{s+k} \le C(r,s)\left(h^{s-r} + \Delta t^{s-r+k(1-\frac{r}{s})}\right)$$

and with $p = 1 - \frac{l+r}{s+k}$ and $p' = 1 - \frac{s+k}{l+r}$, we obtain

$$h^s \Delta t^{-(l+r)} \le C(l,r,k,s)\left(h^{s-s\frac{l+r}{s+k}} + \Delta t^{s+k-(l+r)}\right).$$

Hence, with $C = C(m_1,m_2,l,r,k,s)$,

$$\|u - \Pi_{h,\Delta t}^{m_1,m_2}[u]\|_{\Gamma;\, l;\, r,r} \le C\left(h^{s-r} + h^{s-s\frac{l+r}{s+k}} + \Delta t^{s+k-(l+r)} + \Delta t^{s-r+k(1-\frac{r}{s})}\right)\|u\|_{\Gamma;\, k;\, s,s}$$

which proves the claim for $l, r < 0$.

Now let $l, r > 0$. There holds

$$\|u - \Pi_{h,\Delta t}^{m_1,m_2}[u]\|_{H^{l+r}(I,L^2(\Gamma))} \le \|u - q_{h,m_1}[u]\|_{H^{l+r}(I,L^2(\Gamma))} + C\|u - r_{\Delta t,m_2}[u]\|_{H^{l+r}(I,L^2(\Gamma))}.$$

By (3.161), $u \in H^{k+s\theta}(\mathbb{R}, H^{(1-\theta)s}(\Gamma))$ for any $\theta \in [0,1]$. Let $\theta = \frac{l+r}{s+k}$. Using (3.162) with $\mu = l + r$, $\rho = s - s\theta$ and $\kappa = 0$, we estimate the second term by

$$\begin{aligned}\|u - q_{h,m_1}[u]\|_{H^{l+r}(I,L^2(\Gamma))} &\le Ch^{s-s\theta}\|u\|_{H^{l+r}(I,H^{(1-\theta)s}(\Gamma))} \le Ch^{s-s\theta}\|u\|_{H^{\theta s+k}(I,H^{(1-\theta)s}(\Gamma))} \\ &\le Ch^{s-s\frac{l+r}{s+k}}\|u\|_{\Gamma;\, k;\, s,s} \qquad (3.165)\end{aligned}$$

where the second inequality holds as $l + r \le k + s\frac{l+r}{s+k}$ (note that $0 \le k\left(1 - \frac{l+r}{s+k}\right)$ to see this). The last inequality follows from Lemma 3.15 and holds for arbitrary $\theta \in [0,1]$. For the first term, we obtain, by (3.162) with $\mu = 0$, $\lambda = l + r$ and $\sigma = s + k$,

$$\|u - r_{\Delta t,m_2}[u]\|_{H^{l+r}(I,L^2(\Gamma))} \le C\Delta t^{s+k-(l+r)}\|u\|_{H^{s+k}(I,L^2(\Gamma))}. \qquad (3.166)$$

On the other hand,

$$\|u - \Pi_{h,\Delta t;\, 0,l}^{m_1,m_2}[u]\|_{H^l(\mathbb{R},H^r(\Gamma))} \le \|u - r_{\Delta t,m_2}^l[u]\|_{H^l(\mathbb{R},H^r(\Gamma))} + \|r_{\Delta t,m_2}^l\left[u - q_{h,m_1}[u]\right]\|_{H^l(\mathbb{R},H^r(\Gamma))}$$

by the triangle inequality. Let $\theta = 1 - \frac{r}{s}$, which implies $(1-\theta)s = r$. Using (3.163) with $\lambda = l$, $\mu = r$ and $\sigma = k + \theta s = k + s - r$, we estimate the first term by

$$\|u - r_{\Delta t,m_2}^l[u]\|_{H^l(I,H^r(\Gamma))} \le C\Delta t^{s+k-r-l}\|u\|_{H^{\theta s+k}(I,H^{(1-\theta)s}(\Gamma))} \le C\Delta t^{s+k-(l+r)}\|u\|_{\Gamma;\, k;\, s,s} \qquad (3.167)$$

where the last inequality is again due to Lemma 3.15. Only for the second term we actually need to take the higher order projection operator in time which is continuous with respect to the $H^l(\mathbb{R})$ norm. By (3.162) with $\mu = l$, $\kappa = r$ and $\rho = s$,

$$\begin{aligned}\|r_{\Delta t,m_2}^l\left[u - q_{h,m_1}[u]\right]\|_{H^l(\mathbb{R},H^r(\Gamma))} &\le C\|u - q_h^{m_1}[u]\|_{H^l(\mathbb{R},H^r(\Gamma))} \le Ch^{s-r}\|u\|_{H^l(\mathbb{R},H^s(\Gamma))} \\ &\le Ch^{s-r}\|u\|_{H^k(\mathbb{R},H^s(\Gamma))}. \qquad (3.168)\end{aligned}$$

Putting estimates (3.165), (3.166), (3.167) and (3.168) together implies

$$\begin{aligned}\|u - \Pi_{h,\Delta t;\, 0,l}^{m_1,m_2}[u]\|_{\Gamma;\, l;\, r,r} &= \|u - \Pi_{h,\Delta t;\, 0,l}^{m_1,m_2}[u]\|_{H^{l+r}(\mathbb{R},L^2(\Gamma))} + \|u - \Pi_{h,\Delta t;\, 0,l}^{m_1,m_2}[u]\|_{H^l(\mathbb{R},H^r(\Gamma))} \\ &\le C\left(h^{s-r} + h^{s-s\frac{l+r}{s+k}} + \Delta t^{s+k-(l+r)}\right)\|u\|_{\Gamma;\, k;\, s,s}\end{aligned}$$

which proves the result that was claimed for $l, r > 0$. ∎

The following result, that translates (3.157) to the setup of the σ-dependent norms, was shown in [20, Sections 5.1 and 5.2]. Let $u \in \mathcal{H}^k_\sigma(\mathbb{R},\mathbb{R})$. Then there holds the approximation property

$$\|u - r_{\Delta t,m_2}[u]\|_{\sigma,l,\mathbb{R}} \leq C(m_2)\Delta t^{k-l}|u|_{\sigma,k,\mathbb{R}} \tag{3.169}$$

with $m_2 - 1 \leq l \leq m_2$ and $l \leq k \leq m_2 + 1$.

Remark 3.55 (On Equation 3.169)
$l = 0$ in (3.169) is [20, (5.6)], $l = \frac{1}{2}$ is [20, (5.7)], $l = -\frac{1}{2}$ is [20, (5.8)]. Note that only [20, (5.6)] is actually proven in [20]. But it is easy to show the bound for $l \in \mathbb{Z}$ by proceeding similarly, and the non-integer case follows immediately by interpolation.

Combining the approximation properties (3.156) and (3.169), we obtain, for $r = l = 0$,

$$\begin{aligned}
& \|u - r_{\Delta t,m_2}\left[q_{h,m_1}[u]\right]\|_{\sigma,0,L^2(\Gamma)} \\
\leq\ & \|u - q_{h,m_1}[u]\|_{\sigma,0,L^2(\Gamma)} + \|q_{h,m_1}[u] - r_{\Delta t,m_2}\left[q_{h,m_1}[u]\right]\|_{\sigma,0,L^2(\Gamma)} \\
\leq\ & C(m_1)h^s\|u\|_{\sigma,0,H^s(\Gamma)} + C(m_2)\Delta t^k\|q_{h,m_1}[u]\|_{\sigma,k,L^2(\Gamma)} \\
\leq\ & C(m_1,m_2)\left(h^s + \Delta t^k\right)\|u\|_{\sigma,k,H^s(\Gamma)}
\end{aligned} \tag{3.170}$$

where the last inequality is due to the fact that the projection operator q_{h,m_1} is stable with respect to $L^2(\Gamma)$. This estimate is entirely similar to [53, (5.22)], [125, (7.7)].

Analogously to Proposition 3.52, we obtain Proposition 3.56 from (3.170).

Proposition 3.56 (Approximation Property for $\mathcal{H}^k_\sigma(\mathbb{R}, H^s(\Gamma))$)
Let $u \in \mathcal{H}^k_\sigma(\mathbb{R}, H^s(\Gamma))$ with $0 < s \leq m_1 + 1$ and $0 < k \leq m_2 + 1$. Let $r \leq s$ and $l \leq k$ such that $lr \geq 0$. Then, if $l, r \leq 0$,

$$\|u - \Pi^{m_1,m_2}_{h,\Delta t}[u]\|_{\sigma,l,H^r(\Gamma)} \leq C\left(h^{s-r} + \Delta t^{k-l}\right)\|u\|_{\sigma,k,H^s(\Gamma)} \tag{3.171}$$

with $C = C(m_1,m_2) > 0$. For $l, r \geq 0$, we need to replace $\Pi^{m_1,m_2}_{h,\Delta t}$ in (3.171) by $\Pi^{m_1,m_2}_{h,\Delta t;0,l}$ or $\Pi^{m_1,m_2}_{h,\Delta t;r,0}$ to guarantee the continuity estimate (3.172) in the proof in this case.

Proof
Let $l, r \leq 0$ first. Then

$$\begin{aligned}
\|u - \Pi^{m_1,m_2}_{h,\Delta t}[u]\|_{\sigma,l,H^r(\Gamma)} &\leq \|u - q_{h,m_1}[u]\|_{\sigma,l,H^r(\Gamma)} + \|q_{h,m_1}[u] - q_{h,m_1}\left[r_{\Delta t,m_2}[u]\right]\|_{\sigma,l,H^r(\Gamma)} \\
&\leq C(m_1)h^{s-r}\|u\|_{\sigma,l,H^s(\Gamma)} + C(m_2)\Delta t^{k-l}\|q_{h,m_1}[u]\|_{\sigma,k,H^r(\Gamma)} \\
&\leq C(m_1)h^{s-r}\|u\|_{\sigma,l,H^s(\Gamma)} + C(m_2)\Delta t^{k-l}\|q_{h,m_1}[u]\|_{\sigma,k,L^2(\Gamma)} \\
&\leq C(m_1)h^{s-r}\|u\|_{\sigma,l,H^s(\Gamma)} + \tilde{C}(m_2)\Delta t^{k-l}\|u\|_{\sigma,k,L^2(\Gamma)} \\
&\leq C(m_1,m_2)\left(h^{s-r} + \Delta t^{k-l}\right)\|u\|_{\sigma,k,H^s(\Gamma)}
\end{aligned} \tag{3.172}$$

where the third inequality is due to [92, Theorem 4.2.2], and the fourth inequality holds due to the $L^2(\Gamma)$-stability of the projection operator q_{h,m_1}.

Now let $l, r > 0$. If $\Pi^{m_1,m_2}_{h,\Delta t}$ is replaced by $\Pi^{m_1,m_2}_{h,\Delta t;r,0}$ we obtain, instead of (3.172), the estimate

$$C_1h^{s-r}\|u\|_{\sigma,l,H^s(\Gamma)} + C_2\Delta t^{k-l}\|q^r_{h,m_1}[u]\|_{\sigma,k,H^r(\Gamma)} \leq C_1h^{s-r}\|u\|_{\sigma,l,H^s(\Gamma)} + C_2\Delta t^{k-l}\|u\|_{\sigma,k,H^r(\Gamma)}.$$

The rest remains unchanged. ∎

It remains to consider the approximation properties for the energy space-time Sobolev spaces $H^{k;s,s}_{\sigma,\Gamma}$. From (3.111), we know that $\|u\|_{\sigma,\Gamma;k;s,s} \sim \|e^{-\sigma t}u\|_{\Gamma;k;s,s}$, where the equivalence constants depend only on s and σ_0 (Lemma 3.43). Thus, for $k = 0$,

$$\|u\|^2_{\sigma,\Gamma;0;s,s} \sim \|e^{-\sigma t}u\|^2_{\Gamma;s,s} = \|e^{-\sigma t}u\|^2_{L^2(\mathbb{R},H^s(\Gamma))} + \|e^{-\sigma t}u\|^2_{H^s(\mathbb{R},L^2(\Gamma))}. \tag{3.173}$$

Recalling $\|u\|_{\sigma,k,H^s(\Gamma)} = \|e^{-\sigma t}\frac{\partial^k u}{\partial t^k}\|_{L^2(\mathbb{R}_{\geq 0},H^s(\Gamma))}$ and (3.169), this means that the weight factor $e^{-\sigma t}$ in the $H^{s,s}_\Gamma$-norm in (3.173) does not affect the approximation properties of $H^{s,s}_\Gamma$ (Proposition 3.52). Similarly, $H^{k;s,s}_{\sigma,\Gamma}$ inherits the approximation properties of $H^{k;s,s}_\Gamma$ (Proposition 3.54). For reference, we summarise this in Proposition 3.57.

Proposition 3.57 (Approximation Property for $H^{k;s,s}_{\sigma,\Gamma}$)
Let $u \in H^{k;s,s}_{\sigma,\Gamma}$. Then there holds, with s,k,r,l,α,β as in Proposition 3.54,

$$\|u - \Pi^{m_1,m_2}_{h,\Delta t}[u]\|_{\sigma,\Gamma;l;r,r} \leq C\left(h^\alpha + \Delta t^\beta\right)\|u\|_{\sigma,\Gamma;k;s,s} \tag{3.174}$$

with $C = C(l,r,k,s,m_1,m_2) > 0$. Again, for $l,r > 0$, we need to replace $\Pi^{m_1,m_2}_{h,\Delta t}$ in (3.174) by $\Pi^{m_1,m_2}_{h,\Delta t;0,l}$

3.4.1 Inverse Estimates

It is well known that, for globally uniform meshes, $s \in [0,1]$ and $q_h \in V^1_h$, there holds [55, Theorem 4.1], [133, Theorem 4.4.3 and Remark 4.4.4]

$$\|q_h\|_{H^s(\Gamma)} \leq Ch^{-s}\|q_h\|_{L^2(\Gamma)} \tag{3.175}$$

with $C = C\left(K(\mathcal{T}_S)\right)$, and, for $s \in [-1,0]$ and $q_h \in V^p_h$, $p \geq 0$, there holds [55, Theorem 4.6], [133, Theorem 4.4.3 and Remark 4.4.4]

$$\|q_h\|_{L^2(\Gamma)} \leq Ch^s\|q_h\|_{H^s(\Gamma)} \tag{3.176}$$

with $C = C\left(p,K(\mathcal{T}_S)\right)$. The estimates (3.175) and (3.176) are known as *inverse inequalities*. Bamberger and Ha-Duong show that the weight function $e^{-\sigma t}$ in the classical norms does not affect these inequalities, and that in fact, for $\beta_{\Delta t} \in V^q_{\Delta t}$, $q \geq 0$, and $s \leq 0$, there holds, analogously to (3.176) [20, Lemme 2 and the accompanying Corollaire]

$$\left\|e^{-\sigma t}\beta_{\Delta t}\right\|_{L^2(\mathbb{R})} \leq C\Delta t^s\left\|e^{-\sigma t}\beta_{\Delta t}\right\|_{H^s(\mathbb{R})} \tag{3.177}$$

with $C = C\left(\sigma,q,K(\mathcal{T}_T)\right)$. Indeed, estimates (3.176) and (3.177) can be combined so that there holds

$$\left\|p_{h,\Delta t}\right\|_{\sigma,0,L^2(\Gamma)} \leq C\Delta t^k h^s\left\|p_{h,\Delta t}\right\|_{\sigma,k,H^s(\Gamma)} \tag{3.178}$$

for $p_{h,\Delta t} \in V^p_h \otimes V^q_{\Delta t}$ and $C = C\left(\sigma,p,q,K(\mathcal{T}_S),K(\mathcal{T}_T)\right)$, since

$$\begin{aligned}
\left\|p_{h,\Delta t}\right\|^2_{\sigma,0,L^2(\Gamma)} &= \int_{\mathbb{R}_{\geq 0}} e^{-2\sigma t}\left\|p_{h,\Delta t}(\cdot,t)\right\|^2_{L^2(\Gamma)}\,dt = \int_{\mathbb{R}_{\geq 0}}\int_\Gamma\left(e^{-\sigma t}p_{h,\Delta t}(x,t)\right)^2\,dx\,dt \\
&= \left\|\left\|e^{-\sigma t}p_{h,\Delta t}(x,t)\right\|_{L^2(\mathbb{R}_{\geq 0})}\right\|^2_{L^2(\Gamma)} \\
&\leq C\Delta t^{2k}\left\|\left\|\Lambda^k\left(e^{-\sigma t}p_{h,\Delta t}(x,t)\right)\right\|_{L^2(\mathbb{R}_{\geq 0})}\right\|^2_{L^2(\Gamma)} \\
&= C\Delta t^{2k}\left\|\left\|\Lambda^k\left(e^{-\sigma t}p_{h,\Delta t}(x,t)\right)\right\|_{L^2(\Gamma)}\right\|^2_{L^2(\mathbb{R}_{\geq 0})} \\
&\leq Ch^{2s}\Delta t^{2k}\left\|\left\|\Lambda^k\left(e^{-\sigma t}p_{h,\Delta t}(x,t)\right)\right\|_{H^s(\Gamma)}\right\|^2_{L^2(\mathbb{R}_{\geq 0})} \\
&= Ch^{2s}\Delta t^{2k}\left\|p_{h,\Delta t}\right\|^2_{\sigma,k,H^s(\Gamma)}.
\end{aligned} \tag{3.179}$$

Regarding the spaces $H_\Gamma^{r,s}$, there hold inverse inequalities of the type

$$\left\|p_{h,\Delta t}\right\|_{\Gamma;\,0,0} \leq C \max\left\{h^r, \Delta t^s\right\} \left\|p_{h,\Delta t}\right\|_{\Gamma;\,r,s} \tag{3.180}$$

for $r, s \leq 0$ [125, Lemma 7.4], with $C = C\left(p, q, K(\mathcal{T}_S), K(\mathcal{T}_T)\right)$. Similarly,

$$\left\|p_{h,\Delta t}\right\|_{\Gamma;\,0;\,0,0} \leq C\Delta t^k \max\left\{h^s, \Delta t^s\right\} \left\|p_{h,\Delta t}\right\|_{\Gamma;\,k;\,s,s} \tag{3.181}$$

with $C = C\left(p, q, K(\mathcal{T}_S), K(\mathcal{T}_T)\right)$, and

$$\left\|p_{h,\Delta t}\right\|_{\sigma,\Gamma;\,0;\,0,0} \leq C\Delta t^k \max\left\{h^s, \Delta t^s\right\} \left\|p_{h,\Delta t}\right\|_{\sigma,\Gamma;\,k;\,s,s} \tag{3.182}$$

for $k, s \leq 0$, with $C = C\left(\sigma, p, q, K(\mathcal{T}_S), K(\mathcal{T}_T)\right)$.

Chapter 4

A Priori Error Estimates and some Energy Considerations

In this chapter, we analyse the variational formulation of our problem. In particular, this study involves a priori error estimates and error measures.

In Section 4.1, the weak form of problem (P) and its discrete counterpart are re-introduced in a form that is suitable for studies with the function spaces introduced in Chapter 3. The properties of the underlying bilinear form are investigated, in particular with regard to the solution's energy.

A best approximation property and stability estimates for the continuous and the discrete solution are stated in Section 4.2. Most of these results are well known. On the other hand, a best approximation property for the Galerkin time domain Boundary Element Method has not been stated this explicitly to our knowledge, and not at all for the space-time energy spaces. The approximation properties of Section 3.4 are then used to conclude theoretical convergence rates, and their practical relevance is discussed.

In Section 4.3, an alternative error measure for approximations to (P) is studied. It is similar to a result by Holm et al. [91] for the time harmonic Helmholtz problem. The estimates we obtain provide an error measure for problems with unknown exact solution that has some theoretical justification, unlike other measures currently used in the literature. Further, the error measure's implementation does not yield any implementational overhead, as we report in Section 4.3.2. In Section 4.3.3, we provide some numerical experiments, using this alternative error measure.

4.1 The Variational Indirect Single Layer Problem and the Wave's Energy

Let us consider the transient problem (P) with Dirichlet boundary datum f. We represent the solution u of (P) by an indirect Single Layer ansatz, i.e. $u = S[p]$ with unknown density $p \in \mathcal{H}^2_\sigma(\mathbb{R}, H^{-1/2}(\Gamma))$ respectively $p \in H^{2;\,-1/2,-1/2}_{\sigma,\Gamma}$, or another appropriate function space. As in (3.154), we write

$$a^V_\sigma(p,q) = \int_{\mathbb{R}_{\geq 0}} e^{-2\sigma t} \left\langle V[\dot{p}](\cdot,t), q(\cdot,t) \right\rangle \, dt \tag{4.1}$$

for $p \in \mathcal{H}^2_\sigma(\mathbb{R}, H^{-1/2}(\Gamma))$, $q \in \mathcal{L}^2_\sigma(\mathbb{R}, H^{-1/2}(\Gamma))$ respectively $p \in H^{2;-1/2,-1/2}_{\sigma,\Gamma}$, $q \in L^{0;-1/2,-1/2}_{\sigma,\Gamma}$. The variational form of the problem is to find $p \in \mathcal{H}^2_\sigma(\mathbb{R}, H^{-1/2}(\Gamma))$ such that

$$a^V_\sigma(p,q) = \int_{\mathbb{R}_{\geq 0}} e^{-2\sigma t} \left\langle \dot{f}(\cdot,t), q(\cdot,t) \right\rangle \, dt \tag{4.2}$$

for all $q \in \mathcal{L}^2_\sigma(\mathbb{R}, H^{-1/2}(\Gamma))$, with $f \in \mathcal{H}^1_\sigma(\mathbb{R}, H^{1/2}(\Gamma))$. We further seek to find an approximation $p_N \in V_N \subseteq \mathcal{H}^2_\sigma(\mathbb{R}, H^{-1/2}(\Gamma))$ to p such that

$$a^V_\sigma(p_N, q_N) = \int_{\mathbb{R}_{\geq 0}} e^{-2\sigma t} \left\langle \dot{f}(\cdot,t), q_N(\cdot,t) \right\rangle \, dt \tag{4.3}$$

for all $q_N \in W_N \subseteq \mathcal{L}^2_\sigma(\mathbb{R}, H^{-1/2}(\Gamma))$. For practical purposes, in particular for direct integral equations, it can be useful to replace the right hand side function f in (4.3) by a approximation $f_N \in V_N$; see [145, p. 270] and Appendix A.5. One then seeks to find the solution $\tilde{p}_N \in V_N$ of the *perturbed problem*

$$a^V_\sigma(\tilde{p}_N, q_N) = \int_{\mathbb{R}_{\geq 0}} e^{-2\sigma t} \left\langle \dot{f}_N(\cdot,t), q_N(\cdot,t) \right\rangle \, dt \tag{4.4}$$

for all $q_N \in W_N$.

We obtain the variational form (2.13), for which we study the computation of the matrix entries in Chapter 2, with $\sigma = 0$, which violates the assumption $\sigma > 0$ established in Section 3.2.1. This ambiguity is addressed in Section 4.3.

By (4.2) and (4.3), we obtain the *Galerkin orthogonality*

$$a^V_\sigma(p - p_N, q_N) = 0 \tag{4.5}$$

for all $q_N \in W_N$ and, in particular,

$$a^V_\sigma(p, p_N) = a^V_\sigma(p_N, p_N). \tag{4.6}$$

In practice, $V_N = W_N$ is always chosen.

Let us collect some further properties of the bilinear form $a^V_\sigma(\cdot,\cdot)$. Integrating by parts, we find

$$\begin{aligned} a^V_\sigma(p,q) &= \left[e^{-2\sigma t} \langle V[p](\cdot,t), q(\cdot,t) \rangle \right]_{t=0}^{t\to\infty} - \int_{\mathbb{R}_{\geq 0}} \left\langle V[p](\cdot,t), \frac{\partial}{\partial t} \left(e^{-2\sigma t} q(\cdot,t) \right) \right\rangle \, dt \\ &= 0 - \int_{\mathbb{R}_{\geq 0}} (-2\sigma) e^{-2\sigma t} \langle V[p](\cdot,t), q(\cdot,t) \rangle + e^{-2\sigma t} \langle V[p](\cdot,t), \dot{q}(\cdot,t) \rangle \, dt \\ &= -a^V_\sigma(q,p) + 2\sigma \int_{\mathbb{R}_{\geq 0}} e^{-2\sigma t} \langle V[p](\cdot,t), q(\cdot,t) \rangle \, dt \end{aligned} \tag{4.7}$$

where, in the last step, we have used that the Single Layer operator is symmetric with respect to the space variables x, y, i.e.

$$\langle V[\dot{p}](\cdot,t), q(\cdot,t) \rangle = \langle V[q](\cdot,t), \dot{p}(\cdot,t) \rangle . \tag{4.8}$$

In particular, (4.7) means that the bilinear form $a^V_\sigma(\cdot,\cdot)$ is *non-symmetric*. An immediate consequence of (4.7) is

$$a^V_\sigma(p,p) = \sigma \int_{\mathbb{R}_{\geq 0}} e^{-2\sigma t} \langle V[p](\cdot,t), p(\cdot,t) \rangle \, dt. \tag{4.9}$$

Let us recall the definition of the energy (3.11),

$$E_\Omega[u](t) = \frac{1}{2} \int_\Omega |\nabla u(x,t)|^2 + \dot{u}(x,t)^2 \, dx$$

where, using the notation of (P), $\Omega = \mathbb{R}^n \setminus \Omega^-$ with $\Omega^- \subseteq \mathbb{R}^n$ being a bounded domain. As u solves the homogeneous wave equation (1.1a), we obtain, using Green's formula,

$$0 = \int_\Omega (\ddot{u} - \Delta u)\dot{u}\, dx = \int_\Omega \ddot{u}\dot{u} + \nabla u \cdot \nabla \dot{u}\, dx - \int_\Gamma \frac{\partial u}{\partial n}\dot{u}\, ds_x. \tag{4.10}$$

Since

$$\dot{E}_\Omega[u](t) = \frac{1}{2}\int_\Omega 2\nabla u(x,t)\cdot\nabla\dot{u}(x,t) + 2\dot{u}(x,t)\ddot{u}(x,t)\, dx$$

and with the representation $u = S[p]$ in $\Omega \times \mathbb{R}_{\geq 0}$, we obtain the identity [54, p. 12], [81, (53)]

$$\dot{E}_\Omega[u](t) = \langle V[\dot{p}](\cdot,t), p(\cdot,t)\rangle \tag{4.11}$$

from (4.10). Further, using integration by parts,

$$\int_{\mathbb{R}_{\geq 0}} e^{-2\sigma t} E_\Omega[u](t)\, dt = -\frac{1}{2\sigma}\left[e^{-2\sigma t}E_\Omega[u](t)\right]_{t=0}^{t\to\infty} + \frac{1}{2\sigma}\int_{\mathbb{R}_{\geq 0}} e^{-2\sigma t}\dot{E}_\Omega[u](t)\, dt$$

and therefore [81, p. 20], using (4.10),

$$a_\sigma^V(p,p) = 2\sigma \int_{\mathbb{R}_{\geq 0}} e^{-2\sigma t} E_\Omega[u](t)\, dt. \tag{4.12}$$

We note that, by (3.101), $\int_{\mathbb{R}_{\geq 0}} e^{-2\sigma t}E_\Omega[u](t)\, dt$ is an equivalent norm in the space $H^{0;\,1,1}_{\sigma,\Omega}$, with

$$a_\sigma^V(p,p) = \frac{\sigma}{2\pi}\|u\|^2_{\sigma,\Gamma;\,0;\,1,1} \tag{4.13}$$

for $u = S[p]$. We denote this *energy norm* by $|||\cdot|||$, i.e.

$$|||p|||^2 := a_\sigma^V(p,p). \tag{4.14}$$

We stress that, differently to, for instance, the energy norm induced by the Single Layer operator for the Laplace equation, which is known to be equivalent to the $H^{-1/2}(\Gamma)$-norm, it is unclear whether the energy norm $|||\cdot|||$ is equivalent to any norm on $\Gamma \times \mathbb{R}_{\geq 0}$. In fact, we only know that, by Corollaries 3.50 a) (ii) and 3.51 a) (ii),

$$C_1\|p\|^2_{\sigma,\Gamma;\,0;\,-1/2,-1/2} \;\leq\; a_\sigma^V(p,p) = |||p|||^2 \;\leq\; C_2\|p\|^2_{\sigma,\Gamma;\,1;\,-1/2,-1/2} \tag{4.15}$$

and, by Corollaries 3.50 a) (i) and 3.51 a) (i),

$$C_3\|p\|^2_{\sigma,-1/2,H^{-1/2}(\Gamma)} \;\leq\; a_\sigma^V(p,p) = |||p|||^2 \;\leq\; C_4\|p\|^2_{\sigma,1,H^{-1/2}(\Gamma)} \tag{4.16}$$

with $C_i = C_i(\Gamma,\sigma_0)$ for $i = 1,\dots,4$.

Remark 4.1
a) If we use the representation $u = D[\varphi]$ in $\Omega \times \mathbb{R}_{\geq 0}$, we obtain [6, (2.14)]

$$\dot{E}_\Omega[u](t) = \langle W[\varphi](\cdot,t), \dot{\varphi}(\cdot,t)\rangle\,. \tag{4.17}$$

in place of (4.11).

b) It does not matter whether we take the time derivative in the ansatz function or in the test function in the variational formulation (4.2) *from the perspective of the mathematical analysis. However, by* (4.7)*, there holds*

$$\begin{aligned} a_\sigma^V(p,q) &= \int_{\mathbb{R}_{\geq 0}} e^{-2\sigma t} \langle V[\dot{p}](\cdot,t), q(\cdot,t)\rangle \, dt \\ &= -\int_{\mathbb{R}_{\geq 0}} e^{-2\sigma t} \langle V[p](\cdot,t), \dot{q}(\cdot,t)\rangle \, dt + 2\sigma \int_{\mathbb{R}_{\geq 0}} e^{-2\sigma t} \langle V[p](\cdot,t), q(\cdot,t)\rangle \, dt \\ &\neq \int_{\mathbb{R}_{\geq 0}} e^{-2\sigma t} \langle V[p](\cdot,t), \dot{q}(\cdot,t)\rangle \, dt. \end{aligned} \tag{4.18}$$

On the other hand, if p solves the variational problem (4.2)*,*

$$\begin{aligned} &\int_{\mathbb{R}_{\geq 0}} e^{-2\sigma t} \langle V[p](\cdot,t), \dot{q}(\cdot,t)\rangle \, dt \\ = &\int_{\mathbb{R}_{\geq 0}} e^{-2\sigma t} \langle f(\cdot,t), \dot{q}(\cdot,t)\rangle \, dt + 2\sigma \int_{\mathbb{R}_{\geq 0}} e^{-2\sigma t} \langle (V[p]-f)(\cdot,t), q(\cdot,t)\rangle \, dt \end{aligned}$$

where the extra term vanishes since the solution p of the weak problem (4.2) *also solves the operator equation. We therefore conclude that, while the bilinear forms are not equal to each other, solving one variational problem provides us with a solution for the other, and vice versa.*

In practical computations, as outlined in Chapter 2, the parameter σ is set to zero, and in this case there is no extra term as in (4.18)*, i.e.*

$$\int_0^T \langle V[\dot{p}](\cdot,t), q(\cdot,t)\rangle \, dt = -\int_0^T \langle V[p](\cdot,t), \dot{q}(\cdot,t)\rangle \, dt \tag{4.19}$$

since we assume p and q to vanish at T.

4.2 Best Approximation Property, Stability and A Priori Error Estimates

In this section, we study the best approximation property of the Galerkin method (4.3) and its stability. First we consider a general statement given by Costabel [54] *without proof* and discuss it.

Theorem 4.2 (Costabel [54, p. 10f.])
Let X be some Hilbert space with norm $\|\cdot\|_1$ and let $a(\cdot,\cdot)$ be a bilinear form on $X \times X$. Further let $X_0 \supseteq X$ with norm $\|\cdot\|_0$ such that X is continuously embedded into X_0. Assume that the bilinear form $a(\cdot,\cdot)$ is bounded on X, i.e. there exists a number $M > 0$ such that

$$|a(u,v)| \leq M|u|_1|v|_1$$

for all $u, v \in X$, and that $a(\cdot,\cdot)$ is elliptic on X_0, i.e. there exists a number $\alpha > 0$ such that

$$\alpha\|u\|_0^2 \leq |a(u,u)|$$

for all $u \in X$. Finally, let $X_N \subseteq X$ be a finite dimensional approximation space.

Then, for the variational problem Find $u \in X$ such that, for some $f \in X'$,

$$a(u,v) = \langle f, v\rangle$$

for all $v \in X$ *and for its discrete counterpart* Find $u \in X_N$ such that

$$a(u_N, v_N) = \langle f, v_N \rangle$$

for all $v_N \in X_N$*, there holds the* stability estimate 'with a loss'

$$\|u_N\|_0 \leq C\|u\|_1. \tag{4.20}$$

and the best approximation estimate 'with a loss'

$$\|u - u_N\|_0 \leq C \inf_{w_N \in X_N} \|u - w_N\|_1. \tag{4.21}$$

We suspect that Theorem 4.2 is not meant as an actual result, but rather as some sort of work schedule for results which one *would like* to show. Without additional information (a bound on $\frac{\|\cdot\|_0}{\|\cdot\|_1}$, which does not exist), however, it seems to be impossible to prove the result above in its generality. On the other hand, Costabel seems to use this result when he states [54, Theorem 2.4], where he obtains the best approximation estimate

$$\|p - p_N\|_{\sigma,\Gamma;\,0;-1/2,-1/2} \leq C \inf_{q_N \in W_N} \|p - q_N\|_{\sigma,\Gamma;\,1;-1/2,-1/2}. \tag{4.22}$$

for the solution of (4.2) respectively (4.3). By gut feeling, one should think that one would lose at least two orders of regularity in time, due to the mapping properties of the Single Layer operator and since we need to use a time derivative in either the ansatz or the test function for positive definiteness. Such a result can actually be proven:

Lemma 4.3 (Best Approximation Property for the Single Layer Problem)
Let $p \in H^{2;-1/2,-1/2}_{\sigma,\Gamma}$ *respectively* $p \in \mathcal{H}^{5/2}_{\sigma}(\mathbb{R}, H^{-1/2}(\Gamma))$*. Then the best approximation estimates*

$$\|p - p_N\|_{\sigma,\Gamma;\,0;-1/2,-1/2} \leq C \inf_{q_N \in W_N} \|p - q_N\|_{\sigma,\Gamma;\,2;-1/2,-1/2} \tag{4.23}$$

and

$$\|p - p_N\|_{\sigma,-1/2,H^{-1/2}(\Gamma)} \leq C \inf_{q_N \in W_N} \|p - q_N\|_{\sigma,5/2,H^{-1/2}(\Gamma)} \tag{4.24}$$

hold for the indirect Single Layer problem (4.2) *and its approximation* (4.3)*. The positive constants* $C = C(\Gamma, \sigma)$ *are independent of the approximation spaces* W_N*.*

There further hold the best approximation estimates

$$\|p - \tilde{p}_N\|_{\sigma,\Gamma;\,0;-1/2,-1/2} \leq C \inf_{q_N \in W_N} \|p - q_N\|_{\sigma,\Gamma;\,2;-1/2,-1/2} \quad + \quad \|f - f_N\|_{\sigma,\Gamma;\,1;\,1/2,1/2} \tag{4.25}$$

and

$$\|p - p_N\|_{\sigma,-1/2,H^{-1/2}(\Gamma)} \leq C \inf_{q_N \in W_N} \|p - q_N\|_{\sigma,5/2,H^{-1/2}(\Gamma)} \quad + \quad \|f - f_N\|_{\sigma,3/2,H^{1/2}(\Gamma)} \tag{4.26}$$

for the indirect Single Layer problem (4.2) *and the perturbed approximation* (4.4)*, with the same constant* $C = C(\Gamma, \sigma)$*.*

Proof
By Corollary 3.50 a) (ii), by the Galerkin orthogonality (4.5), by (4.7) and by the triangle inequality, there holds

$$\begin{aligned} & C_1\|p-p_N\|^2_{\sigma,\Gamma;\,0;-1/2,-1/2} \\ \leq\ & a^V_\sigma(p-p_N,p-p_N) = \left|a^V_\sigma(p-p_N,p-p_N)\right| = \left|a^V_\sigma(p-p_N,p-q_N)\right| \\ =\ & \left|-a^V_\sigma(p-q_N,p-p_N) + 2\sigma\int_{\mathbb{R}_{\geq 0}} e^{-2\sigma t}\,\langle V[p-p_N](\cdot,t),p-q_N(\cdot,t)\rangle\ dt\right| \\ \leq\ & \left|a^V_\sigma(p-q_N,p-p_N)\right| + 2\sigma\left|\int_{\mathbb{R}_{\geq 0}} e^{-2\sigma t}\,\langle V[p-p_N](\cdot,t),p-q_N(\cdot,t)\rangle\ dt\right| \end{aligned} \tag{4.27}$$

for every $q_N \in W_N$, with $C_1 = C_1(\Gamma,\sigma_0)$. For the second term in (4.27), we use the symmetry of V with respect to the space variables (4.8) and obtain, using Lemma 3.44 and the mapping property (3.140),

$$\begin{aligned} & \left|\int_{\mathbb{R}_{\geq 0}} e^{-2\sigma t}\,\langle V[p-p_N](\cdot,t),p-q_N(\cdot,t)\rangle\ dt\right| = \left|\int_{\mathbb{R}_{\geq 0}} e^{-2\sigma t}\,\langle V[p-q_N](\cdot,t),p-p_N(\cdot,t)\rangle\ dt\right| \\ \leq\ & \|V[p-q_N]\|_{\sigma,\Gamma;\,0;\,1/2,1/2}\ \|p-p_N\|_{\sigma,\Gamma;\,0;-1/2,-1/2} \\ \leq\ & C_2\|p-q_N\|_{\sigma,\Gamma;\,1;-1/2,-1/2}\ \|p-p_N\|_{\sigma,\Gamma;\,0;-1/2,-1/2} \end{aligned} \tag{4.28}$$

and, similarly, for the first term in (4.27),

$$\begin{aligned} & \left|a^V_\sigma(p-q_N,p-p_N)\right| = \left|\int_{\mathbb{R}_{\geq 0}} e^{-2\sigma t}\,\langle V[\dot p-\dot q_N](\cdot,t),p-p_N(\cdot,t)\rangle\ dt\right| \\ \leq\ & \|V[\dot p-\dot q_N]\|_{\sigma,\Gamma;\,0;\,1/2,1/2}\ \|p-p_N\|_{\sigma,\Gamma;\,0;-1/2,-1/2} \\ \leq\ & C_3\|\dot p-\dot q_N\|_{\sigma,\Gamma;\,1;-1/2,-1/2}\ \|p-p_N\|_{\sigma,\Gamma;\,0;-1/2,-1/2} \end{aligned} \tag{4.29}$$

with $C_i = C_i(\Gamma,\sigma_0)$ for $i = 2,3$. Combining estimates (4.27), (4.28) and (4.29) we obtain, with $C_4 = C_4(\Gamma,\sigma) := \max\{2\sigma C_2, C_3\}$,

$$\begin{aligned} & C_1\|p-p_N\|^2_{\sigma,\Gamma;\,0;-1/2,-1/2} \\ \leq\ & C_4\|p-p_N\|_{\sigma,\Gamma;\,0;-1/2,-1/2}\ \left(\|p-q_N\|_{\sigma,\Gamma;\,1;-1/2,-1/2} + \|\dot p-\dot q_N\|_{\sigma,\Gamma;\,1;-1/2,-1/2}\right) \\ \leq\ & C_4\|p-p_N\|_{\sigma,\Gamma;\,0;-1/2,-1/2}\ \|p-q_N\|_{\sigma,\Gamma;\,2;-1/2,-1/2} \end{aligned}$$

which gives (4.23).

(4.24) is shown absolutely similarly, the only difference being that we start from

$$C_1\|p-p_N\|^2_{\sigma,-1/2,H^{-1/2}(\Gamma)} \leq a^V_\sigma(p-p_N,p-p_N)$$

in this case, which holds due to Corollary 3.50 a) (i).

To show (4.25), we observe that, by (4.3) and (4.4),

$$a^V_\sigma(p_N-\tilde p_N,q_N) = \int_{\mathbb{R}_{\geq 0}} e^{-2\sigma t}\left\langle\left(\dot f-\dot f_N\right)(\cdot,t),q_N(\cdot,t)\right\rangle\ dt \tag{4.30}$$

for any $q_N \in W_N = V_N$, and thus, by Corollary 3.50 a) (ii), by choosing $q_N = p_N - \tilde p_N$ in (4.30) and by the Cauchy-Schwarz inequality,

$$C_1\|p_N-\tilde p_N\|^2_{\sigma,\Gamma;\,0;-1/2,-1/2} \leq \left|a^V_\sigma(p_N-\tilde p_N,p_N-\tilde p_N)\right| \leq \|p_N-\tilde p_N\|_{\sigma,\Gamma;\,0;-1/2,-1/2}\|\dot f-\dot f_N\|_{\sigma,\Gamma;\,0;\,1/2,1/2}.$$

Therefore,

$$C_1\|p_N-\tilde p_N\|_{\sigma,\Gamma;\,0;-1/2,-1/2} \leq \|f-f_N\|_{\sigma,\Gamma;\,1;\,1/2,1/2}. \tag{4.31}$$

(4.25) then follows from the triangle inequality in combination with (4.23) and (4.31), and (4.26) is shown in the same way. ∎

Remark 4.4 (Best Approx. Property for the Single Layer P. in the Energy Norm)
Due to the Galerkin orthogonality (4.5)*, there holds*

$$|||p - p_N|||^2 = a_\sigma^V(p - p_N, p - p_N) = a_\sigma^V(p - p_N, p - q_N)$$

similarly to (4.27)*. Using* (4.15) *in the form* $\|p - p_N\|_{\sigma,\Gamma;\,0;\,-1/2,-1/2} \le C\,|||p - p_N|||$*, with* $C = C(\Gamma, \sigma_0)$*, we obtain, by* (4.28) *and* (4.29)*,*

$$|||p - p_N||| \le \tilde{C} \inf_{q_N \in W_N} \|p - q_N\|_{\sigma,\Gamma;\,2;\,-1/2,-1/2} \tag{4.32}$$

with $\tilde{C} = \tilde{C}(\Gamma, \sigma)$*. This inequality also implies* (4.23) *and* (4.24) *via* (4.15) *and* (4.16)*, respectively.*

Similar variants of (4.24) *and of the statements of Corollary 4.5 and Remark 4.6 that involve the energy norm follow analogously. Regarding Lemma 4.7, we refer to Remark 4.8 below.*

Regarding stability, the loss is indeed of the same order.

Corollary 4.5 (Stability of the Discrete Solution for the Single Layer Problem)
Under the assumptions of Lemma 4.3 and with $C = C(\Gamma, \sigma_0) > 0$*, the stability estimates*

$$\|p_N\|_{\sigma,\Gamma;\,0;-1/2,-1/2} \le C\|p\|_{\sigma,\Gamma;\,2;-1/2,-1/2} \tag{4.33}$$

and

$$\|p_N\|_{\sigma,-1/2,H^{-1/2}(\Gamma)} \le C\|p\|_{\sigma,5/2,H^{-1/2}(\Gamma)} \tag{4.34}$$

hold.

For the perturbed problem, the stability estimates

$$\|\tilde{p}_N\|_{\sigma,\Gamma;\,0;-1/2,-1/2} \le C\left(\|p\|_{\sigma,\Gamma;\,2;-1/2,-1/2} + \|f - f_N\|_{\sigma,\Gamma;\,1;\,1/2,1/2}\right) \tag{4.35}$$

and

$$\|\tilde{p}_N\|_{\sigma,-1/2,H^{-1/2}(\Gamma)} \le C\left(\|p\|_{\sigma,5/2,H^{-1/2}(\Gamma)} + \|f - f_N\|_{\sigma,3/2,H^{1/2}(\Gamma)}\right) \tag{4.36}$$

hold.

Proof
The proof is similar to the one of Lemma 4.3: Using the identity (4.6),

$$\begin{aligned} C_1\|p_N\|^2_{\sigma,\Gamma;\,0;\,-1/2,-1/2} \le a_\sigma^V(p_N, p_N) = |a_\sigma^V(p, p_N)| &\le \|V[\dot{p}]\|_{\sigma,\Gamma;\,0;\,1/2,1/2}\ \|p_N\|_{\sigma,\Gamma;\,0;-1/2,-1/2} \\ &\le C_2\|\dot{p}\|_{\sigma,\Gamma;\,1;\,1/2,1/2}\ \|p_N\|_{\sigma,\Gamma;\,0;-1/2,-1/2} \end{aligned}$$

with $C_i = C_i(\Gamma, \sigma_0)$ for $i = 1, 2$, which gives (4.33), and again the proof of (4.34) is analogous.

To show (4.35) and (4.36), one has to use the identity (4.30). ∎

Remark 4.6 (Stability of the Continuous and Discrete solutions)
Obviously, combining the variational formulations (4.2) *and* (4.3) *with Corollary 3.50 a), we obtain, for suitable functions f, bounds on the continuous solutions [81, (41) and Theorem 3(2)]*

$$\|p\|_{\sigma,\Gamma;\,0;-1/2,-1/2} \le C\|f\|_{\sigma,\Gamma;\,1;\,1/2,1/2} \qquad \|p\|_{\sigma,-1/2,H^{-1/2}(\Gamma)} \le C\|f\|_{\sigma,3/2,H^{1/2}(\Gamma)} \tag{4.37}$$

and on the discrete solutions

$$\|p_N\|_{\sigma,\Gamma;\,0;-1/2,-1/2} \le C\|f\|_{\sigma,\Gamma;\,1;\,1/2,1/2} \qquad \|p_N\|_{\sigma,-1/2,H^{-1/2}(\Gamma)} \le C\|f\|_{\sigma,3/2,H^{1/2}(\Gamma)} \tag{4.38}$$

as well, with $C = C(\Gamma, \sigma_0)$.

The estimates in (4.38) *look more favourable than estimates* (4.33) *and* (4.34) *in terms of assumed temporal regularity, but one should note that, here, we estimate the norm of* p_N *by the norm of the right hand side* f*, whereas Corollary 4.5 relates the norms of* p *and* p_N *to each other.*

We have included Corollary 4.5 here in particular to relate to Costabel's statement (Theorem 4.2). Note that (4.37) *is also an immediate consequence of Lemma 3.27 and Remark 3.28 d).*

Bamberger and Ha-Duong [20] prove an a priori error estimate as well. In the proof of [20, Théorème 5], they obtain another kind of best approximation property, which is in fact (4.40) below. We repeat the proof here in brief.

Lemma 4.7 (Best Approx. Property for the Single Layer P. as in [20, Théorème 5]) *Let* $p \in H^{1;0,0}_{\sigma,\Gamma}$ *respectively* $p \in \mathcal{H}^{3/2}_{\sigma}(\mathbb{R}, L^2(\Gamma))$*. Then the best approximation estimates*

$$\|p - p_N\|_{\sigma,\Gamma;\,0;-1/2,-1/2} \leq C \max\left\{1, \frac{1}{\sqrt{h}}, \frac{1}{\sqrt{\Delta t}}\right\} \inf_{q_N \in W_N} \|p - q_N\|_{\sigma,\Gamma;\,1;\,0,0} \tag{4.39}$$

and

$$\|p - p_N\|_{\sigma,-1/2,H^{-1/2}(\Gamma)} \leq C \max\left\{1, \frac{1}{\sqrt{h}}\right\} \inf_{q_N \in W_N} \|p - q_N\|_{\sigma,3/2,L^2(\Gamma)} \tag{4.40}$$

with $C = C\,(\Gamma, \sigma, p, q, K(\mathcal{T}_S), K(\mathcal{T}_T))$ *hold for the indirect Single Layer problem* (4.2) *and its approximation* (4.3)*.*

There further hold the best approximation estimates

$$\|p - \tilde{p}_N\|_{\sigma,\Gamma;\,0;-1/2,-1/2} \leq C \max\left\{1, \frac{1}{\sqrt{h}}, \frac{1}{\sqrt{\Delta t}}\right\} \inf_{q_N \in W_N} \|p - q_N\|_{\sigma,\Gamma;\,1;\,0,0} \;+\; \|f - f_N\|_{\sigma,\Gamma;\,1;\,1/2,1/2} \tag{4.41}$$

and

$$\|p - p_N\|_{\sigma,-1/2,H^{-1/2}(\Gamma)} \leq C \max\left\{1, \frac{1}{\sqrt{h}}\right\} \inf_{q_N \in W_N} \|p - q_N\|_{\sigma,3/2,L^2(\Gamma)} \;+\; \|f - f_N\|_{\sigma,3/2,H^{1/2}(\Gamma)} \tag{4.42}$$

for the indirect Single Layer problem (4.2) *and the perturbed approximation* (4.4)*, with the same constant* C*.*

Note that only the classical spaces are considered in [20].

Proof
By Corollary 3.50 a) (ii) and by the Galerkin orthogonality (4.5),

$$\begin{aligned} C_1 \|p_N - q_N\|^2_{\sigma,\Gamma;\,0;\,-1/2,-1/2} &\leq a^V_\sigma(p_N - q_N, p_N - q_N) \\ &= a^V_\sigma(p_N - p, p_N - q_N) + a^V_\sigma(p - q_N, p_N - q_N) \\ &= a^V_\sigma(p - q_N, p_N - q_N) \end{aligned} \tag{4.43}$$

for any $q_N \in W_N$, with $C_1 = C_1(\Gamma, \sigma_0)$. Using Lemma 3.44 for the first inequality, and $p_N - q_N \in W_N$, the fact that V does not lose regularity as an operator mapping from $L^2_{\sigma,\Gamma}$ to $L^2_{\sigma,\Gamma}$ (see (3.37)) and the inverse inequality (3.182) for the second inequality, we obtain

$$\begin{aligned} \left|a^V_\sigma(p - q_N, p_N - q_N)\right| &\leq \|V[\dot{p} - \dot{q}_N]\|_{\sigma,\Gamma;\,0;\,0,0}\; \|p_N - q_N\|_{\sigma,\Gamma;\,0;\,0,0} \\ &\leq C_2 \max\left\{\frac{1}{\sqrt{h}}, \frac{1}{\sqrt{\Delta t}}\right\} \|\dot{p} - \dot{q}_N\|_{\sigma,\Gamma;\,0;\,0,0}\; \|p_N - q_N\|_{\sigma,\Gamma;\,0;-1/2,-1/2} \end{aligned} \tag{4.44}$$

with $C_2 = C_2(\Gamma, \sigma, p, q, K(\mathcal{T}_S), K(\mathcal{T}_T))$, and hence

$$\|p_N - q_N\|_{\sigma,\Gamma;\,0;-1/2,-1/2} \le C \max\left\{\frac{1}{\sqrt{h}}, \frac{1}{\sqrt{\Delta t}}\right\} \|p - q_N\|_{\sigma,\Gamma;\,1;\,0,0} \tag{4.45}$$

with $C = C(\Gamma, \sigma, p, q, K(\mathcal{T}_S), K(\mathcal{T}_T)) := \frac{C_1}{C_2}$. Thus, by the triangle inequality and (4.45),

$$\begin{aligned}
\|p - p_N\|_{\sigma,\Gamma;\,0;-1/2,-1/2} &\le \inf_{q_N \in W_N} \left\{\|p - q_N\|_{\sigma,\Gamma;\,0;-1/2,-1/2} + \|p_N - q_N\|_{\sigma,\Gamma;\,0;-1/2,-1/2}\right\} \\
&\le \inf_{q_N \in W_N} \left\{\|p - q_N\|_{\sigma,\Gamma;\,0;-1/2,-1/2} + C \max\left\{\frac{1}{\sqrt{h}}, \frac{1}{\sqrt{\Delta t}}\right\} \|p - q_N\|_{\sigma,\Gamma;\,1;\,0,0}\right\} \\
&\le C \max\left\{1, \frac{1}{\sqrt{h}}, \frac{1}{\sqrt{\Delta t}}\right\} \inf_{q_N \in W_N} \|p - q_N\|_{\sigma,\Gamma;\,1;\,0,0}
\end{aligned} \tag{4.46}$$

which is (4.39).

To prove (4.40), we need to proceed in a slightly different manner. Due to Corollary 3.50 a) (i), there holds

$$C_1 \|p_N - q_N\|^2_{\sigma,-1/2,H^{-1/2}(\Gamma)} \le a^V_\sigma(p - q_N, p_N - q_N) \tag{4.47}$$

for any $q_N \in W_N$ in place of (4.43), with $C_1 = C_1(\Gamma, \sigma_0)$. Further, using (3.37) as for the proof of (4.39) and the inverse inequality (3.178), we obtain

$$\begin{aligned}
\left|a^V_\sigma(p - q_N, p_N - q_N)\right| &\le \|V[\dot{p} - \dot{q}_N]\|_{\sigma,\,1/2,L^2(\Gamma)} \, \|p_N - q_N\|_{\sigma,-1/2,L^2(\Gamma)} \\
&\le C_2 \frac{1}{\sqrt{h}} \|\dot{p} - \dot{q}_N\|_{\sigma,\,1/2,L^2(\Gamma)} \, \|p_N - q_N\|_{\sigma,-1/2,H^{-1/2}(\Gamma)}
\end{aligned}$$

with $C_2 = C_2(\Gamma, \sigma, p, q, K(\mathcal{T}_S), K(\mathcal{T}_T))$. The result now follows similarly to the one above.

(4.41) and (4.42) are shown in the same way as (4.25) and (4.26) in Lemma 4.3. ∎

Remark 4.8 (Best Approx. Property for the Single Layer P. in the Energy Norm) *By* (4.43) *and* (4.44) *and since* $\|p_N - q_N\|_{\sigma,\Gamma;\,0;\,-1/2,-1/2} \le C_1 \,|\!|\!|p_N - q_N|\!|\!|$ *by* (4.15)*, with* $C_1 = C_1(\Gamma, \sigma_0)$*, there holds*

$$|\!|\!|p_N - q_N|\!|\!| \le C_2 \max\left\{\frac{1}{\sqrt{h}}, \frac{1}{\sqrt{\Delta t}}\right\} \|p - q_N\|_{\sigma,\Gamma;\,1;\,0,0}$$

with $C_2 = C_2(\Gamma, \sigma, p, q, K(\mathcal{T}_S), K(\mathcal{T}_T))$ *for any* $q_N \in W_N$*.* (4.15) *further gives*

$$|\!|\!|p - q_N|\!|\!| \le C_3 \|p - q_N\|_{\sigma,\Gamma;\,1;\,-1/2,-1/2}$$

with $C_3 = C_3(\Gamma, \sigma_0)$*, and hence* $|\!|\!|p - q_N|\!|\!| \le C_3 \|p - q_N\|_{\sigma,\Gamma;\,1;\,0,0}$*. Proceeding as in* (4.46)*, we obtain, by the triangle inequality, an analogue to* (4.39)*,*

$$|\!|\!|p - p_N|\!|\!| \le C \max\left\{1, \frac{1}{\sqrt{h}}, \frac{1}{\sqrt{\Delta t}}\right\} \inf_{q_N \in W_N} \|p - q_N\|_{\sigma,\Gamma;\,1;\,0,0}. \tag{4.48}$$

A similar variant of (4.40) *follows analogously. As in Remark 4.4, the energy error estimates imply* (4.39) *and* (4.40) *via* (4.15) *and* (4.16)*, respectively.*

Comparing the two estimates in Lemmas 4.3 and 4.7, we note that both are of the same quality: The norms on the right hand sides of the estimates in Lemma 4.7 are higher by one temporal order but one spatial order lower than the ones in Lemma 4.3. One may argue that the estimates in Lemma 4.7 are more balanced, as we lose one order in both space and time or one order in space and $\frac{3}{2}$ orders in time, respectively. On the other hand, the estimates in Lemma 4.3 show that the spatial regularity in the best approximation estimate is the same as the one for the time harmonic problem, as one would expect. From a more theoretical point of view we further remark that the proof of Lemma 4.7 employs inverse estimates. As a consequence, the constants in the best approximation estimates depend on the approximation space W_N and the underlying mesh.

However, only the estimates in Lemma 4.7 can be combined with the approximation properties given in Section 3.4 in order to obtain convergence rates, since the approximation properties can only be applied when the spatial and temporal order are either both positive or both negative. Then, by (4.40) and Proposition 3.56 with $l = \frac{3}{2}$ and $r = 0$, we obtain

$$\|p - p_N\|_{\sigma,-1/2,H^{-1/2}(\Gamma)} \leq C \max\left\{1, \frac{1}{\sqrt{h}}\right\}\left(h + \Delta t^{1/2}\right)\|p\|_{\sigma,2,H^1(\Gamma)} \quad \lesssim \quad \mathcal{O}\left(h^{1/2} + h^{-1/2}\Delta t^{1/2}\right)$$

at most for $m_1 = 0$, $m_2 = 1$, and

$$\|p - p_N\|_{\sigma,-1/2,H^{-1/2}(\Gamma)} \leq C \max\left\{1, \frac{1}{\sqrt{h}}\right\}\left(h^2 + \Delta t^{3/2}\right)\|p\|_{\sigma,3,H^2(\Gamma)} \quad \lesssim \quad \mathcal{O}\left(h^{3/2} + h^{-1/2}\Delta t^{3/2}\right)$$

at most for $m_1 = 1$, $m_2 = 2$, and so on. This means that, by using a $h\Delta t$-version with fixed ratio $\frac{h}{\Delta t}$, we can expect no convergence for $m_1 = 0$, $m_2 = 1$ and convergence of order 1 for $m_1 = 1$, $m_2 = 2$ in theory.

For the energy spaces, on the other hand, by (4.39) and Proposition 3.57 with $l = 1$ and $r = 0$, we obtain

$$\begin{aligned}\|p - p_N\|_{\sigma,\Gamma;\,0;-1/2,-1/2} &\leq C \max\left\{1, \frac{1}{\sqrt{h}}, \frac{1}{\sqrt{\Delta t}}\right\}\left(h^{1/2} + \Delta t\right)\|p\|_{\sigma,\Gamma;\,1;\,1,1} \\ &\lesssim \mathcal{O}\left(\max\left\{h^{-1/2}, \Delta t^{-1/2}\right\}\left(h^{1/2} + \Delta t\right)\right)\end{aligned}$$

at most for $m_1 = 0$, $m_2 = 0$, and

$$\begin{aligned}\|p - p_N\|_{\sigma,\Gamma;\,0;-1/2,-1/2} &\leq C \max\left\{1, \frac{1}{\sqrt{h}}, \frac{1}{\sqrt{\Delta t}}\right\}\left(h^{3/2} + \Delta t^3\right)\|p\|_{\sigma,\Gamma;\,1;\,1,1} \\ &\lesssim \mathcal{O}\left(\max\left\{h^{-1/2}, \Delta t^{-1/2}\right\}\left(h^{3/2} + \Delta t^3\right)\right)\end{aligned}$$

at most for $m_1 = 1$, $m_2 = 1$, and so on. Here, for a $h\Delta t$-version with fixed ratio $\frac{h}{\Delta t}$, we can expect no convergence for $m_1 = 0$, $m_2 = 0$ and convergence of order 1 for $m_1 = 1$, $m_2 = 1$ in theory.

For $m_1 = 0$, $m_2 = 1$, which has also been used for the classical spaces, the estimate is

$$\begin{aligned}\|p - p_N\|_{\sigma,\Gamma;\,0;-1/2,-1/2} &\leq C \max\left\{1, \frac{1}{\sqrt{h}}, \frac{1}{\sqrt{\Delta t}}\right\}\left(h^{2/3} + \Delta t^2\right)\|p\|_{\sigma,\Gamma;\,2;\,1,1} \\ &\lesssim \mathcal{O}\left(\max\left\{h^{-1/2}, \Delta t^{-1/2}\right\}\left(h^{2/3} + \Delta t^2\right)\right)\end{aligned}$$

at most.

Convergence rate estimates for the perturbed problem (4.4) can be derived in the same way. The order of convergence of the additional term of type $\|f - f_N\|$ in these estimates depends on the type of approximation used to obtain f_N.

Lemmas 4.3 and 4.7 both estimate the error in norms that cannot be computed exactly, even when the exact solution is known. The error in the space-time L^2-norm,

$$\|p - p_N\|_{\sigma,0,L^2(\Gamma)} = \|p - p_N\|_{\sigma,\Gamma;\,0;\,0,0} = \|e^{-\sigma t}\,(p - p_N)\,\|_{L^2(\mathbb{R}_{\geq 0},L^2(\Gamma))}$$

however, is easily computable. Theoretical error estimates can be derived by using the inverse inequalities provided in Section 3.4.1, similarly to [145, Lemma 12.2].

Corollary 4.9 (to Lemma 4.7)
Under the assumptions of Lemma 4.7, there hold the error estimates

$$\begin{aligned} C\|p - p_N\|_{\sigma,\Gamma;\,0;0,0} \quad \leq \quad & \|p - \Pi_{h,\Delta t}^{m_1,m_2}[p]\|_{\sigma,\Gamma;\,0;0,0} + \max\left\{\frac{1}{\sqrt{h}}, \frac{1}{\sqrt{\Delta t}}\right\} \|p - \Pi_{h,\Delta t}^{m_1,m_2}[p]\|_{\sigma,\Gamma;\,0;-1/2,-1/2} \\ & + \max\left\{\frac{1}{\sqrt{h}}, \frac{1}{\sqrt{\Delta t}}\right\} \max\left\{1, \frac{1}{\sqrt{h}}, \frac{1}{\sqrt{\Delta t}}\right\} \inf_{q_N \in W_N} \|p - q_N\|_{\sigma,\Gamma;\,1;\,0,0} \end{aligned} \tag{4.49}$$

and

$$\begin{aligned} C\|p - p_N\|_{\sigma,0,L^2(\Gamma)} \quad \leq \quad & \|p - \Pi_{h,\Delta t}^{m_1,m_2}[p]\|_{\sigma,0,L^2(\Gamma)} + \frac{1}{\sqrt{h}}\frac{1}{\sqrt{\Delta t}} \|p - \Pi_{h,\Delta t}^{m_1,m_2}[p]\|_{\sigma,-1/2,H^{-1/2}(\Gamma)} \\ & + \frac{1}{\sqrt{h}}\frac{1}{\sqrt{\Delta t}} \max\left\{1, \frac{1}{\sqrt{h}}\right\} \inf_{q_N \in W_N} \|p - q_N\|_{\sigma,3/2,L^2(\Gamma)} \end{aligned} \tag{4.50}$$

with $C = C\,(\Gamma, \sigma, p, q, K(\mathcal{T}_S), K(\mathcal{T}_T))$.

Proof
By the triangle inequality, the inverse inequality (3.178) and the triangle inequality again,

$$\begin{aligned} \|p - p_N\|_{\sigma,0,L^2(\Gamma)} \quad \leq \quad & \|p - \Pi_{h,\Delta t}^{m_1,m_2}[p]\|_{\sigma,0,L^2(\Gamma)} + \|\Pi_{h,\Delta t}^{m_1,m_2}[p] - p_N\|_{\sigma,0,L^2(\Gamma)} \\ \leq \quad & \|p - \Pi_{h,\Delta t}^{m_1,m_2}[p]\|_{\sigma,0,L^2(\Gamma)} + Ch^{-1/2}\Delta t^{-1/2}\|\Pi_{h,\Delta t}^{m_1,m_2}[p] - p_N\|_{\sigma,-1/2,H^{-1/2}(\Gamma)} \\ \leq \quad & \|p - \Pi_{h,\Delta t}^{m_1,m_2}[p]\|_{\sigma,0,L^2(\Gamma)} + Ch^{-1/2}\Delta t^{-1/2}\|p - \Pi_{h,\Delta t}^{m_1,m_2}[p]\|_{\sigma,-1/2,H^{-1/2}(\Gamma)} \\ & + Ch^{-1/2}\Delta t^{-1/2}\|p - p_N\|_{\sigma,-1/2,H^{-1/2}(\Gamma)} \end{aligned}$$

where $C = C\,(\sigma, p, q, K(\mathcal{T}_S), K(\mathcal{T}_T))$ is the constant from (3.178). (4.50) then follows from Lemma 4.7.

The proof of (4.49) is similar, but here one uses the inverse inequality (3.182) instead of (3.178). ∎

Remark 4.10 (Corollary 4.9 for the Perturbed Problem)
Since, by (3.182) *and* (4.31),

$$\begin{aligned} C\|p_N - \tilde{p}_N\|_{\sigma,\Gamma;\,0;\,0,0} \quad & \leq \quad \max\left\{h^{-1/2}, \Delta t^{-1/2}\right\} \|p_N - \tilde{p}_N\|_{\sigma,\Gamma;\,0;-1/2,-1/2} \\ & \leq \quad \max\left\{h^{-1/2}, \Delta t^{-1/2}\right\} \|f - f_N\|_{\sigma,\Gamma;\,1;\,1/2,1/2} \end{aligned}$$

and, by (3.179) *and similarly,*

$$C\|p_N - \tilde{p}_N\|_{\sigma,0,L^2(\Gamma)} \leq h^{-1/2}\Delta t^{-1/2}\|p_N - \tilde{p}_N\|_{\sigma,-1/2,H^{-1/2}(\Gamma)} \leq h^{-1/2}\Delta t^{-1/2}\|f - f_N\|_{\sigma,3/2,H^{1/2}(\Gamma)}$$

we obtain estimates on the error terms

$$\|p - \tilde{p}_N\|_{\sigma,\Gamma;\,0;\,0,0} \qquad \textit{and} \qquad \|p - \tilde{p}_N\|_{\sigma,0,L^2(\Gamma)}$$

immediately from the estimates in Corollary 4.9 and the triangle inequality.

(4.49) and (4.50) both estimate the error in the same norm. However, the convergence estimates one can derive from (4.49) are slightly more favourable than the ones that can be derived from (4.50):

(4.50) and Proposition 3.56 yield

$$\begin{aligned}\|p - p_N\|_{\sigma,0,L^2(\Gamma)} \;\lesssim\;& \left(h + \Delta t^2\right)\|p\|_{\sigma,2,H^1(\Gamma)} \;+\; h^{-1/2}\Delta t^{-1/2}\left(h^{3/2} + \Delta t^{5/2}\right)\|p\|_{\sigma,2,H^1(\Gamma)} \\ &+ h^{-1/2}\Delta t^{-1/2}\max\left\{1, h^{-1/2}\right\}\left(h + \Delta t^{1/2}\right)\|p\|_{\sigma,2,H^1(\Gamma)} \\ \lesssim\;& \mathcal{O}\left(\Delta t^{-1/2} + h^{-1}\right)\end{aligned}$$

at most for $m_1 = 0$, $m_2 = 1$, and

$$\begin{aligned}\|p - p_N\|_{\sigma,0,L^2(\Gamma)} \;\lesssim\;& \left(h^2 + \Delta t^3\right)\|p\|_{\sigma,3,H^2(\Gamma)} \;+\; h^{-1/2}\Delta t^{-1/2}\left(h^{5/2} + \Delta t^{7/2}\right)\|p\|_{\sigma,3,H^2(\Gamma)} \\ &+ h^{-1/2}\Delta t^{-1/2}\max\left\{1, h^{-1/2}\right\}\left(h^2 + \Delta t^{3/2}\right)\|p\|_{\sigma,3,H^2(\Gamma)} \\ \lesssim\;& \mathcal{O}\left(h\Delta t^{-1/2} + h^{-1}\Delta t\right)\end{aligned}$$

at most for $m_1 = 1$, $m_2 = 2$, and so on. In both cases, convergence of a $h\Delta t$-version cannot be guaranteed in theory.

(4.49) and Proposition 3.57, on the other hand, yield

$$\begin{aligned}\|p - p_N\|_{\sigma,\Gamma;\,0;0,0} \;\lesssim\;& \left(h + \Delta t^2\right)\|p\|_{\sigma,\Gamma;\,1;1,1} \;+\; \max\left\{h^{-1/2}, \Delta t^{-1/2}\right\}\left(h^{5/4} + \Delta t^{5/2}\right)\|p\|_{\sigma,\Gamma;\,1;1,1} \\ &+ \max\left\{h^{-1/2}, \Delta t^{-1/2}\right\}\max\left\{1, h^{-1/2}, \Delta t^{-1/2}\right\}\left(h^{1/2} + \Delta t\right)\|p\|_{\sigma,\Gamma;\,1;1,1} \\ \lesssim\;& \mathcal{O}\left(\max\left\{h^{-1}, \Delta t^{-1}\right\}\left(h^{1/2} + \Delta t\right)\right)\end{aligned}$$

at most for $m_1 = 0$, $m_2 = 0$, and

$$\begin{aligned}\|p - p_N\|_{\sigma,\Gamma;\,0;0,0} \;\lesssim\;& \left(h^2 + \Delta t^4\right)\|p\|_{\sigma,\Gamma;\,2;2,2} \;+\; \max\left\{h^{-1/2}, \Delta t^{-1/2}\right\}\left(h^{9/4} + \Delta t^{9/2}\right)\|p\|_{\sigma,\Gamma;\,2;2,2} \\ &+ \max\left\{h^{-1/2}, \Delta t^{-1/2}\right\}\max\left\{1, h^{-1/2}, \Delta t^{-1/2}\right\}\left(h^{3/2} + \Delta t^{3}\right)\|p\|_{\sigma,\Gamma;\,2;2,2} \\ \lesssim\;& \mathcal{O}\left(\max\left\{h^{-1}, \Delta t^{-1}\right\}\left(h^{3/2} + \Delta t^{3}\right)\right)\end{aligned}$$

at most for $m_1 = 1$, $m_2 = 1$, and so on. In the first case, a $h\Delta t$-version does not guarantee any convergence, while the theoretical rate of convergence in the second case is of order 1/2.

For $m_1 = 0$, $m_2 = 1$, which has also been used for the classical spaces, the estimate is

$$\begin{aligned}\|p - p_N\|_{\sigma,\Gamma;\,0;0,0} \;\lesssim\;& \left(h + \Delta t^3\right)\|p\|_{\sigma,\Gamma;\,2;1,1} \;+\; \max\left\{h^{-1/2}, \Delta t^{-1/2}\right\}\left(h^{7/6} + \Delta t^{7/2}\right)\|p\|_{\sigma,\Gamma;\,2;1,1} \\ &+ \max\left\{h^{-1/2}, \Delta t^{-1/2}\right\}\max\left\{1, h^{-1/2}, \Delta t^{-1/2}\right\}\left(h^{2/3} + \Delta t^{2}\right)\|p\|_{\sigma,\Gamma;\,2;1,1} \\ \lesssim\;& \mathcal{O}\left(\max\left\{h^{-1}, \Delta t^{-1}\right\}\left(h^{2/3} + \Delta t^{2}\right)\right)\end{aligned}$$

at most.

This slight improvement in the theoretical order of convergence is probably what Ha-Duong [81, p. 32] means when stating that some of the approximation properties and interpolation theorems in [20] 'can certainly be improved in the framework of the functional spaces used in this paper [i.e. the Energy spaces]'.

4.3 An Energy Error Estimate

A general problem regarding the validation of numerical schemes to approximate the solutions of scattering problems is that there are not many reference solution available. The only non-trivial exact solution to problem (P) we are aware of are the circular waves discussed in Section 1.3.1. In three space dimensions, for the indirect Single Layer problem $V[p] = g$ on a sphere, (non-physical) reference solutions have recently been derived by Sauter and Veit [135].

The same problem occurs for the exterior Helmholtz problem. For this problem, it has been shown by Holm et al. [91] that the relation

$$|\Re\left(\langle V_\omega[p], p\rangle\right) - \Re\left(\langle V_\omega[p_N], p_N\rangle\right)| \lesssim \|p - p_N\|^2_{H^{-1/2}(\Gamma)} \lesssim |\Re\left(\langle V_\omega[p], p\rangle\right) - \Re\left(\langle V_\omega[p_N], p_N\rangle\right)| \quad (4.51)$$

holds, where the constants hidden in $\lesssim$ are mesh-independent. The term

$$\sqrt{|\Re\left(\langle V_\omega[p], p\rangle\right) - \Re\left(\langle V_\omega[p_N], p_N\rangle\right)|} \quad (4.52)$$

is thus an equivalent measure for the approximation error, where the number $\Re\left(\langle V_\omega[p], p\rangle\right)$ that involves the unknown exact solution ψ, can be approximated by Aitken's extrapolation method. This error measure has been used for numerical validation in [113], for instance. (4.51) implies that the convergence rates that one obtains by computing the error in this way are the same as the ones expected for the error in the $\|\cdot\|_{H^{-1/2}(\Gamma)}$-norm [91, (5.6)].

In the existing literature on time domain Boundary Element Methods, estimates of the type

$$\|p - p_N\|^2_{\sigma,0,L^2(\Gamma)} \approx \|p\|^2_{\sigma,0,L^2(\Gamma)} - \|p_N\|^2_{\sigma,0,L^2(\Gamma)} \quad (4.53)$$

are sometimes used; for example in [28, p. 18] or [69, p. 18]. Alas, there is in fact no Galerkin orthogonality that would justify the use of (4.53) to approximate the error in the space-time L^2-norm. On the other hand, the experiments in the cited literature give very reasonable results.

4.3.1 Estimating the Energy Error

In this section, we explore whether a result similar to (4.51) can be derived for the time dependent case, where the energy norm is given by (4.14). By (4.12) (first identity), (4.5) (second identity), (4.7) (fourth identity), (4.6) (fifth identity) and (4.9) and (4.14) (seventh identity) there holds, similarly to [91, p. 116],

$$\begin{aligned}
\int_{\mathbb{R}_{\geq 0}} e^{-2\sigma t} E_\Omega[u - u_N](t)\, dt &= \frac{1}{2\sigma} \underbrace{a^V_\sigma(p - p_N, p - p_N)}_{= |||p - p_N|||^2} = \frac{1}{2\sigma} a^V_\sigma(p - p_N, p) \\
&= \frac{1}{2\sigma}\left(a^V_\sigma(p,p) - a^V_\sigma(p_N,p)\right) \\
&= \frac{1}{2\sigma}\left(a^V_\sigma(p,p) + a^V_\sigma(p,p_N) - 2\sigma \int_{\mathbb{R}_{\geq 0}} e^{-2\sigma t} \langle V[p](\cdot,t), p_N(\cdot,t)\rangle\, dt\right) \\
&= \frac{1}{2\sigma}\left(a^V_\sigma(p,p) + a^V_\sigma(p_N,p_N) - 2\sigma \int_{\mathbb{R}_{\geq 0}} e^{-2\sigma t} \langle V[p](\cdot,t), p_N(\cdot,t)\rangle\, dt\right) \\
&= \frac{1}{2\sigma}\left(a^V_\sigma(p,p) - a^V_\sigma(p_N,p_N) + 2\left(a^V_\sigma(p_N,p_N) - \sigma \int_{\mathbb{R}_{\geq 0}} e^{-2\sigma t} \langle V[p](\cdot,t), p_N(\cdot,t)\rangle\, dt\right)\right) \\
&= \frac{1}{2\sigma}\left(|||p|||^2 - |||p_N|||^2\right) - \int_{\mathbb{R}_{\geq 0}} e^{-2\sigma t} \langle V[p - p_N](\cdot,t), p_N(\cdot,t)\rangle\, dt.
\end{aligned} \quad (4.54)$$

Using the Cauchy-Schwarz inequality and (3.37), the additional term in (4.54) is

$$\begin{aligned}\left| \int_{\mathbb{R}_{\geq 0}} e^{-2\sigma t} \left\langle V[p - p_N](\cdot, t), p_N(\cdot, t) \right\rangle \, dt \right| &\leq \|V[p - p_N]\|_{\sigma,0,L^2(\Gamma)} \|p_N\|_{\sigma,0,L^2(\Gamma)} \\ &\leq C \|p - p_N\|_{\sigma,0,L^2(\Gamma)} \|p_N\|_{\sigma,0,L^2(\Gamma)} \end{aligned} \tag{4.55}$$

with $C = C(\Gamma)$. As a consequence of estimates (4.54) and (4.55), we obtain

$$|||p - p_N|||^2 \leq \left| |||p|||^2 - |||p_N|||^2 \right| + 2\sigma \, C \|p - p_N\|_{\sigma,0,L^2(\Gamma)} \|p_N\|_{\sigma,0,L^2(\Gamma)}$$

and

$$\left| |||p|||^2 - |||p_N|||^2 \right| \leq |||p - p_N|||^2 + 2\sigma \, C \|p - p_N\|_{\sigma,0,L^2(\Gamma)} \|p_N\|_{\sigma,0,L^2(\Gamma)}.$$

The inverse estimate (3.179) and the stability estimate (4.37) in Remark 4.6 imply that the term $\|p_N\|_{\sigma,\Gamma;0;-1/2,-1/2}$ is bounded with

$$\|p_N\|_{\sigma,0,L^2(\Gamma)} \leq C_1 h^{-1/2} \Delta t^{-1/2} \|p_N\|_{\sigma,-1/2,H^{-1/2}(\Gamma)} \leq C_1 C_2 h^{-1/2} \Delta t^{-1/2} \|f\|_{\sigma,3/2,H^{1/2}(\Gamma)}$$

with $C_1 = C_1(\sigma, p, q, K(\mathcal{T}_S), K(\mathcal{T}_T))$ and $C_2 = C_2(\Gamma, \sigma_0)$. We set $\tilde{C} := C_1 C_2 \|f\|_{\sigma,3/2,H^{1/2}(\Gamma)}$, so that $\tilde{C} = \tilde{C}(\sigma, p, q, K(\mathcal{T}_S), K(\mathcal{T}_T), \Gamma, f)$. Then, similarly to [91, (5.3) and (5.4)],

$$|||p - p_N|||^2 \leq \left| |||p|||^2 - |||p_N|||^2 \right| + C\tilde{C} h^{-1/2} \Delta t^{-1/2} \|p - p_N\|_{\sigma,0,L^2(\Gamma)} \tag{4.56}$$

and

$$\left| |||p|||^2 - |||p_N|||^2 \right| \leq |||p - p_N|||^2 + C\tilde{C} h^{-1/2} \Delta t^{-1/2} \|p - p_N\|_{\sigma,0,L^2(\Gamma)}. \tag{4.57}$$

A bound on the term $\|p - p_N\|_{\sigma,0,L^2(\Gamma)}$ is given by Corollary 4.9, which indicates that it vanishes for approximation spaces consisting of higher-order polynomials.

However, for lower-order approximations, there is no theoretical guarantee that the non-energy norm terms in (4.56) and (4.57) converge to zero for growing N. Even if they converge to zero, their rate of decrease would be expected to be smaller than the one of the other respective bounding terms in (4.56) and (4.57). However, unlike for (4.53), there is at least some justification to use the terms $\left| |||p|||^2 - |||p_N|||^2 \right|$ to estimate the approximation error in the many cases where the exact solution is unknown.

4.3.1.1 What about the Presence of σ?

The problem with the type of analysis we conduct here has been pointed out often, for example in [136, p. 46]: While in theory one assumes $\sigma \geq \sigma_0$ for some $\sigma_0 > 0$ for the temporal weight factor $e^{-2\sigma t}$ present in the norms and bilinear forms (Section 3.2.1), one usually sets $\sigma = 0$ in practical computations, as we did in Chapter 2. In fact, Aimi et al. investigate the bilinear form

$$a_E^V(p, q) := \int_0^T \left\langle V[\dot{p}](\cdot, s), q(\cdot, s) \right\rangle \, ds \tag{4.58}$$

in [5]. By (4.11) and since the energy is by the definition always positive, there holds for $t \geq 0$ [81, (58)]

$$E_\Omega[u](t) = \int_0^t \left\langle V[\dot{p}](\cdot, s), p(\cdot, s) \right\rangle \, ds \;\geq\; 0 \tag{4.59}$$

and thus

$$a_E^V(p, p) = E_\Omega[u](T). \tag{4.60}$$

One could carry out an analysis similar to the one in the previous section and obtain a result similar to (4.54) and (4.66) below, but this would then only give estimates for the energy at the end of the temporal computation interval, i.e. $E_\Omega[u](T)$. This quantity is not a space-time norm, but it is 'the' energy norm induced by the bilinear form $a_E^V(\cdot,\cdot)$.

On the other hand we know that $\int_0^T E_\Omega[u](t)\,dt$ is an equivalent norm in the space $H_\Omega^{0;\,1,1}$. By (4.59), there holds [81, p. 22]

$$\int_0^T E_\Omega[u](t)\,dt = \int_0^T \int_0^t \langle V[\dot p](\cdot,s), p(\cdot,s)\rangle\,ds\,dt = \int_0^T (T-s)\,\langle V[\dot p](\cdot,s), p(\cdot,s)\rangle\,ds \tag{4.61}$$

where the second equality is due to the fact that, for $F(t) \coloneqq \int_0^t f(s)\,ds$ with $f(0) = 0$, there holds $F'(t) = f(t)$, and thus

$$\frac{\partial}{\partial t}\left(\int_0^t (t-s) f(s)\,ds\right) = \frac{\partial}{\partial t}\left(tF(t) - \int_0^t s f(s)\,ds\right) = F(t) + tF'(t) - (tf(t) - 0) = F(t).$$

Consequently, $\int F(t)\,dt = \int_0^t (t-s) f(s)\,ds$, and hence (4.61).

We denote the induced bilinear form by

$$a_T^V(p,q) \coloneqq \int_0^T (T-s)\,\langle V[\dot p](\cdot,s), q(\cdot,s)\rangle\,ds. \tag{4.62}$$

for which, by (4.61), the relation

$$a_T^V(p,p) = \int_0^T E_\Omega[u](t)\,dt \tag{4.63}$$

holds, which corresponds to (4.12).

Remark 4.11 (Comment on the Different Bilinear Forms)
Let us try to relate the bilinear forms $a_T^V(\cdot,\cdot)$ and $a_E^V(\cdot,\cdot)$, given by (4.58) *and* (4.62)*, respectively, to each other. We note that, for $\tilde q(x,s) \coloneqq (T-s)q(x,s)$,*

$$a_T^V(p,q) = a_E^V(p,\tilde q).$$

The bilinear form $a_T^V(\cdot,\cdot)$ is therefore less suitable for implementation: Its kernel does not depend on the difference $t-s$ any longer, due to the additional factor of $T-s$, and the corresponding linear systems can therefore not be reduced to a MOT scheme, as discussed in Section 2.3. The same is true for the bilinear form $a_\sigma^V(\cdot,\cdot)$ when, in accordance with the theoretical reasoning, a temporal weight factor $e^{-2\sigma t}$ with $\sigma > 0$ is used. Atle [10, p. 59] has done computations for this case. He reports that the programme then ran 'much slower than in the case $[\sigma = 0]$', and that 'the method is only useful for $[\sigma = 0]$'.

Despite its practical ineptness, let us investigate the bilinear form $a_T^V(\cdot,\cdot)$ further. In place of (4.7),

$$\begin{aligned} a_T^V(p,q) &= \left[(T-s)\,\langle V[p](\cdot,t), q(\cdot,t)\rangle\right]_{s=0}^{s=T} - \int_0^T \left\langle V[p](\cdot,s), \frac{\partial}{\partial s}\left((T-s)q(\cdot,s)\right)\right\rangle ds \\ &= -\int_0^T \langle V[p](\cdot,s), -q(\cdot,s)\rangle + (T-s)\,\langle V[p](\cdot,s), \dot q(\cdot,s)\rangle\,ds \\ &= -a_T^V(q,p) + \int_0^T \langle V[p](\cdot,s), q(\cdot,s)\rangle\,ds \end{aligned} \tag{4.64}$$

and thus in place of (4.9),

$$2a_T^V(p,p) = \int_0^T \langle V[p](\cdot,s), p(\cdot,s)\rangle \; ds. \tag{4.65}$$

The Galerkin orthogonality equations (4.5) and (4.6) remain valid for the corresponding variational problems when we replace the bilinear form $a_\sigma^V(\cdot,\cdot)$ by $a_T^V(\cdot,\cdot)$. We can therefore proceed in the same way as for (4.54) and obtain

$$\begin{aligned} & \int_0^T E_\Omega[u-u_N](t)\; dt \\ = \;& a_T^V(p,p) - a_T^V(p_N,p_N) - \int_0^T \langle V[p-p_N](\cdot,s), p_N(\cdot,s)\rangle \; ds \\ = \;& \int_0^T E_\Omega[u](s)\; ds - \int_0^T E_\Omega[u_N](s)\; ds - \int_0^T \langle V[p-p_N](\cdot,s), p_N(\cdot,s)\rangle \; ds \end{aligned} \tag{4.66}$$

where the additional term would need further investigation.

Finally, let us consider what happens when the bilinear form $a_E^V(\cdot,\cdot)$ is used. For any $t \geq 0$, let

$$a_E^V(p,q;t) \coloneqq \int_0^t \langle V[\dot{p}](\cdot,s), q(\cdot,s)\rangle \; ds \tag{4.67}$$

with $a_E^V(p,q;T) = a_E^V(p,q)$ as in (4.58) and $a_E^V(p,p;t) = E_\Omega[u](t)$. If we want to solve $a_E^V(p,q;t) = \int_0^t \left\langle \dot{f}(\cdot,s), q(\cdot,s)\right\rangle \; ds$ for any test function q and $t \geq 0$, and the corresponding discrete problem $a_E^V(p_N,q_N;t) = \int_0^t \left\langle \dot{f}(\cdot,s), q_N(\cdot,s)\right\rangle \; ds$ for any discrete test function q_N, we obviously obtain results similar to (4.5) and (4.6). Integration by parts yields, as in (4.7),

$$a_E^V(p,q;t) = -a_E^V(q,p;t) + \langle V[p](\cdot,t), q(\cdot,t)\rangle\,.$$

Using all these relations, there holds

$$\begin{aligned} E_\Omega[u-u_N](t) &= a_E^V(p,p;t) + a_E^V(p_N,p_N;t) - \langle V[p](\cdot,t), p_N(\cdot,t)\rangle \\ &= E_\Omega[u](t) - E_\Omega[u_N](t) - \langle V[p-p_N](\cdot,t), p_N(\cdot,t)\rangle \end{aligned} \tag{4.68}$$

which, in turn, yields (4.54) and (4.66).

4.3.2 Practical Computation of the Scattered Wave's Energy

In Section 4.3.1, we considered the error in the energy norm induced by the bilinear form $a_\sigma^V(\cdot,\cdot)$, which is related to the scattered wave's energy via (4.12) and (4.60). We investigate how the energy norm can be computed in practice.

Assume that the approximation is given by (2.16), i.e. $p_N(x,t) = \sum_{m=1}^{M_T}\sum_{i=1}^{N_S} p_i^m \beta^m(t)\varphi_i(x)$. Using (2.28) (for the second identity) and $\mathcal{U}^l = 0$ for $l < 0$ (for the fifth identity), we obtain

$$\begin{aligned} \int_0^T \langle V[\dot{p}_N](\cdot,t), p_N(\cdot,t)\rangle \; dt &= \sum_{n=1}^{M_T}\sum_{j=1}^{N_S} p_j^n \int_0^T \langle V[\dot{p}_N](\cdot,t), \beta^n(t)\varphi_j\rangle \; dt \\ &= \sum_{n=1}^{M_T}\sum_{j=1}^{N_S} p_j^n \left(\sum_{m=1}^{M_T}\sum_{i=1}^{N_S} \mathcal{U}_{i,j}^{n-m} p_i^m\right) = \sum_{m,n=1}^{M_T}\sum_{i,j=1}^{N_S} p_j^n \mathcal{U}_{i,j}^{n-m} p_i^m \\ &= \sum_{m,n=1}^{M_T} (\vec{p}^{\,m})^T \mathcal{U}^{n-m}\vec{p}^{\,n} = \sum_{n=1}^{M_T}\sum_{m=1}^{n} (\vec{p}^{\,m})^T \mathcal{U}^{n-m}\vec{p}^{\,n} \end{aligned} \tag{4.69}$$

Using (4.59), there consequently holds

$$E_\Omega[u_N](T) = \sum_{n=1}^{M_T} \sum_{m=1}^{n} (\vec{p}^m)^T \mathcal{U}^{n-m} \vec{p}^n \tag{4.70}$$

for $u_N = S[p_N]$. We shall refer to this quantity as the *final energy* of the approximation u_N.

What if we want to compute the energy at other times t? We restrict ourselves to those times which correspond to mesh points of the time mesh, i.e. $t = t_k = k\Delta t$. If we assume that the basis functions are numbered in ascending order, we can truncate the sum in (4.69) at some number smaller than M_T. To compute the energy at time $t = t_k$, all the entries for $n \geq M_T^k$ are zero, where $M_T^k \leq M_T$ denotes the index of the last basis function β^m with support in $[0, t_k]$. Obviously we obtain the quantities

$$E^k := E_\Omega[u](t_k) = \int_0^{t_k} \langle V[\dot{p}_N](\cdot,t), p_N(\cdot,t)\rangle \, dt \tag{4.71}$$

in this way, replacing M_T by M_T^k in (4.69). We can thus approximate the energy $E_\Omega[u](t)$ for every time $t \in [0,T]$ by the piecewise constant function

$$E_N(t) := \sum_{k=1}^{M} \mathbb{1}_{[t_{k-1},t_k)}(t) \, E^k. \tag{4.72}$$

where M is the number of temporal mesh points, i.e. $T = M\Delta t$, as in Section 2.1. We can then approximate the norm that is induced by the bilinear form $a^V_{\sigma=0,T}(\cdot,\cdot)$ via (4.12) by

$$\int_0^T E_\Omega[u_N](t) \, dt \approx \int_0^T E_N(t) \, dt = \sum_{k=1}^{M} E^k \int_0^T \chi_{[t_{k-1},t_k]}(t) \, dt = \Delta t \sum_{k=1}^{M} E^k. \tag{4.73}$$

We shall refer to this quantity as the *integrated energy* of the approximation u_N.

The choice of $\sigma = 0$ is, however, particularly problematical here, since one could not obtain the identity (4.12) from (4.10) and (4.11) in that case, and (4.12) would in fact yield $a^V_{\sigma=0}(p_N, p_N) = 0$. At least for the latter problem, there is some theoretical remedy, since, if u has only support on the finite interval $[0,T]$, there holds, by (4.12),

$$a^V_\sigma(p,p) = 2\sigma \int_0^T e^{-2\sigma t} E_\Omega[u](t) \, dt =: a^V_{\sigma,T}(p,p). \tag{4.74}$$

Hence, using (4.13) for the equality and the fact that $e^{-2\sigma t}$ is decreasing from 1 to $e^{-2\sigma T}$ on $[0,T]$, i.e. $e^{-2\sigma T} \leq e^{-2\sigma t} \leq 1$ for $t \in [0,T]$, for the inequalities, we obtain

$$2\sigma e^{-2\sigma T} \int_0^T E_\Omega[u](t) \, dt \leq a^V_{\sigma,T}(p,p) = \frac{\sigma}{2\pi} \|u\|^2_{\sigma,\Omega;\,0;\,1,1} \leq 2\sigma \int_0^T E_\Omega[u](t) \, dt \tag{4.75}$$

and thus

$$4\pi e^{-2\sigma T} \int_0^T E_\Omega[u](t) \, dt \leq \|u\|^2_{\sigma,\Omega;\,0;\,1,1} = \frac{2\pi}{\sigma} a^V_{\sigma,T}(p,p) \leq 4\pi \int_0^T E_\Omega[u](t) \, dt. \tag{4.76}$$

We note that

$$\lim_{\sigma\to 0} \frac{2\pi}{\sigma} a^V_{\sigma,T}(p,p) = 2\pi \lim_{\sigma\to 0} \int_0^T \frac{e^{-2\sigma t}}{\sigma} \langle V[\dot{p}](\cdot,t), p(\cdot,t)\rangle \, dt = 2\pi \int_0^T \langle V[\dot{p}](\cdot,t), p(\cdot,t)\rangle \, dt$$

where the latter term is the bilinear form used in the implementation.

We further note that the computation of the energy terms (4.70) and (4.73) creates no implementational overhead. We only need the matrices that are computed and stored while running the MOT scheme anyway to compute them.

We remark that both (4.70) and (4.73) are realisations of the energy norm $|||\cdot|||$: By (4.14) and (4.1),

$$|||p_N|||^2 = a^V_{\sigma=0}(p_N, p_N) = \int_0^T \langle V[\dot{p}_N](\cdot,t), p_N(\cdot,t)\rangle \, dt \tag{4.77}$$

which is the left hand side of (4.69) when $\sigma = 0$, but also

$$|||p_N|||^2 = a^V_{\sigma=0}(p_N, p_N) = \int_0^T \langle V[\dot{p}_N](\cdot,t), p_N(\cdot,t)\rangle \, dt \tag{4.78}$$

by (4.12), which is the left hand side of (4.73) when $\sigma = 0$.

While these arguments, based on choosing $\sigma = 0$ in a setup that assumes $\sigma > 0$, obviously stand on shaky ground, the quantity computed in (4.69) is, on the other hand, indeed 'the' energy norm associated with the bilinear form that is used in our implementation (i.e. (4.1) with $\sigma = 0$), which is certainly related to the scattered wave's energy via (4.59). Similarly, (4.73) is an approximation to the integrated scattered wave's energy.

Since other measures to quantify the accuracy of approximations do not present themselves, we have used (4.70) and (4.73) as error measures in some of our experiments. Some first examples are given in Section 4.3.3.

4.3.3 Two Numerical Experiments

4.3.3.1 Circular Wave

Let us consider the Dirichlet problem with circular incident wave and known exact solution that was introduced in Section 1.3.1 and already studied in Section 2.6. As in Section 2.6, we use the direct formulation (1.12) and lowest-order elements in space and time to approximate the solution.

We compute the final energy $E_\Omega[u_N](T)$ via (4.70) and the integrated energy via (4.73) for each approximation. Results are shown in Table 4.1 and Figure 4.1a. Using these experimental quantities and Aitken's extrapolation method, we assume that the the exact values of the final and integrated energy are

$$E_\Omega[u](T) = 19.43150 \quad \text{and} \quad \int_0^T E_\Omega[u](t)\, dt = 39.46782.$$

The energy errors shown in Table 4.1 and Figure 4.1b are then, as indicated in (4.54), computed by

$$\left(|E_\Omega[u](T) - E_\Omega[u_N](T)|\right)^{1/2} \quad \text{and} \quad \left(\left|\int_0^T E_\Omega[u](t)\, dt - \int_0^T E_\Omega[u_N](t)\, dt\right|\right)^{1/2} \tag{4.79}$$

respectively. The corresponding experimental rates of convergence $\alpha_{h,\Delta t}$ are computed by (2.149). We observe that the experimental convergence rate for the final energy error is similar to the one for the approximation error in the space-time L^2-norm. The integrated energy error curve, on the other hand, indicates a convergence rate of smaller order.

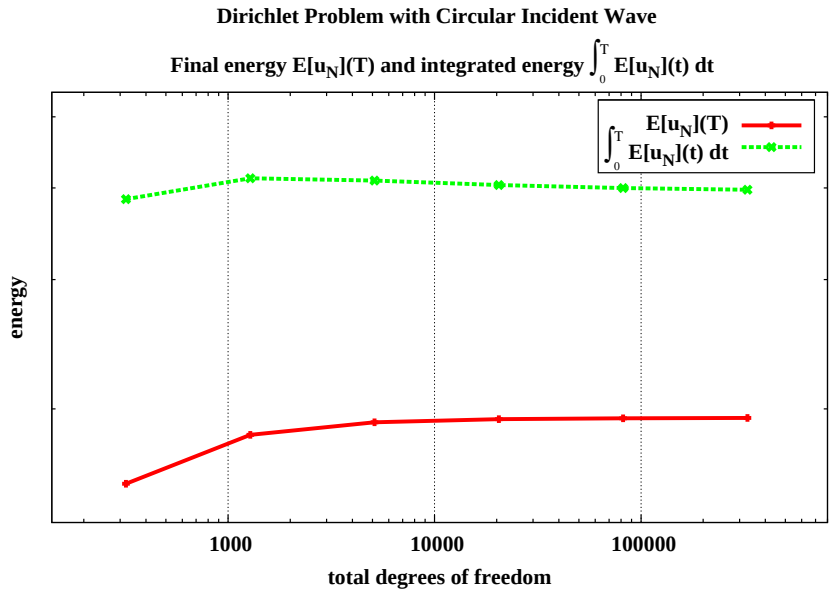

(a) Final energy $E_\Omega[u_N](T)$ and integrated energy $\int_0^T E_\Omega[u_N](t)\,dt$

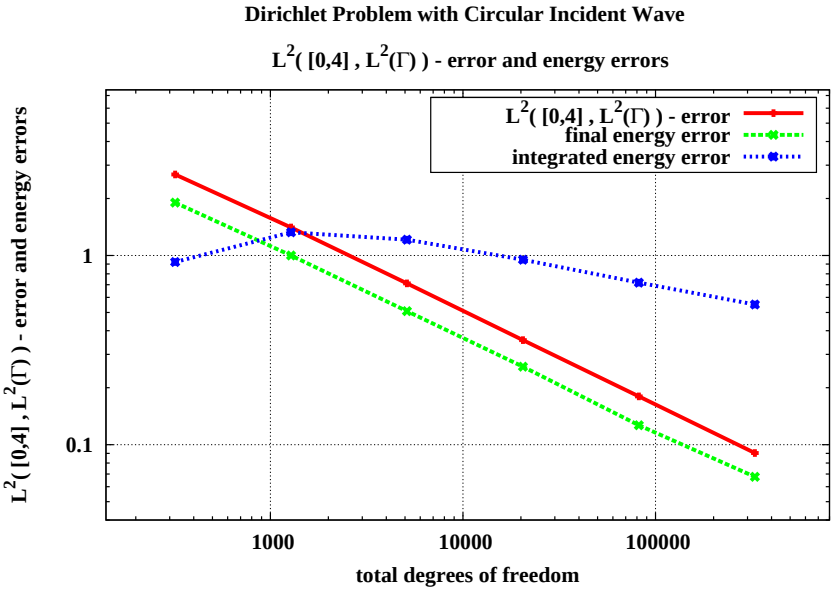

(b) $L^2([0,4], L^2(\Gamma))$-error and final and integrated energy errors

Figure 4.1: Energy and energy error graphs for the problem considered in Section 4.3.3.1

degrees of freedom			final energy (4.70)			integrated energy (4.73)		
TDOF	SDOF	TS	$E_\Omega[u](T)$	energy error	$\alpha_{h,\Delta t}$	$\int_0^T E_\Omega[u](t)\,dt$	energy error	$\alpha_{h,\Delta t}$
320	64	5	15.80865	1.9033791	-	38.61528	0.9233304	-
1280	128	10	18.43334	0.9990806	0.93	41.22481	1.3255154	-0.52
5120	256	20	19.17326	0.5081752	0.98	40.93636	1.2118337	0.13
20480	512	40	19.36469	0.2584802	0.98	40.36877	0.9491844	0.35
81920	1024	80	19.41546	0.1266570	1.03	39.98356	0.7181511	0.40
327680	2048	160	19.43608	0.0676609	0.91	39.77134	0.5509274	0.38
extrapolated value:			19.43150			39.46782		

Table 4.1: Final energy with corresponding energy errors and experimental convergence rates, and integrated energy with corresponding energy errors and experimental convergence rates for the problem considered in Section 4.3.3.1. TDOF and SDOF denote the total and spatial degrees of freedom, respectively, while TS stands for the number of time steps.

4.3.3.2 Plane Incident Wave

We now consider an incident wave for which the exact scattered wave is not known. We choose the plane wave from Example 1.8 a) as the incident wave, and consider two different scatterers, a square scatterer $\Omega = [-1,1]^2$ and a circular scatterer $\Omega = \mathbb{B}_{\sqrt{2}}(0)$. Our choice of the parameter m_F in Example 1.8 a) guarantees that the wave's initial front, at $t = 0$, is the line $x_1 + x_2 = -2$, which intersects both scatterers in one single point, $(x_1, x_2) = (-1,-1)$. Our choice of the parameter k implies that the incident wave hits both scatterers there first, and subsequently progresses in direction $(1,1)$. We split each scatterer's boundary as $\Gamma = \partial\Omega = \Gamma_{\text{lit}} \cup \Gamma_{\text{shadowed}}$ with $\Gamma_{\text{lit}} = \Gamma \cap \left\{ x \in \mathbb{R}^2 \;\middle|\; x_1 + x_2 \leq 0 \right\}$ and $\Gamma_{\text{shadowed}} = \Gamma \setminus \Gamma_0$. The incident plane wave is 'active' on Γ_{lit} for $0 \leq t \leq 2\sqrt{2}$, with $t = 2\sqrt{2} \approx 2.83$ being the time when the wave's tail is the line $x_1 + x_2 = 0$.

We use an indirect approach and represent the solution by a Single Layer potential ansatz $u = S[p]$ with unknown density p. The approximation is done by lowest-order elements in space and time, as in Section 4.3.3.1. We reiterate that the exact density cannot be computed analytically here, and that we, therefore, cannot carry out an error analysis by simply comparing the approximate solution to the exact solution in some norm, as it was possible for the circular wave considered in Sections 2.6 and 4.3.3.1. This implies that we have to rely on alternative error measures.

As in Section 4.3.3.1, we compute the final energy $E_\Omega[u_N](T)$ via (4.70) and the integrated energy via (4.73) for each approximation. We extrapolate the experimental quantities and deduce, by extrapolation, that the the exact values of the final and integrated energy are

$$E_\Omega[u](T) = 157.1270 \quad \text{and} \quad \int_0^T E_\Omega[u](t)\,dt = 269.1102$$

for the square scatterer $\Omega = [-1,1]^2$, and

$$E_\Omega[u](T) = 162.2099 \quad \text{and} \quad \int_0^T E_\Omega[u](t)\,dt = 305.4083$$

for the circular scatterer $\Omega = \mathbb{B}_{\sqrt{2}}(0)$. The energy errors are then again computed by (4.79).

Tables 4.2 and 4.3 and Figure 4.3 show that, for both scatterers, the convergence rates are similar for each of the two error measures. This is somewhat surprising since, due to the corners in the square scatterer, the solution for the circular scatterer could be expected to be more regular.

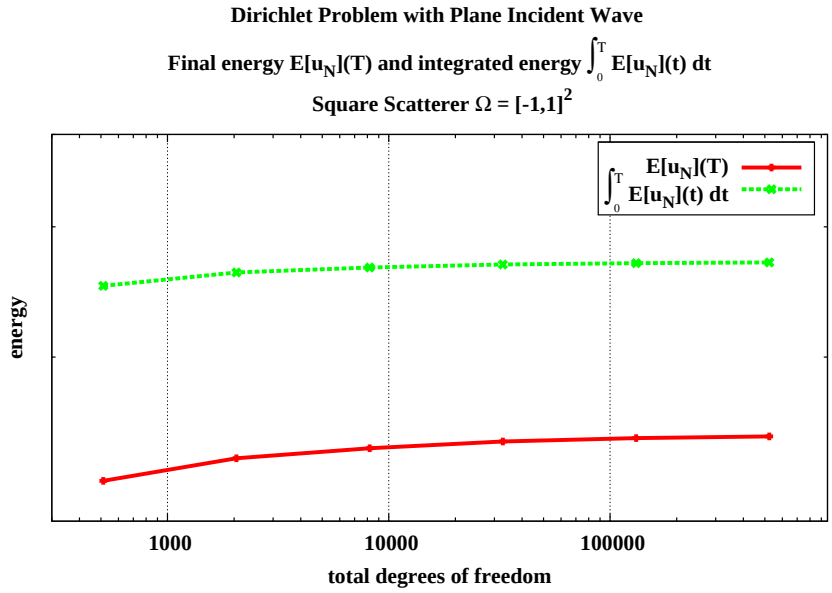

(a) Final energy $E_\Omega[u_N](T)$ and integrated energy $\int_0^T E_\Omega[u_N](t)\ dt$, for square scatterer $\Omega = [-1,1]^2$

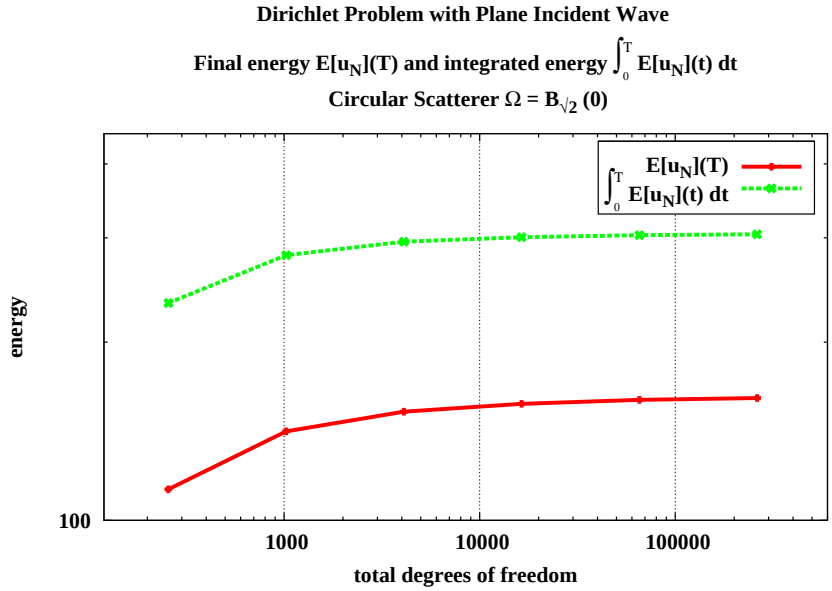

(b) Final energy $E_\Omega[u_N](T)$ and integrated energy $\int_0^T E_\Omega[u_N](t)\ dt$, for circular scatterer $\Omega = \mathbb{B}_{\sqrt{2}}(0)$

Figure 4.2: Energy graphs for the problem considered in Section 4.3.3.2

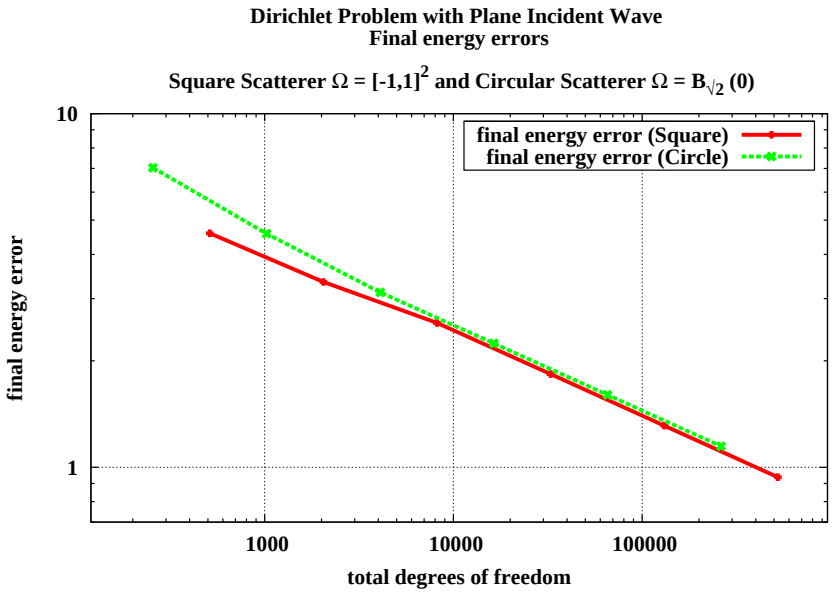

(a) final energy errors

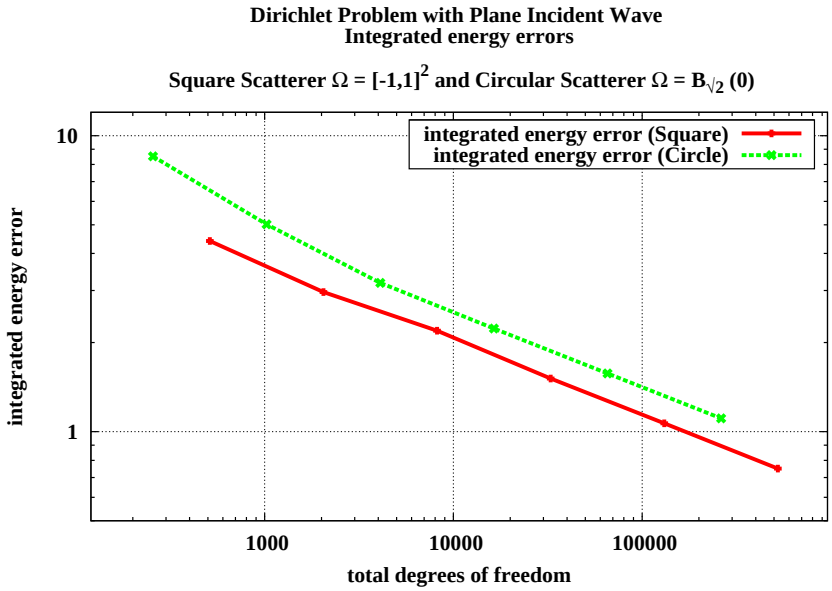

(b) integrated energy errors

Figure 4.3: Energy error graphs for the problem considered in Section 4.3.3.2

degrees of freedom			final energy (4.70)			integrated energy (4.73)		
TDOF	SDOF	TS	$E_\Omega[u](T)$	energy error	$\alpha_{h,\Delta t}$	$\int_0^T E_\Omega[u](t)\,dt$	energy error	$\alpha_{h,\Delta t}$
512	64	8	136.0640	4.5894422	-	249.6822	4.4077205	-
2048	128	16	145.9587	3.3418977	0.46	260.3386	2.9616887	0.57
8192	256	32	150.5723	2.5602109	0.38	264.3026	2.1926240	0.43
32768	512	64	153.7597	1.8350150	0.48	266.8249	1.5117209	0.54
131072	1024	128	155.4061	1.3118232	0.48	267.9719	1.0669114	0.50
524288	2048	256	156.2476	0.9377526	0.48	268.5471	0.7503999	0.51
extrapolated value:			157.1270			269.1102		

Table 4.2: Final energy with corresponding energy errors and experimental convergence rates, and integrated energy with corresponding energy errors and experimental convergence rates for the problem considered in Section 4.3.3.2 with square scatterer $\Omega = [-1,1]^2$. TDOF and SDOF denote the total and spatial degrees of freedom, respectively, while TS stands for the number of time steps.

degrees of freedom			final energy (4.70)			integrated energy (4.73)		
TDOF	SDOF	TS	$E_\Omega[u](T)$	energy error	$\alpha_{h,\Delta t}$	$\int_0^T E_\Omega[u](t)\,dt$	energy error	$\alpha_{h,\Delta t}$
256	32	8	112.8036	7.0289629	-	232.8427	8.5185421	-
1024	64	16	141.2519	4.5779930	0.62	280.2000	5.0207828	0.76
4096	128	32	152.4527	3.1236549	0.55	295.2848	3.1817385	0.66
16384	256	64	157.1895	2.2406294	0.48	300.4336	2.2303946	0.51
65536	512	128	159.6418	1.6025355	0.48	302.9362	1.5722786	0.50
262144	1024	256	160.8956	1.1464380	0.48	304.1786	1.1089004	0.50
extrapolated value:			162.2099			305.4083		

Table 4.3: Final energy with corresponding energy errors and experimental convergence rates, and integrated energy with corresponding energy errors and experimental convergence rates for the problem considered in Section 4.3.3.2 with circular scatterer $\Omega = \mathbb{B}_{\sqrt{2}}(0)$. TDOF and SDOF denote the total and spatial degrees of freedom, respectively, while TS stands for the number of time steps.

Chapter 5

A Posteriori Error Estimates

In this chapter, we study three a posteriori error estimates for the indirect Single Layer problem $V[p] = f$ that was considered in Chapter 4. We investigate if, and how, these error estimates can be localised for subsequent use as error indicators in adaptive algorithms, and their reliability and efficiency.

In Section 4.2, we gave a priori error estimates in the $\|\cdot\|_{\sigma,0,L^2(\Gamma)}$- and $\|\cdot\|_{\sigma,-1/2,H^{-1/2}(\Gamma)}$-norms (and in the corresponding energy space norms). These could be interpolated to obtain error estimates for intermediate norms, but we did not provide any error estimates for weaker norms. These can, in the case of Boundary Element Methods for time independent problems, be obtained by using the Aubin-Nitsche duality technique; see, for instance, [133, Theorem 4.2.7] or [145, Theorem 12.3]. Generalised mapping properties of the type discussed in Section 3.3.2 are employed in the proofs. However, it does not appear to be possible to use the same technique in our setup, due to the presence of the temporal derivative in the weak formulation, and we were not able to derive any a priori estimates on the error in weaker norms. The proofs of a posteriori error estimates use different techniques, which allow us to prove estimates in weaker norms.

The first a posteriori error estimate that is studied in this chapter is residual-based (Section 5.1). We follow methods by Carstensen et al. to obtain two estimates which can both be localised. One of these is of limited practical use with adaptive algorithms (Section 5.1.1), whereas the second one is well suited to steer adaptive algorithms (Section 5.1.2).

The second a posteriori error estimate is of Faermann type (Section 5.2). We employ results by Faermann to localise the spatial $H^{-1/2}(\Gamma)$-norm, and use these to obtain a localised error estimate that can be used to steer adaptive algorithms.

The third a posteriori error estimate, presented in Section 5.3, is called a N-$N/2$-type error bound, after the h-$h/2$ error estimates introduced by Praetorius et al. for elliptic problems. As for the previous two types of error estimates, these can be localised and consequently be used as local error indicators.

In Section 5.4, we investigate whether the estimates derived in Sections 5.1-5.3 for two space dimensions can be adapted to the three dimensional setup, and point out similarities and differences.

In Section 5.5, we present some numerical experiments in which we use the error bounds derived in Sections 5.1-5.3 to estimate the approximation error.

5.1 Residual-Based A Posteriori Error Estimate

The first a posteriori error estimates that we consider are of residual type. The residual $R := V[p_N] - f$, in a certain norm, is clearly an intuitive error measure. In what follows, we justify its use theoretically.

5.1.1 First Residual-Based A Posteriori Error Estimate

We prove a result similar to [38, Theorem 3] respectively [41, Theorem 2]. We cannot apply the referenced results directly since, in our setup, $V : X \to Y$ does not imply $V^{-1} : Y \to X$, as we observed in Remark 3.49 b). The work presented here follows the original ideas closely, adapting them to our setup. We work with the classical spaces $\mathcal{H}^k_\sigma(\mathbb{R}, H^s(\Gamma))$ and provide comments at the end of this section on how corresponding results can be derived for the energy spaces $H^{k;\,s,s}_{\sigma,\Gamma}$.

By Lemma 3.15 and (3.98), there hold the interpolation inequalities

$$\|q\|_{\sigma,0,H^{1/2+s}(\Gamma)} \le \|q\|^{1/2-s}_{\sigma,0,L^2(\Gamma)} \|q\|^{1/2+s}_{\sigma,0,H^1(\Gamma)} \quad \text{and} \quad \|q\|_{\sigma,3/2,H^{1/2+s}(\Gamma)} \le \|q\|^{1/2-s}_{\sigma,3/2,L^2(\Gamma)} \|q\|^{1/2+s}_{\sigma,3/2,H^1(\Gamma)} \tag{5.1}$$

for any $q \in \mathcal{L}^2_\sigma(\mathbb{R}, H^1(\Gamma))$ and $q \in \mathcal{H}^{3/2}_\sigma(\mathbb{R}, L^2(\Gamma))$, respectively, and $s \in \left(-\frac{1}{2}, \frac{1}{2}\right)$. We further recall the definition of the duality product,

$$\langle\!\langle p, q \rangle\!\rangle_\sigma = \int_{\mathbb{R}_{\ge 0}} e^{-2\sigma t} \, \langle \, p(\cdot,t), q(\cdot,t) \, \rangle \, dt \tag{5.2}$$

for $p \in \mathcal{H}^k_\sigma(\mathbb{R}, H^s(\Gamma))$ and $q \in \mathcal{H}^{-k}_\sigma(\mathbb{R}, H^{-s}(\Gamma))$, as in (3.119). Let $f \in \mathcal{H}^{3/2}_\sigma(\mathbb{R}, H^1(\Gamma))$. This means that f is more regular in space compared to if it was assumed to live in the usual energy space $\mathcal{H}^{3/2}_\sigma(\mathbb{R}, H^{1/2+s}(\Gamma))$. Since we are dealing with the integral equation $V[p] = f$, assuming $p \in \mathcal{H}^{5/2}_\sigma(\mathbb{R}, L^2(\Gamma))$ implies $f \in \mathcal{H}^{3/2}_\sigma(\mathbb{R}, H^1(\Gamma))$, by Theorem 3.45 and Remark 3.49. It is thus reasonable to assume $p \in \mathcal{H}^{5/2}_\sigma(\mathbb{R}, L^2(\Gamma))$ at least, to guarantee the desired regularity of f.

Let us now consider the weak forms that were discussed in Chapter 4, given by (4.2) and (4.3): In the continuous and discrete variational formulations, we are looking for functions $p \in \mathcal{H}^{5/2}_\sigma(\mathbb{R}, L^2(\Gamma))$ and $p_N \in V_N \subseteq \mathcal{H}^{5/2}_\sigma(\mathbb{R}, L^2(\Gamma))$, respectively, such that

$$a^V_\sigma(p, q) = \langle\!\langle V[\dot{p}], q \rangle\!\rangle_\sigma = \left\langle\!\!\left\langle \dot{f}, q \right\rangle\!\!\right\rangle_\sigma$$

for any $q \in \mathcal{L}^2_\sigma(\mathbb{R}, L^2(\Gamma))$ (recall that $\dot{p} \in \mathcal{H}^{3/2}_\sigma(\mathbb{R}, L^2(\Gamma))$ implies $V[\dot{p}] \in \mathcal{H}^{1/2}_\sigma(\mathbb{R}, H^1(\Gamma))$), and

$$a^V_\sigma(p_N, q_N) = \langle\!\langle V[\dot{p}_N], q_N \rangle\!\rangle_\sigma = \left\langle\!\!\left\langle \dot{f}, q_N \right\rangle\!\!\right\rangle_\sigma$$

for any $q_N \in W_N \subseteq \mathcal{L}^2_\sigma(L^2(\Gamma))$. Let

$$R := V[p - p_N] = f - V[p_N]$$

be the corresponding residual. By assumption, $f \in \mathcal{H}^{3/2}_\sigma(\mathbb{R}, H^1(\Gamma))$ and $p_N \in \mathcal{H}^{5/2}_\sigma(\mathbb{R}, L^2(\Gamma))$ for any $s \in \left(-\frac{1}{2}, \frac{1}{2}\right)$, so that, by Theorem 3.45, $V[p_N] \in \mathcal{H}^{3/2}_\sigma(\mathbb{R}, H^1(\Gamma))$, and consequently $R \in \mathcal{H}^{3/2}_\sigma(\mathbb{R}, H^1(\Gamma))$. Obviously, recalling (4.5), there holds

$$\left\langle\!\!\left\langle \dot{R}, q_N \right\rangle\!\!\right\rangle_\sigma = \left\langle\!\!\left\langle \dot{R}, q_N \right\rangle\!\!\right\rangle_{\mathcal{L}^2_\sigma(\mathbb{R},L^2(\Gamma))\times(\mathcal{L}^2_\sigma(\mathbb{R},L^2(\Gamma)))^*} = 0 \tag{5.3}$$

for any $q_N \in W_N$, i.e. $\dot{R}$ is orthogonal to the approximation space W_N.

The following result is a corollary to the Hahn-Banach Theorem [8, Folgerung 4.17(1), p. 183], [131, Theorem 3.3].

Theorem 5.1 ([41, Lemma 1])
Let Y be a normed space, and $0 \neq y_0 \in Y$. Then there exists some $y_0^* \in Y^*$ such that

$$\langle y_0, y_0^* \rangle_{Y \times Y^*} = \|y_0\|_Y^2 = \|y_0^*\|_{Y^*}^2.$$

Recall that, due to our assumptions, $R \in \mathcal{H}_\sigma^{3/2}(\mathbb{R}, H^1(\Gamma))$. Taking $Y = \mathcal{H}_\sigma^{1/2}(\mathbb{R}, L^2(\Gamma))$ with $Y^* = \mathcal{H}_\sigma^{-1/2}(\mathbb{R}, L^2(\Gamma))$ (see Lemma 3.44) and $y_0 = \dot{R} \in \mathcal{H}_\sigma^{1/2}(\mathbb{R}, H^1(\Gamma)) \subseteq Y$ in Theorem 5.1, there exists some $y_0^* = \rho \in Y^*$ such that

$$\begin{aligned} \|R\|_{\sigma,3/2,L^2(\Gamma)}^2 = \|\dot{R}\|_{\sigma,1/2,L^2(\Gamma)}^2 &= \left\langle\!\left\langle \dot{R}, \rho \right\rangle\!\right\rangle_{\mathcal{H}_\sigma^{1/2}(\mathbb{R},L^2(\Gamma)) \times \mathcal{H}_\sigma^{-1/2}(\mathbb{R},L^2(\Gamma))} \\ &= \left\langle\!\left\langle \dot{R}, \rho - q_N \right\rangle\!\right\rangle_{\mathcal{H}_\sigma^{1/2}(\mathbb{R},L^2(\Gamma)) \times \mathcal{H}_\sigma^{-1/2}(\mathbb{R},L^2(\Gamma))} \end{aligned} \tag{5.4}$$

for any $q_N \in W_N$, where the first equality is due to Remark 3.38 b), the second equality holds since the duality $\mathcal{L}_\sigma^2(\mathbb{R}, L^2(\Gamma)) \times \mathcal{L}_\sigma^2(\mathbb{R}, L^2(\Gamma))$ is also the duality $\mathcal{H}_\sigma^{1/2}(\mathbb{R}, L^2(\Gamma)) \times \mathcal{H}_\sigma^{-1/2}(\mathbb{R}, L^2(\Gamma))$, and the third equality is due to the Galerkin orthogonality (5.3). By the Cauchy-Schwarz inequality,

$$\begin{aligned} \|\dot{R}\|_{\sigma,1/2,L^2(\Gamma)}^2 &= \inf_{q_N \in W_N} \left\langle\!\left\langle \dot{R}, \rho - q_N \right\rangle\!\right\rangle_{\mathcal{H}_\sigma^{1/2}(\mathbb{R},L^2(\Gamma)) \times \mathcal{H}_\sigma^{-1/2}(\mathbb{R},L^2(\Gamma))} \\ &\leq \|\dot{R}\|_{\sigma,1/2,L^2(\Gamma)} \left(\inf_{q_N \in W_N} \|\rho - q_N\|_{\sigma,-1/2,L^2(\Gamma)} \right) \end{aligned}$$

and thus

$$\|R\|_{\sigma,3/2,L^2(\Gamma)} = \|\dot{R}\|_{\sigma,1/2,L^2(\Gamma)} \leq \inf_{q_N \in W_N} \|\rho - q_N\|_{\sigma,-1/2,L^2(\Gamma)}. \tag{5.5}$$

Since we assumed $R \in \mathcal{H}_\sigma^{3/2}(\mathbb{R}, H^1(\Gamma))$, we obtain, using (5.1),

$$\|R\|_{\sigma,3/2,H^{1/2+s}(\Gamma)} \leq \left(\inf_{q_N \in W_N} \|\rho - q_N\|_{\sigma,-1/2,L^2(\Gamma)}^{1/2-s} \right) \|R\|_{\sigma,3/2,H^1(\Gamma)}^{1/2+s}. \tag{5.6}$$

Due to the mapping properties (Lemma 3.47 and Remark 3.49), there holds

$$\|p - p_N\|_{\sigma,-1/2-2|s|,H^{-1/2+s}(\Gamma)} = \|V^{-1}[R]\|_{\sigma,-1/2-2|s|,H^{-1/2+s}(\Gamma)} \leq C \|R\|_{\sigma,3/2,H^{1/2+s}(\Gamma)} \tag{5.7}$$

for $s \in \left(-\frac{1}{2}, \frac{1}{2}\right)$, with $C = C(\Gamma, \sigma_0, s)$. We thus have the following result.

Lemma 5.2 (Space-Time Version of [41, Theorem 1])
Let ρ be as in (5.4)*, and $R \in \mathcal{H}_\sigma^{3/2}(\mathbb{R}, H^1(\Gamma))$. As discussed above, assuming*

$$p \in \mathcal{H}_\sigma^{5/2}(\mathbb{R}, L^2(\Gamma)), \;\; p_N \in V_N \subseteq \mathcal{H}_\sigma^{5/2}(\mathbb{R}, L^2(\Gamma)) \;\; \textit{and} \;\; f \in \mathcal{H}_\sigma^{3/2}(\mathbb{R}, H^1(\Gamma))$$

guarantees $R \in \mathcal{H}_\sigma^{3/2}(\mathbb{R}, H^1(\Gamma))$.

Then there holds the a posteriori error estimate

$$\|p - p_N\|_{\sigma,-1/2-2|s|,H^{-1/2+s}(\Gamma)} \leq C \|R\|_{\sigma,3/2,H^1(\Gamma)}^{1/2+s} \left(\inf_{q_N \in W_N} \|\rho - q_N\|_{\sigma,-1/2,L^2(\Gamma)}^{1/2-s} \right)$$

for $s \in \left(-\frac{1}{2}, \frac{1}{2}\right)$, with $C = C(\Gamma, \sigma_0, s) > 0$.

Proof
Combine (5.6) and (5.7). ∎

Let $\rho = y_0^\star = \Lambda[\dot{R}] = \ddot{R}$, so that $\|\rho\|_{\sigma,-1/2,L^2(\Gamma)} = \|\dot{R}\|_{\sigma,1/2,L^2(\Gamma)}$. This choice of ρ satisfies (5.4). We now make an even stronger assumption than that of Lemma 5.2 on the residual, and assume that $R \in \mathcal{H}^{5/2}_\sigma(\mathbb{R}, H^1(\Gamma))$. This can be guaranteed if we let $p \in \mathcal{H}^{7/2}_\sigma(\mathbb{R}, L^2(\Gamma))$, $p_N \in V_N \subseteq \mathcal{H}^{7/2}_\sigma(\mathbb{R}, L^2(\Gamma))$ and $f \in \mathcal{H}^{5/2}_\sigma(\mathbb{R}, H^1(\Gamma))$. Using Proposition 3.56 with $l = -\frac{1}{2}$, $r = 0$ and $k = \frac{1}{2}$, $s = 1$ on the term in Lemma 5.2, we obtain the *a posteriori error estimate*

$$\|p - p_N\|_{\sigma,-1/2-2|s|,H^{-1/2+s}(\Gamma)} \leq C\|R\|^{1/2+s}_{\sigma,3/2,H^1(\Gamma)} \left\|\left(h(\mathcal{T}_{S,T}) + \Delta t(\mathcal{T}_{S,T})\right) R\right\|^{1/2-s}_{\sigma,5/2,H^1(\Gamma)} \tag{5.8}$$

with $C = C(\Gamma, \sigma_0, s, m_1, m_2)$, which is similar to the inequality that is [41, Theorem 2].

We are interested in estimating the terms $\|R\|_{\sigma,k,H^1(\Gamma)}$ with $k = \frac{3}{2}, \frac{5}{2}$ further. To do so, we review another result from [41]. Let $f \in H^\theta_0(\Gamma) := \left\{ \psi \in H^\theta(\Gamma) \;\middle|\; \langle 1, \psi\rangle = 0 \right\} \subseteq H^\theta(\Gamma)$. We further define an operator

$$I_s[f](x) := \int_0^{s_x} f(\ y(s_y)\ )\, ds_y + c_{I_s} \tag{5.9}$$

with $x = x(s_x)$, where we assume that the parameter set of the parameterisation of Γ is $[0, S_\Gamma]$. The constant c_{I_s} is fixed by demanding $\langle 1, I_s[f]\rangle = 0$. There holds:

Lemma 5.3 ([41, Lemma 3])
For $\theta \in [0,1]$, the operator $I_s : H^{\theta-1}_0(\Gamma) \to H^\theta_0(\Gamma)$ is an isometry, i.e. $\|I_s[f]\|_{H^\theta(\Gamma)} = \|f\|_{H^{\theta-1}(\Gamma)}$ for $f \in H^{\theta-1}_0(\Gamma)$.

Further, I and $\frac{\partial}{\partial s}$ are inverse to each other, i.e. $\frac{\partial}{\partial s}\left(I_s[f]\right) = f$ for $f \in H^{\theta-1}_0(\Gamma)$ and $I_s\left[\frac{\partial}{\partial s} g\right] = g$ for $g \in H^\theta_0(\Gamma)$.

As an immediate consequence, there holds, for $f \in H^\theta_0(\Gamma)$, $\|\frac{\partial}{\partial s} f\|_{H^{\theta-1}(\Gamma)} = \|I_s\left[\frac{\partial}{\partial s} f\right]\|_{H^\theta(\Gamma)} = \|f\|_{H^\theta(\Gamma)}$, and in particular

$$\left\|\frac{\partial}{\partial s} f\right\|_{L^2(\Gamma)} = \|f\|_{H^1(\Gamma)} \tag{5.10}$$

for $f \in H^1_0(\Gamma)$. $R \in \mathcal{H}^{3/2}_\sigma(\mathbb{R}, H^1(\Gamma))$ implies $R(\cdot, t) \in H^1(\Gamma)$ for (almost) every t. We cannot guarantee $R(\cdot, t) \in H^1_0(\Gamma)$ though, since p_N is defined via the space-time inner product. Analogously to the spaces $H^\theta_0(\Gamma)$ above, let us define spaces

$${}_0\mathcal{H}^k_\sigma(\mathbb{R}, H^\theta(\Gamma)) := \left\{ q \in \mathcal{H}^k_\sigma(\mathbb{R}, H^\theta(\Gamma)) \;\middle|\; \langle\!\langle q, 1\rangle\!\rangle_\sigma = 0 \right\}.$$

By (5.3), $\dot{R} \in {}_0\mathcal{L}^2_\sigma(\mathbb{R}, H^\theta(\Gamma))$. We define the operator

$$\tilde{I}_s[f](x) := \int_{\mathbb{R}_{\geq 0}} e^{-2\sigma t} \int_0^{s_x} f(\ y(s_y), t\ )\, ds_y\, dt + c_{\tilde{I}_s}.$$

Note that $\tilde{I}_s[f](x) = \int_{\mathbb{R}_{\geq 0}} e^{-2\sigma t}\ I_s[f(\cdot, t)](x)\, dt$ if we set $c_{\tilde{I}_s} = \frac{c_{I_s}}{2\sigma}$. We can hence extend Lemma 5.3 from the case of the spaces $H^\theta_0(\Gamma)$ to the case of the spaces ${}_0\mathcal{H}^k_\sigma(\mathbb{R}, H^\theta(\Gamma))$, and we therefore obtain, analogously to (5.10),

$$\left\|\frac{\partial}{\partial s} f\right\|_{\sigma,k,L^2(\Gamma)} = \|f\|_{\sigma,k,H^1(\Gamma)} \tag{5.11}$$

for $f \in {}_0\mathcal{H}^k_\sigma(\mathbb{R}, H^1(\Gamma))$. As a consequence, we obtain Corollary 5.4.

Corollary 5.4 (Space-Time Version of [41, Theorem 2])
Under stronger assumptions than in Lemma 5.2, namely

$$p \in \mathcal{H}^{7/2}_{\sigma}(\mathbb{R}, L^2(\Gamma)), \;\; p_N \in V_N \subseteq \mathcal{H}^{7/2}_{\sigma}(\mathbb{R}, L^2(\Gamma)) \;\; \textit{and} \;\; f \in \mathcal{H}^{5/2}_{\sigma}(\mathbb{R}, H^1(\Gamma))$$

to guarantee $R \in \mathcal{H}^{5/2}_{\sigma}(\mathbb{R}, H^1(\Gamma))$*, there holds the* a posteriori error estimate

$$\|p - p_N\|_{\sigma,-1/2-2|s|,H^{-1/2+s}(\Gamma)} \leq C \left\| \frac{\partial}{\partial s} R \right\|^{1/2+s}_{\sigma,3/2,L^2(\Gamma)} \left\| \left(h(\mathcal{T}_{S,T}) + \Delta t(\mathcal{T}_{S,T})\right) \frac{\partial}{\partial s} R \right\|^{1/2-s}_{\sigma,5/2,L^2(\Gamma)} \tag{5.12}$$

for $s \in \left(-\frac{1}{2}, \frac{1}{2}\right)$*, with* $C = C(\Gamma, \sigma_0, s, m_1, m_2) > 0$.

Remark 5.5 (On Lemma 5.3 and Corollary 5.4)

a) *Note that we have not made use of temporal interpolation in the proof of Lemma 5.3. This is due to the mapping properties of the inverse Single Layer operator. Instead of* (5.7)*, we could have worked with*

$$\|p - p_N\|_{\sigma,-1/2-|s|,H^{-1/2+s}(\Gamma)} \leq C \|R\|_{\sigma,3/2+|s|,H^{1/2+s}(\Gamma)}$$

for $s \in \left(-\frac{1}{2}, \frac{1}{2}\right)$*, with* $C = C(\Gamma, \sigma_0, s)$*. The right hand side term could then only be estimated by* $\|R\|_{\sigma,2,L^2(\Gamma)} \|R\|_{\sigma,2,H^1(\Gamma)}$*, which destroys the usual gain in order due to the interpolation estimate. One could then work with* $Y = \mathcal{H}^1_{\sigma}(\mathbb{R}, L^2(\Gamma))$ *and* $R \in \mathcal{H}^2_{\sigma}(\mathbb{R}, L^2(\Gamma))$*, which would lead to even more severe assumptions on the temporal order of the residual. Consequently,* (5.8) *would then change to*

$$\|p - p_N\|_{\sigma,-1/2-|s|,H^{-1/2+s}(\Gamma)} \leq C \|R\|^{1/2+s}_{\sigma,2,H^1(\Gamma)} \|\left(h(\mathcal{T}_{S,T}) + \Delta t(\mathcal{T}_{S,T})\right) R\|^{1/2-s}_{\sigma,3,H^1(\Gamma)} \tag{5.13}$$

with $C = C(\Gamma, \sigma_0, s, m_1, m_2)$*. See also d) below.*

b) *(a posteriori error estimate for uniform space-time meshes) For a uniform space-time mesh there holds* $h(\mathcal{T}_{S,T}) = h$ *and* $\Delta t(\mathcal{T}_{S,T}) = \Delta t$ *for every* $i = 1, \ldots, N$ *and* $j = 1, \ldots, M$*. For* $s = 0$ *we obtain, by Corollary 5.4,*

$$\|p - p_N\|_{\sigma,-1/2,H^{-1/2}(\Gamma)} \leq C \sqrt{h + \Delta t} \;\; \left\| \frac{\partial}{\partial s} R \right\|_{\sigma,5/2,L^2(\Gamma)}. \tag{5.14}$$

We thus have an estimate for the unknown error that only involves computable quantities. Note that the $\|\cdot\|_{\sigma,-1/2,H^{-1/2}(\Gamma)}$*-error cannot be computed exactly, even when the exact solution is known. The estimate* (5.14) *is the a posteriori analogue of the a priori error estimate* (4.24)*.*

c) *For the energy-based norms, the estimates have to be changed accordingly. We sketch the major differences: Applying Lemma 3.47 and Remark 3.49, we can replace* (5.7) *by*

$$\|p - p_N\|_{\sigma,\Gamma;-2|s|;-1/2+s,-1/2+s} \leq C \|R\|_{\sigma,\Gamma;1;1/2+s,1/2+s}$$

with $C = C(\Gamma, \sigma_0, s)$*, where, by* (3.114)

$$\|\cdot\|^2_{\sigma,\Gamma;0;-1/2,-1/2} \sim \|\cdot\|^2_{\sigma,0,H^{-1/2}(\Gamma)} + \|\cdot\|^2_{\sigma,-1/2,L^2(\Gamma)}$$

in the case $s = 0$*. The term* $\rho = y_0^*$ *in Lemma 5.2 can be chosen as* $\rho = \dot{R} \in Y^*$*, with* $Y = Y^* = H^{0;0,0}_{\sigma,\Gamma} = L^2_{\sigma,\Gamma}$*. If the energy-based norms are used, it further suffices to assume*

$f \in H^{1;1,1}_{\sigma,\Gamma}$ and $p \in H^{2;0,0}_{\sigma,\Gamma}$ to ensure $R \in H^{1;1,1}_{\sigma,\Gamma}$. Regarding the estimate in (5.8)*, one can use Proposition 3.57 with $k = l = r = 0$ and $s = 1$ to obtain*

$$\|p - p_N\|_{\sigma,\Gamma;\,-2|s|;\,-1/2+s,-1/2+s} \leq C\|R\|^{1/2+s}_{\sigma,\Gamma;\,1;\,1,1}\,\|(h(\mathcal{T}_{S,T}) + \Delta t(\mathcal{T}_{S,T}))\,R\|^{1/2-s}_{\sigma,\Gamma;\,1;\,1,1} \tag{5.15}$$

with $C = C(\Gamma, \sigma_0, s, m_1, m_2)$. For $s = 0$, one then obtains the a posteriori analogue

$$\|p - p_N\|_{\sigma,\Gamma;\,0;\,-1/2,-1/2} \leq C\sqrt{h + \Delta t}\|R\|_{\sigma,\Gamma;\,1;\,1,1} \tag{5.16}$$

to the a priori error estimate (4.23)*. As for the a priori error estimates, the regularity assumptions become slightly milder when the energy-based norms are used.*

d) *The assumptions made on temporal regularity appear to be rather severe here. It is, however, well known (see Remark 3.49 b) and the references cited therein) that the mapping properties of the time domain boundary integral operators that can be verified theoretically seem to be unrealistic. Lemmas 4.3 and 4.7, for instance, do not guarantee convergence for lowest order methods in time, which work well and are widely used in practice, as discussed in Section 4.2. See also Remark 5.9 c).*

e) *(implementational detail) For an arbitrary potential P, we use the same method to compute terms of the type $\|\frac{\partial}{\partial s}P[u]\|_{L^2(\Gamma_i)}$ as in [42, p. 2177], i.e.*

$$\frac{\partial}{\partial s}P[u](\vec{x}) \approx \frac{P[u](\vec{x} + \varepsilon\vec{d}_i) - P[u](\vec{x} - \varepsilon\vec{d}_i)}{\varepsilon|\Gamma_i|} \tag{5.17}$$

with $\varepsilon = 10^{-2}$, and $\vec{d}_i$ as in (2.37)*.*

f) *(usage in adaptive algorithms) Using the notation of [41, Section 6], we define*

$$a_{i,j} := \left\|\Lambda^{3/2}\frac{\partial}{\partial s}R\right\|_{\sigma,L^2(T_j),L^2(\Gamma_i)} \quad \text{and} \quad b_{i,j} := \left\|\Lambda^{5/2}\frac{\partial}{\partial s}R\right\|_{\sigma,L^2(T_j),L^2(\Gamma_i)}.$$

Then, for $s = 0$, the terms in the right hand side term of the estimate given in Corollary 5.4 can be written as

$$\left\|\Lambda^{3/2}\frac{\partial}{\partial s}R\right\|^2_{\sigma,0,L^2(\Gamma)} = \sum_{i=1}^{N}\sum_{j=1}^{M} a_{i,j}^2$$

and

$$\left\|(h(\mathcal{T}_{S,T}) + \Delta t(\mathcal{T}_{S,T}))\,\frac{\partial}{\partial s}R\right\|^2_{\sigma,5/2,L^2(\Gamma)} = \sum_{i=1}^{N}\sum_{j=1}^{M}(h_i + \Delta t_j)^2 b_{i,j}^2$$

and thus

$$\|p - p_N\|_{\sigma,-1/2,H^{-1/2}(\Gamma)} \leq C\left(\sum_{i=1}^{N}\sum_{j=1}^{M} a_{i,j}^2\right)^{1/4}\left(\sum_{i=1}^{N}\sum_{j=1}^{M}(h_i + \Delta t_j)^2 b_{i,j}^2\right)^{1/4}. \tag{5.18}$$

The estimate (5.18) *provides an upper bound that can be used to control local error contributions. However, this estimate is not very useful for adaptive computations, as every space-time cell $\Gamma_i \times [t_{j-1}, t_j]$ contributes two error terms, and it is not clear which one should be used to steer the corresponding algorithm, as discussed in [42]. We thus establish another, more practical estimate in the next section.*

g) Carstensen shows in [38] that residual error estimators for the Galerkin Boundary Element Method for the Laplace problem with Dirichlet data are efficient under the assumption of quasi-uniform meshes [38, Theorem 2]. The proof uses a representation of the problem's unknown solution by a series, which is not available for our problem. We therefore do not address the issue of efficiency, i.e. whether an inequality inverse to (5.14) *holds, for the residual error estimator discussed here.*

5.1.2 Second Residual-Based A Posteriori Error Estimate

We first cite a result from [42]. A similar result for three space dimensions is [40, Theorem 3.2].

Proposition 5.6 ([42, Proposition 1])
If $g \in H^1(\Gamma)$ satisfies

$$\langle g, \psi_h \rangle = 0 \tag{5.19}$$

for all $\psi_h \in S_h^0$ then there holds, for $\theta \in [0,1]$,

$$\|g\|_{H^\theta(\Gamma)} \leq \sqrt{2} K^\theta \sum_{i=1}^{N} \left\| \frac{\partial}{\partial s} g \right\|_{L^2(\Gamma_i)} h_i^{1-\theta} (1 + h_i^2)^{\theta/2} \tag{5.20}$$

with $K = K(\mathcal{T}_S)$ as defined in (2.3).

We would like to apply Proposition 5.6 with $g = R$, as it is done in [42]. The approximation p_N that appears in our residual is defined in a weak space-time sense. The residual therefore does not satisfy (5.19), and it is not immediately possible to apply Proposition 5.6. Further on, this estimate does not feature any temporal localisation, only a spatial one. We further remark that, technically, the space-time domain $\Gamma \times [0,T]$ that we consider is a cylinder-without-cap-like or tube-like object; see Figure 6.1. The three dimensional result [40, Theorem 3.2] mentioned above covers the cases of an open surface and the boundary of a closed domain, so the object that we consider does not belong to this class.

Let us introduce some further notation. We set $T_j := [t_{j-1}, t_j]$ for any $j = 1, \ldots, M$, and we further define local norms in time by

$$\|u\|_{\sigma, H^k(T_j), H^s(\Gamma)} := \|\mathbb{1}_{T_j}(t)\ u\|_{\sigma,k,H^s(\Gamma)} = \|e^{-\sigma t} u\|_{H^k(T_j, H^s(\Gamma))}. \tag{5.21}$$

We know from (5.3) that the orthogonality relation $\left\langle\!\left\langle \dot{R}, q_N \right\rangle\!\right\rangle_\sigma = 0$ for every $q_N \in W_N$ holds. This leads us to the next result.

Lemma 5.7 (Space-Time Version of [42, Proposition 1])
Let the function $g \in \mathcal{H}^1_\sigma(\mathbb{R}, H^1(\Gamma))$ satisfy

$$\langle\!\langle g, q_N \rangle\!\rangle_\sigma = 0 \tag{5.22}$$

for every $q_N \in W_N$. Then the estimate

$$\|g\|_{\sigma,0,H^\theta(\Gamma)} \leq 2\,(K_1 K_2)^\theta \sum_{i=1}^{N} \sum_{j=1}^{M} \left(1 + h_i^2 \Delta_j^2\right)^{\theta/2} (h_i \Delta_j)^{1-\theta} \left\| \frac{\partial}{\partial s} g \right\|_{\sigma, H^1(T_j), L^2(\Gamma_i)}$$

holds, with $K_1 = K(\mathcal{T}_S)$ and $K_2 = K(\mathcal{T}_T)$ as defined in (2.3), *and for $\theta \in [0,1]$.*

Proof
We consider a) first. We follow the proof of [42, Proposition 1]. Let us first note that the estimates [42, (23), (24)] in the proof of [42, Proposition 1] are purely algebraic. However, we need to adapt them slightly for our case and cannot apply them directly. For this reason, we present the proof in its entirety here.

In this proof, we use the following notation: We define a space-time L^1-norm and a space-time L^∞-norm by

$$\|u\|_{\sigma,L^1([0,T]),L^1(\Gamma)} := \|e^{-\sigma t}u\|_{L^1([0,T],L^1(\Gamma))} \quad \text{and} \quad \|u\|^2_{\sigma,L^\infty([0,T]),L^\infty(\Gamma)} := \left(\sup_{t\in[0,T]}\sup_{x\in\Gamma}\left|e^{-\sigma t}u\right|\right)^2$$

with obvious localisations, analogously to (5.21)

Let $q_N(x,t) = \mathbb{1}_{\Gamma_i}(x)\ \mathbb{1}_{T_j}(t)$ in (5.22). Then

$$\int_{T_j}\int_{\Gamma_i} e^{-2\sigma t} g(x,t)ds\ dt = 0$$

for every space-time cell $\Gamma_i \times T_j$, and thus there exists a pair $(y_{i,j},\tau_{i,j}) \in \Gamma_i \times T_j$ such that $e^{-2\sigma\tau_{i,j}} g(y_{i,j},\tau_{i,j}) = 0$, and hence $g(y_{i,j},\tau_{i,j}) = 0$, for every $\Gamma_i \times T_j$. For $0 \le i \le N-1$ and $0 \le j \le M$, we define continuous piecewise functions

$$\tilde{g}_{i,j}(x,t) := \begin{cases} e^{-\sigma t}g(x,t) & (x,t) \in \{\, y \in \Gamma_i \cup \Gamma_{i+1} \mid y \text{ between } y_i \text{ and } y_{i+1} \,\} \\ & \qquad \times \{\, s \in T_j \cup T_{j+1} = [t_{j-1},t_{j+1}] \mid s \text{ between } \tau_j \text{ and } \tau_{j+1} \,\} \\ 0 & \text{else} \end{cases}$$

with $\Gamma_N = \Gamma_0$ and $t_{-1} := \tau_{-1} := 0$, $t_{M+1} := \tau_{M+1} := t_M = T$. We note that $\tilde{g}_{i,j} \in \mathcal{H}^1_\sigma(\mathbb{R}, H^1(\Gamma))$ again. Writing $\operatorname{supp}\tilde{g}_{i,j} := \tilde{\Gamma}_i \times \tilde{T}_j$ with $\tilde{T}_j := [\tau_{j-1},\tau_j]$, we observe that

$$\|\tilde{g}_{i,j}\|^2_{L^2([0,T],H^\theta(\Gamma))} = \int_0^T \|\tilde{g}_{i,j}(\cdot,t)\|^2_{H^\theta(\Gamma)}\,dt = \int_{\tilde{T}_j} e^{-2\sigma t}\|g(\cdot,t)\|^2_{H^\theta(\tilde{\Gamma}_i)}\,dt = \|g\|^2_{\sigma,L^2(\tilde{T}_j),H^\theta(\tilde{\Gamma}_i)}. \tag{5.23}$$

Hence, by the triangle inequality,

$$\|g\|_{\sigma,0,H^\theta(\Gamma)} = \left\|\sum_{i=0}^{N-1}\sum_{j=0}^{M}\tilde{g}_{i,j}\right\|_{L^2([0,T],H^\theta(\Gamma))} \le \sum_{i=0}^{N-1}\sum_{j=0}^{M}\|\tilde{g}_{i,j}\|_{L^2([0,T],H^\theta(\Gamma))}. \tag{5.24}$$

By interpolation (inequality; see [114, Lemma B.1] respectively (5.1)) and by (5.23) (equality), there holds

$$\|\tilde{g}_{i,j}\|_{L^2([0,T],H^\theta(\Gamma))} \le \|\tilde{g}_{i,j}\|^\theta_{L^2([0,T],H^1(\Gamma))}\|\tilde{g}_{i,j}\|^{1-\theta}_{L^2([0,T],L^2(\Gamma))} = \|g\|^\theta_{\sigma,L^2(\tilde{T}_j),H^1(\tilde{\Gamma}_i)}\|g\|^{1-\theta}_{\sigma,L^2(\tilde{T}_j),L^2(\tilde{\Gamma}_i)}. \tag{5.25}$$

We use the decomposition $\Gamma_i = \Gamma_{i,i-1} \cup \Gamma_{i,i}$ with $\Gamma_{i,i-1} := \Gamma_i \cap \tilde{\Gamma}_{i-1}$ and $\Gamma_{i,i} := \Gamma_i \cap \tilde{\Gamma}_i$, illustrated in Figure 5.1. Note that this also gives the decomposition $\tilde{\Gamma}_i = \Gamma_{i,i} \cup \Gamma_{i+1,i}$. Similarly, $T_j = T_{j,j-1} \cup T_{j,j}$ with $T_{j,j-1} := [t_{j-1},\tau_j]$ and $T_{j,j} := [\tau_j,t_j]$, and $\tilde{T}_j = T_{j,j} \cup T_{j+1,j}$.

As $y_i \in \Gamma_{i,k}$ for $k = i-1, i$ and $\tau_j \in T_{j,l}$ for $l = j-1, j$, there exists a root of g in every sub-cell $\Gamma_{i,k} \times T_{j,l}$. Using the fundamental theorem of calculus (and writing $g' = \frac{\partial}{\partial s}g$),

$$g(x,t) = \int^t \int^x \frac{\partial}{\partial t}\left(g'(y,s)\right)\,ds_y\,ds + C$$

for $(x,t) \in \Gamma_{i,k} \times T_{j,l}$ and some $C \in \mathbb{R}$.

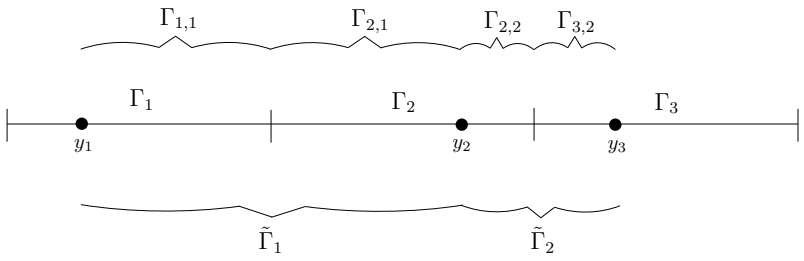

Figure 5.1: Decomposition of Γ_i and $\tilde{\Gamma}_i$, respectively, as used in the proof of Lemma 5.7.

Due to the existence of a root, $C = 0$, and thus

$$\begin{aligned}
&\|g\|^2_{\sigma,L^\infty(T_{j,l}),L^\infty(\Gamma_{i,k})} \\
= &\left(\sup_{t\in T_{j,l}}\sup_{x\in\Gamma_{i,k}} |e^{-\sigma t}g(x,t)|\right)^2 = \left(\sup_{t\in T_{j,l}}\sup_{x\in\Gamma_{i,k}} \left|\int^t\int^x \frac{\partial}{\partial t}\left(\left(e^{-\sigma t}g(x,t)\right)'\right)\, ds_y\, ds\right|\right)^2 \\
\leq &\left(\sup_{t\in T_{j,l}}\sup_{x\in\Gamma_{i,k}} \int^t\int^x \left|\frac{\partial}{\partial t}\left(\left(e^{-\sigma t}g(x,t)\right)'\right)\right| ds_y\, ds\right)^2 \leq \left\|\frac{\partial}{\partial t}\left(\left(e^{-\sigma t}g\right)'\right)\right\|^2_{L^1(T_{j,l},L^1(\Gamma_{i,k}))}.
\end{aligned}$$

Combining

$$\|u\|_{\sigma,L^2(T_{j,l}),L^2(\Gamma_{i,k})} \leq \sqrt{|\Gamma_{i,k}||T_{j,l}|}\|u\|_{\sigma,L^\infty(T_{j,l}),L^\infty(\Gamma_{i,k})}$$

and Jensen's inequality

$$\|u\|_{L^1(T_{j,l},L^1(\Gamma_{i,k}))} \leq \sqrt{|\Gamma_{i,k}||T_{j,l}|}\|u\|_{L^2(T_{j,l},L^2(\Gamma_{i,k}))}$$

with the previous estimate gives

$$\begin{aligned}
\|g\|_{\sigma,L^2(T_{j,l}),L^2(\Gamma_{i,k})} &\leq \sqrt{|\Gamma_{i,k}||T_{j,l}|}\|g\|_{\sigma,L^\infty(T_{j,l}),L^\infty(\Gamma_{i,k})} \\
&\leq \sqrt{|\Gamma_{i,k}||T_{j,l}|}\left\|\frac{\partial}{\partial t}\left(\left(e^{-\sigma t}g\right)'\right)\right\|_{L^1(T_{j,l},L^1(\Gamma_{i,k}))} \\
&\leq |\Gamma_{i,k}||T_{j,l}|\left\|\frac{\partial}{\partial t}\left(\left(e^{-\sigma t}g\right)'\right)\right\|_{L^2(T_{j,l},L^2(\Gamma_{i,k}))}
\end{aligned}$$

i.e. $\|g\|_{\sigma,L^2(T_{j,l}),L^2(\Gamma_{i,k})} \leq |\Gamma_{i,k}||T_{j,l}|\|g'\|_{\sigma,H^1(T_{j,l}),\Gamma_{i,k}}$. Using the interpolation estimate (5.25) and the definition of the $H^1(\tilde{\Gamma}_i)$-norm,

$$\|\tilde{g}_{i,j}\|_{L^2([0,T],H^\theta(\Gamma))} \leq \left(\|g\|^2_{\sigma,L^2(\tilde{T}_j),L^2(\tilde{\Gamma}_i)} + \|g'\|^2_{\sigma,L^2(\tilde{T}_j),L^2(\tilde{\Gamma}_i)}\right)^{\theta/2}\|g\|^{1-\theta}_{\sigma,L^2(\tilde{T}_j),L^2(\tilde{\Gamma}_i)}.$$

The first term can now be estimated as

$$
\begin{aligned}
& \|g\|^2_{\sigma,L^2(\tilde{T}_j),L^2(\tilde{\Gamma}_i)} + \|g'\|^2_{\sigma,L^2(\tilde{T}_j),L^2(\tilde{\Gamma}_i)} \\
= \quad & \Big(\|g\|_{\sigma,L^2(T_{j,j}),L^2(\Gamma_{i,i})} + \|g\|_{\sigma,L^2(T_{j+1,j}),L^2(\Gamma_{i,i})} \\
& \quad + \|g\|_{\sigma,L^2(T_{j,j}),L^2(\Gamma_{i+1,i})} + \|g\|_{\sigma,L^2(T_{j+1,j}),L^2(\Gamma_{i+1,i})} \Big)^2 \\
& + \Big(\|g'\|_{\sigma,L^2(T_{j,j}),L^2(\Gamma_{i,i})} + \|g'\|_{\sigma,L^2(T_{j+1,j}),L^2(\Gamma_{i,i})} \\
& \quad + \|g'\|_{\sigma,L^2(T_{j,j}),L^2(\Gamma_{i+1,i})} + \|g'\|_{\sigma,L^2(T_{j+1,j}),L^2(\Gamma_{i+1,i})} \Big)^2 \\
\leq \quad & \Big(|\Gamma_{i,i}||T_{j,j}|\|g'\|_{\sigma,H^1(T_{j,j}),L^2(\Gamma_{i,i})} + |\Gamma_{i,i}||T_{j+1,j}|\|g'\|_{\sigma,H^1(T_{j+1,j}),L^2(\Gamma_{i,i})} \\
& \quad + |\Gamma_{i+1,i}||T_{j,j}|\|g'\|_{\sigma,H^1(T_{j,j}),L^2(\Gamma_{i+1,i})} + |\Gamma_{i+1,i}||T_{j+1,j}|\|g'\|_{\sigma,H^1(T_{j+1,j}),L^2(\Gamma_{i+1,i})} \Big)^2 \\
& + \Big(\|g'\|_{\sigma,L^2(T_{j,j}),L^2(\Gamma_{i,i})} + \|g'\|_{\sigma,L^2(T_{j+1,j}),L^2(\Gamma_{i,i})} \\
& \quad + \|g'\|_{\sigma,L^2(T_{j,j}),L^2(\Gamma_{i+1,i})} + \|g'\|_{\sigma,L^2(T_{j+1,j}),L^2(\Gamma_{i+1,i})} \Big)^2
\end{aligned}
$$

and the second term as

$$
\begin{aligned}
& \|g\|_{\sigma,L^2(\tilde{T}_j),L^2(\tilde{\Gamma}_i)} \\
= \quad & \|g\|_{\sigma,L^2(T_{j,j}),L^2(\Gamma_{i,i})} + \|g\|_{\sigma,L^2(T_{j+1,j}),L^2(\Gamma_{i,i})} \\
& + \|g\|_{\sigma,L^2(T_{j,j}),L^2(\Gamma_{i+1,i})} + \|g\|_{\sigma,L^2(T_{j+1,j}),L^2(\Gamma_{i+1,i})} \\
\leq \quad & |\Gamma_{i,i}||T_{j,j}|\|g'\|_{\sigma,H^1(T_{j,j}),L^2(\Gamma_{i,i})} + |\Gamma_{i,i}||T_{j+1,j}|\|g'\|_{\sigma,H^1(T_{j+1,j}),L^2(\Gamma_{i,i})} \\
& + |\Gamma_{i+1,i}||T_{j,j}|\|g'\|_{\sigma,H^1(T_{j,j}),L^2(\Gamma_{i+1,i})} + |\Gamma_{i+1,i}||T_{j+1,j}|\|g'\|_{\sigma,H^1(T_{j+1,j}),L^2(\Gamma_{i+1,i})}.
\end{aligned}
$$

Hence

$$
\begin{aligned}
& \|\tilde{g}_{i,j}\|_{L^2([0,T],H^\theta(\Gamma))} \\
\leq \quad & \Bigg(\Big(|\Gamma_{i,i}||T_{j,j}|\|g'\|_{\sigma,H^1(T_{j,j}),L^2(\Gamma_{i,i})} + |\Gamma_{i,i}||T_{j+1,j}|\|g'\|_{\sigma,H^1(T_{j+1,j}),L^2(\Gamma_{i,i})} \\
& \quad + |\Gamma_{i+1,i}||T_{j,j}|\|g'\|_{\sigma,H^1(T_{j,j}),L^2(\Gamma_{i+1,i})} + |\Gamma_{i+1,i}||T_{j+1,j}|\|g'\|_{\sigma,H^1(T_{j+1,j}),L^2(\Gamma_{i+1,i})} \Big)^2 \\
& + \Big(\|g'\|_{\sigma,H^1(T_{j,j}),L^2(\Gamma_{i,i})} + \|g'\|_{\sigma,H^1(T_{j+1,j}),L^2(\Gamma_{i,i})} \\
& \quad + \|g'\|_{\sigma,H^1(T_{j,j}),L^2(\Gamma_{i+1,i})} + \|g'\|_{\sigma,H^1(T_{j+1,j}),L^2(\Gamma_{i+1,i})} \Big)^2 \Bigg)^{\theta/2} \\
& \Bigg(|\Gamma_{i,i}||T_{j,j}|\|g'\|_{\sigma,H^1(T_{j,j}),L^2(\Gamma_{i,i})} + |\Gamma_{i,i}||T_{j+1,j}|\|g'\|_{\sigma,H^1(T_{j+1,j}),L^2(\Gamma_{i,i})} \\
& \quad + |\Gamma_{i+1,i}||T_{j,j}|\|g'\|_{\sigma,H^1(T_{j,j}),L^2(\Gamma_{i+1,i})} + |\Gamma_{i+1,i}||T_{j+1,j}|\|g'\|_{\sigma,H^1(T_{j+1,j}),L^2(\Gamma_{i+1,i})} \Bigg)^{1-\theta}. \qquad (5.26)
\end{aligned}
$$

Analogously to the estimate $(a+b)^2 + (\alpha a + \beta b)^2 \leq \left(a\sqrt{1+\alpha^2} + b\sqrt{1+\beta^2}\right)^2$ used in [42], there holds, for positive $a, b, c, d, \alpha, \beta, \gamma, \delta$ the estimate

$$
(a+b+c+d)^2 + (\alpha\gamma a + \alpha\delta b + \beta\gamma c + \beta\delta d)^2 \leq 2\left(a\sqrt{1+\alpha^2\gamma^2} + b\sqrt{1+\alpha^2\delta^2} + c\sqrt{1+\beta^2\gamma^2} + d\sqrt{1+\beta^2\delta^2}\right)^2
$$

since, for $a_i, b_i \geq 0$ and due to $(a+b)^2 \leq 2(a^2+b^2)$ (Young's inequality),

$$\left(\sum_i a_i\right)^2 + \left(\sum_i b_i\right)^2 \leq \left(\sum_i a_i + b_i\right)^2 \leq \left(\sum_i \sqrt{2}\sqrt{a_i^2+b_i^2}\right)^2 = 2\left(\sum_i a_i \sqrt{1+\left(\frac{a_i}{b_i}\right)^2}\right)^2 \tag{5.27}$$

which gives the claimed inequality with $a_1 = a, a_2 = b, a_3 = c, a_4 = d$ and $b_1 = \alpha\gamma a, b_2 = \alpha\delta b, b_3 = \beta\gamma c, b_4 = \beta\delta d$.

With $|\Gamma_{i+1,i}| \leq |\Gamma_{i+1}| = h_{i+1}$, $|\Gamma_{i,i}| \leq h_i$ and $|T_{j+1,j}| \leq \Delta_{j+1}$, $|T_{j,j}| \leq \Delta_j$, we obtain

$$\begin{aligned}
&\left(\frac{1}{\sqrt{2}}\right)^\theta \|\tilde{g}_{i,j}\|_{L^2([0,T],H^\theta(\Gamma))} \quad \leq \quad \|\tilde{g}_{i,j}\|_{L^2([0,T],H^\theta(\Gamma))} \\
\leq \;& \Big(\sqrt{1+h_i^2\Delta_j^2}\|g'\|_{\sigma,H^1(T_{j,j}),L^2(\Gamma_{i,i})} + \sqrt{1+h_i^2\Delta_{j+1}^2}\|g'\|_{\sigma,H^1(T_{j+1,j}),L^2(\Gamma_{i,i})} \\
&\quad + \sqrt{1+h_{i+1}^2\Delta_j^2}\|g'\|_{\sigma,H^1(T_{j,j}),L^2(\Gamma_{i+1,i})} + \sqrt{1+h_{i+1}^2\Delta_{j+1}^2}\|g'\|_{\sigma,H^1(T_{j+1,j}),L^2(\Gamma_{i+1,i})}\Big)^\theta \\
&\Big(h_i\Delta_j\|g'\|_{\sigma,H^1(T_{j,j}),L^2(\Gamma_{i,i})} + h_i\Delta_{j+1}\|g'\|_{\sigma,H^1(T_{j+1,j}),L^2(\Gamma_{i,i})} \\
&\quad + h_{i+1}\Delta_j\|g'\|_{\sigma,H^1(T_{j,j}),L^2(\Gamma_{i+1,i})} + h_{i+1}\Delta_{j+1}\|g'\|_{\sigma,H^1(T_{j+1,j}),L^2(\Gamma_{i+1,i})}\Big)^{1-\theta}.
\end{aligned} \tag{5.28}$$

In [42], it is exploited that the function

$$f(t) := K^{1-s}\left(1-\lambda+\lambda t^s\right) - \left(1-\lambda+\lambda t\right)^s$$

with $K \geq 1$ is positive for $t \in [1,K]$ and $\lambda \in [0,1]$, to show that

$$(a+b)^{1-s}(\alpha a + \beta b)^s \leq K^{1-s}(a\alpha^s + b\beta^s)$$

for positive a, b, α, β, $s \in [0,1]$ and $\frac{\alpha}{\beta} \leq K$.

Similarly, if we define

$$f(t,\tilde{t}) := K_1^{1-s}K_2^{1-s}\left(1-\lambda-\mu+\lambda t^s+\mu\tilde{t}^s\right) - \left(1-\lambda-\mu+\lambda t+\mu\tilde{t}\right)^s \tag{5.29}$$

with $K_1, K_2 \geq 1$ for $t \in [1,K_1]$, $\tilde{t} \in [1,K_2]$ and $\lambda, \mu \in [0,1]$, we have $f(1,1) = K_1^{1-s}K_2^{1-s} - 1 \geq 0$. Further,

$$\frac{\partial f}{\partial t} = \lambda s\left(K_1^{1-s}K_2^{1-s}t^{s-1} - \left(1-\lambda-\mu+\lambda t+\mu\tilde{t}\right)^{s-1}\right) \geq \lambda s\left(K_2^{1-s} - \left(1-\lambda-\mu+\lambda t+\mu\tilde{t}\right)^{s-1}\right) \geq 0.$$

Similarly, $\frac{\partial f}{\partial \tilde{t}} \geq 0$, and therefore $f \geq 0$ on the plane $[1,K_1]\times[1,K_2]$. Assuming, without loss of generality (possibly renaming pairs of variables, otherwise), $t = \frac{\alpha}{\gamma} \in [1,K_1]$, $\tilde{t} = \frac{\beta}{\gamma} \in [1,K_2]$, we obtain

$$K_1^{1-s}K_2^{1-s}\left((1-\lambda-\mu)\gamma^s + \lambda\alpha^s + \mu\beta^s\right) \geq \left((1-\lambda-\mu)\gamma + \lambda\alpha + \mu\beta\right)^s. \tag{5.30}$$

For $\lambda = \frac{a}{a+b+c}$, $\mu = \frac{a}{a+b+c}$ with $1-\lambda-\mu = \frac{c}{a+b+c}$, we obtain

$$(a+b+c)^{1-s}(\alpha a+\beta b+\gamma c)^s \leq K_1^{1-s}K_2^{1-s}(a\alpha^s + b\beta^s + c\gamma^s). \tag{5.31}$$

Obviously, this result can be extended to the case of eight variables instead of six in a similar way. We set

$$a := \sqrt{1+h_i^2\Delta_j^2}\|g'\|_{\sigma,H^1(T_{j,j}),L^2(\Gamma_{i,i})} \qquad \alpha := \frac{h_i\Delta_j}{\sqrt{1+h_i^2\Delta_j^2}}$$

$$b := \sqrt{1+h_i^2\Delta_{j+1}^2}\|g'\|_{\sigma,H^1(T_{j,j+1}),L^2(\Gamma_{i,i})} \qquad \beta := \frac{h_i\Delta_{j+1}}{\sqrt{1+h_i^2\Delta_{j+1}^2}}$$

$$c := \sqrt{1+h_{i+1}^2\Delta_j^2}\|g'\|_{\sigma,H^1(T_{j,j}),L^2(\Gamma_{i,i+1})} \qquad \gamma := \frac{h_{i+1}\Delta_j}{\sqrt{1+h_{i+1}^2\Delta_j^2}}$$

$$d := \sqrt{1+h_{i+1}^2\Delta_{j+1}^2}\|g'\|_{\sigma,H^1(T_{j,j+1}),L^2(\Gamma_{i,i+1})} \qquad \delta := \frac{h_{i+1}\Delta_{j+1}}{\sqrt{1+h_{i+1}^2\Delta_{j+1}^2}}$$

and note that

$$\frac{\gamma}{\delta} \le K_2 \text{ if } \frac{h_{i+1}\Delta_j}{h_{i+1}\Delta_{j+1}} = \frac{\Delta_j}{\Delta_{j+1}} \le K_2 \qquad \text{and} \qquad \frac{\beta}{\delta} \le K_1 \text{ if } \frac{h_i\Delta_{j+1}}{h_{i+1}\Delta_{j+1}} = \frac{h_i}{h_{i+1}} \le K_1.$$

This also implies $\frac{\alpha}{\delta} = \frac{h_i\Delta_j}{h_{i+1}\Delta_{j+1}} \le K_1K_2$.

Applying the estimate (5.31) with $s = 1-\theta$ (and eight variables instead of six) to (5.28), we obtain

$$\begin{aligned}(K_1K_2)^{-\theta}\|\tilde{g}_{i,j}\|_{L^2([0,T],H^\theta(\Gamma))} \le\ & \left(1+h_i^2\Delta_j^2\right)^{\theta/2}(h_i\Delta_j)^{1-\theta}\|g'\|_{\sigma,H^1(T_{j,j}),L^2(\Gamma_{i,i})} \\ &+ \left(1+h_i^2\Delta_{j+1}^2\right)^{\theta/2}(h_i\Delta_{j+1})^{1-\theta}\|g'\|_{\sigma,H^1(T_{j+1,j}),L^2(\Gamma_{i,i})} \\ &+ \left(1+h_{i+1}^2\Delta_j^2\right)^{\theta/2}(h_{i+1}\Delta_j)^{1-\theta}\|g'\|_{\sigma,H^1(T_{j,j}),L^2(\Gamma_{i+1,i})} \\ &+ \left(1+h_{i+1}^2\Delta_{j+1}^2\right)^{\theta/2}(h_{i+1}\Delta_{j+1})^{1-\theta}\|g'\|_{\sigma,H^1(T_{j+1,j}),L^2(\Gamma_{i+1,i})}\end{aligned} \tag{5.32}$$

and, consequently by (5.24),

$$\begin{aligned}&(K_1K_2)^{-\theta}\|g\|_{\sigma,0,H^\theta(\Gamma)} \\ \le\ & \sum_{i=0}^{N-1}\sum_{j=0}^{M}\left(1+h_i^2\Delta_j^2\right)^{\theta/2}(h_i\Delta_j)^{1-\theta}\Big(\ \|g'\|_{\sigma,H^1(T_{j,j}),L^2(\Gamma_{i,i})} + \|g'\|_{\sigma,H^1(T_{j,j-1}),L^2(\Gamma_{i,i})} \\ &\qquad + \|g'\|_{\sigma,H^1(T_{j,j}),L^2(\Gamma_{i,i-1})} + \|g'\|_{\sigma,H^1(T_{j,j-1}),L^2(\Gamma_{i,i-1})}\Big).\end{aligned}$$

This implies

$$\|g\|_{\sigma,0,H^\theta(\Gamma)} \le 2\,(K_1K_2)^\theta\sum_{i=1}^{N}\sum_{j=1}^{M}\left(1+h_i^2\Delta_j^2\right)^{\theta/2}(h_i\Delta_j)^{1-\theta}\|g'\|_{\sigma,H^1(T_j),L^2(\Gamma_i)} \tag{5.33}$$

as claimed. ∎

Having Proposition 5.7 and the results of the previous section at hand, we now obtain, in addition to Corollary 5.4, another a posteriori estimate on the error term $\|p-p_N\|_{\sigma,-1/2-2|s|,H^{-1/2+s}(\Gamma)}$ for $s \in \left(-\frac{1}{2},\frac{1}{2}\right)$, which features only local quantities on the right hand side.

Corollary 5.8 (Space-Time Version of [42, Theorem 1])
Let the assumptions of Corollary 5.4 hold. Then there holds the a posteriori error estimate

$$\begin{aligned} &\|p - p_N\|_{\sigma,-1/2-2|s|,H^{-1/2+s}(\Gamma)} \\ \leq\ & 2\, C_{V^{-1}} \left(K_1 K_2\right)^{s+1/2} \sum_{i=1}^{N} \sum_{j=1}^{M} \left(1 + h_i^2 \Delta_j^2\right)^{1/4+s/2} \left(h_i \Delta_j\right)^{1/2-s} \|\Lambda^{5/2} R'\|_{\sigma,L^2(T_j),L^2(\Gamma_i)} \end{aligned}$$

for $s \in \left(-\frac{1}{2}, \frac{1}{2}\right)$, where $C_{V^{-1}} = C_{V^{-1}}(\Gamma, \sigma_0, s)$ is the norm of the inverse Single Layer operator V^{-1} as in Lemma 3.47, and K_1, K_2 are as in Proposition 5.7.

Proof
By (5.7),

$$\begin{aligned} \|p - p_N\|_{\sigma,-1/2-2|s|,H^{-1/2+s}(\Gamma)} &= \|V^{-1}[R]\|_{\sigma,-1/2-2|s|,H^{-1/2+s}(\Gamma)} \\ &\leq C_{V^{-1}} \|R\|_{\sigma,3/2,H^{1/2+s}(\Gamma)} = C_{V^{-1}} \|\Lambda^{3/2} R\|_{\sigma,0,H^{1/2+s}(\Gamma)}. \end{aligned}$$

By assumption, $R \in \mathcal{H}^{5/2}_{\sigma}(\mathbb{R}, H^1(\Gamma))$, and therefore $\Lambda^{3/2} R \in \mathcal{H}^{1}_{\sigma}(\mathbb{R}, H^1(\Gamma))$. This allows us to apply Proposition 5.7 with $\theta = \frac{1}{2} + s$ to bound the term $\|\Lambda^{3/2} R\|_{\sigma,0,H^{1/2+s}(\Gamma)}$, which yields the claim. ∎

Remark 5.9 (On Lemma 5.7 and Corollary 5.8)

a) *It is not clear whether a modification of Lemma 5.7 that makes use of energy-based norms instead of the classical norms, such as the one discussed in Remark 5.5 b) for the first a posteriori error estimate, can be proven.*

b) *(usage in adaptive algorithms) As in Remark 5.5 e), we consider the case $s = 0$ and write $a_{i,j} := \|\Lambda^{5/2} R'\|_{\sigma,L^2(T_j),L^2(\Gamma_i)}$. By Corollary 5.8 and using $(1 + h_i^2 \Delta_j^2)^{1/4} \leq C(\Gamma, T)$,*

$$\|p - p_N\|_{\sigma,-1/2,H^{-1/2}(\Gamma)} \leq 2\, C_{V^{-1}} C(\Gamma, T) \left(K_1 K_2\right)^{1/2} \sum_{i=1}^{N} \sum_{j=1}^{M} h_i^{1/2} \Delta_j^{1/2} a_{i,j}.$$

One would thus use the terms $h_i^{1/2} \Delta_j^{1/2} a_{i,j}$ to steer an adaptive algorithm.

c) *We have only made use of spatial interpolation here, namely for the estimates* (5.1) *and* (5.25)*, and therefore broken-order temporal norms appear in the right hand sides of the estimates. One could, alternatively, use a 'double interpolation' in space and time to get rid of the broken-order terms. However, since the temporal order within the mapping properties is obscure anyway, we have used R in place of any $\Lambda^s R$ terms in $a_{i,j}$ in our practical computations, i.e. the terms*

$$\tilde{a}_{i,j} := \|R'\|_{\sigma,L^2(T_j),L^2(\Gamma_i)} \tag{5.34}$$

which gave reasonable results. We further note that the error indicators $\tilde{a}_{i,j}$ are always heuristically reasonable.

5.2 Faermann-Type A Posteriori Error Estimate

We now consider the type of a posteriori error estimates introduced by Faermann. The main idea behind these estimates is, in short, to find bounds involving local measures for the broken-order norms that naturally appear when dealing with Boundary Element Methods and which are, crucially, non-additive. We begin with a result by Faermann.

Lemma 5.10 ([67, Lemma 2.5])
Let $I \subseteq \mathbb{R}$ be an arbitrary interval. Then, for any $\mu \in (0,1)$ and $v \in H^\mu(I)$,

$$\|v\|^2_{L^2(I)} \leq \frac{1}{2}|I|^{2\mu}|v|^2_{H^\mu(I)} + \frac{1}{|I|}\left|\int_I v(x)\,dx\right|^2. \tag{5.35}$$

Faermann uses this result in the proof of [67, Lemma 2.7] and estimates the term $\left|\int_{S_i} v(x)\,dx\right|^2$ in (5.35) for any $v \in H^\mu(\Gamma)$ that is orthogonal to V_h^p, where $S_i = \operatorname{supp}\varphi_i^p$, by

$$\left|\int_{S_i} v(x)\,dx\right| = \left|\int_{S_i} v(x)\left(1-\varphi_i^p\right)\,dx\right| \leq \|v\|_{L^2(S_i)}\|1-\varphi_i^p\|_{L^2(S_i)}.$$

In [67, Lemma 2.6], it is shown that

$$\|1-\varphi_i^p\|_{L^2(S_i)} \leq C^{1/2}|S_i|^{1/2}$$

with constants $C = C(p, K(\mathcal{T}_S)) \in [0,1)$ (given in explicit form for $p = 0,1,2$) and $K(\mathcal{T}_S)$ as in (2.3). Consequently,

$$\frac{1}{|S_i|}\left|\int_{S_i} v(x)\,dx\right|^2 \leq C\|v\|^2_{L^2(S_i)}$$

and hence, by Lemma 5.10 and with the same constant $C = C(p, K(\mathcal{T}_S))$,

$$\|v\|^2_{L^2(S_i)} \leq \frac{1}{2(1-C)}|S_i|^{2\mu}|v|^2_{H^\mu(S_i)}. \tag{5.36}$$

Alternatively, one can use the Cauchy-Schwarz inequality and obtains

$$\left|\int_{S_i} v(x)\,dx\right| \leq |S_i|^{1/2}\|v\|_{L^2(S_i)} \tag{5.37}$$

where, due to the Galerkin orthogonality,

$$\|v\|^2_{L^2(S_i)} = \int_{S_i} v^2(x)\,dx = \int_{S_i} v(x)\left(v(x)-\alpha\varphi_i^p\right)\,dx$$

for any $\varphi_i^p \in V_h$ and any $\alpha \in \mathbb{R}$. Therefore, due to the Cauchy-Schwarz inequality and (3.156),

$$\|v\|_{L^2(S_i)} \leq \inf_{w_i \in \operatorname{span}\{\varphi_i^p\}} \|v-w_i\|_{L^2(S_i)} \leq C|S_i|^\mu |v|_{H^\mu(S_i)} \tag{5.38}$$

where the constant $C = C(p)$ depends only on p in the two dimensional case. Similarly to (5.36), there consequently holds

$$\|v\|^2_{L^2(S_i)} \leq \left(\frac{1}{2}+C^2\right)|S_i|^{2\mu}|v|^2_{H^\mu(S_i)} \tag{5.39}$$

for any $v \in H^\mu(S_i)$ that is orthogonal to V_h^p, where the factor $\left(\frac{1}{2}+C^2\right)$ is now no longer known explicitly. However, this alternative approach will prove to be helpful when dealing with the time dependent case.

Note that, for $v \in L^2((0,T), H^\mu(I))$, the estimate (5.35) in Lemma 5.10 can be adapted to

$$\int_0^T \|v(\cdot,t)\|^2_{L^2(I)}\,dt = \|v\|^2_{L^2((0,T),L^2(I))} \leq \frac{1}{2}|I|^{2\mu}\|v\|^2_{L^2((0,T),H^\mu(I))} + \frac{1}{|I|}\int_0^T \left|\int_I v(x,t)\,dx\right|^2 dt \tag{5.40}$$

where the last term can, similarly to (5.37), be estimated by

$$\begin{aligned}\frac{1}{|I|}\int_0^T \left|\int_I v(x,t)\,dx\right|^2 dt &\le \frac{1}{|I|}\int_0^T \left(\int_I |v(x,t)|\,dx\right)^2 dt \\ &\le \frac{1}{|I|}\int_0^T \left(|I|^{1/2}\left(\int_I |v(x,t)|^2\,dx\right)^{1/2}\right)^2 dt = \|v\|^2_{L^2((0,T),L^2(I))}.\end{aligned}$$

By taking $I = (0,T)$ in Lemma 5.10 and integrating over an arbitrary interval $I \subseteq \mathbb{R}$ there holds, by (5.40),

$$\|v\|^2_{L^2((0,T),L^2(I))} \le \frac{1}{2}|T|^{2\kappa}\|v\|^2_{H^\kappa((0,T),L^2(I))} + \|v\|^2_{L^2((0,T),L^2(I))} \tag{5.41}$$

for any $v \in H^\kappa((0,T),L^2(I))$ with $\kappa \in (0,1)$. Combining (5.40) and (5.41), we obtain

$$\|v\|^2_{L^2((0,T),L^2(I))} \le \frac{1}{4}\left(|I|^{2\mu}+|T|^{2\kappa}\right)\|v\|^2_{L^2((0,T),H^\mu(I))\cap H^\kappa((0,T),L^2(I))} + \|v\|^2_{L^2((0,T),L^2(I))} \tag{5.42}$$

for any $v \in L^2((0,T),H^\mu(I)) \cap H^\kappa((0,T),L^2(I))$.

If we assume orthogonality in the form $\int_0^T \int_I v(x,t) w_N(x,t)\,dx\,dt = 0$ for any $w_N \in V_N$, we obtain a bound similar to (5.38),

$$\|v\|^2_{L^2(T_j,L^2(S_i))} \le \inf_{w_{i,j}\in \operatorname{span}\left\{\varphi_i^p \beta_j^q\right\}} \|v - w_{i,j}\|^2_{L^2(T_j,L^2(S_i))}$$

where $S_i \times T_j = \operatorname{supp}\left(\varphi_i^p \beta_j^q\right)$. Applying the approximation properties (Proposition 3.52), we obtain

$$\|v\|^2_{L^2(T_j,L^2(S_i))} \le C_1\left(|S_i|^\mu + |T_j|^\kappa\right)^2 \|v\|^2_{L^2(T_j,H^\mu(S_i))\cap H^\kappa(T_j,L^2(S_i))}$$

with $C_1 = C_1(p,q,\mu,\kappa)$ depending only on p,q and μ,κ, and therefore

$$\|v\|^2_{L^2(T_j,L^2(S_i))} \le \left(\frac{1}{4}+2C_1\right)\left(|S_i|^{2\mu}+|T_j|^{2\kappa}\right)\|v\|^2_{L^2(T_j,H^\mu(S_i))\cap H^\kappa(T_j,L^2(S_i))}. \tag{5.43}$$

By [39, Lemma 4.2], [67, Lemma 2.3] there holds, for any $v \in L^2((0,T),H^\mu(\Gamma))$ and after integrating over $(0,T)$, the estimate

$$\|v\|^2_{L^2((0,T),H^\mu(\Gamma))} \le \sum_{i=1}^N \|v\|^2_{L^2((0,T),H^\mu(\Gamma_i\cup\Gamma_{i+1}))} + C_2\sum_{i=1}^N d_i^{-2\mu}\|v\|^2_{L^2((0,T),L^2(\Gamma_i))} \tag{5.44}$$

where $C_2 = C_2(\gamma,\mu)$ depends only on the parameterisation γ of Γ and on μ, and [39, (4.2)] $d_i := \operatorname{dist}(\Gamma_i, \Gamma \setminus (\Gamma_{i-1}\cup\Gamma_i\cup\Gamma_{i+1})) = \min\{|\Gamma_{i-1}|,|\Gamma_{i+1}|\}$, with $\Gamma_{N+1} := \Gamma_1$ and $\Gamma_0 := \Gamma_N$.

Similarly, for any $H^\kappa((0,T),L^2(\Gamma))$,

$$\|v\|^2_{H^\kappa((0,T),L^2(\Gamma))} \le \sum_{j=0}^M \|v\|^2_{H^\kappa(T_j\cup T_{j+1},L^2(\Gamma))} + C_3\sum_{j=1}^M d_j^{-2\kappa}\|v\|^2_{L^2(T_j,L^2(\Gamma))} \tag{5.45}$$

where $C_3 = C_3(\kappa)$ depends only on κ, and

$$d_j := \operatorname{dist}(T_j, (0,T)\setminus(T_{j-1}\cup T_j\cup T_{j+1})) = \min\{|T_{j-1}|,|T_{j+1}|\}$$

with $T_0 \coloneqq T_{M+1} \coloneqq \varnothing$. Combining the last two estimates, and using the fact that the L^2-norm is always additive, we obtain

$$\begin{aligned}\|v\|^2_{L^2((0,T),H^\mu(\Gamma))\cap H^\kappa((0,T),L^2(\Gamma))} \quad \leq \quad & \sum_{i=1}^{N}\sum_{j=0}^{M}\Big(\|v\|^2_{L^2(T_j,H^\mu(\Gamma_i\cup\Gamma_{i+1}))} + \|v\|^2_{H^\kappa(T_j\cup T_{j+1},L^2(\Gamma_i))}\Big) \\ & + C_4\sum_{i=1}^{N}\sum_{j=1}^{M}\left(d_i^{-2\mu}+d_j^{-2\kappa}\right)\|v\|^2_{L^2(T_j,L^2(\Gamma_i))} \end{aligned} \tag{5.46}$$

for any $v \in L^2((0,T),H^\mu(\Gamma)) \cap H^\kappa((0,T),L^2(\Gamma))$, where

$$C_4 = C_4(\gamma,\mu,\kappa) \coloneqq \max\left\{C_2(\gamma,\mu), C_3(\kappa)\right\}.$$

Using (5.43) and setting $\tilde{C}_1(p,q,\mu,\kappa) \coloneqq \left(\frac{1}{4} + 2C_1(p,q,\mu,\kappa)\right)$, we obtain

$$\left(d_i^{-2\mu}+d_j^{-2\kappa}\right)\|v\|^2_{L^2(T_j,L^2(\Gamma_i))} \leq \tilde{C}_1\left(d_i^{-2\mu}+d_j^{-2\kappa}\right)\left(|S_i|^{2\mu}+|T_j|^{2\kappa}\right)\|v\|^2_{L^2(T_j,H^\mu(S_i))\cap H^\kappa(T_j,L^2(S_i))} \tag{5.47}$$

for any $i \in \{1,\dots,N\}$, $j \in \{1,\dots,M\}$. Clearly, $d_i^{-2\mu}|S_i|^{2\mu} \leq K(\mathcal{T}_{S,T})^{2\mu}$ and $d_j^{-2\kappa}|T_j|^{2\kappa} \leq K(\mathcal{T}_{S,T})^{2\kappa}$. However, to bound the terms $d_j^{-2\kappa}|S_i|^{2\mu}$ and $d_i^{-2\mu}|T_j|^{2\kappa}$ as well, we assume $\kappa = \mu$ from here on. These terms can be bounded with the help of the global mesh constant $q(\mathcal{T}_{S,T})$, namely $d_j^{-2\mu}|S_i|^{2\mu} \leq q(\mathcal{T}_{S,T})^{2\mu}$ and $d_i^{-2\mu}|T_j|^{2\mu} \leq q(\mathcal{T}_{S,T})^{2\mu}$. With

$$C = C(\gamma,\mu,p,q,K(\mathcal{T}_{S,T}),K(\mathcal{T}_{S,T}),q(\mathcal{T}_{S,T})) > 0$$

we then have

$$\begin{aligned} & \|v\|^2_{L^2((0,T),H^\mu(\Gamma))\cap H^\mu((0,T),L^2(\Gamma))} \\ \leq \quad & \sum_{i=1}^{N}\sum_{j=0}^{M}\Big(\|v\|^2_{L^2(T_j,H^\mu(\Gamma_i\cup\Gamma_{i+1}))} + \|v\|^2_{H^\mu(T_j\cup T_{j+1},L^2(\Gamma_i))}\Big) \\ & + C_4\tilde{C}_1\left(K(\mathcal{T}_{S,T})^{2\mu} + 2q(\mathcal{T}_{S,T})^{2\mu} + K(\mathcal{T}_{S,T})^{2\mu}\right)\sum_{i=1}^{N}\sum_{j=1}^{M}\|v\|^2_{L^2(T_j,L^2(\Gamma_i))} \\ \leq \quad & C\sum_{i=1}^{N}\sum_{j=0}^{M}\Big(\|v\|^2_{L^2(T_j,H^\mu(\Gamma_i\cup\Gamma_{i+1}))} + \|v\|^2_{H^\mu(T_j\cup T_{j+1},L^2(\Gamma_i))}\Big) \end{aligned} \tag{5.48}$$

for any $v \in L^2((0,T),H^\mu(\Gamma)) \cap H^\mu((0,T),L^2(\Gamma))$ that is orthogonal to V_N, similarly to [67, Theorem 2.2], and therefore:

Lemma 5.11 (Space-Time Version of [67, Theorem 2.2])
Let $v \in L^2((0,T),H^\mu(\Gamma)) \cap H^\mu((0,T),L^2(\Gamma))$ satisfy $\int_0^T \int_\Gamma v(x,t)w_N(x,t)\,ds_x\,dt = 0$ for any $w_N \in V_N$, and $\mu \in (0,1)$. Then there exists a constant $C = C(\gamma,\mu,p,q,K(\mathcal{T}_{S,T}),K(\mathcal{T}_{S,T}),q(\mathcal{T}_{S,T}))$ such that

$$\|v\|^2_{L^2((0,T),H^\mu(\Gamma))\cap H^\mu((0,T),L^2(\Gamma))} \leq C\sum_{i=1}^{N}\sum_{j=0}^{M}\Big(\|v\|^2_{L^2(T_j,H^\mu(\Gamma_i\cup\Gamma_{i+1}))} + \|v\|^2_{H^\mu(T_j\cup T_{j+1},L^2(\Gamma_i))}\Big).$$

We note that the bound in Lemma 5.11 involves the global constant $q(\mathcal{T}_{S,T})$ and is therefore more restrictive than the bounds proven by Faermann for the spatial case that involve only local quantities.

Obviously, Lemma 5.11 can be used with the spaces $H_\Gamma^{\mu;\mu,\mu}$ if v is assumed to have finite support, and consequently, due to (3.111), also with the spaces $H_{\sigma,\Gamma}^{\mu;\mu,\mu}$.

By Lemma 3.47 there holds, for any $\mu \in (0,1)$,

$$\|V^{-1}[R]\|_{\sigma,\Gamma;\,0;\,\mu-1,\mu-1} \le C_{V^{-1}} \|R\|_{\sigma,\Gamma;\,1+2|\mu-1/2|;\,\mu,\mu} = C_{V^{-1}} \|\dot R\|_{\sigma,\Gamma;\,2|\mu-1/2|;\,\mu,\mu}$$

or

$$\|V^{-1}[R]\|_{\sigma,\Gamma;\,\mu-2|\mu-1/2|;\,\mu-1,\mu-1} \le C_{V^{-1}} \|\dot R\|_{\sigma,\Gamma;\,\mu;\,\mu,\mu}$$

with $C_{V^{-1}} = C_{V^{-1}}(\Gamma,\sigma_0,\mu)$. In terms of $s \in \left(-\frac12,\frac12\right)$, this is

$$\|p-p_N\|_{\sigma,\Gamma;\,s+1/2-2|s|;\,s-1/2,s-1/2} = \|V^{-1}[R]\|_{\sigma,\Gamma;\,s+1/2-2|s|;\,s-1/2,s-1/2} \le C_{V^{-1}} \|\dot R\|_{\sigma,\Gamma;\,s+1/2;\,s+1/2,s+1/2}.$$

By (5.3), $\dot R$ is orthogonal to V_N, and Lemma 5.11 can therefore be applied with $v = \Lambda^{s+1/2}\dot R$ to bound the term on the right hand side, and therewith the error term on the left hand side. This proves reliability in the form

$$\|p-p_N\|_{\sigma,\Gamma;\,s+1/2-2|s|;\,s-1/2,s-1/2} \le C \sum_{i=1}^N \sum_{j=0}^M b_{i,j} \tag{5.49}$$

with $b_{i,j} := \|e^{-\sigma t}\Lambda^{s+1/2}\dot R\|_{L^2(T_j,H^{s+1/2}(\Gamma_i\cup\Gamma_{i+1}))} + \|e^{-\sigma t}\Lambda^{s+1/2}\dot R\|_{H^{s+1/2}(T_j\cup T_{j+1},L^2(\Gamma_i))}$. Note that the error term in (5.49) also bounds the error in the $\|\cdot\|_{\sigma,\Gamma;\,s-2|s|;\,s-1/2,s-1/2}$-norm, which seems to be the more natural norm.

Regarding efficiency, we can proceed as in [67, Theorem 3.1] to see that the first term in the estimate in Lemma 5.11 can be bounded by

$$\sum_{i=1}^N \sum_{j=0}^M \|v\|^2_{L^2(T_j,H^\mu(\Gamma_i\cup\Gamma_{i+1}))} = \sum_{i=1}^N \|v\|^2_{L^2((0,T),H^\mu(\Gamma_i\cup\Gamma_{i+1}))} \le 2\|v\|^2_{L^2((0,T),H^\mu(\Gamma))}$$

and the second, similarly, by

$$\sum_{i=1}^N \sum_{j=0}^M \|v\|^2_{H^\mu(T_j\cup T_{j+1},L^2(\Gamma_i))} \le 2\|v\|^2_{H^\mu((0,T),L^2(\Gamma))}.$$

Hence we have an inverse estimate to the one of Lemma 5.11,

$$\sum_{i=1}^N \sum_{j=0}^M \left(\|v\|^2_{L^2(T_j,H^\mu(\Gamma_i\cup\Gamma_{i+1}))} + \|v\|^2_{H^\mu(T_j\cup T_{j+1},L^2(\Gamma_i))}\right) \le 2\|v\|^2_{L^2((0,T),H^\mu(\Gamma))\cap H^\mu((0,T),L^2(\Gamma))}$$

for any $v \in L^2((0,T),H^\mu(\Gamma))\cap H^\mu((0,T),L^2(\Gamma))$. Using the mapping properties (Theorem 3.46), we obtain

$$\|R\|_{\sigma,\Gamma;\,s+1/2;\,s+1/2,s+1/2} = \|V\,[p-p_N]\,\|_{\sigma,\Gamma;\,s+1/2;\,s+1/2,s+1/2} \le C\|p-p_N\|_{\sigma,\Gamma;\,s+3/2;\,s-1/2,s-1/2}$$

with $C = C(\Gamma,\sigma_0,s)$. Taking $v = R$, we can therefore conclude efficiency, but not for the error indicators $b_{i,j}$ defined above.

Note that a bound for the classical space-time norms cannot be derived in a similar way. Applying [67, Lemma 2.3] twice, one can only show

$$\begin{aligned}
&\|v\|^2_{H^\kappa((0,T),H^\mu(\Gamma))}\\
\le\ & \sum_{i=1}^N \sum_{j=0}^M \|v\|^2_{H^\kappa(T_j\cup T_{j+1},H^\mu(\Gamma_i\cup\Gamma_{i+1}))} + C_\kappa \sum_{i=1}^N \sum_{j=0}^M d_j^{-2\kappa}\|v\|^2_{L^2(T_j,H^\mu(\Gamma_i\cup\Gamma_{i+1}))}\\
&+C_\mu \sum_{i=1}^N \sum_{j=0}^M d_i^{-2\mu}\|v\|^2_{H^\kappa(T_j\cup T_{j+1},L^2(\Gamma_i))} + C_\kappa C_\mu \sum_{i=1}^N \sum_{j=0}^M d_i^{-2\mu} d_j^{-2\kappa}\|v\|^2_{L^2(T_j,L^2(\Gamma_i))}
\end{aligned}$$

where the term $d_i^{-2\mu} d_j^{-2\kappa} \|v\|^2_{L^2(T_j, L^2(\Gamma_i))}$ cannot be bounded. One can, however, use $\|v\|_{H^\mu((0,T),H^\mu(\Gamma))} \leq \|\Lambda^\mu v\|_{L^2((0,T),H^\mu(\Gamma))\cap H^\mu((0,T),L^2(\Gamma))}$ to derive bounds, for instance

$$\begin{aligned}\|p - p_N\|_{\sigma,-2-2|\mu-1/2|+\mu,H^{\mu-1}(\Gamma)} &= \|V^{-1}[R]\|_{\sigma,-2-2|\mu-1/2|+\mu,H^{\mu-1}(\Gamma)} \leq C_{V^{-1}} \|R\|_{\sigma,\mu,H^\mu(\Gamma)} \\ &\leq C_{V^{-1}} \|\dot{R}\|_{L^2((0,T),H^\mu(\Gamma))\cap H^\mu((0,T),L^2(\Gamma))}.\end{aligned}$$

In terms of $s \in \left(-\frac{1}{2}, \frac{1}{2}\right)$, this is

$$\|p - p_N\|_{\sigma,s-3/2-2|s|,H^{s-1/2}(\Gamma)} \leq C_{V^{-1}} \|\dot{R}\|_{L^2((0,T),H^{s-1/2}(\Gamma))\cap H^{s-1/2}((0,T),L^2(\Gamma))}. \tag{5.50}$$

The term on the right hand side of (5.50) is bounded by Lemma 5.11.

We note that, in contrast to the estimates in Corollaries 5.4 and 5.8, the estimated error norm is weaker by one temporal order for $s = 0$. In practice, we use

$$\sum_{i=1}^{N} \sum_{j=0}^{M} \|R\|^2_{L^2(T_j, H^{1/2}(\Gamma_i \cup \Gamma_{i+1}))} \tag{5.51}$$

as an error estimator, where the $H^{1/2}(\Gamma_i \cup \Gamma_{i+1})$-norm [39, (3.3)], [67, (1.6)]

$$\|v\|^2_{H^{1/2}(\Gamma_i \cup \Gamma_{i+1})} = \int_{\Gamma_i \cup \Gamma_{i+1}} \int_{\Gamma_i \cup \Gamma_{i+1}} \frac{|v(x) - v(y)|^2}{|x - y|^2} \, ds_y \, ds_x \tag{5.52}$$

is approximated by graded quadrature.

5.3 N-$N/2$-Type A Posteriori Error Estimate

A posteriori error estimators of h-$h/2$-type for Boundary Element Methods have enjoyed considerable research interest recently. These error estimates are based on the computation of the difference of two approximations, one on the current grid and one on the corresponding globally refined grid, in a certain norm. Praetorius et al. [60, 72] have studied such error estimators for the Single Layer integral equation of the Laplace problem, which is also known as Symm's integral equation, and for the hypersingular integral equation [61].

Compared to other types of error estimators, h-$h/2$-type error estimators for Symm's integral equation have some striking advantages: They are easily (yet expensively) calculated, and their implementation leads to almost no computational overhead. They are always efficient and, using a (standard and reasonable) saturation assumption, reliable. As the residual error estimators, they are further an intuitive error bound. In what follows, we investigate how these error estimators can be adapted to our time dependent setup.

We begin with some general observations. The aforementioned works by Praetorius et al. have all been done in a setup in which the bilinear form corresponding to the problem is symmetric. Since the bilinear form $a^V_\sigma(\cdot,\cdot)$ of the problem that we study is not symmetric, we drop this assumption and consider an arbitrary, non-symmetrical bilinear form $b(\cdot,\cdot)$ that induces the energy norm $|||p|||^2_b := b(p,p)$. As before, we write p and p_N for the problem's exact solution and its approximation, both given by weak formulations involving $b(\cdot,\cdot)$. Further, let X_N be the current approximation space, and let $\hat{X}_N \supseteq X_N$ be the approximation space of the same polynomial order with underlying spatial and temporal meshes that have both been refined uniformly, in which an approximation $\hat{p}_N \in \hat{X}_N$ is computed. Assuming a Galerkin orthogonality of type (5.3), there

holds, since $p_N \in X_N \subseteq \hat{X}_N$,

$$\begin{aligned}
\|\!|p - p_N|\!\|_b^2 &= b(p - p_N, p - p_N) \\
&= b(p - \hat{p}_N, p - \hat{p}_N) + b(\hat{p}_N - p_N, p - \hat{p}_N) + \underbrace{b(p - \hat{p}_N, \hat{p}_N - p_N)}_{=0} + b(\hat{p}_N - p_N, \hat{p}_N - p_N) \\
&= \|\!|p - \hat{p}_N|\!\|_b^2 + \|\!|\hat{p}_N - p_N|\!\|_b^2 + b(\hat{p}_N - p_N, p - \hat{p}_N). \qquad (5.53)
\end{aligned}$$

If the bilinear form $b(\cdot,\cdot)$ is symmetric, the non-norm term in (5.53) vanishes, and one can conclude $\|\!|\hat{p}_N - p_N|\!\|_b \leq \|\!|p - p_N|\!\|_b$ without any further assumptions. This immediately implies efficiency of the error estimator

$$\eta := \|\!|\hat{p}_N - p_N|\!\|_b . \qquad (5.54)$$

In the non-symmetrical case, however, we cannot even determine the sign of $b(\hat{p}_N - p_N, p - \hat{p}_N)$. In fact, we can only show that $b(\hat{p}_N - p_N, p - \hat{p}_N) \leq \|\!|p - p_N|\!\|_b^2$. Praetorius et al. impose the *saturation assumption*

$$\|\!|p - \hat{p}_N|\!\|_b \leq \kappa \, \|\!|p - p_N|\!\|_b \qquad (5.55)$$

with $\kappa \in (0,1)$ to prove reliability. A saturation assumption of the type (5.55) has been proven to hold for some Finite Element problem in [123], but it is not clear whether these also hold for other cases.

Since

$$\eta = \|\!|\hat{p}_N - p_N|\!\|_b \leq \|\!|p - p_N|\!\|_b + \|\!|p - \hat{p}_N|\!\|_b \leq (1 + \kappa) \, \|\!|p - p_N|\!\|_b$$

the error estimator η is always efficient if (5.55) is assumed. Further, by the triangle inequality and (5.55),

$$\|\!|p - p_N|\!\|_b \leq \|\!|p - \hat{p}_N|\!\|_b + \eta \leq \kappa \, \|\!|p - p_N|\!\|_b + \eta$$

and η is thus reliable in the form $\eta \geq (1 - \kappa) \, \|\!|p - p_N|\!\|_b$ with the same κ-dependent constant as in the symmetric case for error estimators of this type. Combining both estimates, we get

$$\frac{\eta}{1 + \kappa} \leq \|\!|p - p_N|\!\|_b \leq \frac{\eta}{1 - \kappa}.$$

This means that efficiency still holds, but only under the saturation assumption (5.55), and with a less favourable constant. We further note that, differently to the symmetric case, reliability is not equivalent to the saturation assumption here.

The error estimator η cannot immediately be used as an error indicator in adaptive algorithms in general. In the case of Symm's integral equation, the energy norm is equivalent to the $H^{-1/2}(\Gamma)$-norm, which cannot be localised. Praetorius et al. [60, 72] therefore introduce an equivalent error estimator that involves only the localisable $L^2(\Gamma)$-norm. In our case, it is not even clear if the energy norm induced by the bilinear form $a_\sigma^V(\cdot,\cdot)$ is equivalent to some space-time norm, or to which, as discussed in Section 4.1. We, therefore, cannot proceed in an entirely similar way here, and our results are less satisfactory, due to the hideous mapping properties of the time domain Single Layer operator discussed in Section 3.3.2. However, we can still find computable and localisable upper and lower bounds on η. From here onwards, we replace the abstract bilinear form $b(\cdot,\cdot)$ and the induced energy norm $\|\!|\cdot|\!\|_b$ by our bilinear form $a_\sigma^V(\cdot,\cdot)$ and its underlying energy norm $\|\!|\cdot|\!\|$, given by (4.14). Since the underlying mesh size does not solely depend on the spatial mesh size h in the space-time setup, we use the term $h\Delta t$-$(h\Delta t)/2$-*type* or N-$N/2$-*type error estimators* for the error estimators η.

Let us consider reliability first. By the inverse inequality (3.179), there holds

$$h^{1/2} \|q_N\|_{\sigma,-1/2,L^2(\Gamma)} \leq C_1 \|q_N\|_{\sigma,-1/2,H^{-1/2}(\Gamma)}$$

for any $q_N \in V_N$, with $C_1 = C_1(\sigma, p, q, K(\mathcal{T}_S), K(\mathcal{T}_T))$. Further, by (4.16),

$$\|q\|_{\sigma,-1/2,H^{-1/2}(\Gamma)} \leq C_2 \,|\!|\!| q |\!|\!|$$

for any $q \in \mathcal{H}^{-1/2}_\sigma(\mathbb{R}, H^{-1/2}(\Gamma))$, with $C_2 = C(\Gamma, \sigma_0)$. Hence

$$h^{1/2}\|q_N\|_{\sigma,-1/2,L^2(\Gamma)} \leq C_1 C_2 \,|\!|\!| q_N |\!|\!|$$

for any $q_N \in V_N \cap \mathcal{H}^{-1/2}_\sigma(\mathbb{R}, H^{-1/2}(\Gamma))$, and in particular

$$h^{1/2}\|p_N - \hat{p}_N\|_{\sigma,-1/2,L^2(\Gamma)} \leq C_1 C_2 \,|\!|\!| p_N - \hat{p}_N |\!|\!| = \eta \tag{5.56}$$

which proves reliability of η.

The proof of efficiency is more involved. To begin, we set $V := \mathcal{H}^{-1/2}_\sigma(\mathbb{R}, H^{-1/2}(\Gamma))$, and we define the *Galerkin projection* $\mathbb{G}_N : V \to V_N$ implicitly by, for $p \in V$,

$$a^V_\sigma(\mathbb{G}_N[p], v_N) = a^V_\sigma(p, v_N)$$

for every $v_N \in V_N$. By the definition, $a^V_\sigma(\mathbb{G}_N[p_N], v_N) = a^V_\sigma(\mathbb{G}_N[\hat{p}_N], v_N)$ for any $v_N \in V_N$, and thus

$$a^V_\sigma(\mathbb{G}_N[p_N] - \mathbb{G}_N[\hat{p}_N], v_N) = a^V_\sigma(p_N - \mathbb{G}_N[\hat{p}_N], v_N) = 0 \tag{5.57}$$

for every $v_N \in V_N$.

By (5.57), and since $\mathbb{G}_N[p_N] - \mathbb{G}_N[\hat{p}_N] \in V_N$, there holds $|\!|\!| p_N - \mathbb{G}_N[\hat{p}_N] |\!|\!| = 0$. With the triangle inequality, we obtain

$$|\!|\!| p_N - \hat{p}_N |\!|\!| = |\!|\!| \mathbb{G}_N[\hat{p}_N] - \hat{p}_N |\!|\!| \tag{5.58}$$

as a consequence.

Further, by the definition, $a^V_\sigma(\mathbb{G}_N[p_N], v_N) = a^V_\sigma(p_N, v_N)$ for any $v_n \in V_N$, and therefore, with $\mathbb{G}_N[p_N] - p_N \in V_N$,

$$|\!|\!| \mathbb{G}_N[p_N] - p_N |\!|\!| = 0. \tag{5.59}$$

(5.58) and (5.59) give

$$|\!|\!| p_N - \hat{p}_N |\!|\!| = |\!|\!| \mathbb{G}_N[\hat{p}_N] - \hat{p}_N |\!|\!| = |\!|\!| (p_N - \hat{p}_N) - \mathbb{G}_N\left[p_N - \hat{p}_N\right] |\!|\!| \,. \tag{5.60}$$

In terms of the Galerkin projection, (4.40) in conjunction with Remark 4.8 implies

$$|\!|\!| p - \mathbb{G}_N[p] |\!|\!| \leq C_3 \max\left\{1, h^{-1/2}\right\} \inf_{q_N \in V_N} \|p - q_N\|_{\sigma,3/2,L^2(\Gamma)}$$

for $p \in \mathcal{H}^{3/2}_\sigma(\mathbb{R}, L^2(\Gamma))$, with $C_3 = C_3(\Gamma, \sigma, p, q, K(\mathcal{T}_S), K(\mathcal{T}_T))$. With $p = p_N - \hat{p}_N$ and $q_N = \Pi_{h,\Delta t}[p_N - \hat{p}_N]$, we obtain

$$\eta = |\!|\!| p_N - \hat{p}_N |\!|\!| \leq C_3 \max\left\{1, h^{-1/2}\right\} \|p_N - \hat{p}_N - \Pi_N[p_N - \hat{p}_N]\|_{\sigma,3/2,L^2(\Gamma)}$$

and thus, by Proposition 3.56, efficiency of η in the form

$$\eta \leq C_3 \max\left\{1, h^{-1/2}\right\} C_4 \,(h + \Delta t)\, \|p_N - \hat{p}_N\|_{\sigma,5/2,H^1(\Gamma)} \tag{5.61}$$

with $C_4 = C_4(p, q)$. In particular, if a $h\Delta t$-version is used, there holds

$$\eta \leq C_3 C_4 h^{1/2} \|p_N - \hat{p}_N\|_{\sigma,5/2,H^1(\Gamma)}.$$

We note that both the reliability estimate (5.56) and the efficiency estimate (5.61) feature a localisable spatial norm. However, these spatial norms are different, and so is the temporal norm. In practice, we use the term

$$h^{1/2}\|p_N - \hat{p}_N\|_{\sigma,0,L^2(\Gamma)} \tag{5.62}$$

to estimate the error.

5.4 Notes on the Three Dimensional Case

In this thesis, we work in a two dimensional setup. However, with regard to further research, it is also worth commenting on the case of three space dimensions briefly. A posteriori error estimates could certainly be useful in three space dimensions as well, but space-time adaptive methods would effectively require the handling of four dimensional space-time mesh elements, which appears to be unrealistic.

5.4.1 Residual-Based Error Estimates

We first note that we did not use any assumptions on the spatial dimension in the proofs of the results of Section 5.1.1, and they therefore also hold for $n = 3$. The same is not true for the results of Section 5.1.2. Carstensen, Maischak and Stephan [40] show that a three dimensional equivalent of Proposition 5.6 holds by using a partition of unity of Γ [40, Theorem 3.2], since it is not possible to use the same techniques as in [42] for $n = 3$. We have, however, failed to adapt this result to the space-time setup.

5.4.2 Faermann-Type Error Estimates

Let us introduce some notation first. Similarly to the two dimensional case (Section 2.1) and as in [68, Section 2], we assume that $\Gamma \subseteq \mathbb{R}^3$ is polygonal with faces P_i, such that $\Gamma = \bigcup_i P_i$. Each face P_i can be identified with a polygon $D \subseteq \mathbb{R}^2$.

We discretise any such polygon $D \subseteq \mathbb{R}^2$ by a triangular mesh $\mathcal{T}_S(D) = \Delta_D = \{\Gamma_1, \dots, \Gamma_N\}$, such that (a) $D = \bigcup_{i=1}^N \Gamma_i$, and (b) for $i \neq j$, each pair of triangles $\Gamma_i, \Gamma_j \in \Delta_D$ intersects in either a common vertex or a common edge, or $\Gamma_i \cap \Gamma_j = \varnothing$. By $\operatorname{diam}(\Gamma_i)$ and $\operatorname{width}(\Gamma_i)$ we denote the *diameter* (the length of the longest edge) and the *width* (the radius of the largest incircle) of Γ_i. We further write $\mathcal{N}_{\Delta_D}$ for the *set of nodal points* of Δ_D, and

$$\omega_\nu := \bigcup \{\, \Gamma_i \in \Delta_D \;\mid\; \nu \in \Gamma_i \,\}$$

for the *neighbourhood of a nodal point* $\nu \in \mathcal{N}_\Delta$, and

$$\omega_{\Gamma_i} := \bigcup \{\, \Gamma_j \in \Delta_D \;\mid\; \Gamma_i \cap \Gamma_j \neq \varnothing \,\}$$

for the *neighbourhood of a triangle* $\Gamma_i \in \Delta_D$. An illustration of these domains can be found in [68, Figure 2.1].

As in [68], an admissible mesh Δ on Γ is then given by $\Delta = \bigcup_i \Delta_{P_i}$ if we assume that for each nodal point $\nu \in \mathcal{N}_{\Delta_{P_i}}$ with $\nu \in \partial P_i \cap \partial P_j$ there also holds $\nu \in \mathcal{N}_{\Delta_{P_j}}$.

The three dimensional equivalent of Lemma 5.10 is Lemma 5.12.

Lemma 5.12 ([68, Lemma 3.4])
Let $D \subseteq \mathbb{R}^2$ be an arbitrary polygonal domain. Then, for any $\mu \in (0,1)$ and $v \in H^\mu(D)$,

$$\|v\|^2_{L^2(D)} \leq \frac{1}{2} \frac{\operatorname{diam}(D)^{2+2\mu}}{\operatorname{area}(D)} |v|^2_{H^\mu(D)} + \frac{1}{\operatorname{area}(D)} \left| \int_D v(x)\, dx \right|^2 . \tag{5.63}$$

In what follows, we proceed as for two space dimensions and consider a function $v \in H^\mu(\Gamma)$ that is orthogonal to V_h^p, and let $S_i \subseteq \mathbb{R}^2$ be the set of support of an arbitrary function $\varphi_i^p \in V_h^p$. (5.37) is then replaced by

$$\left| \int_{S_i} v(x)\, dx \right| \leq \operatorname{area}(S_i)^{1/2} \, \|v\|_{L^2(S_i)} \tag{5.64}$$

and (5.38) still holds, but the constant C now depends on the *shape regularity constant* [133, Definition 4.1.12]

$$\kappa(\Delta_D) := \max\left\{ \frac{\operatorname{diam}(\Gamma_i)}{\operatorname{width}(\Gamma_i)} \quad | \quad \Gamma_i \in \Delta_D \right\} \geq 1 \tag{5.65}$$

as well, i.e.

$$\|v\|_{L^2(S_i)} \leq \inf_{w_i \in \operatorname{span}\{\varphi_i^p\}} \|v - w_i\|_{L^2(S_i)} \leq C \operatorname{area}(S_i)^{\mu} |v|_{H^\mu(S_i)} \tag{5.66}$$

with $C = C(p, \kappa(\Delta_D))$. We note that $\kappa(\Delta_D) = 1$ in two space dimensions.

In place of (5.39), we obtain

$$\|v\|^2_{L^2(S_i)} \leq \max\left\{\frac{1}{2}, C^2\right\} \left(\frac{\operatorname{diam}(S_i)^{2+2\mu}}{\operatorname{area}(S_i)} + \operatorname{area}(S_i)^{2\mu} \right) |v|^2_{H^\mu(S_i)} \tag{5.67}$$

for any $v \in H^\mu(S_i)$ that is orthogonal to V_h^p.

Further, (5.40) is replaced by, for $v \in L^2((0,T), H^\mu(D))$,

$$\|v\|^2_{L^2((0,T),L^2(D))} \leq \frac{1}{2} \frac{\operatorname{diam}(D)^{2+2\mu}}{\operatorname{area}(D)} \|v\|^2_{L^2((0,T),H^\mu(D))} + \frac{1}{\operatorname{area}(D)} \int_0^T \left| \int_D v(x,t)\, dx \right|^2 dt \tag{5.68}$$

where

$$\frac{1}{\operatorname{area}(D)} \int_0^T \left| \int_S v(x,t)\, dx \right|^2 dt \leq \|v\|^2_{L^2((0,T),L^2(D))}.$$

Similarly, (5.41) changes to

$$\|v\|^2_{L^2((0,T),L^2(D))} \leq \frac{1}{2} |T|^{2\kappa} \|v\|^2_{H^\kappa((0,T),L^2(D))} + \|v\|^2_{L^2((0,T),L^2(D))} \tag{5.69}$$

for any $v \in H^\kappa((0,T), L^2(D))$ with $\kappa \in (0,1)$. The combination of (5.68) and (5.69) then gives

$$\|v\|^2_{L^2((0,T),L^2(D))} \leq \frac{1}{4} \left(\frac{\operatorname{diam}(D)^{2+2\mu}}{\operatorname{area}(D)} + |T|^{2\kappa} \right) \|v\|^2_{L^2((0,T),H^\mu(D)) \cap H^\kappa((0,T),L^2(D))} + \|v\|^2_{L^2((0,T),L^2(D))} \tag{5.70}$$

for any $v \in L^2((0,T), H^\mu(D)) \cap H^\kappa((0,T), L^2(D))$, which is analogous to (5.42).

The approximation properties (Proposition 3.52) give

$$\|v\|^2_{L^2(T_j,L^2(S_i))} \leq C_1 \left(\operatorname{diam}(S_i)^{\mu} + |T_j|^{\kappa} \right)^2 \|v\|^2_{L^2(T_j,H^\mu(S_i)) \cap H^\kappa(T_j,L^2(S_i))}$$

with $C_1 = C_1(p, q, \mu, \kappa, \kappa(\Delta_D))$, and therefore, by the same arguments as in the two dimensional case,

$$\|v\|^2_{L^2((0,T),L^2(S_i))} \leq \tag{5.71}$$
$$\left\{ \frac{1}{4} \left(\frac{\operatorname{diam}(S_i)^{2+2\mu}}{\operatorname{area}(S_i)} + |T|^{2\kappa} \right) + 2C_1 \left(\operatorname{diam}(S_i)^{2\mu} + |T_j|^{2\kappa} \right) \right\} \|v\|^2_{L^2((0,T),H^\mu(S_i)) \cap H^\kappa((0,T),L^2(S_i))}$$

for any $v \in L^2((0,T), H^\mu(S_i)) \cap H^\kappa((0,T), L^2(S_i))$ that is orthogonal to V_N.

Instead of using [67, Lemma 2.3], as we did for (5.44), we now integrate over $(0,T)$ in the inequality in [68, Lemma 3.2] and obtain, for any $D \subseteq R^2$ and any $v \in L^2((0,T), H^\mu(D))$, the estimate

$$\|v\|^2_{L^2((0,T),H^\mu(D))} \leq \sum_{\nu \in \mathcal{N}_{\Delta_D}} \|v\|^2_{L^2((0,T),H^\mu(\omega_\nu))} + C_2 \sum_{\Gamma_i \in \Delta_D} d_i^{-2\mu} \|v\|^2_{L^2((0,T),L^2(\Gamma_i))} \tag{5.72}$$

with $C_2 = C_2(\mu)$, and [68, (2.4)] $d_i := \operatorname{dist}(\Gamma_i, D \setminus \omega_{\Gamma_i})$.

Similarly to inequality (5.45), there holds

$$\|v\|^2_{H^\kappa((0,T),L^2(\Gamma))} \le \sum_{j=0}^{M} \|v\|^2_{H^\kappa(T_j \cup T_{j+1}, L^2(\Gamma))} + C_3 \sum_{j=1}^{M} d_j^{-2\kappa} \|v\|^2_{L^2(T_j, L^2(\Gamma))} \tag{5.73}$$

for any $H^\kappa((0,T),L^2(\Gamma))$ in three space dimensions, with $C_3 = C_3(\kappa)$. Combining these two estimates as in the two dimensional case, see (5.46), we obtain

$$\begin{aligned} \|v\|^2_{L^2((0,T),H^\mu(\Gamma))\cap H^\kappa((0,T),L^2(\Gamma))} \quad \le \quad & \sum_{\nu \in \mathcal{N}_{\Delta_D}} \sum_{j=0}^{M} \left(\|v\|^2_{L^2(T_j, H^\mu(\omega_\nu))} + \|v\|^2_{H^\kappa(T_j \cup T_{j+1}, L^2(\omega_\nu))} \right) \\ & + C_4 \sum_{\Gamma_i \in \Delta_D} \sum_{j=1}^{M} \left(d_i^{-2\mu} + d_j^{-2\kappa} \right) \|v\|^2_{L^2(T_j, L^2(\Gamma_i))} \end{aligned} \tag{5.74}$$

for any $v \in L^2((0,T),H^\mu(\Gamma)) \cap H^\kappa((0,T),L^2(\Gamma))$ with $C_4 = C_4(\mu,\kappa) := \max\{C_2, C_3\}$. Estimating the terms $\|v\|_{L^2(T_j,L^2(\Gamma_i))}$ by (5.71), it is crucial to bound the second term in the three dimensional analogue of (5.47),

$$\begin{aligned} & \left(d_i^{-2\mu} + d_j^{-2\kappa} \right) \|v\|^2_{L^2(T_j, L^2(\Gamma_i))} \\ \le \quad & \left(d_i^{-2\mu} + d_j^{-2\kappa} \right) \left\{ \frac{1}{4} \left(\frac{\operatorname{diam}(\Gamma_i)^{2+2\mu}}{\operatorname{area}(\Gamma_i)} + |T|^{2\kappa} \right) + 2C_1 \left(\operatorname{diam}(\Gamma_i)^{2\mu} + |T_j|^{2\kappa} \right) \right\} \\ & \qquad \|v\|^2_{L^2((0,T),H^\mu(\Gamma_i))\cap H^\kappa((0,T),L^2(\Gamma_i))} \end{aligned} \tag{5.75}$$

further. The assumed shape regularity (5.65) implies [68, (3.23)]

$$\frac{\operatorname{diam}(\Gamma_i)^2}{\operatorname{area}(\Gamma_i)} \le C_5 \qquad \text{and} \qquad \frac{\operatorname{diam}(\Gamma_i)}{d_i} \le C_5 \tag{5.76}$$

with $C_5 = C_5(\kappa(\Delta_D))$ for every $\Gamma_i \in \Delta_D$, where one uses, for the first inequality, the geometrical estimate $\sqrt{27}\,\frac{\operatorname{width}(\Gamma_i)^2}{\operatorname{area}(\Gamma_i)} \le 1$, and [133, p. 530] $d_i \ge C(\kappa(\Delta_D))\operatorname{diam}(\Gamma_i)$ for the second. As in two space dimensions, we have to restrict ourselves to the case $\kappa = \mu$ to bound the terms $d_j^{-2\kappa}\operatorname{diam}(S_i)^{2\mu}$ and $d_i^{-2\mu}|T_j|^{2\kappa}$ as well, and again they can only be bounded by the global constant $q(\mathcal{T}_{S,T})$. We then obtain

$$\begin{aligned} & \left(d_i^{-2\mu} + d_j^{-2\mu} \right) \left\{ \frac{1}{4} \left(\frac{\operatorname{diam}(\Gamma_i)^{2+2\mu}}{\operatorname{area}(\Gamma_i)} + |T|^{2\mu} \right) + 2C_1 \left(\operatorname{diam}(\Gamma_i)^{2\mu} + |T_j|^{2\mu} \right) \right\} \qquad (5.77) \\ \le \quad & \left(d_i^{-2\mu} + d_j^{-2\mu} \right) \left(\frac{1}{4} \max\{1, C_4\} + 2C_1 \right) \left(\operatorname{diam}(\Gamma_i)^{2\mu} + |T_j|^{2\mu} \right) \\ \le \quad & \left(\frac{1}{4} \max\{1, C_5\} + 2C_1 \right) \left(C_4^{2\mu} + 2q(\mathcal{T}_{S,T}) + K(\mathcal{T}_T)^{2\mu} \right) =: C_6(p, q, \mu, \kappa(\Delta_D), q(\mathcal{T}_{S,T}), K(\mathcal{T}_T)) \end{aligned}$$

and consequently, from (5.72) and (5.77) and (5.77), an analogue of the estimate in Lemma 5.11, i.e.

$$\|v\|^2_{L^2((0,T),H^\mu(\Gamma))\cap H^\mu((0,T),L^2(\Gamma))} \le C \sum_{\nu \in \mathcal{N}_{\Delta_D}} \sum_{j=0}^{M} \left(\|v\|^2_{L^2(T_j, H^\mu(\omega_\nu)} + \|v\|^2_{H^\mu(T_j \cup T_{j+1}, L^2(\omega_\nu))} \right) \tag{5.78}$$

with $C = C(p, q, \mu, \kappa(\Delta_D), q(\mathcal{T}_{S,T}), K(\mathcal{T}_T))$.

5.4.3 N-$N/2$ Error Estimates

The results of Section 5.3 do not involve any assumptions on the spatial dimension, and thus still hold for $n = 3$. However, the dependence of the constants on the parameters involved changes slightly. For instance, as we mentioned in Section 5.4.2, the constant C in the approximation estimate (3.156) now depends on the shape regularity constant κ, defined by (5.65), as well, which subsequently affects the constants that appear in the estimates discussed in Section 5.3. We do not elaborate on this any further.

5.5 Numerical Experiment

In this section we present some numerical experiments in which realisations of the a posteriori error estimates introduced in Sections 5.1, 5.2 and 5.3 are used to quantify the approximation error. Technical data on the code and on the equipment the experiments were performed on are given in Section 6.2.

We consider the same problem as in Section 2.6, of which we know the exact solution. However, since we cannot compute any other error norms, we compare the a posteriori error estimates only to the space-time L^2-error. In what follows, we denote by

$$\eta^R_{h,\Delta t} = \|R'\|_{\sigma,0,L^2(\Gamma)} \tag{5.79}$$

the a posteriori error estimator of residual type (see Remarks 5.5 b) and 5.9 c)) used in the experiments, by

$$\eta^F_{h,\Delta t} = \sum_{i=1}^{N}\sum_{j=0}^{M} \|R\|^2_{L^2(T_j,H^{1/2}(\Gamma_i\cup\Gamma_{i+1}))} \tag{5.80}$$

the a posteriori error estimator of Faermann type (5.51) used in the experiments, and by

$$\eta^N_{h,\Delta t} = |||\hat{p}_N - p_N||| \tag{5.81}$$

the N-$N/2$ error estimator (see (5.54) and (5.62)) used in the experiments.

Results are presented in Table 5.1 and Figure 5.2. We observe an experimental convergence rate of $\frac{3}{2}$ for all three error estimators, compared to the experimental convergence rate of 1 we observed for the space-time L^2-error. This appears reasonable, since the spatial error norm estimated in all case is the $H^{-1/2}(\Gamma)$-norm. On the other hand, of course, there remains a wide gap between theoretical error estimates and experimental results, which is, again, due to the apparently unrealistic mapping properties of the time domain boundary integral operators involved. This issue has been discussed in Section 3.3.2.

We further note that, while the error curves for the residual and N-$N/2$-type error estimators in Figure 5.2 are almost parallel, the Faermann error estimators nearly coincide with their residual counterparts in the beginning, but decrease at a slower rate for larger degrees of freedom. The reason for this is probably an insufficiently accurate evaluation of the broken-order error norm (5.52).

degrees of freedom			residual (5.79)		Faermann (5.80)		N-$N/2$ (5.81)	
TDOF	SDOF	TS	$\eta^R_{h,\Delta t}$	$\alpha_{h,\Delta t}$	$\eta^F_{h,\Delta t}$	$\alpha_{h,\Delta t}$	$\eta^N_{h,\Delta t}$	$\alpha_{h,\Delta t}$
80	16	5	0.7301119	-	0.6766216	-	4.5072746	-
320	32	10	0.3314411	1.14	0.3637185	0.90	1.7008228	1.41
1280	64	20	0.0988636	1.75	0.1060899	1.78	0.6137240	1.47
5120	128	40	0.0342029	1.53	0.0398010	1.41	0.2330997	1.40
20480	256	80	0.0121167	1.50	0.0197873	1.00	0.0821900	1.50

Table 5.1: A posteriori error estimators $\eta^{\{R,F,N\}}_{h,\Delta t}$ as defined in (5.79), (5.80), (5.81), and corresponding experimental convergence rates $\alpha_{h,\Delta t}$ for the problem considered in Section 5.5. TDOF and SDOF denote the total and spatial degrees of freedom, respectively, while TS stands for the number of time steps.

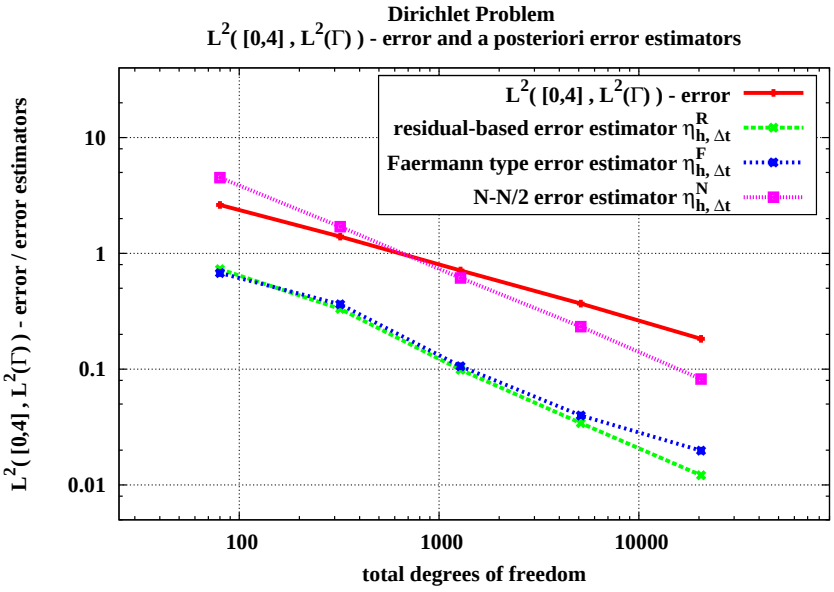

Figure 5.2: $L^2([0,4], L^2(\Gamma))$-error and a posteriori error estimators for the problem considered in Section 5.5.

Chapter 6

Adaptive Strategies and Numerical Experiments

In this chapter, we present two adaptive schemes that can be used with the time domain Boundary Element Method, and numerical experiments in which these schemes are applied.

The two adaptive schemes are introduced in Section 6.1.

The first one, presented in Section 6.1.1, focuses on spatial modifications of the underlying mesh while leaving the uniform temporal mesh unchanged, and can therefore be used with an adaption of the MOT scheme (Algorithm 2.1).

The second adaptive scheme, presented in Section 6.1.2, is based on a changed perspective on the computational domain, in which we do not seek to decouple the global linear system any longer. Computation times and storage requirements consequently increase, but we gain the chance to work with more flexible meshes.

Numerical experiments in which these two adaptive strategies are employed are considered and discussed in Section 6.2.

6.1 Adaptive Strategies

In the literature review in Section 1.1.2, the use of adaptive schemes for the wave equation has been thoroughly motivated. Further, we observed in Section 4.2 that the time domain Boundary Element Method is unconditionally stable and should, therefore, be well suited to be used with adaptive schemes. The a posteriori error estimates established in Chapter 5 give a theoretical foundation for error indicators that can be used with adaptive methods.

We have mentioned in the introduction that there are, generally, two different possible strategies that can be used in adaptive schemes for time dependent problems, see Figure 1.4 in particular. In what follows, we describe their implementation in detail. Advantages and disadvantages of both were also discussed in Section 1.1.2. We have implemented and conducted numerical experiments using both strategies.

6.1.1 Adaptivity with a Time-Marching Scheme

In this section, we use meshes of type (2.2) that are uniform in time but of arbitrary form in space. Their design is assumed to be steered by local error indicators. The strategy we present here is sketched in Figure 1.4a. Since the temporal mesh sizes are assumed to be uniform, this

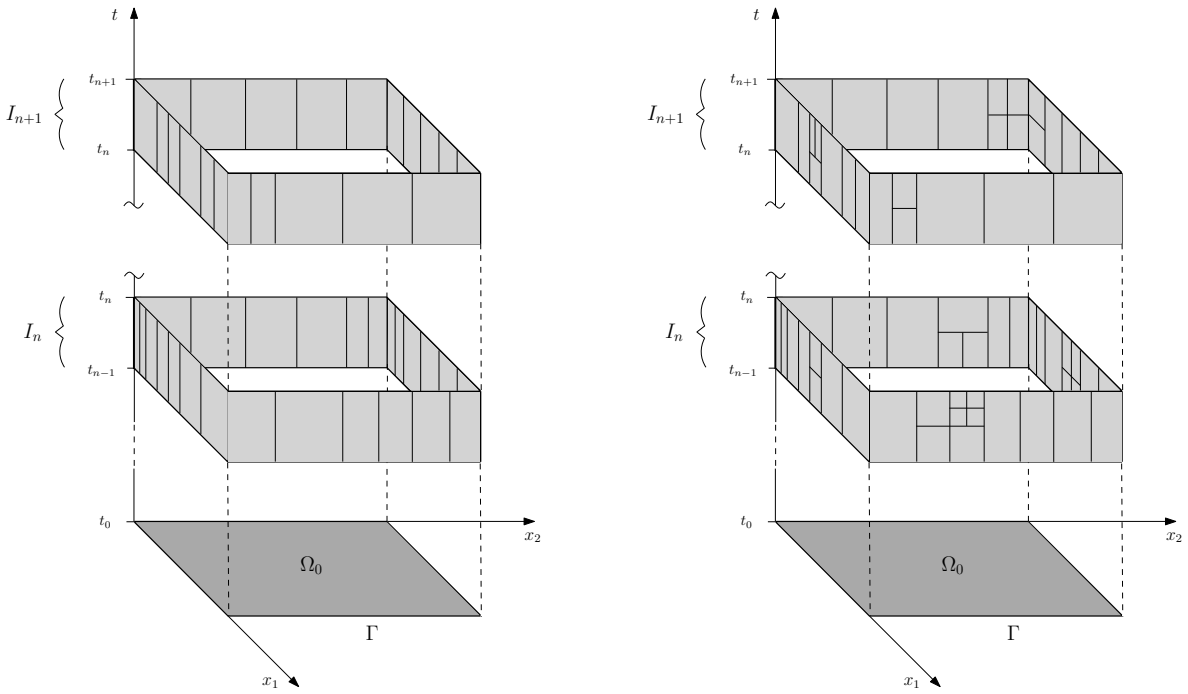

(a) Adaptivity with a time-marching scheme

(b) Adaptivity with a all-at-once scheme (pseudo-3D mesh)

Figure 6.1: Two possible realisations of adaptive meshes for time dependent problems. After [150, Figure 2.1a].

strategy is suitable to be used with a MOT scheme. However, the MOT scheme used here is more costly than the standard one for uniform spatial meshes. This is because previously computed matrices cannot be re-used here, since they would not comply with the current time step's mesh. Therefore, the complete history of matrices has to be recomputed which is, however still computationally cheaper than dealing with the full linear system (2.30).

Temporal adaptivity can be realised, but only by restarting the scheme with a smaller or larger global temporal mesh size. In what follows, we therefore focus on spatial adaptivity. A typical space-time mesh that results from this strategy is sketched in Figure 6.1a. As the illustration shows, mesh elements can be refined and coarsened (or de-refined) throughout the computations within this strategy. While the implementation of refinement procedures is rather straightforward, the implementation of coarsening procedures is more involved and less frequently used. The reason for the latter is probably that coarsening strategies are only suitable for time dependent problems, where different meshes can be used for different time steps. For elliptic problems, on the other hand, coarsening is not really applicable.

We give a brief review of our implementation, in which we restrict ourselves to the case of line elements, as used for the two dimensional Boundary Element Method. We use the same data structure that is described in Sections 1.1.2 and 1.2 of the monograph by Schmidt and Siebert [138]. Its most important features are:

- The initial mesh is represented by a list of so-called *macro elements* that cannot be coarsened any further.
- Every macro element is the root of a binary tree, see Figure 6.2. When an element is refined, it is split into two new elements, each of them half the size of the original element,

as shown in Figure 6.3. We call the original element the *father* of its *sons*, the two new elements. In these terms, every element has either two sons or no son.

- Any node of one of the binary trees is called a *leaf* if it has no son. In particular every macro element that has not been refined so far is a leaf. All the leafs form the current mesh; see Figure 6.2(b) for an illustration.

- An element can only be coarsened together with its brother element. This means that any element that is marked for coarsening is only coarsened if its brother element has also been marked for coarsening. If this is indeed the case, the two brother elements are removed from the current mesh and replaced by their common father element, as shown in Figure 6.3. We thus understand mesh coarsening as the inverse operation to mesh refinement.

The refinement and coarsening procedure is outlined in Algorithm 6.1.

Algorithm 6.1 General refinement and coarsening procedure

Input: mesh $\{\Gamma_1, \ldots, \Gamma_N\}$ with corresponding error indicators $\eta_1, \ldots, \eta_N$, refinement and coarsening criterion
Output: refinement and coarsening flags for the mesh elements

```
1  for all element Γ_i , i = 1,...,N do
2    if η_i fulfils the refinement criterion then
3      mark Γ_i for refinement
4    else if η_i fulfils the coarsening criterion then
5      set Γ_j := brother(Γ_i)
6      if η_j fulfils the coarsening criterion then
7        mark Γ_i and Γ_j for coarsening
8      end if
9    end if
10 end for
```

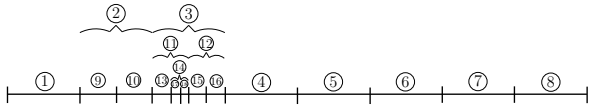

(a) Mesh that has been refined locally.

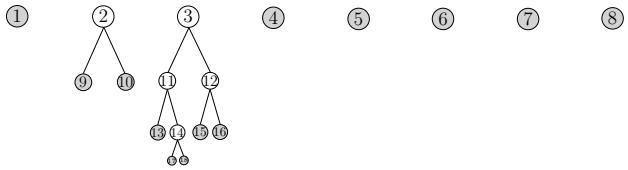

(b) Mesh representation by binary trees. The elements of the current mesh are highlighted.

Figure 6.2: Binary tree data structure for 2D BEM meshes.

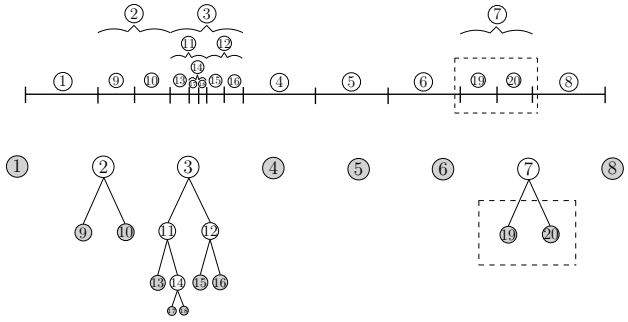

Figure 6.3: Refinement of mesh element 7.

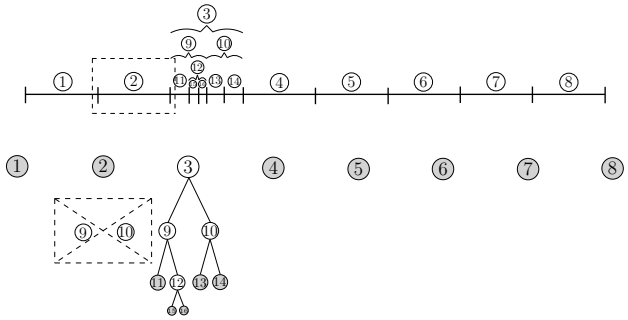

Figure 6.4: Coarsening of elements 9 and 10.

Some refinement and coarsening criteria (as used in lines 2 and 4, 6 of Algorithm 6.1, respectively) are presented in [138, Sections 1.5]. We collect them in Definition 6.1.

Definition 6.1 (Popular Refinement and Coarsening Criteria)
Let $0 < \Theta_{cor} < \Theta_{ref} < 1$, and assume that a mesh $\{\Gamma_1, \ldots, \Gamma_N\}$ of N elements with corresponding, previously computed, error indicators $\eta_1, \ldots, \eta_N$ is given.

- maximum strategy *[138, pp. 44/47]: η_i fulfils the refinement criterion if $\eta_i > \Theta_{ref} \max_k \eta_k$ and η_i fulfils the coarsening criterion if $\eta_i < \Theta_{cor} \max_k \eta_k$, where $\eta = \sum_{k=1}^{N} \eta_k$.*
- equidistribution strategy *[138, pp.44/48, with $p = 1$]: η_i fulfils the refinement criterion if $\eta_i > \Theta_{ref} \frac{\eta}{N}$ and η_i fulfils the coarsening criterion if $\eta_i < \Theta_{cor} \frac{\eta}{N}$.*
- fixed-rate strategy *[26, p. 48]: η_i fulfils the refinement criterion if η_i is one of the $100 \cdot \Theta_{ref}$ % largest error indicators and η_i fulfils the coarsening criterion if η_i is one of the $100 \cdot \Theta_{cor}$ % smallest error indicators.*
- 'Dörfler marking' *or* 'guaranteed error reduction strategy' *[101], [138, p. 45]: η_i fulfils the refinement criterion if $\Gamma_i \in \mathcal{K}_{ref}$, where $\mathcal{K}_{ref} \subseteq \{\Gamma_1, \ldots, \Gamma_N\}$ is a set of elements such that $\Theta_{ref}^2 \sum_{i=1}^{N} \eta_i^2 \leq \sum_{\Gamma_i \in \mathcal{K}_{ref}} \eta_i^2$. The set $\mathcal{K}_{ref}$ can be computed using [138, Algorithm 1.20].*

  Coarsening for this strategy is described in [26, p. 48, fixed-error reduction*]: η_i fulfils the refinement criterion if $\Gamma_i \in \mathcal{K}_{cor}$, where $\mathcal{K}_{cor} \subseteq \{\Gamma_1, \ldots, \Gamma_N\}$ is a set of elements such that $\Theta_{cor}^2 \sum_{i=1}^{N} \eta_i^2 \geq \sum_{\Gamma_i \in \mathcal{K}_{cor}} \eta_i^2$. The refinement and coarsening parameters are chosen such that $1 - \Theta_{ref} > \Theta_{cor}$.*
- 'explicit error control strategy'*: η_i fulfils the refinement criterion if $\eta_i > \Theta_{ref}$ and η_i fulfils the coarsening criterion if $\eta_i < \Theta_{cor}$. In this case, the refinement and coarsening parameters are error bounds and not ratios.*

Remark 6.2 (On the Choice of the Coarsening Parameter [138, Section 1.5.3])
One needs to take care when choosing the coarsening parameter Θ_{cor}. It should be chosen in a way that ensures that the newly de-refined elements are not immediately marked for refinement again in the next iteration step. Bangerth and Rannacher [26, p. 18] suggest to take $\Theta_{cor} = \frac{1}{4}\Theta_{ref}$. The same strategy is also chosen in other research articles that deal with adaptive methods for hyperbolic problems, such as [22, p. 36], [36, p. 224], [128, p. 37], [150, p. 1972].

In the literature on parabolic problems it is often suggested to proceed in the following way: The coarsening is done first, then the solution and the error indicators are re-computed on the new mesh. Let Γ_i^1, Γ_i^2 be two elements that were marked for coarsening and which were subsequently replaced by their common father element Γ_i^c. Let η_i^1, η_i^2, η_i^c be the corresponding error indicators. The decision on whether to keep the new mesh or to neglect is then based on whether $\eta_i^1 + \eta_i^c$ and $\eta_i^2 + \eta_i^c$ fulfil the coarsening criterion (lines 4,6 of Algorithm 6.1). See [124, p. 19 and flow chart 6.4.4] or [138, Section 1.5.3 and Algorithm 1.25].

Several possible adaptive procedures for time dependent problems are given in [138, p. 49]. We collect them in Definition 6.3.

Definition 6.3 (Adaptive Strategies for Time Dependent Problems)
Let $\mathcal{M}^m = \mathcal{M}(t^m)$ be the mesh for time step t^m, where 'the mesh' here means the final mesh after k_m modifications $\mathcal{M}^{m,1}, \ldots, \mathcal{M}^{m,k_m}$ of the initial mesh $\mathcal{M}^{m,0}$ for time step t^m, i.e. $\mathcal{M}^m = \mathcal{M}^{m,k_m}$.

(i) explicit strategy*: $\mathcal{M}^{m,0} = \mathcal{M}^{m-1,k_{m-1}}$; $k_m = 1$ for all m. The problem is only solved once per time step, on the mesh $\mathcal{M}^{m,0}$.*

(ii) semi-implicit strategy*: similar to (i); but the problem is solved twice per time step, i.e.* $k_m = 2$.

(iii) implicit strategy A*:* $\mathcal{M}^{m,0} = \mathcal{M}^{m-1,k_{m-1}}$*;* k_m *is variable (the mesh is modified until the desired accuracy is achieved in every time step).*

(iv) implicit strategy B*:* $\mathcal{M}^{m,0} = \mathcal{M}^*$ *where* $\mathcal{M}^*$ *denotes some, usually uniform, coarse mesh;* k_m *is variable as in (iii). No explicit coarsening is done. Instead, this is rather a global coarsening at the start of each time step.*

Numerous other strategies can be found in the literature as well.

The full adaptive scheme that can be used with the MOT scheme is sketched as a pseudo code in Algorithm 6.2.

Algorithm 6.2 Adaptive Procedure for TD-BEM with the MOT scheme

Input: initial spatial mesh $\{\Gamma_1, \ldots, \Gamma_N\}$, global temporal mesh size Δt and number of time steps M, refinement and coarsening criterion, adaptive strategy

Output: sequence of meshes $\mathcal{M}^{m,k}$ with $m = 1, \ldots, M$, $k = 1, \ldots, k_m$ and corresponding solutions

1 **for all** time step $t_m = j\Delta t$, $m = 1, \ldots, M$ **do**
2 **for all** modification steps $k = 0, \ldots, k_m - 1$ **do**
3 recompute matrices $\mathcal{U}^0, \ldots, \mathcal{U}^{m-1}$ {with basis functions corresponding to meshes $\mathcal{M}^{m,k}$ versus $\mathcal{M}^{n,k_n}$ for matrices $\mathcal{U}^n$ for $n = 1, \ldots, m-1$ and to meshes $\mathcal{M}^{m,k}$ versus $\mathcal{M}^{m,k}$ for matrix $\mathcal{U}^0$}
4 compute solution $\vec{p}^{\,m,k}$ on mesh $\mathcal{M}^{m,k}$ via the MOT scheme (Algorithm 2.1)
5 compute error indicators
6 set refinement and coarsening marks via Algorithm 6.1, using the chosen refinement and coarsening criterion
7 modify the current mesh $\mathcal{M}^{m,k}$ according to the chosen adaptive strategy and obtain mesh $\mathcal{M}^{m,k+1}$
8 **end for**
9 **end for**

Remark 6.4 (on Algorithm 6.2)

a) The refinement and coarsening criterion and the adaptive strategy in the input list of Algorithm 6.2 can be chosen out of the ones given in Definitions 6.1 and 6.3. If strategy (iii) or (iv) in Definition 6.3 is chosen, the for *loop in line 2 of Algorithm 6.2 would be replaced by a* while *loop.*

b) Note that the recomputation of the matrices in line 3 saves projecting previous solutions to the current mesh.

c) Temporal adaptivity can be realised by adding a temporal error indicator that forces the algorithm to restart with $2\Delta t$ *or* $\frac{\Delta t}{2}$*, if the temporal error indicator is too small or too large, respectively. The solutions obtained from the previous computations with* Δt *can then be projected to the new temporal mesh. Alternatively, the algorithm can be fully restarted from* $m = 1$.

6.1.2 Adaptivity with a All-At-Once Scheme

In this section, we allow more general meshes of type (2.1), in which we do not treat the temporal domain separately from the spatial domain. Instead, we remind ourselves of the fact that our computational domain is basically a space-time cylinder. We discretise this computational domain by what we call a pseudo-3D mesh that allows variable step sizes in both directions, i.e. in space and in time. A typical space-time mesh of this kind is sketched in Figure 6.1b. Note that, as opposed to Figure 6.1a, this method enables us to treat every space-time mesh cell $\Gamma_i \times T_m$ just in the way that one would treat a rectangular surface element in a three dimensional Boundary Element Method. In particular, refinements in different directions (along the space or the time axis) are, in principle, possible. In our implementation, however, we simply split each space-time mesh cell into four equally-sized subcells. This strategy was sketched in Figure 1.4b.

In particular, we need to handle non-uniform temporal meshes here, which were explicitly included in our studies on the computation of the matrix entries in Chapter 2. Non-uniform temporal meshes seem to be better suited for usage with the time domain Galerkin Boundary Element Method, but they have also recently been introduced for the Convolution Quadrature Boundary Element Method [106, 107].

The price one has to pay for this increase in flexibility are larger computation times. The MOT scheme (Algorithm 2.1) cannot be used in this case any more. Instead, the full linear system (2.30) has to be stored and solved, which increases the storage requirements and the computation time for the setup and the solution of the linear system considerably.

Even though the procedure used here should be clear, since it so strongly resembles the well known procedure for adaptive methods for time independent problems, we provide the pseudo code for this adaptive scheme in Algorithm 6.3.

Algorithm 6.3 Adaptive Procedure for TD-BEM with Pseudo-3D Meshes

Input: initial space-time mesh $(\mathcal{T}_S \times \mathcal{T}_T)^0 := \{\Gamma_1, \ldots, \Gamma_N\} \times \{T_1, \ldots, T_M\}$, refinement criterion, adaptive strategy, maximum number of refinement levels K

Output: sequence of meshes $(\mathcal{T}_S \times \mathcal{T}_T)^k$, $k = 1, \ldots, K$ and corresponding solutions

1 **for all** refinement steps $k = 0, \ldots, K-1$ **do**
2 compute matrices $\mathcal{U}^{m,n}$ of the linear system (2.30), and solve it
3 compute error indicators
4 set refinement marks, using the chosen refinement criterion
5 modify the current space-time mesh $(\mathcal{T}_S \times \mathcal{T}_T)^k$ according to the chosen adaptive strategy and obtain next space-time mesh $(\mathcal{T}_S \times \mathcal{T}_T)^{k+1}$
6 **end for**

6.2 Numerical Experiments

In what follows, we present the results of several numerical experiments that were conducted to test our implementation and the theoretical estimates. A detailed description of the quadrature scheme used and some first validational examples were given in Chapter 2. The algorithms provided there and in this chapter were implemented as an extension to the software package *maiprogs* [111], which is written in Fortran 95. All numerical experiments were run on the School of Information Systems, Computing and Mathematics' servers that feature 24 kernels with 2.5 GHz and 64 GB RAM. The code is designed to make as much use as possible of the large number of available kernels. In particular, the computations of the matrix entries and local error indicators, which involve numerical quadrature and can therefore be very costly, are run in parallel.

6.2.1 Periodic Plane Incident Wave

In this section we compare the results of numerical experiments with periodic plane incident waves for the transient and time harmonic case. In the transient case, we take a setup similar to the one used in Section 4.3.3.2, which, in turn, is the one of Example 1.8 a), i.e.

$$u^{\mathrm{inc}}(x,t) = -A\cos\left(k\cdot x+\varphi_0-\omega t\right)H\left(k\cdot x-\omega t+m_F\right) \tag{6.1}$$

with $k = \pi\,(1,1)$, $\omega = \sqrt{2}\pi$, $\varphi_0 = \frac{7}{2}\pi$. Differently to the referred setup, this periodic incident wave has no tail, and it therefore persists indefinitely where it has arrived at the scatterer. We expect that, once the incident wave has fully arrived at the obstacle, a steady state is reached, in which the scattered wave becomes time harmonic. We consider the case of a square scatterer $\Omega = [-1,1]^2$ and represent the unknown scattered wave by a Single Layer ansatz. Due to the direction of the plane wave, the boundary of the scatterer can be divided into a lit region $\Gamma_{\mathrm{lit}} := ([-1,1]\times\{-1\})\cup(\{-1\}\times[-1,1])$ and a shadowed region $\Gamma_{\mathrm{shadowed}} := \Gamma\setminus\Gamma_{\mathrm{lit}}$. Problems of similar type have been considered for crack domains $\Omega = \Gamma = [0,1]\times\{0\}$ in [5, p. 1229f.] and [33].

In order to verify our computational results for the transient case we compare them to the results obtained in an experiment with the time harmonic counterpart of the transient scattering problem: We consider the Dirichlet Helmholtz problem with the real part of the time harmonic part of the transient incident wave as the boundary datum, i.e.

$$u^{\mathrm{inc}}(x) = -A\cos\left(k\cdot x+\varphi_0\right) \tag{6.2}$$

and use, as in the transient case, a Single Layer approach to represent the solution. We emphasise that (6.2) is not a solution of the time harmonic problem. It is a solution of the homogeneous Helmholtz equation and obviously fits the boundary condition, but it does not, as every time harmonic plane wave [122, Section 2.6.4], satisfy the Sommerfeld radiation condition posed at infinity. By using a representation of the solution in terms of boundary layer potentials, however, the Sommerfeld radiation condition is automatically guaranteed.

Plots of the scattered wave in the time harmonic case and in the transient case (at different times) are shown in Figures 6.7 and 6.10, respectively. Figure 6.10 suggests that, indeed, a steady state is reached, in which a time harmonic wave is excited periodically. The nature of this wave seems to be similar to the one shown in Figure 6.7. A strict verification of this observation, however, does not seem to be possible.

Due to the corners of the domain, we expect singularities in the solution in both the harmonic and the transient case, even though the respective incident waves are smooth [58]. Indeed, regions with relatively steep gradients can be observed in the respective plots of both cases (Figures 6.7 and 6.10). The use of adaptive methods is, therefore, appealing. However, since the exact

solution is unknown, we cannot state any expectations on possible improvements regarding the convergence rates.

The adaptive experiments were run with the following setup: For the time independent problem and for Algorithm 6.3, we used the fixed-rate strategy with $\Theta = 0.9$. For Algorithm 6.2, we also used the fixed-rate strategy with $\Theta_{\text{ref}} = 0.9$ and $\Theta_{\text{cor}} = 0.6$. Residual error indicators were used in each case.

6.2.1.1 Time Harmonic Signal

We follow [91] for the computation of the energy error and the error indicators for the time harmonic signal. Let p_h denote the approximation of the solution to the indirect Helmholtz Single Layer equation. Then the energy error is computed by (4.52), and we use the residual error indicator

$$\eta_i = |\Gamma_i|^{1/2} \left\| \frac{\partial}{\partial s} \left(V[p_h] - f \right) \right\|_{L^2(\Gamma_i)} . \tag{6.3}$$

A plot of the approximation via the representation formula in the truncated exterior domain $[-5,5]^2 \setminus [-1,1]^2$ around the scatterer $[-1,1]^2$ is given in Figure 6.7. The matrices in all time harmonic experiments are computed analytically using the *maiprogs* implementation of [112]. However, the series expansion of the Helmholtz kernel function used for the analytical computation is only valid for small arguments $|x-y|$, and we therefore use the reference implementation [9, 119], and see also Appendix B, to compute the values of the representation formula in the exterior domain.

A plot of the energy error (4.52) for the uniform and adaptive versions is shown in Figure 6.5a, while the corresponding error estimators (6.3) are shown in Figure 6.5b. The experimental convergence rates are of order $\frac{2}{3}$ for the uniform version, and the reliability constant is approximately $\frac{1}{4}$. The convergence rates clearly increase for the adaptive version. For the error estimators, it is larger than $\frac{3}{2}$, the expected convergence rate for regular solutions which the adaptive algorithm is expected to restore. The energy error curve shows some unexpected plateaus and looks generally unconvincing. This is probably due to the fact that we used the results of the uniform version to extrapolate the exact solution's energy norm, which may not be precise enough.

Some of the meshes obtained using the adaptive algorithm based on the residual error indicators (6.3) are presented in Figure 6.6. We observe that the mesh is refined symmetrically and strongly around the corners $(-1,-1)$, $(-1,1)$ and $(1,-1)$. The shadowed part of the boundary Γ_{shadowed} remains relatively coarse throughout the refinement process.

6.2.1.2 Transient Signal

In order to compare the results for the time harmonic and time dependent problems, we have plotted the approximation via the representation formula in the exterior domain $[-5,5]^2 \setminus [-1,1]^2$ in Figure 6.10 at different times. We observe that, as expected, the solution becomes harmonic for larger times, and that there appear to be singularities of similar type as for the harmonic case.

Regarding the adaptivity, we have used both adaptive schemes introduced in Section 6.1 for the transient problem. Some of the meshes obtained by using the adaptive time-marching scheme (Algorithm 6.2) are shown in Figure 6.9, while some of the pseudo-3D meshes obtained by the adaptive all-at-once scheme (Algorithm 6.3) are shown in Figure 6.11.

We observe a similar refinement pattern in the pseudo-3D meshes to the meshes for the time harmonic problem shown in Figure 6.6. Again, the regions around the corners are strongly and symmetrically refined where the incident signal has arrived, while the shadowed region remains

comparably coarse. The meshes shown in Figure 6.9 are different. They are, comprehensively, heavily refined around the corner $(-1,-1)$, where the incident wave first hits the scatterer, for smaller times. However, the mesh continues to be adapted very finely there also for larger times, and it is not as much refined along the two lit edges as one would expect. This could be due to a bad choice of Θ_{ref} and Θ_{cor}, but similar meshes were also obtained for different choices of these parameters.

The energy error (see Section 4.3) and the error estimator curves shown in Figure 6.5 are also of different characters for the two adaptive schemes. The adaptive time-marching scheme suffers from the fact that the initial error is propagated via the first solution vector that appears on the right hand sides of the linear systems solved throughout the MOT scheme. The convergence rates can therefore not be expected to be of a higher order than the ones for the uniform scheme. Figure 6.5 confirms that indeed the convergence order does not increase. A step in the pseudo-3D scheme, on the other hand, is effectively equivalent to a restart of the MOT scheme with a more suitable mesh, and the corresponding error curves therefore decrease more quickly at first. It was this phenomenon that initially triggered the introduction of the pseudo-3D meshes. However, after an initial pre-asymptotic period, in which the error curve based on the adaptive pseudo-3D scheme decreases at a higher rate than the one for the uniform version, the rate of convergence appears to be the same. This indicates that the solution of the transient problem is of higher regularity, which would explain why the rate of convergence does not improve asymptotically.

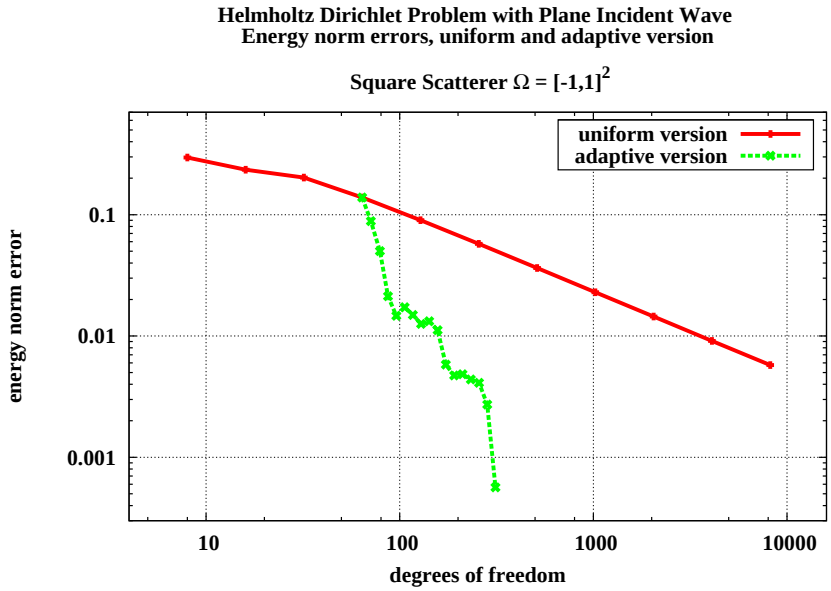

(a) energy errors

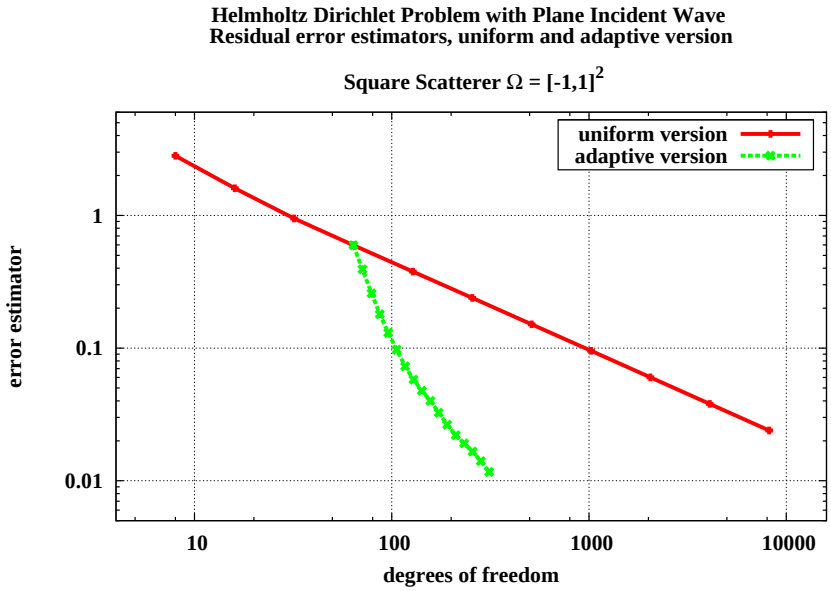

(b) residual error estimators

Figure 6.5: Error plots for the time harmonic problem considered in Section 6.2.1.1.

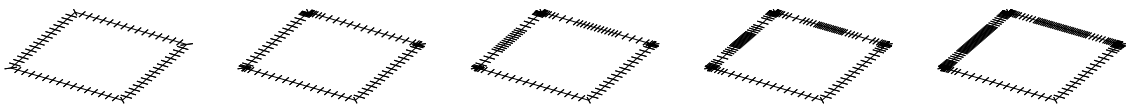

(a) mesh 1 (b) mesh 4 (c) mesh 7 (d) mesh 10 (e) mesh 13

Figure 6.6: Some meshes obtained by using the adaptive version for the time harmonic problem considered in Section 6.2.1.1. The corner $(-1,-1)$ is on the top.

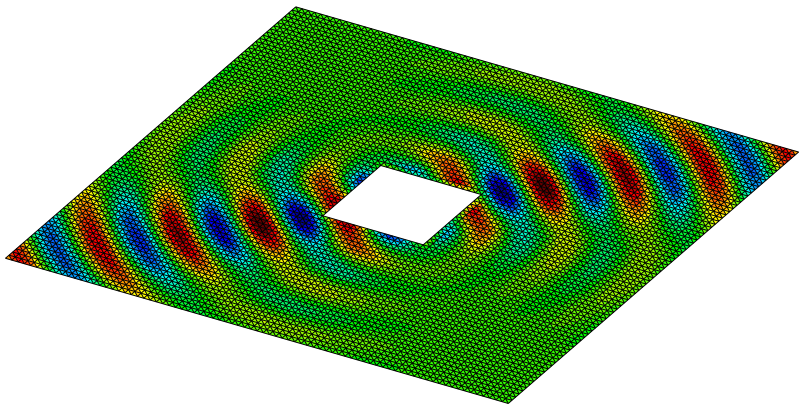

Figure 6.7: Plot of the solution of the time harmonic problem considered in Section 6.2.1.1, using the representation formula in the truncated exterior domain $[-5,5]^2 \setminus [-1,1]^2$. The corner $(-1,-1)$ is on the top.

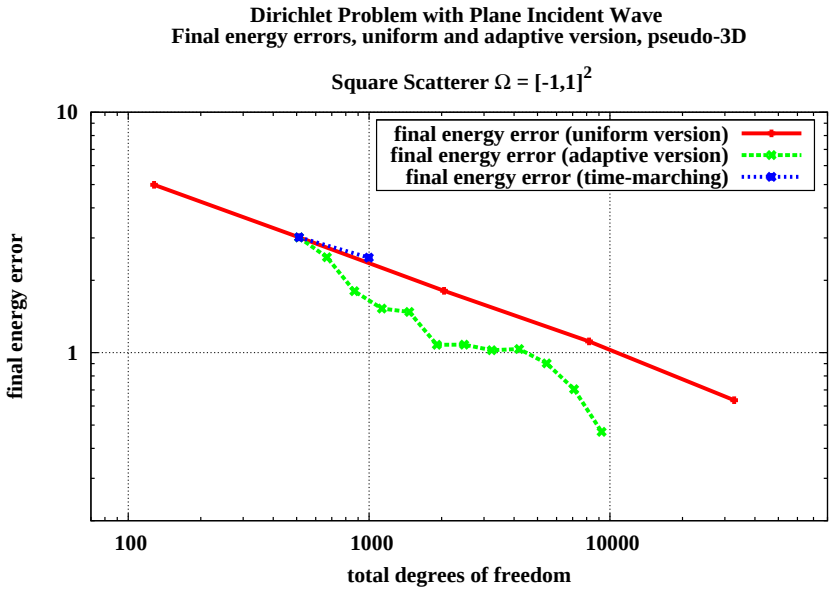

(a) energy errors

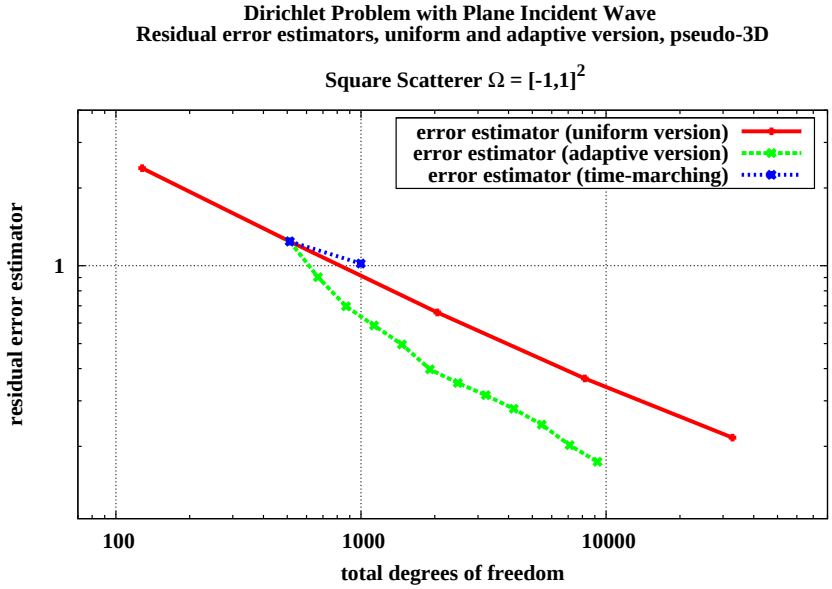

(b) residual error estimators

Figure 6.8: Error plots for the transient problem considered in Section 6.2.1.2.

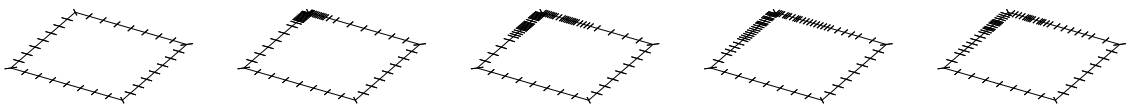

(a) initial mesh (b) $t = 0.6$, mesh 2 (c) $t = 1.0$, mesh 2 (d) $t = 1.4$, mesh 2 (e) $t = 1.8$, mesh 2

Figure 6.9: Some meshes obtained by using the adaptive version of the time-marching scheme (Algorithm 6.2) for the problem considered in Section 6.2.1.2. The corner $(-1, -1)$ is on the top.

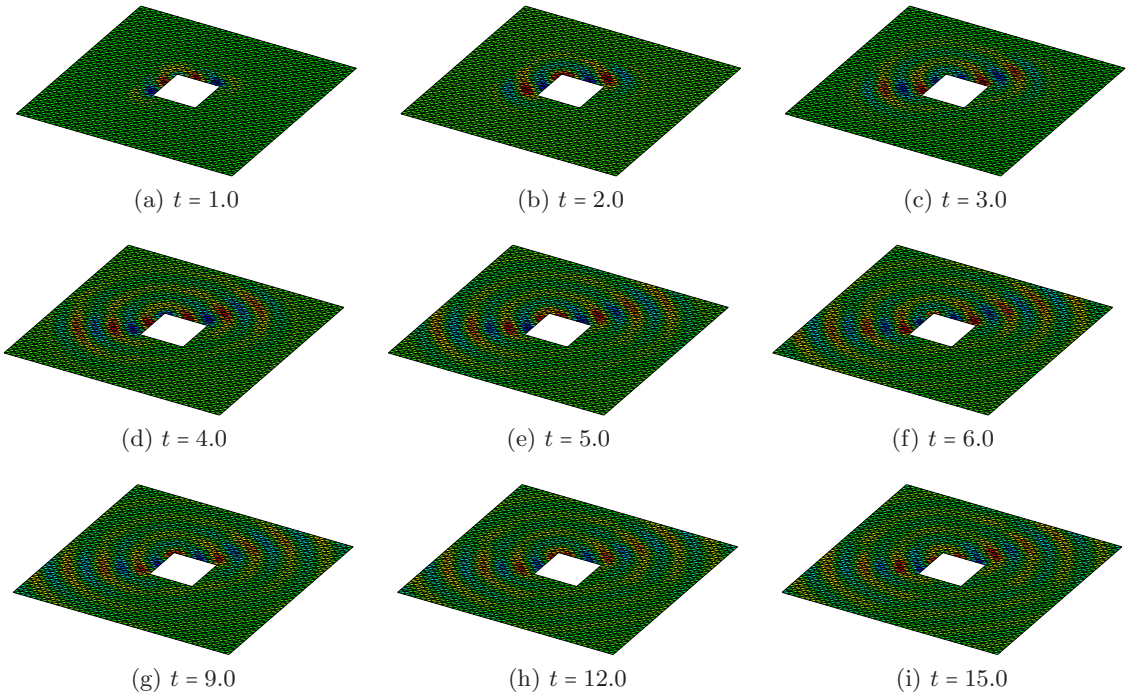

(a) $t = 1.0$ (b) $t = 2.0$ (c) $t = 3.0$

(d) $t = 4.0$ (e) $t = 5.0$ (f) $t = 6.0$

(g) $t = 9.0$ (h) $t = 12.0$ (i) $t = 15.0$

Figure 6.10: Plot of the solution of the transient problem considered in Section 6.2.1.2, using the representation formula in the truncated exterior domain $[-5,5]^2 \setminus [-1,1]^2$ at different times. The corner $(-1,-1)$ is on the top.

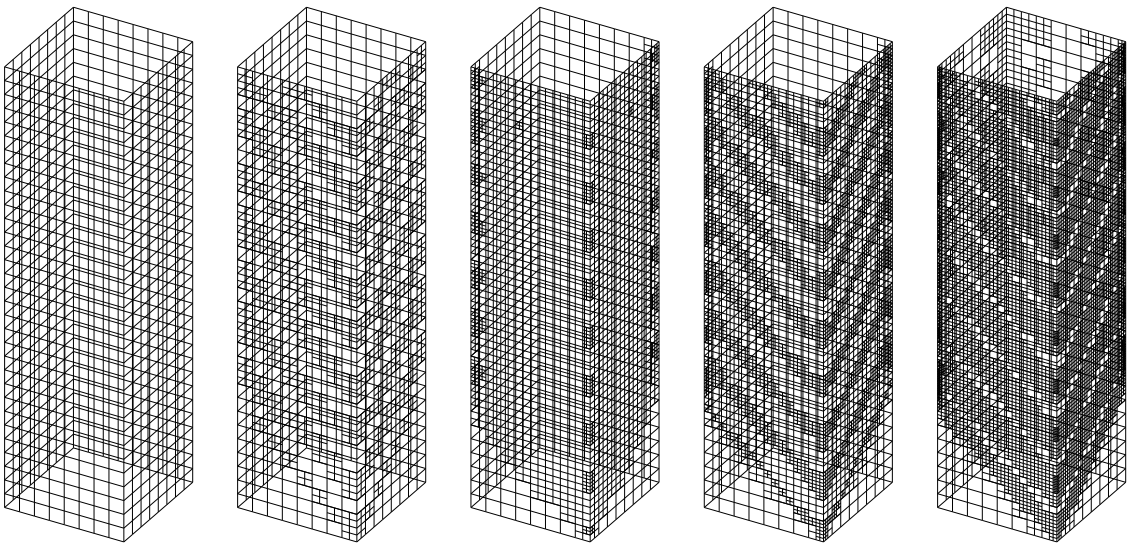

(a) mesh 1 (b) mesh 3 (c) mesh 5 (d) mesh 7 (e) mesh 9

Figure 6.11: Some meshes obtained by using the adaptive version for the transient case (Algorithm 6.3) for the problem considered in Section 6.2.1.2. The corner $(-1,-1)$ is on the bottom.

6.2.2 Box Pulse

In the experiment presented in this section, we use a box pulse of the type presented in Section 1.3.2 with length $\lambda = 0.05$, moving with a velocity of $\frac{1}{\sqrt{2}}$ space units per time unit, as the incident signal of the scattering problem with scatterer $[-1,1]^2$. We only consider the transient problem here. The box pulse is non-smooth, which appears to have an effect on the regularity of the solution of the problem: Unlike to the previous experiment, the convergence order for the adaptive version is genuinely higher than the one of the uniform version, even for large degrees of freedom, as we observe in Figure 6.12. The meshes that result from the adaptive algorithm, shown in Figure 6.13, are heavily refined along the part of the surface of the space-time cylinder where the box pulse moves along the scatterer.

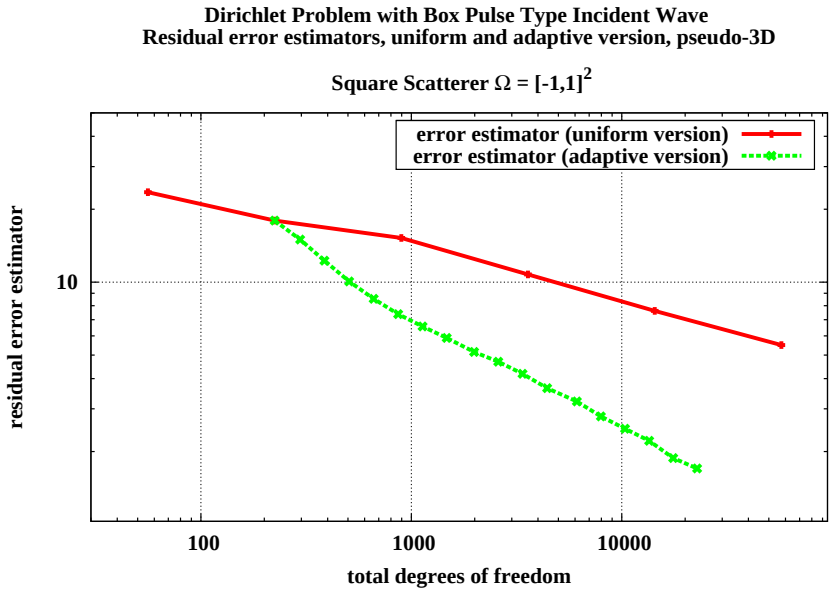

Figure 6.12: Residual error estimators for the transient problem considered in Section 6.2.2.

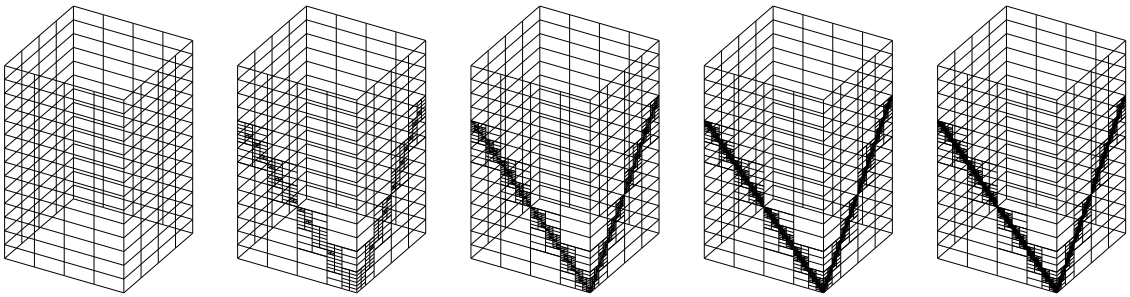

(a) mesh 1 (b) mesh 4 (c) mesh 7 (d) mesh 10 (e) mesh 13

Figure 6.13: Some meshes obtained by using the adaptive version for the transient case (Algorithm 6.3) for the problem considered in Section 6.2.2. The corner $(-1,-1)$ is on the bottom.

6.2.3 Box Pulse and Plane Wave from Different Directions

In our last experiment we consider, again, the square scatterer $[-1,1]^2$. The scatterer is hit by a plane wave of the type considered in Section 6.2.1.2 right from the start of the computation. A box pulse travelling at a velocity of $1.25 \cdot \sqrt{2}$ space units per time unit arrives at the corner $(1,-1)$ at $t = 1$, and leaves the lit part of the scatterer at $t = 1.805$. As in Section 6.2.2, the solution of the problem seems to be non-regular, since the adaptive version improves the converge rate, as Figure 6.14 shows. The meshes shown in Figure 6.15 show that elements are refined heavily in the region where the box pulse moves along the scatterer, while the plane incident wave is also, though less heavily, tracked by the adaptive scheme.

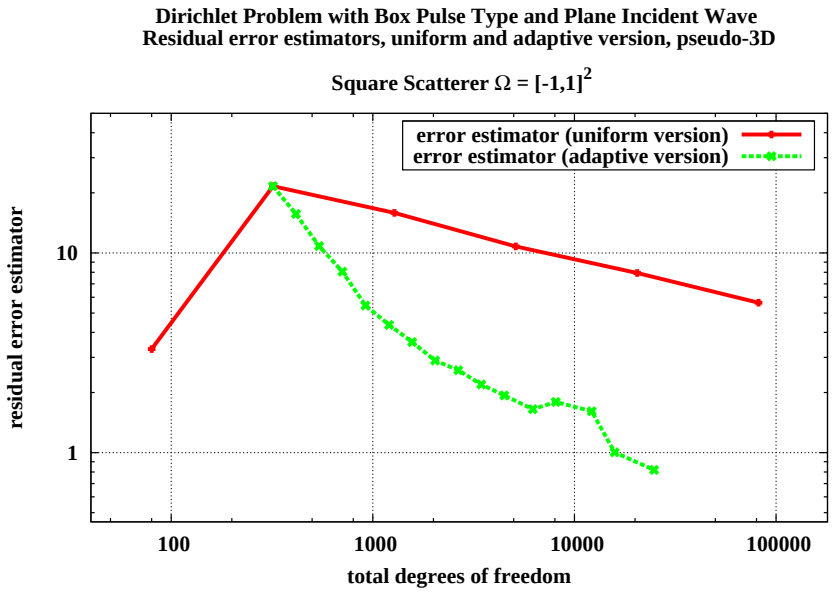

Figure 6.14: Residual error estimators for the transient problem considered in Section 6.2.3.

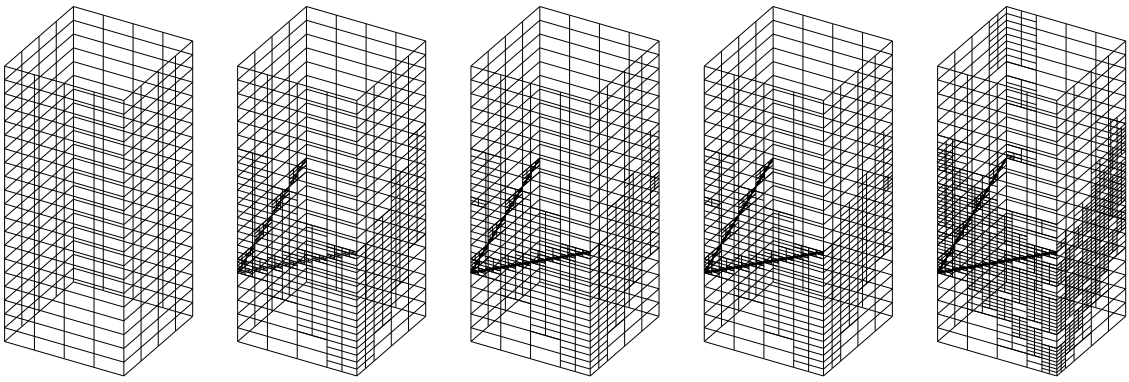

(a) mesh 1 (b) mesh 4 (c) mesh 7 (d) mesh 10 (e) mesh 13

Figure 6.15: Some meshes obtained by using the adaptive version for the transient case (Algorithm 6.3) for the problem considered in Section 6.2.3. The corner $(-1,-1)$ is on the bottom.

Chapter 7

Conclusions and Further Research

In this final chapter, we review the main results presented in this work and make suggestions for further research.

7.1 Conclusions

This thesis mainly makes two contributions to the field of time domain Boundary Element Methods. On the theoretical side, it provides generalised mapping results for the operators involved and introduces a posteriori error estimates to this field. On the implementational side, it provides a full integration scheme that can be used with non-uniform meshes and introduces a flexible self-adaptive algorithm that allows refinements in both the spatial and temporal direction.

In Chapter 2, we developed and analysed in detail a full spatial quadrature scheme for the Galerkin time domain Boundary Element Method in two space dimensions in which the temporal integrals are computed analytically. Traditionally, uniform temporal meshes have been preferred for time domain Boundary Element Methods, which lead to special structure of the linear system matrix which can be exploited to obtain a computationally cheap marching-on-in-time (MOT) scheme. We did not restrict ourselves to these uniform meshes but explicitly allowed arbitrary temporal meshes.

In Chapter 3, we derived generalised mapping properties for time domain boundary layer potentials and operators. Most of the analysis was done in the frequency domain, where we analysed the mapping properties of the Helmholtz boundary layer potentials and operators and obtained generalised mapping properties which are explicit in the wavenumber. These were subsequently transferred to the space-time domain. We compared these novel results to the well known ones for the energy spaces and pointed out some deficiencies. The mapping properties were used in Chapters 4 and 5 to derive a priori and a posteriori error estimates for the Single Layer problem, respectively. Regarding the a priori estimates, some of them are well known and some of them fill gaps in the existing literature. We further discussed the use of the energy norm as an alternative error measure, with particular regard to problems whose exact solution is not known. The three types of a posteriori error estimates which we presented were studied with special regard to their localisation, which allows their use in self-adaptive algorithms. Both the a priori and a posteriori error estimates suffer from the poor mapping properties of the time domain boundary layer operators which manifest themselves in strong assumptions on the regularity of the given data and of the solution, and in low theoretical orders of convergence. However, our first numerical experiments in Chapters 2, 4 and 5 showed that convergence rates similar to the ones for time independent problems can be expected in practice, and that the convergence orders

that can be proven theoretically are too pessimistic.

In Chapter 6, we presented two self-adaptive algorithms, of which the first can be used with the computationally cheaper MOT scheme while the latter allows more flexible space-time meshes, which we call pseudo-3D meshes, at the cost of increased computation times. Our numerical experiments strongly indicate that the use of self-adaptive methods based on pseudo-3D meshes is advantageous in this setup. The experiments further show that these methods are effective and lead to improved convergence rates for problems with non-smooth input data.

7.2 Suggestions for Further Research

The wide field of wave modelling, of which the problem and methods considered in this thesis are only a minor branch, is certain to continue to receive a vast amount of future research interest in engineering, mathematics and physics, due to its practical importance and the academic challenges within it. Particularly with regard to applications, it might be worth considering to adapt approaches used in these related fields to time domain Boundary Element Methods. Some of these approaches are collected in what follows.

One interesting future research direction could be the study of other types of approximation spaces. So-called *numerical-asymptotic boundary integral methods* for time harmonic scattering problems which 'combine conventional piecewise polynomial approximations with high-frequency asymptotics to build basis functions suitable for representing the oscillatory solutions' are currently very actively studied. An account on recent progresses in this field is given by Chandler-Wilde et al. [44]. Several types of non-polynomial approximation spaces have also been used for voluminous methods for wave propagation problems, see, for instance, [121] and the references cited therein.

Time domain Boundary Element Methods, on the other hand, are still almost exclusively used with piecewise polynomial basis functions, the only exception known to the author being the recent works by Sauter and Veit [134, 152] that are discussed in the introduction. It is further worth remarking that even their approach features a tensor product decomposition of the ansatz and test functions into a spatial and a temporal part. This is clearly advantageous in terms of computational cost, but it might not be sufficient to represent the scattered wave precisely enough. In the present age of fast multi-core computers, it could therefore be worthwhile to implement and analyse schemes with basis functions that do not separate the space and time variables.

Different types of approximation space basis functions could also be used to treat singularities and thus present an alternative to adaptive schemes. Such approaches are used in the engineering community for time harmonic scattering problems, for example with the so-called *Wave Based Method* in [58]. However, this method is volumetric in nature, and it has not been mathematically analysed so far, nor has it been used with Boundary Element Methods.

hp-adaptive methods have been studied and successfully implemented for numerous time independent problems [91, 146], and it therefore appears to be attractive to transfer this approach to time domain Boundary Element Methods. However, higher-order temporal polynomial approximations are reported to be even more prone to instabilities than low-order approximations, and they have therefore rarely been used in practice [34, p. 53].

Different types of error estimators, in addition to the ones studied in Chapter 5 which could, to some extent, be adapted to the time dependent setup, have been applied and analysed for elliptic problems. *Steinbach error estimators* [140, 144], [39, Section 2.6.4], that represent the approximation error by a truncated Neumann series, and *Babuška-Rheinboldt error estimators* [39, Section 6], [66] could be of interest for further research. On the theoretical side, we mention

that convergence of error estimators and adaptive algorithms for Finite Element Methods can be proven under the assumption that Dörfler marking (see Definition 6.1) is used. Similar convergence results have recently been proven for $h - h/2$-error estimators [12] and for residual error estimators [11, 70, 71] for Boundary Element Methods for Symm's integral equation. It would certainly be of interest to prove analogous results for time dependent problems.

The mathematical analysis of the time domain Boundary Element Method is, on the whole, still in an inadequate state. Consequences are the counter-intuitive mapping properties of the potentials and operators involved, and the resulting overly pessimistic error estimates elaborated in Chapters 3 to 5. We cited in Remark 3.49 b) Ha-Duong's speculation, that these shortcomings are probably due to the chosen functional framework, which might not be entirely suitable for the analysis of the time domain Boundary Element Method. The quest for a more suitable framework has been an open problem for more than two decades. No attempts to tackle it were made in this work. Instead, we worked within the existing framework. It remains a huge intellectual challenge to design function spaces in which more plausible mapping properties could be proven.

Transient transmission problems, which can be used to model different media around a scatterer, have been treated by coupling time domain Boundary Element Methods with Discontinuous Galerkin Finite Element Methods in [1], and by different coupling schemes in earlier doctoral theses in the French school. Adaptive methods could be useful in this context as well.

Bibliography

[1] Abboud, T., Joly, P., Rodríguez, J., and Terrasse, I. Coupling discontinuous Galerkin methods and retarded potentials for transient wave propagation on unbounded domains. *J. Comput. Phys. 230*, 15 (2011), 5877–5907.

[2] Adams, R. A., and Fournier, J. J. F. *Sobolev spaces*, vol. 140 of *Pure and Applied Mathematics*. Academic Press, Amsterdam, 2003.

[3] Aimi, A., Diligenti, M., and Guardasoni, C. Numerical integration schemes for space-time hypersingular integrals in energetic Galerkin BEM. *Numer. Algorithms 55*, 2–3 (2010), 145–170.

[4] Aimi, A., Diligenti, M., and Guardasoni, C. On the energetic Galerkin boundary element method applied to interior wave propagation problems. *J. Comp. Appl. Math. 235*, 7 (2011), 1746–1754.

[5] Aimi, A., Diligenti, M., Guardasoni, C., Mazzieri, I., and Panizzi, S. An energy approach to space-time Galerkin BEM for wave propagation problems. *Internat. J. Numer. Methods Engrg. 80*, 9 (2009), 1196–1240.

[6] Aimi, A., Diligenti, M., and Panizzi, S. Energetic Galerkin BEM for wave propagation Neumann exterior problems. *CMES Comput. Model. Eng. Sci. 58*, 2 (2010), 185–219.

[7] Ainsworth, M., and Oden, J. T. *A posteriori error estimation in finite element analysis*. Pure and Applied Mathematics. Wiley, New York, NY, 2000.

[8] Alt, H.-W. *Lineare Funktionalanalysis: eine anwendungsorientierte Einführung*. Springer, Berlin, 2006.

[9] Amos, D. E. Algorithm 644: A portable package for Bessel functions of a complex argument and nonnegative order. *ACM Trans. Math. Software 12*, 3 (1986), 265–273. Available for download at `http://www.netlib.org/toms/644` (in Fortran 77).

[10] Atle, A. *Approximation of Integral Equations for Wave Scattering*. PhD thesis, Skolan för informations- och kommunikationsteknik, Kungliga Tekniska högskolan, Stockholm, 2006.

[11] Aurada, M., Feischl, M., Führer, T., Karkulik, M., and Praetorius, D. Efficiency and optimality of some weighted-residual error estimator for adaptive 2D boundary element methods. Tech. Rep. 15/2012, Institut für Analysis und Scientific Computing, Technische Universität Wien, 2012.

[12] Aurada, M., Ferraz-Leite, S., and Praetorius, D. Estimator reduction and convergence of adaptive BEM. *Appl. Numer. Math. 62*, 6 (2012), 787–801.

[13] Babuška, I., and Guo, B. Q. Regularity of the solution of elliptic problems with piecewise analytic data. I. Boundary value problems for linear elliptic equation of second order. *SIAM J. Math. Anal. 19*, 1 (1988), 172–203.

[14] Babuška, I., and Guo, B. Q. Regularity of the solution of elliptic problems with piecewise analytic data. II. The trace spaces and application to the boundary value problems with nonhomogeneous boundary conditions. *SIAM J. Math. Anal. 20*, 4 (1989), 763–781.

[15] Babuška, I., and Rheinboldt, W. C. A-posteriori error estimates for the finite element method. *Int. J. Numer. Methods Eng. 12*, 10 (1978), 1597–1615.

[16] Babuška, I., and Rheinboldt, W. C. Error estimates for adaptive finite element computations. *SIAM J. Numer. Anal. 15*, 4 (1978), 736–754.

[17] Babuška, I., and Strouboulis, T. *The finite element method and its reliability.* Numerical Mathematics and Scientific Computation. Clarendon Press, Oxford, 2001.

[18] Bachelot, A., Bounhoure, L., and Pujols, A. Couplage éléments finis–potentiels retardés pour la diffraction électromagnétique par un obstacle hétérogène. *Numer. Math. 89*, 2 (2001), 257–306.

[19] Bagçi, H., Yilmaz, A. E., Jin, J.-M., and Michielssen, E. Time domain adaptive integral method for surface integral equations. In *Modeling and computations in electromagnetics: a volume dedicated to Jean-Claude Nédélec*, H. Ammari, Ed., vol. 59 of *Lect. Notes Comput. Sci. Eng.* Springer, Berlin, 2008, pp. 65–104.

[20] Bamberger, A., and Ha-Duong, T. Formulation variationnelle espace-temps pour le calcul par potentiel retardé de la diffraction d'une onde acoustique (I). *Math. Methods Appl. Sci. 8*, 3 (1986), 405–435.

[21] Bamberger, A., and Ha-Duong, T. Formulation variationnelle pour le calcul de la diffraction d'une onde acoustique par une surface rigide. *Math. Methods Appl. Sci. 8*, 4 (1986), 598–608.

[22] Bangerth, W., Geiger, M., and Rannacher, R. Adaptive Galerkin finite element methods for the wave equation. *Comput. Meth. Appl. Math. 10*, 1 (2010), 3–48.

[23] Bangerth, W., Grote, M., and Hohenegger, C. Finite element method for time dependent scattering: nonreflecting boundary condition, adaptivity, and energy decay. *Comput. Methods Appl. Mech. Engrg. 193*, 23–26 (2004), 2453–2482.

[24] Bangerth, W., and Rannacher, R. Finite element approximation of the acoustic wave equation: error control and mesh adaptation. *East-West J. Numer. Math. 7*, 4 (1999), 263–282.

[25] Bangerth, W., and Rannacher, R. Adaptive finite element techniques for the acoustic wave equation. *J. Comput. Acoust. 9*, 2 (2001), 575–591.

[26] Bangerth, W., and Rannacher, R. *Adaptive finite element methods for differential equations.* Lectures in mathematics: ETH Zürich. Birkhäuser, Basel, 2003.

[27] Banjai, L. Multistep and multistage convolution quadrature for the wave equation: algorithms and experiments. *SIAM J. Sci. Comput. 32*, 5 (2010), 2964–2994.

[28] Banjai, L., Lubich, C., and Melenk, J. M. Runge-Kutta convolution quadrature for operators arising in wave propagation. *Numer. Math. 119*, 1 (2011), 1–20.

[29] Banjai, L., and Sauter, S. A. Rapid solution of the wave equation in unbounded domains. *SIAM J. Numer. Anal. 47*, 1 (2008/09), 227–249.

[30] Banjai, L., and Schanz, M. Wave propagation problems treated with convolution quadrature and BEM. In *Fast Boundary Element Methods in Engineering and Industrial Applications*, U. Langer, M. Schanz, O. Steinbach, and W. L. Wendland, Eds., vol. 59 of *Lect. Notes Comput. Sci. Eng.* Springer, Berlin, 2011, pp. 65–104.

[31] Bänsch, E. Adaptive finite element techniques for the Navier-Stokes equations and other transient problems. In *Adaptive finite and boundary element methods*, C. A. Brebbia and M. H. Aliabadi, Eds., Internat. Ser. Comput. Engrg. Computational Mechanics Publications, Southampton, 1993, pp. 47–76.

[32] Bécache, E. *Résolution par une méthode d'équation intégrales d'un problème de diffraction d'ondes élastiques transitoires par une fissure.* PhD thesis, Centre de Mathématiques Appliquées, École Polytechnique, Université de Paris VI – Pierre et Marie Curie, 1991.

[33] Bécache, E. A variational boundary integral equation method for an elastodynamic antiplane crack. *Internat. J. Numer. Methods Engrg. 36*, 6 (1993), 969–984.

[34] Bécache, E. Equations intégrales pour l'équation des ondes. Cours de l'école des ondes, INRIA, 1994. Available for download at `http://www-rocq.inria.fr/~becache/cours_eqinteg.ps.gz`.

[35] Bécache, E., and Ha-Duong, T. A space-time variational formulation for the boundary integral equation in a 2D elastic crack problem. *RAIRO Modél. Math. Anal. Numér. 28*, 2 (1994), 141–176.

[36] Bernardi, C., and Süli, E. Time and space adaptivity for the second-order wave equation. *Math. Models Methods Appl. Sci. 15*, 2 (2005), 199–225.

[37] Bieterman, M. B., and Babuška, I. The finite element method for parabolic equations. I. A posteriori error estimation. *Numer. Math. 40*, 3 (1982), 339–371.

[38] Carstensen, C. Efficiency of a posteriori BEM-error estimates for first-kind integral equations on quasi-uniform meshes. *Math. Comp. 65*, 213 (1996), 69–84.

[39] Carstensen, C., and Faermann, B. Mathematical foundation of a posteriori error estimates and adaptive mesh-refining algorithms for boundary integral equations of the first kind. *Eng. Anal. Bound. Elem. 25*, 7 (2001), 497–509.

[40] Carstensen, C., Maischak, M., and Stephan, E. P. A posteriori error estimate and h-adaptive algorithm on surfaces for Symm's integral equation. *Numer. Math. 90*, 2 (2001), 197–213.

[41] Carstensen, C., and Stephan, E. P. A posteriori error estimates for boundary element methods. *Math. Comp. 64*, 210 (1995), 483–500.

[42] Carstensen, C., and Stephan, E. P. Adaptive boundary element methods for some first kind integral equations. *SIAM J. Numer. Anal. 33*, 6 (1996), 2166–2183.

[43] Chandler-Wilde, S. N., Graham, I. G., Langdon, S., and Lindner, M. Condition number estimates for combined potential boundary integral operators in acoustic scattering. *J. Integral Equations Appl. 21*, 2 (2009), 229–279.

[44] Chandler-Wilde, S. N., Graham, I. G., Langdon, S., and Spence, E. A. Numerical-asymptotic boundary integral methods in high-frequency acoustic scattering. *Acta Numer. 21* (2012), 89–305.

[45] Chappell, D. J. A convolution quadrature Galerkin boundary element method for the exterior Neumann problem of the wave equation. *Math. Methods Appl. Sci. 32*, 12 (2009), 1585–1608.

[46] Chappell, D. J. Convolution quadrature Galerkin boundary element method for the wave equation with reduced quadrature weight computation. *IMA J. Numer. Anal. 31*, 2 (2011), 640–666.

[47] Chappell, D. J., and Harris, P. J. On the choice of coupling parameter in the time domain Burton-Miller formulation. *Quart. J. Mech. Appl. Math. 62*, 4 (2009), 431–450.

[48] Chen, J. T., Chen, K. H., and Chen, C. T. Adaptive boundary element method of time-harmonic exterior acoustics in two dimensions. *Comput. Methods Appl. Mech. Engrg. 191*, 31 (2002), 3331–3345.

[49] Chen, Q., Haddar, H., Lechleiter, A., and Monk, P. A sampling method for inverse scattering in the time domain. *Inverse Problems 26*, 8 (2010), 085001.

[50] Chung, Y.-S., Sarkar, T. K., Jung, B. H., Salazar-Palma, M., Ji, Z., Jang, S., and Kim, K. Solution of time domain electric field integral equation using the Laguerre polynomials. *IEEE Trans. Antennas Propag. 52*, 9 (2004), 2319–2328.

[51] Colton, D., and Kress, R. *Integral equation methods in scattering theory*, vol. 93 of *Pure and Applied Mathematics*. John Wiley & Sons, New York, NY, 1983.

[52] Costabel, M. Boundary integral operators on Lipschitz domains: elementary results. *SIAM J. Math. Anal. 19*, 3 (1988), 613–626.

[53] Costabel, M. Boundary integral operators for the heat equation. *Int. Eqs. Oper. Theo. 13*, 4 (1990), 498–552.

[54] Costabel, M. Time-dependent problems with the boundary integral equation method. In *Encyclopedia of Computational Mechanics*, E. Stein, R. de Borst, and J. R. Hughes, Eds. John Wiley & Sons, Chichester, 2004, pp. 703–721.

[55] Dahmen, W., Faermann, B., Graham, I. G., Hackbusch, W., and Sauter, S. A. Inverse inequalities on non-quasi-uniform meshes and application to the mortar element method. *Math. Comp. 73*, 247 (2004), 1107–1138.

[56] Dautray, R., and Lions, J. L. *Mathematical analysis and numerical methods for science and technology. Vol. 2: Functional and variational methods.* Springer, Berlin, 1988.

[57] Davies, P. J., and Duncan, D. B. Stability and convergence of collocation schemes for retarded potential integral equations. *SIAM J. Numer. Anal. 42*, 3 (2004), 1167–1188.

[58] Deckers, E., Bergen, B., van Genechten, B., Vandepitte, D., and Desmet, W. An efficient Wave Based Method for 2D acoustic problems containing corner singularities. *Comput. Methods Appl. Mech. Engrg. 241–244* (2012), 286–301.

[59] El Gharib, J. *Méthode des potentiels retardés pour l'acoustique.* PhD thesis, École Polytechnique, Palaiseau, 1999.

[60] Erath, C., Ferraz-Leite, S., Funken, S. A., and Praetorius, D. Energy norm based a posteriori error estimation for boundary element methods in two dimensions. *Appl. Numer. Math. 59*, 11 (2009), 2713–2734.

[61] Erath, C., Funken, S. A., Goldenits, P., and Praetorius, D. Simple error estimators for the Galerkin BEM for some hypersingular integral equation in 2D. To appear in *Applicable Anal.*, DOI:10.1080/00036811.2012.661045.

[62] Ergin, A. A., Shanker, B., and Michielssen, E. Fast evaluation of three-dimensional transient wave fields using diagonal translation operators. *J. Comput. Phys. 146*, 1 (1998), 157–180.

[63] Ergin, A. A., Shanker, B., and Michielssen, E. Analysis of transient wave scattering from rigid bodies using a Burton-Miller approach. *J. Acoust. Soc. Am. 106*, 5 (1999), 2396–2404.

[64] Eriksson, K., Estep, D., Hansbo, P., and Johnson, C. Introduction to adaptive methods for differential equations. *Acta Numer. 4* (1995), 105–158.

[65] Eriksson, K., and Johnson, C. Adaptive finite element methods for parabolic problems. I. A linear model problem. *SIAM J. Numer. Anal. 28*, 1 (1991), 43–77.

[66] Faermann, B. Local a-posteriori error indicators for the Galerkin discretization of boundary integral equations. *Numer. Math. 79*, 1 (1998), 43–76.

[67] Faermann, B. Localization of the Aronszajn-Slobodeckij norm and application to adaptive boundary element methods. i. The two-dimensional case. *IMA J. Numer. Anal. 20*, 2 (2000), 203–234.

[68] Faermann, B. Localization of the Aronszajn-Slobodeckij norm and application to adaptive boundary element methods. ii. The three-dimensional case. *Numer. Math. 92*, 3 (2002), 467–499.

[69] Falletta, S., Monegato, G., and Scuderi, L. A space-time BIE method for nonhomogeneous exterior wave equation problems. The Dirichlet case. *IMA J. Appl. Math. 32*, 1 (2012), 202–226.

[70] Feischl, M., Karkulik, M., Melenk, J. M., and Praetorius, D. Quasi-optimal convergence rate for an adaptive boundary element method. Tech. Rep. 28/2011, Institut für Analysis und Scientific Computing, Technische Universität Wien, 2011.

[71] Feischl, M., Karkulik, M., Melenk, J. M., and Praetorius, D. Residual a-posteriori error estimates in BEM: Convergence of h-adaptive algorithms. Tech. Rep. 21/2011, Institut für Analysis und Scientific Computing, Technische Universität Wien, 2011.

[72] Ferraz-Leite, S., and Praetorius, D. Simple a posteriori error estimators for the h-version of the boundary element method. *Computing 83*, 4 (2008), 135–162.

[73] Friedman, M. B., and Shaw, R. P. Diffraction of pulses by cylindrical obstacles of arbitrary cross section. *Trans. ASME Ser. E. J. Appl. Mech. 29*, 1 (1962), 40–46.

[74] Georgoulis, E. H., Lakkis, O., and Makridakis, C. A posteriori $L^\infty(L^2)$-error bounds in finite element approximation of the wave equation. `arXiv:1003.3641v1`, 2010.

[75] Geranmayeh, A. *Time Domain Boundary Integral Equations Analysis*. PhD thesis, Fachbereich Elektrotechnik und Informationstechnik, Technische Universität Darmstadt, 2011.

[76] Geranmayeh, A., Ackermann, W., and Weiland, T. Temporal discretization choices for stable boundary element methods in electromagnetic scattering problems. *Appl. Numer. Math. 59* (2009), 2751–2773.

[77] Guardasoni, C. *Wave Propagation Analysis with Boundary Element Method*. PhD thesis, Università Statale di Milano, 2010.

[78] Ha-Duong, T. Space-time variational formulas and calculations of retarded potential. vol. I of *Boundary Elements VII*. Springer, Southampton, 1985, pp. 5.51–5.60.

[79] Ha-Duong, T. *Équations intégrales pour la résolution numérique de problèmes de diffraction d'ondes acoustiques dans* $\mathbb{R}^3$. PhD thesis, Université de Paris VI – Pierre et Marie Curie, 1987.

[80] Ha-Duong, T. On the transient acoustic scattering by a flat object. *Japan J. Appl. Math. 7*, 3 (1990), 489–513.

[81] Ha-Duong, T. On retarded potential boundary integral equations and their discretisation. In *Topics in Computational Wave Propagation: Direct and Inverse Problems*, M. Ainsworth, P. Davis, D. B. Duncan, P. A. Martin, and B. Rynne, Eds., vol. 31 of *Lect. Notes Comput. Sci. Eng.* Springer, Berlin, 2003, pp. 301–336.

[82] Ha-Duong, T., Ludwig, B., and Terrasse, I. A Galerkin BEM for transient acoustic scattering by an absorbing obstacle. *Internat. J. Numer. Methods Engrg. 57*, 13 (2003), 1845–1882.

[83] Hackbusch, W. *Integral equations: theory and numerical treatment*, vol. 120 of *International Series of Numerical Mathematics*. Birkhäuser, Basel, 1995.

[84] Hackbusch, W., Kress, W., and Sauter, S. A. Sparse convolution quadrature for time domain boundary integral formulations of the wave equation. *IMA J. Numer. Anal. 29*, 1 (2009), 158–179.

[85] Haque, M. Z., and Moore, P. K. Comparison of *hp*-adaptive error estimates for second order hyperbolic systems. *J. Numer. Math. 10*, 1 (2010), 1–24.

[86] Hardy, G. H., Littlewood, J. E., and Pólya, G. *Inequalities*. Cambridge University Press, Cambridge, 1934.

[87] Hargreaves, J. A., and Cox, T. J. A transient boundary element method model of Schroeder diffuser scattering using well mouth impedance. *J. Acoust. Soc. Am. 124*, 5 (2008), 2942–2951.

[88] He, D. *Local space-time adaptive finite element methods for the wave equation on unbounded domains*. PhD thesis, Department of Mechanical Engineering, Clemson University, 2003.

[89] Hiptmair, R., Hoppe, R. H. W., Joly, P., and Langer, U. Computational electromagnetism and acoustics. Tech. Rep. 05/2007, Mathematisches Forschungsinstitut Oberwolfach, 2007.

[90] Hiptmair, R., Hoppe, R. H. W., Joly, P., and Langer, U. Computational electromagnetism and acoustics. Tech. Rep. 10/2010, Mathematisches Forschungsinstitut Oberwolfach, 2010.

[91] Holm, H., Maischak, M., and Stephan, E. P. The *hp*-version of the boundary element method for Helmholtz screen problems. *Computing 57*, 2 (1996), 105–134.

[92] Hsiao, G. C., and Wendland, W. L. *Boundary integral equations*, vol. 164 of *Applied Mathematical Sciences*. Springer, Berlin, 2008.

[93] Huang, W., and Russell, R. D. *Adaptive Moving Mesh Methods*, vol. 174 of *Applied Mathematical Sciences*. Springer, New York, NY, 2011.

[94] Hughes, T. J. R., and Hulbert, G. M. Space-time finite element methods for elastodynamics: Formulations and error estimates. *Comput. Methods Appl. Mech. Eng. 66*, 3 (1988), 339–363.

[95] Ji, Z., Sarkar, T. K., Jung, B. H., Chung, Y.-S., Salazar-Palma, M., and Mengtao, Y. A stable solution of time domain electric field integral equation for thin-wire antennas using the Laguerre polynomials. *IEEE Trans. Antennas Propag. 52*, 10 (2004), 2641–2649.

[96] Johnson, C. Discontinuous Galerkin finite element methods for second order hyperbolic problems. *Comput. Methods Appl. Mech. Eng. 107*, 1–2 (1993), 117–129.

[97] Jung, B. H., Sarkar, T. K., Chung, Y.-S., Salazar-Palma, M., and Ji, Z. Time-domain combined field integral equation using Laguerre polynomials as temporal basis functions. *Int. J. Numer. Model. 17*, 3 (2004), 251–268.

[98] Khoromskij, B. N., Sauter, S. A., and Veit, A. Fast quadrature techniques for retarded potentials based on TT/QTT tensor approximation. *Comput. Meth. Appl. Math. 11*, 3 (2011), 342–362.

[99] Kneubühl, F. K. *Repetitorium der Physik*. Teubner, Stuttgart, 1982.

[100] Kress, W., and Sauter, S. A. Numerical treatment of retarded boundary integral equations by sparse panel clustering. *IMA J. Numer. Anal. 28*, 1 (2008), 162–185.

[101] Kreuzer, C., and Siebert, K. G. Decay rates of adaptive finite elements with Dörfler marking. *Numer. Math. 117*, 4 (2011), 679–716.

[102] Kröner, A. Adaptive finite element methods for optimal control of second order hyperbolic equations. *Comput. Methods Appl. Math. 11*, 2 (2011), 214–240.

[103] Laliena, A. R., and Sayas, F.-J. Theoretical aspects of the application of convolution quadrature to scattering of acoustic waves. *Numer. Math. 112*, 4 (2009), 637–678.

[104] Lions, J. L., and Magenes, E. *Non-homogeneous boundary value problems and applications. Vol. I*, vol. 181 of *Die Grundlehren der mathematischen Wissenschaften*. Springer, Berlin, 1972.

[105] Lions, J. L., and Magenes, E. *Non-homogeneous boundary value problems and applications. Vol. II*, vol. 182 of *Die Grundlehren der mathematischen Wissenschaften*. Springer, Berlin, 1972.

[106] López-Fernández, M., and Sauter, S. A. A generalized Convolution Quadrature with variable time stepping. Tech. Rep. 17-2011, Institut für Mathematik, Universität Zürich, 2011.

[107] López-Fernández, M., and Sauter, S. A. Generalized Convolution Quadrature with variable time stepping. Part II: Algorithm and numerical results. Tech. Rep. 09-2012, Institut für Mathematik, Universität Zürich, 2012.

[108] Lubich, C. On the multistep time discretization of linear initial-boundary value problems and their boundary integral equations. *Numer. Math. 67*, 3 (1994), 365–389.

[109] Lubich, C. Convolution quadrature revisited. *BIT 44*, 3 (2004), 503–514.

[110] Ludwig, M. *BEM für elastodynamische Probleme*. Diploma thesis, Institut für Angewandte Mathematik, Leibniz Universität Hannover, April 2007.

[111] Maischak, M. The software package maiprogs, 2012. For informations on *maiprogs*, see `http://www.ifam.uni-hannover.de/~maiprogs/`.

[112] Maischak, M. The analytical computation of the Galerkin elements for the Laplace, Lamé and Helmholtz equation in 2D-BEM. Tech. Rep. 95-15, Institut für Angewandte Mathematik, Leibniz Universität Hannover, 1999.

[113] Maischak, M., Mund, P., and Stephan, E. P. Adaptive multilevel BEM for acoustic scattering. *Comput. Methods Appl. Mech. Engrg. 150*, 1–4 (1997), 351–367.

[114] McLean, W. *Strongly elliptic systems and boundary integral equations.* Cambridge University Press, Cambridge, 2000.

[115] Melenk, J. M. Mapping properties of combined field Helmholtz boundary integral operators. Tech. Rep. 01/2010, Institut für Analysis und Scientific Computing, Technische Universität Wien, 2010.

[116] Melenk, J. M., and Sauter, S. A. Convergence analysis for finite element discretizations of the Helmholtz equation with Dirichlet-to-Neumann boundary conditions. *Math. Comp. 79*, 272 (2010), 1871–1914.

[117] Melenk, J. M., and Sauter, S. A. Wavenumber explicit convergence analysis for Galerkin discretizations of the Helmholtz equation. *SIAM J. Numer. Anal. 49*, 3 (2011), 1210–1243.

[118] Michielssen, E., Shanker, B., Aygun, K., Lu, M., and Ergin, A. Plane-wave time-domain algorithms and fast time-domain integral equation solvers. In *Review of Radio Science 1999-2002*, W. R. Stone, Ed. IEEE Press / Wiley Interscience, New York, NY, 2002, pp. 181–200.

[119] Miller, A. Transactions on Mathematical Software (TOMS) Algorithm 644, written in Fortran 90, 2012. Available for download at `http://jblevins.org/mirror/amiller/toms644.zip`.

[120] Mitzner, K. M. Numerical solution for transient scattering from a hard surface of arbitrary shape – retarded potential technique. *J. Acoust. Soc. Am. 42*, 2 (1967), 391–397.

[121] Moiola, A., Hiptmair, R., and Perugia, I. Plane wave approximation of homogeneous Helmholtz solutions. *Z. Angew. Math. Phys. 62*, 5 (2011), 809–837.

[122] Nédélec, J.-C. *Acoustic and electromagnetic equations: integral representations for harmonic problems*, vol. 144 of *Applied Mathematical Sciences*. Springer, New York, NY, 2001.

[123] Nochetto, R. H., and Dörfler, W. Small data oscillation implies the saturation assumption. *Numer. Math. 91*, 1 (2002), 1–12.

[124] Nochetto, R. H., Schmidt, A., and Verdi, C. A posteriori error estimation and adaptivity for degenerate parabolic problems. *Math. Comp. 69*, 229 (2000), 1–24.

[125] Noon, P. J. *The Single Layer Heat Potential and Galerkin Boundary Element Methods for the Heat Equation.* PhD thesis, University of Maryland, College Park, 1988.

[126] Oden, J. T., Prudhomme, S., and Demkowicz, L. A posteriori error estimation for acoustic wave propagation problems. *Arch. Comput. Meth. Eng. 12*, 4 (2005), 343–389.

[127] Ostermann, E. *Numerical Methods for Space-Time Variational Formulations of Retarded Potential Boundary Integral Equations.* PhD thesis, Institut für Angewandte Mathematik, Leibniz Universität Hannover, 2009.

[128] Picasso, M. Numerical study of an anisotropic error estimator in the $L^2(H^1)$ norm for the finite element discretization of the wave equation. *SIAM J. Sci. Comput. 32*, 4 (2010), 2213–2234.

[129] Piessens, R., de Doncker-Kapenga, E., Überhuber, C. W., and Kahaner, D. *QUADPACK: a subroutine package for automatic integration*, vol. 1 of *Springer Series in Computational Mathematics*. Springer, Berlin, 1983.

[130] Rademacher, A. *Adaptive Finite Element Methods for Nonlinear Hyperbolic Problems of Second Order.* PhD thesis, Fakultät für Mathematik, Technische Universität Dortmund, 2009.

[131] Rudin, W. *Functional analysis.* International series in pure and applied mathematics. McGraw-Hill, New York, NY, 1991.

[132] Safjan, A., and Oden, J. T. High-order Taylor-Galerkin and adaptive *h-p* methods for second-order hyperbolic systems: Application to elastodynamics. *Comput. Methods Appl. Mech. Eng. 103*, 1–2 (1993), 187–230.

[133] Sauter, S. A., and Schwab, C. *Boundary Element Methods*, vol. 39 of *Springer Series in Computational Mathematics*. Springer, Berlin, 2011.

[134] Sauter, S. A., and Veit, A. A Galerkin method for retarded boundary integral equations with smooth and compactly supported temporal basis functions. To appear in *Numer. Math.*, DOI:10.1007/s00211-012-0483-7.

[135] Sauter, S. A., and Veit, A. A Galerkin method for retarded boundary integral equations with smooth and compactly supported temporal basis functions. Part ii: implementation and reference solutions. Tech. Rep. 03-2011, Institut für Mathematik, Universität Zürich, 2011.

[136] Sayas, F.-J. Retarded potentials and time domain boundary integral equations: a road-map. Lecture Notes, Workshop on Theoretical and Numerical Aspects of Inverse Problems and Scattering Theory, Universidad Autónoma de Madrid, April 4 - July 8, 2011. Available for download at `http://www.math.udel.edu/~fjsayas/TDBIE.pdf`.

[137] Schmich, M., and Vexler, B. Adaptivity with dynamic meshes for space-time finite element discretizations of parabolic equations. *SIAM J. Sci. Comput. 30*, 1 (2007/08), 369–393.

[138] Schmidt, A., and Siebert, K. G. *Design of adaptive finite element software: the finite element toolbox ALBERTA*, vol. 42 of *Lecture Notes in Computational Science and Engineering*. Springer, Berlin, 2005.

[139] Schneider, P. J., and Eberly, D. H. *Geometric tools for computer graphics*. Morgan Kaufmann, Amsterdam, 2004.

[140] Schulz, H., and Steinbach, O. A new a posteriori error estimator in adaptive direct boundary element methods: the Dirichlet problem. *Calcolo 37*, 2 (2000), 79–96.

[141] Schwab, C. Variable order composite quadrature of singular and nearly singular integrals. *Computing 53*, 2 (1994), 173–194.

[142] Shaw, R. P. Boundary integral equation methods applied to wave problems. In *Developments in boundary element methods*, P. Banerjee and R. Butterfield, Eds. Elsevier, London, 1979, pp. 121–153.

[143] Shi, Y., and Chen, R. S. Analysis of transient electromagnetic scattering using Hermite polynomials. In *IEEE Antennas and Propagation Society International Symposium (Albuquerque, NM, 2006)* (Piscataway, NJ, 2006), IEEE Operations Center, pp. 3895–3898.

[144] Steinbach, O. Adaptive boundary element methods based on computational schemes for Sobolev norms. *SIAM J. Sci. Comput. 22*, 2 (2000), 604–616.

[145] Steinbach, O. *Numerical approximation methods for elliptic boundary value problems. Finite and Boundary Elements*. Springer, New York, NY, 2008.

[146] Stephan, E. P. The *h-p* boundary element method for solving 2- and 3-dimensional problems. *Comput. Methods Appl. Mech. Engrg. 133*, 3–4 (1996), 183–208.

[147] Terrasse, I. *Résolution mathématique et numérique des équations de Maxwell instationnaires par une méthode de potentiels retardés*. PhD thesis, École Polytechnique, Palaiseau, 1993.

[148] Terrasse, I., and Abboud, T. Modélisation des phénomènes de propagation d'ondes. Lecture notes, Programme d'approfondissement sciences de l'ingénieur, simulation et modélisation, École Polytechnique, Palaiseau, 2007. Available for download at `http://catalogue.polytechnique.fr/site.php?id=123&fileid=684`.

[149] Thompson, L. L. A review of finite-element methods for time-harmonic acoustics. *J. Acoust. Soc. Am. 119*, 3 (2006), 1315–1330.

[150] Thompson, L. L., and He, D. Adaptive space-time finite element methods for the wave equation on unbounded domains. *Comput. Methods Appl. Mech. Engrg. 194*, 18–20 (2005), 1947–2000.

[151] Trèves, F. *Basic linear partial differential equations*, vol. 62 of *Pure and Applied Mathematics*. Academic Press, New York, NY, 1975.

[152] Veit, A. *Numerical methods for time-domain boundary integral equations*. PhD thesis, Mathematisch-Naturwissenschaftliche Fakultät, Universität Zürich, 2011.

[153] Verfürth, R. *A review of a posteriori error estimation and adaptive mesh-refinement techniques*. Wiley-Teubner Series in Advances in Numerical Mathematics. Wiley-Teubner, Chichester, 1996.

[154] Wilcox, C. H. *Scattering theory for the d'Alembert equation in exterior domains*, vol. 442 of *Lecture Notes in Mathematics*. Springer, Berlin, 1975.

[155] Yilmaz, A. E., Jin, J.-M., and Michielssen, E. Time domain adaptive integral method for surface integral equations. *IEEE Trans. Antennas Propag. 52*, 10 (2004), 2692–2708.

[156] Zhu, M.-D., Zhou, X.-L., and Yin, W.-Y. An adaptive marching-on-in-order method with FFT-based blocking scheme. *IEEE Antenn. Wireless Propag. Lett. 9* (2010), 436–439.

[157] Zienkiewicz, O. C. The background of error estimation and adaptivity in finite element computations. *Comput. Methods Appl. Mech. Engrg. 195*, 4–6 (2006), 207–213.

Appendix A

Notes on the Analytical Computation of the Temporal Integrals

This appendix is concerned with the analytical computation of integrals of the type (2.18),

$$\Upsilon^{q;\,m,n}(r) = \int_0^\infty \int_0^\infty H(t-s-r)\kappa(s,t;r)\ \beta^{m,q_1}(s)\beta^{n,q_2}(t)\ ds\ dt$$

which appear as the temporal part of the general form of the matrix entries (2.15).

We consider different types of basis functions with arbitrary kernel in Section A.1, and with the kernels of the Single Layer, Double Layer and Hypersingular operators in Section A.2.

A.1 Computation of some General Temporal Integrals

In this section we use the notation

$$\bar{k}(s,t;r) \coloneqq \int k(s,t;r)\ ds \tag{A.1}$$

$$K(s,t;r) \coloneqq \int \bar{k}(s,t;r)\ dt = \int\int k(s,t;r)\ ds\ dt \tag{A.2}$$

$$\tilde{K}(t;r) \coloneqq \int \lim_{s\to t-r} \bar{k}(s,t;r)\ dt \tag{A.3}$$

for integrals of the type (2.24), and

$$K_\alpha(s;r) \coloneqq \int k(s,\alpha;r)\ ds \tag{A.4}$$

for integrals of the type (2.36).

In what follows, we consider ansatz and test functions of different polynomial degrees in the integrals (2.18) and (2.33) with arbitrary kernel κ, and the analytical computation of their temporal part. Each case features some considerations that hold for arbitrary temporal meshes, followed by simplifications that are only valid for uniform temporal meshes. We give indications on the non-uniform case in Remark A.1 in Section A.1.4.

A.1.1 Piecewise Linear Ansatz and Piecewise Constant Test Functions

We consider integrals of the type (2.18) with $q_1 = 1$, $q_2 = 0$,

$$\begin{aligned}
&\Upsilon_{L,C}(r) := \Upsilon^{(1,0);\,m,n}(r)\\
=\;& \int_0^\infty \int_0^\infty H(t-s-r)\kappa(s,t;r)\beta^m(s)\gamma^n(t)\;ds\;dt\\
=\;& \frac{1}{\Delta t}\sum_{i=0,1}(-1)^i \int_{t_{n-1}}^{t_n}\int_{t_{m+i-1}}^{t_{m+i}} H(t-s-r)\kappa(s,t;r)(s-t_{m+2i-1})\;ds\;dt\\
=\;& \frac{1}{\Delta t}\sum_{i=0,1}(-1)^i \Upsilon_{L,C}^{m+i,n}(r) \qquad\qquad (A.5)
\end{aligned}$$

with β^m and γ^n as in (2.10) and

$$\Upsilon_{L,C}^{m+i,n}(r) := \int_{t_{n-1}}^{t_n}\int_{t_{m+i-1}}^{t_{m+i}} H(t-s-r)k(s,t;r)\;ds\;dt \qquad (A.6)$$

for $i \in \{0,1\}$, which is an integral of the type (2.20) with kernel $k(s,t;r) = \kappa(s,t;r)(s-t_{m+2i-1})$. Using notation (A.3), the kernels $\bar{k}$, K and $\tilde{K}$ are of the form

$$\begin{aligned}
\bar{k}(s,t;r) &= \bar{k}_1(t-s;r) + (\alpha-s)\bar{k}_0(t-s;r)\\
K(s,t;r) &= K_0(t-s;r) + (\alpha-s)K_1(t-s;r)\\
\tilde{K}(t;r) &= \tilde{K}_0(t;r) + (t-\alpha)^2\tilde{K}_1(r) \qquad\qquad (A.7)
\end{aligned}$$

for $\alpha \in \mathbb{R}$, where

$$\begin{aligned}
\bar{k}_0(t-s;r) &= -\int \kappa(s,t;r)\;ds \qquad \bar{k}_1(t-s;r) = -\int\int \kappa(s,t;r)\;ds\;ds\\
K_0(t-s;r) &= \int \bar{k}_1(t-s;r)\;dt = -\int\int\int \kappa(s,t;r)\;ds\;ds\;dt\\
K_1(t-s;r) &= \int \bar{k}_0(t-s;r)\;dt = -\int\int \kappa(s,t;r)\;ds\;dt\\
\tilde{K}_0(t;r) &= t(r\bar{k}_0(r;r) + \bar{k}_1(r;r)) \qquad \tilde{K}_1(r) = -\frac{1}{2}\bar{k}_0(r;r)
\end{aligned}$$

We thus write $\bar{k}(t-s,\alpha-s;r)$, $K(t-s,\alpha-s;r)$ and $\tilde{K}(t,t-\alpha;r)$ instead of $\bar{k}(s,t;r)$, $K(s,t;r)$ and $\tilde{K}(t;r)$. There holds the relation

$$\tilde{K}(t_1,t_1-\alpha;r) - \tilde{K}(t_2,t_2-\alpha;r) = (t_1-t_2)\left(\bar{k}_1(r;r) + (r+\alpha-\frac{1}{2}(t_1+t_2))\bar{k}_0(r;r)\right). \qquad (A.8)$$

By (2.24) we can now express $\Upsilon^i_{L,C}$ in terms of K and $\tilde{K}$,

$$\begin{aligned}
\Upsilon^{m+i,n}_{L,C}(r) = \quad & \mathbb{1}_{D_{l-i-1}}(r)\Big(\quad K(t_{l-i},\alpha-t_{m+i};r) - K(t_{l-i-1},\alpha-t_{m+i};r) \\
& \qquad - \quad K(t_{l-i+1},\alpha-t_{m+i-1};r) + K(t_{l-i},\alpha-t_{m+i-1};r)\Big) \\
& +\mathbb{1}_{E_{l-i-1}}(r)\Big(\quad \tilde{K}(r+t_{m+i},r+t_{m+i}-\alpha;r) - \tilde{K}(t_{n-1},t_{n-1}-\alpha;r) \\
& \qquad + \quad K(t_{l-i},\alpha-t_{m+i-1};r) + K(t_{l-i},\alpha-t_{m+i};r) \\
& \qquad - \quad K(r,\alpha-t_{m+i};r) - K(t_{l-i+1},\alpha-t_{m+i-1};r)\Big) \\
& +\mathbb{1}_{E_{l-i}}(r)\Big(\quad \tilde{K}(t_n,t_n-\alpha;r) - \tilde{K}(r+t_{m+i-1},r+t_{m+i-1}-\alpha;r) \\
& \qquad - \quad K(t_{l-i+1},\alpha-t_{m+i-1};r) + K(r,\alpha-t_{m+i-1};r)\Big)
\end{aligned}$$

Inserting $\alpha = t_{m+2i-1}$, $i \in \{0,1\}$,

$$\begin{aligned}
\Upsilon^{m+i,n}_{L,C}(r) = \Upsilon^{l,i}_{L,C}(r) = \quad & \mathbb{1}_{D_{l-i-1}}(r)\Big(\quad K(t_{l-i},t_{i-1};r) - K(t_{l-i-1},t_{i-1};r) \\
& \qquad - \quad K(t_{l-i+1},t_i;r) + K(t_{l-i},t_i;r)\Big) \\
& +\mathbb{1}_{E_{l-i-1}}(r)\Big(\quad \tilde{K}(r+t_{m+i},r+t_{-i+1};r) - \tilde{K}(t_{n-1},t_{l-2i};r) \\
& \qquad + \quad K(t_{l-i},t_i;r) + K(t_{l-i},t_{i-1};r) \\
& \qquad - \quad K(r,t_{i-1};r) - K(t_{l-i+1},t_i;r)\Big) \\
& +\mathbb{1}_{E_{l-i}}(r)\Big(\quad \tilde{K}(t_n,t_{l-2i+1};r) - \tilde{K}(r+t_{m+i-1},r+t_{-i};r) \\
& \qquad - \quad K(t_{l-i+1},t_i;r) + K(r,t_i;r)\Big) \\
=: \mathbb{1}_{D_{l-i-1}}(r)F^D_{L,C}(l,i;r) & + \mathbb{1}_{E_{l-i-1}}(r)F^{E_p}_{L,C}(l,i;r) + \mathbb{1}_{E_{l-i}}(r)F^{E_c}_{L,C}(l,i;r)
\end{aligned}$$

In summary, using (A.5),

$$\begin{aligned}
& (\Delta t)\Upsilon_{L,C}(r) \\
= \quad & \sum_{i=0,1}(-1)^{l,i}\Upsilon^i_{L,C}(r) \\
= \quad & \mathbb{1}_{D_{l-2}}(r)\left(F^D_{L,C}(l,0;r) - F^D_{L,C}(l,1;r)\right) \quad + \quad \mathbb{1}_{E_{l-2}}(r)\left(F^D_{L,C}(l,0;r) - F^{E_p}_{L,C}(l,1;r)\right) \\
& +\mathbb{1}_{E_{l-1}}(r)\left(F^{E_p}_{L,C}(l,0;r) - F^{E_c}_{L,C}(l,1;r)\right) \quad + \quad \mathbb{1}_{E_l}(r)\left(F^{E_c}_{L,C}(l,0;r)\right) \\
=: \quad & \mathbb{1}_{D_{l-2}}(r)F^D_{L,C}(l;r) + \mathbb{1}_{E_{l-2}}(r)F^{E_{pp}}_{L,C}(l;r) + \mathbb{1}_{E_{l-1}}(r)F^{E_p}_{L,C}(l;r) + \mathbb{1}_{E_l}(r)F^{E_c}_{L,C}(l;r). \qquad \text{(A.9)}
\end{aligned}$$

A.1.2 Piecewise Constant Ansatz and Test Functions

We consider integrals of the type (2.18) with $q_1, q_2 = 0$,

$$\begin{aligned}
\Upsilon_{C,C}(r) := \Upsilon^{(0,0);\,m,n}(r) \quad &= \quad \int_0^\infty \int_0^\infty H(t-s-r)\kappa(s,t;r)\gamma^m(s)\gamma^n(t)\; ds\; dt \\
&= \quad \int_{t_{n-1}}^{t_n}\int_{t_{m-1}}^{t_m} H(t-s-r)\kappa(s,t;r)\; ds\; dt \qquad \text{(A.10)}
\end{aligned}$$

with γ^m and γ^n as in (2.10). $\Upsilon_{C,C}$ is immediately given by (2.20), and with $K(s,t;r) = K(t-s;r)$, $\tilde{K}(t;r) = t\bar{k}(r;r)$ and $k(s,t;r) = \kappa(s,t;r)$ we obtain, by (2.24)

$$\begin{aligned}
\Upsilon_{C,C}(r) = \Upsilon^l_{C,C}(r) &= \mathbb{1}_{D_{l-1}}(r)\,(2K(t_l;r) - K(t_{l-1};r) - K(t_{l+1};r)) \\
&\quad + \mathbb{1}_{E_{l-1}}(r)\left(\tilde{K}(r+t_m;r) - \tilde{K}(t_{n-1};r) + 2K(t_l;r) - K(r;r) - K(t_{l+1};r)\right) \\
&\quad + \mathbb{1}_{E_l}(r)\left(\tilde{K}(t_n;r) - \tilde{K}(r+t_{m-1};r) - K(t_{l+1};r) + K(r;r)\right). \\
&= \mathbb{1}_{D_{l-1}}(r)\,(2K(t_l;r) - K(t_{l-1};r) - K(t_{l+1};r)) \\
&\quad + \mathbb{1}_{E_{l-1}}(r)\left((r-t_{l-1})\bar{k}(r;r) + 2K(t_l;r) - K(r;r) - K(t_{l+1};r)\right) \\
&\quad + \mathbb{1}_{E_l}(r)\left((t_{l+1}-r)\bar{k}(r;r) - K(t_{l+1};r) + K(r;r)\right). \\
&=: \mathbb{1}_{D_{l-1}}(r)F^D_{C,C}(l;r) + \mathbb{1}_{E_{l-1}}(r)F^{E_p}_{C,C}(l;r) + \mathbb{1}_{E_l}(r)F^{E_c}_{C,C}(l;r). \qquad \text{(A.11)}
\end{aligned}$$

A.1.3 Piecewise Linear Ansatz and Derivatives of Piecewise Constant Test Functions

We consider integrals of the type (2.33) with $q_1 = 1$,

$$\begin{aligned}
&\Upsilon_{L,\dot{C}}(r) = \Upsilon^{(1,-1);m,n}(r) \\
&= \int_0^\infty \int_0^\infty H(t-s-r)\kappa(s,t;r)\beta^m(s)\dot{\gamma}^n(t)\; ds\; dt \\
&= \int_0^\infty \int_0^\infty H(t-s-r)\kappa(s,t;r)\left(\sum_{i=0,1}\frac{1}{\Delta t}(-1)^i(s-t_{m+2i-1})\mathbb{1}_{T_{m+i}}(s)\right)\dot{\gamma}^n(t)\; ds\; dt \\
&= \frac{1}{\Delta t}\sum_{i=0,1}(-1)^i\int_{t_{m+i-1}}^{t_{m+i}}\left(H(t_{n-1}-s-r)\kappa(s,t_{n-1};r) - H(t_n-s-r)\kappa(s,t_n;r)\right)(s-t_{m+2i-1})\; ds \\
&= \frac{1}{\Delta t}\sum_{i,j=0,1}(-1)^{i+j+1}\int_{t_{m+i-1}}^{t_{m+i}}\kappa(s,t_{n-j};r)(s-t_{m+2i-1})H(t_{n-j}-s-r)\; ds. \qquad \text{(A.12)}
\end{aligned}$$

Let

$$\Upsilon^{m+i}_{\alpha,\beta}(r) := \int_{t_{m+i-1}}^{t_{m+i}} H(\alpha-s-r)\kappa(s,\alpha;r)(s-\beta)\; ds \qquad \text{(A.13)}$$

which is an integral of the type (2.34) with kernel $k(s,\alpha,\beta;r) := \kappa(s,\alpha;r)(s-\beta)$ and $\alpha = t_{n-j}$, $\beta = t_{m+2i-1}$. By (2.35),

$$\Upsilon^{m+i}_{\alpha,\beta}(r) = \begin{cases} \int_{t_{m+i-1}}^{t_{m+i}} k(s,\alpha,\beta;r)ds & \text{if } r < \alpha - t_{m+i} \\ \int_{t_{m+i-1}}^{\alpha-r} k(s,\alpha,\beta;r)ds & \text{if } \alpha - t_{m+i} < r < \alpha - t_{m+i-1} \end{cases}.$$

Inserting $\alpha = t_{n-j}$, we thus distinguish $r < t_{l-j-i}$ and $t_{l-j-i} < r < t_{l-j-i+1}$. Hence, with $\beta = t_{m+2i-1}$,

$$\begin{aligned}
\Upsilon^{m+i}_{t_{n-j},t_{m+2i-1}}(r) &= \mathbb{1}_{D_{l-j-i}}(r)\int_{t_{m+i-1}}^{t_{m+i}} k(s,t_{n-j},t_{m+2i-1};r)\; ds \\
&\quad + \mathbb{1}_{E_{l-j-i}}(r)\int_{t_{m+i-1}}^{t_{n-j}-r} k(s,t_{n-j},t_{m+2i-1};r)\; ds. \qquad \text{(A.14)}
\end{aligned}$$

The structure of the kernels we consider allows us to write $K_{\alpha-s}(\beta-s;r)$ instead of $K_\alpha(s;r)$ in (A.4). Then, with $\alpha = t_{n-j}$, $\beta = t_{m+2i-1}$,

$$\begin{aligned}
&\Upsilon^{m+i}_{t_{n-j},t_{m+2i-1}}(r) =: \Upsilon^{l;i,j}_{L,\dot C}(r)\\
= \quad & \mathbb{1}_{D_{l-j-i}}(r)\big(\quad K(t_{n-j}-t_{m+i}, t_{m+2i-1}-t_{m+i};r)\\
& \qquad\qquad - K(t_{n-j}-t_{m+i-1}, t_{m+2i-1}-t_{m+i-1};r)\big)\\
& +\mathbb{1}_{E_{l-j-i}}(r)\big(\quad K(t_{n-j}-(t_{n-j}-r), t_{m+2i-1}-(t_{n-j}-r);r)\\
& \qquad\qquad - K(t_{n-j}-t_{m+i-1}, t_{m+2i-1}-t_{m+i-1};r)\big)\\
= \quad & \mathbb{1}_{D_{l-j-i}}(r)\big(K(t_{l-j-i}, t_{i-1};r) - K(t_{l-j-i+1}, t_i;r)\big)\\
& +\mathbb{1}_{E_{l-j-i}}(r)\big(K(r, r-t_{l-2i-j+1};r) - K(t_{l-j-i+1}, t_i;r)\big)\\
=: \quad & \mathbb{1}_{D_{l-j-i}}(r)F^D_{L,\dot C}(l,i,j;r) + \chi_{E_{l-j-i}}(r)F^E_{L,\dot C}(l,i,j;r). \qquad \text{(A.15)}
\end{aligned}$$

In summary, using (A.12),

$$\begin{aligned}
&\Delta t\Upsilon_{L,\dot C}(r)\\
= \quad & \sum_{i,j=0,1}(-1)^{i+j+1}\Upsilon^{l;i,j}_{L,\dot C}(r)\\
= \quad & \mathbb{1}_{D_{l-2}}(r)\Big(-F^D_{L,\dot C}(l,0,0;r) - F^D_{L,\dot C}(l,1,1;r) + F^D_{L,\dot C}(l,0,1;r) + F^D_{L,\dot C}(l,1,0;r)\Big)\\
& +\mathbb{1}_{E_{l-2}}(r)\Big(-F^D_{L,\dot C}(l,0,0;r) - F^E_{L,\dot C}(l,1,1;r) + F^D_{L,\dot C}(l,0,1;r) + F^D_{L,\dot C}(l,1,0;r)\Big)\\
& +\mathbb{1}_{E_{l-1}}(r)\Big(-F^D_{L,\dot C}(l,0,0;r) + F^E_{L,\dot C}(l,0,1;r) + F^E_{L,\dot C}(l,1,0;r)\Big)\\
& +\mathbb{1}_{E_l}(r)\Big(-F^E_{L,\dot C}(l,0,0;r)\Big)\\
=: \quad & \mathbb{1}_{D_{l-2}}(r)F^D_{L,\dot C}(l;r) + \mathbb{1}_{E_{l-2}}(r)F^{E_{pp}}_{L,\dot C}(l;r) + \mathbb{1}_{E_{l-1}}(r)F^{E_p}_{L,\dot C}(l;r) + \mathbb{1}_{E_l}(r)F^{E_c}_{L,\dot C}(l;r). \qquad \text{(A.16)}
\end{aligned}$$

A.1.4 Piecewise Constant Ansatz and Derivatives of Piecewise Constant Test Functions

We consider integrals of the type (2.33) with $q_1 = 0$,

$$\begin{aligned}
\Upsilon_{C,\dot C}(r) \quad &= \quad \Upsilon^{(0,-1);m,n}(r) = \int_0^\infty\int_0^\infty H(t-s-r)\kappa(s,t;r)\gamma^m(s)\dot\gamma^n(t)\,ds\,dt\\
&= \quad \sum_{j=0,1}(-1)^{j+1}\int_{t_{m-1}}^{t_m} H(t_{n-j}-s-r)\kappa(s,t_{n-j};r)\,ds\\
&= \quad \sum_{j=0,1}(-1)^{j+1}\Upsilon^m_{t_{n-j}}(r) \qquad \text{(A.17)}
\end{aligned}$$

with $\Upsilon^m_{t_{n-j}}$ as in (2.36). We define $K(\alpha-s;r) := \int\kappa(s,\alpha;r)\,ds$. Clearly,

$$\begin{aligned}
\Upsilon^m_{t_{n-j}}(r) =: \Upsilon^l_j(r) \quad &= \quad \mathbb{1}_{D_{l-j}}(r)\left(K(t_{n-j}-t_m;r) - K(t_{n-j}-t_{m-1};r)\right)\\
&\quad +\mathbb{1}_{E_{l-j}}(r)\left(K(t_{n-j}-(t_{n-j}-r);r) - K(t_{n-j}-t_{m-1};r)\right)\\
&= \quad \mathbb{1}_{D_{l-j}}(r)\big(K(t_{l-j};r) - K(t_{l-j+1};r)\big) + \mathbb{1}_{E_{l-j}}(r)\big(K(r;r) - K(t_{l-j+1};r)\big)\\
&=: \quad \mathbb{1}_{D_{l-j}}(r)F^D_{C,\dot C}(l,j;r) + \mathbb{1}_{E_{l-j}}(r)F^E_{C,\dot C}(l,j;r). \qquad \text{(A.18)}
\end{aligned}$$

In summary,

$$\begin{aligned}\Upsilon_{C,\dot{C}}(r) &= \sum_{j=0,1}(-1)^{j+1}\Upsilon_j^l(r) = \Upsilon_1^l(r) - \Upsilon_0^l(r)\\ &= \mathbb{1}_{D_{l-1}}(r)\left(F^D_{C,\dot{C}}(l,1;r) - F^D_{C,\dot{C}}(l,0;r)\right)\\ &\quad +\mathbb{1}_{E_{l-1}}(r)\left(F^E_{C,\dot{C}}(l,1;r) - F^D_{C,\dot{C}}(l,0;r)\right) \;+\; \mathbb{1}_{E_l}(r)\left(-F^E_{C,\dot{C}}(l,0;r)\right)\\ &=: \mathbb{1}_{D_{l-1}}(r)F^D_{C,\dot{C}}(l;r) + \mathbb{1}_{E_{l-1}}(r)F^{E_p}_{C,\dot{C}}(l;r) + \mathbb{1}_{E_l}(r)F^{E_c}_{C,\dot{C}}(l;r). \qquad (A.19)\end{aligned}$$

Remark A.1 (Non-Uniform Temporal Meshes)
Note that the simplification (A.19) *can only be done if the underlying temporal mesh is uniform. If the temporal mesh is non-uniform, one has to keep* (A.18) *in its l-independent form, i.e.*

$$\begin{aligned}\Upsilon^m_{t_{n-j}}(r) &= \mathbb{1}_{[0,t_{n-j}-t_m]}(r)\left(K(t_{n-j}-t_m;r) - K(t_{n-j}-t_{m-1};r)\right)\\ &\quad +\mathbb{1}_{[t_{n-j}-t_m,t_{n-j-1}-t_{m-1}]}(r)\left(K(t_{n-j}-(t_{n-j}-r);r) - K(t_{n-j}-t_{m-1};r)\right)\end{aligned}$$

and treat the terms $\Upsilon^m_{t_{n-1}}$ *and* $\Upsilon^m_{t_n}$ *in* (A.17) *separately. Instead of integrating over one discrete light disc and two discrete light rings as in* (A.19)*, one then has to integrate over two discrete light discs and two discrete light rings instead.*

Similar considerations need to be made for the other types of basis functions. In Section A.1.1, for instance, (A.5) *is replaced by*

$$\Upsilon_{L,C}(r) = \sum_{i=0,1}(-1)^i\frac{1}{\Delta t_{m+i-1}}\Upsilon^{m+i,n}_{L,C}(r)$$

where $\Upsilon^{m+i,n}_{L,C}(r)$ *has to be kept in its l-independent form. Recomputing* $\Upsilon^{m+i,n}_{L,C}(r)$ *for non-uniform temporal meshes, there are contributions from two discrete light discs and six discrete light rings. For a uniform temporal mesh, as shown in* (A.9)*, one has to integrate over one discrete light disc and three discrete light rings only instead.*

A.1.5 Derivatives of Piecewise Constant Ansatz and Piecewise Constant Test Functions

Finally we consider integrals of the type

$$\Upsilon_{\dot{C},C}(r) = \Upsilon^{(-1,0);m,n}(r) = \int_0^\infty\int_0^\infty H(t-s-r)\kappa(s,t;r)\dot{\gamma}^m(s)\gamma^n(t)\,ds\,dt. \qquad (A.20)$$

By theoretical considerations (see Remark 4.1), we have

$$\Upsilon_{\dot{C},C} = -\Upsilon_{C,\dot{C}} \qquad (A.21)$$

which is given by (A.19).

A.2 Explicit Analytical Temporal Integration of the Kernels of some Time Domain Boundary Integral Operators

In this section, we consider particular examples of temporal integrals of the types studied in Section A.1, with the kernels of the four time domain boundary integral operators given in Definition 1.4.

A.2.1 Notations

Let us define functions

$$S(a) := S(a;r) := \sqrt{a^2 - r^2} \qquad \text{and} \qquad L(a) := L(a;r) := \ln\left(a + \sqrt{a^2 - r^2}\right). \tag{A.22}$$

The derivatives with respect to a are

$$S'(a) = \frac{a}{\sqrt{a^2 - r^2}} = \frac{a}{S(a)} \qquad \text{and} \qquad L'(a) = \frac{1}{\sqrt{a^2 - r^2}} = \frac{1}{S(a)}. \tag{A.23}$$

The integrals given in Table A.1 will prove to be useful in what follows.

$$\int \frac{1}{S(t-s)} ds = -L(t-s) \tag{A.24}$$

$$\int L(t-s) dt = (t-s)L(t-s) - S(t-s) \tag{A.25}$$

$$\int L(t-s) ds = -\int L(t-s) dt = -(t-s)L(t-s) + S(t-s) \tag{A.26}$$

$$\int S(t-s) dt = \frac{1}{2}\left((t-s)S(t-s) - r^2 L(t-s)\right) \tag{A.27}$$

$$\int S(t-s) ds = -\int S(t-s) dt = \frac{1}{2}\left(r^2 L(t-s) - (t-s)S(t-s)\right) \tag{A.28}$$

$$\int (t-s)L(t-s) dt = \frac{1}{2}\left((t-s)^2 L(t-s) - \frac{1}{2}(t-s)S(t-s) - \frac{1}{2}r^2 L(t-s)\right) \tag{A.29}$$

$$\int (t-s)^2 L(t-s) dt = \frac{1}{3}\left((t-s)^3 L(t-s) - \frac{1}{3}(t-s)^2 S(t-s) - \frac{2}{3}r^2 S(t-s)\right) \tag{A.30}$$

$$\int (t-s)S(t-s)^{n-2} dt = \frac{1}{n}S(t-s)^n \qquad (n \geq 3) \tag{A.31}$$

$$\int \frac{s-\beta}{S(\alpha-s)(\alpha-s+r)} ds = (\beta-s)\left(\frac{(\alpha-s)-r}{rS(\alpha-s)}\right) + L(\alpha-s) - \frac{1}{r}S(\alpha-s) \tag{A.32}$$

$$\int \frac{(\alpha-s)-r}{rS(\alpha-s)} ds = L(\alpha-s) - \frac{1}{rS(\alpha-s)} \tag{A.33}$$

$$\int (\beta-s)\frac{(\alpha-s)-r}{rS(\alpha-s)} ds = (\beta-\alpha-\frac{r}{2})L(\alpha-s) + \frac{1}{2r}(s+\alpha+2(r-\beta))S(\alpha-s) \tag{A.34}$$

$$= (\beta-s)(L(\alpha-s) - \frac{1}{r}S(\alpha-s)) + (\alpha-s)(-L(\alpha-s) + \frac{1}{2r}S(\alpha-s)) + (-\frac{r}{2}L(\alpha-s) + S(\alpha-s))$$

Table A.1: Table of integrals for the analytical computation of temporal integrals of matrix entries for temporal basis functions of low polynomial order, with S, L as in (A.22) and $\alpha, \beta \in \mathbb{R}$.

Functions of type (A.22) appear as parts of the kernel functions (2.18) of the spatial boundary integrals. For this reason, we also need to analyse their behaviour as kernel functions in r. We compute

$$\frac{\partial}{\partial x_i} S(a;r) = -\frac{x_i - y_i}{S(a;r)} \qquad \text{and} \qquad \frac{\partial}{\partial x_i} L(a;r) = -\frac{x_i - y_i}{S(a;r)} \frac{1}{a + \sqrt{a^2 - r^2}} \tag{A.35}$$

for $r = \sqrt{(x_1-y_1)^2+(x_2-y_2)^2}$. Since $\lim_{r\to a} S(a;r) = 0$, the spatial derivatives of S and L are both singular for $r \to a$. We observe in the following that $r = a$ typically corresponds to the boundary of a light disc or of a light ring. This means that we need to take particular care of the singularities in the derivatives when we integrate over these domains. After studying some exemplary cases, we summarise in Section A.3 some properties of all the spatial kernel functions that we consider in Sections A.2.2, A.2.3 and A.2.4. An abstract class of spatial kernel functions that includes all the kernel functions considered in this section is analysed in Section 2.5.

A.2.2 The Time Domain Single Layer Operator

A.2.2.1 The Time Domain Single Layer Operator with Piecewise Constant Ansatz and Test Functions

The time domain Single Layer operator is given by (1.8),

$$V[\varphi](x,t) = \int_\Gamma \int_{\mathbb{R}_{\geq 0}} G(t-s,|x-y|)\ \varphi(y,s)\ ds\ ds_y \tag{A.36}$$

for $(x,t) \in \Gamma \times \mathbb{R}_{\geq 0}$. We compute the bilinear form as indicated by (2.26), and with p_N, q_N as in (2.16),

$$\begin{aligned} & b_V(p_N,q_N) := \int_0^\infty \langle V[p_N](\cdot,t), q_N(\cdot,t)\rangle\, dt \\ = & \frac{1}{2\pi}\sum_{m=1}^{M_T}\sum_{i=1}^{N_S} p_i^m \iint_{\Gamma\times\Gamma}\int_{t_{n-1}}^{t_n}\int_{t_{m-1}}^{t_m} \frac{H(t-s-r)}{S(t-s;r)}\gamma^m(s)\gamma^n(t)\ ds\ dt\ \varphi_i(y)\varphi_j(x)\ ds_x\ ds_y \\ = & \frac{1}{2\pi}\sum_{m=1}^{M_T}\sum_{i=1}^{N_S} p_i^m \iint_{\Gamma\times\Gamma} \Upsilon_{C,C}^{V;m,n}(r)\ \varphi_i(y)\varphi_j(x)\ ds_x\ ds_y \end{aligned} \tag{A.37}$$

where

$$\Upsilon_{C,C}^{V;m,n}(r) = \int_{t_{n-1}}^{t_n}\int_{t_{m-1}}^{t_m} H(t-s-r)\frac{1}{S(t-s;r)}\ ds\ dt \tag{A.38}$$

is a realisation of (A.10). We can compute $\Upsilon_{C,C}^{V;m,n} = \Upsilon_{C,C}^{V;l}$ analytically, using the results of Section A.1.2. Here, $\kappa(s,t;r) = \frac{1}{S(t-s;r)}$, and thus, by (A.24) and (A.25),

$$\begin{aligned} \bar{k}(t-s;r) &= -L(t-s;r) && \text{(A.39)}\\ K(t-s;r) &= S(t-s;r) - (t-s)L(t-s;r) && \text{(A.40)}\\ K(r;r) &= S(r;r) - rL(r;r) = -r\ln r && \text{(A.41)}\\ \bar{k}(r;r) &= -\ln r. && \text{(A.42)} \end{aligned}$$

$\Upsilon_{C,C}^{V;l}$ is then immediately given by (A.11), with

$$\begin{aligned} F_{C,C}^{D}(l;r) &= -S(t_{l-1};r) + 2S(t_l;r) - S(t_{l+1};r) + t_{l-1}L(t_{l-1};r) - 2t_lL(t_l;r) + t_{l+1}L(t_{l+1};r)\\ F_{C,C}^{E_p}(l;r) &= 2S(t_l;r) - S(t_{l+1};r) + t_{l-1}\ln r - 2t_lL(t_l;r) + t_{l+1}L(t_{l+1};r)\\ F_{C,C}^{E_c}(l;r) &= -S(t_{l+1};r) - t_{l-1}\ln r + t_{l+1}L(t_{l+1};r). \end{aligned} \tag{A.43}$$

A.2.2.2 The Time Domain Single Layer Operator with Piecewise Constant Ansatz and Derivatives of Piecewise Constant Test Functions

For this choice of basis functions, we replace $\int_0^\infty \int_0^\infty \frac{H(t-s-r)}{S(t-s;r)}\ \gamma^m(s)\gamma^n(t)ds\ dt$ in (A.37) by

$$\int_0^\infty \int_0^\infty \frac{H(t-s-r)}{S(t-s;r)}\ \gamma^m(s)\dot{\gamma}^n(t)ds\ dt =: \Upsilon^{V;m,n}_{C,\dot{C}}(r) \tag{A.44}$$

which is a realisation of (A.18) with $\kappa(t-s;r) = \frac{1}{S(t-s;r)}$. Therefore $\Upsilon^{V;m,n}_{C,\dot{C}} = \Upsilon^{V;l}_{C,\dot{C}}$ is given by (A.19) with

$$\begin{aligned} K(\alpha-s;r) &= -L(\alpha-s;r) && \text{(A.45)}\\ K(r;r) &= -\ln r && \text{(A.46)} \end{aligned}$$

which gives

$$\begin{aligned} F^{D}_{C,\dot{C}}(l;r) &= -L(t_{l-1};r) + 2L(t_l;r) - L(t_{l+1};r)\\ F^{E_p}_{C,\dot{C}}(l;r) &= -\ln r + 2L(t_l;r) - L(t_{l+1};r)\\ F^{E_c}_{C,\dot{C}}(l;r) &= \ln r - L(t_{l+1};r). \end{aligned} \tag{A.47}$$

A.2.2.3 The Time Domain Single Layer Operator with piecewise linear ansatz and constant test functions

For this choice of basis functions, we replace $\int_0^\infty \int_0^\infty \frac{H(t-s-r)}{S(t-s;r)}\ \gamma^m(s)\gamma^n(t)ds\ dt$ in (A.37) by

$$\int_0^\infty \int_0^\infty \frac{H(t-s-r)}{S(t-s;r)}\ \beta^m(s)\gamma^n(t)ds\ dt =: \Upsilon^{V;m,n}_{L,C}(r). \tag{A.48}$$

(A.48) is an integral of the type (A.5) with kernel $\kappa(s,t;r) = \frac{1}{S(t-s;r)}$. We thus need to compute the antiderivatives of the kernel $k(s,t;r) = \frac{s-\alpha}{S(t-s;r)}$ for $\alpha = t_{m+2i-1}$. Then

$$\begin{aligned} \bar{k}(t-s,\alpha-s;r) &= \underbrace{-(t-s)L(t-s;r) + S(t-s;r)}_{=\bar{k}_1(t-s;r)} + (\alpha-s)\underbrace{L(t-s;r)}_{=\bar{k}_0(t-s;r)}\\ &= (\alpha-t)L(t-s;r) + S(t-s;r) && \text{(A.49)} \end{aligned}$$

$$\begin{aligned} K(t-s,\alpha-s;r) &= \frac{1}{2}\left(\frac{3}{2}(t-s)S(t-s;r) - \frac{r^2}{2}L(t-s;r) - (t-s)^2L(t-s;r)\right)\\ &\quad +(\alpha-s)\left((t-s)L(t-s;r) - S(t-s;r)\right) && \text{(A.50)} \end{aligned}$$

$$K(r,\alpha-s;r) = -\frac{3}{4}r^2\ln r + (\alpha-s)r\ln r \tag{A.51}$$

$$\tilde{K}(t,t-\alpha;r) = \tilde{K}(t-\alpha;r) = \int (\alpha-t)\ln r\ dt = -\frac{1}{2}(t-\alpha)^2\ln r \tag{A.52}$$

Thus

$$\begin{aligned} &\tilde{K}(r+t_{m+i}, r+t_{m+i}-\alpha;r) - \tilde{K}(t_{n-1}, t_{n-1}-\alpha;r)\\ &= -\frac{1}{2}\left((r+t_{m+i}-\alpha)^2 - (t_{n-1}-\alpha)^2\right)\ln r = -\frac{1}{2}\left((r+t_{-i+1})^2 - t_{l-2i}^2\right)\ln r\\ &= -\frac{1}{2}(t_{l-i-1}-r)(t_{l-3i+1}+r)\ln r && \text{(A.53)} \end{aligned}$$

and

$$\begin{aligned}
&\tilde{K}(t_n, t_n-\alpha; r) - \tilde{K}(r+t_{m+i-1}, r+t_{m+i-1}-\alpha; r)\\
=\ & -\frac{1}{2}\left((t_n-\alpha)^2 - (r+t_{m+i-1}-\alpha)^2\right)\ln r = -\frac{1}{2}\left(t_{l-2i+1}^2 - (r+t_{-i})^2\right)\ln r\\
=\ & -\frac{1}{2}(t_{l-i+1}-r)(t_{l-3i+1}+r)\ln r. \qquad \text{(A.54)}
\end{aligned}$$

$\Upsilon_{L,C}^{V;m,n} = \Upsilon_{L,C}^{V;l}$ is then given by (A.9), with

$$\begin{aligned}
F_{L,C}^{D}(l;r) &= K(t_{l-2},0;r) - K(t_{l-1},-\Delta t;r) - K(t_{l-1},0;r) - K(t_{l-1},\Delta t;r)\\
&\quad + K(t_l,-\Delta t;r) + K(t_l,0;r) + K(t_l,\Delta t;r) - K(t_{l+1},0;r)\\
F_{L,C}^{E_{pp}}(l;r) &= \frac{1}{2}\left\{(t_{l-2}-r)(t_{l-2}+r) - \frac{3}{2}r^2\right\}\ln r - K(t_{l-1},-\Delta t;r) - K(t_{l-1},0;r) - K(t_{l-1},\Delta t;r)\\
&\quad + K(t_l,-\Delta t;r) + K(t_l,0;r) + K(t_l,\Delta t;r) - K(t_{l+1},0;r)\\
F_{L,C}^{E_{p}}(l;r) &= \frac{1}{2}\left\{-(t_{l-1}-r)(t_{l+1}+r) + \frac{3}{2}r^2 - r\Delta t\right\}\ln r\\
&\quad + K(t_l,-\Delta t;r) + K(t_l,0;r) + K(t_l,\Delta t;r) - K(t_{l+1},0;r)\\
F_{L,C}^{E_{c}}(l;r) &= \frac{1}{2}\left\{-(t_{l+1}-r)(t_{l+1}+r) - \frac{3}{4}r^2\right\}\ln r - K(t_{l+1},0;r). \qquad \text{(A.55)}
\end{aligned}$$

The function K that appears in all form terms is given by (A.50).

A.2.3 The Time Domain Double Layer Operator

A.2.3.1 The Time Domain Double Layer Operator with Piecewise Constant Ansatz and Test Functions

The time domain Double Layer operator is given by (1.10),

$$K[\varphi](x,t) = \int_\Gamma \int_{\mathbb{R}_{\geq 0}} n_y \cdot \nabla_x G(t-s, |x-y|)\ \varphi(y,s)\ ds\ ds_y \qquad \text{(A.56)}$$

for $(x,t) \in \Gamma \times \mathbb{R}_{\geq 0}$. The adjoint time domain double layer operator is given by (1.9),

$$K'[p](x,t) = \int_\Gamma \int_{\mathbb{R}_{\geq 0}} n_x \cdot \nabla_x G(t-s, |x-y|)\ p(y,s)\ ds\ ds_y \qquad \text{(A.57)}$$

for $(x,t) \in \Gamma \times \mathbb{R}_{\geq 0}$.

Remark A.2 (On the Adjoint Time Domain Double Layer Operator)
Note that $\int_0^\infty \langle K[\varphi](\cdot,t), p(\cdot,t)\rangle\, dt \neq \int_0^\infty \langle \varphi(\cdot,t), K'[p](\cdot,t)\rangle\, dt$ *in general [34, p. 16], due to the structure of the fundamental solution. In particular,* $G(t-s,|x-y|) \neq G(s-t,|x-y|)$ *in general. The operator* K^* *that is dual to* K *in the sense that* $\int_0^\infty \langle K[\varphi](\cdot,t), p(\cdot,t)\rangle\, dt = \int_0^\infty \langle \varphi(\cdot,t), K^*[p](\cdot,t)\rangle\, dt$ *is*

$$K^*[p](x,t) = \int_\Gamma \int_0^\infty n_x \cdot \nabla_x G(s-t, |x-y|)\ p(y,s)\ ds\ ds_y \qquad \text{(A.58)}$$

for $(x,t) \in \Gamma \times \mathbb{R}_{\geq 0}$.

Nevertheless, for functions with independent space and time variables, and therewith in particular for piecewise polynomial functions of type (2.16), there holds, by simply renaming the variables, the following trivial result.

Lemma A.3 (The Adjoint Time Domain Double Layer Matrix)
There holds

$$\int_0^\infty \left\langle K'\left[\gamma^m\varphi_i\right](\cdot,t), \gamma^n(t)\varphi_j\right\rangle \, dt = \int_0^\infty \left\langle K\left[\gamma^n\varphi_j\right](\cdot,t), \gamma^m(t)\varphi_i\right\rangle \, dt. \tag{A.59}$$

This implies $K'^{,l} = \left(K^l\right)^T$.

Integrating by parts, the double layer operator (A.56) can be rewritten as [4, (2.9)], [34, (17)]

$$K\left[\varphi\right](x,t) = \int_\Gamma \frac{n_y\cdot(x-y)}{r} \int_0^\infty G(t-s,r)\left(\dot\varphi(y,s) + \frac{\varphi(y,s)}{t-s+r}\right) \, ds \, ds_y \tag{A.60}$$

for $(x,t) \in \Gamma\times\mathbb{R}_{\geq 0}$. Inserting the definition of G,

$$K\left[\varphi\right](x,t) = \frac{1}{2\pi}\int_\Gamma \frac{n_y\cdot(x-y)}{r} \int_0^\infty H(t-s-r)\left(\frac{\varphi(y,s)}{(t-s+r)S(t-s;r)} + \frac{\dot\varphi(y,s)}{S(t-s;r)}\right) \, ds \, ds_y.$$

One finds that K has a singularity of order $\frac{1}{2}$ for $s\to t-r$. Approximating the terms in the bilinear form that corresponds to the Double Layer operator as in (A.37), we obtain

$$\begin{aligned}
& b_K(p_N,q_N) := \int_0^\infty \langle K[p_N](\cdot,t), q_N(\cdot,t)\rangle \, dt \\
= \; & \frac{1}{2\pi}\sum_{m=1}^{M_T}\sum_{i=1}^{N_S} p_i^m \iint_{\Gamma\times\Gamma} \frac{n_y\cdot(x-y)}{r}\Bigg\{ \int_{t_{n-1}}^{t_n}\int_{t_{m-1}}^{t_m} H(t-s-r)\frac{1}{S(t-s;r)(t-s+r)} \, ds \, dt \\
& \qquad + \sum_{j=0,1}(-1)^{j+1}\int_{t_{n-1}}^{t_n} H(t-t_{m-j}-r)\frac{1}{S(t-s;r)} \, dt\Bigg\} \varphi_i(y)\varphi_j(x) \, ds_x \, ds_y \\
= \; & \frac{1}{2\pi}\sum_{m=1}^{N_t}\sum_{i=1}^{N_s} p_i^m \iint_{\Gamma\times\Gamma} \frac{n_y\cdot(x-y)}{r}\left(\Upsilon_{C,C}^{K;m,n}(r) + \Upsilon_{\dot C,C}^{K;m,n}(r)\right) \, \varphi_i(y)\varphi_j(x) \, ds_x \, ds_y
\end{aligned} \tag{A.61}$$

with

$$\Upsilon_{C,C}^{K;m,n}(r) = \int_{t_{n-1}}^{t_n}\int_{t_{m-1}}^{t_m} H(t-s-r)\frac{1}{S(t-s;r)(t-s+r)} \, ds \, dt \tag{A.62}$$

$$\Upsilon_{\dot C,C}^{K;m,n}(r) = \sum_{j=0,1}(-1)^{j+1}\int_{t_{n-1}}^{t_n} H(t-t_{m-j}-r)\frac{1}{S(t-s;r)} \, dt \tag{A.63}$$

Let us consider $\Upsilon_{C,C}^{K;m,n} = \Upsilon_{C,C}^{K;l}$ first. The function is a realisation of (A.10) with kernel $\kappa(s,t;r) = \frac{1}{S(t-s;r)(t-s+r)}$, and therefore

$$\bar k(t-s;r) = \frac{r-(t-s)}{rS(t-s;r)} \tag{A.64}$$

$$K(t-s;r) = \frac{1}{r}\left(rL(t-s;r) - S(t-s;r)\right) \tag{A.65}$$

$$K(r;r) = \frac{1}{r}\left(rL(r;r) - S(r;r)\right) = \ln r \tag{A.66}$$

$$\tilde K(t;r) = \int \lim_{s\to t-r}\frac{r-(t-s)}{rS(t-s;r)} \, dt = -\int \lim_{s\to t-r}\frac{S(t-s;r)}{r(t-s)} \, dt = 0 \tag{A.67}$$

by de l'Hôpital's rule. $\Upsilon^{K;l}_{C,C}$ is then given by (A.11), with

$$\begin{aligned}
F^{D}_{C,C}(l;r) &= \frac{1}{r}\left\{S(t_{l-1};r) - 2S(t_l;r) + S(t_{l+1};r)\right\} - L(t_{l-1};r) + 2L(t_l;r) - L(t_{l+1};r)\\
F^{E_p}_{C,C}(l;r) &= \frac{1}{r}\left\{-2S(t_l;r) + S(t_{l+1};r)\right\} - \ln r + 2L(t_l;r) - L(t_{l+1};r)\\
F^{E_c}_{C,C}(l;r) &= \frac{1}{r}S(t_{l+1};r) + \ln r - L(t_{l+1};r).
\end{aligned} \tag{A.68}$$

Secondly we consider $\Upsilon^{K;m,n}_{\dot{C},C}$, which is a realisation of (A.20) with kernel $\kappa(s,t;r) = \frac{1}{S(t-s;r)}$. By (A.21), we have

$$\Upsilon^{K;m,n}_{\dot{C},C} = \Upsilon^{K;l}_{\dot{C},C} = -\Upsilon^{K;l}_{C,\dot{C}} \tag{A.69}$$

with $\Upsilon^{K;l}_{C,\dot{C}}$ as in (A.44).

A.2.3.2 The Time Domain Double Layer Operator with Piecewise Linear Ansatz and Piecewise Constant Test Functions

For this choice of basis functions, we replace $\Upsilon^{K;m,n}_{C,C}$ and $\Upsilon^{K;m,n}_{C,\dot{C}}$ in (A.61) by

$$\Upsilon^{K;m,n}_{L,C}(r) := \int_0^\infty \int_0^\infty \frac{H(t-s-r)}{S(t-s;r)(t-s+r)}\ \beta^m(s)\gamma^n(t)\ ds\ dt \tag{A.70}$$

which is a realisation of (A.5) with kernel $\kappa(s,t;r) = \frac{1}{S(t-s;r)(t-s+r)}$, and

$$\begin{aligned}
\Upsilon^{K;m,n}_{\dot{L},C}(r) &:= \int_0^\infty \int_0^\infty \frac{H(t-s-r)}{S(t-s;r)}\ \dot{\beta}^m(s)\gamma^n(t)\ ds\ dt\\
&= \frac{1}{\Delta t}\Big(\int_0^\infty \int_0^\infty \frac{H(t-s-r)}{S(t-s;r)}\gamma^m(s)\gamma^n(t)\ ds\ dt\\
&\qquad - \int_0^\infty \int_0^\infty \frac{H(t-s-r)}{S(t-s;r)}\gamma^{m+1}(s)\gamma^n(t)\ ds\ dt\Big)
\end{aligned} \tag{A.71}$$

which is the sum of two integrals of the type (A.10) with kernel $k(s,t;r) = \frac{1}{S(t-s;r)}$. Hence $\Upsilon^{K;m,n}_{\dot{L},C} = \Upsilon^{K;l}_{\dot{L},C} = \Upsilon^{V;l}_{C,C} + \Upsilon^{V;l-1}_{C,C}$ with $\Upsilon^{V;l}_{C,C}$ as in (A.38). We therefore do not need to consider this term any further.

For $\Upsilon^{K;m,n}_{L,C} = \Upsilon^{K;l}_{L,C}$, with $k(s,t;r) = \kappa(s,t;r)(s-\alpha)$ and $\alpha = t_{m+2i-1}$,

$$\bar{k}(t-s,\alpha-s;r) = (\alpha-s)\left(-\frac{(r-(t-s))}{rS(t-s;r)}\right) + L(t-s;r) - \frac{1}{r}S(t-s;r) \tag{A.72}$$

$$\begin{aligned}
K(t-s,\alpha-s;r) &= ((t-s)L(t-s;r) - S(t-s;r)) - \frac{1}{2r}\left((t-s)S(t-s;r) - r^2L(t-s;r)\right)\\
&\quad +(\alpha-s)\left(\frac{1}{r}S(t-s;r) - L(t-s;r)\right)
\end{aligned} \tag{A.73}$$

$$K(r,\alpha-s;r) = \frac{3}{2}r\ln r + (\alpha-s)(-\ln r). \tag{A.74}$$

$$\tag{A.75}$$

For $\tilde{K}(t,t-\alpha;r)$, we first note that, by de l'Hôpital's rule,

$$\begin{aligned}\lim_{s\to t-r}\frac{(s-\alpha)(r-(t-s))}{rS(t-s;r)} &= \lim_{s\to t-r}\frac{r-(t-s)+(s-\alpha)}{r\frac{t-s}{S(t-s;r)}(-1)}\\ &= -\lim_{s\to t-r}\frac{S(t-s;r)(2s-t+r-\alpha)}{r(t-s)} = 0\end{aligned}$$

and therefore

$$\tilde{K}(t,t-\alpha;r) = \tilde{K}(t;r) = \int \ln r\ dt = t\ln r. \tag{A.76}$$

Thus

$$\tilde{K}(r+t_{m+i},r+t_{-i+1};r) - \tilde{K}(t_{n-1},t_{l-2i};r) = (r-t_{l-i-1})\ln r \tag{A.77}$$

and

$$\tilde{K}(t_n,t_{l-2i+1};r) - \tilde{K}(r+t_{m+i-1},r+t_{-i};r) = (-r+t_{l-i+1})\ln r \tag{A.78}$$

$\Upsilon_{L,C}^{K;l}$ is then given by (A.9), with

$$\begin{aligned}F_{L,C}^{D}(l;r) &= K(t_{l-2},0;r) - K(t_{l-1},-\Delta t;r) - K(t_{l-1},0;r) - K(t_{l-1},\Delta t;r)\\ &\quad + K(t_l,-\Delta t;r) + K(t_l,0;r) + K(t_l,\Delta t;r) - K(t_{l+1},0;r)\\ F_{L,C}^{E_{pp}}(l;r) &= \left(\frac{1}{2}r+t_{l-2}\right)\ln r - K(t_{l-1},-\Delta t;r) - K(t_{l-1},0;r) - K(t_{l-1},\Delta t;r)\\ &\quad + K(t_l,-\Delta t;r) + K(t_l,0;r) + K(t_l,\Delta t;r) - K(t_{l+1},0;r)\\ F_{L,C}^{E_{p}}(l;r) &= -3r\ln r + K(t_l,-\Delta t;r) + K(t_l,0;r) + K(t_l,\Delta t;r) - K(t_{l+1},0;r)\\ F_{L,C}^{E_{c}}(l;r) &= \left(\frac{1}{2}r+t_{l+1}\right)\ln r - K(t_{l+1},0;r).\end{aligned} \tag{A.79}$$

A.2.3.3 The Time Domain Double Layer Operator with Piecewise Linear Ansatz and Derivatives of Piecewise Constant Test Functions

For this choice of basis functions, we replace $\Upsilon_{C,C}^{K;m,n}$ and $\Upsilon_{C,\dot{C}}^{K;m,n}$ in (A.61) by

$$\Upsilon_{L,\dot{C}}^{K;m,n}(r) := \int_0^\infty\int_0^\infty \frac{H(t-s-r)}{S(t-s;r)(t-s+r)}\ \beta^m(s)\dot{\gamma}^n(t)\ ds\ dt \tag{A.80}$$

which is a realisation of (A.12) with kernel $\kappa(s,t;r) = \frac{1}{S(t-s;r)(t-s+r)}$, and

$$\begin{aligned}\Upsilon_{\dot{L},\dot{C}}^{K;m,n}(r) &:= \int_0^\infty\int_0^\infty \frac{H(t-s-r)}{S(t-s;r)}\ \dot{\beta}^m(s)\dot{\gamma}^n(t)\ ds\ dt\\ &= \frac{1}{\Delta t}\Big(\int_0^\infty\int_0^\infty \frac{H(t-s-r)}{S(t-s;r)}\gamma^m(s)\dot{\gamma}^n(t)\ ds\ dt\\ &\qquad -\int_0^\infty\int_0^\infty \frac{H(t-s-r)}{S(t-s;r)}\gamma^{m+1}(s)\dot{\gamma}^n(t)\ ds\ dt\Big)\\ &= \frac{1}{\Delta t}\left(\int_0^\infty \langle V[\gamma^m],\dot{\gamma}^n(t)\rangle\ dt - \int_0^\infty \left\langle V[\gamma^{m+1}],\dot{\gamma}^n(t)\right\rangle\ dt\right)\end{aligned} \tag{A.81}$$

which is the sum of two integrals of the type (A.18) with kernel $\kappa(t-s;r) = \frac{1}{S(t-s;r)}$, i.e.

$$\Upsilon_{\dot{L},\dot{C}}^{K;m,n} = \Upsilon_{\dot{L},\dot{C}}^{K;l} = \Upsilon_{C,\dot{C}}^{V;l} + \Upsilon_{C,\dot{C}}^{V;l-1}. \tag{A.82}$$

The functions $\Upsilon^{V;l-i}_{C,\dot{C}}$, $i \in \{0,1\}$, were computed in (A.44).

For $\Upsilon^{K;m,n}_{L,\dot{C}} = \Upsilon^{K;l}_{L,\dot{C}}$, with kernel

$$k(s,\alpha,\beta;r) = \kappa(s,\alpha;r)(s-\beta) = -\frac{(\beta-s)}{S(\alpha-s;r)(\alpha-s+r)}$$

and $\beta = t_{m+2i-1}$ we obtain, replacing t and α in (A.72) by α and β, respectively,

$$K(\alpha-s,\beta-s;r) = (\beta-s)\left(-\frac{S(\alpha-s;r)}{r\sqrt{(\alpha-s)^2+r^2}}\right) + L(\alpha-s;r) - \frac{1}{r}S(\alpha-s;r) \quad \text{(A.83)}$$

$$K(r,\beta-s;r) = K(r;r) = \ln r \quad \text{(A.84)}$$

$\Upsilon^{K;l}_{L,\dot{C}}$ is then given by (A.16), with

$$\begin{aligned}
F^{D}_{L,\dot{C}}(l;r) &= -K(t_{l-2},0;r) + K(t_{l-1},-\Delta t;r) + K(t_{l-1},0;r) + K(t_{l-1},\Delta t;r) \\
&\quad -K(t_l,-\Delta t;r) - K(t_l,0;r) - K(t_l,\Delta t;r) + K(t_{l+1},0;r) \\
F^{E_{pp}}_{L,\dot{C}}(l;r) &= -\ln r + K(t_{l-1},-\Delta t;r) + K(t_{l-1},0;r) + K(t_{l-1},\Delta t;r) \\
&\quad -K(t_l,-\Delta t;r) - K(t_l,0;r) - K(t_l,\Delta t;r) + K(t_{l+1},0;r) \\
F^{E_{p}}_{L,\dot{C}}(l;r) &= 2\ln r - K(t_l,-\Delta t;r) - K(t_l,0;r) - K(t_l,\Delta t;r) + K(t_{l+1},0;r) \\
F^{E_{c}}_{L,\dot{C}}(l;r) &= -\ln r + K(t_{l+1},0;r). \quad \text{(A.85)}
\end{aligned}$$

A.2.4 The Time Domain Hypersingular Boundary Integral Operator

A.2.4.1 The Time Domain Hypersingular Boundary Integral Operator with Piecewise Linear Ansatz and Piecewise Constant Test Functions

The time domain hypersingular boundary integral operator is given by (1.11),

$$-W[\varphi](x,t) = \lim_{x'\in\Omega\to x} n_x \cdot \nabla_{x'} \left(\int_\Gamma \int_{\mathbb{R}_{\geq 0}} n_y \cdot \nabla_{x'} G(t-s,|x'-y|)\ \varphi(y,s)\ ds\ ds_y \right) \quad \text{(A.86)}$$

for $(x,t) \in \Gamma \times \mathbb{R}_{\geq 0}$. Using integration by parts, Bécache [32, p. 90], [33, (7)-(9)], [34, (34)] shows

$$\begin{aligned}
&-\int \langle W[\varphi](\cdot,t),\psi(\cdot,t)\rangle\ dt \\
&= \frac{1}{2\pi}\iint_{\Gamma\times\Gamma}\int_0^\infty\int_0^\infty \frac{H(t-s-r)}{S(t-s;r)}\ \frac{d\varphi(y,s)}{ds_y}\ ds\ \frac{d\psi(x,t)}{ds_x}\ dt\ d\Gamma_x d\Gamma_y \\
&\quad -\frac{1}{2\pi}\iint_{\Gamma\times\Gamma} n_y\cdot n_x \int_0^\infty\int_0^\infty \frac{H(t-s-r)}{S(t-s;r)}\ \dot{\varphi}(y,s)\ ds\ \dot{\psi}(x,t)\ dt\ d\Gamma_x d\Gamma_y \\
&= \int_0^\infty \left\langle V\left[\frac{d\varphi(y,s)}{ds_y}\right], \frac{d\psi(x,t)}{ds_x}\right\rangle dt - \int_0^\infty \left\langle V\left[\dot{\varphi}(y,s)\right], n_y\cdot n_x\ \dot{\psi}(x,t)\right\rangle dt. \quad \text{(A.87)}
\end{aligned}$$

The hypersingular kernel of (A.86) is thus regularised to a weakly singular one in the weak form (A.87). Approximating the terms in the bilinear form that corresponds to the hypersingular

boundary integral operator as in (A.37) and (A.61), we obtain

$$
\begin{aligned}
& b_W(p_N, q_N) \\
:= \; & \frac{1}{2\pi} \sum_{m=1}^{N_t} \sum_{i=1}^{N_s} \phi_i^m \Bigg\{ \iint_{\Gamma\times\Gamma} \int_0^\infty \int_0^\infty \frac{H(t-s-r)}{S(t-s;r)} \, \beta^m(s)\gamma^n(t) \, ds \, dt \, \frac{d\varphi_i(y)}{ds_y} \frac{d\varphi_j(x)}{ds_x} \, ds_x \, ds_y \\
& \qquad - \iint_{\Gamma\times\Gamma} n_y \cdot n_x \int_0^\infty \int_0^\infty \frac{H(t-s-r)}{S(t-s;r)} \, \dot\beta^m(s)\dot\gamma^n(t) \, ds \, dt \, \varphi_i(y)\varphi_j(x) \, ds_x \, ds_y \Bigg\} \\
=: \; & \frac{1}{2\pi} \sum_{m=1}^{N_t} \sum_{i=1}^{N_s} p_i^m \Bigg\{ \quad \iint_{\Gamma\times\Gamma} \Upsilon_{L,C}^{W;m,n}(r) \, \frac{d\varphi_i(y)}{ds_y} \frac{d\varphi_j(x)}{ds_x} \, ds_x \, ds_y \\
& \qquad - \iint_{\Gamma\times\Gamma} n_y \cdot n_x \Upsilon_{\dot L,\dot C}^{W;m,n}(r) \, \varphi_i(y)\varphi_j(x) \, ds_x \, ds_y \Bigg\}. \qquad \text{(A.88)}
\end{aligned}
$$

where

$$
\Upsilon_{L,C}^{W;m,n}(r) := \int_0^\infty \int_0^\infty \frac{H(t-s-r)}{S(t-s;r)} \beta^m(s)\gamma^n(t) \, ds \, dt \qquad \text{(A.89)}
$$

and

$$
\Upsilon_{\dot L,\dot C}^{W;m,n}(r) := \int_0^\infty \int_0^\infty \frac{H(t-s-r)}{S(t-s;r)} \dot\beta^m(s)\dot\gamma^n(t) \, ds \, dt. \qquad \text{(A.90)}
$$

(A.89) does not need any further consideration, since $\Upsilon_{\dot L,\dot C}^{W;m,n} = \Upsilon_{L,C}^{W;;} = \Upsilon_{L,C}^{W;l} = \Upsilon_{L,C}^{V;l}$, which was computed in (A.48).

(A.90) is the difference of two integrals of the type (A.17) with kernel $\kappa(s,t;r) = \frac{1}{S(t-s;r)}$,

$$
\begin{aligned}
& \Upsilon_{\dot L,\dot C}^{W;m,n}(r) \qquad \text{(A.91)} \\
= \; & \int_0^\infty \int_0^\infty \frac{H(t-s-r)}{S(t-s;r)} \dot\beta^m(s)\dot\gamma^n(t) \, ds \, dt \\
= \; & \int_0^\infty \int_0^\infty \frac{H(t-s-r)}{S(t-s;r)} \gamma^m(s)\dot\gamma^n(t) \, ds \, dt - \int_0^\infty \int_0^\infty \frac{H(t-s-r)}{S(t-s;r)} \gamma^{m+1}(s)\dot\gamma^n(t) \, ds \, dt \\
= \; & \Upsilon_{C,\dot C}^{V;l}(r) + \Upsilon_{C,\dot C}^{V;l-1}(r).
\end{aligned}
$$

The functions $\Upsilon_{C,\dot C}^{V;l-i}$, $i \in \{0,1\}$, were computed in (A.44).

A.3 Typical Singularities in the Spatial Kernel Functions on Discrete Domains

The spatial kernel functions for the Single Layer operator, depending on the type of temporal basis functions used, are given by (A.43), (A.47) and (A.55). In each case, we observe the following types of singularities:

S1. On the discrete light discs $D_{l-1} = \{ (x,y) \in \Gamma\times\Gamma \mid |x-y| \le t_{l-1} \}$, singularities in the derivatives of S and L appear at the outer boundary, i.e. at $r = |x-y| = t_{l-1}$.

S2. On the discrete light rings $E_{l-1} = \{ (x,y) \in \Gamma\times\Gamma \mid t_{l-1} \le |x-y| \le t_l \}$ and, similarly, on E_{l-2} and E_l, two types of singularities appear:

(i) singularities of type $\ln r$, which need to be taken into account if the inner boundary of the discrete light ring is equal to zero, i.e. if $E_{l-1} = D_l$ (or $E_{l-2} = D_{l-1}$ or $E_l = D_{l+1}$, respectively), and

(ii) singularities in the derivatives of S and L that appear at the outer boundary, i.e. at $r = t_l$ (or $r = t_{l-1}$ or $r = t_{l+1}$, respectively).

In particular, there are *no singularities* in the kernel functions at $r = 0$ on the discrete light discs and, apart from the special case 2.(i), *no singularities* in the kernel functions at the inner boundary of the discrete light rings. This analysis also covers the hypersingular boundary integral operator after integrating by parts; see (A.87).

The spatial kernel functions for the Double Layer operator, depending on the type of temporal basis functions used, are given by (A.68), (A.79) and (A.85). In each case, we observe the following types of singularities:

D1. On the discrete light discs D_{l-1}, singularities of type $\frac{(x-y)\cdot n_y}{r^2}$ appear at the outer boundary, i.e. at $r = |x-y| = t_{l-1}$. Additionally, singularities in the derivatives of S and L appear at the outer boundary, i.e. at $r = |x-y| = t_{l-1}$.

D2. On the discrete light rings $E_{l-1} = \{\ (x,y) \in \Gamma \times \Gamma \ \mid \ t_{l-1} \le |x-y| \le t_l\ \}$ and, similarly, on E_{l-2} and E_l, two types of singularities appear:

(i) singularities of type $\frac{(x-y)\cdot n_y}{r^2}$, which need to be taken into account if the inner boundary of the discrete light ring is equal to zero, i.e. if $E_{l-1} = D_l$ (or $E_{l-2} = D_{l-1}$ or $E_l = D_{l+1}$, respectively), and

(ii) singularities in the derivatives of S and L that appear at the outer boundary, i.e. at $r = t_l$ (or $r = t_{l-1}$ or $r = t_{l+1}$, respectively).

A.4 Evaluation of Time Domain Boundary Integral Operators with Discrete Density

Post-processing tasks such as the computation of local error indicators, or the computation of the solution in the exterior domain around the scatterer via a representation formula, require the evaluation of time domain boundary integral operators with piecewise polynomial densities. We briefly sketch the analytical evaluation of the temporal integrals in this section. The spatial integration is again done by numerical quadrature.

Let p_N be given by (2.16), and let P be the model time domain boundary integral operator defined by (2.11). Then

$$P[p_N](x,t) = \sum_{m=1}^{M_T} \sum_{i=1}^{N_S} p_i^m \, P\left[\beta^{m,q_1}(s)\varphi_i^{p_1}(y)\right](x,t) \tag{A.92}$$

where

$$P\left[\beta^{m,q_1}(s)\varphi_i^{p_1}(y)\right](x,t) = \int_\Gamma \int_0^\infty H(t-s-r)\kappa(s,t;r)\,\beta^{m,q_1}(s)\varphi_i^{p_1}(y)\,ds\,ds_y$$

and $r = |x-y|$ as in (2.18). Similarly to (2.34), we restrict ourselves to integrals of type

$$\int_\Gamma \int_{t_{m-1}}^{t_m} H(t-s-r)k(s,t;r)\,ds\,\varphi_i^{p_1}(y)\,ds_y =: \int_\Gamma \Upsilon^m(r,t)\varphi_i^{p_1}(y)\,ds_y \tag{A.93}$$

where $k(s,t;r) := \kappa(s,t;r)\beta^{m,q_1}(s)|_{[t_{m-1},t_m)}$. Using $\alpha = t$ in (2.35), we obtain, analogously to (2.36),

$$\Upsilon_t^m(r) = \Upsilon^m(r,t) = \mathbb{1}_{[0,t-t_m)}(r)\int_{t_{m-1}}^{t_m} k(s,t;r)\,ds + \mathbb{1}_{[t-t_m,t-t_{m-1})}(r)\int_{t_{m-1}}^{t-r} k(s,t;r)\,ds. \quad \text{(A.94)}$$

The underlying domain decomposition is sketched in Figure A.1.

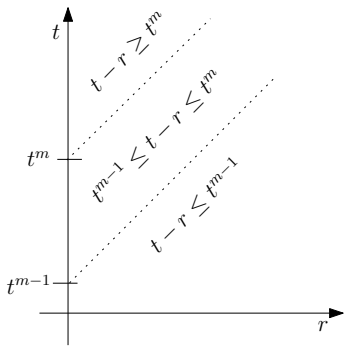

Figure A.1: Domain decomposition for potential evaluations.

Example A.4

a) For piecewise constant basis functions in time, i.e. $q_1 = 0$, and the corresponding Single Layer operator kernel $k(s,t;r) = \kappa(s,t;r) = \frac{1}{2\pi}\frac{1}{\sqrt{(t-s)^2-r^2}} = \frac{1}{2\pi}\frac{1}{S(t-s;r)}$ (using the notation of (A.22)) there holds, by (A.24) and similarly to Section A.2.2.2,

$$\int k(s,t;r)\,ds = -L(t-s;r)$$

and hence

$$\begin{aligned}&\Upsilon^m(r,t)\\ =\ &\mathbb{1}_{[0,t-t_m)}(r)\left(L(t-t_{m-1};r) - L(t-t_m;r)\right) + \mathbb{1}_{[t-t_m,t-t_{m-1})}(r)\left(L(t-t_{m-1};r) - \underbrace{L(r;r)}_{=\ln r}\right).\end{aligned}$$

b) For the same setup and the temporal part of the adjoint Double Layer operator kernel as given by (A.60), $k(s,t;r) = \kappa(s,t;r) = \frac{1}{(t-s+r)S(t-s;r)}$, there holds, by (A.64),

$$\int k(s,t;r)\,ds = \frac{r-(t-s)}{rS(t-s;r)}$$

and hence

$$\Upsilon^m(r,t) = \mathbb{1}_{[0,t-t_m)}(r)\left(\frac{r-(t-t_m)}{rS(t-t_m;r)} - \frac{r-(t-t_{m-1})}{rS(t-t_{m-1};r)}\right) + \mathbb{1}_{[t-t_m,t-t_{m-1})}(r)\left(-\frac{r-(t-t_{m-1})}{rS(t-t_{m-1};r)}\right).$$

Remark A.5 (On Equation (A.92))

In particular, there holds

$$P[p_N|_{T_m}](x,t) = \sum_{i=1}^{N_S} p_i^m P\left[\beta^{m,q_1}(s)\varphi_i^{p_1}(y)\right](x,t).$$

This is of course trivial, but also important as, in practice, we store one approximation for each time interval. Hence, if we want to compute $P[p_N](x,t)$ for some $t \in [t_{M-1}, t_M]$, we compute $\sum_{m=1}^{M} P[p_N|_{[t_{M-1},t_M]}](x,t)$.

A.5 Computation of the Right Hand Sides

In this section, we briefly explain how we compute right hand side terms of the type (2.29), i.e.

$$\int_0^\infty \langle I[f](\cdot,t), q_N(\cdot,t)\rangle \, dt = \int_0^\infty \int_\Gamma \langle f(x,t), q_N(x,t)\rangle \, ds_x \, dt \tag{A.95}$$

with test function $q_N \in V_{h,\Delta t}^{p_2,q_2}$. One can obviously approximate (A.95) directly by quadrature. Alternatively, and this is the option that we consider here, one can approximate f by a discrete function $f_N \in V_{h,\Delta t}^{p_1,q_1}$ and compute the resulting simple integrals analytically. Note that this also allows us to approximate right hand side terms of the type $\int_0^\infty \langle P[f](\cdot,t), q_N(\cdot,t)\rangle \, dt$, with P as in (2.11), as matrix-vector multiplications, using the the routines that compute the matrices that correspond to the bilinear forms computed in Section A.2.

A.5.1 Approximation by Piecewise Constant Functions in Time

We approximate f by piecewise constant functions in time, i.e. $q_1 = 0$, and hence

$$f_N(x,t) = \sum_{m=1}^{N_t} \sum_{i=1}^{N_s} f_i^m \varphi_i(x) \gamma^m(t) \tag{A.96}$$

with $f_i^m = f(x_i, t_m)$. The term (A.95) can then be evaluated analytically, depending on the degree of the temporal test function.

a) $q_2 = -1$: Choosing $q_N(x,t) = \varphi_j(x)\dot{\gamma}^n(t)$, there holds

$$\int_0^\infty \langle I[f_N](\cdot,t), q_N(\cdot,t)\rangle \; dt = \int_\Gamma \sum_{i=1}^{N_s} \varphi_i(x)\varphi_j(x) \; ds_x \; \int_0^\infty \sum_{m=1}^{N_t} \gamma^m(t)\dot{\gamma}^n(t) f_i^m \; dt \tag{A.97}$$

where

$$\begin{aligned} &\int_0^\infty \sum_{m=1}^{N_t} \gamma^m(t)\dot{\gamma}^n(t) f_i^m \; dt = \int_0^\infty \sum_{m=1}^{N_t} \gamma^m(t)(\delta_{t_{n-1}}(t) - \delta_{t_n}(t)) f_i^m \; dt \\ = &\sum_{m=1}^{N_t} \left(\gamma^m(t_{n-1}) - \gamma^m(t_n)\right) f_i^m \; dt = \sum_{m=1}^{N_t} \left(\delta^{m,n-1} - \delta^{m,n}\right) f_i^m \; dt = f_i^{n-1} - f_i^n. \end{aligned} \tag{A.98}$$

Hence

$$\int_0^\infty \langle I[f_N](\cdot,t), q_N(\cdot,t)\rangle \; dt = \sum_{i=1}^{N_s} \int_\Gamma \varphi_i(x)\varphi_j(x) \; ds_x \; (f_i^{n-1} - f_i^n). \tag{A.99}$$

b) $q_2 = 0$: Choosing $q_N(x,t) = \varphi_j(x)\gamma^n(t)$, there holds

$$\int_0^\infty \langle I[f_N](\cdot,t), q_N(\cdot,t)\rangle \; dt = \int_\Gamma \sum_{i=1}^{N_s} \varphi_i(x)\varphi_j(x) \; ds_x \; \int_0^\infty \sum_{m=1}^{N_t} \gamma^m(t)\gamma^n(t) f_i^m \; dt \tag{A.100}$$

where

$$\int_0^\infty \sum_{m=1}^{N_t} \gamma^m(t)\gamma^n(t) f_i^m \; dt = \int_{t_{n-1}}^{t_n} \sum_{m=1}^{N_t} \delta^{m,n} f_i^m \; dt = \Delta t f_i^n. \tag{A.101}$$

Hence

$$\int_0^\infty \langle I[f_N](\cdot,t), q_N(\cdot,t)\rangle \; dt = \Delta t \sum_{i=1}^{N_s} \int_\Gamma \varphi_i(x)\varphi_j(x) \; ds_x \; f_i^n. \tag{A.102}$$

Note that the terms $\int_\Gamma \varphi_i(x)\varphi_j(x)\; ds_x$ in (A.99) and (A.102) correspond to entries of the spatial mass matrix, which can easily be calculated.

A.5.2 Approximation by Piecewise Linear Functions in Time

We approximate f by piecewise linear functions in time, i.e. $q_1 = 1$, and hence

$$f_N(x,t) = \sum_{m=1}^{N_t} \sum_{i=1}^{N_s} f_i^m \varphi_i(x)\beta^m(t) \tag{A.103}$$

with $f_i^m = f(x_i, t_m)$. We multiply f_N by a test function q_N and integrate over Γ and $(0,\infty)$ to approximate (A.95).

a) $q_2 = -1$: Choosing $q(x,t) = \varphi_j(x)\dot{\gamma}^n(t)$, there holds

$$\int_0^\infty \langle I[f_N](\cdot,t), q_N(\cdot,t)\rangle \; dt = \int_\Gamma \sum_{i=1}^{N_s} \varphi_i(x)\varphi_j(x) \; ds_x \; \int_0^\infty \sum_{m=1}^{N_t} \beta^m(t)\dot{\gamma}^n(t) f_i^m \; dt \tag{A.104}$$

where

$$\begin{aligned}
&\int_0^\infty \sum_{m=1}^{N_t} \beta^m(t)\dot{\gamma}^n(t) f_i^m \; dt \\
= \; &\int_0^\infty \sum_{m=1}^{N_t} \left(\frac{t - t_{m-1}}{\Delta t} \mathbb{1}_{T_m}(t) - \frac{t - t_{m+1}}{\Delta t} \mathbb{1}_{T_{m+1}}(t) \right) (\delta_{t_{n-1}}(t) - \delta_{t_n}(t)) f_i^m \; dt \\
= \; &\left(\left(\frac{t_{n-1} - t_{m-1}}{\Delta t} \delta^{m,n-1} - \frac{t_{n-1} - t_{m+1}}{\Delta t} \delta^{m+1,n-1} \right) \right. \\
- \; &\left. \left(\frac{t_n - t_{m-1}}{\Delta t} \delta^{m,n} - \frac{t_n - t_{m+1}}{\Delta t} \delta^{m+1,n} \right) \right) f_i^m \\
= \; &\left(\frac{t_{n-1} - t_{n-2}}{\Delta t} f_i^{n-1} - 0 \right) - \left(\frac{t_n - t_{n-1}}{\Delta t} f_i^n - 0 \right) \\
= \; &f_i^{n-1} - f_i^n.
\end{aligned} \tag{A.105}$$

Hence

$$\int_0^\infty \langle I[f_N](\cdot,t), q_N(\cdot,t)\rangle \; dt = \sum_{i=1}^{N_s} \int_\Gamma \varphi_i(x)\varphi_j(x) \; ds_x \; (f_i^{n-1} - f_i^n). \tag{A.106}$$

b) $q_2 = 0$: Choosing $q_N(x,t) = \varphi_j(x)\gamma^n(t)$, there holds

$$\int_0^\infty \langle I[f_N](\cdot,t), q_N(\cdot,t)\rangle \; dt = \int_\Gamma \sum_{i=1}^{N_s} \varphi_i(x)\varphi_j(x) \; ds_x \; \int_0^\infty \sum_{m=1}^{N_t} \beta^m(t)\gamma^n(t) f_i^m \; dt \tag{A.107}$$

where

$$\begin{aligned}
&\int_0^\infty \sum_{m=1}^{N_t} \beta^m(t)\gamma^n(t) f_i^m \; dt \\
= &\int_0^\infty \sum_{m=1}^{N_t} \left(\frac{t-t_{m-1}}{\Delta t} \mathbb{1}_{T_m}(t) - \frac{t-t_{m+1}}{\Delta t} \mathbb{1}_{T_{m+1}}(t) \right) \mathbb{1}_{T_n}(t) f_i^m \; dt \\
= &\frac{1}{\Delta t} \int_{t_{n-1}}^{t_n} \sum_{m=1}^{N_t} \left((t-t_{m-1})\delta^{m,n} - (t-t_{m+1})\delta^{m+1,n} \right) f_i^m \; dt \\
= &\frac{1}{\Delta t} \int_{t_{n-1}}^{t_n} (t-t_{n-1}) f_i^n - (t-t_{n+1}) f_i^{n-1} \; dt \\
= &\frac{1}{\Delta t} \left(f_i^n \left[\frac{(t-t_{n-1})^2}{2} \right]_{t=t_{n-1}}^{t=t_n} - f_i^{n-1} \left[\frac{(t-t_{n+1})^2}{2} \right]_{t=t_{n-1}}^{t=t_n} \right) = \frac{\Delta t}{2} \left(f_i^n + f_i^{n-1} \right). \quad \text{(A.108)}
\end{aligned}$$

Hence

$$\int_0^\infty \langle I[f_N](\cdot,t), q_N(\cdot,t) \rangle \; dt = \frac{\Delta t}{2} \sum_{i=1}^{N_s} \int_\Gamma \varphi_i(x)\varphi_j(x) \; ds_x \; (f_i^n + f_i^{n-1}). \quad \text{(A.109)}$$

As in Section A.5.1, the terms $\int_\Gamma \varphi_i(x)\varphi_j(x) \; ds_x$ in (A.106) and (A.109) correspond to entries of the spatial mass matrix, which can easily be calculated.

Remark A.6 (Time Derivatives in the Right Hand Side Function)
Assuming that we take the time derivative in the right hand side function and not in the test function, we obtain, by theoretical considerations outlined in Remark 4.1,

$$\int_0^\infty \left\langle I[\dot{f}_N](\cdot,t), q_N(\cdot,t) \right\rangle \; dt = - \int_0^\infty \langle I[f_N](\cdot,t), \dot{q}_N(\cdot,t) \rangle \; dt$$

for any type of temporal basis function.

Appendix B

Notes on the Implementation of the Convolution Quadrature Boundary Element Method

This appendix provides a brief introduction to the Convolution Quadrature Boundary Element Method that we use in Section 2.6 for the validation of the implementation of the Galerkin scheme. The general introduction to the method in Section B.1 is followed by details on the relevant kernel functions, i.e. the ones of the time domain Single Layer, Double Layer and hypersingular operators, in Section B.2.

B.1 The Convolution Quadrature Boundary Element Method

The temporal kernel of the time domain Single Layer operator (1.8), and the ones of the other time domain boundary integral operators given in Definition 1.4, can be written as a convolution,

$$\left(k_V(\cdot,|x-y|) * \varphi(\cdot,y)\right)(t) = \int_0^t k_V(t-s,|x-y|)\varphi(s,y)\,ds. \tag{B.1}$$

The idea of the Convolution Quadrature Method [109] is to approximate convolutions of the type

$$(f * g)(t) = \int_0^t f(t-s)g(s)\,ds \tag{B.2}$$

at $t = t_n$ by a discrete convolution $f *_{\Delta t} g$,

$$(f * g)(t_n) \approx (f *_{\Delta t} g)(t_n) := \sum_{j=0}^{n} \omega_{n-j}^{\Delta t} g_j \tag{B.3}$$

where $g_j := g(\cdot, t_j)$, with unknown weights $\omega_{n-j}^{\Delta t} = \omega_{n-j}^{\Delta t}[f]$. These weights are implicitly given by the power series [29, (3.3)]

$$\hat{f}\left(\frac{\gamma(\xi)}{\Delta t}\right) = \sum_{n=0}^{\infty} \omega_n^{\Delta t}[f]\xi^n \tag{B.4}$$

for $|\xi| < 1$, where γ is a given rational function, the quotient of the generating polynomials [29]. By applying the inverse z-transform, one finds [29, (3.5)]

$$\omega_j^{\Delta t}[f] = \frac{1}{2\pi i}\int_C \frac{\hat{f}\left(\frac{\gamma(\xi)}{\Delta t}\right)}{\xi^{j+1}}\,d\xi \tag{B.5}$$

with $C = \mathbb{B}_r(0)$, $r < 1$. Applying the inverse discrete Fourier transform, one obtains [29]

$$\omega_j^{\Delta t}[f](r) \approx \frac{r^{-j}}{L} \sum_{l=0}^{L-1} \hat{f}\left(\frac{\gamma(r\xi_L^{-l})}{\Delta t}\right) \xi_L^{lj} \tag{B.6}$$

where $\xi_L = e^{\frac{2\pi i}{L}}$.

Let $N_{\Delta t}$ be the number of points in a uniform temporal grid, i.e. $N_{\Delta t}\Delta t = T$. The usual choice for L and r in (B.6) is [69, p.13]

$$L = N_{\Delta t} \quad \text{or} \quad L = 2\ N_{\Delta t} \quad \text{and} \quad r = \varepsilon^{-N_{\Delta t}}$$

where ε is the desired accuracy. We further choose

$$\gamma(\xi) = \sum_{i=1}^{2} \frac{1}{i}(1-\xi)^i = \frac{1}{2}(\xi-1)(\xi-3) = \frac{3}{2} - 2\xi + \frac{1}{2}\xi^2$$

which also seems to be the standard choice in the literature.

B.2 The Time Domain Single Layer, Double Layer and Hypersingular Operator Kernel Functions

For the kernel of the time domain Single Layer operator (1.8), one obtains [29]

$$\hat{k}_V(\tau, d) = \mathcal{L}\left[k_V(\cdot, d)\right](\tau, d) = \frac{1}{2\pi} K_0(d\tau) = \frac{i}{4} H_0^{(1)}(id\tau) \tag{B.7}$$

where $K_0(x) = \frac{\pi}{2} i H_0^{(1)}(ix)$ is the *modified Bessel function of the second kind of order zero* (also known as the *MacDonald function of order zero*), and $H_0^{(1)}$ is the *Hankel function of the first kind of order zero*. We use the reference implementation [9, 119] of the Hankel functions for our numerical experiments.

For the time domain Double Layer operator (1.10), one needs the derivatives of the respective functions. There holds $K_0' = -K_1$ and, similarly, $\left(H_0^{(1)}\right)' = -H_1^{(1)}$. Since the temporal Laplace transform used here is space-invariant, there holds

$$\mathcal{L}\left[\nabla_x k_V(\cdot, d)\right] = \nabla_x \mathcal{L}\left[k_V(\cdot, d)\right](\tau, d) = \nabla_x \hat{k}_V(\tau, d)$$

where $d = |x - y|$. With $\frac{\partial}{\partial x_i}|x-y| = \frac{x_i - y_i}{|x-y|}$, $i = 1, 2$, one then obtains

$$\nabla_x K_0(d\tau) = -\left(\frac{\tau}{d} K_1(d\tau)\right)(x-y) \quad \text{and} \quad \nabla_x H_0^{(1)}(id\tau) = -\left(\frac{i\tau}{d} H_1^{(1)}(id\tau)\right)(x-y).$$

Therefore

$$\hat{k}_K(\tau, d) = -\frac{i}{4}\left(\frac{i\tau}{d} H_1^{(1)}(id\tau)\right)\ n_y \cdot (x-y) = \frac{1}{4}\left(\frac{\tau}{d} H_1^{(1)}(id\tau)\right)\ n_y \cdot (x-y) \tag{B.8}$$

is the kernel of the Double Layer operator.

For the time domain hypersingular boundary integral operator (1.11), one needs to differentiate again. There holds

$$\frac{1}{x}\frac{d}{dx}(xH_1^{(1)}) = \frac{1}{x}\left(H_1^{(1)} + x\left(H_1^{(1)}\right)'\right) = H_0^{(1)}$$

and thus $\left(H_1^{(1)}\right)' = H_0^{(1)} - \frac{1}{x}H_1^{(1)}$. Further

$$\frac{\partial}{\partial y_i}\left(n_y \cdot (x-y)\right) = -\left(n_y\right)_i \quad \text{and} \quad \frac{\partial}{\partial y_i}|x-y| = -\frac{x_i - y_i}{|x-y|}.$$

Therefore

$$\begin{aligned}
\frac{\partial}{\partial y_i}\left(\frac{\tau}{d}H_1^{(1)}(id\tau)\right) &= -\tau d^{-2}(-1)(x_i-y_i)d^{-1}H_1^{(1)}(id\tau) \\
&\quad + \frac{\tau}{d}\left(H_0^{(1)}(id\tau) - \frac{1}{id\tau}H_1^{(1)}(id\tau)\right)(-1)(x_i-y_i)d^{-1}i\tau \\
&= \tau d^{-2}\left(d^{-1}H_1^{(1)}(id\tau) - i\tau H_0^{(1)}(id\tau) + d^{-1}H_1^{(1)}(id\tau)\right)(x_i-y_i) \\
&= \tau d^{-2}\left(2d^{-1}H_1^{(1)}(id\tau) - i\tau H_0^{(1)}(id\tau)\right)(x_i-y_i)
\end{aligned}$$

and thus

$$\begin{aligned}
\frac{\partial}{\partial y_i}\hat{k}_K(\tau,d) &= \frac{1}{4}\left\{\frac{\partial}{\partial y_i}\left(\frac{\tau}{d}H_1^{(1)}(id\tau)\right)\left(n_y\cdot(x-y)\right) + \left(\frac{\tau}{d}H_1^{(1)}(id\tau)\right)\frac{\partial}{\partial y_i}\left(n_y\cdot(x-y)\right)\right\} \\
&= \frac{1}{4}\Big\{\ \tau d^{-2}\left(2d^{-1}H_1^{(1)}(id\tau) - i\tau H_0^{(1)}(id\tau)\right)\left(n_y\cdot(x-y)\right)(x_i-y_i) \\
&\qquad - \left(\frac{\tau}{d}H_1^{(1)}(id\tau)\right)\left(n_y\right)_i\Big\}
\end{aligned}$$

which gives, finally,

$$\begin{aligned}
&\nabla_y\left(\hat{k}_K(\tau,d)\right) \\
&= \frac{1}{4}\left\{\left(\left(\frac{2\tau}{d^3}H_1^{(1)}(id\tau) - \frac{i\tau^2}{d^2}H_0^{(1)}(id\tau)\right)\left(n_y\cdot(x-y)\right)\right)(x-y) - \left(\frac{\tau}{d}H_1^{(1)}(id\tau)\right)n_y\right\} \quad \text{(B.9)}
\end{aligned}$$

Alternatively one can, as for the Galerkin time domain Boundary Element Method, integrate by parts in the bilinear form that corresponds to the hypersingular boundary integral operator, to obtain a weakly singular instead of a hypersingular kernel. By (A.87) there holds, in convolution notation,

$$-\langle W[\varphi](\cdot,t),\psi(\cdot,t)\rangle = \iint_{\Gamma\times\Gamma}\left(k_V * \ddot{\varphi}\right)(y,t)\ \psi(x,t)\ n_x\cdot n_y\ +\ \left(k_V * \frac{d\varphi}{ds}\right)(y,t)\ \frac{d\psi}{ds}(x,t)\ ds_x ds_y. \quad \text{(B.10)}$$

We write $k_{W,1} := k_V * \ddot{\varphi}$ and $k_{W,2} := k_V$. Using integration by parts one has $k_{W,1} = \ddot{k}_V * \varphi$ and therefore $\hat{k}_{W,1}(\tau,d) = \tau^2\hat{k}_V(\tau,d)$. This representation has also been used by Chappell in the three dimensional case; see [45, (51)].